

# 2014 Medical Imaging

9-14 February 2014

**Technical Summaries** 

www.spie.org/mi

#### Location

Town & Country Resort and Convention Center San Diego, California, USA

Conference and Courses

15-20 February 2014







#### Symposium Chairs:



Ehsan Samei, Duke Univ. (USA)



David Manning, Lancaster Univ. (UK)

#### Contents

9033:	Physics of Medical Imaging
9034:	Image Processing
9035:	Computer-Aided Diagnosis99
9036:	Image-Guided Procedures, Robotic Interventions, and Modeling
9037:	Image Perception, Observer Performance, and Technology Assessment
9038:	Biomedical Applications in Molecular, Structural, and Functional Imaging
9039:	PACS and Imaging Informatics: Next Generation and Innovations
9040:	Ultrasonic Imaging and Tomography 202
9041:	Digital Pathology

Click on the Conference Title to be sent to that page

SPIE would like to express its deepest appreciation to the symposium chairs, conference chairs, program committees, session chairs, and authors who have so generously given their time and advice to make this symposium possible.

The symposium, like our other conferences and activities, would not be possible without the dedicated contribution of our participants and members. This program is based on commitments received up to the time of publication and is subject to change without notice.

### 2014 Medical Imaging

15–20 February 2014 Town & Country Resort and

Convention Center San Diego, California, USA

Cooperating Organizations:

American Association of Physicists in Medicine

**American Physiological Society** 

Computer Assisted Radiology and Surgery

**DICOM Standards Committee** 

**Medical Image Perception Society** 

Radiological Society of North America

Society for Imaging Informatics in Medicine

**World Molecular Imaging Society** 











Monday - Thursday 17-20 February 2014

Part of Proceedings of SPIE Vol. 9033 Medical Imaging 2014: Physics of Medical Imaging



9033-1, Session 1

## Noninvasive functional assessment of coronary artery disease using cardiac CT imaging and computational fluid dynamics (Keynote Presentation)

Charles A. Taylor, HeartFlow, Inc. (United States) and Stanford Univ. (United States)

Heart disease resulting from atherosclerosis in the coronary arteries is the cause of nearly one-third of all global deaths. The severity of coronary artery disease and the consequent effect on blood flow to the heart are difficult to measure, yet this information is critical for treating patients. Currently, the gold-standard for assessing the functional significance of coronary artery disease involves invasive measurement of pressure in the coronary arteries at the time of diagnostic cardiac catheterization, but this procedure is expensive and poses risk to the patient. A recent breakthrough in imaging technologies with CT scanners and computational fluid dynamics is enabling an inexpensive and potentially safer diagnostic tool to emerge. Broad application of this technology could reduce annual health care costs nationally by billions of dollars and save thousands of lives each year. Based on research funded by the National Science Foundation and the National Institutes of Health, HeartFlow is able to analyze a patient's coronary CT scan images and, using high performance computing and computational fluid dynamics, to solve for coronary blood flow and pressure. Clinical data has demonstrated significant improvements in diagnostic accuracy as compared to other noninvasive technologies. HeartFlow employs a service model whereby patient data is uploaded through a secure web browser, processed on-site using custom software and high performance computing platforms and transmitted back to the ordering physician through a secure web browser. This analysis enables the physician to quickly determine the best treatment without invasive diagnostic cardiac catheterization.

9033-2. Session 1

## Simulation evaluation of quantitative myocardial perfusion assessment from dynamic cardiac CT

Michael D. Bindschadler, Univ. of Washington (United States); Dimple Modgil, The Univ. of Chicago (United States); Kelley R. Branch, Univ. of Washington (United States); Patrick J. La Rivière, The Univ. of Chicago (United States); Adam M. Alessio, Univ. of Washington (United States)

Contrast enhancement on cardiac CT provides valuable information about myocardial perfusion and methods have been proposed to assess perfusion with static and dynamic acquisitions. There is no consensus on the best approach to ensure 1) sufficient diagnostic accuracy for clinical decisions and 2) low radiation doses for patient safety. This work uses a thorough dynamic CT simulation and several accepted blood flow estimation techniques to evaluate perfusion assessment across a range of acquisition and estimation scenarios. Simulated CT acquisitions used a validated CT simulator incorporating polyenergetic data acquisition. Time attenuation curves were extracted for multiple regions around the myocardium and used to estimate flow. In total, >2,700 independent realizations of dynamic sequences were generated and multiple perfusion estimation methods were applied to each of these. Evaluation of quantitative kinetic modeling yielded perfusion estimates with a root mean square error (RMSE) of ~0.6 ml/g/min, averaged across multiple scenarios. Semi-quantitative modeling and qualitative static imaging resulted in significantly more error. For quantitative methods, a similar dose reduction through reduced temporal sampling or through reduced

tube current had comparable impact on perfusion estimate fidelity. On average, half dose acquisitions increased the RMSE of estimates by only 18% suggesting that substantial dose reductions may be possible in the context of quantitative myocardial blood flow estimation. In conclusion, quantitative model-based dynamic cardiac CT perfusion assessment is capable of accurately estimating perfusion across a range of cardiac outputs and tissue perfusion states, outperforms comparable static perfusion estimates, and is relatively robust to noise and temporal subsampling.

9033-3, Session 1

### A combined local and global motion estimation and compensation method for cardiac CT

Qiulin Tang, Beshan S. Chiang, Toshiba Medical Research Institute USA (United States); Akin Akinyemi, Toshiba Medical Visualization Systems Europe, Ltd. (United Kingdom); Alexander A. Zamyatin, Toshiba Medical Research Institute USA (United States); Bibo Shi, Ohio Univ. (United States); Satoru Nakanishi, Toshiba Medical Research Institute USA (United States)

A new motion estimation and compensation method for cardiac computed tomography (CT) was developed. By combining two motion estimation (ME) approaches the proposed method estimates the local and global cardiac motion and then preforms motion compensated reconstruction. The combined motion estimation method has two parts: one is the local motion estimation, which estimates the coronary artery motion by using coronary artery tree tracking and registration; the other one is the global motion estimation, which estimates the entire cardiac motion estimation by image registration. There are two approaches to combine the coronary artery motion and entire cardiac motion to obtain the final cardiac motion. First one is to use a linear combination of them directly. The second one is to use the coronary artery motion as a prior for global motion estimation. We use the backproject-then-warp method proposed by Pack et al. to perform motion compensation reconstruction (MCR). The proposed method was evaluated with 5 patient data and improvements in sharpness of both coronary arteries and heart chamber boundaries were obtained.

9033-4, Session 2

## Dose reduction assessment in dynamic CT myocardial perfusion imaging in a porcine balloon-induced-ischemia model

Rachid Fahmi, Brendan L. Eck, Case Western Reserve Univ. (United States); Xiaorong Zhou, Univ. Hospitals of Cleveland (United States); Mani Vembar, Philips Healthcare (United States); Hiram G. Bezerra M.D., Univ. Hospitals of Cleveland (United States); David L. Wilson, Case Western Reserve Univ. (United States)

Dynamic myocardial CT perfusion (D-MCTP) is a high resolution, non-invasive technique for assessing myocardial blood flow (MBF), which in concert with coronary CT angiography would enable CT to provide a comprehensive, fast analysis of both coronary anatomy and functional flow. Since radiation exposure (RE) is an issue in dynamic acquisitions, we investigated acquisition parameters and low dose reconstruction methods. Partial scan acquisitions and reductions in tube output (kVp and/or mAs) can reduce RE at the expense of reducing image quality and hampering accurate MBF quantification. We assess D-MCTP in a porcine model before and after induced-ischemia using different kVp/mAs combinations and reconstructions (FBP and iDose4-Philips). Each animal











underwent LAD stent implantation followed by partial-balloon inflation with FFR assessment of occlusion severity. CT images were acquired at end-systole using a 256-slice MDCT (Brilliance-iCT-Philips), and 20mL of iodine flushed by 20mL of saline at 4mL/s, both before (FFR=1) and after (FFR<0.8) balloon inflation. Deformable 3D-registration and spatiotemporal bilateral filtering were applied to reduce motion and partial-scan artifacts. Beam-hardening-correction removed artifacts often perceived as perfusion deficits. Absolute MBF was measured by a deconvolution-based approach using singular value decomposition (SVD). Arterial input function was estimated from the LV-cavity near the aortic valve. ROIs in both LAD and remote territories were assessed for both baseline and occluded conditions. MBF was measured in these ROIs and their ratios compared to FFR values. Preliminary results show that iDose4 reconstruction leads to good correlation between MBF measurements and FFR values even for lower dose acquisitions.

9033-5, Session 2

### Estimating lesion volume in low-dose chest CT: How low can we go?

Stefano Young, Michael F. McNitt-Gray, Univ. of California, Los Angeles (United States)

PURPOSE: To examine the potential for dose reduction in chest CT studies whose primary purpose is to output lesion volumes (e.g. therapymonitoring applications).

METHODS: We developed a workflow to simulate reduced-dose chest CT scans and measure lesion volumes as follows: (1) Add noise to the raw clinical data to simulate a lower reference-mAs setting, (2) reconstruct the simulated, reduced-mAs data on the clinical workstation, and (3) import the reduced-mAs reconstructions into our quantitative imaging database for lesion contouring. We asked one reader to contour 9 different lesions (one per patient) at the clinical reference-mAs level (100%) and 10 fractions of the clinical mAs (50,25,15,10,7,5,4,3,2,1%). The reader was given approximate lesion coordinates and he could work on the clinical and reduced-mAs scans in any order, but the mAs fractions were hidden to reduce bias. Finally, we compared the clinical-mAs contours with reduced-mAs contours as a surrogate for true volume estimation. Contouring accuracy was defined as the average percent difference between the reduced-mAs contour volume and its corresponding clinical-mAs contour volume.

RESULTS: Contouring accuracy appeared to be consistent (> 80%) down to simulated reference-mAs levels corresponding to less than 10% of current clinical settings at our institution.

CONCLUSIONS: For a simple lung-lesion-contouring task, the referencemAs settings at our institution may be an order-of-magnitude higher than necessary. However, these preliminary results are limited by potential recall bias, a small patient cohort, and an overly-simplified task. Therapy monitoring involves checking for new lesions, which may influence the reader's mAs threshold for acceptable performance.

9033-6, Session 2

### A biological phantom for evaluation of CT image reconstruction algorithms

Jochen Cammin, George S. Fung, Elliot K. Fishman, Johns Hopkins Outpatient Ctr. (United States); Jeffrey H. Siewerdsen, Joseph W. Stayman, Johns Hopkins Univ. (United States); Katsuyuki Taguchi, Johns Hopkins Outpatient Ctr. (United States)

In recent years, iterative algorithms have become popular in diagnostic CT imaging to reduce noise or radiation dose to the patient. The non-linear nature of these algorithms leads to non-linearities in the imaging chain. However, the methods to assess the performance of CT imaging systems were developed assuming the linear process of filtered backprojection (FBP). Those methods may not be suitable any longer

when applied to non-linear systems. In order to evaluate the imaging performance, a phantom is typically scanned and the image quality is measured using various indices. For reasons of practicality, cost, and durability, those phantoms often consist of simple water containers with uniform cylinder inserts. However, these phantoms do not represent the rich structure and patterns of real tissue accurately. As a result, the measured image quality or detectability performance for lesions may not reflect the performance on clinical images. The discrepancy between estimated and real performance may be even larger for iterative methods with their tendency to produce "plastic-like" images with homogeneous patterns. Consequently, more realistic phantoms should be used to assess the performance of iterative algorithms. We designed and constructed a biological phantom consisting of porcine organs and tissue that models a human abdomen, including liver lesions. We scanned the phantom on a clinical CT scanner and compared basic image quality indices between FBP and an image processing approach to reduce noise based on total-variation minimization (TVmin).

9033-7, Session 2

## Impact of norm selections on the performance of four-dimensional cone-beam computed tomography (4DCBCT) using PICCS

Yinsheng Li, Jie Tang, Guang-Hong Chen, Univ. of Wisconsin-Madison (United States)

In 4D CBCT, projection data were retrospectively sorted into different phase bins to mitigate motion blur and thus to increase the temporal resolution. Projection view in each phase bin is insufficient to reconstruct a streak-free image using Filtered Backprojection (FBP). An image reconstruction framework known as Prior Image Constrained Compressed Sensing (PICCS) has been used to mitigate the undersampled artifacts. To date, published studies have employed the L1 norm in the minimization of the objective function, as the L1 norm has been shown to promote sparsity in compressed sensing studies. However, the norm p does not necessarily need to be unity. The purpose of this study is two-fold: (1) How does image quality depend on the Lp norm used in the minimization of the objective function? (2) In the minimization of the Lp norm, is there any improvement in image quality, when alternative weighting strategies are used, such as the iterative reweighted methods?

Both numerical motion phantom and real scanned patient data were used to investigate how the performance of the PICCS algorithm depends on the norm selection. In this study, the minimization strategy for employing Lp norms is discussed. The performance of Lp norm PICCS is compared with and without incorporating an iterative reweighted strategy. Image quality is evaluated in terms of reconstruction accuracy and motion recoverability.

9033-8, Session 2

### 3D image-based scatter estimation and correction for multi-detector CT imaging

Martin Petersilka, Thomas Allmendinger, Karl Stierstorfer, Siemens Healthcare (Germany)

The aim of this work is to implement and evaluate a 3D image-based approach for the estimation of scattered radiation in multi-detector CT. Based on a reconstructed CT image volume, the scattered radiation contribution is calculated in 3D fan-beam geometry in the framework of a point-scatter kernel (PSK) model of scattered radiation. The PSK model is based on the calculation of elemental scatter contributions propagating the rays from the focal spot to the detector across the object for defined interaction points on a 3D fan beam grid. Each interaction point in 3D leads to an individual elemental 2D scatter distribution on











the detector. The sum of all elemental contributions represents the total scatter intensity distribution on the detector. Our proposed PSK depends on the scattering angle (defined by the interaction point and the considered detector channel) and the line integral between the interaction point on a 3D fan beam ray and the line integral between the interaction point on a 9D fan beam ray and the intersection of the same ray with the detector. The PSK comprises single- and multiple scattering as well as the angular selectivity characteristics of the anti-scatter grid on detector. Our point-scatter kernels were obtained from a low-noise Monte-Carlo simulation of water-equivalent semi-spheres with different radii for a particular CT scanner geometry. The model allows obtaining noise-free scatter intensity distribution estimates with a lower computational load compared with Monte-Carlo methods. In this work, we give a description of the algorithm and the proposed PSK. Furthermore, we compare resulting scatter intensity distributions (obtained for numerical phantoms) to Monte-Carlo results.

9033-9, Session 2

### Small animal lung imaging with a benchtop in-line X-ray phase-contrast system

Alfred Garson III, Washington Univ. in St. Louis (United States); Enrique Izaguirre, Scott & White Healthcare (United States); Samantha Price, Huifeng Guan, Sunil Vasireddi, Mark A. Anastasio, Washington Univ. in St. Louis (United States)

X-ray phase-contrast (XPC) imaging methods are well-suited for lung imaging applications due to the weakly absorbing nature of lung tissue and the strong refractive effects associated with tissue-air inter-faces. Until recently, XPC lung imaging had only been accomplished with synchrotron experiments with lung images exhibiting a speckled appearance attributed to multiple refractions of X-rays as they traverse through air-tissue interfaces of alveoli. We investigate the manifestation of speckle in propagation-based XPC images of mouse lungs acquired in situ by use of a benchtop imager. The key contributions of the work are: a) the demonstration that lung speckle can be observed by use of a benchtop XPC imaging system employing a polychromatic tubesource; b) a systematic experimental investigation of how the texture of the speckle pattern depends on the parameters of the imaging system; and c) the application of speckle texture analysis for identifying regions of abnormal lung tissue. In particular, we present results demonstrating analysis of speckle texture is a promising technique for identifying regions of ra- diation induced lung damage (RILD). Our analyses consists of image texture characterization based on the statistical properties of pixel intensity values in projection images. Results are compared with those from XPC tomography that exhibit details of lung structure possessing exceptional quality and spatial resolution . Finally, the physiological changes to alveoli associated with RILD are modeled with simple lung phantoms based on hollow microspheres of differing size and distributions. The dependence of the detected X-ray signal on alveoli structural properties is investigated.

9033-10, Session 3

## Fast data acquisitions in X-ray differential phase contrast imaging using a new grating design

Yongshuai Ge, Ke Li, Guang-Hong Chen, Univ. of Wisconsin-Madison (United States)

Grating interferometer-based x-ray differential phase contrast imaging (DPCI) often uses a time-consuming phase stepping procedure that requires sequential movements of a grating and multiple x-ray exposures to extract phase information. To accelerate the data acquisition speed of DPCI and improve the mechanical stability of the grating interferometer, a novel interferometer setup was developed and experimentally integrated into a DPCI benchtop system. In this new interferometer, the original

one-dimensional analyzer G2 grating was divided into separate rows, each with a horizontal offset where the lateral shift from row to row is equal to a quarter of the period of the x-ray interference fringe pattern. By performing phase retrieval using detector counts of four neighboring pixels along the vertical direction, the complete differential phase contrast (DPC) signal at each detector pixel can be extracted. Therefore, this method completely removes the need to perform phase stepping and requires only a single x-ray exposure to generate a DPC image. Initial physical phantom experiments demonstrated that the new interferometer design can generate DPC images with high accuracy at the same data acquisition time as that used in the conventional absorption x-ray imaging. Thus, this new breakthrough is expected to greatly facilitate the transition of DPCI to clinical applications.

9033-11, Session 3

### Slit-scanning differential phase-contrast mammography: first experimental results

Ewald Roessl, Heiner Daerr, Thomas Koehler, Gerhard Martens, Udo van Stevendaal, Philips Technologie GmbH (Germany)

The demand for a large field-of-view (FOV) and the stringent requirements for a stable acquisition geometry rank among the major obstacles for the translation of grating-based, differential phase-contrast techniques from the laboratory to clinical applications. While for state-of-the-art Full-Field-Digital Mammography (FFDM) FOVs of 24 cm x 30 cm are common practice, the specifications for mechanical stability are naturally derived from the detector pixel size which ranges between 50 ?m to 100 ?m. However, in grating-based, phase-contrast imaging, the relative placement of the gratings in the interferometer must be guaranteed to within micro-meter precision. In this work, we report on first, experimental results on a phase-contrast x-ray imaging system based on the Philips MicroDoseTM L30 mammography unit. With the proposed approach we achieve a FOV of about 7 cm x 18 cm by the use of the slit-scanning technique. The demand for mechanical stability on a micrometer scale was relaxed by the specific interferometer design, i.e., a rigid, actuatorfree mount of the phase-grating G1 with respect to the analyzer-grating G2 onto a common steel frame. The image acquisition and formation processes are described and first phase-contrast images of a test object are presented. A brief discussion of the shortcomings of the current approach is given, including the level of remaining image artifacts and the relatively inefficient usage of the total available x-ray source output.

9033-12. Session 3

## A multi-channel image reconstruction method for grating-based X-ray phase-contrast computed tomography

Qiaofeng Xu, Alex Sawatzky, Mark A. Anastasio, Washington Univ. in St. Louis (United States)

In this work, we report on the development of advanced multi-channel (MC) image reconstruction algorithms for grating-based X-ray phasecontrast computed tomography (GB-XPCT). The MC reconstruction methods we have developed operate by concurrently, rather than independently as is done conventionally, reconstructing tomographic images of the three object properties (absorption, refractive index, ultrasmall-angle scattering). By jointly estimating the object properties by use of an appropriately defined penalized weighted least squares (PWLS) estimator, the 2nd order statistical properties of the object property sinograms, including correlations between them, can be fully exploited to improve the variance vs. resolution tradeoff of the reconstructed images as compared to existing methods. Channel-independent regularization strategies are proposed. To solve the MC reconstruction problem, we developed advanced algorithms based on the proximal point algorithm and the augmented Lagrangian method. By use of experimental and computer-simulation data, we demonstrate that by exploiting inter-











channel noise correlations, MC reconstruction methods can improve image quality in GB XPCT. We also establish that MC reconstruction methods can facilitate reductions in data-acquisition times and doses in GB-XPCT.

9033-13, Session 3

## Simultaneous implementation of low dose and high sensitivity capabilities in differential phase contrast and dark-field imaging with laboratory x-ray sources

Alessandro Olivo, Charlotte K. Hagen, Thomas P. Millard, Fabio A. Vittoria, Paul C. Diemoz, Marco Endrizzi, Univ. College London (United Kingdom)

We present a development of the laboratory-based implementation of edge-illumination (EI) x-ray phase contrast imaging (XPCI) that simultaneously enables low-dose and high sensitivity. Lab-based EI-XPCI simplifies the set-up with respect to other methods, as it only requires two optical elements, the large pitch of which relaxes the alignment requirements. Albeit in the past it was erroneously assumed that this would reduce the sensitivity, we demonstrate quantitatively that this is not the case.

We discuss a system where the pre-sample mask open fraction is smaller than 50%, and a large fraction of the created beamlets hits the apertures in the detector mask. This ensures that the majority of photons traversing the sample are detected i.e. used for image formation, optimizing dose delivery. We show that the sensitivity depends on the dimension of the part of each beamlet hitting the detector apertures, optimized in the system design. We also show that the aperture pitch does not influence the sensitivity. Compared to previous implementations, we only reduced the beamlet fraction hitting the absorbing septa on the detector mask, not the one falling inside the apertures: the same number of x-rays per second is thus detected, i.e. the dose is reduced but not at the expense of exposure time.

We also present an extension of our phase-retrieval algorithm enabling the extraction of ultra-small-angle scattering by means of only one additional frame, with all three frames acquired within dose limits imposed by e.g. clinical mammography, and easy adaptation to labbased phase-contrast x-ray microscopy implementations.

9033-14, Session 3

## Cramer-Rao lower bound in differential phase contrast imaging and its application in the optimization of data acquisition system

Ke Li, Yongshuai Ge, Guang-Hong Chen, Univ. of Wisconsin-Madison (United States)

Object detectability in medical images is fundamentally noise limited, and x-ray differential phase contrast imaging (DPCI) is no exception. Unlike conventional absorption-based x-ray imaging that involves the logarithmic transform of the detector readouts, DPCI uses a algorithmic phase retrieval procedure to obtain the phase shift information from the same set of detector readouts. As a result, its noise performance is expected to behave differently than x-ray absorption imaging. In this work, we are interested in evaluating the lowest achievable noise variance in DPC images using the Cramer-Rao lower bound (CRLB) estimation method. We found that the noise variance in images obtained by algorithmic phase retrieval is always higher than the value estimated by the CRLB, which implies the sub-optimality of current phase retrieval method and the necessity of incorporating statistical signal estimation theory into DPCI in order to optimize its noise performance and dose efficiency. We also found that the lower bound of the noise variance in DPCI is directly related to the total number of phase steps, therefore an

optimal phase stepping scheme can be established under the guideline of the CRLB method.

9033-15, Session 3

### Statistical signal estimation methods in X-ray differential phase contrast imaging

Yongshuai Ge, Ke Li, Guang-Hong Chen, Univ. of Wisconsin-Madison (United States)

X-ray differential phase contrast imaging (DPCI) uses a Fouriertransform-based analytical method to retrieve phase shift information of the x-rays, which carries important information about the object being imaged. The Fourier method was derived by modeling the measured x-ray intensity modulations generated by the phase stepping routine as sinusoidal functions, which is oversimplified since noises induced by the quantum fluctuations of the x-rays and by the electronic fluctuations of the readout hardware were entirely ignored by the model. Based on the statistical probability distribution function of the detected x-ray intensities in DPCI, we developed a new iterative phase retrieval method that simultaneously maximize the statistical likelihood of the three estimated physical quantities in DPCI, including the phase signal, the conventional absorption signal, and the dark field signal. Our numerical simulations demonstrate that this new iterative method outperformed the Fourier method by minimizing the noise variance in the estimated results, therefore the dose efficiency of DPCI is expected to be further improved by this method.

9033-16, Session 3

## Investigation of in-line X-ray phase-contrast tomosynthesis using an advanced iterative algorithm

Huifeng Guan, Qiaofeng Xu, Alfred Garson III, Mark A. Anastasio, Washington Univ. in St. Louis (United States)

Tomosynthesis is a practical technique for section imaging that provides a greater level of 3D information than planar radiography but at lower dose than CT. Even with limited depth resolution, tomosynthesis is useful for resolving superimposed structures that are projected onto the 2D plane of x-ray detector. In-line (or propagation-based) X-ray phase-contrast (XPC) imaging is an emerging modality based on Fresnel diffraction theory. Phase-contrast edge enhancement occurs at the boundary between different media enabling improved conspicuity in projection images. It is natural to combine these two concepts and to explore the idea of "XPC tomosynthesis" for 3D characterization of weakly absorbing objects. We have made the following contributions in this work. 1) We have developed an advanced iterative reconstruction algorithm that employs total variation (TV) regularization. We showed the advantage of iterative algorithm in reconstruction accuracy and noise suppression; 2) Based on the XPC tomography imaging model, we investigate and evaluate the ability of tomosynthesis to preserve phase-contrast information; 3) We demonstrate that phase-contrast tomosynthesis provides better depth resolution than conventional (absorption-based) tomosynthesis; and 4) We propose and demonstrate a novel variant of XPC tomosynthesis employing an offset detector to increase the field-of-view without sacrificing spatial resolution.

9033-500, Session PL

### The emerging role of quantitative imaging biomarkers

John C. Gore, Vanderbilt Univ. Medical Ctr. (United States)

The development and applications of quantitative imaging biomarkers











are essential goals for modern biomedical imaging science. Imaging biomarkers are growing in their diversity and impact, and are of particular importance in the evaluation of novel drugs and treatments. In cancer, molecular imaging using PET and optical methods report directly on cellular events and characteristics, and are complemented by MRI, CT and US methods that measure downstream effects such as changes in tumor volume, cell density, tissue vascular properties and blood flow. These are being applied in evaluating new drugs and in clinical trials, and are proving useful in cancer management, especially to evaluate treatment response. Integrating multiple data sets from different modalities such as PET and MRI can provide a more comprehensive view of tumor metabolic and physiological state. In neuroscience, quantitative brain morphometry is used to characterize and distinguish subject groups and identify structural variants in individuals which correlate with behavior and function. PET studies of neurotransmitters and their transporters are well established and provide direct evidence of whether drugs hit specific targets, along with their in vivo binding properties. Functional MRI based on BOLD (blood oxygen level dependent) signals provides unique insights into neural circuits and inter-regional functional connectivities, which may be quantified to assess changes with treatment, development, degeneration or as an index of severity of disease. Pharmaceutical MRI uses similar measurements to evaluate the actions of drugs and specific signaling pathways in the brain. In diabetes and metabolic disorders, measures of tissue composition, physiology and metabolism provide quantitative indices of disease risk and progression. Overall, there are numerous such biomarkers under development in many different areas of application in each modality, and these activities define much of the research in current imaging science.

9033-17, Session 4

### Removing blooming artifacts with binarized deconvolution in cardiac CT

Christian Hofmann, Friedrich-Alexander-Univ. Erlangen-Nürnberg (Germany); Michael Knaup, German Cancer Research Center (DKFZ) (Germany); Marc Kachelriess, Deutsches Krebsforschungszentrum (Germany)

With modern CT scanners detection and classification of coronary artery disease has become a routine application in cardiac CT. It poses a desirable non-invasive alternative to the invasive coronary angiography which is the current clinical gold standard. However the accuracy depends on the spatial resolution of the imaging system. The limited spatial resolution leads to blooming artifacts arising from hyper-dense calcification deposits in the arterial walls. This blooming leads to an overestimation of the degree of luminal narrowing and to loss of the morphology of the calcified region. We propose an imagebased algorithm which aims at removing the blooming and estimating the correct CT-value and morphology of the calcification. The method is based on the assumption, that each calcification consists of a region which has an almost constant density and attenuation. This knowledge is incorporated into an iterative deconvolution algorithm in image space. We quantitatively assess the accuracy of the proposed algorithm on analytically simulated phantom data. Qualitative results of clinical patient data are presented as well. In both cases the proposed method outperforms the compared algorithms. The initial patient data results are promising. However, an ex vivo study has to be done to confirm the quantitative results of the simulation study with real specimen.

9033-18, Session 4

### Automatic cable artifact removal for cardiac C-arm CT imaging

Christian Haase, Dirk Schäfer, Philips Technologie GmbH (Germany); Michael Kim, S. James Chen, John D. Carroll M.D., Univ. of Colorado (United States); Peter G. Eshuis, Philips

Healthcare (Netherlands); Olaf Dössel, Karlsruher Institut für Technologie (Germany); Michael Grass, Philips Technologie GmbH (Germany)

Cardiac C-arm computed tomography (CT) imaging on interventional C-arm systems can be applied in various areas of interventional cardiology ranging from structural heart disease and electrophysiology interventions to valve procedures in hybrid operating rooms. In contrast to conventional CT systems, the reconstruction field of view (FOV) of C-arm systems is limited to a region of interest in cone-beam (along the patient axis) and fan-beam (in the transaxial plane) direction. Hence, highly X-ray opaque objects (e.g. pacing leads from patient implants or cables from the interventional setup) outside the reconstruction field of view, yield streak artifacts in the reconstruction volume. To decrease the impact of these streaks a cable tracking approach on the 2D projection sequences with subsequent interpolation is applied. The proposed approach uses the fact that the projected position of objects outside the reconstruction volume depends strongly on the projection perspective. By tracking candidate points over multiple projections only objects outside the reconstruction volume are segmented in the projections.

The method is quantitatively evaluated based on 30 simulated CT data sets. The 3D root mean square deviation to a reference image could be reduced for all cases by an average of 50 % (min 16 %, max 76 %). Image quality improvement is shown for clinical whole heart data sets acquired on an interventional C-arm system.

9033-19. Session 4

## Ringing artifact reduction for metallic objects in direct digital radiography detectors with stationary antiscatter grids

Dong Sik Kim, Hankuk Univ. of Foreign Studies (Korea, Republic of); Sanggyun Lee, DRTECH Corp. (Korea, Republic of)

In digital radiography imaging, the antiscatter grid is usually employed to obtain clear projected images by absorbing scattered x-ray beams. However, due to the stationary antiscatter, the grid artifact appears in the obtained x-ray image as stripes if a linear grid is considered. In order to alleviate the grid artifact, band-stop filters (BSFs) can be used and may cause annoying ringing artifact especially for metallic objects. In this paper, in order to reduce the ringing artifact while applying BSFs to alleviate the grid artifact, a spatial prefiltering technique, which is called the gradient-reduction filter, is proposed. The gradient-reduction filter can remove steep edges in the obtained x-ray images especially for metallic objects and can prevent the grid-artifact BSFs from yielding serious ringing artifact. The structure of the gradient-reduction filter is similar to that of the Crawford noise-reduction filter. However, the nonlinear function in the gradient-reduction filter has decreasing slopes as its input increases contrary to the Crawford filter case. Through extensive experiments for real digital x-ray images, which are obtained from a direct digital radiography detector, we can see the superior ringingartifact reduction performance comparing to the conventional filtering approaches especially when the x-ray image has metallic objects.

9033-20, Session 4

### Algorithms for optimizing CT fluence control

Scott S. Hsieh, Norbert J. Pelc, Stanford Univ. (United States)

The ability to customize the incident x-ray fluence in CT via beam-shaping filters or mA modulation is known to improve image quality without increasing radiation dose. Previous work has shown that complete control of x-ray fluence (ray-by-ray fluence modulation) would further improve dose efficiency. While complete control of fluence is not currently possible, emerging concepts such as dynamic attenuators and inverse-geometry CT allow nearly complete control to be realized. Optimally using ray-by-ray fluence modulation requires solving a very











high-dimensional optimization problem. Most optimization techniques fail or only provide approximate solutions. We present efficient algorithms for minimizing mean or peak variance given a fixed dose limit. The reductions in variance can easily be translated to reduction in dose, if the original variance was sufficiently low. For mean variance, a closed form solution is derived. The peak variance problem is recast as iterated, weighted mean variance minimization, and at each iteration it is possible to bound the distance to the optimal solution. We apply our algorithms in simulations of the thorax and abdomen. In simulations, peak variance reductions of 45% and 65% are demonstrated in the abdomen and thorax, respectively, compared to a bowtie filter alone. Mean variance shows smaller gains (about 15%).

9033-21, Session 4

### Towards in-vivo K-edge imaging using a new semi-analytical calibration method

Carsten O. Schirra, Philips Research North America (United States); Axel Thran, Heiner Daerr, Ewald Roessl, Roland M. Proksa, Philips Research Labs. (Germany)

Flat field calibration methods are commonly used in CT to correct system imperfections. Unfortunately, they cannot be applied in energy-resolving CT when using bow-tie filters owing to spectral distortions imprinted by the filter. This work presents a novel semi-analytical calibration method for photon counting spectral CT systems which efficiently compensates pile-up effects at fourfold increased photon flux compared to a previously published method without degradation of image quality. The obtained reduction of the scan time enabled the first K-edge imaging in-vivo.

The method employs a calibration measurement with a set of flat sheets of only a single absorber material and utilizes an analytical attenuation model to predict the expected photon counts, taking into account system properties such as x-ray spectrum and detector response. From the ratios of the measured x-ray intensities and the corresponding simulated photon counts, a look-up table is generated. By use of this look-up table, measured photon-counts can be corrected yielding data nearly in line with the analytical model. The corrected data show low pixel-to-pixel variations and pile-up effects are mitigated. Consequently, operations like material decomposition based on the same analytical model yield accurate results

The method was validated on a spectral CT animal scanner prototype equipped with a bow-tie filter in a phantom experiment and in-vivo animal study. The level of artifacts in resulting images is considerably lower than in images generated with the previously published method. First in-vivo K-edge images of a rabbit selectively depict vessel occlusion by an ytterbium-based thermoresponsive polymer.

9033-22, Session 5

### Regularization design and control of change admission in prior-image-based reconstruction

Hao Dang, Jeffrey H. Siewerdsen, Joseph W. Stayman, Johns Hopkins Univ. (United States)

The image properties of all reconstruction methods can be controlled through various parameter selections. Traditionally, reconstruction parameters are used to specify a particular noise and resolution tradeoff. The introduction of reconstruction methods that incorporate prior image information has demonstrated dramatic improvements in dose utilization and image quality, but has greatly complicated the selection of reconstruction parameters associated with the magnitude of information used from prior images. While a noise-resolution tradeoff still exists, other potentially detrimental effects are possible with poor parameter values including the possible introduction of false features and the failure to incorporate sufficient prior information to gain any improvements.

Traditional parameter selection methods such as heuristics based on similar imaging scenarios are subject to error and suboptimal solutions while exhaustive searches can involve a large number of time-consuming iterative reconstructions. We propose a novel approach that prospectively determines optimal prior image regularization strength to accurately admit specific anatomical changes without performing full iterative reconstructions. This approach leverages analytical approximations to the implicitly defined prior image-based reconstruction solution and predictive metrics used to estimate imaging performance. The proposed method is investigated in a phantom experiments and the shift-variance and data-dependence of optimal prior strength is explored. Optimal regularization based on the predictive approach is shown to agree well with traditional exhaustive reconstruction searches, while yielding substantial reductions in computation time. This suggests great potential of the proposed methodology in allowing for prospective patient-, data-, and change-specific customization of prior-image penalty strength to ensure accurate reconstruction of specific anatomical changes.

9033-23, Session 5

### Novel iterative reconstruction method for optimal dose usage in redundant CT - acquisitions

Herbert K. Bruder, Rainer Raupach, Thomas Allmendinger, Steffen G. Kappler, Johan Sunnegardh, Karl Stierstorfer, Thomas G. Flohr, Siemens Healthcare (Germany)

In CT imaging, a variety of applications exist where reconstructions are SNR and/or resolution limited. However, if the measured data provide redundant information, a composite image data with high SNR can be computed. These composite image volumes will generally compromise spectral information and/or spatial resolution and/or temporal resolution.

This brings us to the idea of transferring the high SNR of the composite image volume to the low SNR (but high resolution) 'source' image data.

It was shown that the SNR of CT image data can be improved using iterative reconstruction [1]. We present a novel iterative reconstruction method enabling optimal dose usage of re-dundant CT measurements of the same body region. The generalized update equation is formulated in image space without further referring to raw data after initial reconstruction of source and composite image volumes. The update equation consists of a linear combination of the previous update, a correction term constrained by the source data, and a regularization prior initialized by the composite data.

The efficiency of the method is demonstrated for four different applications. (i) Cardiac Imaging: the optimal phase image ('best phase') can be improved by transferring all applied radiation exposure into that image. (ii) Spectral Imaging with photon counting: we have analysed material decomposition from dual energy data of our photon counting prototype scan-ner: the material images can be significantly improved transferring the good noise statistics of the 20 keV threshold image data to each of the material images. (iii) High temporal resolution helical reconstruction: splitting up reconstruction of redundant helical acquisition data into a short scan reconstruction with Tam window and a simultaneous reconstruction of all the data optimizes the temporal resolution without degrading the SNR. (iv) Liver Imaging: Reconstructions of multi-phase liver data can be optimized by utilizing the noise statistics of com-bined data from all measured phases.

In all these cases, we show that - at constant patient dose - SNR can efficiently be transferred from the composite image to the source image data maintaining resolution properties of source data.











9033-24, Session 5

## FINESSE: a Fast Iterative Non-linear Exact Sub-space SEarch based algorithm for CT imaging

Katharina Schmitt, The Univ. of Utah (United States) and Friedrich-Alexander-Univ. Erlangen-Nürnberg (Germany); Harald Schöndube, Karl Stierstorfer, Siemens AG (Germany); Joachim Hornegger, Friedrich-Alexander-Univ. Erlangen-Nürnberg (Germany); Frédéric Noo, The Univ. of Utah (United States)

Statistical iterative image reconstruction has become the subject of strong, active research in X-ray computed tomography (CT), primarily because it may allow a significant reduction in dose imparted to the patient. However, developing an algorithm that converges fast while allowing parallelization so as to obtain a product that can be used routinely in the clinic is challenging. In this work, we present a novel algorithm that combines the strength of two popular methods. A preliminary investigation of this algorithm was performed, and strongly encouraging initial results are reported.

9033-25, Session 5

### A new approach to regularized iterative CT image reconstruction

Christian Hofmann, Friedrich-Alexander-Univ. Erlangen-Nürnberg (Germany); Michael Knaup, German Cancer Research Center (DKFZ) (Germany); Marc Kachelriess, Deutsches Krebsforschungszentrum (Germany)

Significant efforts have been done to develop image reconstruction algorithms which outperform standard filtered backprojection methods with the aim to lower the noise and maintain spatial resolution. The underlying motivation is to further reduce patient dose. Vendors and researchers try to achieve this aim by incorporating a priori knowledge into the reconstruction process by adding an additional constraints to the objective function of the iterative reconstruction algorithm, which penalizes strong variations between neighboring voxels. Many penalty terms have been proposed like q-generalized Gaussian Markov random fields, total variation (TV) and Huber penalty or other anisotropic filters. Regularization approaches in general pose a resolution noise trade-off.

One has to choose several regularization parameters carefully to not achieve an unaccustomed image impression (noise texture, staircase effect) or to loose anatomical information due to strong regularization. It can be a challenging task to find robust parameter settings. Driven by the desire to combine the wanted image properties of regularization results with various parameter settings to overcome this trade-off, we propose a new method to incorporate regularization in iterative reconstruction. The idea is to generate basis images which emphasize certain image properties like high resolution, high low contrast detectability or low noise. These images could be regularized reconstructions, post reconstruction filtered images, or reference reconstructions like filtered back-projection (FBP). Each basis image on its own may suffer from certain deficiencies due to strong regularization so they might be not anatomically correct on their own. By combining the desired properties of each basis image one can generate an image with lower noise and maintained high contrast resolution thus improving the resolution noise trade-off. We conducted a phantom simulation study and a preliminary patient study to investigate our approach. We compared the proposed method against filtered backprojection (FBP) and a penalized weighted least squares algorithm (PWLS) with a TV penalty term. The proposed method achieved the highest contrast and lowest noise at the same time.

9033-26, Session 5

## A practical statistical polychromatic image reconstruction for computed tomography using spectrum binning

Meng Wu, Stanford Univ. (United States); Qiao Yang, Friedrich-Alexander Univ. Erlangen-Nürnberg (Germany); Andreas K. Maier, Friedrich-Alexander-Univ. Erlangen-Nürnberg (Germany); Rebecca Fahrig, Stanford Univ. (United States)

Polychromatic statistical reconstruction algorithms have very high computational demands due to hard optimization problems and large number of spectrum bins. We want to develop a more practical algorithm that has a simpler optimization problem, a faster numerical solver, and requires only little prior knowledge. In this paper, a modified optimization problem for polychromatic statistical reconstruction algorithms is proposed. The modified optimization problem utilizes the idea of determining scanned materials based on a first pass FBP reconstruction to fix the ratios between photoelectric and Compton scattering components of all image pixels. The reconstruction of a density image is easy to solve by a separable quadratic surrogate algorithm that is also applicable the multi-material case. In addition, a spectrum binning method is introduced to reduce the full spectrum information. The energy bins sizes and attenuations are optimized based on the true spectrum and object. Then the expected line integral values computed by a few energy bins only are very closed to the true polychromatic values. Thus both the problem size and computational demand caused by the large number of energy bins to model a full spectrum are reduced. Simulation showed that three energy bins using the generalized spectrum binning method could provide an accurate approximation of the polychromatic X-ray signals. The average absolute error of the logarithmic detector signal is less than 0.003 for a 120 kVp spectrum. The proposed modified optimization problem and spectrum binning approach can effectively suppress beam hardening artifacts while providing low noise images.

9033-27, Session 5

## Investigation of an efficient short-scan C-arm reconstruction method with radon-based redundancy handling

Frank Dennerlein, Holger Kunze, Siemens AG (Germany)

The short-scan Feldkamp David Kress (FDK) method for C-arm CT reconstruction involves a heuristic ray-based weighting scheme to handle data redundancies. This scheme is known to be approximate and it often creates low frequency image artifacts in regions away from the central axial plane. Alternative algorithms, such as the one proposed by Defrise and Clack (DC), can handle data redundancy in a theoretically exact manner and thus notably improve image quality. The DC algorithm, however, is computationally more complex than FDK, as it requires a shift-variant 2D filtering of the data instead of a efficient 1D filtering. In this paper, a modification of the original DC algorithm is investigated, which applies the efficient FDK filtering scheme whereever possible and the DC filtering scheme only where it is required. This modification leads to a more efficient implementation of the DC algorithm, in which filtering effort can be reduced by 40%, and makes the DC method more attractive for use in an interventional imaging environment.











9033-28, Session 6

### Statistical Image Reconstruction with fast convergence via denoised orderedsubset statistically penalized algebraic reconstruction technique (DOS-SPART)

Yinsheng Li, Jie Tang, Guang-Hong Chen, Univ. of Wisconsin-Madison (United States)

Statistical Image Reconstruction (SIR) has been extensively explored in CT community due to its potentially enable the low dose or ultra-low dose data acquisition while highly maintain the acceptable image quality for clinical diagnosis. Due to the huge dynamic range of photon statistical weighting and non-linearity of the regularizer, the minimization of single objective function is computationally intensive. In this study, we propose a new implementation scheme for SIR reconstruction methods that decompose the single objective function minimization problem into a shift-invariant minimization (reconstruction) problem and a shift-variant image denoising problem to provide accelerated convergence.

To deal with the non-linearity (due to the square root property) in the TV denoising problem, an auxiliary link variable was used to replace a pair of variables with grouped image pixels via an equality constraint. The Augmented Lagrangian (AL) method is then used to convert the constrained problem into a series of equivalent unconstrained problems and Alternative Directions Multiplier Method (ADMM) can be used to exactly solve the constrained denoising problem. Hence, the denoising problem with a TV prior can be further separated into two quadratic minimization problems with purely analytical solutions, as well as a direct multiplier updating. The proposed reconstruction framework is amenable to efficient parallelization and can be straightforwardly extended into cone-beam, multislice detector or helical geometry. In the results section, both noise-spatial resolution tradeoff and convergence behaviour were used to present the feasibility and advantages of the new framework.

9033-29, Session 6

## Toward a dose reduction strategy using model-based reconstruction with limited-angle tomosynthesis

Eri Haneda, J. Eric Tkaczyk, GE Global Research (United States); Giovanni J. Palma, Razvan Iordache, GE Healthcare France (France); Scott Zelakiewicz, GE Global Research (United States); Serge L. Muller, GE Healthcare France (France); Bruno De Man, GE Global Research (United States)

Model-based iterative reconstruction (MBIR) is an emerging technique for several imaging applications including medical CT, PET, transportation security, and microscopy. Its success derives from an ability to preserve image resolution and perceived diagnostic quality under impressively reduced signal level. MBIR typically uses a cost optimization framework which models system geometry, photon statistics, and prior knowledge of reconstructed volume. The challenge of tomographic geometries is that the inverse problem becomes more ill-posed. The volumetric image solution is not uniquely determined by the incompletely sampled projection data. Furthermore, low signal level conditions introduce additional challenges due to noise. A big advantage of MBIR for limited-views and limited-angle is that it provides a framework for constraining the solution consistent with prior knowledge of expected image characteristics. In this study, we analyze the MBIR reconstruction capabilities by inspecting the influence of prior modeling components for limited-views, limited-angle tomography under low dose environment in simulation. The comparison to ground truth shows MBIR with regularization achieves higher level of fidelity and lower level of blurring/streaking artifacts compared to other state of the art iterative reconstructions especially for microcalcification.

9033-30, Session 6

## Enhancing tissue structures with iterative image reconstruction for digital breast tomosynthesis

Emil Y. Sidky, Ingrid S. Reiser, The Univ. of Chicago Medical Ctr. (United States); Robert M. Nishikawa, Univ. of Pittsburgh (United States)

Digital breast tomosynthesis (DBT) is developing rapidly as an alternative screening imaging modality to two-view projection mammography. While exposing the subject to similar X-ray dose, DBT provides some depth information, which can help to distinguish suspicious masses from normal, overlapping tissue structures. The initial clinical experience with DBT indicates improvements in sensitivity and specificity relative to digital mammography, yet there may be further room for improvement for DBT by employing advanced iterative image reconstruction (IIR) algorithms.

In this abstract, we design an IIR algorithm for enhancing tissue structure contrast. The algorithm takes advantage of a data fidelity term, which compares the derivative of the DBT projections withthe derivative of the estimated projections. This derivative data fidelity is sensitive to the edges of tissue structure projections, and as a consequence minimizing the corresponding the data-error term brings out structure information in the reconstructed volumes. The method has the practical advantages that few iterations are required and that direct region-of-interest (ROI) reconstruction is possible with the proposed derivative data fidelity term. Both of these advantages reduce the computational burden of the IIR algorithm and potentially make it feasible for clinical application.

The algorithm is demonstrated on clinical data acquired on a Hologic DBT scanner.

9033-31, Session 6

### Estimation of sparse null space functions for compressed sensing in SPECT

Joyeeta M. Mukherjee, Univ. of Massachusetts Medical School (United States); Emil Y. Sidky, The Univ. of Chicago Medical Ctr. (United States); Michael A. King, Univ. of Massachusetts Medical School (United States)

Compressed sensing (CS) is a novel sensing paradigm that asserts exact recovery of a sparse signal from far fewer measurements than the number of unknowns. CS techniques have led to gains in imaging speed, image quality, radiation dose reduction and other benefits. Successful applications of CS may be found in MRI , CT , and optical imaging . In this work we investigate the applicability of CS in SPECT for cardiac imaging application using a multi-pinhole stationary SPECT camera. The objective is to investigate which sparse system configurations are not only indistinguishable by the system but also indistinguishable by a sparsity exploiting reconstruction method. We achieve this by reconstructing the system null space with an additional sparsity constraint. In this paper, we present a proof of principle on the technique. We will test the method with realistic modeling of increasingly sparse multi-pinhole geometries and an ensemble of cardiac XCAT phantoms with and without defects.

9033-32, Session 6

## Whole-body PET parametric imaging employing direct 4D nested reconstruction and a generalized non-linear Patlak model

Nicolas Karakatsanis, Arman Rahmim, Johns Hopkins Univ. (United States)











Graphical analysis is employed in the research setting to provide quantitative estimation of PET tracer kinetics from dynamic images at a single bed. Recently, we proposed a multi-bed dynamic acquisition framework enabling clinically feasible whole-body parametric PET imaging by employing post-reconstruction parameter estimation. In addition, by incorporating linear Patlak modeling within the system matrix, we enabled direct 4D reconstruction in order to effectively circumvent noise amplification in dynamic whole-body imaging. However, direct 4D Patlak reconstruction exhibits a relatively slow convergence due to the presence of non-sparse spatial correlations in temporal kinetic analysis. In addition, the standard Patlak model does not account for reversible uptake, thus underestimating the influx rate Ki. We have developed a novel whole-body PET parametric reconstruction framework in the STIR platform, a widely employed open-source reconstruction toolkit, a) enabling accelerated convergence of direct 4D multi-bed reconstruction, by employing a nested algorithm to decouple the temporal parameter estimation from the spatial image update process, and b) enhancing the quantitative performance particularly in regions with reversible uptake, by pursuing a non-linear generalized Patlak 4D nested reconstruction algorithm.

A set of published kinetic parameters and the XCAT phantom were employed for the simulation of dynamic multi-bed acquisitions. Quantitative analysis on the Ki images demonstrated considerable acceleration in the convergence of the nested 4D whole-body Patlak algorithm. In addition, our simulated and patient whole-body data in the post-reconstruction domain indicated the quantitative benefits of our extended generalized Patlak 4D nested reconstruction for tumor diagnosis and treatment response monitoring.

9033-33, Session 7

### Rapid scatter estimation for CBCT using the Boltzmann transport equation

Mingshan Sun, Varian Medical Systems, Inc. (United States); Alex Maslowski, Todd Wareing, Greg Failla, Transpire, Inc. (United States); Josh M. Star-Lack, Varian Medical Systems, Inc. (United States)

Scatter in cone-beam computed tomography (CBCT) is a significant problem that degrades image contrast, uniformity and CT number accuracy. One means of estimating and correcting for detected scatter is through an iterative deconvolution method also known as scatter kernel superposition (SKS). While the SKS approach is efficient, clinically significant errors on the order 2-4% (20-40 HU) still remain. We have previously shown that the kernel method can be improved by perturbing the kernel parameters based on reference data provided by limited Monte Carlo simulations of a first-pass reconstruction. In this work, we replace the Monte Carlo modeling with a deterministic Boltzmann solver (AcurosCTS) to generate the reference scatter data in a dramatically reduced time. In addition, the algorithm is improved so that instead of adjusting kernel parameters, we directly perturb the SKS scatter estimates. Studies were conducted on simulated data and on a large pelvis phantom scanned on a tabletop system. The new method reduced average reconstruction errors from 2.3% to 1.5%, and significantly improved visualization of low contrast objects. In total, 24 projections were simulated and AcurosCTS execution time was 22 sec/projection on an 8-core machine. We are porting AcurosCTS to the GPU, and current run-times are approximately 5 sec/projection using two GPU's running in parallel.

9033-34, Session 7

### A patient-specific scatter artifacts correction method

Wei Zhao, Guang-Hong Chen, Stephen Brunner, Univ. of Wisconsin-Madison (United States)

This paper provides a fast and patient-specific scatter artifact correction method for flat-panel detector based cone-beam computed tomography (CBCT) imaging, which can be employed to correct scatter artifacts on existing CBCT scanners without extra scan or extra hardware support. Due to increased irradiated volumes, scatter artifacts are often present in flat panel detector based CBCT system, causing degraded images. In this study, we propose a novel scatter artifact correction strategy that combines the residual of the raw projection data and the polychromatic reprojection, with the analytical convolution based scatter estimation model. The residual is employed to calibrate the free parameters of the convolution-based model. The final scatter distribution was calculated using the accurate scatter convolution model with calibrated parameters. The method was evaluated with Monte Carlo simulation and real CBCT data.

9033-35, Session 7

### Development and evaluation of a novel designed breast CT system

Claudia Braun, Oleg Tischenko, Helmut Schlattl, Christoph Hoeschen, Helmholtz Zentrum München GmbH (Germany)

The performance of a novel designed x-ray CT scanning geometry is investigated. Composed of a specially designed tungsten collimation mask and a high resolution flat panel detector, this scanning geometry provides high efficient data acquisition allowing dose reduction potentially up to 50%.

In recent years a special type of scanning geometry has been proposed. A first prototype of this geometry, named CTDOR (CT with Dual Optimal Reading). Despite many drawbacks, resulting images have shown promising potential of dual reading. The approach of gaining two subsets of data has anew been picked up and come to terms with a novel designed CT scanner for breast imaging. The main idea consists of collimating the X-ray beam through a specially designed shielding mask thereby reducing radiation dose without compromising image quality. This is achieved by hexagonally sampled Radon transform image reconstruction with the especially suitable OPED algorithm.

This work now presents the development and evaluation of the novel designed breast CT system emphasizing on image quality metrics. Therefore simulated phantom data were obtained to test the performance of the scanning device and compared to a standard 3rd generation scanner. Retaining advantages such as scatter-correction potential and 3D-capability, the proposed CT system yields high resolution images for breast diagnostics in low energy ranges. Assuming similar sample size and applied dose, it is expected that the novel designed breast CT system in conjunction with OPED outperforms the standard 3rd generation CT system combined with FBP.

9033-36, Session 7

#### Effective one step-iterative fiducial markerbased compensation for involuntary motion in weight-bearing C-arm cone-beam CT scanning of knees

Jang-Hwan Choi, Stanford Univ. (United States); Andreas K. Maier, Martin Berger, Friedrich-Alexander-Univ. Erlangen-Nürnberg (Germany); Rebecca Fahrig, Stanford Univ. (United States)

We previously introduced three different fiducial marker-based correction methods (2D projection shifting, 2D projection warping, and 3D image warping) for patients' involuntary motion in the lower body during weight-bearing C-arm CT scanning. The 3D warping method performed better than 2D methods since it could more accurately take into account the lower body motion in 3D.











However, as the 3D warping method applies different rotational and translational movement to the reconstructed image for each projection frame, distance-related weightings were slightly twisted and thus resulted in overlaying background noise over the entire image. In order to suppress background noise and artifacts (e.g. metallic marker-caused streaks), the 3D warping method has been improved by incorporating bilateral filtering and a Landweber type iteration in one step.

A series of projection images of five healthy volunteers standing at various flexion angles were acquired using a C-arm conebeam CT system with a flat panel. A horizontal scanning trajectory of the C-arm was calibrated to generate projection matrices. Using the projection matrices, the static reference marker coordinates in 3D were estimated and used for the improved 3D warping method.

The improved 3D warping method effectively reduced background noise down below the noise level of 2D methods and also eliminated metallic streaks. Thus, improved visibility of soft tissue structures (e.g. fat and muscle) was achieved as well as sharp bone edges. Any high resolution weight-bearing conebeam CT systems can apply this method for motion compensation.

9033-37, Session 8

## Evaluation of low contrast detectability after scatter correction in digital breast tomosynthesis

Koen Michielsen, Katholieke Univ. Leuven (Belgium); Andreas Fieselmann, Siemens Healthcare (Germany); Lesley Cockmartin, Johan Nuyts, Katholieke Univ. Leuven (Belgium)

Projection images from digital breast tomosynthesis acquisitions can contain a large fraction of scattered x-rays due to the absence of an antiscatter grid before the detector. In order to produce quantitative results, this should be accounted for in reconstruction algorithms. We examine the possible improvement in signal difference to noise ratio (SDNR) for low contrast spherical densities while applying a scatter correction.

Hybrid patient data were created by combining real patient data with attenuation profiles of spherical masses acquired with matching exposure settings. Scatter in these cases was estimated using Monte-Carlo based scattering kernels. All cases were reconstructed using filtered backprojection (FBP) with and without beam hardening correction and two maximum likelihood methods for transmission tomography, with and without quadratic smoothing prior (MAPTR and MLTR). For all methods, images were reconstructed with and without scatter correction. SDNR of the inserted spheres was calculated by subtracting the reconstructions with and without inserted template and measuring the signal and noise in these difference images.

SDNR improved by 3.7% (p=0.0005) for MLTR and by 6.6% (p=0.0005) for MAPTR. It was unchanged for regular FBP (p=0.96) and for FBP with beam hardening correction (p=0.092).

These results show that the effect of scatter correction depends on the reconstruction algorithm, with SDNR improving significantly for both iterative methods, possibly due to their inherent noise model, while the FBP results were unchanged because the scatter correction modifies low frequency information, which is mostly ignored in the reconstruction due to the high pass filter.

9033-38, Session 8

## An experimental study of practical computerized scatter correction methods for prototype digital breast tomosynthesis

Ye-Seul Kim, Hye-Suk Park, Hee-Joung Kim, Haeng-hwa Lee, Yonsei Univ. (Korea, Republic of); Young-Wook Choi, JaeGu Choi, Korea Electrotechnology Research Institute (Korea, Republic of) Digital breast tomosynthesis (DBT) is a technique developed to overcome limitations of conventional digital mammography by reconstructing slices through the breast from projections acquired at different angles. In developing and optimizing DBT, the x-ray scatter reduction technique remains a significant challenge due to the projection geometry and radiation dose limitations. The most common approach for scatter reduction technique is a beam-stop-array (BSA) algorithm while this method has a concern of additional exposure to acquire the scatter distribution. The compressed breast is roughly symmetric and scatter profiles from projections acquired at axially opposite angle are similar to a mirror image from each other. The purpose of this study was to apply the BSA algorithm acquiring only two scans with a beam stop array, which estimates scatter distribution with minimum additional exposure. The results of scatter correction with angular interpolation were comparable to those of scatter correction with all scatter distributions at each angle and exposure increase was less than 13%. This study demonstrated the influence of scatter correction by BSA algorithm with minimum exposure which indicates the potential for practical application in clinic.

9033-39, Session 8

## Optimizing the acquisition geometry for digital breast tomosynthesis using the Defrise phantom

Raymond J. Acciavatti, Alice Chang, Laura Woodbridge, Andrew D. A. Maidment, The Univ. of Pennsylvania Health System (United States)

In cone beam computed tomography (CT), it is common practice to use the Defrise phantom for image quality assessment. The phantom consists of a stack of plastic plates with low frequency spacing. Because the x-ray beam may traverse multiple plates, the spacing between plates can appear blurry in the reconstruction, and hence modulation provides a measure of image quality. This study considers the potential merit of using the Defrise phantom in digital breast tomosynthesis (DBT), a modality with a smaller projection range than CT. To this end, a Defrise phantom was constructed and subsequently imaged with a commercial DBT system. It was demonstrated that modulation is dependent on position and orientation in the reconstruction. Modulation is preserved over a broad range of positions along the chest wall if the input frequency is oriented in the tube travel direction. By contrast, modulation is degraded with increasing distance from the chest wall if the input frequency is oriented in the posteroanterior (PA) direction. A theoretical framework was then developed to model these results. Reconstructions were calculated in an acquisition geometry designed to improve modulation. Unlike current geometries in which the x-ray tube motion is restricted to the plane of the chest wall, we consider a geometry with an additional component of tube motion along the PA direction. In simulations, it is shown that the newly proposed geometry improves modulation at positions distal to the chest wall. In conclusion, this study demonstrates that the Defrise phantom is a tool for optimizing DBT systems.

9033-40, Session 8

## Increased microcalcification visibility in lumpectomy specimens using a stationary digital breast tomosynthesis system

Andrew W. Tucker, Yueh Z. Lee M.D., Cherie M. Kuzmiak M.D., Jabari Calliste, Jianping Lu, Otto Zhou, The Univ. of North Carolina at Chapel Hill (United States)

Current digital breast tomosynthesis (DBT) systems have been shown to have diminished microcaclification (MC) visibility compared to 2D mammography systems. Rotating gantry DBT systems require mechanical motion of the X-ray source which causes motion blurring











of the focal spot, thus reducing spatial resolution. We have developed a stationary DBT (s-DBT) technology that uses a carbon nanotube (CNT) based X-ray source array in order to acquire all the projections images without any mechanical motion. It is capable of producing full tomosynthesis datasets with zero motion blur. It has been shown to have significantly higher spatial resolution than continuous motion DBT systems. An s-DBT system also allows for a wider angular span without increasing the acquisition time. A larger angular span covers a larger portion of the Fourier domain, thus decreasing the tissue overlap. In this study, we compare tomosynthesis imaging of MCs, in lumpectomy specimens, between an s-DBT system and a rotating gantry DBT system. Results show that s-DBT produces better MC sharpness and reduced tissue overlap over continuous motion DBT systems.

9033-41, Session 8

### **Evaluation of imaging geometry for stationary chest tomosynthesis**

Jing Shan, Andrew W. Tucker, The Univ. of North Carolina at Chapel Hill (United States); Yueh Z. Lee M.D., The Univ. of North Carolina School of Medicine (United States); Michael D. Heath, Xiaohui Wang, David H. Foos, Carestream Health, Inc. (United States); Jianping Lu, Otto Zhou, The Univ. of North Carolina at Chapel Hill (United States)

Chest tomosynthesis is a low-dose 3-D imaging modality that has been shown to improve the detection sensitivity for small lung nodules compared to 2D chest radiography. We have recently demonstrated the feasibility of stationary digital chest tomosynthesis (s-DCT) using a distributed CNT x-ray source array. The technology has the potential to increase the imaging resolution and speed by eliminating source motion. In addition, the flexibility in the spatial configuration of the individual sources allows new tomosynthesis imaging geometries beyond the linear scanning mode used in the conventional systems, which may reduce the image artifacts. In this paper, we report the preliminary results on the effects of the tomosynthesis imaging geometry on the image quality. The study was performed using a bench-top s-DCT system consisting of a CNT x-ray source array and a flat-panel detector. System MTF and ASF are used as quantitative measurement of the in-plane and in-depth resolution. In this study tomosynthesis imaging geometries with the x-ray sources arranged in linear, square, rectangular and circular configurations are investigated using comparable imaging doses. Anthropomorphic chest phantom images were acquired and reconstructed to tomosynthesis slices for image quality assessment. It is found that wider angular coverage results in better in-depth resolution, while the angular span has little impact on the in-plane resolution in the linear geometry. Square imaging geometry leads to a more isotropic in-plane resolution.

9033-42, Session 9

#### CT calibration and dose minimization in image-based material decomposition with energy-selective detectors

Sebastian Faby, Stefan Kuchenbecker, David Simons M.D., Heinz-Peter Schlemmer M.D., Deutsches Krebsforschungszentrum (Germany); Michael Lell M.D., Friedrich-Alexander-Univ. Erlangen-Nürnberg (Germany); Marc Kachelriess, Deutsches Krebsforschungszentrum (Germany) and Friedrich-Alexander-Univ. Erlangen-Nürnberg (Germany)

Possible advantages of energy-selective photon counting detectors compared to dual energy CT shall be evaluated in the case of a typical dual energy application: Image-based material decomposition into an iodine and a water material image. Apart from a possibly smaller spectral overlap between the low and the high energy information, a photon

counting detector will probably offer more than the two necessary energy bins. In this case additional degrees of freedom are gained that allow minimizing the noise in the material images. We propose an imagebased method that determines optimal bin image weighting factors for material decomposition with respect to minimal material image noise. This is equal to maximizing the CNR since the contrast in the material images is kept constant by the calibration that our algorithm uses to find a first solution for the material decomposition task. Then the noise in each bin image is considered to determine the optimal weighting factors. Results indicate that a perfect photon counting detector with four bins outperforms the dual energy CT technique by a noise reduction of 15% in the water image and 45% in the iodine image. Limited detector energy resolution has only a small impact on the achieved noise reduction, the photon counting detector performs still better than the dual energy technique. Only if degrading detector effects like charge sharing and K-escape peaks are taken into account, the performance of our proposed method drops below the one of the dual energy CT.

9033-43, Session 9

### Segmented targeted least squares estimator for material decomposition in multi bin PCXDs

Paurakh L. Rajbhandary, Scott S. Hsieh, Norbert J. Pelc, Stanford Univ. (United States)

We present a fast, noise-efficient, and accurate targeted least squares estimator (TLSE) for material separation using photon-counting X-ray detectors (PCXDs) with multiple energy bin capability for the overdetermined case (more energy bins than basis materials). The proposed estimator uses a novel method of incorporating ray-dependent weighting that allows noise to be homogenous and close to the Cramer-Rao Lower Bound (CRLB) throughout the operating range. We explore Cartesian and average-energy contour segmentation of the basis material space for TLSE, and show that iso-average-energy contours require fewer segments compared to using Cartesian segmentation for similar performance. We compare the iso-average-energy TLSE to other proposed estimators - including the gold standard MLE and the A-Table [1] in terms of variance, bias and computational efficiency. Iso-average energy TLSE achieves an average variance within 4% of CRLB, an average bias of (2.59  $\pm$  0.12) x 10-5 cm. Using the same protocol, the gold standard Maximum Likelihood Estimator (MLE) showed average bias and variance-to-CRLB ratio of (2.77  $\pm$  0.06) x 10-5 cm and 1.035  $\pm$  0.001 but was 50 times slower in our simulation. Compared to A-Table method, TLSE also demonstrated significant advantage, as TLSE uses locally optimized parameter that gives a more homogenous variance-to-CRLB profile in the operating region. We show that variance-to-CRLB for TLSE is lower by as much as ~40% than A-Table method in the peripheral region of operation (thin or thick objects).

9033-44, Session 9

### Pooling optimal combinations of energy thresholds in spectroscopic CT

Thomas Koenig, Marcus Zuber, Elias Hamann, Karlsruher Institut für Technologie (Germany); Armin Runz, German Cancer Research Center (Germany); Michael Fiederle, Freiburger Materialforschungszentrum (Germany); Tilo Baumbach, Karlsruher Institut für Technologie (Germany)

Photon counting detectors used in spectroscopic CT are often based on small pixels and therefore offer only limited space to include energy discriminators and their associated counters in each pixel cell. For this reason, it is important to use the available energy thresholds as efficiently as possible in order to achieve an optimized material contrast at a radiation dose as low as possible. Unfortunately, the complexity of











evaluating every possible combination of energy thresholds, given a fixed number of counters, rapidly increases with the resolution at which this search is performed, and makes brute-force approaches to this problem infeasible. In this work, we introduce methods from machine learning, in particular sparse regression, to perform a feature selection to determine optimal combinations of energy thresholds. We will demonstrate how methods enforcing row-sparsity on a linear regression's coefficient matrix can be applied to the multiple response problem in spectroscopic CT, i.e. the case in which a single set of energy thresholds is sought to simultaneously discriminate a multitude of materials in an optimal way. These methods are applied to CT images experimentally obtained with a Medipix3RX detector operated in charge summing mode and with a CdTe sensor at a pixel pitch of 110 µm. We will show that sparse regression successfully chooses four out of 20 possible threshold positions that allow discriminating PMMA, iodine and gadolinium in a contrast agent phantom. In our conference contribution, we will also discuss the role of noise and covariance, investigate overfitting and introduce confidence intervals for variable importance.

9033-45, Session 9

## Effects of energy-bin acquisition methods on noise properties in photon-counting spectral CT

Taly Gilat-Schmidt, Kevin C. Zimmerman, Marquette Univ. (United States); Emil Y. Sidky, The Univ. of Chicago (United States)

Spectral CT with photon-counting detectors has the potential to improve material decomposition and contrast-to-noise ratio (CNR) compared to conventional CT. This work compared the noise properties of two general energy-bin acquisition methods: (1) energy bins acquired from the same spectrum noise realization (e.g., simultaneous energy bin measurements), and (2) energy bins acquired from different spectrum noise realizations (e.g., sequential or checkerboard acquisitions). For both types of acquisitions, the transmission through slabs of acrylic and aluminum were simulated and measured on a prototype system. The energy-bin noise standard deviation and covariance were compared for both acquisition methods. Simulations were performed to compare both methods with respect to noise in material decomposition estimates and the CNR in image-based weighted images. Both the experimental and simulation results indicated increased energy-bin noise when energy measurements were acquired from different spectrum realizations and positive noise correlations across energy bins when energy measurements were acquired from one source realization. The noise increased by a factor of 2 for the lowest energy bin, with the noise penalty decreasing with increasing bin energy. The simulation results demonstrated a factor of 1.6 to 2.5 increase in noise in material decomposition estimates when acquiring from different spectrum realizations. Despite the decreased energy-bin noise, energy measurements from one spectrum realization reduced the CNR in image-based-weighted images by a factor of 0.8, due to increased correlation between bins. Overall, the investigated acquisition methods demonstrated differences in noise magnitude and correlation, affecting material decomposition estimates and CNR.

9033-46, Session 9

## Photon counting CT at elevated X-ray tube currents: contrast stability, image noise and multi-energy performance

Steffen G. Kappler, Andre Henning, Bjoern Kreisler, Friederike Schöck, Karl Stierstorfer, Thomas G. Flohr, Siemens AG (Germany)

The energy-selectivity of photon counting detectors provides contrast enhancement and enables new material-identification techniques for clinical Computed Tomography (CT). Patient dose considerations and the resulting requirement of efficient X-ray detection suggest the use of CdTe

or CdZnTe as detector material. The finite signal pulse duration of several nanoseconds present in those detectors requires strong reduction of the pixel size to achieve feasible count rates in the high-flux regime of modern CT scanners. Residual pulse pile-up effects in scans with high X-ray fluxes still can limit two key properties of the counting detector, namely count-rate linearity and spectral linearity.

We have used our research prototype scanner with CdTe-based counting detector and 225µm small pixels to investigate these effects in CT imaging scenarios at elevated X-ray tube currents. We present measurements of CT images and provide a detailed analysis of contrast stability, image noise and multi-energy performance achieved with different phantom sizes at various X-ray tube settings.

9033-47, Session 9

## Direct spectral recovery using X-ray fluorescence measurements for material decomposition applications of photon counting spectral X-ray detectors

Tom Campbell-Ricketts, Mini Das, Univ. of Houston (United States)

Spectral x-ray measurements using pixelated photon counting spectral x-ray detectors (PCSXD) are subject to significant spectral distortion. For detectors with small pixel size, charge sharing between adjacent electrodes often dominates this distortion. In material decomposition applications, a popular spectral recovery technique employs a calibration phantom with known spectral properties. This works due to the similarity of the attenuation properties of the phantom and the material to be studied. However this approach may be too simplistic for clinical imaging applications as it assumes the homogeneity (and knowledge) of exactly the properties whose variation accounts entirely for the diagnostic content of the spectral data obtained by the photon counting detector. It will also be difficult to find the right calibration phantom for varying patient size and tissue densities on a case-by-case basis. Thus, it is desirable to develop direct correction strategies, based on the objectively measurable response of the detector. We present investigations into direct, calibration-free recovery of distorted spectral x-ray measurements with the Medipix detector. We model analytically the distortion of a spectral signal in a PCSXD by applying Gaussian broadening and charge sharing. The model parameters are fitted to the measured fluorescence of several metals. We will investigate experimentally the application of this recovery method to calibration-free material decomposition with a focus on breast imaging. While we are demonstrating the methodology using Medipix detectors, it should be applicable to other PCXDs as well.

9033-48, Session 10

## Energy weighting improves the image quality of spectral mammograms: implementation on a photon-counting mammography system

Johan Berglund, Henrik Johansson, Philips Home Healthcare Solutions (Sweden); Hanns-Ingo Maack, Philips GmbH Healthcare (Germany); Erik Fredenberg, Philips Home Healthcare Solutions (Sweden)

In x-ray imaging, contrast information content varies with photon energy. It is therefore possible to improve image quality by assigning different weights to photons of different energies, a technique known as energy weighting. In this work, energy weighting was implemented and evaluated on a commercially available spectral (energy-resolving) photon-counting mammography system. Phantom measurements revealed that energy weighting improves the contrast-to-noise ratio by about 4%. Computer simulations confirmed that a similar improvement can be expected for real breast tissue. In addition, a practical hands-on











formula for calculating the optimal weight from the image pixel values was derived. A reader study showed that the image quality improvement by energy weighting was detectable in a set of screening mammograms. Using different weights at different spatial frequencies has the potential to further improve image quality.

9033-49, Session 10

#### Spectral lesion characterization on a photoncounting mammography system

Klaus Erhard, Philips Research (Germany); Erik Fredenberg, Philips Healthcare (Sweden); Hanno Homann, Ewald Roessl, Philips Research (Germany)

Spectral X-ray imaging allows to differentiate between two given tissue types, provided their spectral absorption characteristics differ measurably. In mammography, this method is used clinically to determine a composition of the breast into an adipose and glandular tissue compartment, from which the glandular tissue fraction and hence the volumetric breast density (VBD) can be computed. Another interesting application of this technique is the characterization of lesions with spectral mammography. In particular round lesions are relatively easily detected by experienced radiologists, but are often difficult to characterize as benign or malignant without further diagnostic workup. Here, a method is described that aims at discriminating cysts from tumors directly on a spectral mammogram, obtained with a calibrated spectral mammography system and using a hypothesis-testing algorithm based on a maximum likelihood approach. The method includes a parametric model describing the lesion shape, compression height variations and breast composition. With the maximum likelihood algorithm, the model parameters are estimated separately for cyst and tumor tissue. The resulting ratio of the maximum likelihood values is used for the final tissue characterization. Initial results using simulations and phantom measurements are presented.

9033-50, Session 10

### Amorphous selenium direct detection CMOS digital x-ray imager with 25 micron pixel pitch

Christopher C. Scott, Shiva Abbaszadeh, Sina Ghanbarzadeh, Univ. of Waterloo (Canada); Gary Allan, Michael Farrier, Teledyne DALSA (Canada); Karim S. Karim, Univ. of Waterloo (Canada)

We have developed a high resolution amorphous selenium (a-Se) direct detection imager using a large-area compatible back-end fabrication process on top of a state-of-the-art CMOS active pixel sensor having 25 micron pixel pitch. Integration of a-Se with CMOS technology requires overcoming a-Se/CMOS interfacial strain, which initiates nucleation of crystalline selenium and results in high detector dark currents. A CMOScompatible polyimide buffer layer was used to planarize the backplane and provide a low stress and thermally stable surface for a-Se. The buffer layer inhibits crystallization and provides detector stability that is not only a performance factor but also critical for favorable long term costbenefit considerations in the application of CMOS digital x-ray imagers in medical practice. The detector structure is comprised of a polyimide (PI) buffer layer, the a-Se layer, and a gold (Au) top electrode. The PI layer is applied by spin-coating and is patterned using dry etching to open backplane bond pads for wire bonding. Thermal evaporation is used to deposit the a-Se and Au layers, and the detector is operated at 15 V/ µm in hole collection mode (i.e. a positive bias on the Au top electrode). Preliminary images demonstrating high spatial resolution have been obtained from a first prototype imager.

9033-51, Session 10

### Reflection properties of scintillator-septum candidates for a pixelated MeV detector

Mihye Shin, Stanford Univ. (United States); Josh M. Star-Lack, Varian Medical Systems, Inc. (United States); Martin Janecek, Lawrence Berkeley National Lab. (United States); Eric Abel, Daniel Shedlock, Varian Medical Systems, Inc. (United States); Rebecca Fahrig, Stanford Univ. (United States)

In order to predict and improve performance of pixelated detectors, it is important to understand the optical properties of the basic unit of the scintillating structure. We have used a device composed of a laser and detectors for measuring the optical reflectance of unit samples. A sample has scintillator, glue, and septum (reflector) layer, and each sample has a different scintillator surface (polished/rough) and/or reflector (ESR film/aluminum-sputtered ESR film) condition. A high-refractive-index hemisphere was attached on the top surface of a sample to increase the maximum incidence angle at the scintillator-glue interface from 27° to 52°. The sample including ESR film demonstrated average reflectance approximately 1.3 times higher than that from the sample with aluminumsputtered ESR film as a reflector, and the polished surface condition showed higher reflectance than the rough-cut surface condition. We have also developed an analytical model based on Snell's law and Fresnel equations, whose results match experimental data fairly well. Using the analytical simulation, potential unit structures implemented by combinations of other materials can be inspected before being machined. However, the model cannot take into account the surface conditions or imperfections, as is shown by miss-match from the roughcut sample. The measured reflection coefficients can be used as input to Monte Carlo simulation to determine the performance metrics of an assembled pixelated detector, nonetheless, transmission and absorption through the unit structure are required to provide a complete description of performance. A new measurement device to permit probing of these additional parameters is being assembled and tested.

9033-52, Session 10

#### Initial steps toward the realization of large area arrays of single photon counting pixels based on polycrystalline silicon TFTs

Albert K. Liang, Martin Koniczek, Larry E. Antonuk, Youcef El-Mohri, Qihua Zhao, Hao Jiang, Univ. of Michigan (United States)

Active matrix flat-panel imagers (AMFPIs) have become ubiquitous in medical imaging environments. The development of these useful x-ray imaging technologies was a direct consequence of the emergence of thin-film electronics fabrication that enabled creation of inexpensive, large area transistor backplanes for television, desktop computer and laptop displays. Now, a guarter-century after the initial conception of AMFPIs, the demands of the tablet and smartphone markets have led to new fabrication technologies that are enabling the rise of potentially game-changing medical devices: large area x-ray imagers offering single photon-counting (SPC) capabilities. Such devices would be based on arrays of pixels, each of which would comprise circuits for signal amplification and discrimination, along with event counters and fast readout logic. In place of the single amorphous silicon thin-film transistor (a-Si TFT) typically present in each pixel of an AMFPI array, each single photon counting array pixel will employ many (on the order of 10^2 to 10^3) TFTs based on semiconductor materials, such as polycrystalline silicon (poly-Si), that offer considerably higher mobilities than a-Si. Compared to conventional AMFPI imagers that simply measure fluence, the novel energy binning capabilities of large area SPC imagers could have a profound impact upon medicine. In this presentation, progress toward the development of the first SPC prototypes based on poly-Si will be reported, the capabilities of such circuits (based on circuit simulations and early measurements) will be described, and prospects











for incorporation of further capabilities will be discussed. The research is supported by NIH grant R01-EB000558.

9033-53, Session 11

## X-ray fluorescence molecular imaging of high-Z tracers: investigation of a novel analyzer based setup

Bernhard H. Müller, Ludwig-Maximilians-Univ. München (Germany) and Helmholtz Zentrum München GmbH (Germany); Christoph Hoeschen, Helmholtz Zentrum München GmbH (Germany); Florian J. Grüner, Univ. Hamburg (Germany); Thorsten R. Johnson, Ludwig-Maximilians-Univ. München (Germany)

A novel X-ray fluorescence imaging setup for the in vivo detection of high-Z tracer distributions is investigated for its application in molecular imaging. The setup uses an energy resolved detection method based on a Bragg reflecting analyzer array together with a multiple scatter reducing radial collimator. The aim of this work is to investigate the potential application of this imaging method to in vivo imaging in humans. A proof of principle experiment modeling a partial setup for the detection of gold nano-particles was conducted in order to test the feasibility of the proposed imaging method. Furthermore a Monte Carlo simulation of the complete setup was created in order to quantify the dependence of the image quality to the applied radiation dose and to the geometrical collimator parameters as well as to the analyzer crystal properties. The Monte Carlo simulation quantifies the signal-to-noise ratio per radiation dose and its dependence on the collimator parameters. Thereby the parameters needed for a dose efficient in vivo imaging of gold nanoparticle based tracer distributions are quantified. However also a number of problems are found like the fluorescence emission as well as scatter from the collimator material obscuring the tracer fluorescence and the potentially large scan time.

9033-54, Session 11

## Monte Carlo simulations of dose enhancement around gold nanoparticles used as X-ray imaging contrast agents and radio sensitizers

Weibo Li, Marie Müllner, Matthias B. Greiter, Helmholtz Zentrum München GmbH (Germany); Caroline Bissardon, Helmholtz Zentrum München GmbH (Germany) and Univ. Claude Bernard Lyon 1 (France); Wenzhang Xie, Helmholtz Zentrum München GmbH (Germany) and Tsinghua Univ. (China); Helmut Schlatll, Uwe Oeh, Christoph Hoeschen, Helmholtz Zentrum München GmbH (Germany)

Gold nanoparticles were demonstrated as X-ray imaging contrast agents and radiosensitizers in mice. However the translational medical applications of gold nanoparticles in clinic need further detail information on the biological effects related to the enhanced doses in malignant and healthy cells. The idea of enhancing radiotherapy with high-Z materials, especially gold foils was initiated in our research unit in 1980s. Recently, efforts were advanced experimentally and theoretically to investigate the potential improvement of imaging and radiotherapy with gold nanoparticles. Initially the present work attempts to validate the dose enhancement effects of gold nanoparticles to cancer cells; secondly, it intends to explore the possibilities of nanoparticles serving as X-ray imaging contrast agents and to find out the adverse effects on healthy cells in the vicinity of the particles. Three Monte Carlo codes, namely PENELOPE-2011, EGSnrc and GEANT4-DNA, were used to simulate the local energy depositions and the resulting dose enhancements of gold nanoparticles. The diameters of those nanoparticles are assumed

to be 2 nm, 15 nm, 50 nm, 100 nm and 200 nm, respectively. The X-ray energy spectra are 60 kVp, 80 kVp, 100 kVp, 150 kVp with filtering of 2.7 mm Al for projection radiography, and 8 mm Al for 100 kVp and 150 kVp for computed tomography. The cell survival fractions with and without gold nanoparticles were experimentally accomplished to validate the simulated effect and to verify the basic principle of simulated dose enhancements for understanding the physical imaging and for implication to the radiotherapy.

9033-55, Session 11

#### Small-animal microangiography using phasecontrast X-ray imaging and gas as contrast agent

Ulf Lundström, Daniel H. Larsson, KTH Royal Institute of Technology (Sweden); Ulrica K. Westermark, Karolinska Institutet (Sweden); Anna Burvall, Hans M. Hertz, KTH Royal Institute of Technology (Sweden)

We investigate the possibility of using propagation-based phasecontrast X-ray imaging with gas as contrast agent to visualize the microvasculature of both healthy mouse tissue and tumors. The radiation dose required for absorption X-ray imaging is proportional to the minus fourth power of the structure size to be detected. This makes small vessels impossible to image at reasonable radiation doses using the absorption of conventional iodinated contrast agents. Propagation-based phase contrast gives enhanced contrast for high spatial frequencies by moving the detector away from the sample to let phase variations in the transmitted X-rays develop into intensity variations at the detector. Blood vessels are normally difficult to observe in phase contrast even with iodinated contrast agents as the density difference between blood and most tissues is relatively small. By injecting gas into the blood stream this density difference can be greatly enhanced giving strong phase contrast. One possible gas to use is carbon dioxide, which is a clinically accepted X-ray contrast agent. The gas is injected into the blood stream of patients to temporarily displace the blood in a region and thereby reduce the X-ray absorption in the blood vessels. We show that this method can be used to image blood vessels down to 8 µm in diameter in healthy tissue and down to 15 µm in tumors in mouse ears. The low dose requirements of this method indicate a potential for live small-animal imaging and longitudinal studies of angiogenesis.

9033-56, Session 11

### Small-animal dark-field radiography for pulmonary emphysema evaluation

Andre Yaroshenko, Technische Univ. München (Germany); Felix G. Meinel, Katharina Hellbach, Ludwig-Maximilians-Univ. Hospital München (Germany); Martin Bech, Technische Univ. München (Germany) and Lund Univ., Medical Radiation Physics (Sweden); Astrid Velroyen, Mark Müller, Technische Univ. München (Germany); Fabian Bamberg, Konstantin Nikolaou, Maximilian F. Reiser M.D., Ludwig-Maximilians-Univ. Hospital München (Germany); Önder A. Yildirim, Oliver Eickelberg, Helmholtz Zentrum München GmbH (Germany) and Comprehensive Pneumology Ctr. (Germany); Franz Pfeiffer, Technische Univ. München (Germany)

Chronic obstructive pulmonary disease (COPD) is one of the leading causes of morbidity and mortality worldwide and emphysema is one of its main components. The disorder is characterized by irreversible destruction of the alveolar walls and enlargement of distal airspaces. Despite the severe changes in the lung tissue morphology, conventional chest radiographs have only a limited sensitivity for the detection of mild











to moderate emphysema. X-ray dark-field is an imaging modality that can significantly increase the visibility of lung tissue on radiographic images. The dark-field signal is generated by coherent, small-angle scattering of x-rays on the air-tissue interfaces in the lung. Therefore, morphological changes in the lung can be clearly visualized on dark-field images. This is demonstrated by a preclinical study with a small-animal emphysema model, performed both ex vivo and in vivo. To generate a murine model of pulmonary emphysema, female C57BL/6N mice were treated with a single orotracheal application of porcine pancreatic elastase (100 U/ kg body weight) dissolved in phosphate-buffered saline (PBS). Control mice received PBS. The mice were imaged using a small-animal dark-field scanner. While conventional x-ray transmission radiography images revealed only subtle indirect signs of the pulmonary disorder, the difference between healthy and emphysematous lungs could be clearly directly visualized on the dark-field images. The dose applied to the animals is compatible with longitudinal studies. The imaging results correlate well with pulmonary function tests and histology. The results of this study reveal the high potential of dark-field radiography for clinical lung imaging.

9033-57, Session 11

## Compton coincidence volumetric imaging: a new x-ray volumetric imaging modality based on Compton scattering

Xiaochao Xu, William Beaumont Hospital (United States)

Compton scattering is a dominant interaction during radiography and computed tomography x-ray imaging. However, the scattered photons are not used for extracting imaging information, but seriously degrade image quality. Here we introduce a new scheme that overcomes most of the problems associated with existing Compton scattering imaging schemes and allows Compton scattered photons to be effectively used for imaging. In our scheme, referred as Compton coincidence volumetric imaging (CCVI), a collimated monoenergetic x-ray beam is directed onto a thin semiconductor detector. A small portion of the photons is Compton scattered by the detector and their energy loss is detected. Some of the scattered photons intersect the imaging object, where they are Compton scattered a second time. The finally scattered photons are recorded by an areal energy resolving detector panel around the object. The two detectors work in coincidence mode. CCVI images the spatial electron density distribution in the imaging object. Similar to PET imaging, the event location can be located within a curve; therefore the imaging reconstruction algorithms are also similar to those of PET. Two statistical iterative imaging reconstruction algorithms are tested. Our study verifies the feasibility of CCVI in imaging acquisition and reconstruction. Various aspects of CCVI are discussed. If successfully implemented, it will offer a great potential for imaging dose reduction compared with x-ray CT. Furthermore, a CCVI modality will have no moving parts, which potentially offers cost reduction and faster imaging speed.

9033-58, Session 11

## Apparatus and fast method for cancer cell classification based on high harmonic coherent diffraction imaging in reflection geometry

Michael Zürch, Friedrich-Schiller-Univ. Jena (Germany); Stefan Foertsch, Friedrich-Schiller-Univ. Jena (Germany) and Siemens AG (Germany); Mark Matzas, Siemens AG (Germany); Katharina Pachmann, Friedrich-Schiller-Univ. Jena (Germany); Rainer Kuth, Siemens AG (Germany); Christian Spielmann, Friedrich-Schiller-Univ. Jena (Germany) and Abbe School of Photonics (Germany) and Helmholtz Institute Jena (Germany)

In cancer treatment it is highly desirable to identify and /or classify individual cancer cells in real time. Nowadays, the standard method is PCR which is costly and time-consuming. Here we present a different approach to rapidly classify cell types: we measure the pattern of coherently diffracted extreme ultraviolet radiation (XUV radiation at 38nm wavelength) allowing to distinguish different single breast cancer cell types. The output of our laser driven XUV light source is focused onto a single unstained and unlabeled cancer cell and the resulting diffraction pattern is measured in reflection geometry. As we will further show, the outer shape of the object can be retrieved from the diffraction pattern with sub-micron resolution. For classification it is often not necessary to retrieve the image, it is only necessary to compare the diffraction patterns which can be regarded as a spatial fingerprint of the specimen. For a proof-of-principle experiment MCF7 and SKBR3 breast cancer cells were pipetted on gold-coated silica slides. From illuminating each single cell and measuring a diffraction pattern we could distinguish between them. Owing the short bursts of coherent soft x-ray light, one could also image temporal changes of the specimen, i.e. studying changes upon drug application once the desired specimen is found by the classification method. This lab-sized equipment may allow fast classification of any kind of cells, bacteria or even viruses in the near future.

9033-59, Session 12

## Patient-specific minimum-dose imaging protocols for statistical image reconstruction in C-arm cone-beam CT using correlated noise injection

Adam S. Wang, Joseph W. Stayman, Yoshito Otake, Akhil J. Khanna, Gary L. Gallia, Jeffrey H. Siewerdsen, Johns Hopkins Univ. (United States)

PURPOSE: A newly developed method for accurately portraying the impact of low-dose imaging techniques in C-arm cone-beam CT (CBCT) is presented and validated, allowing for identification of minimum-dose protocols suitable to a given imaging task on a patient-specific basis in scenarios that require repeat intraoperative scans.

METHOD: To accurately simulate lower-dose techniques and account for object-dependent noise levels (x-ray quantum noise and detector electronics noise) and correlations (detector blur), noise of the proper magnitude and correlation was injected into the projections from an initial CBCT acquired at the beginning of a procedure. The resulting noisy projections were then reconstructed to yield images that accurately depict the low-dose image quality in both filtered backpro-jection and statistical image reconstruction. Validation studies were conducted on a mobile C-arm, with the noise injection method applied to an anthropomorphic head phantom and cadaveric torso across a range of lower-dose techniques.

RESULTS: Comparison of synthesized and real CBCT images across a full range of techniques demonstrated accurate noise magnitude (within ~3%) and correlation (matching noise-power spectrum, NPS). Other image quality characteristics (e.g., spatial resolution, contrast, beam hardening, and scatter) remained intact and were realistically presented across reconstruction methods, including statistical reconstruction, which potentially enables further dose reduction but where accurate prediction of low-dose limits might otherwise be difficult.

CONCLUSION: Generating synthesized images for a broad range of protocols gives a useful method to select minimum-dose techniques that accounts for complex factors of imaging task, patient-specific anatomy, and physician preference.











9033-60, Session 12

### Prospective optimization of CT under tube current modulation: I. organ dose

Xiaoyu Tian, Duke Univ. (United States); Xiang Li, Cleveland State Univ. (United States); William P. Segars, Donald Frush M.D., Ehsan Samei, Duke Univ. (United States)

The purpose of this study was to prospectively estimate organ dose in chest and abdominopelvic CT exams under tube current modulation (TCM). CTDIvol-normalized-organ dose coefficients for fixed tube current were first estimated as the prediction basis using a validated Monte Carlo simulation program and 150 computational phantoms. Clinical patients were further optimally matched with one or a group of computational phantoms in terms of anatomy, body habitus, and body landmarks. To account for the effect of TCM scheme, a regional CTDIvol was computed from the mA modulation profile for each organ. The prediction accuracy was quantified by comparing the predicted organ dose and the simulated organ dose with Monte Carlo program. The predicted organ dose values under TCM were illustrated as a function of patient size for chest and abdominopelvic scans. To our knowledge, this work is one of the first attempts to predict organ dose under multiple TCM schemes by including the largest number of computational phantoms up to date.

9033-61, Session 12

### Patient-specific, scanner-independent organ dose estimates for head CT exams

Kyle McMillan, Maryam Khatonabadi, Univ. of California, Los Angeles (United States); Maria A. Zankl, Helmholtz Zentrum München GmbH (Germany); John J. DeMarco, Christopher H. Cagnon, Michael F. McNitt-Gray, Univ. of California, Los Angeles (United States)

The purpose of this study is to develop a method for determining patient-specific, scanner-independent organ dose estimates for head CT exams. Monte Carlo simulations of 64-slice MDCT scanners from three major manufacturers were performed to obtain dose to brain and lens of the eye for seven patient models from the GSF family of voxelized phantoms ranging from pediatric to adult. Organ doses for each scanner were normalized by corresponding 16 cm CTDIvol values and averaged across all three scanners to obtain scanner-independent CTDIvol-toorgan-dose conversion coefficients for each patient model. The outer perimeter of each patient was measured at the first slice superior to the eyes to describe patient head size. Coefficients of variation (CoVs) were calculated before and after normalization of organ doses by CTDIvol to demonstrate the validity of scanner-independent CTDIvol-to-organ-dose conversion coefficients for each patient model. The relationship between CTDIvol-to-organ-dose conversion coefficients and patient head size was also examined by analyzing normalized organ dose averaged across all scanners as a function of head size to determine if a correlation exists. The range of CoVs across all organs and patient models before and after CTDIvol normalization was 9.87%-21.78% and 0.75%-10.39%, respectively. An exponential relationship between CTDIvol-to-organdose conversion coefficients and patient head size was observed with correlation coefficients greater than 0.92 for each organ evaluated. These results indicate that head CT organ dose may be accurately estimated with: (a) organ dose normalized by CTDIvol to account for scanner variation and (b) head perimeter to account for patient size variation.

9033-62, Session 12

### Size-specific dose evaluation on a prototype orthopedic CBCT system

Samuel Richard, Nathan Packard, John Yorkston, Carestream Health, Inc. (United States)

Patient specific dose evaluation and reporting is becoming increasingly important for x-ray imaging systems. Even imaging systems with lower patient dose such as CBCT scanners for extremities can benefit from accurate and size-specific dose assessment and reporting. This paper presents CTDI dose measurements performed on a prototype CBCT extremity imaging system across a range of body part sizes (5, 10, 16, and 20 cm effective diameter) and kVp (70, 80, and 90 kVp - with 0.1 mm Cu added filtration). The ratio of the CTDI measurements for the 5, 10, and 20 cm phantoms over the CTDI measurements for the 16 cm phantom were calculated and results were compared to sizespecific dose estimates conversion factors (AAPM Report 204), which were evaluated on a conventional CT scanner. Due to the short scan nature of the system (220 degree acquisition angle), the dependence of CTDI values on the initial angular orientation of the phantom with respect to the imager was also evaluated. The study demonstrated that for a 220 degree acquisition sequence, the initial angular position of the conventional CTDI phantom with respect to the scanner does not significantly affect CTDI measurements (varying by less than 2% overall across the range of possible initial angular positions). The size-specific conversion factor was found to be comparable to the Report 204 factors for the large phantom size (20 cm) but lower, by up to 19%, for the 5 cm phantom (i.e., 1.29 for CBCT vs 1.54 for CT). The factors dependence on kVp was minimal, but dependence was most significant at 90 kVp. These results indicate that specific conversion factors need to be used for CBCT systems with short scans in order to provide more accurate dose reporting across the range of body sizes found in extremity scanners.

9033-63, Session 12

## Monte Carlo investigation of backscatter factors for skin dose determination in interventional neuroradiology procedures

Artur Omar, Karolinska Univ. Hospital (Sweden); Hamza Benmakhlouf, Karolinska Univ. Hospital (Sweden) and Univ. of Stockholm (Sweden); Maria Marteinsdottir, Robert Bujila, Patrik Nowik, Karolinska Univ. Hospital (Sweden); Pedro Andreo, Stockholm Univ. (Sweden) and Karolinska Univ. Hospital (Sweden)

Complex interventional and diagnostic x-ray angiographic (XA) procedures may yield patient skin doses exceeding the threshold for radiation induced skin injuries. Skin dose is conventionally determined by converting the incident air kerma free-in-air into entrance surface air kerma, a process that requires the use of backscatter factors. Subsequently, the entrance surface air kerma is converted into skin kerma using mass energy-absorption coefficient ratios tissue-to-air, which for the photon energies used in XA is identical to the skin dose. The purpose of this work was to investigate how the cranial bone in neurointerventional procedures affects backscatter factors for incident clinical kilovoltage spectra.

The PENELOPE Monte Carlo system was used to calculate backscatter factors at the entrance surface of a spherical and a cubic water phantom that includes a cranial bone layer. The simulations were performed for different clinical x-ray spectra, field sizes, and thicknesses of the bone layer.

The results show a reduction of up to 15% when a cranial bone layer is included in the simulations, compared with conventional backscatter factors calculated for a homogeneous water phantom. The reduction increases for thicker bone layers, "softer" incident beam qualities, and











larger field sizes, indicating that, due to the increased photoelectric cross-section of cranial bone compared to water, the bone layer acts primarily as an absorber of low-energy photons.

For neurointerventional procedures, backscatter factors calculated at the entrance surface of a water phantom containing a cranial bone layer increase the accuracy of the skin dose determination.

9033-64, Session 13

### Design of anthropomorphic textured phantoms for CT performance evaluation

Justin B. Solomon, Duke Univ. (United States); François O. Bochud, Ctr. Hospitalier Univ. Vaudois (Switzerland); Ehsan Samei, Duke Univ. (United States)

Commercially available computed tomography (CT) technologies such as iterative reconstruction (IR) have the potential to enable reduced patient doses while maintaining diagnostic image quality. However, systematically determining safe dose reduction levels for IR algorithms is a challenging task due to their non-linear nature. Most attempts to evaluate IR algorithms rely on measurements made in uniform phantoms. Such measurements may overstate the dose reduction potential of IR because they don't account for the complex relationship between anatomical variability and image quality. The purpose of this study was to design anatomically informed textured phantoms for CT performance evaluation. Two phantoms were designed to represent lung and softtissue texture. The lung phantom includes intricate vessel-like structures along with embedded nodules (spherical, lobulated, and spiculated). The soft tissue phantom was designed based on a three-dimensional clustered lumpy background with included low-contrast lesions (spherical and anthropomorphic). The phantoms were built using rapid prototyping (3D printing) technology and imaged on a modern multi-slice clinical CT scanner. The phantom images provide highly realistic background textures with spectral content similar to real patient images. Further, the phantoms allow for performance evaluation for several important imaging tasks such as low-contrast lesion detectability and lung nodule volumetric assessment. Different analysis strategies and observer models can be implemented to assess CT performance in the presence of background texture.

9033-65. Session 13

## The development of a population of 4D pediatric XCAT phantoms for CT imaging research and optimization

Hannah Norris, Yakun Zhang, Jack Frush, Gregory M. Sturgeon, Anum Minhas M.D., Donald Frush M.D., Ehsan Samei, William P. Segars, Duke Univ. (United States)

With the increased use of CT examinations, the associated radiation dose has become a large concern, especially for pediatrics. Much research has focused on reducing radiation dose through new scanning and reconstruction methods. Computational phantoms provide an effective and efficient means for evaluating image quality, patient-specific dose, and organ-specific dose in CT. We previously developed a set of highlydetailed 4D reference pediatric XCAT phantoms at ages of newborn, 1, 5, 10, and 15 years with organ and tissues masses matched to ICRP Publication 89 values. We now extend this reference set to a series of 73 pediatric phantoms of a variety of ages and weight percentiles, representative of the population at large. High resolution PET-CT data was reviewed by a practicing experienced radiologist for anatomic regularity and was then segmented with manual and semi-automatic methods to form a target model. A Multi-Channel Large Deformation Diffeomorphic Metric Mapping (MC-LDDMM) algorithm was used to calculate the transform from the best age matching pediatric reference phantom to the patient target. The transform was used to complete the

target, filling in the non-segmented structures and defining models for the cardiac and respiratory motions. The complete phantoms, consisting of thousands of structures, were then manually inspected for anatomical accuracy. 3D and 4D CT data was simulated from the phantoms to demonstrate their ability to generate realistic, patient quality imaging data. The population of pediatric phantoms developed in this work provides a vital tool to investigate dose reduction techniques in 3D and 4D pediatric CT.

9033-66, Session 13

#### Construction of anthropomorphic hybrid, dual-lattice voxel models for optimizing image quality and dose in radiography

Nina Petoussi-Henss, Janine Becker, Matthias B. Greiter, Helmut Schlattl, Maria A. Zankl, Christoph Hoeschen, Helmholtz Zentrum München GmbH (Germany)

In radiography there is generally a conflict between the best image quality and the lowest possible patient dose. A proven method of dosimetry is the simulation of radiation transport in virtual human models. However, while the resolution of these voxel models is adequate for most dosimetric purposes, they cannot provide the required organ fine structures necessary for the assessment of the imaging quality.

The aim of this work is to develop hybrid/dual-lattice voxel models as well as simulation methods by which patient dose and image quality for typical radiographic procedures can be determined. The results will provide a basis to investigate by means of simulations the relationships between patient dose and image quality for various imaging parameters and develop methods for their optimization.

A hybrid phantom, based on NURBS (Non Linear Uniform Rational B-Spline) and PM (Polygon Mesh) surfaces, has been constructed from an existing voxel phantom of a female patient. The organs of the hybrid phantom can be then scaled and deformed in a non-uniform way i.e. organ by organ; they can be, thus, adapted to patient characteristics without losing their anatomical realism. Furthermore, one lobe of the lung of this model has been substituted by a high resolution lung voxel model, resulting in a dual-lattice geometry model. "Dual lattice" means in this context the combination of voxel models with different resolution.

Monte Carlo simulations of radiographic imaging were performed with the code EGS4nrc, modified such as to perform dual lattice transport. First results are presented for a thorax examination.

9033-67, Session 13

## Population of 100 realistic, patient-based computerized breast phantoms for multimodality imaging research

William P. Segars, Duke Univ. Medical Ctr. (United States); Alexander I. Veress, Univ. of Washington (United States); Jered R. Wells, Gregory M. Sturgeon, Nooshin Kiarashi, Joseph Y. Lo, Ehsan Samei, James T. Dobbins III, Duke Univ. Medical Ctr. (United States)

Breast imaging is an important area of research with many new techniques being investigated to further reduce the morbidity and mortality of breast cancer through early detection. Computerized phantoms can provide an essential tool to quantitatively compare new imaging systems and techniques. Current phantoms, however, lack sufficient realism in depicting the complex 3D anatomy of the breast. In this work, we created one-hundred detailed 3D computational breast phantoms based on high-resolution CT datasets from normal patients. The CT data was segmented using a semi-automatic method developed in our laboratory. Six segmentation classes were defined to account for different fibroglandular and skin densities. Each set of segmented











data was used to create a mathematically defined phantom that could be incorporated into the female version of the 4D extended cardiactorso (XCAT) phantom, a whole-body model of the human anatomy. The phantoms were defined using a combination of NURBS and subdivision surfaces. Based on actual human data in vivo, the phantoms provide a more realistic model of the breast anatomy and its variation in a population. To make the phantoms applicable to different modalities that may or may not require compression, we developed a finite-element application in FEBio to simulate different compression states of the breast. The breast phantoms and the simulation tools developed for them were incorporated into user-friendly software to be distributed for breast imaging research. There, the phantoms will provide the necessary foundation to quantitatively evaluate and compare existing and emerging breast imaging devices and techniques.

9033-68, Session 13

## A second generation of physical anthropomorphic 3D breast phantoms based on human subject data

Adam C. Nolte, Nooshin Kiarashi, Ehsan Samei, William P. Segars, Joseph Y. Lo, Duke Univ. (United States)

Previous fabrication of anthropomorphic breast phantoms has demonstrated their viability as a model for 2D (mammography) and 3D (tomosynthesis) breast imaging systems. Further development of these models will be essential for the evaluation of breast x-ray systems. There is also the potential to use them as the ground truth in virtual clinical trials. The first generation of phantoms was segmented from patient dedicated breast computed tomography data and fabricated into physical models using high-resolution 3D printing. Two variations were made. The first was a multi-material model (doublet) printed with two photopolymers to represent glandular and adipose tissues with the greatest physical contrast available, mimicking 75% and 35% glandular tissue. The second model was printed with a single 75% glandular equivalent photopolymer (singlet) to represent glandular tissue, which can be filled independently with an adipose equivalent material such as oil. For this study, we have focused on improving the latter, the singlet phantom. First, the temporary oil filler has been replaced with a permanent 0% glandular equivalent urethane based polymer. This offers more realistic contrast as compared to the multi-material approach at the expense of air bubbles and pockets that form during the filling process. Second, microcalcification clusters have been included in the singlet model via crushed eggshells, which have very similar chemical composition to calcifications in vivo. The results from these alterations demonstrate significant improvement over the first generation of anthropomorphic physical phantoms.

9033-69, Session 13

## Automatic insertion of simulated microcalcification clusters in a software breast phantom

Varsha G. Shankla, The Univ. of Pennsylvania Health System (United States); David D. Pokrajac, Delaware State Univ. (United States); Susan P. Weinstein, Emily F. Conant M.D., Andrew D. A. Maidment, Predrag R. Bakic, The Univ. of Pennsylvania Health System (United States)

Software phantoms developed and validated previously for 3D breast imaging are extended to automatically include realistic clusters of simulated microcalcifications (MC). X-ray projections of these phantoms are simulated using polyenergetic ray tracing method to model clinical mammographic image acquisition. This automated generation of synthetic mammograms is used in preclinical validation of breast imaging systems. We introduce a strategy to automatically

place MC clusters at an anatomically informed location within the 3D breast phantom. To validate the automatic insertion strategy, a 2AFC observer study has been designed to compare two placement methods, 'Directed' and 'Random'. The directed method is predicated based on the probability distribution function of potential cluster locations. This probability distribution function can be estimated using anatomical assumptions about cluster locations (e.g., within the dense tissue regions); alternatively, it can be estimated from a set of potential locations manually selected by radiologists. Conversely, the random method was chosen so that the MCs are located anywhere within the phantom volume. During the trial, a radiologist observer selects between the two simulated phantom images, one from each method. Furthermore, we ask questions that probe the rationale behind the observer's selection. Based upon the recorded observer's choices during the 2AFC study, we can test the statistical significance of the difference between the two placement methods. The preferred method will be included as a default feature of the software breast phantom generation code.

9033-70, Session 14

### Cascaded systems analysis of photon counting detectors

Jennifer Xu, Wojciech Zbijewski, Joseph W. Stayman, Grace J. Gang, Katsuyuki Taguchi, Johns Hopkins Univ. (United States); Erik Fredenberg, Philips Women's Healthcare (Sweden); John A. Carrino, Jeffrey H. Siewerdsen, Johns Hopkins Univ. (United States)

Purpose: Photon counting detector (PCD) CT systems are an emerging technology with applications in low-dose and spectral tomographic imaging. This paper develops an analytical model capable of predicting the imaging performance characteristics of PCDs, including the system gain, modulation transfer function (MTF), noise-power spectrum (NPS), and detective quantum efficiency (DQE).

Methods: A cascaded systems analysis model that tracks the propagation of quanta through the imaging chain was developed and parameterized according to the physical properties of a silicon-strip PCD employed on a newly developed PCD-CT imaging bench. The detector signal response, MTF, and NPS were measured as a function of dose (50-100 kVp, 1-7 mA), detector threshold and readout mode, and compared to theoretical predictions.

Results: The detector mean signal exhibited a highly linear response across the system operating range and agreed well with theoretical prediction. The MTF and NPS also demonstrated reasonable agreement with model predictions. Analysis of DQE as a function of exposure conditions, threshold, and readout mode revealed important considerations for system optimization. For example, readout with and without charge sharing and at various levels of threshold exhibited spatial-frequency-dependent effects in the DQE that can be leveraged to enhance performance with respect to high- and low-frequency imaging tasks.

Conclusions: The proposed theoretical model demonstrated agreement with measured PCD performance, provides a useful basis for understanding complex dependencies in PCD imaging performance, and offers an important guide to task-based optimization in developing new PCD-CT systems.

9033-71, Session 14

## Detector system comparison using relative CNR for specific imaging tasks related to neuro-endovascular image-guided interventions (neuro-EIGIs)

Brendan M. Loughran, Swetadri Vasan Setlur Nagesh, Vivek Singh, Ciprian N. Ionita, Amit Jain, Daniel R. Bednarek, Stephen











Rudin, Toshiba Stroke and Vascular Research Ctr. (United States)

Neuro-EIGIs require visualization of very small endovascular devices and small vessels. A Microangiographic Fluoroscope (MAF) x-ray detector was developed to improve on the standard flat panel detector's (FPD's) ability to visualize small objects during neuro-EIGIs. To assess performance between the FPD and MAF imaging systems, specific imaging tasks related to those encountered during neuro-EIGIs were used to assess contrast to noise ratio (CNR) of spatially varying objects and the relative CNR for each system. A bar phantom was placed at a fixed distance from the x-ray focal spot which mimics a clinical imaging geometry and was imaged by both detector systems. Imaging was done without an anti-scatter grid and using the same conditions for each system including: the same x-ray beam quality, collimator position, source to imager distance (SID), and source to object distance (SOD). Spatial frequency dependent relative contrasts were found for both imaging systems using the peak and trough signals from the bar phantom line pairs. The relative noise was found using mean background signal and background noise for varying detector exposures. From these, spatial frequency dependent CNRs were found for each system. Relative CNR was also found to compare imaging system performance. The MAF also utilizes a temporal filter to reduce the overall image noise and effects of using this filter on the MAF spatial frequency dependent CNR were investigated. The relative CNR for the detector system comparison demonstrated that the MAF has superior CNRs for all spatial frequencies and exposures investigated for this specific imaging task.

9033-72, Session 14

### Method for measuring the intensity profile of a CT fan-beam filter

Bruce R. Whiting, Univ. of Pittsburgh (United States); Andreea C. Dohatcu, Univ. of Pittsburgh Medical Ctr. (United States)

Research on CT systems often requires knowledge of intensity as a function of angle in the fan-beam, due to the presence of bowtie filters, for studies such as dose reduction simulation, Monte Carl dose calculations, or statistical reconstruction algorithms. Since manufacturers consider the x-ray bowtie filter design to be proprietary information, several methods have been proposed to measure the beam intensity profile independently: 1) calculate statistical properties of noise in acquired sinograms (requires access to raw data files, which is also vendor proprietary); 2) measure the waveform of a dosimeter located away from the isocenter (requires dosimeter equipment costing > \$10K). We present a novel method that is inexpensive (parts costing ~\$50 from any hardware store, using GafChromic XR film at ~\$3 per measurement), requires no proprietary information, and can be performed in a few minutes. A fixture is built from perforated steel tubing, which forms an aperture that selectively samples the intensity at a particular fan-beam angle in a rotating gantry. Two exposures (1x & 2x) are made and selfdeveloping radiochromic film (GafChromic XR- Ashland Inc.) is then scanned on an inexpensive PC document scanner. An analysis method is described that linearizes the measurements for relative exposure. The resultant profile is corrected for geometric effects (1/L^2 fall-off, gantry dwell time) and background exposure, providing a noninvasive estimate of the CT fan beam intensity present in an operational CT system. This method will allow researchers to conveniently measure parameters required for modeling the effects of bowtie filters in clinical scanners.

9033-73, Session 14

### Prospective optimization of CT under tube current modulation: II. image quality

Xiaoyu Tian, Christopher Smitherman, Olav Christianson, Donald Frush M.D., Ehsan Samei, Duke Univ. (United States)

The purpose of this study was to prospectively determine size- and task-

based image quality indices on a patient-specific basis for chest and abdominopelvic CT scans. Model observer metric of detectability index (d') was derived as a surrogate of task-based diagnostic accuracy. The detectability index incorporated the noise (NPS), resolution (MTF), and the exam indication (task function). The noise (NPS) was characterized as a function of patient size and scanner characteristics (kVp, mAs, slice thickness, and reconstruction algorithm). The resolution (MTF) was modeled as task-based MTF, a function of contrast and noiselevel corresponding to the clinical feature of interest. The NPS and MTF were measured using a variable-size, multi-inserts phantom on two CT scanner models (GE HD 750 and Siemens Definition Flash). The prediction accuracy was quantified using physical quantities presented on the patient images as a gold standard. Detectability index for liver lesions with size and contrast ranges were derived for each patient. The prediction methods show good accuracy for both FBP and IR reconstruction with 8% discrepancy between predicted noise and true noise magnitude. Such prospectively determination of patient- and taskbased image quality enables optimized diagnosis performance with the minimum amount of radiation dose. The quantitative relationship between image quality and radiation dose can be the basis of dose/quality optimization by enabling the operator to select an operating point for a particular exam before it is initiated.

9033-74, Session 14

## A task-based comparison of two reconstruction algorithms for digital breast tomosynthesis

Ravi Mahadevan, Duke Univ. (United States); Lynda C. Ikejimba, Yuan Lin, Carl E. Ravin Advanced Imaging Labs. (United States); Ehsan Samei, Joseph Y. Lo, Duke Univ. (United States) and Carl E. Ravin Advanced Imaging Labs. (United States)

Digital breast tomosynthesis (DBT) generates 3-D reconstructions of the breast by taking X-Ray projections at various angles around patient. DBT improves cancer detection as it minimizes tissue overlap that is present in traditional 2-D mammography. In this work, two methods of reconstruction, filtered back projection (FBP) and the Newton-Raphson (N-R) statistical iterative reconstruction were used to create 3-D reconstructions from phantom images acquired on a breast tomosynthesis system. The task based image analysis method was used to compare the performance of each reconstruction technique. The task simulated a 10mm lesion within the breast containing iodine concentrations between 2.1mg/ml and 8.6mg/ml. The MTF was calculated using the reconstruction of an edge phantom, and the NPS was measured with a structured breast phantom (CIRS 020) over different exposure levels. The detectability index d' was calculated to assess image quality of the reconstructed phantom images. Initial results with unsubtracted tomosynthesis images indicated that the N-R statistical reconstruction yields a higher detectability than the conventional FBP across a wide dose range of 1 to 3 mGy. Moreover, N-R reconstruction of unsubtracted, low-energy tomosynthesis also outperformed FBP of dual energy subtracted tomosynthesis. At the conference, we will compare N-R vs FBP reconstructions for four tomosynthesis modes: conventional (without contrast), unsubtracted contrast-enhanced, temporal subtraction, and dual energy.

9033-75, Session 15

### A refined methodology for modeling volume quantification performance in CT

Baiyu Chen, Ehsan Samei, Duke Univ. (United States)

CT quantification of lung nodule volume depends on the precision of the quantification. To enable the evaluation of quantification precision, we previously developed a mathematical model that related precision to image resolution and noise properties in uniform backgrounds in











terms of an estimability index (e'). The e' was shown to predict empirical precision across 54 imaging and reconstruction protocols, but with different correlation qualities for FBP and iterative reconstruction (IR) due to the non-linearity of IR impacted by anatomical structure. To better account for the non-linearity of IR, this study aimed to refine the noise characterization of the model in the presence of textured backgrounds. Repeated scans of an anthropomorphic lung phantom were acquired. Subtracted images were used to measure the image quantum noise, which was then used to adjust the noise component of the e' calculation measured from a uniform region. In addition to the model refinement, the validation of the model was further extended to 2 nodule sizes (5 and 10 mm) and 2 segmentation algorithms. Results showed that the magnitude of IR's quantum noise was significantly higher in structured backgrounds than in uniform backgrounds (ASiR, 30-50%; MBIR, 100-200%). With the refined model, the correlation between e' values and empirical precision no longer depended on reconstruction algorithm. In conclusion, the model with refined noise characterization accommodated the nonlinearity of iterative reconstruction in structured background, and further showed successful prediction of quantification precision across a variety of nodule sizes, dose levels, slice thickness, reconstruction algorithms, and segmentation software.

9033-76, Session 15

#### The role played by internal noise in Channelized Hotelling Observer (CHO) study of detectability index: differential phase contrast CT versus conventional CT

Xiangyang Tang, Emory Univ. (United States); Yi Yang, The Winship Cancer Institute of Emory Univ. (United States)

The CHO model, wherein internal noise plays an important role to account for the psychological uncertainty in human visual perception, has found extensive applications in the assessment of image quality in nuclear medicine, mammography and the conventional CT. Recently, we extended its application to investigating the detectability index of differential phase contrast (DPC) CT – an emerging CT technology with the potential of increasing the capability in soft tissue differentiation. We found that the quantitative determination of internal noise in the CHO study of DPC-CT's detectability index should differ from that in the conventional CT. It is believed that the root cause of such a difference lies in the distinct noise morphology between the DPC-CT and conventional CT. In this paper, we present the preliminary results and investigate the adequate strategies to quantitatively determine the internal noise of CHO model for its application in the assessment of image quality in DPC-CT.

9033-77, Session 15

### Towards continualized task-based resolution modeling in PET imaging

Saeed Ashrafinia, Nicolas Karakatsanis, Hassan Mohy-ud-Din, Arman Rahmim, Johns Hopkins Univ. (United States)

We propose a generalized resolution modeling (RM) framework, including extensive task-based optimization, wherein we continualize the conventionally discrete framework of RM vs. no RM, to include varying degrees of RM. The proposed framework has the advantage of providing a trade-off between the enhanced contrast recovery by RM and the reduced inter-voxel correlations in the absence of RM, and to enable improved task performance. The investigated context was that of oncologic lung FDG PET imaging. Given a realistic blurring kernel of FWHM h ('true PSF'), we performed iterative EM including RM using a wide range of 'modeled PSF' kernels with varying widths h?. In our simulations, h = 6mm, while h? varied from 0 (no RM) to 12mm, thus considering both underestimation and overestimation of the true PSF. Detection task performance was performed using prewhitened (PWMF) and non-prewhitened matched filter (NPWMF) observers. It

was demonstrated that an underestimated resolution blur (h? = 4mm) enhanced task performance, while slight over-estimation (h? = 7mm) also achieved enhanced performance. The latter is ironically attributed to the presence of ringing artifacts. Nonetheless, in the case of the NPWMF, the increasing inter-voxel correlations with increasing values of h? degrade detection task performance, and underestimation of the true PSF provides the optimal task performance. The proposed framework also achieves significant improvement of reproducibility, which is critical in quantitative imaging tasks such as treatment response monitoring.

9033-78, Session 15

## CT x-ray tube voltage optimisation and image reconstruction evaluation using visual grading analysis

Xiaoming Zheng, Ted M. Kim, Rob Davidson, Charles Sturt Univ. (Australia); Seongju Lee, Cheongil Shin, Seoul National Univ. Hospital (Korea, Republic of); Sook Yang, Dongshin Univ. (Korea, Republic of)

The purposes of this work were to find an optimal x-ray voltage for CT imaging and to determine the diagnostic effectiveness of image reconstruction techniques by using the visual grading analysis (VGA). Images of the PH-5 CT abdomen phantom (Kagaku Co, Kyoto) were acquired by the Toshiba Aquillion One 320 slices CT system with various exposures (from 10 to 580 mAs) under different tube peak voltages (80, 100 and 120 kVp). The images were reconstructed by employing the FBP and the AIDR 3D iterative reconstructions with Mild, Standard and Strong FBP blending. Image quality was assessed by measuring noise, contrast to noise ratio and human observer's VGA scores. The CT dose index CTDIv was obtained from the values displayed on the images. The best fit for the curves of the image quality VGA vs dose CTDIv is a logistic function from the SPSS estimation. A threshold dose Dt is defined as the CTDIv at the just acceptable for diagnostic image quality and a figure of merit (FOM) is defined as the slope of the standardised logistic function. The Dt and FOM were found to be 5.4, 8.1 and 9.1 mGy and 0.47, 0.51 and 0.38 under the tube voltages of 80, 100 and 120 kVp, respectively, from images reconstructed by the FBP technique. The Dt and FOM values were lower from the images reconstructed by the AIDR 3D in comparison with the FBP technique. The optimal x-ray peak voltage for the imaging of the PH-5 abdomen phantom by the Aquillion One CT system was found to be at 100 kVp. The images reconstructed by the FBP are more diagnostically effective than that by the AIDR 3D but with a higher dose Dt to the patients.

9033-79, Session 15

### High-performance soft-tissue imaging in extremity cone-beam CT

Wojciech Zbijewski, Joseph W. Stayman, Abdullah Al Muhit, Gaurav Thawait, Johns Hopkins Univ. (United States); Nathan Packard, Robert A. Senn, Dong Yang, John Yorkston, Carestream Health, Inc. (United States); John A. Carrino, Jeffrey H. Siewerdsen, Johns Hopkins Univ. (United States)

Purpose: We report a clinical performance study of an extremity conebeam CT (CBCT) system, which indicates the need for improvement of soft-tissue image quality. To this end, a rapid Monte Carlo (MC) scatter correction is proposed, and Penalized Likelihood (PL) reconstruction is evaluated for noise management.

Methods: Ten cadaveric hands and 10 knees were scanned on extremity CBCT and multi-detector CT (MDCT) using established protocols (80 kVp, 10 mGy for CBCT and 120 kVp, ~30 mGy for MDCT). Four observers rated clinically relevant imaging tasks for preference (MDCT vs. CBCT) on a 5-point scale. The accelerated MC scatter correction involved fast MC simulation with low number of photons implemented on











a GPU (~6x1e6 photons/sec), followed by Gaussian kernel smoothing in the detector plane and across projection angles. PL reconstructions were investigated for reduction of imaging dose for projections acquired at ~2

Results: CBCT was rated equivalent/superior (median score=0) to MDCT for bone tasks and slightly inferior (median= 1) for soft-tissue tasks due to scatter and noise caused by limited tube output. The rapid scatter estimation yielded root-mean-squared-errors of scatter projections of ~15% of peak scatter intensity for 5x1e6 photons/projection (runtime ~0.6 sec/projection) and 25% improvement in fat-muscle contrast in reconstructions of a cadaveric knee. PL reconstruction largely restored soft-tissue visualization at 2 mGy dose to that of 10 mGy FBP image.

Conclusion: The combination of rapid (5-10 minutes/scan) MC-based, patient-specific scatter correction and PL reconstruction offers an important means to overcome the current limitations of extremity CBCT in soft-tissue imaging.

9033-80, Session 15

#### Analyzing the performance of ultrasonic B-mode imaging for breast lesion diagnosis

Sara Bahramian, Univ. of Illinois at Urbana-Champaign (United States); Craig K. Abbey, Univ. of California, Santa Barbara (United States); Michael F. Insana, Univ. of Illinois at Urbana-Champaign (United States)

We studied the performance of ultrasonic B-mode imaging over a range of visual tasks related to breast lesion diagnosis to find a closed-form expression for SNR that in many cases uncouples task and instrument features. This integral expression over spatial frequency predicts idealobserver performance from the product of task and instrument spectra using B-mode images. Comparing these predictions to performance of ideal observer applied to the RF data we find that post-detection processing discards as much as half of the task information recorded, primarily at high spatial frequencies. We discuss that simple changes in post processing can recover this information.

Previously, we derived the performance of the ideal observer (area under the ROC curve) for a range of diagnostic tasks at the acquisition stage of image formation; i.e., using RF echo signals before the display stage. From that analysis, we related optimal performance to the diagnostic task and instrumentation spectra. The latter quantity we called the acquisition information spectrum (AIS), which is analogous to noise-equivalent quanta (NEQ) in photon imaging. The advance in this paper is to extend those results to the display stage of image formation, which involves demodulation, envelope detection, and gray-scale compression. Image formation is described through traditional Fourier techniques of signal analysis and through a parallel analysis of information. This revealed exactly how task information is handled at each step. Furthermore, using a model observer, whose performance relative to human observers is known, we performed Monte-Carlo simulations to verify the analytic expression of performance.

9033-81, Session PSWed

#### Investigation of the potential causes of partial scan artifacts in dynamic CT myocardial perfusion imaging

Yinghua Tao, Michael A. Speidel, Timothy P. Szczykutowicz, Guang-Hong Chen, Univ. of Wisconsin-Madison (United States)

In recent years, there have been several findings regarding to CT number variations across time in dynamic myocardial perfusion studies with short scan gated reconstruction, as the view angle range corresponding to the short scan acquisition for a given cardiac phase can vary from one cardiac cycle to another due to the asynchrony between heart rate and

gantry rotation speed. Referred as partial scan artifact (PSA), results have shown that this type of artifact may prevent accurate quantitative myocardial perfusion measurements. However, most studies used a dual-source scanner and only investigated the influence of scatter. In this study, we investigate additional potential causes of PSA, including beam hardening and noise, using numerical simulations. In addition, we investigate partial scan artifact in a single source 64-slice diagnostic CT scanner in vivo data sets, and its effect on perfusion analysis. Results indicated that among all three factors investigated, scatter can cause obvious partial scan artifact in dynamic myocardial perfusion imaging. Further, scatter is a low frequency phenomenon and is not heavily dependent on the changing contrasts, as both the frequency method and the virtual scan method are effective in reducing partial scan artifact. However, PSA does not necessarily lead to different perfusion maps compared to the full scan, because perfusion maps are usually generated with a curve fitting procedure.

9033-82, Session PSWed

#### Quantification of microarchitectural anisotropy in bone with diffraction enhanced imaging

Dean M. Connor Jr., Meenal Mehrotra, Amanda C. LaRue, Medical Univ. of South Carolina (United States)

Purpose: The purpose of this study is to determine if diffraction enhanced imaging (DEI) can quantify anisotropy in bone microarchitecture.

Background: Osteoporosis is characterized by low bone mass and microarchitectural deterioration of bone. A non-invasive tool for measuring the degree of anisotropy (DA) in bone microarchitecture will help clinicians better assess fracture risk in osteoporotic patients. DEI detects small angular deflections in an x-ray beam, and is only sensitive to angular changes in one plane. If the beam is refracted by multiple anisotropic microstructures (e.g. osteocyte lacunae and pores) in bone, the angular spreading can be measured with DEI and differences in the amount of spreading for different bone orientations is indicative of the DA in bone microarchitecture.

Method: An x-ray-tube based DEI system was used to collect an array of DEI reflectivity profiles measured through bovine cortical bone samples with the bones oriented with the bone axis in the plane perpendicular to the propagation of the x-ray beam. Micro-CT images of the bones were obtained using a Scanco uCT40 ex vivo scanner, and the DA of the pore structure was quantified using BoneJ.

Results: The maximum and minimum measured reflectivity profile widths through bone varied by a factor of two; this suggests that the microarchitecture is preferentially aligned with the bone axis in a 2-to-1 ratio. The DA for the cortical pores was 0.6, which agrees with DEI's anisotropy measure.

Conclusions: The preliminary findings of this study suggest that DEI is sensitive to anisotropy in bone microarchitecture.

9033-83, Session PSWed

#### Assessment of phase based dose modulation for improved dose efficiency in cardiac CT on an anthropomorphic motion phantom

Adam Budde, GE Healthcare (United States) and Univ. of Wisconsin-Madison (United States); Roy A. Nilsen, Brian E. Nett, GE Healthcare (United States)

State of the art automatic exposure control modulates the tube current across view angle and Z based on patient anatomy for use in axial full scan reconstructions. Cardiac CT, however uses a fundamentally different image reconstruction which uses a temporal weighting to reduce motion artifacts. This paper describes a phase based mA modulation that goes











beyond axial and ECG modulation; it uses knowledge of the temporal view weighting to improve dose efficiency in cardiac CT scanning. Using physical phantoms and synthetic noise emulation, we measure how knowledge of sinogram temporal weighting and the prescribed cardiac phase can be used to improve dose efficiency. First, we validated that a synthetic CT noise emulation method produced realistic image noise. Next, we used the CT noise emulation method to simulate mA modulation on scans of a physical anthropomorphic phantom which features 60 beats per minute motion in the heart. The CT noise emulation method matched noise to lower dose scans across the image within 1.5% relative error. Using this noise emulation method to simulate modulating the mA while keeping the total dose constant, the image noise was reduced by an average of 6.2%, demonstrating improved dose efficiency. Radiation dose reduction in cardiac CT can be achieved while maintaining the same level of image noise through phase based dose modulation.

9033-84, Session PSWed

### Image registration for motion estimation in cardiac CT

Bibo Shi, Ohio Univ. (United States); Gene Katsevich, Princeton Univ. (United States); Beshan S. Chiang, Toshiba Medical Research Institute USA (United States); Alexander I. Katsevich, Univ. of Central Florida (United States); Alexander A. Zamyatin, Toshiba Medical Research Institute USA (United States)

Motion estimation is a very important challenge in CT-based cardiac imaging. In this paper, we use image registration for estimating cardiac motion, and then perform motion-compensated reconstruction. Instead of reconstructing the entire cardiac cycle, we concentrate only on improving image quality at a quiet cardiac phase. The main focus of this paper is to explore accelerated algorithms for image registration, which is the key step in our motion estimation algorithm. We compare three gradient based optimization approaches for motion estimation, including simple gradient descent, the Nesterov accelerated descent, and conjugate gradient algorithms, based on speed and reconstruction image quality. Image quality evaluation is based on a thorough quantitative analysis of image quality metrics, including motion artifact metrics, as well as visual inspection of clinical images. The results show that accelerated gradient methods provide significant speedup over conventional gradient descent with no loss of image quality.

9033-85, Session PSWed

# A novel Region of Interest (ROI) imaging technique for biplane imaging in interventional suites: high-resolution small field-of-view imaging in the frontal plane and dose-reduced, large field-of-view standard-resolution imaging in the lateral plane

Swetadri Vasan Setlur Nagesh, Ciprian N. Ionita, Daniel R. Bednarek, Stephen Rudin, Toshiba Stroke and Vascular Research Ctr. (United States)

Image-guided interventional treatment of neuro-vascular conditions such as aneurysms, stenosed arteries, and thrombosis make use of treatment devices such as stents, coils, and balloons which have very small feature sizes, 10's of microns to a few 100's of microns, hence demand a high resolution imaging system. The current state-of-the-art flat panel detector (FPD) has about 200-um pixel size with the Nyquist of 2.5 lp/mm. For higher-resolution imaging a charge-coupled device (CCD) based Micro-Angio Fluoroscope (MAF-CCD) with a pixel size of 35um (Nyquist of 11 lp/mm) was developed and previously reported. Although the detector addresses the high resolution needs, the field-of-view is limited to 3.5 cm

x 3.5 cm, much smaller than current FPDs. During the use of the MAF-CCD for delicate parts of the intervention, it may be desirable to have real-time monitoring outside the MAF field-of-view with a low dose, and lower, but acceptable, quality image.

To address this need, a novel imaging technique for biplane imaging systems has been designed, using an MAF-CCD in one plane (frontal plane) and a dose-reduced standard large field-of-view imager in the other plane (lateral plane). The dose reduction is achieved by using a combination of ROI fluoroscopy and spatially different temporal filtering, a technique that has been previously presented.

In order to evaluate this technique a stent deployment procedure was done on an aneurysm phantom, placed inside a human skull. A vessel phantom was used to demonstrate the usefulness of this technique under Digital Subtraction Angiography (DSA) conditions.

9033-86, Session PSWed

#### Quantitative analysis of artifacts in 4D DSA: the relative contributions of beam hardening and scatter to vessel drop out behind highly attenuating structures

James R. Hermus, Timothy P. Szczykutowicz, Brian Davis, Erick L. Oberstarb, Martin Wagner, Charles M. Strother, Charles A. Mistretta, Univ. of Wisconsin-Madison (United States)

4D DSA a new method for creating a time series of 3D angiographic volumes using the data normally acquired for a rotational 3D DSA volume. Typically volumes are created at 30 fps providing an acceleration of 150-300 relative to conventional 3D DSA which provides a single angiographic volume per rotation. The time-resolved volumes are generated using the temporal information contained in the projections normally acquired for 3D rotational DSA. The injection protocol is altered to allow the initial angular projections to display inflow. A constraining volume is reconstructed using the acquired projections and has proven to be adequate in spite of the nonuniform intensity in the acquired projections. An alternative strategy is to acquire the constraining image in a second rotation following a single injection. This second rotation provides a somewhat better constraining image but is usually not necessary. The time frames generated during the rotation can experience signal variations in regions where highly attenuating anatomy causes angle-dependent signal loss due to beam hardening or incorrect logarithmic transformation due to high local scatter fraction. In this work initial correction for the scatter component has been implemented using a previously published simple scatter correction algorithm. Restoration of the projection signal behind dental implants is illustrated. Further studies designed to quantitate the relative roles of scatter and beam hardening are under way.

9033-87, Session PSWed

## Calibration-free coronary artery measurements for interventional device sizing using inverse geometry x-ray fluoroscopy: in vivo validation

Michael T. Tomkowiak, Amish N. Raval, Michael S. Van Lysel, Univ. of Wisconsin-Madison (United States); Tobias Funk, Triple Ring Technologies, Inc. (United States); Michael A. Speidel, Univ. of Wisconsin-Madison (United States)

Proper sizing of interventional devices such as angioplasty balloons and stents to match lesion length and vessel reference diameters improves procedural efficiency and therapeutic outcomes. We have developed a novel method using inverse geometry x-ray fluoroscopy and tomosynthesis to automatically determine vessel dimensions without











magnification calibration or optimal views. To validate this method in vivo, we compared results to intravascular ultrasound (IVUS) and coronary computed tomography angiography (CCTA) in a healthy porcine model. Coronary angiography was performed using Scanning-Beam Digital X-ray (SBDX), an inverse geometry fluoroscopy system that performs multiplane digital x-ray tomosynthesis. From a single frame, 3D reconstruction of the arteries was performed by localizing the depth of vessel lumen edges from tomographic blur. The 3D centerline was used to calculate length and diameter measurements in physical units. End-diastolic diameter and length measurements were compared to measurements from IVUS and CCTA, respectively. Coronary arteries in three healthy swine were measured and compared. Average length error was -0.49  $\pm$ 1.76 mm (SBDX - CCTA, mean ± 1 SD) based on segments with CCTA lengths ranging from 6 mm to 73 mm. Average diameter error was 0.07  $\pm$ 0.27 mm (SBDX - minimum IVUS diameter, mean ± 1 SD) using vessels with IVUS diameters ranging from 2.1 mm to 3.6 mm. Coronary artery measurements from the proposed method agree with gold standard imaging, providing automatic, calibration-free interventional device sizing.

9033-88, Session PSWed

## Necessary forward model specification accuracy for basis material decomposition in spectral CT

Hans Bornefalk, Mats Persson, Mats E. Danielsson, KTH Royal Institute of Technology (Sweden)

Basis material decomposition in spectral CT is a method where the energy dependence of the linear attenuation coefficient of each voxel is expressed as a function of only two or three basis functions. This allows removal of beam hardening artifacts, k-edge imaging and more accurate tissue quantification.

One method for basis decomposition in spectral CT relies upon accurate physical characterization the imaging chain, the so called forward model. Misspecifications to the model will make maximum likelihood estimates of the basis coefficient line integrals (conventionally denoted A\_1 and A\_2) biased and result in reconstructed images that are also biased. As so many interesting applications of spectral CT rely upon basis decomposition it is of interest to present a method whereby the tolerance, i.e. required accuracy of the forward model, can be determined. This paper does so and presents results for a particular system.

The result are presented in a way that allows easy comparison of the bias and the statistical uncertainty. As the mean square error of any estimate is the sum of the squared bias and the variance, the

square root of the Cramér-Rao lower bound of the variance is compared to the magnitude of the bias.

The method is of interest to all multibin systems and yields valuable design input when calibration models are selected, as different calibration methods will determine the system parameters to different degrees of certainty.

9033-90, Session PSWed

# A study of the x-ray image quality improvement in the gastrointestinal examination and the examination of the respiratory system based on the new image processing technique

Yuichi Nagai, National Cancer Ctr. (Japan) and Hitachi Medical Corp. (Japan); Mayumi Kitagawa, Jyun Torii, Takumi Iwase, Tomohiko Asou, Kanyu Ihara, National Cancer Ctr. (Japan); Mari Fujikawa, Yumiko Takeuchi, Katsumi Suzuki, Takashi Isiguro, Akio Hara, Hitachi Medical Corp. (Japan)

[Purpose] To achieve better quality of the x-ray fluoroscopic image for the gastrointestinal examination and the examination of the respiratory system, various image processing techniques such as noise reduction method and edge enhancement method have been developed. A recursive filtering which has been used for the purpose of noise reduction so far has a sort of limitation for its effectiveness in case of a moving object exists in the x-ray fluoroscopic image. In other words, the recursive filtering generates residual signals when there is a moving object in the x-ray fluoroscopic image, and these residual signals sometimes disturbs smooth procedure of the examinations. This is because the recursive filtering reduces a noise by adding last few fluoroscopic images. To improve such situation, the Adaptive Noise Reduction [ANR] has been developed as a new noise reduction method. The ANR is brand-new image processing technique which can be detected and then reduced only noise in the x-ray fluoroscopic images regardless the moving object. The target pixel is determined as a noise according to a correlation between the target pixel and its surrounding pixels in the x-ray fluoroscopic images. In addition, the correlation in order to determine the noise can be suitably changed by an x-ray condition and/or a thickness of patient. Therefore, the ANR is a better noise reduction method for the gastrointestinal examination and the examination of the respiratory system because the residual signal caused of the moving object in the x-ray fluoroscopic images is never generated after the ANR. In this presentation, we will explain the effect of the ANR by comparing the ANR images and the conventional recursive filtering

[Methods] We had measured a basic performance of the ANR images using the Noise Power Spectrum [NPS] and the Modulation Transfer Function [MTF]. Moreover, we had also considered a possibility of patient dose reduction during the x-ray examination based on the noise reduction effect by application of the ANR. The NPS was measured while changing an additional x-ray compensated filter such as an aluminum and/or a copper plate prepared on the x-ray R/F table system. The additional x-ray compensated filter used for the evaluation was three types of thickness [H/M/L] and combination for the aluminum and copper plate, which are capable of reducing patient radiation dose by up to approximately 50% at the maximum. As described above, the recursive filtering, which is the conventional noise reduction method, generates the residual signals caused by the moving object in the x-ray fluoroscopic images. Therefore, we also evaluated the amount of residual signals generated by the conventional recursive filtering using the moving subject. And the ANR images and the conventional images in the clinical examination were evaluated by four radiologists.

[Results] From the results of the MTF and the NPS, we confirmed that the ANR reduces the noise in the x-ray fluoroscopic images, without degrading the image resolution of the object. And we confirmed that better NPS can be obtained in comparison with the conventional images by applying the ANR, even if the patient dose is reduced to approximately 50% with the additional x-ray compensated filter. As for the evaluation about the amount of residual signals in the recursive filtering itself, it was possible to reduce the amount of residual signals by changing the processing parameters, but on the other hand it leads to result for the weaken effect of the noise reduction. Consequently, we also confirmed that the combination between the ANR and the conventional recursive filtering is very important for more noise reduction.

[Conclusion] We have performed the evaluation on noise reduction effect of the ANR which is a brad-new noise reduction method, and confirmed that not only it is capable of noise reduction but also it has a possibility of contribution on the reduction of patient radiation dose. According to the evaluation by using the clinical images in the gastrointestinal examination and the examination of the respiratory system, we obtained the result that the ANR images are superior to the conventional images, especially the reduced noise and the decreased residual signals. Furthermore, we think that a combination between the ANR and the conventional recursive filtering is also very important at the clinical situation because various objects are in the x-ray fluoroscopic images and we have to select the suitable technique and parameter according to the clinical objects. Finally, based on our evaluation we believe that the ANR is a suitable technique not only for the noise reduction but also the dose decrease of patient.











9033-91, Session PSWed

#### Relaxation times estimation in MRI

Fabio Baselice, Univ. degli Studi di Napoli Parthenope (Italy); Rocchina Caivano, Aldo Cammarota, IRCCS CROB (Italy); Giampaolo Ferraioli, Vito Pascazio, Univ. degli Studi di Napoli Parthenope (Italy)

Magnetic Resonance Imaging is a very powerful techniques for soft tissue diagnosis. At the present, the clinical evaluation is mainly conducted exploiting the amplitude of the recorded MR image which, in some specific cases, is modified by using contrast enhancements. Nevertheless, spin-lattice (T1) and spin-spin (T2) relaxation times can play an important role in many pathology diagnosis, such as cancer, Alzheimer or Parkinson diseases. Different algorithms for relaxation time estimation have been proposed in literature. In particular, the two most adopted approaches are based on Least Squares (LS) and on Maximum Likelihood (ML) techniques. As the amplitude noise is not zero mean, the first one produces a biased estimator, while the ML is unbiased but at the cost of high computational effort. Recently the attention has been focused on the estimation in the complex, instead of the amplitude, domain. The advantage of working with real and imaginary decomposition of the available data is mainly the possibility of achieving higher quality estimations. Moreover, the zero mean complex noise makes the Least Square estimation unbiased, achieving low computational times.

First results of complex domain relaxation times estimation on real datasets are presented. In particular, a patient with an occipital lesion has been imaged on a 3.0T scanner. Globally, the evaluation of relaxation times allow us to establish a more precise topography of biologically active foci, also with respect to contrast enhanced images.

9033-92, Session PSWed

#### Comparison of the Effect of Simple and Complex Acquisition Trajectories on the 2D SPR and 3D Voxelized Differences for Dedicated Breast CT Imaging

Jainil P. Shah, Steve D. Mann, Duke Univ. (United States); Randolph L. McKinley, ZumaTek, Inc. (United States); Martin P. Tornai, Duke Univ. (United States)

The 2D and 3D scatter-to-primary ratios were characterized for various objects in the FOV of a clinic-ready, cone beam breast CT scanner capable of arbitrary (non-traditional) 3D trajectories. The CT system uses a 30X30 cm2 flat panel imager with 197 micron pixellation, and a Rad 70B x-ray source with an SID of 70cm. A uniform, water-filled cylindrical phantom (13cm diameter) was imaged using this system. Projections were acquired with two different acquisition trajectories: 1) azimuthal orbit without tilt; and 2) saddle orbit following a sinusoidal trajectory around the object. Projection data were acquired in 2X2 binned (394 micron pixels) mode, with and without a beam stop array (BSA). Projections were scatter corrected using the BSA method and the 2D scatter to primary ratio (SPR) was measured on the projections. The data were then reconstructed using an iterative reconstruction algorithm, and the 3D SPR was calculated based on the reconstructed volumes. Results indicate that the 2D SPR is higher on some views for the saddle orbit, due to the longer path length through the volume. However, the 3D SPR is fairly comparable for both trajectories, not considering cone beam sampling artifacts for the simple circular (incompletely sampled) orbit. This indicates that the 3D SPR is a more robust way of evaluating the scatter conditions of an object imaged with an arbitrary trajectory.

9033-93, Session PSWed

### C-arm perfusion imaging with a fast penalized maximum-likelihood approach

Robert Frysch, Tim Pfeiffer, Sebastian Bannasch, Otto-von-Guericke-Univ. Magdeburg (Germany); Steffen Serowy, Univ. Medical Ctr. Magdeburg (Germany); Sebastian Gugel, Otto-von-Guericke-Univ Magdeburg (Germany); Martin Skalej, Univ. Medical Ctr. Magdeburg (Germany); Georg Rose, Otto-von-Guericke-Univ. Magdeburg (Germany)

Perfusion imaging is an essential method for stroke diagnostics. One of the most important factors for a successful therapy is to get the diagnosis as fast as possible. Therefore our approach aims at perfusion imaging (PI) with a cone beam C-arm system providing perfusion information directly in the interventional suite. For PI the imaging system has to provide excellent soft tissue contrast resolution in order to allow the detection of small attenuation enhancement due to contrast agent in the capillary vessels. The limited dynamic range of flat panel detectors as well as the sparse sampling of the slow rotating C-arm in combination with standard reconstruction methods results in limited soft tissue contrast. We choose a penalized maximum-likelihood reconstruction method to get suitable results. To minimize the computational load, the 4D reconstruction task is reduced to several static 3D reconstructions. We also include an ordered subset technique with transitioning to a small number of subsets, which adds sharpness to the image with less iterations while also suppressing the noise. Instead of the standard multiplicative EM correction, we apply a Newton-based optimization to further accelerate the reconstruction algorithm. The latter optimization reduces the computation time by about 50%. Further acceleration is provided by a multi-GPU implementation of the forward and backward projection, which fulfills the demands of cone beam geometry. In this preliminary study we evaluate this procedure on clinical data. Perfusion maps are computed and compared with reference images from magnetic resonance scans. We found a high correlation between both images.

9033-94. Session PSWed

#### Simultaneous motion estimation and motioncompensated image reconstruction (SMEIR) for 4D Cone-beam CT

Jing Wang, Xuejun Gu, The Univ. of Texas Southwestern Medical Ctr. at Dallas (United States)

Image reconstruction and motion estimation in four dimensional conebeam CT (4D-CBCT) are conventionally handled as two sequential steps. Due to the limited number of projections at each phase, the image quality of 4D-CBCT is often degraded, and the accuracy of subsequent motion modeling is decreased by the inferior 4D-CBCT. The objective of this work is to enhance both the image quality of 4D-CBCT and the accuracy of motion modeling with a novel strategy enabling simultaneous motion estimation and motion-compensated image reconstruction (SMEIR). The proposed SMEIR algorithm consists of two alternating steps: 1) model-based image reconstruction to obtain motion-compensated primary CBCT (m-pCBCT) and 2) motion model estimation through an unconstraint optimization to obtain an optimal set of deformation vector fields (DVF) between m-pCBCT and other phases of 4D-CBCT from the projection images directly. The motion-compensated image reconstruction is based on the simultaneous algebraic reconstruction (SART) technique coupled with the total variation minimization. During the forward- and back-projection of SART, measured projections from an entire set of 4D-CBCT are used for the reconstruction of m-pCBCT by utilizing the updated DVF. The DVF is estimated by matching the forward projection of the deformed m-pCBCT and measured projections of other phases of 4D-CBCT. The performance of SMEIR algorithm is quantitatively evaluated on a 4D NCAT phantom and a lung cancer patient. Both image quality of 4D-CBCT and the accuracy of tumor











motion trajectory estimation is substantially improved by SMEIR algorithm as compared to those resulted from conventional sequential 4D-CBCT reconstructions and motion estimation algorithm.

9033-95, Session PSWed

### Three-dimensional image-guided extrapolation for cone-beam CT image reconstruction

Brian E. Nett, GE Healthcare (United States)

In conebeam x-ray computed tomography one source of image artifacts is data truncation in the z (SI) direction. The effects of truncation increase as the cone-angle of the system increases. These artifacts can be separated into high frequency component and low frequency components. The aim of the algorithm proposed here is to compensate for lower frequency artifacts which can be caused by truncation of large objects such as the liver, at the boundary with the lungs. A first pass reconstruction over a larger z range is used, followed by a non-linear transform and then a forward projection in order to estimate the truncated projection data.

9033-96, Session PSWed

#### Anti-scatter grid evaluation for wide-cone CT

Roman Melnyk, John M. Boudry, GE Healthcare (United States); Xin Liu, Missouri Univ. of Science and Technology (United States); Mark Adamak, GE Healthcare (United States)

Scatter is a significant source of image artifacts in wide-cone CT. Scatter management includes both scatter rejection and scatter correction. The common scatter rejection approach is to use an anti-scatter grid (ASG). Conventional CT scanners (with detector coverage less than 40mm along the patient axis) typically employ one-dimensional (1D) ASGs. Such grids are quite effective for small cone angles. For larger cone angles, however, simply increasing the aspect ratio of a 1D ASG is not sufficient. In addition, a 1D ASG offers no scatter rejection along the patient axis. To ensure adequate image quality in wide-cone CT, a two-dimensional (2D) ASG needs to be used.

In this work, we measured the amount of scatter and the degree of image artifacts typically attributable to scatter for four prototype 2D ASG designs, and we compared those to a 1D ASG. The scatter was measured in terms of the scatter-to-primary ratio (SPR). The cupping and ghosting artifacts were assessed through quantitative metrics.

For the 2D ASGs, when compared to the 1D ASG, the SPR decreased by up to 66% and 75% for 35cm water and 48cm polyethylene, respectively, phantoms, at 80-160mm apertures (referenced to isocenter), as measured by one method. As measured by another method, the SPR reduction was 59%-68% at isocenter for the 35cm water phantom at 160mm aperture. The cupping artifact was decreased by up to ~80%. The ghosting artifact was reduced as well.

The results of the evaluation clearly demonstrate the advantage of using a 2D ASG for wide-cone CT.

9033-97, Session PSWed

## Variance-based iterative image reconstruction from few views in limited-angle C-arm computed tomography

Wissam El Hakimi, Technische Univ. Darmstadt (Germany); Georgios Sakas, Fraunhofer-Institut für Graphische Datenverarbeitung (Germany) C-arm cone beam CT offers CT-like 3D imaging capabilities. The data is oft acquired in less than a short scan, resulting in significant artifacts if conventional analytic formulas are applied. We present a new algorithm to reduce artifacts and enhance the quality of reconstructed 3D volume on the basis of C-arm data.. We make use of the variance of estimated voxel values over all projections to decrease the ground artifact level. The proposed algorithm is less sensitive to data truncation, and does not require explicit estimation of missing data. The number of required images is very low (up to 56 projections), which have several benefits, like significant reduction of patient dose and shortening of the acquisition time. The performance of the proposed method is demonstrated by simulations and clinical data.

9033-98, Session PSWed

### An experimental study on the noise correlation properties of CBCT projection data

Hua Zhang, Southern Medical Univ. (China) and The Univ. of Texas Southwestern Medical Ctr. at Dallas (United States); Luo Ouyang, The Univ. of Texas Southwestern Medical Ctr. at Dallas (United States); Jianhua Ma, Southern Medical Univ. (China); Jing Huang, Southern Medical University (China); Wufan Chen, Southern Medical Univ. (China); Jing Wang, The Univ. of Texas Southwestern Medical Ctr. at Dallas (United States)

Statistics-based image reconstruction and restoration algorithms for cone-beam CT (CBCT) usually model the noise in CBCT projection data at each detector bin as conditionally independent variable. However, due to the coupling effects of x-ray scatter, the electronic noise, the noise originating from the active readout mechanisms and other data calibration processing, noise correlations among the detector bins are introduced. In this study, we systematically investigated the noise correlation properties among the detector bins by analyzing the repeated projection data measurements. The measurements were performed using a TrueBeam™ imaging system with a 4030CB flat panel detector (FPD). A CIRS male pelvis phantom was used to acquire the projection data at six different dose levels from 1.6 mAs down to 0.1 mAs per projection at three fixed angles. To void the influence of the lag effect, lag correction was first implemented on the consecutive repeated projection data. The analyses on repeated measurements showed that the noise correlation coefficients were non-zero between the nearest neighboring bins of CBCT projection data, and the noise correlation coefficients were independent on the dose level. The obtained noise correlation coefficients were then incorporated into the covariance matrix in the penalized weighted least-squares (PWLS) criterion for noise reduction of low-dose CBCT. Reconstruction results showed that the PWLS criterion with consideration of the noise correlation coefficient among neighboring detectors outperforms the PWLS criterion without considering the noise correlation in terms of noise-resolution tradeoff in low-dose CBCT.

9033-99, Session PSWed

## A sinogram based technique for image correction and removal of metal clip artifacts in cone beam breast CT

Tianpeng Wang, Youtao Shen, Yuncheng Zhong, Chao-Jen Lai, The Univ. of Texas M.D. Anderson Cancer Ctr. (United States); Jian Wang, Department of Radiology, First Affilicated Hospital of Xinjiang Medical University (China); Chris C. Shaw, The Univ. of Texas M.D. Anderson Cancer Ctr. (United States)

Cone beam breast CT technique provides true three-dimensional (3D) images of a breast; however, metal clips used for surgical planning can













cause artifacts in the reconstructed images, which may extend to many slices beyond the metals location.

We developed a sinogram based method to remove the metal clips in the projection image data to improve the reconstructed image quality.

First, the original projection data was reconstructed using FDK algorithm to obtain a volumetric image with metal clips and artifacts. Next, the volumetric image was segmented through threshold method to obtain a 3D map of the metal. Projection image data are reorganized into sinograms for correction in the angular space on a pixel-by-pixel basis. The 3D metal map is re-projected onto the detector plane in various projection views to identify angular positions of metal shadows in the sinograms. Signals in the shadow are replaced with interpolated values using signals on the shadow edges as the references. To increase computational efficiency, pixels which miss the metal clips in all views are first identified and exempted from the correction process. The corrected sinogram data were reorganized into projection images for reconstruction of the artifact free images.

Cone beam CT scan data of mastectomy breast specimens are used to demonstrate the feasibility in using this technique for removal of metal clip artifacts. Preliminary results demonstrate that metal clips artifacts are greatly reduced and the image quality improved.

#### 9033-100, Session PSWed

## Preliminary study of region-of-interest image reconstruction with intensity weighting in cone-beam CT using iterative algorithm

Kihong Son, KAIST (Korea, Republic of) and SAMSUNG Medical Ctr. (Korea, Republic of); Jiseoc Lee, Yunjeong Lee, KAIST (Korea, Republic of); Jin Sung Kim, SAMSUNG Medical Ctr. (Korea, Republic of); Seungryong Cho, KAIST (Korea, Republic of)

Cone beam CT (CBCT) was widely used in image-guided radiation therapy (IGRT) for determine the current position of the target and the surrounding normal tissues. Therefore, reduction of radiation dose is the most important feature in new CT techniques or applications. In this study, we implemented a method that combines a sparse-view imaging and an intensity-weighted region-of-interest (IWROI) imaging technique. In addition, we subdivide the reconstructed ROI into inner and outer regions and locally variant weighed TV algorithm (LoWTV) was applied to make ultra-low absorbed dose to the patient. The CT scanning was simulated using XCAT phantom and the total number of projections was 600, and 200. We added noise at the outer regions to make an ROI region. Then, these projection images were reconstructed by use of Feldkamp-Davis-Kress (FDK) algorithm, and LoWTV algorithm. Reconstructed images on a transverse plane are shown in figure 1, and the line profiles for each condition are plotted in figure 2. Difference between LoWTV-200, FDK-200, and FDK-600 (reference image) image scan is represented. ROI reconstructed image from the LoWTV algorithm displays good image quality similar to FDK-200 views at inner ROI region and shows better image quality at outer ROI region. Also, structures and shape of inner and outer ROI region are well reconstructed compared to the reference imaging. As a result, we achieved promising results and believe that the proposed scanning approach can help reduce radiation dose to the patients while preserving good quality images for applications such as IGRT.

#### 9033-101, Session PSWed

### Toward improved cone-beam CT imaging of prostate patient via optimization-based image reconstruction

Xiao Han, The Univ. of Chicago Medical Ctr. (United States); Erik Pearson, The Univ. of Chicago (United States); Emil Y. Sidky,

The Univ. of Chicago Medical Ctr. (United States); Charles A. Pelizzari, The Univ. of Chicago (United States); Xiaochuan Pan, The Univ. of Chicago Medical Ctr. (United States)

Cone-beam CT (CBCT) is an important clinical tool for image-guided radiation therapy (IGRT). Clinical CBCT images are reconstructed by FDK-type algorithms, which have suboptimal quality for challenging tasks such as imaging of prostate patients. In recent years, rapid progress has been made on optimization-based algorithms, which can potentially improve CBCT image quality or relax the data-acquisition requirement. The objective of the work was thus to explore the potential of CBCT prostate imaging enabled by optimization-based reconstruction under conditions of IGRT interest. In the work, data of prostate patients, acquired with clinical protools, were retrospectively collected, from which half-view data sets were formed by extraction at every other view. We then reconstructed images by using the optimization-based algorithm and, for benchmarking purpose, the FDK algorithm, from the full- and half-view data sets. Results show that full-view optimization-based reconstructions are of improved quality than FDK counterparts, with better suppressed noise and artifacts. Furthermore, optimization-based reconstructions from half-view data appear to be comparable to fullview FDK reconstructions. The results have the implications that clinical applications requiring higher CBCT image quality may be enabled by appropriately-designed optimization-based algorithms, and that certain CBCT applications may potentially be accomplished with a reduced amount of imaging dose.

#### 9033-102, Session PSWed

### Reduction of metal artifacts: beam hardening and photon starvation effects

Girijesh Yadava, Debashish Pal, Jiang Hsieh, GE Healthcare (United States)

The presence of metal-artifacts in CT imaging can obscure relevant anatomy and interfere with disease diagnosis. The cause and occurrence of metal-artifacts are primarily due to beam hardening, scatter, partial volume, and photon starvation; however, the contribution to the artifacts from each of them depends on the type of hardware. A comparison of CT images obtained with different metallic hardware in various applications, along with acquisition and reconstruction parameters, helps understand methods for reducing or overcoming such artifacts. In this work, a metal beam hardening correction (BHC) and a projection-completion based metal artifact reduction (MAR) algorithms were developed, and applied on phantom and clinical CT scans with various metallic implants. Stainless-steel and Titanium were used to model and correct for metal beam hardening effect. In the MAR algorithm, the corrupted projection samples are replaced by the combination of original projections and in-painted data obtained by forward projecting a prior image. The data included spine fixation screws, hip-implants, dental-filling, and body extremity fixations, covering range of clinically used metal implants. Comparison of BHC and MAR on different metallic implants was used to characterize dominant source of the artifacts, and conceivable methods to overcome those. Results of the study indicate that beam hardening could be a dominant source of artifact in many spine and extremity fixations, whereas dental and hip implants could be dominant source of photon starvation. The BHC algorithm could significantly improve image quality in CT scans with metallic screws, whereas MAR algorithm could alleviate artifacts in hip-implants and dental-fillings.

#### 9033-103, Session PSWed

### Acquiring tomographic images from panoramic X-ray scanners

Van-Giang Nguyen, Le Quy Don Technical Univ. (Viet Nam); Soo-Jin Lee, Paichai Univ. (Korea, Republic of)











We propose a new method to acquire three-dimensional tomographic images of a large object from a dental panoramic X-ray scanner which was originally designed to produce a panoramic image of the teeth and jaws on a single frame. The method consists of two components; (i) a new acquisition scheme to acquire the tomographic projection data using a narrow detector, and (ii) a dedicated model-based iterative technique to reconstruct images from the acquired projection data. In conventional panoramic X-ray scanners, the suspension arm that keeps the X-ray source and the narrow detector has two moving axes for the angular movement and the linear movement. To acquire the projection data of a large object, we develop a data acquisition scheme that can emulate an acquisition of the projectional view in a large detector by stitching narrow projection images formed by many acquisitions using a narrow detector and propose a trajectory to move the suspension arm accordingly. To reconstruct images from the acquired projection data, an accelerated model-based iterative reconstruction method derived from the ordered subset convex maximum-likelihood expectation-maximization algorithm is used. In this method each subset of the projection data is constructed by collecting narrow projection images to form emulated tomographic projectional views in a large detector. To validate the performance of the proposed method, we tested with a real dental panoramic X-ray system. The experimental results demonstrate that the new method has great potential to enable existing panoramic X-ray scanners to have an additional CT's function of providing useful tomographic images.

9033-104, Session PSWed

### Impact of redundant ray weighting on motion artifact in a statistical iterative reconstruction framework

Yinghua Tao, Jie Tang, Michael A. Speidel, Guang-Hong Chen, Univ. of Wisconsin-Madison (United States)

In recent years, iterative reconstruction methods have been investigated extensively with the aim of reducing radiation dose while maintaining image quality in CT exams. In such a case, redundant data is usually available. In conventional FBP-type reconstructions, redundant data has to be carefully treated by applying a redundant weighting factor, such as Parker weighting. However, such a redundant weight has not been fully studied in a statistical iterative reconstruction framework. In this work, both numerical simulations and in vivo data sets were analyzed to study the impact of redundant weighting schemes on the reconstructed images for both static and moving objects. Results demonstrated that, for a static object, there was no obvious difference in the iterative reconstructions using different redundant weighting schemes, because the redundant data was consistent, and therefore, they all converged to the same solution. On the contrary, for a moving object, due to the inconsistency of the data, different redundant weighting schemes converged to different solutions, depending on the weight given to the data. The redundant weighting, if appropriately selected, can reduce motion-induced artifacts.

9033-105, Session PSWed

### Effective noise reduction and equalization in projection domain

Zhi Yang, Alexander A. Zamyatin, Satoru Nakanishi, Toshiba Medical Research Institute USA (United States)

Streak and noise reduction is critical for low dose CT imaging. In this paper, we proposed two effective projection domain noise reduction schemes. They were derived from (1) a known noise model that connects the noise behavior before (count domain) and after (projection space) the logarithm step; (2) predicted noise reduction from a finite impulse response filter; and (3) preset goals of noise reduction. As the goals, the two proposed schemes try to achieve: (1) noise equalization or (2) equivalent electronic noise suppression, respectively. They both

demonstrated significant noise and streak reduction in both phantom studies and clinical cases while maximally maintaining the resolution of reconstructed images.

9033-106, Session PSWed

### X-ray pulsing methods for reduced-dose computed tomography in PET/CT attenuation correction

Uwe Wiedmann, V. B. Neculaes, Daniel D. Harrison, Evren Asma, GE Global Research (United States); Paul E. Kinahan, Univ. of Washington (United States); Bruno De Man, GE Global Research (United States)

The image quality needed for CT-based attenuation correction (CTAC) is significantly lower than what is used currently for diagnostic CT imaging. Consequently, the X-ray dose required for sufficient image quality with CTAC is relatively small, potentially smaller than the lowest X-ray dose commercial CT scanners can provide. Operating modes have been proposed in which the X-rays are periodically turned on and off during the scan in order to reduce X-ray dose. This study reviews the different methods by which X-rays can be modulated in a CT scanner, and assesses their adequacy for low-dose acquisitions as required for CTAC. Calculations and experimental data are provided to exemplify selected X-ray pulsing scenarios. Our analysis shows that low-dose pulsing is possible but challenging with commercially available CT tubes. Alternative X-ray tube designs such as gridding would lift this restriction. Alternative options for low-dose CT acquisitions with little or no hardware modifications of commercially available CT systems include the addition of strong spectral filtering in order to lower patient dose of the smallest feasible pulses, and continuous non-pulsed acquisitions at significantly reduced tube current.

9033-107, Session PSWed

### Dose, noise and view weights in CT helical scans

Guangzhi Cao, Edgar Chino, Roy A. Nilsen, Jiang Hsieh, GE Healthcare (United States)

The amount of X-ray dose expresses itself as the variation of noise level in image volume after reconstruction in clinical CT scans. Therefore, it is important to understand the interaction between the dose, noise and reconstruction, which helps to guide the design of CT systems and reconstruction algorithms. Based on the fact that most of practical reconstruction algorithms for CT scans are implemented in filtered backprojection, in this work a unified analytical framework is proposed to build the connection between dose, noise and view weighting functions of different reconstruction algorithms in CT helical scans. The proposed framework helps one better understand the relationship between dose and image noise and is instrumental on how to design the view weighting function in reconstruction without extensive simulations and experiments. Even though certain assumptions were made to simply the analytical model, experimental results using both simulation data and real CT scan data show the proposed model is reasonably accurate for objects of human body shape. In addition, based on the proposed framework an analytical expression of optimal dose efficiency as a function of helical pitch is also derived, which suggests a somehow unintuitive but interesting conclusion that the optimal dose efficiency generally varies with helical pitches.











9033-108, Session PSWed

### Volume estimation of multi-density nodules with thoracic CT

Marios A. Gavrielides, Qin Li, Rongping Zeng, Kyle J. Myers, Berkman Sahiner, Nicholas A. Petrick, U.S. Food and Drug Administration (United States)

The purpose of this work was to quantify the effect of surrounding density on the volumetric assessment of lung nodules in a phantom CT study. Eight synthetic spherical nodules were manufactured and enclosed in another sphere of double the diameter and of different density. Different combinations of outer/inner nodule diameters (20/10mm, 10/5mm) and densities (100HU/-630HU, 10HU/-630HU, -630HU/100HU, -630HU/-10HU) were created. All nodules were placed in an anthropomorphic phantom and scanned with a 16-detector row CT scanner. Ten repeat scans were acquired using exposures of 20, 100, and 200mAs, slice collimations of 16x0.75mm and 16x1.5mm, and pitch of 1.2, and were reconstructed with varying slice thicknesses (three for each collimation) using two reconstruction filters (medium and standard). The volumes of the inner nodules were estimated from the reconstructed CT data using a matched-filter approach with templates modeling the characteristics of the multi-density objects. Volume estimation of the inner nodule was assessed using percent bias (PB) defined as 100\*(estimated\_volume true\_volume)/true\_volume and the standard deviation of percent bias (SPB). True volumes of the inner nodules were measured using micro CT imaging. Results show PB values ranging from -11.2 to 11.8% and SPB values ranging from 7.4 to 19.4%. Our study indicates that the volume of multi-density nodules can be measured with relatively small percent bias (in the order of  $\pm 12\%$  or less) when accounting for the properties of surrounding densities. These findings can provide valuable information for the clinical measurement of nodules with surrounding densities such as those caused by inflammation.

9033-109, Session PSWed

## Accelerating ordered-subsets X-ray CT image reconstruction using the linearized augmented Lagrangian framework

Hung Nien, Jeffrey A. Fessler, Univ. of Michigan (United States)

The augmented Lagrangian (AL) method (including its alternating direction variations) is a powerful technique for solving regularized inverse problems using variable splitting. In X-ray CT image reconstruction, it decomposes the original CT problem into several easier and better-conditioned inner minimization problems to accelerate the convergence. Experimental results showed that the acceleration is significant in 2D CT; however, in 3D CT, due to different geometries, it is more difficult to construct a good preconditioner for the inner leastsquares problem, and we have yet to achieve the same acceleration as in 2D CT. In comparison, the ordered-subsets (OS) algorithm is a gradientbased method with a diagonal preconditioner/majorizer that is more conservative but easily applicable to different geometries. Furthermore, by grouping the projections into M ordered subsets that satisfy the "subset balance condition" and updating the image incrementally using the M subset gradients, the OS algorithm effectively runs M times updates, comparing to the standard gradient descent method, thus leading to an M times acceleration at least in early iterations. Note that the AL method can be interpreted as a gradient-based method applied to the Moreau-Yosida regularized dual. In this paper, we show that OS methods are also very effective for accelerating AL methods. In short, with the linearized AL framework, we can arbitrarily increase the step size of the proximal gradient method by decreasing the AL penalty parameter and still guarantee convergence. We also propose a downward continuation approach that avoids tedious parameter tuning in many splitting-based algorithms for fast convergence. Experimental results showed that the proposed algorithm provides significant acceleration and converges much faster than the standard OS algorithm. Please see the 4-page abstract for the details.

9033-110, Session PSWed

## Sinogram rebinning and frequency boosting for high resolution iterative CT reconstruction with focal spot deflection

Jiao Wang, Yong Long, Lin Fu, Xue Rui, GE Global Research (United States); Ella A Kazerooni, Department of Radiology, University of Michigan Hospital (United States); Bruno De Man, GE Global Research (United States)

High resolution CT is important for qualitative feature identification and quantitative measurements for many clinical applications. To optimize the spatial resolution, filtered backprojection (FBP) based methods use various sinogram domain frequency boosting filters to provide flexible control of frequency responses in reconstructed images. In comparison, model-based iterative reconstruction (MBIR) methods usually rely on a single regularization strength parameter to control the image resolution, and there is limited flexibility in controlling the spectral response. Alternatively, MBIR can also improve the spatial resolution by sinogram preprocessing with frequency boosting filters. Focal spot wobbling technology has been introduced to high-end CT scanner to increase the effective detector sampling rate. With higher Nyquist sampling rate along detector channels, we can design frequency boosting filters with a much wider frequency range and recover higher resolution details in the reconstructed images. In this paper, we explore the potential of sinogram rebinning and frequency boosting method for high resolution MBIR from focal spot wobbling data. The proposed method is tested with phantom and clinical data. Compared with MBIR that models native focal spot wobbling geometry, our results show that MBIR from the rebinned geometry with frequency boosting filters can achieve higher resolution and better noise-resolution tradeoff. The proposed method also shows better contrast and sharper details in clinical images.

9033-111, Session PSWed

### A multi-resolution approach to retrospectively-gated cardiac micro-CT reconstruction

Darin P. Clark, G. Allan Johnson, Cristian T. Badea, Ctr. for In Vivo Microscopy (United States) and Duke Univ. (United States)

In preclinical research, micro-CT is commonly used to provide anatomical information; however, there is significant interest in using this technology to obtain functional information in cardiac studies. The fastest acquisition in 4D cardiac micro-CT imaging is achieved via retrospective gating, resulting in irregular angular projections after binning the projections into phases of the cardiac cycle. Under these conditions, analytical reconstruction algorithms, such as filtered back projection, suffer from streaking artifacts. Here, we show the application of a novel multi-resolution, iterative reconstruction algorithm that prevents the introduction of streaking artifacts, while attempting to recover the highest temporal resolution supported by the projection data. We achieve this through a unique combination of two regularization schemes-horizontal regularization of temporal average residuals inspired by robust principal component analysis, and vertical multi-scale regularization in the reconstruction space using data adaptive kernel regression. Here, we illustrate the application of the algorithm to a dynamic 2D phantom with realistic projection acquisition and reconstruction parameters. For the final manuscript, we intend to compare our algorithm with competing algorithms for the reconstruction of in vivo, murine 4D micro-CT data.











9033-112, Session PSWed

### Generalized least-squares CT reconstruction with detector blur and correlated noise models

Joseph W. Stayman, Wojciech Zbijewski, Steven Tilley II, Jeffrey H. Siewerdsen, Johns Hopkins Univ. (United States)

The success and improved dose utilization of statistical reconstruction methods arises, in part, from their ability to incorporate sophisticated models of the physics of the measurement process and noise. Despite the great promise of statistical methods, typical measurement models ignore blurring effects, and nearly all current approaches make the presumption of independent measurements – disregarding noise correlations and a potential avenue for improved image quality and dose reduction. In some imaging systems, such as flat-panel-based conebeam CT, such correlations and blurs can be a dominant factor in limiting the maximum achievable spatial resolution and noise performance. In this work, we propose a novel regularized generalized least-squares reconstruction method that includes models for both system blur and correlated noise in the projection data. We demonstrate through a resolution-noise analysis in simulation studies, that this approach can break through the traditional spatial resolution limits of methods that do not model these physical effects. Specifically, in investigations simulating flat-panel-based CT, reconstructed spatial resolution limits can be improved from ~0.3 mm down to ~0.15 mm. Moreover, in comparison to other approaches that attempt deblurring without a correlation model, superior noise-resolution trade-offs can be found with the proposed approach. These improved imaging characteristics suggest possible application of the approach in scenarios where traditional resolution limits hamper diagnostic utility. Potential imaging targets include (but are not limited to) CBCT mammography (in identification of microcalcifications), temporal bone imaging (visualizing inner ear anatomy), and quantitative bone analysis (based on the fine structure of trabecular bone).

9033-113, Session PSWed

## LBP-based penalized weighted least-squares approach to low-dose cone-beam computed tomography reconstruction

Ming Ma, Huafeng Wang, Yan Liu, Hao Zhang, Stony Brook Univ. (United States); Xianfeng Gu, Stony Brook University (United States); Zhengrong Liang, Stony Brook Univ. (United States)

Cone-beam computed tomography (CBCT) has obtained growing interest of researchers in image reconstruction. The mAs level of the X-ray tube current, in practical application of CBCT, is mitigated in order to reduce the CBCT dose. The lowering of the X-ray tube current, however, results in the degradation of image quality. Thus, low-dose CBCT image reconstruction is in effect a noise problem. To acquire clinically acceptable quality of image, and keep the X-ray tube current as low as achievable in the meanwhile, some penalized weighted leastsquares (PWLS)-based image reconstruction algorithms are developed. One representative strategy in previous work was to model the prior information for solution regularization using an anisotropic penalty term. To enhance the edge preserving and noise suppressing in a finer scale, a novel algorithm combining the local binary pattern (LBP) with penalized weighted least-squares (PWLS), called LBP-PWLS-based image reconstruction algorithm is proposed in this work. The proposed LBP-PWLS algorithm adaptively encourages strong diffusion on the local spot/flat region around a voxel and less diffusion on edge/corner ones by adjusting the penalty for cost, after the LBP is utilized to detect the region around the voxel as spot, flat and edge ones. The LBP-PWLS reconstruction algorithm was evaluated using the sinogram data acquired by a clinical CT scanner from the CatPhan® 600 phantom.

Experimental results on the noise-resolution tradeoff measurement and LBP distribution statistics demonstrated its feasibility and effectiveness in edge preserving and noise suppressing in comparison with a previous PWLS reconstruction algorithm.

9033-114, Session PSWed

### Nonlocal means-based regularizations for statistical CT reconstruction

Hao Zhang, Stony Brook Univ. (United States); Jianhua Ma, Southern Medical University (China); Yan Liu, Hao Han, Stony Brook Univ. (United States); Lihong Li, City University of New York/CSI (United States); Jing Wang, The Univ. of Texas Southwestern Medical Ctr. at Dallas (United States); Zhengrong Liang, Stony Brook Univ. (United States)

Statistical CT reconstruction have shown great potential to reduce radiation dose while maintain satisfactory image quality compared with the conventional filtered backprojection (FBP). Statistical iterative reconstruction (SIR) algorithms reconstruct the CT images by maximizing or minimizing a cost function in a statistical sense, where the cost function usually consists two terms: the data-fidelity term modeling the statistics of measured data, and the regularization term reflecting a prior information. The regularization term plays an critical role for successful image reconstruction. In this study, we proposed a family of generic, convex and edge-preserving regularization terms based on the nonlocal means(NLM) filter, and evaluated one of them as an example where the potential function took the simple quadratic-form. Experimental results using the digital NCAT phantom and physical CatPhan®600 phantom demonstrated that the presented regularization is superior to conventional quadratic-form Gaussian MRF regularization using equal weighting coefficients for neighbors of equal distance.

9033-115. Session PSWed

### Low-dose CT reconstruction with patch based sparsity and similarity constraints

Qiong Xu, Xuanqin Mou, Xi'an Jiaotong Univ. (China)

As the rapid growth of CT based medical application, low-dose CT reconstruction becomes more and more important to human health. Compared with other methods, statistical iterative reconstruction (SIR) usually performs better in low-dose case. However, the reconstructed image quality of SIR highly depends on the appropriate priors' regularization due to the insufficient of low-dose data. The frequentlyused regularization is developed from pixel based prior, such as the similarity of adjacent pixels. This kind of pixel based constraint cannot distinguish noise and structures effectively. Recently, patch based methods, such as dictionary learning and non-local means filter, have outperformed the conventional pixel based methods. Patch is a small area of image, which expresses structural information. In this paper, we propose to use patch based constraint to improve the image quality of low-dose CT reconstruction. In the SIR framework, both patch based sparsity and similarity are considered in the regularization term. On one hand, patch based sparsity is addressed by sparse representation and dictionary learning methods, on the other hand, patch based similarity is addressed by non-local means filter method. We conducted a real data experiment to evaluate the proposed method. The experimental results validate this method can lead to better image with less noise and more detail than other methods in low-count and few-views case.











9033-116, Session PSWed

## Noise study on cone-beam CT FDK image reconstruction by improved area-simulating-volume technique

Yan Liu, Stony Brook Univ. (United States); Jin Wang, The Univ. of Texas Southwestern Medical Ctr. at Dallas (United States); Hao Zhang, Yi Fan, Zhengrong Liang, Stony Brook Univ. (United States)

Previous studies have reported that the volume-weighting technique has advantages over the linear interpolation technique in Feldkamp-Davis-Kress (FDK) method for cone-beam computed tomography (CBCT) image reconstruction. However, directly calculating the volume of the intersection between the pencil beam and the object is a challenge due to the computational complexity. Inspired by previous works in areasimulating volume (ASV) projector for 3D positron emission tomography, we recently proposed an improved SAV (IASV) technique, which can fast calculate the geometric probability of the intersection between the pencil beam X-ray and the object. In order to show the improvements of the IASV technique compared to the conventional linear interpolation technique, the variances images from both theoretical prediction and empirical determination are showed basing on the assumption of the uncorrelated and stationary noise for each detector bin. The digital phantom analysis results show that the variance of the reconstructed image by IASV technique is between to . Meanwhile, the variance of the linear interpolation result is between to , which is about two times larger than the results by IASV technique. Therefore it can be concluded that the IASV-based FDK method can efficiently suppress the non-uniform noise across the full field of view compared to the linear interpolationbased FDK method. The evaluations between the IASV technique and conventional linear interpolation by CatPhan® 600 physical phantom are further analyzed in this paper.

#### 9033-117. Session PSWed

### Mojette tomographic reconstruction for micro CT: a bone and vessels quality evaluation

Henri Der Sarkissian, LUNAM - Univ. de Nantes (France) and KEOSYS (France); Benoit Recur, Australian National Univ. (Australia) and Univ. de Nantes (Australia); Jean-Pierre V. Guédon, Pauline Bléry, LUNAM - Univ. de Nantes (France); Paul Pilet, Yves Amourig, LUNAM - Univ de Nantes (France)

MicroCT represents a modality where the quality of CT reconstruction is very high thanks to the acquisition properties with a large number of projections and almost no noise. The goal of this paper is to challenge a commercial reconstruction software (NRECON Bruker, Belgium) with our proposed Mojette discrete reconstruction scheme from real microCT data. The first study compares different reconstructions according to the number of angles with the same trabecular bone detectability. Next, is the simultaneous analysis of trabecular bone and vessels tree through an animal study (nine Lewis rats), based on the perfusion of vascularization by a contrast agent before euthanasia. Small vessels are filling trabecular holes with almost the same grey levels as the bone. Therefore vessel detectability that can be achieved from the reconstruction algorithm according to the number of projections is a major issue. In this study, we use the classical projections data set which was used to exhibit the vessels from the femur bones after reconstruction. We performed classical Radon FBP from these data to ensure no other preprocessing has been done and the equivalence with the commercial software. The projections were then dispatched into the Mojette domain using a scheme recently proposed. We used then several Mojette algorithms to perform reconstructions. The quality of the result was tested upon the detectability of the smallest vessels that can be seen on the images. We reduced the number of acquired projections below the detectability threshold to compare the algorithms.

9033-118, Session PSWed

#### Two-step iterative reconstruction of regionof-interest with truncated projection in computed tomography

Keisuke Yamakawa, Shinichi Kojima, Hitachi, Ltd. (Japan)

Iteratively reconstructing data only inside the region of interest (ROI) is widely used to acquire CT images in less computation time while maintaining high spatial resolution. A method that subtracts projected data outside the ROI from full-coverage measured data has been proposed. A serious problem with this method is that the accuracy of the measured data confined inside the ROI decreases according to the truncation error outside the ROI. We propose a two-step iterative method that reconstructs image inside the full-coverage in addition to a conventional iterative method inside the ROI to reduce the truncation error inside full-coverage images. Statistical information (e.g., quantumnoise distributions) acquired by detected X-ray photons is generally used in iterative methods as a photon weight to efficiently reduce image noise. Our proposed method applies one of two kinds of weights (photon or constant weights) chosen adaptively by taking into consideration the influence of truncation error. The effectiveness of the proposed method compared with that of the conventional method was evaluated in terms of simulated CT values by using elliptical phantoms and an abdomen phantom. The standard deviation of error and the average absolute error of the proposed method on the profile curve were respectively reduced from 3.4 to 0.4 [HU] and from 2.8 to 0.8 [HU] compared with that of the conventional method. As a result, applying a suitable weight on the basis of a target object made it possible to effectively reduce the errors in CT images.

#### 9033-119, Session PSWed

### Multigrid iterative method with adaptive spatial support for computed tomography reconstruction from few-view data

Ping-Chang Lee, Industrial Technology Research Institute (Taiwan)

Computed tomography (CT) plays a key role in modern medical system, whether it be for diagnosis or therapy. As an increased risk of cancer development is associated with exposure to radiation, reducing radiation exposure in CT becomes an essential issue. Based on the compressive sensing (CS) theory, iterative based method with total variation (TV) minimization is proven to be a powerful framework for few-view tomographic image reconstruction. Multigrid method is an iterative method for solving both linear and nonlinear systems, especially when the system contains a huge number of components. In medical imaging, image background is often defined by zero intensity, thus attaining spatial support of the image, which is helpful for iterative reconstruction. In the proposed method, the image support is not considered as a priori knowledge. Rather, it evolves during the reconstruction process. Based on the CS framework, we proposed a multigrid method with adaptive spatial support constraint. The simultaneous algebraic reconstruction (SART) with TV minimization is implemented for comparison purpose. The numerical result shows: 1. Multigrid method has better performance while less than 60 views of projection data were used, 2. Spatial support highly improves the CS reconstruction, and 3. When few views of projection data were measured, our method performs better than the SART+TV method with spatial support constraint.











9033-120, Session PSWed

## Iterative raw measurements restoration method with penalized weighted least squares approach for low-dose CT

Hisashi Takahashi, Taiga Goto, Koichi Hirokawa, Osamu Miyazaki, Hitachi Medical Corp. (Japan)

Statistical iterative reconstruction and post-log data restoration algorithms for CT noise reduction have been widely studied and these techniques have enabled us to reduce irradiation doses while maintaining image qualities. In low dose scanning, electronic noise becomes obvious and it results in some non-positive signals in raw measurements. The non-positive signal should be converted to positive signal so that it can be log-transformed. Since conventional conversion methods do not consider local variance on the sinogram, they have difficulty of controlling the strength of the filtering. Thus, in this work, we propose a method to convert the non-positive signal to the positive signal by mainly controlling the local variance. The method is implemented in two separate steps. First, an iterative restoration algorithm based on penalized weighted least squares is used to mitigate the effect of electronic noise. The algorithm preserves the local mean and reduces the local variance induced by the electronic noise. Second, smoothed raw measurements by the iterative algorithm are converted to the positive signal according to a function which replaces the non-positive signal with its local mean. In phantom studies, we confirm that the proposed method properly preserves the local mean and reduce the variance induced by the electronic noise, while keeping the variance in the raw data intact. Our technique results in dramatically reduced shading artifacts and can also successfully cooperate with the post-log data filter to reduce streak artifacts.

9033-121, Session PSWed

## Use of depth information from in-depth photon counting detectors for x-ray spectral imaging: a preliminary simulation study

Yuan Yao, Stanford Univ. (United States); Hans Bornefalk, KTH Royal Institute of Technology (Sweden); Scott S. Hsieh, Stanford Univ. (United States); Mats E. Danielsson, KTH Royal Institute of Technology (Sweden); Norbert J. Pelc, Stanford Univ. (United States)

Purpose: Photon counting x-ray detectors (PCXD) may improve dose-efficiency but are hampered by limited count rate. They generally have imperfect energy response. Multi-layer ("in-depth") detectors have been proposed to enable higher count rates but the potential benefit of the depth information has not been explored. We conducted a simulation study to compare in-depth detectors against single layer detectors composed of common materials with different energy responses. Both photon counting and energy integrating modes were studied.

Methods: Polyenergetic projections were simulated through 25cm of water and 1cm of calcium. For PCXD composed of Si or CdTe a 120kVp spectrum was used. For energy integrating x-ray detectors (EIXD) made from CdTe or CsI, spectral imaging was done using 80 and 140kVp and matched dose. Semi-ideal and phenomenological energy response models were used. To compare these detectors, we computed the Cramér-Rao lower bound (CRLB) of the basis material estimates.

Results: For PCXDs with perfect energy response, depth data provides no additional information. For PCXDs with imperfect energy response and for EIXDs the improvement can be significant. E.g., for a CdTe PCXD

with realistic energy response it could reduce the variance by  $\sim 50\%$ . The improvement depends on the x-ray spectrum. For a semi-ideal Si detector and a narrow x-ray spectrum the depth information has minimal advantage. For EIXD, the in-depth detector has consistent variance reduction (15% and 20% for water and calcium).

Conclusions: Depth information is beneficial to spectral imaging for both PCXD and EIXD. The improvement depends critically on the detector energy response.

9033-122, Session PSWed

### Fast model-based restoration of noisy and undersampled spectral CT data

David S. Rigie, Patrick J. La Rivière, The Univ. of Chicago (United States)

In this work we propose a fast, model-based restoration scheme for noisy or undersampled spectral CT data and demonstrate its potential utility with two simulation studies. First, we show how one can denoise photon counting CT images, post-reconstruction, by using a spectrally averaged image formed from all detected photons as a high SNR prior. Next, we consider a slow slew-rate kV switching scheme, where sparse sinograms are obtained at peak voltages of 80 and 140 kVp. We show how the missing views can be restored by using a spectrally averaged, composite sinogram containing all of the views as a fully sampled prior. We have chosen these examples to demonstrate the versatility of the proposed approach and because they have been discussed in the literature before, but we hope to convey that it may be applicable to a fairly general class of spectral CT systems. Comparisons to several sparsity-exploiting, iterative reconstructions are provided for reference.

9033-123, Session PSWed

## Experimental study of two material decomposition methods using multi-bin photon counting detectors

Kevin C. Zimmerman, Marquette Univ. (United States); Emil Y. Sidky, The Univ. of Chicago Medical Ctr. (United States); Taly Gilat Schmidt, Marquette Univ. (United States)

Photon counting detectors with multi-bin pulse height analysis (PHA) are capable of extracting energy dependent information which can be exploited for material decomposition. However, spectral degradations currently limit the performance of these systems. Iterative decomposition algorithms have been previously implemented which require prior knowledge of the source spectrum, detector spectral response, and energy threshold settings. We experimentally investigated two material decomposition methods that do not require explicit knowledge of the source spectrum and spectral response. In the first method, the effective spectrum for each energy bin is estimated from calibration transmission measurements, followed by an iterative maximum likelihood decomposition algorithm. The second investigated method, first proposed and tested through simulations by Alvarez, uses a linearized maximum likelihood estimator which requires calibration transmission measurements. The Alvarez method has the advantage of being noniterative. This study experimentally quantified and compared the material decomposition error and noise resulting from these two methods. The spectral estimation method resulted in 70% error in the estimated basis material length for one decomposition trial, 20-30% error for three trials, and less than 15% error for the other eight trials. The Alvarez method was able to decompose the basis material lengths to within 20% for all but one of the samples, which had 36% error, with error less than 10% for most cases. The standard deviation of the basis material lengths was less than 1 mm for all test points. Future work is planned to decrease the error of these algorithms by improving the calibration techniques.











9033-124, Session PSWed

## Prostate tissue decomposition via DECT using the model based iterative image reconstruction algorithm DIRA

Alexandr Malusek, Maria Magnusson, Michael Sandborg, Robin Westin, Gudrun Alm Carlsson, Linköping Univ. (Sweden)

Better knowledge of elemental composition of patient tissues may improve the accuracy of absorbed dose delivery in brachytherapy. Deficiencies of water-based protocols have been recognized and work is ongoing to implement patient-specific radiation treatment protocols. A model based iterative image reconstruction algorithm DIRA has been developed by the authors to automatically decompose patient tissues to two or three base components via dual-energy computed tomography. Performance of an updated version of DIRA was evaluated for the determination of prostate calcification. A computer simulation using an anthropomorphic phantom showed that the mass fraction of calcium in the prostate tissue was determined with accuracy better than 9%. The calculated mass fraction was little affected by the choice of the material triplet for the surrounding soft tissue. Relative differences between true and approximated values of linear attenuation coefficient and mass energy absorption coefficient for the prostate tissue were less than 6% for photon energies from 1 keV to 2 MeV. The results indicate that DIRA has the potential to improve the accuracy of dose delivery in brachytherapy despite the fact that base material triplets only approximate surrounding soft tissues.

9033-125, Session PSWed

## Investigation of the polynomial approach for material decomposition in spectral X-ray tomography using an energy-resolved detector

Alexandra Potop, Véronique Rebuffel, Jean Rinkel, Andrea Brambilla, CEA-LETI-Minatec (France); Françoise Peyrin, CREATIS-LRMN INSA (France); Loick Verger, CEA-LETI-Minatec (France)

Recent advances in the domain of energy-resolved semiconductor based detectors stimulate research in X-ray computed tomography (CT). However, the imperfections of these detectors induce errors that should be considered for further applications. Charge sharing and pile-up effects due to high photon fluxes can degrade image quality or yield wrong material identification. Basis component decomposition provides separate images of principal components, based on the energy related information acquired in each energy bin. The object is typically either decomposed in photoelectric and Compton physical effects or in basis materials functions.

This work presents a simulation study taking into account the properties of an energy-resolved CdTe detector with flexible energy thresholds in the context of materials decomposition CT. We consider the effects of a first order pile-up model with triangular pulses of a non-paralyzable detector and a realistic response matrix. We address the problem of quantifying mineral content in bone based on a polynomial approach for material decomposition in the case of two and three energy bins. The basis component line integrals are parameterized directly in the projection domain and a conventional filtered back-projection reconstruction is performed to obtain the material component images. We use figures of merit such as noise and bias to select the optimal thresholds and quantify the mineral content in bone. The results obtained with an energy resolved detector for two and three energy bins are compared with the ones obtained for the dual-kVp technique using an integrating-mode detector with filters and voltages optimized for bone densitometry.

9033-126, Session PSWed

### Enabling photon counting detectors with dynamic attenuators

Scott S. Hsieh, Norbert J. Pelc, Stanford Univ. (United States)

Photon-counting x-ray detectors (PCXDs) are being investigated as a replacement for conventional x-ray detectors because they promise several advantages, including better dose efficiency, higher resolution and spectral imaging. However, many of these advantages disappear when the count rate incident on the detector becomes comparable to the detector's characteristic count rate. We recently proposed a dynamic, piecewise-linear attenuator (or beam shaping filter) that can control the flux incident on the detector. This can restrict the operating range of the PCXD to keep the incident count rate below a given limit. We simulated a system with the piecewise-linear attenuator and the PCXD using raw data generated from forward projected DICOM files. We investigated the classic paralyzable and nonparalyzable PCXD as well as a weighted average of the two, with the weights chosen to mimic an existing PCXD (Taguchi et al, Med Phys 2011). The dynamic attenuator has small synergistic benefits with the nonparalyzable detector and large synergistic benefits with the paralyzable detector. Real PCXDs operate somewhere between these models, and the weighted average model still shows large benefits from the dynamic attenuator. We conclude that dynamic attenuators can reduce the count rates necessary for adopting PCXDs.

9033-127, Session PSWed

### Noise balance in pre-reconstruction decomposition in spectral CT

Xiaolan Wang, Yu Zou, Toshiba Medical Research Institute USA (United States)

Spectral CT requires two or more independent measurements for each ray path in order to extract complete energy-dependent information of the object attenuation. The number of required measurements is equivalent to the number of independent basis functions needed to describe the attenuation of the imaged objects. For example, two independent measurements are sufficient if only photoelectric absorption and Compton scattering are dominating. If additional K-edge(s) is present in the energy range of interest, more than two measurements are necessary.

In this study, we present a pre-reconstruction decomposition method that utilizes spectral data redundancy to improve image quality. We assume projection data are acquired with an M-energy-bin photon counting detector that generates M independent measurements and the attenuation of the objects can be described with N (N< M) basis functions. The method addresses un-balanced noise level of data from different energy bins of the photon counting detector. During a CT scan, with the non-uniform attenuation of a typical patient, spectral shape and beam intensity can change drastically from detector to detector, from view to view. As a consequence, a detector unit is subject to significantly varying incident x-ray spectra. Hardware approaches (dynamically adjusting detector energy bins during a scan to maintain a balanced noise level in all energy bins, dynamic bowtie filters, etc.) are limited by the current detector and mechanical technology, and almost not possible to achieve in a typical clinical scan with e.g., 1800 views / 0.5 s.

Our method applies adaptive noise balance weighting to data acquired from different energy bins, post data acquisition and prior data decomposition. The results show substantially improved quality in spectral images reconstructed from photon counting detector data.











9033-128, Session PSWed

### Energy-resolved CT imaging with a photon counting silicon strip detector

Mats Persson, Ben Huber, Staffan Karlsson, Xuejin Liu, Han Chen, Cheng Xu, Moa M. Yveborg, Hans Bornefalk, Mats E. Danielsson, KTH Royal Institute of Technology (Sweden)

Photon counting detectors are promising candidates for use in the next generation of x-ray CT scanners. Among the foreseen benefits are higher spatial resolution, better trade-off between noise and dose, and energy discriminating capabilities.

Silicon is an attractive detector material because of its low cost, mature manufacturing process and short charge carrier collection time. However, it is sometimes claimed to be unsuitable for use in computed tomography because of its low absorption efficiency and high fraction of Compton scatter. The purpose of this work is to demonstrate that, despite these drawbacks, high-quality energy-resolved CT images can be acquired at a competitive dose using a photon counting silicon strip detector with eight energy thresholds developed in our group.

We use a single detector module, consisting of a linear array of 50 0.5\*0.4 mm detector elements, to image a phantom in a table-top lab setup. The phantom consists of a plastic cylinder with circular inserts containing water, fat and aqueous solutions of calcium, iodine and gadolinium, in different concentrations.

We use basis material decomposition to obtain water, calcium, iodine and gadolinium basis images and demonstrate that these basis images can be used to separate and quantify the different materials in the inserts.

9033-129, Session PSWed

### Characterization of a hybrid energy-resolving photon-counting detector

Andrea Zang, Georg Pelzer, Gisela Anton, Friedrich-Alexander-Univ. Erlangen-Nürnberg (Germany); Rafael Ballabriga Sune, CERN (Switzerland); Francesca Bisello, Friedrich-Alexander-Univ. Erlangen-Nürnberg (Germany) and IBA Dosimetry GmbH (Germany); Michael Campbell, Xavier Llopart, CERN (Switzerland); Ina Ritter, Felix Tennert, Friedrich-Alexander-Univ. Erlangen-Nürnberg (Germany); Stefan Wölfel, IBA Dosimetry GmbH (Germany); Winnie S. Wong, CERN (Switzerland); Thilo Michel, Friedrich-Alexander-Univ. Erlangen-Nürnberg (Germany)

Photon-counting detectors in medical x-ray imaging provide a higher dose efficiency than integrating detectors. Even further possibilities for imaging applications arise if the energy of each photon counted is measured as for example K-edge-imaging or optimizing image quality by applying energy weighting factors.

In this contribution we show results of the characterization of the Dosepix detector. This hybrid photon-counting pixel detector allows energy-resolved measurements with a novel concept of energy binning included in the pixel electronics. Based on ideas of the Medipix detector family, it provides three different modes of operation: An integration mode, a photon-counting mode, and an energy binning mode. Here it is possible to set 16

energy thresholds in each pixel individually to derive a binned energy spectrum in every pixel from one measurement. The detector matrix of 16x16 square pixels with 4 rows of small (55µm) and 12 rows of big pixels (220µm) is due to the originally intended use in the field of radiation measurement but the detector concept itself provides potential for imaging applications as well.

We present a spectrum derived in one single pixel as well as using the whole pixel matrix in energy binning mode with a conventional x-ray tube. In addition results concerning the linearity with increasing count

rates are shown. Further measurements regarding energy resolution and evaluations to decrease analog pile up events are topic of current work.

9033-130, Session PSWed

### X-ray light valve (XLV): a novel detectors' technology for digital mammography

Sorin Marcovici, Vladimir N. Sukhovatkin, Peter Oakham, XLV Diagnostics, Inc. (Canada)

The digital mammography markets, particularly in the developing countries, demand quality machines at substantially lower prices than the ones available today. More and more pressure is applied on x-ray detectors' manufacturers to reduce the price of flat panel detectors for digital mammography. XLV presents a unique opportunity to achieve the needed price - performance characteristics for direct conversion, x-ray detectors. The XLV based detectors combine the proven, superior, spatial resolution of a-Se with the simplicity and low cost of liquid crystals and optical scanning.

The x-ray quanta captured by a-Se produce electrical charge pairs that move under an electric field to the top and bottom of a-Se layer. This 2D charge distribution creates at the interface with the liquid crystals a continuous charge image corresponding to the impinging radiation's information. Under the influence of local electrical charges next to them, the liquid crystals twist proportionally to the charges which vary their reflectivity. A scanning light source illuminates the liquid crystals while a pixilated photo-detector, having a 42um pixel size, captures the light reflected by the liquid crystals and converts it in16 bit words transmitted to the machine for image processing.

The paper will describe a novel XLV, 25 cm x 30 cm, flat panel detector structure, its underlying physics as well as its preliminary performance measured on engineering prototypes. In particular, the paper will present the results of measuring XLV detectors' DQE, MTF, dynamic range, low contrast resolution and dynamic behavior. Finally, the paper will briefly introduce the low cost, XLV based, digital mammography machine under development by XLV Diagnostics Inc.

9033-131, Session PSWed

## Characterization of a silicon strip detector for photon-counting spectral CT using monoenergetic photons from 40 keV to 120 keV

Xuejin Liu, Hans Bornefalk, Han Chen, Mats E. Danielsson, Staffan Karlsson, Mats Persson, Cheng Xu, Ben Huber, KTH Royal Institute of Technology (Sweden)

We have developed a segmented silicon strip detector that operates in photon-counting mode and allows pulse-height discrimination with 8 adjustable energy bins. In this work, we determine the energy resolution of the detector using monoenergetic X-ray radiation from 40 keV to 120 keV. We investigate potential deterioration effects due to signal pileup at high input pulse rates, charge-sharing and Compton scattering.

For each incident monochromatic X-ray energy, we obtain integrated count spectra at different photon fluxes. These spectra reflect the detector response from which we can extract the energy resolution and the charge-sharing probability. Furthermore, we use these spectra to energy-calibrate the detector and to determine the pulse-height response homogeneity among the detector elements. The effect of charge-sharing and Compton scattering is quantified with the aid of Monte Carlo simulations and verified on real synchrotron data.

The energy-dependence of the energy resolution is accurately described by Poissonian photon fluctuations and electronic noise. At medium energies on the order of 60 keV we obtained a RMS energy resolution around 1.77 keV. By increasing input photon flux from 0.07·10<sup>8</sup> to













1.6·10<sup>8</sup>photons/mm/s, the RMS energy resolution decreased to approximately 2.10 keV due to pulse pileup. The effects of charge-sharing and Compton scattering on the energy resolution we both found to be negligibly small. The detector shows a pulse-height response variation among the channels below 4%.

9033-132, Session PSWed

## Experimental and theoretical performance analysis for a CMOS-based high resolution image detector

Amit Jain, Daniel R. Bednarek, Stephen Rudin, Toshiba Stroke and Vascular Research Ctr. (United States)

Increasing complexity of endovascular interventional procedures requires superior x-ray imaging quality. Present state-of-the-art x-ray imaging detectors may not be adequate due to their inherent noise and resolution limitations. With recent developments, CMOS based detectors are presenting an option to fulfill the need for better image quality. For this work, a new CMOS detector has been analyzed experimentally and theoretically in terms of sensitivity, MTF and DQE.

The detector (Dexela-1207) features 14-bit image acquisition, a Csl phosphor, 75 ?m pixels and an active area of 12 cm?7 cm with 30 fps frame rate. This detector has two modes of operations with two different full-well capacities: high and low sensitivity. The sensitivity and instrumentation noise equivalent exposure (INEE) were calculated for both modes. The detector modulation-transfer function (MTF), noise-power spectra (NPS) and detective quantum efficiency (DQE) were measured using an RQA5 spectrum. For the theoretical performance evaluation, a linear cascade model with an added aliasing stage was used.

The detector showed excellent linearity in both modes. The sensitivity and the INEE of the detector were found to be 31.55 DN/?R and 0.55 ?R in high sensitivity mode, while they were 9.87 DN/?R and 2.77 ?R in low sensitivity mode. The theoretical and experimental values for the MTF and DQE showed close agreement with good DQE even at fluoroscopic exposure levels.

In summary, the Dexela detector's imaging performance in terms of sensitivity, linear system metrics, and INEE demonstrates that it can overcome the noise and resolution limitations of present state-of-the-art x-ray detectors.

9033-133, Session PSWed

### Measurement of imaging properties of scintillating fiber optic plate

George Zentai, Arundhuti Ganguly, Josh M. Star-Lack, Gary F. Virshup, Daniel Shedlock, Dave Humber, Varian Medical Systems, Inc. (United States)

Scintillating Fiber Optic Plates (SFOP) or Fiber Optic Scintillator (FOS) made with scintillating fiber-glass, were investigated for x-ray imaging. Two different samples (TxWxL = 1cm x 5cm x 5cm) were used; Sample A: 10µm fibers, Sample B: 50µm fibers both with statistically randomize light absorbing fibers placed in the matrix. A customized holder was used to place the samples in close contact with photodiodes in an amorphous silicon flat panel detector (AS1000, Varian), typically used for portal imaging. The detector has a 392µm pixel pitch and in the standard configuration uses a gadolinium oxy-sulphide (GOS) screen behind a copper plate. X-ray measurements were performed at 120 kV (RQA 9 spectrum), 1 MeV (5mm Al filtration) and 6 MeV (Flattening Filter Free) for Sample A and the latter 2 spectra for Sample B. A machined edge was used for MTF measurements. The measurements showed the MTF degraded with increased X-ray energies because of the increase in Compton scattering. However, at the Nyquist frequency of 1.3 lp/mm, the MTF is still high (FOS value vs. Cu+GOS): (a) 39% and 21% at 120kVp for the 10?m FOS and the Cu+GOS arrays, (b) 31%, 39% and 21% at 1MeV and (c) 18%, 3% and 14% at 6MeV for the 10 $\mu$ m FOS, 50 $\mu$ m FOS and the Cu+GOS arrays. The DQE(0) value comparison at similar energies were (a) ~24% and ~13 % for the 10 $\mu$ m (b) 10%, 10% and 7% (c) 17%, ~13% and 1.6% for the 10 $\mu$ m FOS , 50 $\mu$ m FOS and Cu+GOS arrays.

9033-134, Session PSWed

## Optimizing two radioluminescence based quality assurance devices for diagnostic radiology utilizing a simple model

Jan P. Lindström, Karolinska Univ. Hospital (Sweden) and Linköping Univ. (Sweden) and Radicon, Bromma (Sweden); Markus Hulthén, Karolinska Univ. Hospital (Sweden); Gudrun Alm-Carlsson, Michael Sandborg, Linköping Univ. (Sweden)

The extrinsic (absolute) efficiency of a phosphor is expressed as the ratio of light energy emitted per unit area at the phosphor surface to incident x-ray energy fluence. A model described in earlier work has shown that by knowing the intrinsic efficiency, the particle size, the thickness and the light extinction factor ?, it is possible to deduce the extrinsic efficiency for an extended range of particle sizes and layer thicknesses. The model has been tested on Gd2O2S:Tb and ZnS:Cu fluorescent layers utilized in two quality assurance devices, respectively, aimed for the control of light field and radiation field congruence in diagnostic radiology. The first unit is an established device based on both fluorescence and phosphorescence containing an x-ray sensitive phosphor (ZnS:Cu) screen comprising a long afterglow. The other unit is under development and based on a linear CCD sensor which is sensitized to x-rays by applying a Gd2O2S:Tb scintillator. The field profiles and the corresponding edge localizations are then obtained and compared. The properties of the radioluminescent layers are essential for the functionality of the devices and have been optimized utilizing the previously developed and verified model. A theoretical description of the maximization of phosphorescence is also briefly discussed as well as an interesting finding encountered during the development processes: focus wandering. The oversimplistic physical assumptions made in the radioluminescence model have not been found to lead the optimizing process astray. The obtained functionality is believed to be adequate within their respective limitations for both devices.

9033-135, Session PSWed

# Investigation of spatial resolution and temporal performance of SAPHIRE (scintillator avalanche photoconductor with high resolution emitter readout) with integrated electrostatic focusing

David A. Scaduto, Anthony R. Lubinsky, John A. Rowlands, Stony Brook Univ. (United States); Hidenori Kenmotsu, Norihito Nishimoto, Takeshi Nishino, NANOX Japan (Japan); Kenkichi Tanioka, Tokyo Denki Univ. (Japan); Wei Zhao, Stony Brook Univ. (United States)

We have previously proposed SAPHIRE (scintillator avalanche photoconductor with high resolution emitter readout), a novel detector concept with potentially superior spatial resolution and low-dose performance compared with existing flat-panel imagers. The detector comprises a scintillator that is optically coupled to an amorphous selenium photoconductor operated with avalanche gain, known as high-gain avalanche rushing photoconductor (HARP). High resolution electron beam readout is achieved using a field emitter array (FEA). This combination of avalanche gain, allowing for very low-dose imaging, and electron emitter readout, providing high spatial resolution, offers











potentially superior image quality compared with existing flat-panel imagers, with specific applications to fluoroscopy and breast imaging. A prototype HARP sensor with integrated electrostatic focusing and nanospindt FEA readout technology has been fabricated by our industrial collaborator NanoX Japan. This integrated electron-optic focusing approach is scalable and appropriate for fabricating large-area detectors. We will investigate the dependence of spatial resolution on target and focus voltages, and compare the performance of this electrostatic focusing technique with and without mesh-electrode focusing. Temporal performance of the detector will be evaluated by characterizing lag effects. This proposed study represents the first technical evaluation and characterization of the SAPHIRE concept with integrated electrostatic focusing.

#### 9033-136, Session PSWed

# Imaging performance of a thin Lu<sub>2</sub>O<sub>3</sub>:Eu nanophosphor scintillating screen coupled to a high resolution CMOS sensor under X-ray radiographic conditions: comparison with Gd<sub>2</sub>O<sub>2</sub>S:Eu conventional phosphor screen

Ioannis E. Seferis, Univ. of Patras (Greece); C. M. Michail, I. G. Valais, Technological Educational Institute of Athens (Greece); Justyna Zeler, Univeristy of Wroclaw (Poland); Panagiotis F. Liaparinos, Nektarios I. Kalyvas, G. P. Fountos, Technological Educational Institute of Athens (Greece); Eugeniusz Zych, Univ. of Wroclaw (Poland); I. S. Kandarakis, Technological Educational Institute of Athens (Greece); George Panayiotakis, Univ. of Patras (Greece)

The purpose of the present study was to experimentally evaluate the imaging characteristics of the Lu2O3:Eu nanophosphor thin screen coupled to a high resolution CMOS sensor under radiographic conditions. Parameters such as the Modulation Transfer Function (MTF), the Normalized Noise Power Spectrum (NNPS) and the Detective Quantum Efficiency (DQE) were investigated at 70 kVp under three exposure levels (20 mAs, 63 mAs and 90 mAs). Since Lu2O3:Eu emits light in the red wavelength range, the imaging characteristics of a 33.3 mg/cm2 Gd2O2S:Eu conventional phosphor screen were also evaluated for comparison purposes.

The Lu2O3:Eu nanophosphor powder was produced by the combustion synthesis, using urea as fuel. A scintillating screen of 30.2 mg/cm2 was prepared by sedimentation of the nanophosphor powder on a fused silica substrate. The CMOS/Lu2O3:Eu detector's imaging characteristics were evaluated using an experimental method proposed by the International Electrotechnical Commission (IEC) guidelines.

It was found that the CMOS/Lu2O3:Eu nanophosphor system has higher MTF values compared to CMOS/Gd2O2S:Eu sensor/screen combination in the whole frequency range examined. For low frequencies (0 to 2 cycles/mm) NNPS values of the CMOS/ Gd2O2S:Eu system were found 90% higher compared to the NNPS values of the CMOS/Lu2O3:Eu nanophosphor system, whereas from medium to high frequencies (2 to 13 cycles/mm) were found 40% higher. In contrast with the CMOS/Gd2O2S:Eu system, CMOS/Lu2O3:Eu nanophosphor system appears to retain high DQE values in the whole frequency range examined.

Our results indicate that Lu2O3:Eu nanophosphor is a promising scintillator for further research in digital X-ray radiography.

9033-137, Session PSWed

## Physical properties of a new flat panel detector with irradiated side sampling (ISS) technology

Martin Fiebich, Jan M. Burg, Christina Piel, Technische Hochschule Mittelhessen (Germany); Laura Rodenheber, Justus-Liebig-Univ. Giessen (Germany); Petar Penchev, Technische Hochschule Mittelhessen (Germany); Gabriele A. Krombach, Justus-Liebig-Univ. Giessen (Germany)

Flat panel detectors have become the standard technology in projection radiography. Further progress in detector technology will result in an improvement of MTF and DQE. The new detector (FDR D-Evo plus C35i, Fuji, Japan) is based on cesium-iodine crystals and has a change in the detector layout. The read-out electrodes are moved to the irradiated side of the detector. The physical properties of the detector were determined following IEC 62220-1-1 as close as possible. The MTF showed a significant improvement compared to other cesium-iodine based flatpanel detectors. Thereby the DQE is improved to other cesium-iodine based detectors especially for the higher frequencies.

The average distance between the point of interaction of the x-rays in the detector and the light collector is shorter, due to the exponential absorption law in the detector. Thereby there is a reduction in light scatter and light absorption in the cesium-iodine needle crystals. This might explain the improvement of the MTF and DQE results in our measurements. The new detector design results in an improvement in the physical properties of flat-panel detectors. This enables a potential for further dose reductions in clinical imaging.

#### 9033-138, Session PSWed

## MTF characterization in 2D and 3D for a high resolution, large field of view flat panel imager for cone beam CT

Jainil P. Shah, Steve D. Mann, Martin P. Tornai, Duke Univ. (United States); Michelle Richmond, George Zentai, Varian Medical Systems, Inc. (United States)

The 2D and 3D MTFs of a custom made, large 40x30cm2 area, 600-micron CsI-TFT based flat panel imager having 127-micron pixilation, along with the higher resolution fiber-like scintillator structure, were characterized in detail using various techniques. The larger area detector has a reconstructed FOV of 25cm diameter with an 80cm SID. The MTFs were determined with 1X1 (intrinsic) and 2X2 binning. The 2D MTFs were determined using a 50.8 micron tungsten wire and a solid lead edge, and the 3D MTF was measured using a custom made phantom consisting of three nearly orthogonal tungsten wires suspended in an acrylic cubic frame. The projection data was reconstructed in 1x1 and 2x2 binned modes using an iterative OSC algorithm using 16 subsets and 5 iterations. The 2D MTF was ~4% using the wire technique and ~1% using the edge technique at the 3.96 lp/mm Nyquist frequency. The average 3D MTF measured along the wires was ~8% at the Nyquist. As additional verification of the resolution, along with scatter, the Catphan phantom was also imaged, where the 1.7 lp/mm bars were easily observed. This high performance detector is integrated into a dedicated breast SPECT-CT imaging system.











9033-139, Session PSWed

## Comparing analytical and Monte Carlo optical diffusion models in phosphor-based X-ray detectors

Nektarios I. Kalyvas, Panagiotis F. Liaparinos, Technological Educational Institute of Athens (Greece)

Luminescent materials are employed as radiation to light converters in detectors of medical imaging systems, often referred to as phosphor screens. Several processes affect the light transfer properties of phosphors. Amongst the most important is the transmission of light. Light attenuation (absorption and scattering) can be described either through 'diffusion' theory in theoretical models or 'quantum' theory in Monte Carlo methods. Although analytical methods, based on photon diffusion equations, have been preferentially employed to investigate optical diffusion in the past, Monte Carlo simulation models can overcome several of the analytical modelling assumptions. The present study aimed to compare both methodologies and investigate the dependence of the analytical model optical parameters as a function of particle size and light wavelength. For this purpose the light transmission efficiency (LE) and the modulation transfer function (MTF) of Gd2O2S granular phosphor was calculated. This work considered varying grain size (6 - 12 µm) and three different values of light wavelength 420 nm, 545 nm and 610 nm

#### 9033-141, Session PSWed

#### X-ray imaging performance of an intraoral X-ray detector featuring a structured scintillator

Uwe Zeller, Suni Medical Imaging, Inc. (United States); Olof Svenonius, Scint-X AB (Sweden); Dan Brüllmann, Univ. Augenklinik Mainz (Germany); Buon Nguyen, Suni Medical Imaging, Inc. (United States); Anna Sahlholm, Fredrik Jonsson, Scint-X AB (Sweden)

#### Objectives:

Present the feasibility of an intra-oral x-ray detector, featuring a structured scintillator coupled to a commercially available CMOS sensor for dental applications.

#### Methods:

A structured scintillator has been fabricated by filling a deep pore array in silicon with scintillating material [CsI(TI), pore pitch:30.8 µm, hexagonal pattern] and optically coupled to a CMOS sensor [pixel pitch 33 µm].

In vitro images of phantoms, acquired with a dental x-ray source (60kVp, 2mm Al equivalent filtration) have been acquired in comparison to the commercially used CsI(TI) / fiber optic scintillator as typically used in dental x-ray applications.

MTF and SNR data obtained from the detector have been accessed in combination with a dedicated "front-end" filtering algorithm.

#### Results

The x-ray conversion efficiency of the novel scintillator is (as expected) lower compared to the reference version. This change effectively increases the usable dose range for the application, which is limited by the charge capacity of the CMOS sensor.

The resulting MTF yields higher values over the complete spatial frequency range needed for dental intra-oral x-ray imaging, while the SNR properties of the system are, after SW filtration, comparable to the reference.

#### Conclusion

A dental x-ray detector with improved spatial resolution within the range used in dental intra-oral imaging is feasible.

Future work is needed to access the impact of the lower x-ray conversion efficiency and to extend the performance assessment to images with relevant clinical structures like caries lesions, dental implants or root canal instruments.

#### 9033-142, Session PSWed

### Radio-fluorogenic dosimetry with violet diode laser-induced fluorescence

Peter A. Sandwall, Precision Physics, Inc. (United States); Henry Spitz, Howard Elson, Michael Lamba, William Connick, Henry Fenichel, University of Cincinnati (United States)

Radiotherapy is an important component of modern cancer care. While many developing nations have historically been underserved, access to medical linear accelerators is increasing. As such, research on inexpensive devices to monitor and calibrate radiation output is warranted.

The following work describes experiments with an aqueous coumarin based chemical dosimeter, read with an inexpensive 405nm, "bluray" laser and digital camera. Water radiolysis produces hydroxyl free radicals which readily hydroxylate coumarin-3-carboxylic acid (C3CA) to 7-hydroxy-coumarin-3-carboxylic acid (7HO-C3CA). Fluorescent 7HO-C3CA excites in UV to near UV range of 365-405nm and has a visible 455nm blue emission.

Solutions of coumarin-3-carboxlyic acid were irradiated with 6MeV electrons from a Varian Trilogy medical linear accelerator. Aliquots were placed in poly-styrene cuvettes and exposed to 30mW 405nm laser. The laser excited emission was photographed for each aliquot with a filtered digital camera. A line profile was taken of the emission and processed with MATLAB to obtain a dose response curve.

Initial results show a clear dose response in the range of 0.1-50 Gy. This work demonstrates the feasibility of applying inexpensive 405nm lasers to radiation dosimetry with specific application to radiotherapy. Further refinements will include exploration of enhanced imaging techniques and lower dose studies.

#### 9033-143, Session PSWed

# Comparison of different approaches of estimating effective dose from reported exposure data in 3D imaging with interventional fluoroscopy systems

Angelica Svalkvist, Jonny Hansson, Magnus Båth, Sahlgrenska Univ. Hospital (Sweden)

Three-dimensional (3D) imaging with interventional fluoroscopy systems is today a common examination. The examination includes acquisition of two-dimensional projection images, used to reconstruct CT like images of the patient. The resulting patient radiation dose, indicated to be on the same level as a conventional CT scan, needs concern in the optimization process, but determining the radiation doses from this kind of examinations is a challenging task. The aim of this study was to evaluate the uncertainties connected to using simplified methods for estimating the radiation doses from these examinations. In the study the Siemens Artis Zee interventional fluoroscopy system (Siemens Medical Solutions, Erlangen, Germany) was used. Images of anthropomorphic chest and pelvis phantoms were collected. The exposure values obtained were used in Monte Carlo-based calculations of the resulting effective doses, using the computer software PCXMC (STUK, Helsinki, Finland). Calculations were performed both using individual exposure values (kV and mAs) for each projection image and constant mean values (kV/mAs and DAP) for all projections. In addition, the effects of not including all projection images in the calculations were investigated. Preliminary results show that the effective dose from a pelvis examination











using this system is approximately 6 mSv. Only small variations were found between different methods used for dose calculations (variation smaller than 4%). The results thereby indicate that simplified dose calculations, e.g. not accounting for each projection image included in the examination, can be used to estimate the radiation doses from 3D imaging using interventional fluoroscopy systems with reasonable accuracy.

9033-144, Session PSWed

## Improved-resolution real-time skin-dose mapping for interventional fluoroscopic procedures

Vijay K. Rana, Stephen Rudin, Daniel R. Bednarek, Univ. at Buffalo (United States) and Toshiba Stroke and Vascular Research Ctr. (United States)

We have developed a dose-tracking system (DTS) that provides a realtime display of the skin-dose distribution on a 3D patient graphic during fluoroscopic procedures. Radiation dose to individual points on the skin is calculated using exposure and geometry parameters from the digital bus on a Toshiba C-arm unit. To accurately define the distribution of dose, it is necessary to use a high-resolution patient graphic consisting of a large number of elements. In the original DTS version, the patient graphics were obtained from a library of population body scans which consisted of larger-sized triangular elements resulting in poor congruence between the graphic points and the x-ray beam boundary. To improve the resolution without impacting real-time performance, the number of calculations must be reduced and so we created software-designed human models and modified the DTS to read the graphic as a list of vertices of the triangular elements such that common vertices of adjacent triangles are listed once. Dose is calculated for each vertex point once instead of the number of times that a given vertex appears in multiple triangles. By reformatting the graphic file, we were able to subdivide the triangular elements by a factor of 64 times with an increase in the file size of only 1.3 times. This allows a much greater number of smaller triangular elements and improves resolution of the patient graphic without compromising the real-time performance of the DTS and also gives a smoother graphic display for better visualization of the dose distribution.

9033-145. Session PSWed

## Beam hardening and partial beam hardening of the bowtie filter: Effects on dosimetric applications in CT

Xochitl Lopez Rendon, Katholieke Univ. Leuven (Belgium); Guozhi Zhang, Mayo Clinic (United States); Hilde Bosmans, Raymond Oyen, Federica Zanca, Katholieke Univ. Leuven (Belgium)

Purpose: To estimate the consequences on dosimetric applications when a CT bowtie filter is modeled by accounting for beam hardening versus only beam shaping.

Method: A model of source and filtration for a CT scanner was developed as described by Turner et. al. [1]. Fan angle specific exposures were measured with the stationary CT X-ray tube in order to assess the equivalent thickness of Al of the bowtie filter as a function of the fan angle. These thicknesses were used to calculate energy and fan angle specific weighting factors (beam hardening). The effect of beam shaping was studied by giving the photon spectrum a global fan angle specific weighting factor directly retrieved from the measurements.

Percentage differences between the two methods were quantified by calculating the dose in air after passing several water equivalent thicknesses as retrieved from patients with different BMI. Specifically, the maximum water equivalent thickness of the lateral and anterior-posterior dimension and of the corresponding (half) effective diameter were tested.

Results: The largest percentage differences were found for the thickest part of the bowtie filter and they increased with patient size. For a normal patient they ranged from 5.5% at half effective diameter to 16.5% for the lateral dimension; for the most obese patient they ranged from 7.4% to 20.4%, respectively.

Conclusion: The need for simulating the beam hardening of the bowtie filter in Monte Carlo platforms for CT dosimetry will depend on the required accuracy.

9033-146, Session PSWed

## CT-guided brachytherapy of prostate cancer: reduction of effective dose from X-ray examination

Dmitriy Sanin, Vitaliy Birukov M.D., Sergey Rusetskiy, Medical Radiological Research Ctr. (Russian Federation); Pavel Sviridov M.D., Tatiana Volodina M.D., Ctr. of Brachytherapy of Prostate Cancer (Russian Federation)

The technique of the microsources implantation under spiral computed tomography control is used in the Medical Radiological Research Center. In accordance with paragraph 5.4.2. NRP 99 2009 – "medical procedures associated with exposure to patients, must be justified by comparing the diagnostic or therapeutic benefits that they bring with the radiation damage to health that can be caused by the exposure, taking into account available alternatives, that are not connected with the medical exposure". Recommendations of the ICRP (Publication 105): There is a potential to reduce the dose which patient gets from computed tomography (CT). However, actual decrease of the dose depends on specific of system used. It is important for radiologists, medical physicists and CT operators to understand the correlation between the dose of the patient and the image quality and realize that the image quality in CT often higher than necessary for diagnosis.

9033-147, Session PSWed

### X-ray scatter characterization in dedicated breast CT with bowtie filters

Kimberly Kontson, Robert J. Jennings, Univ. of Maryland (United States) and U.S. Food and Drug Administration, Ctr. for Devices and Radiological Health (United States)

The scatter contamination of projection images in cone-beam computed tomography (CT) degrades image quality. The use of bowtie filters in dedicated breast CT can decrease this scatter contribution. Three bowtie filter designs that compensate for one or more aspects of the beammodifying effects due to the differences in path length in a projection have been studied. The first produces the same beam-hardening effect as breast tissue with a single-material design. The second produces the same beam quality and intensity at the detector with a two-material design and the third eliminates the beam-hardening effect by adjusting the bowtie filter thickness such that the same effective attenuation is produced at the detector. We have selected aluminum, boron carbide/ beryllium oxide, and PMMA as the materials for the previously described designs, respectively. These designs have been investigated in terms of their ability to reduce the scatter contamination in projection images acquired in a dedicated breast CT geometry. The magnitude of the scatter was measured as the scatter-to-primary ratio using experimental and Monte Carlo techniques. The distribution of the scatter will also be measured at different locations in the scatter image to produce scatter distribution maps for all three bowtie filter designs as a function of tube voltage and breast diameter. The results of this study will be useful in designing scatter correction methods and understanding the benefits of bowtie filters in dedicated breast CT.











9033-148, Session PSWed

## A simple scatter correction method for dual energy contrast-enhanced digital breast tomosynthesis

Yihuan Lu, Beverly A. Lau, Yue-Houng Hu, Wei Zhao, Gene Gindi, Stony Brook Univ. (United States)

Dual-Energy Contrast Enhanced Digital Breast Tomosynthesis (DE-CEDBT) has the potential to deliver additional diagnostic information for vascularized breast pathology beyond that available from screening DBT. DE-CE-DBT involves a contrast (iodine) injection followed by a low energy (LE) and a high energy (HE) acquisition. These undergo weighted subtraction then reconstruction which ideally shows only the iodinated signal. There is a scatter component in the projection data and, for the HE data, scatter leads to "cupping" artifacts. Scatter can reduce the visibility (as measured by SDNR) and quantitative accuracy (linearity of the reconstructed signal with density of iodine) of the signal. The use of filtered backprojection (FBP) reconstruction ameliorates these types of artifacts since FBP is insensitive to low spatial frequency scatter artifacts, but the use of FBP precludes the advantages of iterative reconstructions. This motivates effective scatter correction (SC) for the HE and LE projection data. We propose a simple SC method, applied at each acquisition angle. It uses scatter-only data at the edge of the image to interpolate a scatter estimate within the breast region. The interpolation has an approximately correct spatial profile but is quantitatively inaccurate. We further correct the interpolated scatter data with the aid of easily obtainable knowledge of SPR (scatter-to-primary ratio) at a single reference point. We validated the SC method using a CIRS breast phantom with iodine inserts. We evaluated its efficacy in terms of SDNR and iodine quantitative accuracy. The SC method is quick to use and may be useful in a clinical setting.

9033-149, Session PSWed

## Development of mammography system using CdTe photon counting detector for the exposure dose reduction

Sho Maruyama, Naoko Niwa, Misaki Yamazaki, Nagoya Univ. Graduate School of Medicine (Japan); Tatsuya Nagano, Telesystems Co., Ltd. (Japan); Yoshie Kodera, Nagoya Univ. Graduate School of Medicine (Japan)

We consider the development of new mammography system using the cadmium telluride (CdTe) photon counting detector for the exposure dose reduction. This system use the high X-ray energy which completely different from the conventional mammography. In this study, we estimated the usefulness of this system by measuring the absorbed dose distribution of phantom depth direction and contrast-to-noise ratio (CNR) at the acrylic step in the several polymethyl methacrylate (PMMA) phantom thicknesses using the Monte Carlo simulation. In addition, we developed a proto-type scanning system based on CdTe detector using shift-and-add method and evaluated its image qualities. CdTe sensor thickness was 1 mm and the pixel size was 0.2 x 0.2 mm2. The result of simulation, in our conditions that tube voltage is 40 kV and tungsten/ barium (W/Ba) as a target/filter, surface dose was reduced more than 60 % compared to conventional conditions. Also about CNR, it became higher than conventional conditions. When we will get the same CNR in PMMA 4 cm, acrylic step 2 mm thickness, it is possible about 35 % dose reduction, and these differences were greater in thick subject. For scanning system, we considered about improvement point from the results of image quality evaluation. This study indicated that by using the high X-ray energy compared to conventional mammography, we can expect a significant exposure dose reduction without loss of image quality. And developed proto-type system is possible to improve image quality by considering the balance of shift-and-add and output of the X-ray tube.

9033-150, Session PSWed

### On imaging with or without grid in digital mammography

Han Chen, Mats E. Danielsson, Björn Cederström, KTH Royal Institute of Technology (Sweden)

The grids used in digital mammography to reduce scattered radiation from the breast are not perfect and lead to partial absorption of primary radiation at the same time as not all of the scattered radiation is absorbed. It has therefore been suggested to remove the grids and correct for effects of scattered radiation using post-processing of the images. In this paper, we study the usefulness of a grid by investigating the possible dose reduction that is achieved when the grid is removed. The dose reduction is determined as a function of the thickness of a PMMA phantom by comparing the contrast-to-noise ratios (CNRs) of images acquired at constant exposure with and without grid. We used a theoretical model that was validated with the aid of Monte Carlo simulations and phantom studies. In order to evaluate the CNR we applied aluminum filters with two different sizes, 4x8 cm2 and 1x1cm2. When the large Al filter was used, the resulting CNR value for the gridless images was overestimated due to a different amount of scattered radiation in the background region and the region covered by Al, a difference that could be eliminated by selecting a region of interest close to the edge of the Al. We found that it is optimal to use a grid above about 4 cm PMMA thickness, while for thinner PMMA removal of the grid leads to a dose saving.

9033-151, Session PSWed

## Estimation of effective x-ray tissue attenuation differences for volumetric breast density measurement

Biao Chen, Chris Ruth, Zhenxue Jing, Baorui Ren, Andrew P. Smith, Ashwini Kshirsagar, Hologic, Inc. (United States)

Breast density has been identified to be a risk factor of developing breast cancer and an indicator of lesion diagnostic obstruction due to masking effect. Volumetric density measurement evaluates fibro-glandular volume, breast volume, and breast volume density measures that have potential advantages over area density measurement in risk assessment. One class of volume density computing methods is based on the finding of the relative fibro-glandular tissue attenuation with regards to the reference fat tissue, and the estimation of the effective x-ray tissue attenuation differences between the fibro-glandular and fat tissue is key to volumetric breast density computing. We have modeled the effective attenuation difference as a function of actual x-ray skin entrance spectrum, breast thickness, fibro-glandular tissue thickness distribution, and detector efficiency. Compared to other approaches, our method has threefold advantages: (1) avoids the system calibration-based creation of effective attenuation differences which may introduce tedious calibrations for each imaging system and may not reflect the spectrum change and scatter induced overestimation or underestimation of breast density; (2) obtains the system specific separate and differential attenuation values of fibro-glandular and fat for each mammographic image; and (3) further reduces the impact of breast thickness accuracy to volumetric breast density. A quantitative breast volume phantom with a set of equivalent fibro-glandular thicknesses has been used to evaluate the volume breast density measurement with the proposed method. The experimental results have shown that the method has significantly improved the accuracy of estimating breast density.











9033-152, Session PSWed

## Improving the spatial resolution characteristics of dedicated cone-beam breast CT technology

Peymon Gazi, Kai Yang, George Burkett, John M. Boone, UC Davis Medical Ctr. (United States)

Dedicated breast CT (bCT) technology may be useful for patients with high risk of developing breast cancer. Previous studies show that bCT outperforms mammography in the visualization of mass lesions, but mammography shows better results in finding microcalcifications. The Breast Tomography Project at UC Davis has led to development of three dedicated breast CT scanners that produce high resolution, fully tomographic images, overcoming tissue superposition effects found in mammography while maintaining an equivalent radiation dose. Over 600 patients have been imaged in an ongoing clinical trial. The latest UC Davis bCT system, code-named Doheny, is expected to be fully developed by October 2013. The main differences between Doheny and the previous generations of bCT system are in using a pulsed x-ray source (generator and tube) instead of continuous x-ray sources and also in using a high speed, low noise x-ray detector with higher sensitivity and smaller pixel pitch compared to the detectors used in the other prototypes of UC Davis bCT. The spatial resolution characteristics of the new scanner were investigated and the results show significant improvement in the overall MTF properties. Based on these results, it was concluded that using the new scanner, the MTF degradation was partially restored and using the new detector resulted in visibility of smaller details in the scanned object.

9033-153, Session PSWed

### Spectrum optimization for computed radiography systems

Johann B. Hummel, Friedrich Semturs, Marcus Kaar, Peter Homolka, Michael Figl, Medizinische Univ. Wien (Austria)

Technical quality assurance (TQA) is one of the key issues in breast screening protocols where the two crucial aspects are image quality and dose. While digital radiography (DR) systems can produce excellent image quality at low dose, it appears often to be difficult with computed radiography (CR) systems to fulfil the requirements for image quality and to keep the dose below the limits. Here, the choice of an optimal spectrum can help to reach the limiting values given by the standards.

To investigate the optimal choice of the spectrum, we calculated the contrast-noise ratio (CNR) for different anode/filter (a/f) combinations depending on the clinical range of tube voltage. This was done for breast thicknesses of 50, 60 and 70 mm. The figure-of-merit to be optimized was the quotient of squared CNR and average glandular dose. The investigated imaging plates were made of BaFBrI:Eu.

We found that the two k-edges of lodine at 33 kV and Barium at 37 kV influence the results significantly. A peak as found in DR systems is followed by two additional peaks resulting from the higher absorption at the k-edges. This can be experienced with all a/f combinations.

9033-155, Session PSWed

## Feasibility study of spectral computed tomography (CT) with gold as a new contrast agent

Marie Müllner, Helmut Schlattl, Uwe Oeh, Christoph Hoeschen, Helmholtz Zentrum München GmbH (Germany); Olaf Dietrich, Ludwig-Maximilians-University Hospital Munich (Germany) A new spectral CT (by Philips) with a photon-counting and energy selective detector provides the possibility to use the additional information, which is held by the energy of the incoming photons. The new CT system is capable of yielding valuable insight into the elemental composition of the tissue and it opens up the way for new CT contrast agents by detecting element-specific K-edge patterns. Gold could be a promising new CT contrast agent. The major goal of this study is to determine the minimum amount of gold which is needed to use it as a spectral CT contrast agent for medical imaging in humans. To reach this goal, Monte Carlo simulations with EGSnrc were performed.

The energy selective detector by Philips has 6 energy bins and the energy thresholds can be selected freely. At the outset of the investigation different energy thresholds were analyzed to determine the best energy thresholds, with respect to detect gold. The K-edge imaging algorithm was then applied to the simulation results with these energy bins. The reconstructed images were evaluated with respect to the signal-to-noise ratio, the contrast-to-noise ratio and the contrast.

The K-edge imaging algorithm is able to convert the information in the six energy bins into three images, which correspond to the photoelectric effect, Compton scattering and gold content. But the algorithm requires very long computing time. The simulations indicate that at least 0.3 to 0.2w% of gold are required to use it as a CT contrast agent in humans.

9033-156, Session PSWed

## Projection-based energy weighting on photon-counting X-ray images in digital subtraction mammography: a feasibility study

Sung-Hoon Choi, Seung-Wan Lee, Yu-Na Choi, Young-Jin Lee, Hee-Joung Kim, Yonsei Univ. (Korea, Republic of)

Contrast media, such as iodine and gadolinium, are generally used to enhance the contrast between target and background materials. Especially in digital subtraction mammography where subtracts the one image (with contrast medium) from the other (anatomical background) for observing the tumor structure, tumors which include more blood vessels than normal tissue could be distinguished through the enhancement of contrast-to-noise ratio (CNR). In order to improve CNR, we adopted projection-based energy weighting for iodine solutions with four different concentrations embedded in a breast phantom (50% adipose and 50% glandular tissues). In this study, a Monte Carlo simulation was used to simulate a 40 mm thickness breast phantom, which has 2.96, 7, 15 and 30 mg/cm3 iodine solutions, and an energy resolving photon-counting system. The input energy spectrum was simulated in a range of 20 to 45 keV in order to reject electronic noise and include k-edge energy of iodine (33.2 keV). The results showed that the projection-based energy weighting improved the CNR by factors of 1.25-3.61 compared to the counting images. Consequently, the CNR of images from the digital subtraction mammography could be improved by the projection-based energy weighting with photon-counting detectors.

9033-157, Session PSWed

## High resolution X-ray fluorescence imaging for a microbeam radiation therapy treatment planning system

Pavel A. Chtcheprov, Christina R. Inscoe, Laurel Burk, Rachel Ger, Hong Yuan, Jianping Lu, The Univ. of North Carolina at Chapel Hill (United States); Sha Chang, Univ. of North Carolina at Chapel Hill (United States); Otto Zhou, The Univ. of North Carolina at Chapel Hill (United States)

Microbeam radiation therapy (MRT) uses an array of high-dose, narrow (~100um) beams separated by a fraction of a millimeter to treat various radio-resistant, deep-seated tumors. MRT has been shown to spare











normal tissue up to 1000Gy of entrance dose while still being highly tumoricidal. Current methods of tumor localization for MRT treatments require MRI and x-ray imaging with subject motion and image registration that contribute to the measurement error. The purpose of this study is to develop a novel form of imaging to quickly and accurately assist in high resolution target positioning for MRT treatments using x-ray fluorescence. The key to this method is using the microbeam to both treat and image. High atomic number contrast media is injected into the phantom or blood pool of the subject prior to imaging. Using a collimated spectrum analyzer, the region of interest is slowly scanned through the MRT beam and the fluorescence signal is recorded for each slice. The signal can be processed to show vascular differences in the tissue and isolate tumor regions. By using the radiation therapy source as the imaging source we eliminate repositioning and registration errors. A phantom study showed that a spatial resolution of a fraction of microbeam width can be achieved by precision translation of the mouse stage. Preliminary results from an animal study showed accurate iodine profusion, confirmed by CT. The proposed image guidance method, using x-ray fluorescence to locate and ablate tumors, can be used as a fast and accurate MRT treatment planning system.

9033-158, Session PSWed

## Development of an MRI fiducial marker prototype for automated MR-US fusion of abdominal images

Christopher P. Favazza, Krzysztof R. Gorny, Mayo Clinic (United States); Michael J. Washburn, GE Healthcare (United States); Nicholas J. Hangiandreou, Mayo Clinic (United States)

External fiducial marker devices are expected to facilitate robust, accurate, and efficient image fusion of MR and other modalities. Automating of this process requires: selection of a suitable marker size and material that is visible across a variety of pulse sequences, design of an appropriate fiducial device, and a robust segmentation algorithm. A set of routinely used abdominal pulse sequences was used to image a variety of marker materials and range of sizes. The most successfully detected marker was 0.5" diameter cylindrical reservoir filled with 1 g/L copper sulfate solution. A fiducial device was designed and fabricated from four such markers arranged in a tetrahedral orientation. The device was imaged on both a phantom and a volunteer and custom developed algorithm was used to detect and segment the individual markers. The individual markers were accurately segmented in all sequences for both the phantom and volunteer. The measured intra-marker spacings matched well with the dimensions of the fiducial device. The average deviation from the actual physical spacings was  $0.63 \pm 0.37$  mm in the volunteer data and 1.02  $\pm$  1.05 mm for the phantom data. These preliminary results suggest that this general fiducial design and detection algorithm could be used for MRI multimodality fusion applications.

9033-159, Session PSWed

### Comparison between optimized GRE and RARE sequences for 19F MRI studies

Chiara D. Soffientini, Politecnico di Milano (Italy); Alfonso Mastropietro, Fondazione I.R.C.C.S. Istituto Neurologico Carlo Besta (Italy) and Politecnico di Milano (Italy); Matteo Caffini, Sara Cocco, Politecnico di Milano (Italy); Ileana Zucca, Alessandro Scotti, Fondazione I.R.C.C.S. Istituto Neurologico Carlo Besta (Italy); Giuseppe Baselli, Politecnico di Milano (Italy); Maria Grazia Bruzzone, Fondazione IRCCS Istituto Neurologico C. Besta (Italy)

In 19F-MRI studies a limiting factor is the presence of a low signal due to the low amount of 19F-nuclei, necessary for biological applications, and the inherent low sensitivity of MRI. Hence, acquiring images using the pulse sequence with the best SNR is a core issue: this is possible if the

acquisition parameters are optimized for the specific 19F compound. In 19F-MRI, multiple-spin-echo (RARE) and gradient-echo (GRE) are the two most frequently used pulse sequence families; therefore we performed an optimization study of GRE pulse sequences based on numerical simulations and experimental acquisitions on fluorinated compounds. We compared GRE performance to optimized RARE sequence.

Images were acquired on a 7T MRI preclinical scanner on phantoms containing different fluorinated compounds. Actual relaxation times (T1, T2, T2\*) were evaluated in order to optimize pulse sequences. Experimental comparison between spoiled GRE and RARE, obtained at a fixed acquisition time and in condition of steady state, suggested that RARE sequence has a better performance than spoiled GRE ( up to 373% higher). Moreover, spoiled GRE is less sensitive to T1 variations at the Ernst angle if a short TR is applied. The use of unbalanced-SSFP shows an increase in SNR compared to both RARE and GRE (up to 77% higher than RARE).

The obtained results confirm the importance of optimization process related to actual relaxation times of fluorinated compounds. GRE was demonstrated to be negligibly influenced by relaxation times compared to RARE. Moreover, potential improvements by considering unbalanced-SSFP were demonstrated and deserve further investigation.

9033-160, Session PSWed

### Noise effects in multi-peak multi-echo chemical shift-based water-fat quantification

Giulio Siracusano, Michele Gaeta, Univ. degli Studi di Messina (Italy); Aurelio La Corte, Univ. degli Studi di Catania (Italy); Carmelo Milazzo, Demetrio Milardi, Univ. degli Studi di Messina (Italy); Placido Bramanti, IRCCS Ctr. Studi Neurolesi Bonino Pulejo (Italy); Giuseppe Pio Anastasi, Giovanni Finocchio, Univ. degli Studi di Messina (Italy)

The signal from a voxel containing water and fat can be written as the sum of two deterministic signals related directly to the percentage of water and fat and a stochastic contribution which can be modeled as a Gaussian process with zero mean, unit variance and an amplitude which depends mainly on the experimental framework analyzed. Despite the main peck of fat and water are characterized by different T2\*, most of the quantification procedures are based on the assumption of a single common decay to be less noise sensitive.

Here we studied how controlled Gaussian noise affect the identification procedure based on a single-R2\* (R2\*=1/T2\*). We identified the stochastic properties of the water, and fat percentage, R2\*, and the field B0. We find that the Fat/Water images based on the mean values of those parameters give rise to an improved resolution. This procedure can be also used to estimate image variance maps that give information on how the percentage of Fat/Water can spread out voxel by voxel with respect to the central value. Although this procedure is developed for fat/water percentage quantification, it is general and can be also considered as a new tool for the post processing analysis of other MRI signals (e.g. diffusion MRI).

9033-161, Session PSWed

## A new resonance-frequency based electrical impedance spectroscopy and its application in biomedical engineering

Sreeram Dhurjaty, Dhurjaty Electronics Consulting LLC (United States); Yuchen Qiu, Univ of Oklahoma (United States); Maxine Tan, Bin Zheng, The Univ. of Oklahoma (United States)

Electrical Impedance Spectroscopy (EIS) has shown promising results for differentiating between malignant and benign tumors, which exhibit different dielectric properties. However, the performance of current EIS











systems has been inadequate and unacceptable in clinical practice. In the last several years, we have been developing and testing a new EIS approach using resonance frequencies for detection and classification of suspicious tumors. From this experience, we identified several limitations of current technologies and designed a new EIS system with a number of new characteristics that include (1) an increased A/D (analog-todigital) sampling frequency, 24 bits, and a frequency resolution of 100 Hz, to increase detection sensitivity (2) automated calibration to monitor and correct variations in electronic components within the system, (3) temperature sensing and compensation algorithms to minimize impact of environmental change during testing, and (4) multiple inductor-switching to select optimum resonance frequencies. We performed a theoretical simulation to analyze the impact of adding these new functions for improving performance of the system. This system was tested using phantoms and pathology-specimens. The theoretical and experimental test results are consistent with each other, and show that this new EIS system possesses improved sensitivity and reproducibility for detecting small impedance variations in tumor cells. The potential of applying this new EIS technology in biomedical applications will be investigated.

9033-164, Session PSWed

## A simple model for deep tissue attenuation correction and large organ analysis of Cerenkov luminescence imaging

Frezghi Habte, Stanford Univ. (United States); Arutselvan Natarajan, UC Davis Cancer Ctr. (United States); Sanjiv S. Gambhir M.D., Stanford Univ. (United States); David S Paik, Stanford Univ. School of Medicine (United States)

Cerenkov luminescence imaging (CLI) is an emerging cost effective modality that uses conventional small animal optical imaging systems and certain radionuclides probes for light emission. CLI has shown good correlation with PET for organs of high uptake such as kidney, spleen, thymus and subcutaneous tumors in mouse models. Since, however, the blue-weighted spectral characteristic of Cerenkov radiation is highly attenuated by tissue, CLI has significant limitations for deep tissue quantitative imaging. Large organs, such as liver, have also shown significantly higher signals due to the contribution of emission of light from finite depth of tissue. In this study, we have developed a simple model that estimates the effective tissue attenuation coefficient to correct for signal intensity per unit volume of large organ with pre-estimated depth and thickness of specific organ within the small animal model. We used several thin slices of ham cut roughly to the size of mouse model as a phantom. We placed a CLI-producing radionuclide source inside the phantom at different tissue depths and imaged it using an IVIS Spectrum Imaging System (Perkin-Elmer, Waltham, MA, USA). For validation, we also performed PET imaging. Finally, we performed small animal studies using both PET and CLI and applied the proposed model to quantitatively analyze and correct the CLI measurements. The result indicates that our model has a capability of correcting the CLI signal with the same order of magnitude as of the partial volume corrected PET measurements compared to the conventional (uncorrected) method.

9033-165, Session PSWed

## Improved attenuation correction for freely moving animal brain PET studies using a virtual scanner geometry

Georgios I. Angelis, Brain & Mind Research Institute (Australia); William J. Ryder, Andre Z. Kyme, Roger R. Fulton, Steven R. Meikle, Brain & Mind Research Institute (Australia) and The Univ. of Sydney (Australia)

Attenuation correction in positron emission tomography brain imaging of freely moving animals can be very challenging since the body of the

animal is often within the field of view and introduces a non negligible attenuating factor that can degrade the quantitative accuracy of the reconstructed images. An attractive approach that avoids the need for a transmission scan involves the generation of the convex hull of the animal's head based on the reconstructed emission images. However, this approach ignores the potential attenuation introduced by the animal's body. In this work, we propose a virtual scanner geometry, which moves in synchrony with the animal's head and discriminates between those events that traverse only the animal's head (and therefore can be accurately compensated for attenuation) and those that might have also traversed the animal's body. For each pose a new virtual scanner geometry was defined and therefore a new system matrix was calculated leading to a time-varying system matrix. This new approach was evaluated on phantom data acquired on the microPET Focus 220 scanner using a custom-made rat phantom. Results showed that when the animal's body is within the FOV and not accounted for during attenuation correction it can lead to bias of up to 10%.

On the contrary, attenuation correction was more accurate when the virtual scanner was employed leading to improved quantitative estimates (bias <2%), without the need to account for the animal's

9033-166, Session PSWed

# Optimization using detective quantum efficiency (DQE) of the high-resolution parallel-hole collimators with CdTe pixelated semiconductor SPECT system

Young-Jin Lee, Dae-Hong Kim, Ye-Seul Kim, Hee-Joung Kim, Yonsei Univ. (Korea, Republic of)

To improve both sensitivity and spatial resolution, a pixelated parallelhole collimator with equal hole and pixel sizes based on CdTe pixelated semiconductor SPECT system can be of a choice. However, the trade-off between sensitivity and spatial resolution is needed before determination of pixelated parallel-hole collimator geometric designs. The purpose of this study was to optimize and evaluate the above-mentioned collimators using detective quantum efficiency (DQE) to determine the best image performance of CdTe pixelated semiconductor SPECT system. The modulation transfer function (MTF) and sensitivity of the various collimator geometric designs with varying septal heights were measured. DQE was then calculated to optimize the collimator geometric designs. According to the results, the DQE decreased with increasing sourceto-collimator distance and decreasing septal height. In conclusion, we successfully optimized the pixelated parallel-hole collimator, and based on our results, we recommended the 15 mm septal height with 4 cm source-to-collimator distance with CdTe pixelated semiconductor SPECT system.

9033-167, Session PSWed

### A novel intra-operative positron imager for rapid localization of tumor margins

Hamid Sabet, Radiation Monitoring Devices, Inc. (United States); Brendan Stack Jr., Univ. of Arkansas for Medical Sciences (United States); Vivek V. Nagarkar, Radiation Monitoring Devices, Inc. (United States)

We report on the development of a compact intra-operative positron imaging probe designed to describe margins of PET- positive lesions. At present most probes on the market are non-imaging, and provide no ancillary information of surveyed areas including clear delineations of malignant tissue. The new probe consists of a novel hybrid scintillator coupled to a compact silicon photomultiplier (SiPM) array with associated front-end electronics packaged in an ergonomic housing. Pulse shape discrimination electronics has been implemented and integrated into the downstream data acquisition system to discriminate against the gamma











background.

The hybrid scintillator consists of a 0.4 mm thick layer of CsI:Tl coupled to a 1 mm thick LYSO crystal. To achieve high spatial resolution, CsI:Tl is pixelated to 0.5x0.5 mm2 pixels using laser ablation. While CsI:Tl acts as beta sensor, LYSO detects the gamma radiation from F-18 source and is used to navigate the probe to the malignant tissue site. These data are also used to effectively suppress gamma response in the beta image, thereby improving SNR and contrast.

The data show that the response in the two scintillators of the hybrid design exposed to a mixed beta/gamma radiation field could be easily distinguished based on pulse shapes, thus enabling effective background suppression. The measured spatial resolution of the probe over its 10x10mm2 effective area is <1.5 mm FWHM. Also, the probe has demonstrated the ability to localize nCi levels of F-18 beta radiation within seconds, even in the presence of strong gamma background.

9033-168, Session PSWed

### Preliminary Monte Carlo simulation of developments of Zr-89 PET imaging protocols

Khalid S. Alzimami, King Saud Univ. (Saudi Arabia); Salem A. Sassi, Riyadh Military Hospital (Saudi Arabia); Nicholas M. Spyrou, Univ. of Surrey (United Kingdom)

The zirconium-89 (Zr-89) has recently drawn significant interest in using immuno-PET in the detection of certain cancers such as breast cancer in comparison to F-18-deoxyglucose. This preliminary study aims to characterize Zr-89 PET imaging performance compared to F-18 and to investigate the optimal energy window settings for Zr-89 PET imaging. For this study, the Siemens Biograph 6 PET scanner geometry was modelled using GATE. More The physics processes were modelled using the low energy electromagnetic processes package including Rayleigh, photoelectric and Compton interactions. GATE allows modeling signal processing including energy and timing resolution blurring and coincidence sorting. A paralyzable dead-time model of 800 ns in order to simulate the dead time at the singles level was applied. Scans were made with energy windows of 425-580, 425-650, and 425-750 keV, in 3D mode. The ROOT output (V.5.14), providing list mode of the detected single events including energy deposited and coordinates of detection within the modelled scanner geometry for each single event, was used to calculate the scatter fraction (SF) and noise equivalent count rate (NECR) results. The SF and NECR measurements were simulated by modeling the NEMA NU-2001 scatter phantom uniformly filled with a solution of water and Zr-89 or F-18. Although, the energy window 425-750 keV for Zr-89 gave the highest NECR, it significantly increases the SF. Using the narrowest energy window (425-585 keV) significantly improves image contrast by reducing the SF by 25% and slightly reduces NECR by 6.8% in comparison to the energy window setting of 425-650 keV.

9033-169, Session PSWed

## Image reconstruction for the new simultaneous whole-body openPET/CT geometry

Yannan Yin, Tokyo Institute of Technology (Japan); Hideaki Tashima, National Institute of Radiological Sciences (Japan); Takashi Obi, Tokyo Institute of Technology (Japan); Taiga Yamaya, National Institute of Radiological Sciences (Japan)

A new simultaneous whole-body PET/CT imaging geometry based on the OpenPET imaging structure has been proposed. In this geometry, multiple x-ray sources are adopted to implement the same field of view at the exactly same time for the simultaneous PET and CT imaging process. In this paper, we conducted further quantitative analysis to the new geometry by computer simulation. Then we examined and compared the iterative and analytical algorithms in terms of image quality, regarding the

features of the geometry. Results indicated better images were acquired with the iterative algorithms under this geometry for the whole-body range rather than the analytical method. Improved reconstruction images were still expected with generalization of modified algorithm for the proposed geometry. Technical implementation of the geometry in clinical application should also be further considered.

9033-170, Session PSWed

# Including the effect of molecular interference in the coherent x-ray scattering modeling in MC-GPU and PENELOPE for the study of novel breast imaging modalities

Bahaa Ghammraoui, Rui Peng, Ivan Suarez, Cecilia Bettolo, Andreu Badal, U.S. Food and Drug Administration (United States)

Purpose: We present upgraded versions of MC-GPU and PENELOPE-Imaging, two open-source Monte Carlo codes for the simulation of radiographic projections and CT. The improvements aim to study breast imaging modalities that rely on the accurate modeling of coherent x-ray scatter.

Methods: The simulation codes were extended to account for the effect of molecular interference in coherent scattering using experimentally measured molecular interference functions. The validity of the new model was tested experimentally using the Energy Dispersive X-Ray Diffraction (EDXRD) technique with a polychromatic x-ray source and an energy-resolved Germanium detector at a fixed scattering angle. Experiments and simulations of a full field digital mammography system with and without a 1D focused antiscatter grid were conducted for additional validation. The modified MC-GPU tool was also used to examine the possibility of characterizing breast cancer within a mathematical breast phantom using the EDXRD technique.

Results: The measured EDXRD spectra were correctly reproduced by the simulation with the modified cose while the previous code using the Independent Atomic Approximation (IAA) leaded to large errors in the predicted diffraction spectra. There was good agreement between the simulated and measured rejection factor for the 1D focused antiscatter grid with both models. The simulation study in a whole breast showed that the x-ray scattering profiles of adipose, fibrosis, cancer and benign tissues are differentiable.

Conclusion: MC-GPU and PENELOPE were successfully extended and validated for accurate modeling of coherent x-ray scatter. The EDXRD technique with pencil-cone geometry in a whole breast was investigated by a simulation study and it was concluded that this technique has the potential to characterize breast cancer lesions.

9033-171, Session PSWed

# Evaluation of the resolving potency of a novel reconstruction filter on periodontal ligament space with dental cone-beam CT: a quantitative phantom study

Yuuki Houno, Nagoya Univ. Graduate School of Medicine (Japan); Toshimitsu Hishikawa, Ken-ichi Gotoh, Munetaka Naitoh, Eiichiro Ariji, Aichi Gakuin Univ. (Japan); Yoshie Kodera, Nagoya Univ. Graduate School of Medicine (Japan)

Diagnosis of the alveolar bone condition is important for the treatment planning of periodontal disease. Especially the determination of marginal bone height and periodontal ligament space is the focus. However, owing to the image blur of the current imaging technique, the thin alveolar bone and the periodontal ligament space is difficult to visualize. In this study, we developed an original periodontal ligament phantom (PLP) and evaluated the image quality of a novel reconstruction filter that











emphasized high frequency component.

PLP was composed from two resin blocks of different materials, the bone equivalent block and the dentine equivalent block. They were assembled to make continuously changing space from 0.0 to 1.0 millimeter that mimics periodontal ligament space. PLP was placed in water and the image was obtained by using Alphard-3030 dental cone-beam CT (Asahi Roentgen Industry Co., Ltd.). Then we reconstructed the projection data with a novel reconstruction filter. The axial images were compared with conventional reconstructed images.

In novel filter reconstruction images, 0.4 millimeter of the space width was confirmable, on the other hand 0.6 millimeter was in conventional images. With our method, the resolving potency of cone-beam CT images was improved.

9033-172, Session PSWed

### Unfiltered Monte Carlo-based tungsten anode spectral model from 20 to 640 kV

Andrew M. Hernandez, Univ. of California, Davis (United States); John M. Boone. UC Davis Medical Ctr. (United States)

A Monte Carlo-based tungsten anode spectral model, conceptually similar to the previously-developed TASMIP model, was developed. This new model provides essentially unfiltered x-ray spectra with better energy resolution and significantly extends the range of tube potentials for available spectra. MCNPX was used to simulate x-ray spectra as a function of tube potential for a conventional x-ray tube configuration with several anode compositions. Thirty five x-ray spectra were simulated and used as the basis of interpolating a complete set of tungsten x-ray spectra (at 1 kV intervals) from 20 to 640 kV. Additionally, rhodium and molybdenum anode x-ray spectra were simulated from 20 to 60 kV. Cubic splines were used to construct piecewise polynomials that interpolate the photon fluence per energy bin as a function of tube potential for each anode material. The tungsten anode spectral model using interpolating cubic splines (TASMICS) generates minimally-filtered (0.8 mm Be) x-ray spectra from 20 to 640 kV with 1 keV energy bins. The rhodium and molybdenum anode spectral models (RASMICS and MASMICS, respectively) generate minimally-filtered x-ray spectra from 20 to 60 kV with 1 keV energy bins. TASMICS spectra showed no statistically significant differences when compared with the empirical TASMIP model, the semi-empirical Birch & Marshall model, and a Monte Carlo spectrum reported in AAPM TG 195. The RASMICS and MASMICS spectra showed no statistically significant differences when compared with their counterpart RASMIP and MASMIP models. Spectra from the TASMICS. MASMICS, and RASMICS models are available in spreadsheet format for interested users.

9033-173, Session PSWed

## 3D X-ray reconstruction using lightfield imaging

Murat Tahtali, Sajib K. Saha, Andrew J. Lambert, Mark R. Pickering, UNSW@ADFA (Australia)

Existing Computed Tomography (CT) systems require full 360 degrees rotation projections. Using the principles of lightfield imaging, only 4 projections under ideal conditions can be sufficient when the object is illuminated with multiple-point X-ray sources. The concept was presented in a previous work with synthetically sampled data from a synthetic phantom. Application to real data requires precise calibration of the physical set up. This current work presents the calibration procedures using a physical 3D phantom consisting of simple geometric shapes. The crucial part of this process is to determine the effective distances of the X-ray paths, which are not possible or very difficult by direct measurements. Instead, they are calculated by tracking the positions of fiducial markers under prescribed source and object movements. Determination of minimal sampling parameters for a targeted

reconstruction resolution using ART will be attempted. The results will be compared with conventional CT scanning performed on the same phantom with the same apparatus.

9033-174, Session PSWed

## Hybrid-model for computed tomography simulations and post-patient collimator design

Horace Xu, Kun Tao, GE Global Research (China); Padmashree GK, GE Healthcare (India); Mingye Wu, GE Global Research (China); Ximiao Cao, GE Healthcare (China); Yong Long, GE Global Research (United States); Ming Yan, Yangyang Yao, GE Global Research (China); Bruno DeMan, GE Global Research (United States)

Ray-tracing based simulation methods are widely used in modeling x-ray propagation, detection and imaging. While most of the existing simulation methods rely on analytical modeling, a novel hybrid approach comprising of statistical modeling and analytical approaches is proposed here.

Our hybrid simulator is a unique combination of analytical modeling for evoking the fundamentals of x-ray transport through ray-tracing, and a look-up-table (LUT) based approach for integrating it with the Monte Carlo simulations that model optical photon-transport within scintillator. The LUT approach for scintillation-based x-ray detection invokes depth-dependent gain factors to account for intra-pixel absorption and light-transport, together with incident-angle dependent effects for inter-pixel x-ray absorption (parallax effect). The model simulates scatter-rejection post-patient collimator as an x-ray shadow on scintillator, while handling its position with respect to the pixel boundary, by a smart over-sampling strategy for high efficiency.

We have validated this simulator for computed tomography systemsimulations, by using real data from GE Brivo CT385. The level of accuracy of image noise and spatial resolution is better than 98%. We have used the simulator for designing the post-patient collimator, and measured modulation transfer function (MTF) for different plate widths.

Validation and simulation study clearly demonstrates that the hybrid simulator is an accurate, reliable, efficient tool for realistic system-level simulations. It could be deployed for research, design and development purposes to model any scintillator-based 2-dimension and 3-dimension x-ray imaging system, while being equally applicable for medical and industrial imaging.

9033-175, Session PSWed

## Physics-based modeling of X-Ray CT measurements with energy-integrating detectors

Yong Long, Hewei Gao, GE Global Research (United States); Mingye Wu, GE Global Research (China); Jed D. Pack, GE Global Research (United States); Horace Xu, Kun Tao, GE Global Research (China); Paul F. Fitzgerald, Bruno De Man, GE Global Research (United States)

Computer simulation tools for X-ray CT are important for research efforts on developing reconstructionmethods, designing new CT architectures, and improving X-ray source and detector technologies. In this paper, we propose a physics-based modeling method for X-ray CT measurements with energy-integrating detectors. It accurately accounts for the dependence characteristics on energy, depth and spatial location of the CT measurements generation process, which is either ignored or over simplified in most existing analytical simulationmethods. Compared with methods based on Monte Carlo simulations, it is computationally much more efficient due to the use of a look-up table for optical











collection efficiency. To model the detected electrons, the proposed model considers five separate effects: energy- and location-dependent absorption of the incident X-rays, conversion of the absorbed X-rays into the emitted optical photons by the scintillator, location-dependent collection of the emitted optical photons, quantum efficiency of converting from optical photons to electrons, and electronic readout noise. We evaluated the proposed method by comparing the noise levels in the reconstructed images from measured data and simulations of a GE LightSpeed VCT system. Using the results of a water phantom at various X-ray tube voltages (kVp) and currents (mA), we demonstrated that the proposed method produces realistic CT simulations. The difference in noise standard deviation between measurements and simulations is approximately 2%.

9033-176, Session PSWed

## Quantification of biological tissue and construction of patient equivalent phantom (skull and chest) for infants (1-5 years old)

Allan F. F. Alves, Diana R. Pina, Fernando Antonio Bacchim Neto, Sergio Marrone Ribeiro, José Ricardo A. Miranda, Univ. Estadual Paulista (Brazil)

Our main purpose in this study was to quantify biological tissue in computed tomography (CT) examinations with the aim of developing two patient equivalent phantoms (PEP). The first is a skull phantom and the second a chest phantom, both specific to infants aged between 1 and 5 years old. This type of phantom is widely used in the development of optimization procedures for radiographic techniques, especially in computed radiography (CR) systems. In order to classify and quantify the biological tissue, we used a computational algorithm developed in Matlab. The algorithm performed a histogram analyzes of each CT slice followed by a Gaussian fitting of each tissue at the CT number of interest. The algorithm also converted the mean thicknesses of the biological tissues (bone, soft, fat, and lung) into the corresponding thicknesses of the simulator material (aluminum, lucite, and air). We retrospectively analyzed 148 CT examinations of infant patients, in which 56 were skull examinations and 92 were chest examinations. We divided the results according to the average anterior-posterior diameter (APD) of each anatomical structure. The results also provided elements to construct a phantom to simulate the infant chest and the skull in the posterioranterior or anterior-posterior (PA/AP) view. Both patient equivalent phantoms developed in this study could be used to assess physical variables such as modulation transfer function (MTF) and detector quantum efficiency (DQE) or perform dosimetric control specific to pediatric protocols.

#### 9033-177, Session PSWed

### Guidewire path simulation using equilibrium of forces

Fernando M. Cardoso, Sergio S. Furuie, Escola Politécnica da Univ. de São Paulo (Brazil)

Vascular diseases are among the major causes of death in developed countries and the treatment of those pathologies may require endovascular interventions, in which the physician utilizes guidewires and catheters through the vascular system to reach the injured vessel region. Several computational studies related to endovascular procedures are in constant development. So, predicting the guidewire path may be of great value for both physicians and researchers. We propose a method to simulate and predict the guidewire and catheter path inside a blood vessel based on equilibrium of forces, which leads, iteratively, to the minimum energy configuration. This technique was validated with physical models using a ?0.33mm stainless steel guidewire. This method presented RMS error, in average, less than 1 mm. Moreover, the algorithm presented low variation (in average, ?=0.03mm) due to the

variation of the input parameters. Therefore, even for a wide range of different parameters configuration, similar results are presented, which makes this technique easier to work with. Since this method is based on basic physics, it is simple, intuitive, easy to learn and easy to adapt.

9033-178, Session PSWed

### Optical crosstalk in CT detectors and its effects on CT images

Hanbean Youn, Soohwa Kam, Jong Chul Han, Ho Kyung Kim, Pusan National Univ. (Korea, Republic of)

We present the method and results of optical photon transport in x-ray CT detectors composed of scintillator and photodiode arrays. We quantify the optical photon leaks from a pixel to neighbors with respect to various detector designs and configurations. Detector designs include reflector, optical grease, and multilayers of a photodiode with different optical parameters. Two different detector configurations are considered: front- and back-side illumination. The quantification of optical crosstalk in CT detectors is further extended to the investigation of its effects on the CT image quality. We expect that this study will be helpful for the CT detector design with less signal crosstalk, hence providing better CT images.

9033-179, Session PSWed

#### A comparison of simulation tools for photoncounting spectral CT

Radin A. Nasirudin, Technische Univ. München (Germany); Petar Penchev, Technische Hochschule Mittelhessen (Germany) and Institut für Medizinische Physik und Strahlenschutz (Germany); Kai Mei, Ernst J. Rummeny M.D., Technische Univ. München (Germany); Martin Fiebich, Technische Hochschule Mittelhessen (Germany) and Institut für Medizinische Physik und Strahlenschutz (Germany); Peter B. Noël, Technische Univ. München (Germany)

Photon-counting detectors (PCD) not only have the advantage of providing spectral information but also offer high quantum efficiencies, producing high image quality in combination with a minimal amount of radiation dose. Due to the clinical unavailability of photon-counting CT, the need to evaluate different CT simulation tools for researching different applications for photon-counting systems is essential. In this work, we investigate two different methods to simulate PCD data: Monte-Carlo based simulation (MCS) and analytical based simulation (AS). The MCS is a general-purpose photon transport simulation based on EGSnrc C++ class library. The AS uses analytical forward-projection in combination with additional acquisition parameters. MCS takes into account all physical effects, but is computationally expensive (several days per CT acquisition). AS is fast (several minutes), but lacks the accurateness of MCS with regard to physical interactions. Both methods are compared by simulating a CT spectrum of 100kV with six energy threshold levels. A modified CTP515 module of the CatPhan 500 phantom is used. For evaluation the simulated projection data are decomposed via a maximum likelihood technique, and reconstructed via standard filtered-back projection (FBP), and. Image quality from both methods is subjectively and objectively assessed. Visually, the difference in the image quality was not significant. When further evaluated, the relative difference was below 4%. As a conclusion, both techniques offer different advantages, while at different stages of development the accelerated calculations via AS can make a significant difference. For the future one could foresee a combined method to join accuracy and speed.











9033-180, Session PSWed

### Optimization of grating-based phase-contrast imaging setup

Pavlo Baturin, Mark E. Shafer, Carestream Health, Inc. (United States)

Phase contrast imaging (PCI) technology has emerged over the last decade as a novel imaging technique capable of probing phase characteristics of an object as complimentary information to conventional absorption properties. In this work, we identified and provided a rationale for optimization of key parameters that determine the performance of a Talbot-Lau PCI system. The study used the Fresnel wave propagation theory and system geometry to predict optimal grating alignment conditions necessary for producing maximum-phase contrast. The moiré fringe pattern frequency and angular orientation produced in the X-ray detector plane were studied as functions of the gratings' axial rotation. The effect of axial displacement between source-to-phase (L) and phase-to-absorption (d) gratings, on system contrast was discussed in detail. The L-d regions of highest contrast were identified, and the dependence of contrast on the energy of the X-ray spectrum was also studied. The predictions made in this study were tested experimentally and showed excellent agreement. The results indicated that the PCI system performance is highly sensitive to alignment. The rationale and recommendations made should serve as guidance in design, development, and optimization of Talbot-Lau PCI systems.

9033-181, Session PSWed

### Design of a compact high-energy setup for x-ray phase-contrast imaging

Markus Schüttler, Technische Univ. München (Germany) and Karlsruhe Institute of Technology (Germany); Andre Yaroshenko, Technische Univ. München (Germany); Martin Bech, Technische Univ. München (Germany) and Medical Radiation Physics (Sweden); Guillaume Potdevin, Andreas Malecki, Michael Chabior, Johannes Wolf, Arne Tapfer, Technische Univ. München (Germany); Jan Meiser, Danays Kunka, Maximilian Amberger, Jürgen Mohr, Karlsruher Institut für Technologie (Germany); Franz Pfeiffer, Technische Univ. München (Germany)

The main shortcoming of conventional biomedical x-ray imaging is the weak soft-tissue contrast, caused by the small differences in the absorption coefficients between different materials. This issue can be addressed by x-ray phase-sensitive imaging approaches, e.g. Talbot-Lau grating interferometry.

The advantage of the three binary grating Talbot-Lau approach is that one can acquire x-ray phase-contrast and dark-field images also with a conventional high-power lab source. However, through the introduction of the three gratings, several constraints are posed on the setup geometry. In general, the grating pitch and the x-ray energy determine the setup dimensions. The minimal length of the setup increases linearly with energy and is proportional to p2, where p is the pitch of the so-called phase grating. Thus, a high-energy (100 keV) compact grating-based setup for x-ray imaging can only be realized if gratings with aspect-ratio of approximately 300 and a pitch of 1-2 µm were available. However, production challenges limit the availability of such gratings.

In this study we consider the use of non-binary phase-gratings as means of designing a more compact grating interferometer for phase-contrast imaging. We present simulation and experimental data for both the monochromatic and polychromatic case. The results reveal that phase gratings with triangular-shaped structures yield fringe visibilities that can be used for imaging purposes at significantly shorter distances than binary gratings. This is a very important result, since it allows to design a compact high-energy setup for imaging. Furthermore, we discuss different techniques to obtain triangular-shaped phase-shifting structures.

9033-182, Session PSWed

### Fabrication of multilayer coated gratings for phase-contrast computed tomography (CT)

Zsolt Marton, Harish B. Bhandari, Vivek V. Nagarkar, Radiation Monitoring Devices, Inc. (United States); Harold H. Wen, National Heart, Lung, and Blood Institute (United States)

The principles of grating interferometry enable X-ray phase contrast imaging using incoherent radiation from standard X-ray tube. This approach is in stark contrast with current imaging methods using coherent synchrotron X-ray sources or micro-focus sources to improve contrast. The gratings interferometer imaging technique is capable of measuring the phase shift of hard X-rays travelling through a sample, which greatly enhances the contrast of low absorbing specimen compared to conventional amplitude contrast images. The key components in this approach are the gratings which consists of alternating layers of high and low Z (atomic number) materials fabricated with high aspect ratios.

Here we report on a novel method of fabricating the grating structures using the technique of electron-beam (e-beam) thin film deposition. Alternating layers of silicon (Z=14) and tungsten (Z=74) were deposited, each measuring 100 nm each, on a specially designed "echelle" substrate, which resulted in an aspect ratio of ~100:1. Fabrication parameters related to the thin film deposition such as geometry, directionality, film adhesion, stress and the resulting scanning electron micrographs will be discussed in detail. Using the e-beam method large-area gratings with precise multilayer coating thicknesses can be fabricated economically circumventing the expensive lithography steps.

9033-183, Session PSWed

### In-line phase-contrast X-ray imaging with dual-energy

Hui-Hsin Lu, Jiun-Lin Kuo, Shih-Chung Lee, Wei-Hsin Wang, Yio-Wha Shau, Industrial Technology Research Institute (Taiwan)

In this work, we reported the studying of x-ray imaging process with dualenergy using an in-line phase-contrast imaging system. The x-ray source in our system is tungsten and two metal filters, 100 um thick samarium and erbium, were used to obtain the x-ray source for getting narrow energy bandwidths. The raw chicken feet were used to be imaged in our system. The distance of source and imaging detector (SID) was 70 cm, and the distances of source and object (SOD) were varied from 5 to 35 cm to get various magnification ratios. The phase-contrast enhancement in soft tissue that is mixed connective tissue of chicken feet is 37.5 % with a magnification ratio of 14, and it is 10.1 % with a magnification ratio of 2. In the result of dual-energy processing result, the contours of soft and bone tissues are easily recognized after the dual-energy imaging process and the patterns on the brightness in grey level value at the edge of soft tissue caused by our in-line phase-contrast x-ray imaging system increases 50.2 %. According to our results, the phase-contrast x-ray imaging with dual-energy demonstrates the capability to enhance the edge of overlaying soft tissue and has the potential to clinical diagnosis in the future.

9033-184, Session PSWed

### Analysis and optimization of a deconvolutionbased information retrieval algorithm in X-Ray grating-based phase-contrast imaging

Florian Horn, Florian L. Bayer, Florian Gräf, Christoph Hertle, Georg Pelzer, Jens Rieger, André Ritter, Thomas Weber, Andrea Zang, Thilo Michel, Gisela Anton, Erlangen Ctr. for Astroparticle Physics (Germany)











Grating-based X-ray phase-contrast imaging is a promising imaging modality to increase soft tissue contrast in comparison to conventional attenuation-based radiography. Complementary and otherwise inaccessible information is provided by the dark-field image, which shows the sub-pixel size granularity of the measured object. This could especially turn out to be useful in mammography, where tumourous tissue is connected with the presence of superfine microcalcifications.\

In addition to the well-established image reconstruction process, an information retrieval process was introduced, which is based on deconvolution of the underlying scattering distribution within a single pixel revealing information about the sample. Subsequently, the different contrast modalities can be calculated out of the scattering distribution. The method already proved to deliver additional information by use of the higher moments of the scattering distribution and possibly reaches better image quality in consideration of an increased contrast-to-noise ratio.\

Several measurements were carried out using melamine foam as a phantom.

We show analyses of the dependency of the deconvolution-based method in regard of the dark-field image on different parameters such as dose, number of iterations of the iterative deconvolution-algorithm performed and created dark-field signal. Usage of the resulting characteristics might be helpful in future applications. The results complete recently published numerical simulations. Furthermore, we show a possibility to overcome the impeded ability to distinguish between areas of strong dark-field signal, that is inherent in the deconvolution-based process.

#### 9033-185, Session PSWed

### Energy weighting in grating-based X-ray phase-contrast imaging

Georg Pelzer, Thomas Weber, Gisela Anton, Friedrich-Alexander-Univ. Erlangen-Nürnberg (Germany); Rafael Ballabriga Sune, CERN (Switzerland); Florian L. Bayer, Friedrich-Alexander-Univ. Erlangen-Nürnberg (Germany); Michael Campbell, CERN (Switzerland); Wilhelm Haas, Florian Horn, Friedrich-Alexander-Univ. Erlangen-Nürnberg (Germany); Xavi Llopart Cudie, CERN (Switzerland); Norbert Michel, CMS-Schnaittach (Germany); Uwe Mollenbauer, IBA Dosimetry GmbH (Germany); Jens Rieger, André Ritter, Ina Ritter, Friedrich-Alexander-Univ. Erlangen-Nürnberg (Germany); Stefan Woelfel, IBA Dosimetry GmbH (Germany); Winnie S. Wong, CERN (Switzerland); Andrea Zang, Thilo Michel, Friedrich-Alexander-Univ. Erlangen-Nürnberg (Germany)

By using an energy-resolving photon-counting detector in grating-based x-ray phase-contrast imaging it is possible to reduce the dose needed and optimize the imaging chain towards highest performance. The advantage of photon- counting detectors in attenuation based imaging, due to their linear energy response, is known. The access to the energies of the photons counted provides even further potential for optimization by applying energy weighting factors. We have evaluated energy weighting for grating-based phase-contrast imaging. Measurements with the hybrid photon-counting detector Dosepix were performed. The novel concept of energy binning implemented in the pixel electronics allows individual storing of the energy information of the incoming photons in 16 energy bins for each pixel. With this technique the full spectral information can be obtained pixel wise from one single acquisition. On the differential phase-contrast data taken, we applied different types of energy weighting factors. The results presented in this contribution demonstrate the advantages of energy-resolved photon-counting in differential phase-contrast imaging. Using a x-ray spectrum centred significantly above the interferometers design energy leads to poor image quality. But with the proposed method and detector the quality was enhanced by 2.8 times in signal-to-noise ratio squared. As this is proportional to dose, energy-resolved photon-counting might be valuable especially for medical applications.

9033-186, Session PSWed

### Comparison of propagation- and gratingbased X-ray phase-contrast imaging techniques with a liquid-metal-jet source

Tunhe Zhou, Ulf Lundström, KTH Royal Institute of Technology (Sweden); Thomas Thüring, Simon Rutishauser, Paul Scherrer Institut (Switzerland) and Swiss Federal Institute of Technology (Switzerland); Daniel H. Larsson, KTH Royal Institute of Technology (Sweden); Marco F. M. Stampanoni, Paul Scherrer Institut (Switzerland) and Swiss Federal Institute of Technology (Switzerland); Christian David, Paul Scherrer Institut (Switzerland); Hans M. Hertz, Anna Burvall, KTH Royal Institute of Technology (Sweden)

X-ray phase-contrast imaging has been developed as an alternative to conventional absorption imaging, partly for its dose advantage over absorption imaging at high resolution. Grating-based imaging (GBI) and propagation-based imaging (PBI) are the two more widely applied phasecontrast techniques with polychromatic laboratory sources. We compare the two methods by experiments and simulations with respect to required dose. Cylindrical PET phantoms with different diameters are used to demonstrate the two methods under the same dose level and exposure time. A simulated comparison of the doses required for detection, with respect to cylinder diameter, is also presented. Simulations are done under the projection approximation using Fresnel diffraction theory. They show, for monochromatic radiation, a dose advantage for PBI for small features but an advantage for GBI at larger features. However GBI suffers more from the introduction of polychromatic radiation, in this case so much that PBI gives lower dose for all investigated feature sizes. Furthermore, we present and compare experimental images of biomedical samples. While those support the dose advantage of PBI, they also highlight GBI's advantage of quantitative reconstruction of multimaterial samples. For all experiments a liquid-metal-jet source was used. Liquid-metal-jet sources are a promising option for laboratorybased phase-contrast imaging due to the relatively high brightness and small spot size.

9033-187, Session PSWed

## Performance and optimization of X-ray grating interferometry

Matteo Abis, Thomas Thüring, Marco F. M. Stampanoni, Paul Scherrer Institut (Switzerland)

A theoretical description of the performance of a Talbot and Talbot-Lau type interferometers is developed, providing a framework for the optimization of the geometry for monochromatic and polychromatic beams.

Analytical formulas for the smallest detectable refraction angle and the visibility of the setup are derived. The polychromatic visibility of the interference fringes is particularly relevant for the design of setups with conventional X-ray tubes, and it is described in terms of the spectrum of the source and the type of beam-splitter grating.

9033-188, Session PSWed

## Increasing the field of view of X-ray phase contrast imaging using stitched gratings on low absorbent carriers

Jan Meiser, Maximilian Amberger, Karlsruher Institut für Technologie (Germany); Marian Willner, Technische Univ. München (Germany); Danays Kunka, Pascal Meyer, Karlsruher











Institut für Technologie (Germany); Frieder Koch, Karlsruher Institut für Technologie (Germany); Alexander Hipp, Helmholtz-Zentrum Geesthacht (Germany); Marco Walter, microworks GmbH (Germany); Franz Pfeiffer, Technische Univ. München (Germany); Jürgen Mohr, Karlsruher Institut für Technologie (Germany)

In the last years grating-based differential X-ray phase contrast imaging (DPCI) has become a technique on the cusp of commercial use after demonstrating its transfer from synchrotron to laboratory X-ray sources. [1-3] Current applications in medical diagnostic like blood vessel inspection or cartilage analyses [4-6] benefit from DPCI's enhanced soft-tissue contrast. The analysis of large objects like hand, knee or breast requires a larger field of view as well as higher photon energies. This poses additional challenges to the imaging setups, especially to the gratings as core elements in DPCI. Nowadays, state-of-the-art grating fabrication of high and narrow structures by the LIGA process provides circular areas of 70 mm in diameter or squared ones of 50 mm edge length. To overcome this limitation, we are developing a method to stitch gratings. Merging single grating tiles on a carrier substrate allows increasing the grating area significantly. The concept's potential has been demonstrated at first using 625 µm silicon wafers as carriers. Silicon works fine for high energies but the intensity loss for lower energies due to absorption becomes important. In this work we report on the first results of a new carrier substrate for the use at lower energies. We tested 150 µm thick polyimide foils put into a frame for stabilization with the grating tiles glued onto them. Testing was performed at an X-ray tube recording and comparing tomography scans of an aortic valve for a polyimide and a silicon carrier substrate. Although the transmission could be improved considerably image reconstruction was more difficult for the polvimide carrier.

9033-189, Session PSWed

#### **Grating-based mammography X-ray system**

Jens Rieger, Florian L. Bayer, Florian Horn, Thilo Michel, Georg Pelzer, André Ritter, Thomas Weber, Gisela Anton, Friedrich-Alexander-Univ. Erlangen-Nürnberg (Germany)

Grating-based X-ray phase-contrast imaging~(XPCI) is a promising modality to increase soft-tissue contrast in medical imaging and especially in the case of mammography. Several groups worldwide have performed investigations on grating-based Talbot-Lau X-ray imaging of breast tissue in laboratory set-ups. Most groups focussed on the soft tissue contrast enhancement of the differential phase image. We present in last years contribution the contrast improvement for calcifications in surrounding breast tissue for the dark-field image. So some really good results for this modality are already shown in laboratory set-ups.

In this contribution, we present the next step to get grating-based X-ray imaging into the clinical routine. We show promising measurements with a grating-based set-up integrated in a conventional mammography system. We can present some flat-field quality measurements of the integrated set-up in comparison to a laboratory based set-up and first measurements of small objects.

In the future, we are going to improve the set-up and take additional measurements of real breast mastectomy samples.

9033-191, Session PSWed

### Effect of coherence loss in differential phase contrast cone beam CT

Weixing Cai, Ruola Ning, Jiangkun Liu, Univ. of Rochester Medical Ctr. (United States)

Coherence property of x-rays is critical in the grating-based differential phase contrast (DPC) imaging because it is the physical foundation that

makes any form of phase contrast imaging possible. Loss of coherence is an important experimental issue, which results in increased image noise and reduced object contrast in DPC images and DPC cone beam CT (DPC-CBCT) reconstructions. In this study, experimental results are investigated to characterize the visibility loss (a measurement of coherence loss) in several different applications, including different-sized phantom imaging, specimen imaging and small animal imaging. Key measurements include coherence loss (relative intensity changes in the area of interest in phase-stepping images), contrast and noise level in retrieved DPC images, and contrast and noise level in reconstructed DPC-CBCT images. The influence of the size and composition of imaged object (uniform object, bones, skin hairs, tissues, and etc) will be quantified. The same investigation is also applied for moiré pattern-based DPC-CBCT imaging with the same exposure dose. A theoretical model is established to relate coherence loss, noise level in phase stepping images (or moiré images), and the contrast and noise in the retrieved DPC images. Experiment results show that uniform objects lead to a small coherence loss even when the attenuation is higher, while objects with large amount of small structures result in huge coherence loss even when the attenuation is small. The theoretical model predicts the noise level in retrieved DPC images, and it also suggests a minimum dose required for DPC imaging to compensate for coherence loss.

9033-192, Session PSWed

## Modulation transfer function analysis in X-ray grating interferometry using wave-optical simulations

Johannes Wolf, Michael Chabior, Technische Univ. München (Germany); Jonathan I. Sperl, GE Global Research Europe (Germany); Andreas Malecki, Technische Univ. München (Germany); Dirk Bequé, Cristina Cozzini, GE Global Research Europe (Germany); Franz Pfeiffer, Technische Univ. München (Germany)

The way conventional X-ray imaging is used in many applications in medical diagnostics or materials science, it is based on the absorption of rays passing through a material. However, an object in the beam path not only attenuates the X-rays but also induces a phase shift on the wave front and leads to small-angle scattering. With a grating interferometer, it is possible to convert all three effects into measurable signals and obtain attenuation, phase-contrast, and dark-field images, respectively, with a single acquisition. While phase contrast increases contrast between materials containing light atoms such as soft tissue, the dark-field signal is able to give information about the inner structure of the object at a sub-pixel scale.

For grating-based X-ray dark-field imaging, it has been shown that the size of the scattering structures has a strong influence on the signal. However, previous studies assumed particles with a specific shape (e.g. spheres or cylinders), which is only an approximation for particles in many practical cases. To uncouple the results from this assumption and gain further knowledge about the signal formation, the present study pursues a more general approach and examines the dependence of the dark-field signal on the spatial frequencies contained in the specimen. For that purpose, we use numerical wave-optical simulations employing a sample with a well-defined spatial frequency to investigate and quantitatively describe the modulation transfer function (MTF) of the grating interferometer. This knowledge will take us further towards the optimization of dark-field setups for specific purposes.











9033-194, Session PSWed

# Pre-computed backprojection based penalized-likelihood (PPL) reconstruction with an edge-preserved regularizer for stationary Digital Breast Tomosynthesis

Shiyu Xu, Southern Illinois Univ. Carbondale (United States); Christina R. Inscoe, Jianping Lu, Otto Zhou, The Univ. of North Carolina at Chapel Hill (United States); Ying Chen, Southern Illinois Univ. Carbondale (United States)

Stationary Digital Breast Tomosynthesis (sDBT) is a carbon nanotube based breast imaging device with fast data acquisition and decent projection resolution. However, three dimensional image reconstruction is faced with the challenges of the incomplete and nonsymmetric sampling geometry due to the sparse views and limited view angle. Of all available reconstruction method, statistical iterative reconstruction appears particularly promising since it provides an accurate statistical modeling and geometric system description. In this paper, we present the application of a non-quadratic regularizer to our previous pre-computed backprojection based penalized-likelihood (PPL) reconstruction. With a fine-tune parameter choice, the significant image quality improvement over conventional techniques is demonstrated. Specifically, decent image resolution, lower noise and higher contrast noise ratio (CNR) have been achieved, concurrently with the reduction of out-of-plane blur.

9033-195, Session PSWed

### Digital breast tomosynthesis reconstruction with an adaptive voxel grid

Bernhard E. H. Claus, GE Global Research (United States); Heang-Ping Chan, Univ. of Michigan (United States)

In digital breast tomosynthesis (DBT) volume datasets are typically reconstructed with an anisotropic voxel size, where the in-plane voxel size typically reflects the detector pixel size (e.g., 0.1 mm), and the slice separation is generally between 0.5-1.0 mm. Increasing the tomographic angle is expected to give better 3D image quality; however, the slice spacing in the reconstruction should be reduced, otherwise one may risk losing fine-scale image detail (e.g., small microcalcifications). An alternative strategy consists of reconstructing on an adaptive voxel grid, where the voxel height at each location is adapted based on the backprojected data at this location, with the goal to improve image quality for microcalcifications. In this paper we present an approach for generating such an adaptive voxel grid. This approach is based on an initial reconstruction at a finer slice-spacing combined with a selection of an "optimal" height for each voxel. This initial step is followed by a (potentially iterative) update acting now on the adaptive grid only. The method is combined with an order-statistics based backprojection (OSBP) strategy in order to minimize out-of-plane artifacts due to highcontrast structures. Initial results are promising and show clear image quality improvements for small microcalcifications, as compared to similar reconstructions on a regular voxel grid.

9033-196, Session PSWed

## List-mode PET image reconstruction for motion correction using the Intel XEON PHI co-processor

William J. Ryder, Georgios I. Angelis, Rezaul Bashar, John E. Gillam, Roger R. Fulton, Steven R. Meikle, The Univ. of Sydney (Australia)

List-mode image reconstruction for motion correction is computationally

expensive as it requires projection of hundreds of millions of rays through a 3D array. To decrease reconstruction time it is possible to use symmetric multiprocessing computers or graphics processing units. The former can have high financial costs, while the latter can require reimplementation of algorithms. The Xeon Phi is a new co-processor card with a Many Integrated Core architecture that can run 4 multiple instruction, multiple data threads per core with each thread having a 512-bit single instruction, multiple data vector register. Thus, it is possible to run in the region of 220 threads simultaneously.

An existing list-mode image reconstruction algorithm was ported to run on the Xeon Phi using pthreads. There were no differences between images reconstructed using the Phi co-processor card and images reconstructed using the same algorithm implemented on a Linux server. However, it was found that the reconstruction runtimes were greater on the Phi than the server. A new version of the image reconstruction code was developed using OpenMP which decreased runtimes to be similar to a dual Xeon Linux server. Data transfer from the host to co-processor card was found to be a rate-limiting step; this needs to be carefully considered in order to maximize runtime speeds.

The Xeon Phi co-processor card has been shown to be an effective compute resource for list-mode image reconstruction and a multi-Phi workstation could be a viable alternative to cluster of computers at a lower cost for medical imaging.

9033-197, Session PSWed

## Factor-scaled optimization transfer based iterative reconstruction with stationary digital breast tomosynthesis (sDBT)

Shiyu Xu, Southern Illinois Univ. Carbondale (United States); Jianping Lu, Otto Zhou, The Univ. of North Carolina at Chapel Hill (United States); Ying Chen, Southern Illinois Univ. Carbondale (United States)

We proposed a factor-scaled optimization transfer (OT) based algorithm to solve the statistical reconstruction in transmission tomography. Compared to a representative OT based method such as separable parabolic surrogate with pre-computed curvature (PC-SPS), our algorithm provides comparable image quality with fewer iterations due to a faster convergence rate. The computational cost at each iteration remains a similar level with PC-SPS. The experiments with sDBT system shows that to achieve comparable reconstructed images, the factor-scaled OT algorithm saves 30% computing time. In general, our proposed method exhibits a tremendous potential to be a iterative method with a parallel computation, a monotonic and global convergence with fast rate.

9033-198, Session PSWed

## Iterative reconstruction of volumetric modulated arc radiotherapy plans using control point basis vectors

Joseph C. Barbiere, Alexander Kapulsky, Alois Ndlovu, Hackensack Univ. Medical Ctr. (United States)

Volumetric Modulated Arc Radiotherapy is an innovative technique currently utilized to efficiently deliver complex treatments. Dose rate, speed of rotation, and field shape are continuously varied as the radiation source rotates about the patient. Patient specific quality assurance is performed to verify that the delivered dose distribution is consistent with the plan formulated in a treatment planning system. The purpose of this work is to present novel methodology using a Gafchromic EBT3 film image of a patient plan in a cylindrical phantom and calculating the delivered MU per control point. Images of two dimensional plan dose matrices and film scans are analyzed using MATLAB with the imaging toolbox. Dose profiles in a ring corresponding to the film position are











extracted from the plan matrices for comparison with the corresponding measured film dose. The plan is made up of a series of individual static Control Points. If we consider these Control Points a set of basis vectors, then variations in the plan can be represented as the weighted sum of the basis. The weighing coefficients representing the actual delivered MU can be determined by any available optimization tool, such as downhill simplex or non-linear programming. In essence we reconstruct an image of the delivered dose. Clinical quality assurance is performed with this technique by computing a patient plan with the measured monitor units and standard plan evaluation tools such as Dose Volume Histograms. Testing of the algorithm with known changes in the reference images indicated a correlation coefficient greater than 0.99.

9033-199, Session PSWed

# Investigation of the quantitative accuracy of 3D iterative reconstruction algorithms in comparison to filtered back projection method: a phantom study

Nouf H. Abuhadi, David Bradley, Univ. of Surrey (United Kingdom); Dev Katarey, Kingston Hospital (United Kingdom); Zsolt Podolyak, Univ. of Surrey (United Kingdom); Salem A. Sassi, Prince Sultan Medical Military City (Saudi Arabia)

The combination of CT-based attenuation correction and scatter correction allows more accurate quantification of radiopharmaceutical distribution in SPECT studies. This study aims to investigate the quantitative accuracy of 3D iterative reconstruction algorithms in comparison to filtered back projection (FBP) methods implemented on cardiac SPECT/CT imaging with and without CT-attenuation and scatter corrections. The study also investigated the effect of respiratory induced cardiac motion on myocardium perfusion quantification. This study was performed on a Siemens Symbian SPECT/CT system using clinical acquisition protocols. Respiratory induced cardiac motion was simulated by imaging a cardiac phantom whilst moving it using a respiratory motion motor

We present a comparison of spatial resolution for FBP and Ordered Subset Expectation Maximization (OSEM) Flash 3D together with and without resporatory induced motion, and with and without attenuation and scatter correction.

Our analyses revealed that the use of Flash 3-D without scatter or attenuation correction has improved Spatial Resolution by 30% relative to FBP. Reduction in Spatial Resolution due to respiratory induced motion was 12% and 38% for FBP and Flash 3-D respectively. The implementation of scatter correction has resulted in a reduction in resolution by upto 6% only, however, application of attenuation correction has resulted in 13% and 26% reduction in spatial resolution for SPECT images reconstructed using FBP and Flash 3-D algorithms respectively.

We conclude that iterative reconstruction (Flash-3D) provides significant improvement in image spatial resolution, however, the effects respiratory induced motion become more evident and require correction if the full potential of these algorithms to be realised. Attenuation and scatter correction may improve image contrast, but may have significant detrimental effect on spatial resolution.

9033-200, Session PSWed

## Focal spot measurements using a digital flat panel detector

Amit Jain, Toshiba Stroke and Vascular Research Ctr. (United States); Ashish S. Panse, Toshiba Stroke and Vascular Research Ctr. (United States) and Univ. at Buffalo (United States); Daniel R. Bednarek, Stephen Rudin, Toshiba Stroke and Vascular Research Ctr. (United States)

Focal spot size is one of the crucial factors that affect the image quality of any x-ray imaging system. It is, therefore, important to measure the focal spot size accurately. In the past, pinhole and slit measurements of x-ray focal spots were obtained using direct exposure film. At present, digital detectors are replacing film in medical imaging so that, although focal spot measurements can be made quickly with such detectors, one must be careful to account for the generally poorer spatial resolution of the detector and the limited usable magnification. For this study, the focal spots of a diagnostic x-ray tube were measured with a 10-µm pinhole using a 194-µm pixel flat panel detector (FPD). The two-dimensional MTF, measured with the Noise Response (NR) Method was used for the correction for the detector blurring. The resulting focal spot sizes based on the FWTM (Full Width at Tenth Maxima) were compared with those obtained with a very high resolution detector with 8-µm pixels. This study demonstrates the possible effect of detector blurring on the focal spot size measurements with digital detectors with poor resolution and the improvement obtained by deconvolution. Additionally, using the NR method for measuring the two-dimensional MTF, any nonisotropies in detector resolution can be accurately corrected for, enabling routine measurement of non-isotropic x-ray focal spots. This work presents a simple, accurate and quick quality assurance procedure for measurements of both digital detector properties and x-ray focal spot size and distribution in modern x-ray imaging systems.

9033-201, Session PSWed

#### Dose reduction in CT with correlatedpolarity noise reduction: context-dependent spatial resolution and noise properties demonstrating two-fold dose reduction with minimal artifacts

James T. Dobbins III, Jered R. Wells, William P. Segars, Duke Univ. (United States)

Correlated-polarity noise reduction (CPNR) is a novel noise reduction technique that uses a statistical approach to reducing noise while maintaining excellent resolution and a "normal" noise appearance. It was demonstrated in application to CT imaging for the first time at SPIE 2013 and showed qualitatively excellent image quality at half of normal CT dose. In this current work, we measure quantitatively the spatial resolution and noise properties of CPNR in CT imaging. To measure the spatial resolution, we developed a metrology approach that is suitable for nonlinear algorithms such as CPNR. We introduce the formalism of Signal Modification Factor, SMF(u,v), which is the ratio in frequency space of the CPNR-processed image divided by the noise-free image, averaged over an ensemble of ROIs in a given anatomical context. SMF is a nonlinear analog to the MTF. We used XCAT computer-generated anthropomorphic phantom images followed by projection space processing with CPNR. The SMF revealed virtually no effect from CPNR on spatial resolution of the images (<7% degradation at all frequencies). Corresponding contextdependent NPS measurements generated with CPNR at half-dose were about equal to the NPS of full-dose images without CPNR. This result demonstrates for the first time the quantitative determination of a twofold reduction in dose with CPNR with less than 7% reduction in spatial resolution. We conclude that CPNR shows strong promise as a noise reduction method for dose reduction in CT. CPNR could also be used in combination with iterative reconstruction techniques for yet further dose

9033-202, Session PSWed

#### Validation of an image-based technique to assess the perceptual quality of clinical chest radiographs with an observer study

Yuan Lin, Kingshuk R. Choudhury, H. Page McAdams, Duke Univ. Medical Ctr. (United States); David H. Foos, Carestream











Health, Inc. (United States); Ehsan Samei, Duke Univ. Medical Ctr. (United States)

We previously proposed a novel image-based technique to assess the perceptual quality of clinical chest radiographs. In this paper, an observer study was designed and conducted to systematically validate this technique and to collect acceptable range information for future applications.

Ten perceptual metrics were involved in this observer study, i.e., lung grey level, lung detail, lung noise, rib-lung contrast, rib sharpness, mediastinum detail, mediastinum noise, mediastinum alignment, subdiaphragm-lung contrast, and subdiaphragm area. For each perceptual metric, three tasks were successively presented to the observers. In each task, six image ROIs were randomly presented in a row and observers were asked to rank the images based only on a designated quality but regardless of the other qualities. A range slider on the top of the images was used for observers to indicate the acceptable range of appearance. Five board-certificated radiologists from Duke participated in this observer study on a DICOM calibrated diagnostic display workstation and under low ambient lighting conditions. The observer data were analyzed in terms of the correlations between the observer ranking order and the algorithmic ranking order, inter-observer variations, and acceptable ranges.

The observer study showed that, for each metric, the averaged ranking orders for all observers were strongly correlated with the algorithmic orders. For the lung grey level, the observer ranking orders completely accorded with the algorithmic ranking orders. For the inter-observer variations in terms of ranking order, no significant differences were found. For the inter-observer variations in terms of acceptable range, only one reader appeared to be systematically out of line with others.

The observer study indicates that the previously proposed technique provides a robust reflection of the perceptual image quality in clinical images. The acceptable ranges can be used as first-hand information for future applications to predict whether certain perceptual metrics of a clinical chest radiographs will be accepted by radiologists.

9033-203, Session PSWed

## Relative object detectability (ROD): a new metric for comparing x-ray image detector performance for a specified object of interest

Vivek Singh, Amit Jain, Daniel R. Bednarek, Stephen Rudin, Univ. at Buffalo (United States)

Relative object detectability (ROD) quantifies the relative performance of two image detectors for a specified object of interest by taking the following ratio: the integral of detective quantum efficiency of a detector weighted by the frequency spectrum of the object divided by that for a second detector. Four different detectors, namely the micro-angiographic fluoroscope (MAF), the Dexela 1207 (Dex) and Hamamatsu C10901D-40 (Ham) CMOS x-ray detectors, and a flat-panel detector (FPD) were compared. The ROD was calculated for six pairs of detectors: (1) Dex/FPD, (2) MAF/FPD, (3) Ham/FPD, (4) Dex/Ham, (5) MAF/Ham and (6) Dex/MAF for wires of 20-mm fixed length, solid spheres ranging in diameter from 100 to 1000 microns, and four simulated iodine-filled blood vessels of outer diameters 0.4 and 0.5 mm, each with wall thicknesses of 0.1 and 0.15 mm.

For each selected pair of detectors, the ROD has a value greater than one for small wire or sphere diameter and decreases monotonically with increasing diameter becoming one above a certain diameter, where both detectors perform equally. The relative detectability of simulated small blood vessels is independent of the vessel wall thickness for the same inner diameter; however, the ROD of the pairs compared here increase appreciably with decreasing inner diameter even if the outer diameter is the same so that the wall thickness increases. In summary, the ROD can be a useful figure of merit to evaluate relative performance of two detectors for a given imaging task.

9033-204, Session PSWed

# Experimental characterization of the noise performance of statistical model based iterative reconstruction (MBIR) in a clinical CT system

Ke Li, Jie Tang, Guang-Hong Chen, Univ. of Wisconsin-Madison (United States)

To reduce dose in CT, the statistical model based iterative reconstruction (MBIR) method has been introduced for clinical use. Due to the nonlinearity of this method, the noise characteristics of MBIR are expected to differ from those of FBP. This paper investigated the unique noise characteristics of images generated with MBIR acquired on a state-of-the-art clinical CT system. A water phantom was scanned at seven different exposure levels. At each exposure level, the scan was repeated 50 times to generate a noise ensemble for statistical analysis. The acquired data were reconstructed using both FBP and MBIR. Local noise power spectra (NPS) were assessed at five ROIs at different locations. We found that: (1) At each exposure level, the NPS of MBIR is lower than that of FBP at all frequencies; (2) The shape of the NPS of MBIR was not consistent across exposure levels, but rather experienced a shift of the peak towards lower frequencies at lower exposures; (3) The noise distribution is more uniform in MBIR than in FBP; (4) The noise variance in MBIR images is inversely proportional to two-fifth power of the exposure level. These results indicate that the well known relationship between image noise and exposure level has been significantly modified to account for a more gradual change of noise with respect to radiation dose. In addition, the linear dependence of image quality on the exposure level has been modified due to the shift in the peaks of the NPS in MBIR with exposure levels.

9033-205, Session PSWed

## Comparison of deconvolution techniques to measure directional MTF of FDK reconstruction

Changwoo Lee, Junhan Park, Youngjun Ko, Jongduk Baek, Yonsei Univ. (Korea, Republic of)

To measure a spatial resolution of CT scanner, several methods have been developed using bar pattern, wires and thin plates. While these approaches are effective to measure two dimensional MTF, it is not easy to measure directional MTF using those phantoms. To overcome these limitations, Thornton et al. proposed a method to measure directional MTF using sphere phantoms, which is effective only when the cone angle is small. Recently, Baek et al. developed a method to estimate the directional MTF even with a larger cone angle, but the proposed method was analyzed using a noiseless data set. In this work, we present Wiener and Richardson-Lucy(RL) deconvolution techniques to estimate the directional MTF, and compare the estimation performance with that of the previous methods (i.e., Thornton's and Baek's methods). To estimate directional MTF, we reconstructed a sphere object centered at (0.01 cm, 0.01 cm, 10.01 cm) using FDK algorithm, and then calculated plane integrals of the reconstructed sphere object and the ideal sphere object. The plane integrals of sphere objects were used to estimate the directional MTF using Wiener and RL deconvolution techniques. The estimated directional MTF was compared with the ideal MTF calculated from a point object, and showed an excellent agreement.











9033-206, Session PSWed

## Detector and imaging performance of a pre-clinical spectral CT system using CZT detectors bonded to Medipix3RX

Alexander Cherlin, Ian Radley, Kromek (United Kingdom); Philip H. Butler, MARS Bioimaging Ltd. (New Zealand) and Univ. of Canterbury (New Zealand) and CERN (Switzerland); Anthony P. H. Butler, MARS Bioimaging Ltd. (New Zealand) and Univ. of Otago (New Zealand) and CERN (Switzerland); Stephen T. Bell, MARS Bioimaging Ltd. (New Zealand); Marcus Clyne, ILR (New Zealand); Michael Prokesch, Handong Li, eV Products (United States)

The development of high count rate (10^7 - 10^8 counts/s/mm^2) CdZnTe (CZT) detectors for single photon counting energy-resolving CT systems requires a joint effort from detector and CT system designers. In this talk we present the MARS scanner - the first commercially available pre-clinical spectral CT scanner developed by the MARS team. It utilizes Kromek eV-CZT detectors bonded to the Medipix3RX ASICs. The CZT detectors are manufactured from the material grown by various methods at Kromek-eV and are bonded using a novel hybridisation process. The detector assemblies installed into the MARS scanner were used for the initial detector performance characterisation and then for the evaluation of new imaging performance capabilities which have arisen due to combining CZT detectors with the charge summing mode in the Medipix3RX ASIC. In particular, we shall present results of the assessment of biomarkers using the K-edge imaging approach and demonstrate a capability of simultaneous decomposition of up to six materials. The structural, functional and molecular information that can be obtained with the MARS scanner provides biomedical researchers with an imaging capability today that is of real practical use and not an experimental laboratory setup.

Along with presenting imaging performance of the system, we discuss the advantages of the detector and process technologies. We present detector development and characterisation results with an emphasis on the idea of utilising small pixel configurations (55–110 µm).

9033-207, Session PSWed

### A spectral CT technique using balanced K-edge filter set

Yothin Rakvongthai, Massachusetts General Hospital (United States); William Worstell, Photo Diagnostic Systems Inc. (United States) and Massachusetts General Hospital (United States); Georges El Fakhri, Jinsong Ouyang, Massachusetts General Hospital (United States)

In this work, we propose a novel spectral computed tomography (CT) approach that combines a conventional CT scanner with a Ross spectrometer to obtain quasi-monoenergetic measurements. The Ross spectrometer, which is a generalization of a Ross filter pair, is a set of balanced K-edge filters whose thicknesses are such that the transmitted spectra through any two filters are nearly identical except in the energy band between their respective K-edges. The proposed approach is based on these specially designed filters, which are used to synthesize a set of quasi-monoenergetic sinograms whose reconstruction yields energy-dependent attenuation coefficient (mu\_E) images. In this way, we are able to collect data using conventional CT data acquisition electronics, then to synthesize spectral CT datasets with highly stable, rate-independent energy bin boundaries. This approach avoids the chromatic distortion due to event pile-up which can cause difficulties with single photon spectrometry-based methods. To validate our Ross Spectrometer CT concept, we performed phantom studies and acquired data with a balanced filter set consisting of thin foils of silver, tin, cerium, samarium, dysprosium and tungsten. For each energy bin, a synthesized quasi-monoenergetic CT image was reconstructed using the standard Feldkamp-Davis-Kress (FDK) algorithm operating on the logarithmic ratio of corresponding energy-resolved intensity and blank sinogram pairs. The reconstructed attenuation coefficients showed satisfactorily good agreement with NIST reference values of mu\_E for water. The proposed spectral CT technique is potentially feasible and holds promise to provide a more accurate and cost-effective alternative to single-photon counting spectral CT techniques.

9033-208, Session PSWed

#### A flat-field correction method for photoncounting-detector-based micro-CT

So E. Park, Jae G. Kim, Mohammed A. A. Hegazy, Min H. Cho, Soo Yeol Lee, Kyung Hee Univ. (Korea, Republic of)

As low-dose computed tomography becomes a hot issue in the field of clinical x-ray imaging, photon counting detectors have drawn great attention as alternative x-ray image sensors. Even though photoncounting image sensors have several advantages over the integrationtype sensors, such as low noise and high DQE, they are known to be more sensitive to the various experimental conditions like temperature. Particularly, time-varying detector response during the CT scan is troublesome in photon-counting-detector-based CTs. To correct the time-varying response of the image sensor during the CT scan, we developed a flat-field correction method together with an automated scanning mechanism. We acquired the flat-field images and projection data every view alternatively. When we took the flat-field image, we moved down the imaging sample away from the field-of-view with aid of computer controlled linear positioning stage. Then, we corrected the flat-field effects view-by-view with the flat-field image taken at given view. With a CdTe photon-counting image sensor (XRI-UNO, IMATEK), we took CT images of small bugs. The CT images reconstructed with the proposed flat-field correction method were much superior to the ones reconstructed with the conventional flat-field correction method.

9033-209, Session PSWed

## Initial development of a nested SPECT-CT system with fully suspended CT sub-system for dedicated breast imaging

Jainil P. Shah, Steve D. Mann, Duke Univ. (United States); Randolph L. McKinley, ZumaTek, Inc. (United States); Martin P. Tornai, Duke Univ. (United States)

A fully suspended, stand-alone cone beam CT system capable of complex trajectories, in addition to a simple circular trajectory, has previously been developed and shown to eliminate cone beam sampling insufficiencies and have better sampling close to the chest wall for pendant breast CT imaging. A hybrid SPECT-CT system with the SPECTonly capable of complex 3D trajectories has already been implemented and is currently in use. Here, these two systems are integrated into one hybrid system where each individual component is capable of traversing complex, arbitrary orbits around a pendant breast and anterior chest wall in a common field of view. The integration also involves key hardware upgrades: a new high resolution 40X30cm2 flat panel CT imager with an 8mm bezel edge on two sides for closer to chest wall access, a new x-ray source, and a unique tilting mechanism to enable the spherical trajectories. A novel method to tilt the gantry about a virtual center of rotation using a goniometric cradle and mounted ball bearings is developed and included in the new gantry, illustrating the flexibility of the integrated system.











9033-210, Session PSWed

#### Phase contrast portal imaging for imageguided microbeam radiation therapy

Keiji Umetani, Japan Synchrotron Radiation Research Institute (Japan); Takeshi Kondoh, Kobe Univ. (Japan)

High-dose radiation destroys cancer cells in radiation therapy. Microbeam radiation therapy (MRT) is an experimental form of radiation treatment with greater potential to improve the treatment of many types of cancer than that of customary broad-beam radiation treatment. MRT uses a vertical parallel array of closely spaced laminar microbeams of synchrotron radiation and might not cause severe side-effects of irradiation because of the high tolerance of normal tissues to X-ray microbeams.

Portal imaging for geometric verification in image-guided radiation therapy is performed to adjust the patient's position to administer the prescribed dose correctly within the prescribed tumor region. However, conventional portal images have less image contrast than diagnostic X-ray images have because portal imaging uses a therapeutic high-energy X-ray beam. Photon interactions with the patient occur mainly by Compton scattering.

We applied a synchrotron-radiation phase-contrast technique to portal imaging to improve the MRT accuracy in experiments using small animals. For a high-contrast edge enhancement effect in propagation-based phase-contrast imaging, an X-ray imaging detector is installed 0.2–6.0 m downstream from an object. In this study, rat skull images were obtained by phase-contrast imaging and conventional portal imaging for the evaluation of image contrast improvement. Compared to conventional portal imaging, the parietal and frontal bones were visualized clearly in phase-contrast imaging for positioning brain lesions with respect to the skull structures.

#### 9033-211, Session PSWed

### Rotating and semi-stationary multi-beamline architecture study for cardiac CT imaging

Jiao Wang, Paul F. Fitzgerald, Hewei Gao, Yannan Jin, GE Global Research (United States); Ge Wang, Rensselaer Polytechnic Institute (United States); Bruno De Man, GE Global Research (United States)

Over the past decade, there has been lots of research on the next generation cardiac CT architecture and corresponding reconstruction algorithms. Multiple cardiac CT concepts have been published, including third-generation single source CT with wide cone coverage, dual source CT, and electron-beam CT, etc. Among these cardiac CT architectures. triple source CT offers an approximately three-fold advantage in temporal resolution in half-scan mode, which can significantly reduce motion artifacts due to the moving heart and lung. In this paper, we describe a triple source CT architecture with all three beamlines limited to the cardiac field-of-view (FOV) in order to eliminate the radiation dose outside the cardiac region. We also demonstrated the capability of still performing full FOV imaging in non-cardiac mode by shifting the detectors. Ring source dual rotating detector CT offers the opportunity to provide high temporal resolution at the cost of a full ring stationary source. With this kind of semi-stationary architecture, we find that the azimuthal blur effect can be severer than in a non-stationary CT system. We also propose novel scanning modes to reduce the azimuthal blur in ring source CT.

9033-212, Session PSWed

### Determination of minor and trace elements in kidney stones by x-ray fluorescence analysis

Anjali Srivastava, Brianne J. Heisinger, Vaibhav Sinha, Hyong Koo Lee, Xin Liu, Missouri Univ. of Science and Technology (United States); Mingliang Qu, Xinhui Duan, Shuai Leng, Cynthia H. McCollough, Mayo Clinic (United States)

The determination of accurate material composition of a kidney stone is crucial for understanding the formation of the kidney stone as well as for preventive therapeutic strategies. Radiations probing instrumental activation analysis techniques are excellent tool for identification of involved materials present in the kidney stone. In particular, x-ray fluorescence (XRF) can be very useful for the determination of minor and trace materials in the kidney stone. The X-ray fluorescence measurements were performed at the Radiation Measurements and Spectroscopy Laboratory (RMSL) of department of nuclear engineering of Missouri University of Science & Technology and different kidney stones were acquired from the Mayo Clinic, Rochester, Minnesota. Presently, experimental studies in conjunction with analytical techniques were used to determine the exact composition of the kidney stone. A new type of experimental set-up was developed and utilized for XRF analysis of the kidney stone. The correlation of applied radiation source intensity, emission of X-ray spectrum from involving elements and absorption coefficient characteristics were analyzed. To verify the experimental results with analytical calculation, several sets of kidney stones were analyzed using XRF technique. The elements which were identified from this techniques are Silver (Ag), Aluminum (Al), Bromine (Br), Calcium (Ca), Chlorine (Cl), Chromium (Cr), Potassium (K), Magnesium (Mg), Manganese (Mn), Sodium (Na), Phosphorous (P), Sulfur (S), Selenium (Se), Strontium (Sr), Titanium (Ti). This paper presents a new approach for exact detection of accurate material composition of kidney stone materials using XRF instrumental activation analysis technique.

9033-213, Session PSWed

## Workflow for the use of a high-resolution image detector in endovascular interventional procedures

Raman Rana, Brendan M. Loughran, Swetadri Vasan Setlur Nagesh, Toshiba Stroke and Vascular Research Ctr. (United States) and Univ. at Buffalo (United States); Liza Pope, TSVRC, University at Buffalo (United States); Ciprian N. Ionita, Toshiba Stroke and Vascular Research Ctr. (United States) and Univ. at Buffalo (United States); Adnan Siddiqui, Ning Lin, TSVRC, University at Buffalo (United States); Daniel R. Bednarek, Stephen Rudin, Toshiba Stroke and Vascular Research Ctr. (United States) and Univ. at Buffalo (United States)

Endovascular image-guided intervention (EIGI) has become the primary interventional therapy for the most widespread vascular pathologies. These procedures involve the insertion of a catheter into the femoral artery, which is then threaded under fluoroscopic guidance to the site of the pathology to be treated. Flat Panel Detectors (FPDs) are normally used for EIGIs; however, once the catheter is guided to the pathological site, high-resolution imaging capabilities can be used for accurately guiding a successful endovascular treatment. The Micro-Angiographic Fluoroscope (MAF) detector provides needed high-resolution, high-sensitivity, and real-time imaging capabilities.

The MAF enabled with a Control, Acquisition, Processing, Image Display and Storage System (CAPIDS) was installed and aligned on a detector changer attached to the C-arm of a clinical angiographic unit. CAPIDS was developed and implemented using LabVIEW software and provides a user-friendly interface that enables control of several clinical radiographic imaging modes of the MAF including: fluoroscopy, roadmapping,











radiography, and digital-subtraction-angiography (DSA). Using the automatic controls, the MAF detector can be moved to the deployed position, in front of a standard FPD, whenever higher resolution is needed during angiographic or interventional vascular imaging procedures. To minimize any possible negative impact to image guidance with the two detector systems, it is essential to have a well-designed workflow that enables smooth deployment of the MAF at critical stages of clinical procedures. For the ultimate success of this new imaging capability, a clear understanding of the workflow design is essential. This presentation provides a detailed description and demonstration of such a workflow design.

#### 9033-214, Session PSWed

### Feasibility of active sandwich detectors for single-shot dual-energy imaging

Seungman Yun, Jong Chul Han, Dong Woon Kim, Hanbean Youn, Ho Kyung Kim, Pusan National Univ. (Korea, Republic of); Jesse Tanguay, Ian A. Cunningham, Robarts Research Institute (Canada)

We revisit the doubly-layered detector configuration for single-shot dual-energy x-ray imaging. Using a pair of photodiode arrays coupled to phosphor screens and thin metal sheets, we construct sandwiched detector configuration. Designs of this sandwich detector, such as phosphor screen thicknesses, and filter material and thickness, are optimized by theoretical calculations and experimental measurements. The imaging performance of the sandwich detector is also be reported by using quantitative measurements of image quality. We expect that the active sandwich detector will provide motion-artifact-free tissue-specific images with a reasonable image quality.

#### 9033-215, Session PSWed

## Scatter correction method with primary modulator for dual energy digital radiography: a preliminary study

Byung-Du Jo, Hee-Joung Kim, Dae-Hong Kim, Young-Jin Lee, Pil-Hyun Jeon, Yonsei Univ. (Korea, Republic of)

In conventional digital radiography with dual energy subtraction technique, a significant fraction of the detected photons has been known as scatter component within the body. Scattered radiation can significantly deteriorate image quality in diagnostic x-ray imaging system. Various methods of scatter correction including non-measurementbased and measurement-based methods have been proposed in the past. Both of methods can reduce scatter artifacts in the image. However, non-measurement-based methods require a homogeneous object, moreover, insufficiency of correction. Therefore, we employed a measurement-based method to be able to correct scatter components of inhomogeneous object from dual energy digital radiography (DEDR) image. We performed a simulation study using a Monte Carlo Simulation with primary modulator for DEDR system. The primary modulator, which has 'checker-board-pattern', is used to modulate the primary radiation. Water-filled cylindrical phantoms which have variable size were used to quantify imaging performance. For scatter estimation, we used Discrete Fourier Transform filtering, e.g. Gaussian low pass - high pass filter with the cut-off frequency. The primary modulation method was evaluated using cylindrical phantom with a DEDR system. Although boundary effect has been arisen during the processing of scatter correction, the scatter components using primary modulator was accurately removed. The results show that contrast-to-noise ratio (CNR) was increased from 1.87 to 2.13 and root mean square error (RMSE) reduced from 78.78 to 30.13. The results on a cylindrical phantom demonstrated accuracy of scatter correction and improvement of image quality. These results suggested that the scatter correction method with primary modulator is useful for DEDR system.

9033-216, Session PSWed

### Assessing and improving cobalt-60 digital tomosynthesis image quality

Matthew B. Marsh, Kingston Regional Cancer Ctr. (Canada); L. John Schreiner, Cancer Ctr. of Southeastern Ontario (Canada); Andrew Kerr, Kingston Regional Cancer Ctr. (Canada)

Image guidance capability is an important feature of modern radiotherapy linacs, and future cobalt-60 units will be expected to have similar capabilities. Imaging in the treatment beam is an appealing option, for reasons of simplicity and cost, but the dose needed to produce cone beam CT images in a Co-60 treatment beam is too high for this modality to be clinically useful. Digital tomosynthesis (DT) offers a quasi-3D image, of sufficient quality to identify bony anatomy or fiducial markers, while delivering a much lower dose than CBCT.

A series of experiments were conducted on a prototype Co-60 cone beam imaging system to quantify the resolution, selectivity, geometric accuracy and contrast sensitivity of Co-60 DT. Although the resolution was severely limited by the penumbra cast by the ~2 cm diameter source, it was possible to identify high contrast objects on the order of 1 mm in width, and bony anatomy in anthropomorphic phantoms was clearly recognizable. Low contrast sensitivity down to electron density differences of 3% was obtained, for uniform features of similar thickness. The conventional shift-and-add reconstruction algorithm was compared to several variants of the FDK filtered backprojection algorithm result. The Co-60 DT images were obtained with a total dose of 5 to 15 cGy each.

We conclude that, should Co-60 radiotherapy units be upgraded and modernized, filtered backprojection DT in the treatment beam is a versatile and promising modality that would be well suited to image guidance requirements.

#### 9033-217, Session PSWed

#### 2D and 3D registration methods for dualenergy contrast-enhanced digital breast tomosynthesis

Kristen C. Lau, Susan Roth, Andrew D. A. Maidment, Univ. of Pennsylvania (United States)

Dual-energy contrast-enhanced digital breast tomosynthesis (DE CE-DBT) uses an iodinated contrast agent to image the three-dimensional breast vasculature. The University of Pennsylvania has an ongoing DE CE-DBT clinical study in patients with known breast cancers. The breast is compressed continuously and imaged at 4 time points (1 pre-contrast; 3 post-contrast). DE images are obtained by a weighted logarithmic subtraction of the high-energy (HE) and low-energy (LE) image pairs. In temporal subtraction, post-contrast images are subtracted from the pre-contrast image. This hybrid temporal subtraction of the DE images is performed to analyze iodine uptake, but suffers from motion artifacts. Employing image registration to correct for motion enhances the ability to evaluate the vascular kinetics of breast tumours in DE CE-DBT. Registration using ANTS (Advanced Normalization Tools) is performed in an iterative manner. Mutual information optimization first corrects largescale motions. Normalized cross-correlation optimization then iteratively corrects fine-scale misalignment. Two methods have been evaluated; the 2D method uses a slice-by-slice approach, while the 3D method is a volumetric approach accounting for out-of-plane breast motion. Our results demonstrate that iterative registration qualitatively improves with each iteration (total 5 iterations). Motion artifacts near the edge of the breast are corrected effectively and the appearance of structures (e.g. blood vessels, surgical clip) are better visualized. Statistical and clinical evaluations of registration accuracy in DE-CBT images are currently under investigation.











9033-218, Session PSWed

## Optimization of exposure parameters based on the polychromatic cascaded model of X-ray detectors

Kwang Eun Jang, Jongha Lee, Younghun Sung, SeungDeok Lee, Samsung Advanced Institute of Technology (Korea, Republic of)

Digital breast tomosynthesis (DBT) is an emerging modality for breast cancer screening. To maximize its diagnostic performances, exposure parameters such as the scan angle, number of views, peak voltage, and flux need to be properly determined. Due to the large number of variables, it is challenging to optimize those parameter with real experiments.

In this paper, we present a numerical platform for optimizing the exposure parameters of DBT, which can enhance the diagnostic performance with an efficient manner. It is mainly founded upon two pillars: a realistic simulator capable of synthesizing projections under low-dose conditions, and a numerical examiner that predicts the reconstruction quality under given exposure condition.

To develop a realistic simulator that takes many aspects into account, such as polychromatic nature, correlation with adjacent pixels, and statistical distribution, we combine two currently existing viewpoints on modeling the data acquisition in X-ray imaging. The first approach mainly concerns overall statistical properties of measurements, which assumes that acquired data exhibit some stochastic distribution, such as compound Poisson distribution. In the other approach, each stage of the image formation is modeled as a linear system and the whole acquisition process is described by the cascaded sub-systems. The proposed acquisition model encompasses both aspects.

To predict the diagnostic performance for given exposure parameters, we adapt spectral metrics to construct the numerical examiner.

In the following communication, we will describe the optimization scheme in detail and present results from numerical and experimental DBT systems.

9033-219, Session PSWed

## A vacuum sealed miniature x-ray tube based on carbon nanotube emitters for intraoral x-ray image

Hyun Jin Kim, Jun Mok Ha, Hamid Saeed Raza, Sung Oh Cho, KAIST (Korea, Republic of)

We have fabricated a vacuum-sealed miniature x-ray tube with the diameter of 7 mm and length of 47 mm for intraoral x-ray image using carbon nanotube (CNT) field emitters. Our vacuum-sealed miniature x-ray tube can be placed inside a mouth to reduce the un-necessary exposure of patient to x-ray and have uniform x-ray spatial distributions. A vacuum-sealed miniature x-ray tube is consisted of x-ray target, ceramic tube (alumina), CNT emitter, getter and focusing electrode. A conical shaped transmission-type tungsten (W) target with a thickness of 1.5 µm is used in the vacuum-sealed miniature x-ray tube to produce x-ray with uniform spatial distribution. A getter is used to maintain high level vacuum and ceramic tube is applied for electrical insulation of vacuum sealed miniature x-ray tube. CNTs are used as electrons source of the production of x-ray. The fabricated miniature x-ray tube can be stably and reliably operated up to 60kV without any vacuum pump and produces x-ray with uniform spatial distribution. The fabricated miniature x-ray tube has a simple diode structure unlike the complex structure reported in the literature. We have obtained x-ray radiography of teeth phantom and animal teeth. The quality of the images is very good with high resolution. We also used the vacuum-sealed miniature x-ray tube to have x-ray images of the USB flash drive. All the images are obtained at different angles by rotating the x-ray detector and USB flash drive. We found no difference in the quality of the x-ray images. The worthmentioning point is that our vacuum- sealed miniature x-ray tube has the capability to obtain x-ray images in multi-directions.

9033-220, Session PSWed

## Transmission x-ray characteristics of an ultrananocrystalline diamond cold cathode based X-ray source

Edwin J. Grant, Chrystian M. Posada, Missouri Univ. of Science and Technology (United States); Ralu Divan, Anirudha V. Sumant, Dan Rosenmann, Liliana Stan, Argonne National Lab. (United States); Ashish Avachat, Carlos H. Castano, Hyong Koo Lee, Missouri Univ. of Science and Technology (United States)

We previously reported on electron emission results from our novel cold cathode field emission array (FEA) X-ray source based on planarized ultra-nano-crystalline diamonds (UNCD) field emitters. Our prototype cathode consists of a small 3 x 3 pixel Field Emission Array (FEA) with a pixel to pixel pitch of 500 µm. The prototype yielded field emission turnon voltages as low as 4.69 V/µm with electron current densities of 6.42 mA/cm2 at electric fields lower than 20 V/µm. This work continues upon the previous feasibility simulations along with the design, fabrication and experimental results of electron field emission work to include X-ray generation. The flat-panel X-ray source is being constructed as an alternative for general X-ray use and medical imaging, such as; radiography, Computed Tomography (CT) and tomosynthesis. Additional interest includes using the device as a portable X-ray source, due to its lower power consumption versus traditional X-ray thermionic type sources.

The extracted electrons from the cathode are accelerated by a high voltage bias of 30 kVp to reach a final kinetic energy of 30 keV or lower. The electrons then bombard a tungsten transmission target anode where they generate X-rays by characteristic and Bremsstrahlung interactions. The generated X-rays are then counted and characterized with a low energy (> 3 keV) Ortec GLP series X-ray detector. Several key X-ray generation properties are measured, such as, X-ray energy spectrum, X-ray intensity and X-ray angular distribution.

9033-221, Session PSWed

### Model predictions for the WAXS signals of healthy and malignant breast duct biopsies

Robert J. LeClair, Laurentian Univ. (Canada)

A wide-angle x-ray scatter (WAXS) measurement could potentially be used to determine whether a biopsy of a breast duct is healthy or malignant. A ductal carcinoma in situ (DCIS) occurs when the epithelial cells lining the wall start to replicate and invade the duct interior. Since cells are composed mainly of water a WAXS signal of DCIS should contain a larger component due to water. A model approximates that a breast duct biopsy consists of connective tissue (c.t.) and cells. For a 2 mm diameter 3.81 mm thick healthy duct the volumes in cubic mm are 11.56 c.t. and 0.41 cells whereas 6.64 c.t. and 5.33 cells for DCIS. A two compartment WAXS model provided predictions of the ratio of the number of 6 degree scattered photons Ns to the incident number N0. The differential linear scattering coefficients Us of c.t. and cells for scatter angle of 6 degrees were used for calculations. The Us of cells was approximated by the sum 0.714 Us[water] + 0.286 Us[c.t.]. Although the 28.6% component of the cell is not c.t. the differences found here should be a lower limit for the particular case. The ratios Ns(E)/N0(E) were higher for DCIS by mean=18.5% between 32 keV < E < 45 keV. The increase in scatter signal occurs because the Us of cells in this range are higher than that of c.t. by mean=45.4%. This work suggests that DCIS could potentially be diagnosed via energy dispersive WAXS measurements.











9033-222, Session PSWed

### X-ray coherent scatter imaging for surgical margin detection: a Monte Carlo study

Manu N. Lakshmanan, Anuj J. Kapadia, Duke Univ. Medical Ctr. (United States); Brian P Harrawood, Duke University Medical Center (United States); David J. Brady, Duke Univ. (United States); Ehsan Samei, Duke Univ. Medical Ctr. (United States)

Screening mammography of breast cancer is non-specific as fewer than 20% of women with positive mammograms ultimately prove to have cancer. Coherent scatter x-ray imaging instead directly images the molecular structure of the sample and has been shown to be strongly dependent on disturbances in the collagen structure of breast tissue that occur at the onset of cancer. Therefore, we have designed a coherent scatter x-ray imaging system in the GEANT4 Monte Carlo code for the testing of coherent scatter imaging for breast cancer detection. The development of the simulation required modifying the way that GEANT4 simulates coherent scatter physics as well as obtaining diffraction profiles for breast samples from the literature. The resulting coherent scatter diffraction images we obtain in the simulation show that the signals from healthy and malignant tissue are markedly different. We show that when the subtraction of a scatter image acquired from a healthy breast is applied to the image from a breast containing a tumor, that the malignant tissue signal can be isolated for use in confirming the presence of cancer. In addition, we demonstrate for aluminum and graphite test samples a coded aperture decomposition technique for identifying the scatter signals that come from different axial locations along the beam and that can be used as a more effective method for isolating and identifying signal from cancerous tumors in the breast. This coded aperture coherent scatter imaging system therefore can be used to form an imaging system with higher specificity for cancer detection than screening mammography.

9033-223, Session PSWed

## Limitations of anti-scatter grids when used with high resolution image detectors

Vivek Singh, Amit Jain, Daniel R. Bednarek, Stephen Rudin, Univ. at Buffalo (United States)

Anti-scatter grids are used in fluoroscopic systems to improve image quality by absorbing scattered radiation. A stationary Smit Rontgen X-ray grid (line density 70 lines/cm, grid ratio 13:1) was used with a flat panel detector (FPD) of pixel size 194 micron and a high-resolution CMOS detector, the Dexela 1207 of pixel size, 75 microns. To investigate the effectiveness of the grid, a simulated artery block was placed in a modified uniform frontal head phantom and imaged with both the FPD and the Dexela for both small and larger fields of view (FOV).

The contrast improved for both detectors with the grid but more so for the larger FOV. The contrast-to-noise ratio (CNR) increases for the FPD but degrades dramatically for the Dexela. Since the total noise in a single frame increases substantially for the Dexela compared to the FPD when the grid is used, the CNR is degraded. The increase in the quantum noise per frame was similar for both detectors for both FOVs when the grid is used due to the attenuation of radiation, but the fixed pattern noise caused by the grid was very high for the Dexela compared to the FPD and caused a drastic reduction of CNR.

Thus this grid should not be used with high-resolution fluoroscopic detectors because the CNR is decreased and the visibility of low contrast details would be reduced. An anti-scatter grid of different design would be required to deal with the problem of scatter for high resolution detectors.

9033-224, Session PSWed

## The beam stop array algorithm considering geometric effect in digital breast tomosynthesis

Haeng-hwa Lee, Ye-Seul Kim, Hye-Suk Park, Hee-Joung Kim, Yonsei Univ. (Korea, Republic of); JaeGu Choi, Young-Wook Choi, Korea Electrotechnology Research Institute (Korea, Republic of)

Scatter radiation in medical imaging influences on the image quality as decreasing image contrast and contributing to a non-uniform background. Scatter correction method for digital breast tomosynthesis (DBT) has been searched for many years which includes beam stop array (BSA) algorithm.

However, it is known that there is an effect concerning geometric characteristics due to the radiation beam path and finite thickness of disc in BSA. The BSA algorithm compensating geometric effect can obtain better primary image than conventional BSA method. The purpose of this paper was to evaluate contrast, noise and contrast-to-noise ratio (CNR) between conventional BSA algorithm and BSA algorithm compensating geometric effect. The conventional BSA algorithm was that the primary image was obtained by subtracting scatter image obtained by BSA from original image. Compensation of geometric effect by multiplying the SF proportion by scatter distribution with BSA can be performed. Compared with BSA method compensating geometric effect from the conventional BSA method, the contrast, relative noise and CNR were increased while thin phantoms such as 2 cm and 3 cm breast do not show significant high scatter intensity, thus the increase rate of CNR is not high compared to the thicker breast. The compensation of geometric effect could improve image quality by increasing contrast nearly double compared with the original image.

9033-225, Session PSWed

## Scatter reduction for high resolution image detectors with a region of interest attenuator

Amit Jain, Daniel R. Bednarek, Stephen Rudin, Toshiba Stroke and Vascular Research Ctr. (United States)

Compton scatter is the main interaction of x-rays with objects undergoing radiographic and fluoroscopic imaging procedures. Such scatter is responsible for reducing image signal to noise ratio which can negatively impact object detection especially for low contrast objects. To reduce scatter, possible methods are smaller fields-of-view, larger air gaps and the use of an anti-scatter grid. Deployment of an anti-scatter grid is not well suited for high resolution imagers due to the unavailability of high line density grids so as to prevent grid-line artifacts. Similarly, air gaps can increase geometric unsharpness hence degrading image resolution. Region of interest imaging (ROI); however, can be used not only for dose reduction but also for scatter reduction in the ROI. For ROI imaging, the ROI region receives unattenuated x-rays while the outside or peripheral region receives x-rays reduced in intensity by a ROI attenuator. The total scatter within the ROI, however, is caused by both, unattenuated ROI x-rays and attenuated outside x-rays. The effective scatter fraction in the ROI can be calculated from the primary and scatter x-ray intensity within the ROI. In this study, the scatter fraction for various kVp's, air-gaps and field sizes was measured for a uniform head equivalent phantom. The effective scatter fraction was calculated using the derived effective scatter fraction formula and validated with experimental measurements.

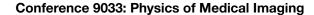
Use of a ROI attenuator is an effective way to reduce both scatter and patient dose while maintaining the superior image quality of high resolution detectors.













9033-226, Session PSWed

### Potential use of a single scatter model in breast CBCT applications

Curtis V. Laamanen, Robert J. LeClair, Laurentian Univ. (Canada)

A model based on singly scattered photons could potentially be used to correct for scatter effects in breast CBCT applications. Consider a phantom consisting of a 14 cm diameter 10.5 cm long cylindrical 50:50 mixture of fibroglandular and fat tissue with 21 cylindrical segments along its central axis. One group of segments were 2 mm in diameter with compositions 0:100, 20:80, 35:65, 50:50, 65:35, 80:20, and 100:0. The remaining two groups had diameters of 5 mm and 10 mm. The distances from the point source to phantom isocenter and to detector were respectively 58 cm and 86 cm. GEANT4 was used to acquire one projection with a 60 kV tungsten anode HVL of 3.7 mm Al beam at a dose of 6/300 = 0.02 mGy. The energy incident signals due to primary (EISp) and scatter (EISs) were computed for detector pixels along the central axis of phantom. The scatter model was used to generate a projection of EISs for a homogeneous 50:50 phantom. The latter was subtracted from the GEANT4 data to yield an estimation of EISp. The estimation was 1.017 pm 0.012 relative to the GEANT4 EISp. Refinements of the model are needed and an image analysis will provide further insight.









Sunday - Tuesday 16-18 February 2014

Part of Proceedings of SPIE Vol. 9034 Medical Imaging 2014: Image Processing



9034-1, Session 1

## An adaptive grid for graph-based segmentation in retinal OCT

Andrew Lang, Aaron Carass, Peter A. Calabresi, Howard S. Ying, Jerry L. Prince, Johns Hopkins Univ. (United States)

Graph-based methods for retinal layer segmentation have proven to be popular due to their efficiency and accuracy. These methods build a graph with nodes at each voxel location, and edges connecting the nodes encoding constraints for each layer's thickness and smoothness. In this work, we explore deforming the regular voxel grid to allow adjacent vertices in the graph to more closely follow the natural curvature of the retina. The grid is constructed by fixing nodes locations based on a regression model of each layer's thickness relative to the overall retina thickness, thus generating a subject specific grid. Graph vertices are not at voxel locations, which allows for control over the resolution that the graph represents. By incorporating soft constraints between adjacent nodes, segmentation on this grid will favor smoothly varying surfaces consistent with the shape of the retina. Therefore, in regions where the cost of segmenting a particular surface is weak, possibly due to poor signal or image artifacts, a realistically shaped surface will result. Our final segmentation method consists of two stages: first, an initial estimate of each boundary is found on a deformed coarsely-sampled grid, and second, we refine each layer to a finer scale by solving for each surface only in the local region around our previous estimate. Our method is shown to be both efficient and have improved boundary accuracy over traditional grid construction.

9034-2, Session 1

## Automated Vessel Shadow Segmentation of Fovea-centered Spectral-domain Images from Multiple OCT Devices

Jing Wu, Bianca S. Gerendas M.D., Sebastian M. Waldstein M.D., Christian Simader M.D., Ursula Schmidt-Erfurth M.D., Medizinische Univ. Wien (Austria)

Spectral-domain Optical Coherence Tomography (SD-OCT) is a non-invasive modality for acquiring high-resolution, three-dimensional (3D) cross-sectional volumetric images of the retina and the subretinal layers. SD-OCT also allows the detailed imaging of retinal pathology, aiding clinicians in the diagnosis of sight degrading diseases such as agerelated macular degeneration (AMD) and glaucoma. Disease diagnosis, assessment, and treatment will require a patient to undergo multiple OCT scans, possibly using multiple scanners, to accurately and precisely gauge disease activity, progression and treatment success. However, cross-vendor imaging and patient movement may result in poor scan spatial correlation potentially leading to incorrect diagnosis or treatment analysis. Image registration can be used to precisely compare disease states by registering differing 3D scans to one another. In order to align 3D scans from different time-points and vendors, landmarks are required, the most obvious being the retinal vasculature.

Presented here is a fully automated cross-vendor method for retinal vessel segmentation from fovea centred 3D SD-OCT scans based on vessel shadows. Noise filtered OCT scans are flattened based on vendor retinal layer segmentation, to extract the retinal pigment epithelium (RPE) layer of the retina. Voxel based layer profile analysis and k-means clustering is used to extract candidate vessel shadow regions from the RPE layer. An image processing method for vessel segmentation of the OCT constructed projection image is then applied to optimize the accuracy of OCT vessel shadow segmentation through the removal of false positive shadow regions such as those caused by exudates and cysts. Validation of segmented vessel shadows uses ground truth vessel shadow regions identified by expert graders at the Vienna Reading

Center (VRC). The results presented here are intended to show the feasibility of this method for the accurate and precise extraction of retinal vessel shadows from multiple vendor 3D SD-OCT scans for use in intravendor and cross-vendor 3D OCT registration, 2D fundus registration and actual retinal vessel segmentation.

Initial results show that for the vendor scans tested, all segmented vessel shadow regions correlate with cross-grader averaged ground truth, totaling 95% of all segmented shadows. However, 5% of total segmented regions did not correlate with ground truth, totaling 25 of 503 segmented regions. This indicates successful segmentation of the vessel shadows by a sensitivity tuned system using the method outlined here with a low tendency for over-inclusion. For or the purposes of a detection system, having all ground truth vessel shadow regions detected and verified is promising for use as landmarks for registration.

9034-4, Session 1

## Automatic nipple detection on 3D images of an automated breast ultrasound system (ABUS)

Mandana Javanshir Moghaddam, Tao Tan, Nico Karssemeijer, Bram Platel, Radboud Univ. Nijmegen Medical Ctr. (Netherlands)

Recent studies have demonstrated that applying Automated Breast Ultrasound in addition to mammography in women with dense breasts can lead to additional detection of small, early stage breast cancers which are occult in corresponding mammograms. In this paper, we proposed a fully automatic method for detecting the nipple location in 3D ultrasound breast images acquired from Automated Breast Ultrasound Systems. The nipple location is a valuable landmark to report the position of possible abnormalities in a breast or to guide image registration. To detect the nipple location, all images were normalized. Subsequently, features have been extracted in a multi scale approach and classification experiments were performed using a gentle boost classifier to identify the nipple location. The method was applied on a dataset of 100 patients with 294 different 3D ultrasound views from Siemens and U-systems acquisition systems. Our database is a representative sample of cases obtained in clinical practice by four medical centers. The automatic method could accurately locate the nipple in 90% of AP (Anterior-Posterior) views and in 79% of the other views.

9034-5, Session 1

## Cancer therapy prognosis using quantitative ultrasound spectroscopy and a kernel-based metric

Mehrdad J. Gangeh, Univ. of Toronto (Canada) and Sunnybrook Health Sciences Ctr. (Canada); Amr Hashim, Anoja Giles, Gregory J. Czarnota, Sunnybrook Health Sciences Ctr. (Canada)

In this study, a kernel-based metric based on the Hilbert-Schmidt independence criterion (HSIC) is proposed in a computer-aided-prognosis system to monitor cancer therapy effects. In order to induce tumour cell death, sarcoma xenograft tumour-bearing mice were injected with microbubbles followed by ultrasound and X-ray radiation therapy successively as a new anti-vascular treatment. High frequency (central frequency 30 MHz) ultrasound imaging was performed before and at different times after treatment and using spectroscopy, quantitative ultrasound (QUS) parametric maps were derived from the radiofrequency (RF) signals. The intensity histogram of midband fit parametric maps was computed to represent the pre- and post-treatment images. Subsequently, the HSIC-based metric between pre- and post-treatment samples were computed for each animal as a measure of distance between the two distributions. The HSIC-based metrics computes the











distance between two distributions in a reproducing kernel Hilbert space (RKHS), meaning that by using a kernel, the input vectors are non-linearly mapped into a different, possibly high dimensional feature space. Computing the population means in this new space, enhanced group separability (compared to, e.g., Euclidean distance in the original feature space) is ideally obtained. The pre- and post-treatment parametric maps for each animal were thus represented by a dissimilarity measure, in which a high value of this metric indicated more treatment effect on the animal. It was shown in this research that this metric has a high correlation with cell death and if it was used in supervised learning, a high accuracy classification was obtained using a k-nearest-neighbor (k-NN) classifier.

9034-158, Session 1

### Locally Constrained Active Contour: A Region-Based Level Set for Ovarian Cancer Metastasis Segmentation

Jianfei Liu, Duke Univ. (United States); Jianhua Yao, Shijun Wang, National Institutes of Health (United States); Marius George Linguraru, Children's National Medical Ctr. (United States); Ronald M. Summers M.D., National Institutes of Health (United States)

Accurate segmentation of ovarian cancer metastases is clinically useful to evaluate tumor growth and determine follow-up treatment. However, because of their location in the peritoneum, ovarian cancer metastases have a wider variety and complexity of shapes compared to metastases within solid organs such as the liver. To address this complexity, we present a region-based level set algorithm with localization constraints to segment ovarian cancer metastases. Our approach is modified from region-based level set, the Chan-Vese model, in which an active contour is driven by region competition. To reduce over-segmentation, we constrain the level set propagation within a narrow image band by embedding a dynamic localization function. The metastasis intensity prior knowledge is also estimated from image regions within the level set initialization. The localization function and intensity prior force the level set to stop at the desired metastasis boundaries. Our approach was validated on 19 ovarian cancer metastases with radiologistlabeled ground-truth on contrast-enhanced CT scans from 15 patients. The comparison between our algorithm and geodesic active contour indicated that the volume overlap was 75±10% vs. 56±6%, the Dice coefficient was 83±8% vs. 63±8%, and the average surface distance was 2.2±0.6mm vs. 4.4±0.9mm. Experimental results demonstrated that our algorithm outperformed traditional level set algorithms.

9034-6, Session 2

## Multiscale feature learning on pixels and super-pixels for seminal vesicles MRI segmentation

Qinquan Gao, Akshay Asthana, Tong Tong, Daniel Rueckert, Philip Edwards, Imperial College London (United Kingdom)

We propose a nearly automatic learning-based approach to segment the seminal vesicles (SV) via random forest classifiers. The proposed discriminative approach relies on the decision forest using high-dimensional multi-scale context-aware spatial, textual and descriptor-based features at both pixel and super-pixel levels. After affine transformation to a template space, the relevant high-dimensional multi-scale features are extracted and random forest classifiers are learned based on the masked region of the seminal vesicles from the most similar atlases. Using these classifiers, an intermediate probabilistic segmentation is obtained for the test images. Then, a graph-cut based refinement is applied to this intermediate probabilistic representation of each voxel to get the final segmentation. We apply this approach to

segment the seminal vesicles from 15 1.5T and 15 3T MRI T2 training images of the prostate, which presents a particularly challenging segmentation task. The results show that the multi-scale approach and the augmentation of the pixel based features with super-pixel based features enhances the discriminative power of the learnt classifier which leads to a better quality segmentation in some very difficult cases. The results are compared to the radiologist labeled ground truth using leave-one-out cross-validation. An average Dice metric of 0.7249 and Hausdorff surface distance of 7.0803 mm are achieved, which is a good result for this difficult task and demonstrates improvement compared to single scale features

9034-7, Session 2

### Failure analysis for model-based organ segmentation using outlier detection

Axel Saalbach, Irina Waechter-Stehle, Philips Technologie GmbH (Germany); Cristian Lorenz, Philips Technologie GmbH, Innovative Technologies, Research Laboratories (Germany); Jürgen Weese, Philips Technologie GmbH (Germany)

During the last years Model-Based Segmentation (MBS) techniques have been used in a broad range of medical applications. In clinical practice, such techniques are increasingly employed for diagnostic purposes and treatment decisions. However, it is not guaranteed that a segmentation algorithm will converge towards the desired solution. In specific situations as in the presence of rare anatomical variants (which cannot be represented) or for images with an extremely low quality, a meaningful segmentation might not be feasible. At the same time, an automated estimation of the segmentation reliability is commonly not available. In this paper we present an approach for the identification of segmentation failures using concepts from the field of outlier detection. The approach is validated on a comprehensive set of Computed Tomography Angiography (CTA) images by means of Receiver Operating Characteristic (ROC) analysis. Encouraging results in terms of an Area Under the ROC Curve (AUC) of up to 0.959 were achieved.

9034-8, Session 2

#### Brain abnormality segmentation based on L1norm minimization

Ke Zeng, Guray Erus, Manoj Tanwar, Christos A. Davatzikos, Univ. of Pennsylvania (United States)

We present a method that uses sparse representations to model the inter-individual variability of healthy anatomy from a limited number of normal medical images. Abnormalities in MR images are then defined as deviations from the normal variation. More precisely, we model an abnormal (pathological) signal as the superposition of a normal part that has a sparse representation under an example-based dictionary, and an abnormal part. Motivated by a dense error correction scheme recently proposed for sparse signal recovery, we use L1-norm minimization to separate the normal and abnormal parts of the signal. We extend the existing framework, which was mainly used on robust face recognition in a discriminative setting, to address challenges of brain image analysis, particularly the high dimensionality and low sample size problem. The dictionary is constructed from local image patches extracted from training images aligned using smooth transformations, together with minor perturbations of those patches. A multi-scale sliding-window scheme is applied to capture anatomical variations ranging from fine and localized to coarser and more global. The statistical significance of the abnormal part is obtained by comparison to its empirical distribution through cross-validation, and is used to assign an abnormality score to each voxel. In our validation experiments the method is applied for segmenting abnormalities on 2-D slices of FLAIR images, and we obtain segmentation results consistent with the expert-defined masks.











9034-9, Session 2

## Towards a comprehensive CT image segmentation for thoracic organ radiation dose estimation and reporting

Cristian Lorenz, Heike Ruppertshofen, Torbjörn Vik, Philips Research (Germany); Peter Prinsen, Jens Wiegert, Philips Research (Netherlands)

Administered dose of ionizing radiation during medical imaging is an issue of increasing concern for the patient, for the clinical community, and for respective regulatory bodies. CT radiation dose is currently estimated based on a set of very simplifying assumptions which do not take the actual body geometry and organ specific doses into account. This makes it very difficult to accurately report imaging related administered dose and to track it for different organs over the life of the patient. In this paper this deficit is addressed in a two-fold way. In a first step, the absorbed radiation dose in each image voxel is estimated based on a Monte-Carlo simulation of X-ray absorption and scattering. In a second step, the image is segmented into tissue types with different radio sensitivity. In combination this allows to calculate the effective dose as a weighted sum of the individual organ doses. The main purpose of this paper is to assess the feasibility of automatic organ specific dose estimation. With respect to a commercially applicable solution and respective robustness and efficiency requirements, we investigated the effect of dose sampling rather than integration over the organ volume. We focused on the thoracic anatomy as the exemplary body region, imaged frequently by CT. For image seg-mentation we applied a set of available approaches which allowed us to cover the main thoracic radio-sensitive tissue types. We applied the dose estimation approach to 10 thoracic CT datasets and evaluated segmentation accuracy and administered dose and could show that organ specific dose estimation can be achieved.

9034-10, Session 2

### Neuromuscular fiber segmentation through particle filtering and discrete optimization

Thomas Dietenbeck, Univ. de Lyon (France) and Czech Technical Univ. in Prague (Czech Republic); François Varray, Univ. de Lyon (France); Jan Kybic, Czech Technical Univ. in Prague (Czech Republic); Olivier Basset, Univ. de Lyon (France); Christian Cachard, Univ. Claude Bernard Lyon 1 (France)

We present an algorithm to segment a set of parallel, intertwined and bifurcating fibers from 3D images, targeted for the identification of neuronal fibers in very large sets of 3D confocal microscopy images. The method consists of preprocessing, local calculation of fiber probabilities, seed detection, tracking by particle filtering, global supervised seed clustering and final voxel segmentation. The preprocessing uses a novel random local probability filtering (RLPF). The fiber probabilities computation is performed using SVM using steerable filters and the RLPF outputs as features. The global segmentation is solved by discrete optimization. The combination of global and local approaches makes the segmentation robust, yet the individual data blocks can be processed sequentially, limiting memory consumption. The method is automatic but efficient manual interactions are possible if needed. The method is validated on the Neuromuscular Projection Fibers dataset from the Diadem Challenge. On the 15 first blocks present, our method has a 99.4% detection rate. We also compare our segmentation results to a state-of-the-art method. On average, the performances of our method are either higher or equivalent to that of the state-of-the-art method but less user interactions is needed in our approach.

9034-11, Session 2

#### Prostate segmentation in MRI using fused T2weighted and elastography images

Guy Nir, Ramin S. Sahebjavaher, The Univ. of British Columbia (Canada); Ali Baghani, Ultrasonix Medical Corp. (Canada); Ralph Sinkus, King's College London (United Kingdom); Septimiu E. Salcudean, The Univ. of British Columbia (Canada)

Segmentation of the prostate in medical imaging is a challenging and important task for surgical planning and delivery of prostate cancer treatment. Automatic prostate segmentation can improve speed, reproducibility and consistency of the process. In this work, we propose a method for automatic segmentation of the prostate in magnetic resonance elastography (MRE) images. The method utilizes the complementary property of the elastogram and the corresponding T2-weighted image, which are obtained from the phase and magnitude components of the imaging readout signal, respectively. It follows a variational approach to propagate an active contour model based on the combination of region statistics in the elastogram and the edge map of the T2-weighted image. The method is fast and does not require prior shape information. The proposed algorithm is tested on 35 clinical image pairs from five MRE data sets, and is evaluated in comparison with manual contouring. The mean absolute distance between the automatic and manual contours is 1.8mm, with a maximum distance of 5.6mm. The relative area error is 7.6%, and the duration of the segmentation process is 2s per slice.

9034-12, Session 3

### Characterizing growth patterns in longitudinal MRI using image contrast

Avantika Vardhan, Marcel Prastawa, Clement Vachet, The Univ. of Utah (United States); Joseph Piven, Department of Psychiatry, University of North Carolina (United States); Guido Gerig, The Univ. of Utah (United States)

It is crucial to understand the growth patterns of the early brain, in order to study both normal and abnormal neural development. Biophysical and chemical processes such as myelination take place during early brain development, manifesting as changes in the appearance of structural MR (Magnetic Resonance) images. As the brain undergoes maturation, there is a subsequent increase in the contrast between gray matter and white matter as observed in structural MRI. In this work, gray-white matter contrast is proposed as an effective measure of appearance which is relatively invariant to location, scanner type, and conditions of scan. To validate this, contrast is computed over various cortical regions for repeated MRI of a human adult phantom, scanned using different scanners, locations, and at different times. It is shown that contrast shows less variability compared to intensity-based measures, demonstrating that it is less dependent on external factors and scanning conditions. In addition, longitudinal MR scans of the early brain, belonging to healthy controls and Down's Syndrome (DS) patients, were analyzed using the contrast measure. The Gompertz function was used to model subject-specific trajectories of contrast changing with time, and distinct trajectories were observed for the two populations. Statistical parameters were extracted from the contrast modeling and showed large differences between groups. The preliminary applications of contrast based analysis indicates its future potential to reveal new information not covered by conventional volumetric or deformation-based analysis, particularly for distinguishing between normal and abnormal growth patterns.











9034-13, Session 3

### Registration of organs with sliding interfaces and changing topologies

Floris F. Berendsen, Alexis N. T. J. Kotte, Max A. Viergever, Josien P. W. Pluim, Univ. Medical Ctr. Utrecht (Netherlands)

Smoothness and continuity assumptions on the deformation field in deformable image registration do not hold for applications where the imaged objects have sliding interfaces.

Recent extensions to deformable image registration that accommodate for sliding motion of organs are limited to sliding motion along approximately planar surfaces or cannot model sliding that changes the topological configuration in case of multiple organs.

We propose a new extension to free-form image registration that is not limited in this way.

Our method uses a transformation model that consists of uniform B-spline transformations for each organ region separately, which is based on the segmentation in one image.

Since this model can create overlapping regions or gaps between regions, we introduce a penalty term that minimizes this undesired effect.

The penalty term acts on the surfaces of the organ regions and is simultaneously optimized with the image similarity.

To evaluate our method registrations were performed on publicly available inhale-exhale CT scans on which other authors have reported performances also.

Target registration errors are computed by using dense landmark sets that are available with these datasets.

On these data our method outperforms the other methods as concerns target registration error and outperforms the other B-spline based methods in terms of overlap and gap volumes.

A second evaluation of our method was done on synthetic images of which the resulting deformation field shows good properties for sliding along curved boundaries and for changing region topology configurations.

9034-14, Session 3

## Elastic registration of prostate MR images based on state estimation of dynamical systems

Bahram Marami, Robarts Research Institute (Canada) and McMaster Univ. (Canada); Suha Ghoul, Robarts Research Institute (Canada); Shahin Sirouspour, McMaster Univ. (Canada); David W. Capson, Univ. of Victoria (Canada); Sean R. H. Davidson, John Trachtenberg M.D., Ontario Cancer Institute (Canada); Aaron Fenster, Robarts Research Institute (Canada) and Univ. of Western Ontariou (Canada)

Magnetic resonance imaging (MRI) is being used for image-guided biopsy and focal therapy of prostate cancer. A combined rigid and deformable registration technique is proposed to register pre-operative diagnostic 3T MR images, with the identified target tumor(s), to the intra-operative 1.5T MR images. The pre-operative 3T images are acquired with patients in strictly supine position using an endorectal coil, while 1.5T images are obtained intra-operatively just before insertion of the ablation needle with patients in the lithotomy position. The intensity-based optimization routine for estimating the rigid transformation parameters is initialized using three manually selected corresponding points in both images, which is followed by a deformable registration algorithm employing a generic dynamic linear elastic deformation model discretized by the finite element method (FEM). The model is used in a classical state estimation framework to estimate the deformation of the prostate based on a similarity metric between pre- and intra-operative

images. Registration results using 10 sets of prostate MR images showed that the proposed method can significantly improve registration accuracy in terms of target registration error (TRE) for all prostate substructures. The root mean square (RMS) TRE of 46 manually identified fiducial points was found to be 2.48±1.31, 2.59±1.40, and 2.37±1.24 mm for the whole gland (WG), central gland (CG), and peripheral zone (PZ), respectively after deformable registration. Registration results are also evaluated based on the Dice similarity coefficient (DSC), mean absolute surface distances (MAD) and maximum absolute surface distances (MAXD) of the WG and CG in the prostate images.

9034-15, Session 3

### A hybrid biomechanical model-based image registration method for sliding objects

Lianghao Han, David J. Hawkes, Dean C. Barratt, Univ. College London (United Kingdom)

The sliding motion between two anatomic structures, such as lung against the chest wall, liver against surrounding tissues, produces a discontinuous displacement field between their boundaries. Capturing the sliding motion is quite challenging for intensity-based image registration methods in which a smoothness condition has commonly been applied to neighborhood voxels to ensure their deformation consistency. Such smoothness constraints contradict motion physiology at the boundaries of these anatomic structures. Although various regularization schemes have been developed to handle sliding motion under the framework of non-rigid intensity-based image registration, the recovered displacement field may still not be physically plausible. In this study, a new framework that incorporates a patient-specific biomechanical model with a non-rigid image registration scheme for motion estimation of sliding objects has been developed. The patient-specific model provides motion estimation with an explicit simulation of sliding motion, while the subsequent non-rigid image registration compensates for smaller residual of the deformation due to the inaccuracy of the physical model. The algorithm was tested against the results from the published literature using 4D CT data from 10 lung cancer patients. The target registration error (TRE) of 3000 landmarks with the proposed method (1.37±0.84 mm) was significantly lower than that with the popular B-spline based free form deformation (FFD) registration (4.55±4.0mm), and was comparable to the B-spline based FFD registration with the sliding constraint (1.71±1.14mm). The propose method also achieved the best registration performance on the landmarks near the lung surface. Since biomechanical models captured most of the lung deformation, the final estimated deformation field was more physically plausible.

9034-16, Session 3

## Real-time intensity based 2D/3D registration using kV-MV image pairs for tumor motion tracking in image guided radiotherapy

Hugo D. Furtado, Elisabeth Steiner, Markus Stock, Dietmar Georg, Wolfgang Birkfellner, Medizinische Univ. Wien (Austria)

Intra-fractional respiratory motion during radiotherapy is one of the main sources of uncertainty in dose application creating the need to extend the margins of the planning target volume (PTV). Real-time tumor motion tracking by 2D/3D registration using on-board kilo-voltage (kV) imaging can lead to a reduction of the PTV. One limitation of this technique when using one projection image, is the inability to resolve motion along the imaging beam axis. We present a retrospective patient study to investigate the impact of paired portal mega-voltage (MV) and kV images, on registration accuracy.

We used data from twelve patients suffering from non small cell lung cancer undergoing regular treatment at our center. For each patient we acquired a planning CT and sequences of kV and MV images during











treatment. Our evaluation consisted of comparing the accuracy of motion tracking in 6 degrees-of-freedom (DOF) using the anterior-posterior (AP) kV sequence or the sequence of kV-MV image pairs. We use graphics processing unit rendering for real-time performance.

Motion along cranial-caudal direction could accurately be extracted when using only the kV sequence but in AP direction we obtained large errors. When using kV-MV pairs, the average error was reduced from 4.1 mm to 2.1 mm and the motion along AP was successfully extracted. The mean registration time was of 186±36 ms. Our evaluation shows that using kV-MV image pairs leads to improved motion extraction in 6 DOF. Therefore, this approach is suitable for accurate, real-time tumor motion tracking with a conventional LINAC.

9034-17, Session 4

## Active-atlas-based segmentation for automated epicardial fat volume quantification from non-contrast CT

Xiaowei Ding, Univ. of California, Los Angeles (United States) and Cedars-Sinai Medical Ctr. (United States); Demetri Terzopoulos, Univ. of California, Los Angeles (United States); Mariana Diaz-Zamudio, Cedars Sinai Medical Ctr. (United States); Daniel S. Berman, Piotr J. Slomka, Damini Dey, Cedars-Sinai Medical Ctr. (United States) and Univ. of California, Los Angeles (United States)

Epicardial fat volume (EFV) is now regarded as a significant imaging biomarker for cardiovascular risk stratification. Manual or semi-automated quantification of EFV includes tedious and careful contour drawing of pericardium on fine image features. We aimed to develop and validate a fully-automated, accurate algorithm for EVF quantification from non-contrast CT using active atlas.

Active atlas is a knowledge-based model that can segment both the heart and pericardium accurately by initializing the location and shape of the heart in large scale from multiple co-registered atlases and locking itself onto the pericardium actively. The deformation process is driven by pericardium detection, extracting only the white contours representing the pericardium in the CT images. Following this step, we can calculate fat volume within this region (epicardial fat) using preset fat attenuation thresholds.

Epicardial fat volume quantified by the algorithm (69.15  $\pm$  8.25 cm3) and the expert (69.46  $\pm$  8.80 cm3) showed excellent correlation (r = 0.96, p < 0.0001) with no significant differences by comparison of individual data points (p = 0.9). The algorithm achieved a dice overlap of 0.93 (range 0.88 – 0.95). The total time was <60 sec on a standard windows computer. Our results show that fast accurate automated knowledge-based quantification of epicardial fat volume from non-contrast CT is feasible. To our knowledge, this is also the first fully automated algorithms reported for this task.

9034-18, Session 4

### Blood flow quantification using optical flow methods in a body fitted coordinate system

Peter Maday, Richard Brosig, Technische Univ. München (Germany); Juergen Endres, Friedrich-Alexander-Univ. Erlangen-Nürnberg (Germany); Markus Kowarschik, Siemens AG (Germany); Nassir Navab, Technische Univ. München (Germany)

In this paper a blood flow quantification method that is based on a physically motivated 2D flow estimation algorithm is outlined. It yields accurate time varying volumetric flow rate measurements based on digital subtraction angiography (DSA) image sequences, with robustness to significant inter-frame displacements. Based on the 2D flow fields

and a 3D vessel segmentation the time varying volumetric flow rate is estimated. The novelty of the approach lies in the use of a vessel aligned coordinate system for problem formulation. The coordinate functions are generated using the Schwarz-Christoffelcite{driscoll2002schwarz} (SC) map that yields a solution with coordinate lines aligned with the flow streamlines. The solution of the finite difference problem only requires slight modifications compared to the regular grid case. The use of vessel aligned coordinates enables the easy and accurate handling of boundary conditions in the irregular domain of a vessel lumen. Unlike traditional coarse to fine approaches we use an anisotropic scaling strategy in the vessel aligned coordinates that enables the estimation of flows with larger inter frame displacements. The evaluation of our method is based on highly relistic synthetic datasets for a number of cases. Performance measures are obtained with varying flow velocities and acquisition rates.

9034-19, Session 4

### 3D geometric analysis of the aorta in 3D MRA follow-up pediatric image data

Stefan Wörz, Abdulsattar Alrajab, Raoul Arnold, Joachim Eichhorn, Ruprecht-Karls-Univ. Heidelberg (Germany); Hendrik von Tengg-Kobligk, Univ. Bern (Switzerland); Jens-Peter Schenk, Karl Rohr, Ruprecht-Karls-Univ. Heidelberg (Germany)

We introduce a new model-based approach for the segmentation of the thoracic aorta and its main branches from follow-up pediatric 3D MRA image data. For robust segmentation of vessels even in difficult cases (e.g., neighboring structures), we propose a new extended parametric cylinder model which requires only relatively few parameters. The new model is used in conjunction with a two-step fitting scheme for refining the segmentation result yielding an accurate segmentation of the vascular shape. Moreover, we include a novel adaptive background masking scheme used for least-squares model fitting and we describe a spatial normalization scheme to align the segmentation results from follow-up examinations. We have evaluated our proposed approach using different 3D synthetic images and we have successfully applied the approach to follow-up pediatric 3D MRA image data.

9034-20, Session 4

#### Tensor-based tracking of the aorta in phasecontrast MR images

Yoo-Jin Jeong, Anton Malsam, Karlsruher Institut für Technologie (Germany); Sebastian Ley, UniversitätsKlinikum Heidelberg (Germany); Fabian Rengier, Univ. Hospital Heidelberg (Germany) and Deutsches Krebsforschungszentrum (Germany); Rüdiger Dillmann, Roland Unterhinninghofen, Karlsruher Institut für Technologie (Germany)

The velocity-encoded magnetic resonance imaging (PC-MRI) is a valuable technique to measure the blood flow velocity in terms of time-resolved 3D vector fields. For diagnosis, presurgical planning and therapy control of a patient with a cardiovascular disease the monitoring of his hemodynamical situation is crucial. Hence, an accurate and robust segmentation of the vessel of interest is the basis for further methods like the computation of the blood pressure. In the literature there exist some approaches to transfer the methods of processing DT-MR images to PC-MR data, but the potential of this approach is not fully exploited yet. In this paper, we present a method to extract the centerline of the aorta in PC-MR images by applying methods from the DT-MRI. On account of this, the velocity vector fields have to be converted into tensor fields first. In the next step tensor-based features can be derived and by applying a modified tensorline algorithm, the tracking of the vessel course can be accomplished. The method only uses features derived from the tensor imaging without the use of additional morphology information. For evaluation purposes we applied our method to 4 volunteer as well as











26 clinical patient datasets with promising results. In 29 of 30 cases our algorithm accomplished to extract the vessel centerline.

9034-21, Session 4

#### Joint multi-object registration and segmentation of left and right cardiac ventricles in 4D cine MRI

Jan Ehrhardt, Timo Kepp, Univ. zu Lübeck (Germany); Alexander Schmidt-Richberg, Imperial College London (United Kingdom); Heinz Handels, Univ. zu Lübeck (Germany)

The diagnosis of cardiac function based on cine MRI requires the segmentation of cardiac structures in the images, but the problem of automatic cardiac segmentation is still open, due to the imaging characteristics of cardiac MR images and the anatomical variability of the heart.

A simultaneous segmentation of multiple objects has several advantages compared to single object segmentation, because imaging properties of different objects can be modeled and concurrently influence the segmentation process. On the other hand, registration-based segmentation methods preserve topological relations between objects, e.g. that LV and RV blood pools are separated by the myocardium. In this contribution, we present a variational framework for joint segmentation and registration of multiple structures of the heart. To enable the simultaneous segmentation and registration of multiple objects, a shape prior term is introduced into a region competition approach for multi-object level set segmentation. The coupled segmentation and registration was embedded in an image processing pipeline for automatic cardiac segmentation and applied for simultaneous segmentation of myocardium as well as left and right ventricular blood pool in short axis cine MRI images. Two experiments are performed: first, intra-patient 4D segmentation with a given initial segmentation for one time-point in a 4D sequence, and second, atlas-based segmentation of unseen patient data. Evaluation of segmentation accuracy is done by overlap coefficients and surface distances. First results are presented and advantages and limitations of the approach are discussed.

9034-22, Session 4

## Nonrigid motion compensation in B-mode and contrast enhanced ultrasound image sequences of the carotid artery

Diego D. B. Carvalho, Zeynettin Akkus, Johan G. Bosch, Stijn C. H. van den Oord, Erasmus MC (Netherlands); Wiro J. Niessen, Erasmus MC (Netherlands) and Technische Univ. Delft (Netherlands); Stefan Klein, Erasmus MC (Netherlands)

In this work, we investigate nonrigid motion compensation in simultaneously acquired (side-by-side) B-mode ultrasound (BMUS) and contrast enhanced ultrasound (CEUS) image sequences of the carotid artery. These images are acquired to study the presence of intraplaque neovascularization (IPN), which is a marker of plaque vulnerability. IPN quantification is visualized by performing the maximum intensity projection (MIP) on the CEUS image sequence over time. As carotid images contain considerable motion, accurate global nonrigid motion compensation (GNMC) is required prior to the MIP. Moreover, we demonstrate that an improved lumen and plaque differentiation can be obtained by averaging the motion compensated BMUS images over time. We propose to use a previously published 2D+t nonrigid registration method, which is based on minimization of pixel intensity variance over time, using a spatially and temporally smooth B-spline deformation model. The validation compares displacements of plaque points with manual trackings by 3 experts in 11 carotids. The average (±standard deviation) root mean square error (RMSE) was 99±74 μm for longitudinal and 47±18 µm for radial displacements. These results

were comparable with the interobserver variability, and with results of a local rigid registration technique based on speckle tracking, which estimates motion in a single point, whereas our approach applies motion compensation to the entire image. In conclusion, we evaluated that the GNMC technique produces reliable results. Since this technique tracks global deformations, it can aid in the quantification of IPN and the delineation of lumen and plaque contours.

9034-23, Session 5

## Influence of image registration on ADC images computed from free-breathing diffusion MRIs of the abdomen

Jean-Marie Guyader, Erasmus MC (Netherlands); Livia Bernardin, Naomi H. M. Douglas, The Institute of Cancer Research (United Kingdom) and Royal Marsden Hospital (United Kingdom); Dirk H. J. Poot, Erasmus MC (Netherlands); Wiro J. Niessen, Erasmus MC (Netherlands) and Technische Univ. Delft (Netherlands); Stefan Klein, Erasmus MC (Netherlands)

The apparent diffusion coefficient (ADC) is an imaging biomarker providing quantitative information on the diffusion of water in biological tissues. This measurement could be of relevance in oncology drug development, but it suffers from a lack of reliability. ADC images are computed by applying a voxelwise exponential fitting to multiple diffusion-weighted MR images (DW-MRIs) acquired with different diffusion gradients. In the abdomen, respiratory motion induces misalignments in the datasets, creating visible artefacts and inducing errors in the ADC maps. We propose a multistep post-acquisition motion compensation pipeline based on 3D non-rigid registrations. It corrects for motion within each image and brings all DW-MRIs to a common image space. The method is evaluated on 10 datasets of free-breathing abdominal DW-MRIs acquired from healthy volunteers. Regions of interest (ROIs) are segmented in the right part of the abdomen and measurements are compared in the three following cases: no image processing, Gaussian blurring of the raw DW-MRIs and registration. Results show that both blurring and registration improve the visual quality of ADC images, but compared to blurring, registration yields visually sharper images. Measurement uncertainty is reduced both by registration and blurring. For homogeneous ROIs, blurring and registration result in similar median ADCs, which are lower than without processing. In a ROI at the interface between liver and kidney, registration and blurring yield different median ADCs, suggesting that uncorrected motion introduces a bias. Our work indicates that averaging procedures on the scanner should be avoided, as they remove the opportunity to perform motion correction.

9034-24, Session 5

## A new method for joint susceptibility artefact correction and super-resolution for dMRI

Lars Ruthotto, The Univ. of British Columbia (Canada); Siawoosh Mohammadi, Nikolaus Weiskopf, Wellcome Trust Ctr. for Neuroimaging (United Kingdom)

Diffusion magnetic resonance imaging (dMRI) has become increasingly relevant in clinical research and neuroscience. It is commonly carried out using the ultra-fast MRI acquisition technique Echo-Planar Imaging (EPI). While offering crucial reduction of acquisition times, two limitations of EPI are distortions due to varying magnetic susceptibilities of the object being imaged and its limited spatial resolution. In the recent years progress has been made both for susceptibility artefact correction and increasing of spatial resolution using image processing and reconstruction methods. However, so far, the interplay between both problems has not been studied and super-resolution techniques could only be applied along one axis, the slice-select direction, limiting the potential gain in spatial resolution.











In this work we describe a new method for joint susceptibility artefact correction and super-resolution in EPI-MRI that can be used to increase resolution in all three spatial dimensions and in particular increase in-plane resolutions. The key idea is to reconstruct a distortion-free, high-resolution image from a number of low-resolution EPI data that are deformed in different directions. Numerical results on dMRI data of a human brain indicate that this technique has the potential to provide for the first time in-vivo dMRI at mesoscopic spatial resolution (i.e. 500~micron); a spatial resolution that could bridge the gap between white-matter information from ex-vivo histology (about 1 micron) and in-vivo dMRI (about 2000 micron).

9034-25, Session 5

### A dual spherical model for multi-shell diffusion imaging

Yogesh Rathi, Harvard Medical School (United States); Oleg V. Michailovich, Univ. of Waterloo (Canada); Kawin Setsompop, Carl-Fredrik Westin, Harvard Medical School (United States)

Multi-shell diffusion imaging (MSDI) allows to characterize the subtle tissue properties of neurons along with providing valuable information about the ensemble average diffusion propagator. Several methods, both parametric and non-parametric, have been proposed to analyze MSDI data. In this work, we propose a hybrid model, which is non-parametric in the angular domain but parametric in the radial domain. This has the advantage of allowing arbitrary number of fiber orientations in the angular domain, yet requiring as little as two b-value shells in the radial (q-space) domain. Thus, an extensive sampling of the q-space is not required to compute the diffusion propagator.

This model, which we term as the "dual-spherical" model, requires estimation of two functions on the sphere to completely (and continuously) model the entire q-space diffusion signal. Specifically, we formulate the cost function so that the diffusion signal is guaranteed to monotonically decrease with b-value for user-defined range of b-values. This is in contrast to other methods, which do not enforce such a constraint, resulting in in-accurate modeling of the diffusion signal (where the signal values could potentially increase with b-value). We also show the relation of our proposed method with that of diffusional kurtosis imaging and how our model extends the kurtosis model.

We use the standard spherical harmonics to estimate these functions on the sphere and show its efficacy using synthetic and in-vivo experiments. In particular, on synthetic data, we computed the normalized mean squared error and the average angular error in the estimated orientation distribution function (ODF) and show that the proposed technique works better than the existing work which only uses a parametric model for estimating the radial decay of the diffusion signal with b-value.

9034-26, Session 5

## Multi-modal pharmacokinetic modeling for DCE-MRI: using diffusion weighted imaging to constrain the local arterial input function

Valentin Hamy, Univ. College London (United Kingdom); Marc Modat, Univ College London (United Kingdom); Rebecca Shipley, Nikos Dikaios, Jon O. Cleary, David J. Hawkes, Shonit Punwani, Sebastien Ourselin, David Atkinson, Andrew Melbourne, Univ. College London (United Kingdom)

The routine acquisition of multi-modal magnetic resonance imaging data in oncology yields the possibility of combined model fitting of traditionally separate models of tissue structure and function. In this work we hypothesise that diffusion weighted imaging data may help constrain the fitting of pharmacokinetic models to dynamic contrast enhanced (DCE) MRI data. Parameters related to tissue perfusion in the intra-voxel

incoherent motion (IVIM) modelling of diffusion weighted MRI provide local information on how tissue is likely to perfuse that can be utilised to guide DCE modelling via local modification of the arterial input function (AIF). In this study we investigate, based on multi-parametric head and neck MRI of 8 subjects (4 with head and neck tumours), the benefit of incorporating parameters derived from the IVIM model within the DCE modelling procedure. Although we find the benefit of this procedure to be marginal on the data used in this work, it is conceivable that a technique of this type will be of greater use in a different application.

9034-27, Session 5

# Intramyocellular lipid dependence on skeletal muscle fiber type and orientation characterized by diffusion tensor imaging and <sup>1</sup>H-MRS

Sunil Kumar Valaparla, Feng Gao, Muhammad Abdul-Ghani, Geoffrey D. Clarke, The Univ. of Texas Health Science Ctr. at San Antonio (United States)

When muscle fibers are aligned with the B0 field, intramyocellular lipids (IMCL), important for providing energy during physical activity, can be resolved in proton magnetic resonance spectra (1H-MRS). This study determined the influence of muscle fiber type and orientation on IMCL using 1H-MRS and diffusion tensor imaging (DTI). Muscle fiber orientation relative to B0 was estimated by pennation angle (PA) measurements from DTI, providing orientation-specific extramyocellular lipid (EMCL) chemical shift that were used for subject-specific IMCL quantification. Vastus Lateralis (VL), Tibialis Anterior (TA) and Soleus (SO) muscles of 6 healthy subjects were studied on a Siemens 3T MRI/MRS system. Single voxel 1H-MRS were acquired using STEAM (TR=3s, TE=270ms) and DTI was performed using EPI (b=600s/mm2, 30 directions) with center slice indexed to MRS voxel center. PA measured from ROI analysis of primary eigenvectors were PA=19.46±5.43 for unipennate VL, 15.65±3.73 for multipennate SO, and 7.04±3.34 for bipennate TA. Chemical shift (CS) was calculated using [3cos2θ-1] dependence: 0.17±0.02 for VL, 0.18±0.01 for SO and 0.19±0.004 ppm for TA. IMCL-CH2 concentrations from spectral analysis were 12.77±6.3 for VL, 3.07±1.63 for SO and 0.27±0.08 mmol/kg ww for TA. ANOVA analysis produced statistical significance deemed at p<0.05. Small PA's were measured in TA and large CS with clear separation between EMCL and IMCL peaks were observed. Larger variations in PA were measured VL and SO resulting in increased overlap of EMCL on IMCL peaks. These results suggest that DTI incorporated 1H-MRS studies on muscle lipids taking fiber orientation into account produce significant quantitative estimation.

9034-28, Session 6

### A statistical Shape+Pose model for segmentation of wrist CT images

Emran Mohammad Abu Anas, Abtin Rasoulian, The Univ. of British Columbia (Canada); Paul S. John, David R. Pichora, Kingston General Hospital (Canada); Robert N. Rohling, Purang Abolmaesumi, The Univ. of British Columbia (Canada)

In recent years, there has been significant interest to develop a model of the wrist joint that can capture the statistics of shape and pose variations in a patient population. Such model could have several clinical applications such as bone segmentation, kinematic analysis and prosthesis development. In this paper, we present a novel statistical model of the wrist joint based on the analysis of shape and pose variations in carpal bones of a group of subjects. The carpal bones are jointly aligned using a group-wise Gaussian Mixture Model registration technique, where principal component analysis is used to determine the mean shape and the main modes of its variations. The pose statistics are determined by using principal geodesics analysis, where statistics











of similarity transformations between individual subjects and the mean shape are computed in a linear tangent space. We also demonstrate an application of the model for segmentation of wrist CT images and the segmentation results demonstrate the efficacy of the proposed model in its application.

9034-30, Session 6

### A framework for joint image-and-shape analysis

Yi Gao, Allen Tannenbaum, The Univ. of Alabama at Birmingham (United States); Sylvain Bouix, Harvard Medical School (United States)

Techniques in medical image analysis are many times used for the comparison or regression on the intensities of images. In general, the domain of the image is a given Cartesian grids. Shape analysis, on the other hand, studies the similarities and differences among spatial objects of arbitrary geometry and topology. Usually, there is no function defined on the domain of shapes. Recently, there has been a growing needs for defining and analyzing functions defined on the shape space, and a coupled analysis on both the shapes and the functions defined on them. Following this direction, in this work we present a coupled analysis for both images and shapes. As a result, the statistically significant discrepancies in both the image intensities as well as on the underlying shapes are detected. The method is applied on both brain images for the schizophrenia and heart images for atrial fibrillation patients.

9034-31, Session 6

#### Groupwise shape analysis of the hippocampus using spectral matching

Mahsa Shakeri, Ecole Polytechnique de Montréal (Canada); Hervé J. Lombaert, McGill Univ. (Canada); Sarah Lippe, Univ. de Montréal (Canada) and CHU Sainte-Justine (Canada); Samuel Kadoury, Ecole Polytechnique de Montréal (Canada) and CHU Sainte-Justine (Canada)

The hippocampus is a prominent subcortical feature of interest in many neuroscience studies. Its subtle morphological changes often predicate illnesses, including Alzheimer's, schizophrenia or epilepsy. The precise location of structural differences necessitates a reliable correspondence map across a population. In this paper, we propose an automated method for groupwise hippocampal shape analysis in which a spectral matching approach is applied to solve the correspondence problem between shape meshes. The framework generates diffeomorphic correspondence maps across a population, which enables us to create a mean shape. Morphological changes are then located between two groups of subjects. The performance of the proposed method was evaluated on a dataset of 42 hippocampus shapes and compared with a state-of-the-art structural shape analysis approach, using spherical harmonics. Difference maps between mean shapes of two test groups demonstrated that the two approaches showed similar results, while Gaussian curvature measures calculated between matched vertices showed a better fit and reduced variability with spectral matching. However, spherical harmonics based methods may require several hours to find shape differences, while the proposed method provides the same results in only a few seconds.

9034-32, Session 6

## 3D shape analysis of heterochromatin foci based on a 3D spherical harmonics intensity model

Simon Eck, Stefan Wörz, Ruprecht-Karls-Univ. Heidelberg (Germany) and Deutsches Krebsforschungszentrum (Germany); Katharina Müller-Ott, Ruprecht-Karls-Univ. Heidelberg (Germany); Matthias Hahn, Gunnar Schotta, Ludwig-Maximilians-Univ. München (Germany); Karsten Rippe, Ruprecht-Karls-Univ. Heidelberg (Germany); Karl Rohr, Ruprecht-Karls-Univ. Heidelberg (Germany) and Deutsches Krebsforschungszentrum (Germany)

We propose a novel approach for 3D shape analysis of heterochromatin foci in 3D confocal light microscopy images of cell nuclei. The approach is based on a 3D parametric intensity model and uses a spherical harmonics (SH) expansion. The model parameters including the SH coefficients are automatically determined by least-squares fitting of the model to the image intensities. Based on the obtained SH coefficients, a shape descriptor is determined, which enables distinguishing heterochromatin foci based on their 3D shape to characterize compaction states of heterochromatin. Our approach has been successfully applied to real static and dynamic 3D microscopy image data.

9034-33, Session 6

### Improved statistical power with a sparse shape model in detecting an aging effect in the hippocampus and amygdala

Moo K. Chung, Univ. of Wisconsin-Madison (United States); Seung-Goo Kim, Max Planck Institute (Germany); Stacey M. Schaefer, Univ. of Wisconsin-Madison (United States); Carien M. van Reekum, The Univ. of Reading (United Kingdom); Lara Peschke-Schmitz, Matt Sutterer, Richard J. Davidson, Univ. of Wisconsin-Madison (United States)

The sparse regression framework has been widely used in medical image processing and analysis. However, it has been rarely used in anatomical studies. We present a sparse shape modeling framework using the Laplace-Beltrami (LB) eigenfunctions of the underlying shape and show its improvement of statistical power.

Traditionally, the LB-eigenfunctions are used as a basis for intrinsically representing surface shapes as a form of Fourier descriptors. To reduce high frequency noise, only the first few terms are used in the expansion and higher frequency terms are simply thrown away. However, some lower frequency terms may not necessarily contribute significantly in reconstructing the surfaces. Motivated by this idea, we present a LB-based method to filter out only the significant eigenfunctions by imposing a sparse penalty. For dense anatomical data such as deformation fields on a surface mesh, the sparse regression behaves like a smoothing process, which will reduce the error of incorrectly detecting false negatives. Hence the statistical power improves. The sparse shape model is then applied in investigating the influence of age on amygdala and hippocampus shapes in the normal population. The advantage of the LB sparse framework is demonstrated by showing the increased statistical power.











9034-97, Session 6

### Statistical shape and appearance models without one-to-one correspondences

Jan Ehrhardt, Julia Krüger, Heinz Handels, Univ. zu Lübeck (Germanv)

One-to-one correspondences are fundamental for the creating classical statistical shape and appearance models. At the same time the identification of these correspondences is the weak point of such model-based methods. A manual identification of these correspondences is not practical because of the potentially large number of required landmarks. Therefore, different automatic approaches were proposed in the literature. An alternative method was proposed by Hufnagel et al. using correspondence probabilities instead of exact one-to-one correspondences for the model generation.

Active Appearance Models (AAM) represent an extension of this approach, and contain, in addition to the shape, also the appearance information of an object in a set of training images.

However, AAMs also presuppose the existence of one-to-one correspondences.

In this paper, we present a new approach for statistical shape and appearance models with correspondence probabilities. We extended the method of Hufnagel et al. by incorporating appearance information into the model. Therefore, we introduce a point-based image representation combining position and appearance information, which enables affine image registration using the EM-ICP.

Then, we pursue the concept of probabilistic correspondences and use a maximum a-posteriori approach to derive a statistical shape and appearance model.

Model generation and model fitting is then performed by minimizing a global criterion. In contrast to classical AAMs, the preprocessing for identifying the one-to-one correspondences and the warping-step to eliminate the shape differences is no longer required.

In a first evaluation, we show the approaches feasibility and evaluate the model generation and model-based segmentation using 2D lung CT slices.

9034-34, Session 7

### Large scale digital atlases in neuroscience (Keynote Presentation)

Michael J. Hawrylycz, Allen Institute for Brain Science (United States)

Imaging in neuroscience has revolutionized our current understanding of brain structure, architecture and increasingly its function. Many characteristics of morphology, cell type, and neuronal circuitry have been elucidated through methods of neuroimaging. Combining this data in a meaningful, standardized, and accessible manner is the scope and goal of the digital brain atlas. Digital brain atlases are used today in neuroscience to characterize the spatial organization of neuronal structures, for planning and guidance during neurosurgery, and as a reference for interpreting other data modalities such as gene expression and connectivity data.

The field of digital atlasing is extensive and in addition to atlases of the human includes high quality brain atlases of the mouse, rat, rhesus macaque, and other model organisms. Using techniques based on histology, structural and functional magnetic resonance imaging as well as gene expression data, modern digital atlases use probabilistic and multimodal techniques, as well as sophisticated visualization software to form an integrated product. Toward this goal, brain atlases form a common coordinate framework for summarizing, accessing, and organizing this knowledge and will undoubtedly remain a key technology in neuroscience in the future.

Since the development of its flagship project of a genome wide image-

based atlas of the mouse brain, the Allen Institute for Brain Science has used imaging as a primary data modality for many of its large scale atlasing projects. We present an overview of the field of digital atlases in neuroscience, with a focus on the challenges and opportunities for image processing and computation.

9034-35, Session 7

## Smoothness parameter tuning for generalized hierarchical continuous max-flow segmentation

John S. H. Baxter, Martin Rajchl, A. Jonathan McLeod, Ali R. Khan, Jing Yuan, Terry M. Peters, Robarts Research Institute (Canada)

Simultaneous segmentation of multiple anatomical objects from medical images has become of increasing interest to the medical imaging community, especially when information concerning these objects such as grouping or hierarchical relationships can facilitate segmentation. Single parameter Potts models have often been used to address these multi-region problems, but such parameterization is not sufficient when regions have largely different regularization requirements. These problems can be addressed by introducing smoothing hierarchies with capture grouping relationships at the expense of additional parameterization. Tuning of these parameters to provide optimal segmentation accuracy efficiently is still an open problem in optimal image segmentation. This paper presents two mechanisms, one iterative and one very computationally efficient, for estimating optimal smoothness parameters for any arbitrary hierarchical model based on multi-objective optimization theory. These methods are evaluated using 5 segmentations of the brain from the IBSR database containing 35 distinct regions. The iterative estimator provides equivalent performance to the downhill simplex method, taking significantly less computation time (93 vs. 431 minutes), allowing for more complicated models to be used without worry as to prohibitive parameter tuning procedures.

9034-36, Session 7

#### Bilayered anatomically-constrained split-andmerge expectation maximisation algorithm (BiASM) for brain segmentation

Carole H. Sudre, M. Jorge Cardoso, Sébastien Ourselin, Univ. College London (United Kingdom)

Dealing with pathological tissues is a very challenging task in medical brain segmentation. The presence of pathology can indeed bias the ultimate results when the model chosen is not appropriate and lead to missegmentations and errors in the model parameters. Model fit and segmentation accuracy are impaired by the lack of flexibility of the model used to represent the data. In this work, based on a finite Gaussian mixture model, we dynamically introduce extra degrees of freedom so that each anatomical tissue considered is modeled as a mixture of Gaussian components. The choice of the appropriate number of components per tissue class relies on a model selection criterion. Its purpose is to balance the complexity of the model with the quality of the model fit in order to avoid overfitting while allowing flexibility. The parameters optimisation, constrained with the additional knowledge brought by probabilistic anatomical atlases, follows the expectation maximisation (EM) framework. Split-and-merge operations bring the new flexibility to the model along with a data-driven adaptation. The proposed methodology appears to improve the segmentation when pathological tissue are present as well as the model fit when compared to an atlasbased expectation maximisation algorithm with a unique component per tissue class. These improvements in the modelling might bring new insight in the characterisation of pathological tissues as well as in the modelling of partial volume effect.











9034-37, Session 7

### Fast CEUS image segmentation based on self organizing maps

Julie Paire, Univ. d'Auvergne (France); Vincent V. Sauvage, Adélaïde Albouy-Kissi, Instituts Universitaires de Technologie (France); Viviane Ladam Marcus, Claude Marcus, Christine Hoeffel, CHU de Reims (France)

Contrast-enhanced ultrasound (CEUS) has recently become an important technology for lesion detection and characterization. CEUS is used to investigate the perfusion kinetics in tissue over time, which relates to tissue vascularization. In this paper, we present an interactive segmentation method based on the neural networks, which enables to segment malignant tissue over CEUS sequences. We use Self-Organizing-Maps (SOM), an unsupervised neural network, to project high dimensional data to low dimensional space, named a map of neurons. The algorithm gathers the observations in clusters, respecting the topology of the observations space. This means that a notion of neighborhood between classes is defined. Adjacent observations in variables space belong to the same class or related classes after classification. Thanks to this neighborhood conservation property and associated with suitable feature extraction, this map provides user friendly segmentation tool. It will assist the expert in tumor segmentation with fast and easy intervention. We implement SOM on a Graphics Processing Unit (GPU) to accelerate treatment. This allows a greater number of iterations and the learning process to converge more precisely. We get a better quality of learning so a better classification. Our approach allows us to identify and delineate lesions accurately. Our results show that this method improves markedly the recognition of liver lesions and opens the way for future precise quantification of contrast enhancement.

9034-38, Session 8

## Spectral-spatial classification using tensor modeling for head and neck cancer detection of hyperspectral imaging

Guolan Lu, Emory Univ. (United States) and Georgia Institute of Technology (United States); Luma V. Halig, Dongsheng Wang, Zhuo Georgia Chen, Emory Univ. (United States); Baowei Fei, Emory Univ. (United States) and Georgia Institute of Technology (United States)

Survival and quality of life in head and neck cancer are directly linked to the size of the primary tumor at first detection; therefore, early detection of malignant lesions could improve both the incidence and survival. As an emerging technology, hyperspectral imaging (HSI) combines the both chemical specificity of spectroscopy and the spatial resolution of imaging, which may provide a non-invasive diagnostic method for head and neck cancer. In this paper, we introduce a tensor-based computation and modeling framework for the analysis of hyperspectral images to detect head and neck cancer. The proposed spectral-spatial representation keeps the natural structure of hyperspectral data. With the proposed classification framework, we are able to distinguish between malignant tissue and healthy tissue with an average sensitivity of 95.59% and an average specificity of 95.45%.

9034-39, Session 8

### Texture feature analysis for prediction of postoperative liver failure prior to surgery

Amber L. Simpson, Vanderbilt Univ. (United States); Richard K. Do, Memorial Sloan-Kettering Cancer Ctr. (United States); E. Patricia Parada, Pathfinder Therapeutics, Inc. (United States);

Michael I. Miga, Vanderbilt Univ. (United States); William R. Jarnagin, Memorial Sloan-Kettering Cancer Ctr. (United States)

Texture analysis of preoperative CT images of the liver is undertaken in this study. Standard texture features were extracted from portal-venous phase contrast-enhanced CT scans of 30 patients prior to major hepatic resection and correlated to postoperative liver failure. Differences between patients with and without postoperative liver failure were statistically significant for correlation, energy, entropy, and maximum probability texture features (p<0.0001). Though texture features have been used to diagnose and characterize lesions, to our knowledge, parenchymal statistical variation has not been quantified and studied. We demonstrate that texture analysis is a valuable tool for quantifying liver function prior to surgery, which may help to identify and change the preoperative management of patients at higher risk for overall morbidity.

9034-40, Session 8

### Detection and location of 127 anatomical landmarks in diverse CT datasets

Mohammad A. Dabbah, Sean Murphy, Hippolyte Pello, Romain Courbon, Erin Beveridge, Stewart Wiseman, Daniel Wyeth, Ian Poole, Toshiba Medical Visualization Systems Europe, Ltd. (United Kingdom)

The automatic detection and localisation of anatomical landmarks has wide application, including intra and inter-patient registration, study location and navigation, and the targeting of specialised algorithms. In this paper, we demonstrate the automatic detection and localisation of 127 clinically defined landmarks distributed throughout the body, excluding arms. Landmarks are defined on the skeleton, vasculature and major organs.

Our approach builds on that of [1], using classification forests with simple image features which can be efficiently computed. For the training and validation of the method we have used 369 CT volumes on which radiographers and anatomists have marked ground-truth (GT) – that is the locations of all defined landmarks occurring in that volume.

A particular challenge is to deal with the wide diversity of datasets encountered in radiology practice. These include data from all major scanner manufacturers, different extents covering single and multiple body compartments, truncated cardiac acquisitions, with and without contrast. Cases with stents and catheters are also represented.

Validation is by a leave-one-out method, which we show can be efficiently implemented in the context of decision forest methods. Mean location accuracy of detected landmarks is 11.2mm overall; execution time averages 7s per volume on a modern server machine. We also present localisation ROC analysis to characterise detection accuracy that is to decide if a landmark is or is not present in a given dataset.

9034-41, Session 8

## Unsupervised detection of abnormalities in medical images using salient features

Sharon Alpert, Pavel Kisilev, IBM Research - Haifa (Israel)

In this paper we propose a new method for abnormality detection in medical images which is based on the notion of medical saliency. The proposed method is general and is suitable for a variety of detection tasks related to: 1) lesions and microcalcifications (MCC) in mammographic images, 2) stenoses in angiographic images, 3) lesions found in magnetic resonance (MRI) images of brain. The main idea of our approach is that abnormalities manifest as rare events, namely, as salient areas compared to normal tissues. We define the notion of medical saliency by combining local patch information from the lightness channel with geometric shape local descriptors. We demonstrate the efficacy of the proposed method by applying it to various modalities, and to various











abnormality detection problems. Promising results are demonstrated for detection of MCC and of masses in mammographic images, detection of stenoses in angiography images, and detection of lesions in brain MRI. We also demonstrate how the proposed automatic abnormality detection method can be combined with a system that performs supervised classification of mammogram images into normal or cancerous MCC's. We use a well known DDSM mammogram database for the experiment on MCC classification, and obtain 80% accuracy in classifying MCC tumor containing images versus normal ones. In contrast to supervised detection methods, the proposed approach does not rely on ground truth markings, and, as such, is very attractive for big corpus image data processing.

9034-42, Session 8

### Recognizing surgeon's actions during suture operations from video sequences

Ye Li, Jun Ohya, Waseda Univ. (Japan); Toshio Chiba, National Research Institute for Child Health and Development (Japan); Rong Xu, Waseda Univ. (Japan); Hiromasa Yamashita, National Research Institute for Child Health and Development (Japan)

Because of the shortage of nurses in the world, the realization of a robotic nurse that can support surgeries autonomously is very important. More specifically, the robotic nurse should be able to autonomously recognize different situations of surgeries so that the robotic nurse can pass necessary surgical tools to the medical doctors in a timely manner. This paper proposes and explores methods that can classify suture and tying actions during suture operations from the video sequence that observes the surgery scene that includes the surgeon's hands.

First, the proposed methods use skin pixel detection and foreground extraction to detect the hand area. Then, interest points are randomly chosen from the hand area so that their 3D SIFT descriptors are computed. A word vocabulary is built by applying hierarchical K-means to these descriptors, and the words' frequency histogram, which corresponds to the feature space, is computed. Finally, to classify the actions, either SVM (Support Vector Machine), Nearest Neighbor rule (NN) for the feature space or a method that combines "sliding window" with NN is performed.

We collect 53 suture videos and 53 tying videos to build the training set and to test the proposed method experimentally. It turns out that the NN gives higher than 90% accuracies, which are better recognition than SVM.

Negative actions, which are different from either suture or tying action, are recognized with quite good accuracies, while "Sliding window" did not show significant improvements for suture and tying and cannot recognize negative actions.

9034-43, Session 9

#### **Bernd Fischer Commemorative Talk**

Jan Modersitzki, Univ. zu Lübeck (Germany)

This is a commemorative talk on Bernd Fischer, a very active member of the SPIE community. A brief outline on Bernd's scientific trajectory including important stations, contributions and persons in his scientific career will be presented. Bernd's outstanding role as a teacher, supervisor and ambassador for applied mathematics is highlighted. Bernd's major achievements, the foundation of the Institut of Mathematics and Image computing and the foundation of the Fraunhofer MEVIS project group on image registration will be honored. The talk ends with a minute of silence to honor the memory of Bernd Fischer.

9034-44, Session 9

### MR to CT registration of brains using image synthesis

Snehashis Roy, Henry M. Jackson Foundation (United States); Aaron Carass, Amod Jog, Jerry L. Prince, Junghoon Lee, Johns Hopkins Univ. (United States)

Computed tomography (CT) is the standard imaging modality to compute dose on the patient in radiation therapy. Magnetic resonance imaging (MRI) is used along with CT to identify brain structures due to its superior soft tissue contrast. Accurate registration of MR and CT is necessary for accurate delineation of the tumor and critical structures and radiotherapy planning. Mutual information (MI) or its variants are typically used as a similarity metric to register MRI to CT.

However, unlike CT, MRI intensity does not have any tissue-specific meaning. Therefore MI-based MR-CT registration may vary from scan to scan as MI depends on the joint histogram of the images.

In this paper, we propose a fully automatic framework for MR-CT registration by synthesizing a pseudo CT image from MRI using a coregistered pair of MR and CT images as an atlas.

Patches of the subject MRI are matched to the atlas and the synthetic CT patches are estimated in a probabilistic framework. The synthetic CT is registered to the original CT using a deformable registration and the computed deformation is applied to the MRI. Contrary to most existing methods, we do not need any manual intervention such as picking landmarks or regions of interests. The proposed method was validated on 10 brain cancer patient cases, showing 25% improvement in MI and correlation between MR and CT images after registration compared to a state-of-the-art registration method.

9034-45, Session 9

### Fast automatic estimation of the optimization step size for nonrigid image registration

Yuchuan Qiao, Boudewijn P. F. Lelieveldt, Marius Staring, Leiden Univ. Medisch Ctr. (Netherlands)

Image registration is often used in the clinic, for example during radiotherapy and image-guide surgery, but also for general image analysis. Currently, this process is often very slow, yet for intraoperative procedures the speed is crucial. For intensity-based image registration, a nonlinear optimization problem should be solved, usually by (stochastic) gradient descent. This procedure relies on a proper setting of a parameter which controls the optimization step size. This parameter is difficult to choose manually however, since it depends on the input data, optimization metric and transformation model. Previously, the Adaptive Stochastic Gradient Descent (ASGD) method has been proposed that automatically chooses the step size, but it comes at high computational cost. In this paper, we propose a new computationally efficient method to automatically determine the step size, by considering the observed distribution of the voxel displacements between iterations. A relation between the step size and the expectation and variance of the observed distribution is then derived. Experiments have been performed on 3D lung CT data (19 patients) using a nonrigid B-spline transformation model. For all tested dissimilarity metrics (mean squared distance, normalized correlation, mutual information, normalized mutual information), we obtained similar accuracy as ASGD. Compared to ASGD whose estimation time is progressively increasing with the number of parameters, the estimation time of the proposed method is substantially reduced to an almost constant time, from 40 seconds to no more than 1 second when the number of parameters is 100000.











9034-46, Session 9

#### Detection and correction of inconsistencybased errors in non-rigid registration

Tobias Gass, Gàbor Székely, Orcun Goksel, ETH Zurich (Switzerland)

In this paper we present a novel post-processing technique to detect and correct inconsistency-based errors in non-rigid registration. While deformable registration is ubiquitous in medical image computing, assessing its quality has yet been an open problem. We propose a method that predicts local registration errors of existing pairwise registrations between a set of images, while simultaneously estimating corrected registrations. In the solution the error is constrained to be small in areas of high post-registration image similarity, while local registrations are constrained to be consistent between direct and indirect registration paths. The latter is a critical property of an ideal registration process, and has been frequently used to asses the performance of registration algorithms. In our work, the consistency is used as a target criterion, for which we efficiently find a solution using a linear least squares model on a coarse grid of registration control points. We show experimentally that the local errors estimated by our algorithm correlate strongly with true registration errors in experiments with known, dense ground-truth deformations. Additionally, the estimated corrected registrations consistently improve over the initial registrations in terms of average deformation error or TRE for different registration algorithms on both simulated and clinical data, independent of modality (MRI/ CT), dimensionality (2D/3D) and employed primary registration method (demons/Markov random field based).

9034-47, Session 9

## A rib-specific multimodal registration algorithm for fused unfolded rib visualization using PET/CT

Jens N. Kaftan, Marcin Kopaczka, Siemens Molecular Imaging (United Kingdom); Andreas Wimmer, Siemens Computed Tomography (Germany); Günther Platsch, Jerome Declerck, Siemens Molecular Imaging (United Kingdom)

Respiratory motion affects the alignment of PET and CT volumes from PET/CT examinations in a non-rigid manner. This becomes particularly apparent if reviewing fine anatomical structures such as ribs with respect to bone metastasis.

To make this routine task more efficient, a fused unfolded rib visualization for 18F-NaF PET/CT is presented. It allows to review the whole rib cage in a single image. This advanced visualization is enabled by a novel rib-specific registration algorithm that rigidly optimizes the local alignment of each individual rib in both modalities based on a matched filter response function. More specifically, rib centerlines are automatically extracted from CT and subsequently individually aligned to the corresponding bone-specific PET rib uptake pattern.

The proposed method has been validated on 20 PET/CT scans acquired at different clinical sites. It has been demonstrated that the presented rib-specific registration method significantly improves the rib alignment without having to run complex deformable registration algorithms. At the same time, it guarantees that rib lesions are not deformed, which may otherwise affect quantitative measurements such as SUVs. Considering clinically relevant acceptance thresholds, the centerline portion with good alignment improved from 60.6% to 86.7% after registration while approximately 98% can be still considered as acceptably aligned.

9034-48, Session 9

### A symmetric block-matching framework for global registration

Marc Modat, David M. Cash, Pankaj Daga, Gavin P. Winston, John S. Duncan, Sebastien Ourselin, Univ. College London (United Kingdom)

Most registration algorithms suffer from a directionality bias that has been shown to largely impact on subsequent analyses. Several approaches have been proposed in the literature to address this bias in the context of non-linear registration but little work has been done in the context of global registration. We propose a symmetric approach based on a block-matching technique and least trimmed square regression. The proposed method is suitable for multi-modal registration and is robust to outliers in the input images. The symmetric framework is compared to the original asymmetric block-matching technique, outperforming it in terms accuracy and robustness.

9034-49, Session 10

### Statistical label fusion with hierarchical performance models

Andrew J. Asman, Alexander S. Dagley, Bennett A. Landman, Vanderbilt Univ. (United States)

Label fusion is a critical step in many image segmentation frameworks (e.g., multi-atlas segmentation) as it provides a mechanism for generalizing a collection of labeled examples into a single estimate of the underlying segmentation. In the multi-label case, typical label fusion algorithms treat all labels equally - fully neglecting the known, yet complex, anatomical relationships exhibited in the data. To address this problem, we propose a generalized statistical fusion framework using hierarchical models of rater performance. Building on the seminal work in statistical fusion, we reformulate the traditional rater performance model from a multi-tiered hierarchical perspective. This new approach provides a natural framework for leveraging known anatomical relationships and accurately modeling the types of errors that raters (or atlases) make within a hierarchically consistent formulation. Herein, we describe several contributions. First, we derive a theoretical advancement to the statistical fusion framework that enables the simultaneous estimation of multiple (hierarchical) performance models within the statistical fusion context. Second, we demonstrate that the proposed hierarchical formulation is highly amenable to the state-of-the-art advancements that have been made to the statistical fusion framework. Lastly, in an empirical wholebrain segmentation task we demonstrate substantial qualitative and significant quantitative improvement in overall segmentation accuracy.

9034-50, Session 10

### Applying the algorithm assessing quality using registration circuits (AQUIRC) to multiatlas segmentation

Ryan Datteri, Benoit M. Dawant, Vanderbilt Univ. (United States)

Multi-atlas registration-based segmentation is a popular technique in the medical imaging community, used to transform anatomical and functional information from a set of atlases onto a new patient that lacks this information. The accuracy of the projected information on the target image is dependent on the quality of the registrations between the atlas images and the target image. Recently, we have developed a technique called AQUIRC that aims at estimating the error of a non-rigid registration at the local level and was shown to correlate to error in a simulated case. Herein, we extend upon this work by applying AQUIRC at the local level across multiple structures in cases in which non-rigid registration











is difficult. We show that AQUIRC can be used as a method to combine multiple segmentations and increase the accuracy of the projected information on a target image.

9034-51, Session 10

### Robust optic nerve segmentation on clinically acquired CT

Swetasudha Panda, Andrew J. Asman, Michael P. DeLisi, Louise A. Mawn M.D., Robert L. Galloway Jr., Bennett A. Landman, Vanderbilt Univ. (United States)

The optic nerve is a sensitive central nervous system structure, which plays a critical role in many devastating pathological conditions. Several methods have been proposed in recent years to segment the optic nerve automatically, but progress toward full automation has been limited. Multi-atlas methods have been successful for brain segmentation, but their application to smaller anatomies remains relatively unexplored. Herein we evaluate a framework for robust and fully automated segmentation of the optic nerves, eye globes and muscles. We employ a robust registration procedure for accurate registrations, variable voxel resolution and image field-of-view. We demonstrate the efficacy of an optimal combination of SyN registration and a recently proposed label fusion algorithm (Non-local Spatial STAPLE). On a dataset containing 30 highly varying computed tomography (CT) images of the human brain, the optimal registration and label fusion pipeline resulted in a median Dice similarity coefficient of 0.77, symmetric mean surface distance error of 0.55 mm, symmetric Hausdorff distance error of 3.33 mm for the optic nerves. Simultaneously, we demonstrate the robustness of the optimal algorithm by segmenting the optic nerve structure in 316 CT scans obtained from 182 subjects from a thyroid eye disease (TED) patient population.

9034-52. Session 10

### Spatially adapted augmentation of agespecific atlas-based segmentation using patch-based priors

Mengyuan Liu, Sharmishtaa Seshamani, Lisa Harrylock, Averi Kitsch, Univ. of Washington (United States); Steven Miller, The Child & Family Research Institute (Canada); Van Chau, Kenneth Poskitt, Child & Family Research Institute (Canada); Francois Rousseau, Univ. de Strasbourg (France); Colin Studholme, Univ. of Washington (United States)

One of the most common approaches to MRI brain tissue segmentation is to employ an atlas prior to initialize an EM image labeling scheme using a statistical model of MRI intensities. This prior is commonly derived from a set of manually segmented training data from the population of interest. However, in cases where subject anatomy varies significantly from the prior anatomical average model (for example in the case of extreme developmental abnormalities or brain injury), the prior tissue map does not provide adequate information about the observed MRI intensities to ensure the EM algorithm converges to an anatomically accurate labeling of the MRI. In this paper, we present a novel approach for automatic segmentation of such cases. This approach augments the atlas-based EM segmentation by exploring approaches to building a hybrid tissue segmentation scheme that seeks to learn where an atlas prior fails (due to inadequate representation of anatomical variation in the statistical atlas) and make use of an alternative prior derived from a patch driven search of the atlas data. We describe a framework for incorporating this scheme into a 4D age-specific atlas-based segmentation of developing brain anatomy. We compute Voxel Label Accuracy (VLA) maps for the atlas-based and patch-based tissue probabilities, which serve as the weights in computing the priors. The proposed approach was evaluated on a set of MRI brain scans of premature neonates with age ranging

from 27.29 to 46.43 gestational weeks (GWs). Results indicated superior performance compared to conventional atlas-based segmentation method, providing improved segmentation accuracy for gray matter, white matter, ventricles and sulcal CSF regions.

9034-53, Session 10

## Personalized articulated atlas with a dynamic adaptation strategy for bone segmentation in CT or CT/MR head and neck images

Sebastian Steger, Florian Jung, Stefan Wesarg, Fraunhofer-Institut für Graphische Datenverarbeitung (Germany)

This paper presents a novel segmentation method for the joint segmentation of individual bones in CT- or CT/MR- head&neck images. It is based on an articulated atlas for CT images that learned the shape and appearance of the individual bones along with the articulation between them from annotated training instances. First, a novel dynamic adaptation strategy for the atlas is presented in order to increase the rate of successful adaptations. Then, if a corresponding CT image is available the atlas can be enriched with personalized information about shape, appearance and size of the individual bones from that image. Using mutual information, this personalized atlas is adapted to a MR image in order to propagate segmentations.

For evaluation, a head&neck bone atlas created from 15 manually annotated training images was adapted to 58 clinically acquired head&neck CT datasets. Visual inspection showed that the automatic dynamic adaptation strategy was successful for all bones in 86% of the cases. This is a 22% improvement compared to the traditional gradient descent based approach. In leave-one-out cross validation manner the average surface distance of the correctly adapted items was found to be 0.68 mm. In 20 cases corresponding CT/MR image pairs were available and the atlas could be personalized and adapted to the MR image. This was successful in 19 cases.

9034-54, Session 11

#### Intra-voxel analysis in MRI

Fabio Baselice, Michele Ambrosanio, Giampaolo Ferraioli, Vito Pascazio, Univ. degli Studi di Napoli Parthenope (Italy)

A new application of Compressive Sensing (CS) in Magnetic Resonance Imaging (MRI) field is presented. In particular, first results of the Intra Voxel Analysis (IVA) technique are reported. The idea is to exploit CS peculiarities in order to distinguish different contributions inside the same resolution cell, instead of reconstructing images from non fully sampled k-space acquisition. Applied to MRI field, this means the possibility of estimating the presence of different tissues inside the same voxel, i.e. in one pixel of the obtained image. In other words, the method is the first attempt of achieving Spectroscopy-like results starting from each pixel of MR images. In particular, tissues are distinguished each others by evaluating their spin-spin relaxation times. Further mathematical details of the approach are supplied in another manuscript submitted to the SPIE conference. Within this work, first results on clinical dataset, in particular an occipital brain lesion corresponding to a metastatic breast cancer nodule, are reported. Considering a voxel of the lesion area, the approach is able to detect the presence of two tissues, namely the healthy and the cancer related ones, while in another location outside the lesion only the healthy tissue is detected. Of course these are the first results of the proposed methodology, further studies on different types of clinical datasets are required in order to widely validate the approach. Although a single dataset has been considered, results seem both interesting and promising.











9034-55, Session 11

### A new application of compressive sensing in MRI

Fabio Baselice, Giampaolo Ferraioli, Univ. degli Studi di Napoli Parthenope (Italy); Flavia Lenti, Univ. degli Studi dell'Insubria (Italy); Vito Pascazio, Univ. degli Studi di Napoli Parthenope (Italy)

Image formation in Magnetic Resonance Imaging (MRI) is the procedure which allows the generation of the image starting from data acquired in the so called k -space. At the present, many image formation techniques have been presented, working with different k -space filling strategies. Recently, Compressive Sampling (CS) has been successfully used for image formation from non fully sampled k -space acquisitions, due to its interesting property of reconstructing signal from highly undetermined linear systems. The main advantage consists in greatly reducing the acquisition time. Within this manuscript, a novel application of CS to MRI field is presented, named Intra Voxel Analysis (IVA). The idea is to achieve the so-called super resolution, i.e. the possibility of distinguish anatomical structures smaller than the spatial resolution of the image. For this aim, multiple Spin Echo images acquired with different Echo Times are required. The output of the algorithm is the estimation of the number of contributions present in the same pixel, i.e. the number of tissues inside the same voxel, and their spin-spin relaxation times. This allows us not only to identify the number of involved tissues, but also to discriminate them. At the present, simulated case studies have been considered, obtaining interesting and promising results. In particular, a study on the required number of images, on the estimation noise and on the regularization parameter of different CS algorithms has been conducted. As future work, the method will be applied to real clinical datasets, in order to validate the estimations.

ies have been considered, obtaining interesting and promising results. In particular, a study on the required number of images, on the estimation noise and on the regularization parameter of different CS algorithms has been conducted. As future work, the method will be applied to real clinical datasets, in order to validate the estimations.

9034-56, Session 11

#### Novel MRI-derived quantitative biomarker for cardiac function applied to classifying ischemic cardiomyopathy within a Bayesian rule learning framework

Prahlad G. Menon, SYSU-CMU Joint Institute of Engineering (United States); Lailonny Morris, Carnegie Mellon Univ. (United States); Mara Staines, Univ. of Pittsburgh (United States); Joao Lima, The Johns Hopkins Hospital (United States); Daniel C. Lee, Northwestern Univ. (United States); Vanathi Gopalakrishnan, Univ. of Pittsburgh (United States)

Accurate and timely quantification of regional pathological function (hypokinesia / akinesia / dyskinesia) could be vital for early clinical risk assessment and patient management of ischemic heart disease (IHD). In an effort to define objective, clinically useful metrics of pathological remodeling and declining cardiac performance, we demonstrate a promising new paradigm for using a fully 4D (3D + time) characteristic metric of cardiac function extracted from standard short-axis cine SSFP cardiac MRI data, as a novel imaging biomarker of IHD. A novel shapebased technique was developed to establish point-to-point endocardial surface correspondences as the surface evolved over the cardiac cycle and record regional phase-to-phase displacement (P2PD) histories at uniformly spaced endocardial surface points in 20 asymptomatic and 25 IHD patients. The cumulative average and standard deviation in the P2PD curves for healthy and unhealthy patient cohorts were compared over the cardiac cycle using a novel biomarker of RMS error between patient-specific P2PD curve over the cardiac cycle for each patient of the IHD cohort and the cumulative average P2PD curve of the asymptomatic cohort viz. the RMS-P2PD marker. Shape analysis resulted in an objective colored rendering of regional shape deformation to visually establish existence of hypokinetic (yellow), akinetic (green) and dyskinetic (red at systole, red at diastole) regions visually. The IHD patient cohort demonstrated: a) diminished peak P2PD magnitudes; and b) indistinct end-systolic and diastole instants (expected zero velocity instants; as opposed to the asymptomatic cohort. The resulting RMS-P2PD biomarker indices were significantly different for the patient and normal control cohorts (p<0.001). Using Baysian Rule Learning classification framework, it was possible to establish that addition of the RMS-P2PD marker improved accuracy (83.8% to 91.9%) and sensitivity (82.6% to 95.7%) for correctly classifying IHD patients in contrast with that achievable using standard cardiac MRI derived biomarkers (viz. ejection fraction and LV volumes), alone. This pilot study indicates RMS-P2PD marker as a promising early indicator of declining cardiac performance, which may warrant timely, informed and appropriate clinical attention.

9034-57, Session 11

## Correction of dental artifacts within the anatomical surface in PET/MRI using active shape models and k-nearest-neighbors

Claes N. Ladefoged, Rigshospitalet (Denmark) and Univ. of Copenhagen (Denmark); Flemming L. Andersen, Sune H. Keller, Rigshospitalet (Denmark); Thomas Beyer, Ctr. for Medical Physics and Biomedical Engineering (Austria); Liselotte Højgaard, Rigshospitalet (Denmark); François B. Lauze, Univ. of Copenhagen (Denmark)

In combined PET/MR, attenuation correction (AC) is performed indirectly based on the available MR image information. Metal implant-induced susceptibility artifacts and subsequent signal voids challenge MR-based AC. Several papers acknowledge the problem in PET attenuation correction when dental artifacts are ignored, but none of them attempts to solve the problem.

We propose a clinically feasible correction method which combines Active Shape Models (ASM) and k-Nearest-Neighbors (kNN) into a simple approach which finds and correct the dental artifacts within the surface boundaries of the patient anatomy. ASM is used to locate a number of landmarks in an unseen T1-weighted MR-image. We calculate a vector of offsets from each voxel within a signal void to each of the landmarks. We then use kNN to classify each voxel as belonging to an artifact or an actual signal void using this offset vector, and fill the artifact voxels with soft tissue.

We tested the method using fourteen patients without artifacts, and eighteen patients with dental artifacts of varying sizes within the anatomical surface of the head/neck region. Though the method wrongly filled a small volume in the bottom part of a maxillary sinus in two patients without any artifacts, due to their abnormal location, it succeeded in filling all of the artifacts.

9034-3, Session PSMon

### Computer-aided Classification of Liver Tumors in 3D Ultrasound Images with Combined Deformable Model Segmentation and Support Vector Machine

Myungeun Lee, Seoul National Univ. (Korea, Republic of); Jong Hyo Kim, Seoul National Univ. College of Medicine (Korea, Republic of); Moon Ho Park, Ye-Hoon Kim, Yeong Kyeong Seong, Baek Hwan Cho, Kyoung-Gu Woo, Samsung Advanced Institute of Technology (Korea, Republic of)











Segmentation has been a major research topic in medical image analysis for decades and many segmentation methods have been developed for different imaging modalities. However, robust algorithms for correct segmentation of different imaging modalities. Several applications of both qualitative and quantitative medical image analysis rely on the definition of object boundaries. Tumor boundaries have to be precisely defined to compare tumor size and shape before and after treatment.

This paper addresses the problem of semi-automatic segmentation of hepatic tumors from US images. We propose an improved version of a level set algorithm that substantially reduces the problem of convergence in noisy images and demonstrate its performance on 79 typical US images of liver tumors of various sizes. The proposed model combines edge, region, and contour smoothness energies. We extracted qualitative appearance features from three hepatic tumor types and use them to adjust the weights of the energy terms in order to determine an optimized set of parameters for each tumor type.

The paper is organized as follows: first, we explain the segmentation method, feature extraction, and classification. Then the experimental results shows that the proposed method can be segment in clinical images accurately and effectively. Finally, we conclude our paper in Section 4.

9034-29, Session PSMon

## Sparse appearance model-based algorithm for automatic segmentation and identification of articulated hand bones

Fitsum Akilu Reda, Siemens Medical Solutions USA, Inc. (United States) and Vanderbilt Univ. (United States); Zhigang Peng, Siemens Medical Solutions USA, Inc. (United States); Gerardo Hermosillo, Shu Liao, Siemens Medical Solutions USA, Inc., CAD R&D (United States); Yoshihisa Shinagawa, Yiqiang Zhan, Xiang Sean Zhou, Siemens Medical Solutions USA, Inc. (United States)

Automatic and precise segmentation of hand bones is important for many medical imaging applications. Although several previous works address segmentation of bones, automatically segmenting articulated hand bones remains a challenging task. The highly articulated nature of hand bones limits the effectiveness of registration-based segmentation methods. The use of low-level information derived from the image alone is insufficient for detecting bone boundaries and separating bone segments that are in close proximity. In this study, we propose a method that combines an articulated statistical shape model and a local exemplar-based appearance model for automatically segmenting hand bones in CT. Our approach is to perform a hierarchical articulated shape deformation that is driven by a set of local exemplar-based appearance models. Specifically, for each point in the shape model, the local appearance model is described by a set of profiles of low-level image features along the normal of the surface. At run-time, each point in the shape model is deformed to a new point whose image features are close to the appearance model. During the deformation, the shape model is also constrained by an articulation model described by a set of auto-detected landmarks on the finger joints. In this way, the deformation is robust to sporadic false bony edges and is able to fit fingers with large articulations. We validated our method on 23 CT scans and our success rate is 93.14%. This result indicates that our method is viable for automatic segmentation of articulated hand bones in conventional CT.

9034-58, Session PSMon

## Joint source based analysis of multiple brain structures in studying major depressive disorder

Mahdi Ramezani, Abtin Rasoulian, The Univ. of British Columbia (Canada); Tom Hollenstein, Kate Harkness, Ingrid S. Johnsrude,

Queen's Univ. (Canada); Purang Abolmaesumi, The Univ. of British Columbia (Canada)

We propose a joint Source-Based Analysis (jSBA) framework to identify brain structural variations in patients with Major Depressive Disorder (MDD). In this framework, features representing position, orientation and size (i.e. pose), shape, and local tissue composition are extracted. Subsequently, simultaneous analysis of these features within a joint analysis method is performed to generate the basis sources that show significant differences between subjects with MDD and those in healthy control. Moreover, in a cross-validation leave-one-out experiment, we use a Fisher Linear Discriminant (FLD) classifier to identify individuals within the MDD group. Results show that we can classify the MDD subjects with an accuracy of 80% solely based on the information gathered from the joint analysis of pose, shape, and tissue composition in multiple brain structures.

9034-59, Session PSMon

#### A multi-view approach to multi-modal MRI cluster ensembles

Carlos A. Méndez Guerrero, Gloria Menegaz, Univ. degli Studi di Verona (Italy); Paul E. Summers, European Institute of Oncology (Italy)

It has been shown that the combination of multi-modal MRI images improve the discrimination of diseased tissue. However the fusion of dissimilar imaging data for classification and segmentation purposes is not a trivial task, there is an inherent difference in information domains, dimensionality and scales. This work proposes a multi-view consensus clustering methodology for the integration of multi-modal MR images into a unified segmentation of tumoral lesions for heterogeneity assessment. Using a variety of metrics and distance functions this multi-view imaging approach calculates multiple vectorial dissimilarity-spaces for each one of the MRI modalities and makes use of the concepts behind cluster ensembles to combine a set of base unsupervised segmentations into an unified partition of the voxel-based data. The methodology is specially designed for combining DCE-MRI and DTI-MR, for which a manifold learning step is implemented in order to account for the geometric constrains of the high dimensional diffusion information.

9034-60, Session PSMon

## Comparative study of two sparse multinomial logistic regression models in decoding visual stimuli from brain activity of fMRI

Sutao Song, Jinan Univ. (China); Gongxiang Chen, School of Education and Psychology, Jinan University (China); Yu Zhan, Jiacai Zhang, Beijing Normal Univ. (China); Li Yao, Beijing Normal Univ. (China) and Beijing Normal Univ. (China)

Abstract: Recently, sparse algorithms, such as Sparse Multinomial Logistic Regression (SMLR), have been successfully applied in decoding visual information from human brain activity recorded by fMRI, where activities of voxels are combined with sparse weights to predict image contrast. For sparse algorithms, the goal is to learn a classifier whose weights distributed as sparse as possible by introducing some prior belief about the weights. There are two ways to introduce a sparse prior constraints for weights: the Automatic Relevance Determination (ARD-SMLR) and Laplace prior (LAP-SMLR). In this paper, we presented comparison results between the ARD-SMLR and LAP-SMLR models in computational time, classification performance and voxel selection. Results showed that, for real fMRI data (public data of Miyawaki et al., 2008), no significant difference was found in classification accuracy between these two methods when voxels in V1 were chosen as input features (totally 1017 voxels). As for computation time, LAP-SMLR was











superior to ARD-SMLR; the survived voxels for ARD-SMLR was less than LAP-SMLR. Using simulation data, we confirmed the classification performance for the two SMLR models was sensitive to the sparsity of the initial features, when the ratio of relevant features to the initial features was larger than 0.01, ARD-SMLR outperformed LAP-SMLR; otherwise, LAP-SMLR outperformed LAP-SMLR. Simulation data showed ARD-SMLR was more efficient in selecting relevant features.

9034-61, Session PSMon

#### Classification of microscopy images of Langerhans islet

Jan Svihlík, Institute of Chemical Technology (Czech Republic) and Czech Technical Univ. in Prague (Czech Republic); Jan Kybic, Czech Technical Univ. in Prague (Czech Republic); David Habart, Zuzana Berková, Peter Girman, Jan Krí?, Klára Zacharovová, Institute for Clinical and Experimental Medicine (Czech Republic)

Classification of images of Langerhans islet is crucial procedure for optimization of diabetes treatment. Hence, this paper deals with segmentation of microscopy images of Langerhans islets and evaluation of islet parameters such as area, islet diameter, islet equivalent (IE) etc. For all the available images, the ground truth and the islet parameters were independently evaluated by four medical experts in a blinded manner. We utilized linear classifier (perceptron algorithm) and SVM (support vector machine) for image segmentation. All the available image data were segmented and compared with corresponding ground truth. The islet parameters were also evaluated and compared with parameters evaluated by medical experts. The presented fully automatic algorithm analyzes the microscopy images as good as medical experts.

9034-62, Session PSMon

## Classification of normal and pathological aging processes based on brain MRI morphology measures

Jorge L. Perez-Gonzalez, Oscar Yanez-Suarez, Veronica Medina-Banuelos, Univ. Autónoma Metropolitana (Mexico)

Reported studies describing normal and abnormal aging based on anatomical MRI analysis do not consider morphological brain changes, but only volumetric measures to distinguish among these processes. This work presents a classification scheme, based both on size and shape features extracted from brain volumes, to determine different aging stages: healthy adults (HC), mild cognitive impairment (MCI), and Alzheimer's disease (AD). Three support vector machines were optimized and validated for the pair-wise separation of these three classes, using selected features from a set of 3D discrete compactness measures and normalized volumes of several global and local anatomical structures. Our analysis show classification rates of up to 98.3% between HC and AD; of 85% between HC and MCI and of 93.3% for MCI and AD separation. These results outperform those reported in the literature and demonstrate the viability of the proposed morphological indexes to classify different aging stages.

9034-63, Session PSMon

### Support vector machine based IS/OS disruption detection from SD-OCT images

Liyun Wang, Weifang Zhu, Soochow Univ. (China); Jianping Liao, Guangxi Univ. (China); Dehui Xiang, Chao Jin, Soochow Univ. (China); Haoyu Chen, Joint Shantou International Eye Ctr. (China);

Xinjian Chen, Soochow Univ. (China)

In this paper, we sought to find a method to detect the Inner Segment / Outer Segment (IS/OS) disruption region automatically. A support vector machine (SVM) based method was proposed for IS/OS disruption detection. Supervised by the experienced ophthalmologist, the IS/ OS disruption region was labeled in each slice of all subjects using the software of CAVASS. The method includes two parts: training and testing. During the training phase, 7 features from the region around the fovea are calculated which includes: normalized intensity value, gradients on direction of x, y, z, the block intensity mean, block intensity standard deviation, and the block entropy (sub-volume of 3\*3\*3 voxels). Support vector machine (SVM) is utilized as the classification method due to its good generalized ability. In the testing phase, the training model derived is utilized to classify the disruption and non-disruption region of the IS/ OS. The proposed method was tested on 9 patients' SD-OCT images using leave-one-out strategy. The preliminary results demonstrated the feasibility and efficiency of the proposed method.

9034-64, Session PSMon

#### Breast tissue classification in digital breast tomosynthesis images based on global gradient minimization and texture features

Xulei Qin, Emory Univ. (United States); Guolan Lu, Ioannis Sechopoulos, Baowei Fei, Emory Univ. (United States) and Georgia Institute of Technology (United States)

Digital breast tomosynthesis (DBT) is a pseudo-three-dimensional x-ray imaging modality proposed to decrease the effect of tissue superposition present in mammography and therefore increase clinical performance in the detection and diagnosis of breast cancer. Tissue classification in DBT images may be useful in risk assessment, computer-aided detection and radiation dosimetry, among other aspects. However, classifying breast tissue in DBT is a challenging problem because DBT images include complicated structures, image noise, and out-of-plane artifacts due to the limited angular tomographic sampling. In this project, we propose an automatic method to classify fatty and glandular tissue in DBT images. First, the DBT images are pre-processed to enhance the tissue structures and decrease the noises and artifacts. Second, a global smooth filter based on L0 gradient minimization is applied to eliminate detailed structures and enhance large-scale ones. Third, the main regions are extracted and labeled by fuzzy C-mean classification. The texture features are also calculated. Finally, each region is classified into different tissue classes based on both intensity and texture features. The proposed method is validated using five patient images using manual segmentation as the gold standard. The Dice scores and the confusion matrix are utilized to evaluate the classified results. The evaluation results indicate that the proposed method is able to classify glandular and fat tissue from DBT images.

9034-65, Session PSMon

#### A minimum spanning forest based hyperspectral image classification method for cancerous tissue detection

Robert Pike, Samuel K. Pattpm, Emory Univ. (United States); Guolan Lu, Emory Univ. (United States) and Georgia Institute of Technology (United States); Luma V. Halig, Dongsheng Wang, Zhuo Georgia Chen, Emory Univ. (United States); Baowei Fei, Emory Univ. (United States) and Georgia Institute of Technology (United States)

Hyperspectral imaging is a developing modality for cancer detection. The rich information associated with hyperspectral images allow for the examination between cancerous and healthy tissue. This study











focuses on a new method that incorporates support vector machines into a minimum spanning forest algorithm for differentiating cancerous tissue from normal tissue. Spectral information was gathered from tumor bearing mice and was used to test the algorithm. Animal experiments were performed and hyperspectral images were acquired from tumorbearing mice. In vivo imaging experimental results demonstrate the applicability of the proposed classification method for cancer tissue classification on hyperspectral images.

9034-66, Session PSMon

### Protein crystallization image classification with elastic net

Kazunori Okada, Jeffrey Hung, John Collins, Mehari Weldetsion, Oliver Newland, Eric Chiang, San Francisco State Univ. (United States); Steve Guerrero, Genentech Inc. (United States)

Protein crystallization plays a crucial role in pharmaceutical research by supporting the investigation of a protein's molecular structure through X-ray diffraction of its crystal. Due to the rare occurrence of crystals, images must be manually inspected, a laborious process. We develop a solution incorporating a regularized, logistic regression model for automatically evaluating these images. Standard image features, such as shape context, Gabor wavelets, and Fourier transforms, are first extracted to represent the heterogeneous appearance of our images. Then the proposed solution utilizes Elastic Net to perform accurate classification, while simultaneously selecting relevant features due to its L1-regularization, mitigating the effects of our large data set. Its L2-regularization ensures proper operation when the feature number exceeds the sample number. In order to validate the proposed method, we experimentally compare it with naïve Bayes, linear discriminant analysis, random forest, and their two-tier cascade classifiers, by 10-fold cross validation. Our experimental results demonstrate that Elastic Net and random forest achieve 82% accuracy, outperforming other models. In addition, Elastic Net better reduces the false negatives responsible for a high, domain specific risk. To the best of our knowledge, this is the first attempt to apply Elastic Net to classifying protein crystallization images. Performance of 82% accuracy measured with a large pharmaceutical data set also fared well in comparison with those presented in the previous studies, while the reduction of the high-risk false negatives is promising.

9034-67, Session PSMon

#### **Example based lesion segmentation**

Snehashis Roy, Qing He, Henry M. Jackson Foundation (United States); Aaron Carass, Johns Hopkins University (United States); Amod Jog, Johns Hopkins Univ. (United States); Jennifer L Cuzzocreo, Department of Radiology, Johns Hopkins School of Medicine (United States); Daniel S Reich, National Institute of Neurological Disorders and Stroke (United States); Jerry L Prince, Johns Hopkins Univ. (United States); Dzung L. Pham, Henry M. Jackson Foundation (United States)

Lesion segmentation from brain magnetic resonance (MR) images is one of the most challenging problems in the medical imaging community. Automatic and accurate detection of white matter lesions is a significant step toward understanding the progression of many diseases, like Alzheimer's Disease or Multiple Sclerosis. Multi-modal MR images are often used to segment white matter lesions.

Some automated lesion segmentation methods describe the lesion intensities using generative models and then classify the lesions with some combination of heuristics and cost minimization. In contrast, we propose a patch based method, where lesions are found using examples from an atlas containing multi-modal MR images and corresponding manual delineation of lesions. Patches from subject MR images are

matched to patches from an atlas and the lesion memberships are found based on the patch similarity weights. We experiment on \$43\$ subjects with MS having various levels of lesion-load and improve upon a state-of-the-art model based lesion segmentation method. We show significant improvement in Dice coefficient and total lesion volume comparing to their manual segmentations, indicating more accurate delineation of lesions.

9034-68, Session PSMon

## Classification of Essential Tremors (ET) disorder and healthy controls using a masking technique

Rakshatha P. Krishnamurthy, Neelam Sinha, International Institute of Information Technology, Bangalore (India); Jitender Saini, Pramod Pal, National Institute of Mental Health and Neuro Sciences (India)

In this study, a novel method is proposed to build a Resting State fMRI (RS fMRI) classifier to discriminate between healthy controls and data of Essential Tremors (ET) disorder. Distinction between healthy controls and diseased subject's data using RS fMRI is more useful in light of the fact that certain patients suffering from neuropsychiatric disorders may be unable to perform the tasks specified for acquisition. Specifically the neurologic disorder that we consider is ET for the reason that fMRI of this disorder is least explored and hence, functionally affected regions of this disease is not clearly known. Regional Homogeneity (ReHo) feature for healthy controls and ET patients was extracted as a mapping to brain function during resting state. One sample t-test was performed for both normal and patient data and regions with significant ReHo values were procured for both the data. The t-test maps respective to the two data groups, consisting of clusters with significant ReHo values, were used as masks respectively on ReHo maps of each of the groups. These masked ReHo maps were used as features as input to a linear classifier. The performance of the proposed scheme for classification of Healthy controls and ET was evaluated and the resulting generalization rate of the classifier was 100% for a dataset consisting of 11 samples in both the groups. The performance of the proposed masking technique remains to be evaluated with a dataset consisting of a large number of samples for ET and Healthy controls.

9034-69. Session PSMon

### Variability sensitivity of dynamic texture based recognition in clinical CT data

Roland Kwitt, Stephen Aylward, Kitware, Inc. (United States); Sharif Razzaque, InnerOptic Technology, Inc. (United States); Jeffrey Lowell M.D., Washington Univ. School of Medicine in St. Louis (United States)

Dynamic texture recognition using a database of template models has recently shown promising results for the task of localizing anatomical structures in Ultrasound video. In order to understand its clinical value, it is imperative to study the sensitivity with respect to interpatient variability as well as sensitivity to acquisition parameters such as Ultrasound probe angle. Fully addressing patient and acquisition variability issues, however, would require a large database of clinical Ultrasound from many patients, acquired in a multitude of controlled conditions, e.g., using a tracked transducer. Since such data is not readily attainable, we advocate an alternative evaluation strategy using abdominal CT data as a surrogate. In this paper, we describe how to replicate Ultrasound variabilities by extracting subvolumes from CT and interpreting the image material as an ordered sequence of video frames. Utilizing this technique, and based on a database of abdominal CT from 45 patients, we report recognition results on an organ (kidney) recognition task, where we try to discriminate kidney subvolumes/videos from a











collection of randomly sampled negative instances. We demonstrate that (1) dynamic texture recognition is relatively insensitive to inter-patient variation while (2) viewing angle variability needs to be accounted for in the template database. Since naively extending the template database to counteract variability issues can lead to impractical database sizes, we propose an alternative strategy based on automated identification of a small set of representative models.

9034-70, Session PSMon

#### Multi-view learning based robust collimation detection in digital radiographs

Hongda Mao, Rochester Institute of Technology (United States); Zhigang Peng, Siemens Medical Solutions USA, Inc. (United States); Frank Dennerlein, Siemens AG (Germany); Yoshihisa Shinagawa, Yiqiang Zhan, Xiang Sean Zhou, Siemens Medical Solutions USA, Inc. (United States)

In X-ray examinations, it is essential that radiographers carefully use collimation to the appropriate anatomy of interest to minimize the overall integral dose to the patient. The shadow regions are not diagnostically meaningful and can impair the overall image quality. Thus, it is desirable to detect the collimation and exclude the shadow regions to optimize the display of the image. However, due to the large variability of collimated images, collimation detection remains a challenging task. In this paper, we consider a region of interest (ROI) in an image, such as the collimation, can be described by two distinct views, a cluster of pixels within the ROI and the corners of the ROI. Based on this observation, we propose a robust multi-view learning-based strategy for collimation detection in digital radiography. Specifically, one view is from random forests based region detector, which provides pixelwise image classification and each pixel is labeled as in-collimation or out-of-collimation. The other view is from a discriminative, learningbased landmark detector, which detects the corners and localizes the collimation in the image. Nevertheless, given the variability of the images, the detection from either view alone may not be perfect. Therefore, we adopt an adaptive view fusing step to obtain the final detection which combines both region and corner information. We evaluate our algorithm in a database with 665 X-ray images in a wide variety of types and dosages, and obtain a high accuracy (95%), compared with using region detector alone (87%) and landmark detector alone (83%).

9034-71, Session PSMon

#### Adaptive temporal smoothing of sinogram data using Karhunen-Loeve (KL) transform for myocardial blood flow estimation from dose-reduced dynamic CT

Dimple Modgil, The Univ. of Chicago Medical Ctr. (United States); Adam M. Alessio, Michael D. Bindschadler, Univ. of Washington (United States); Patrick J. La Rivière, The Univ. of Chicago Medical Ctr. (United States)

There is a strong need for an accurate and available technique for myocardial blood flow (MBF) estimation to aid in the diagnosis and treatment of coronary artery disease (CAD). Dynamic CT could provide a quick and widely available technique to do so. However, its biggest limitation is the dose imparted to the patient. We are exploring techniques to reduce the patient dose by either reducing the photon flux or by reducing the number of temporal frames in the dynamic CT sequence. Both of these dose reduction techniques result in very noisy data. In order to extract the myocardial blood flow information from the noisy sinograms, we have been looking at several data-domain smoothing techniques. In our previous work, we explored sinogram restoration techniques in both the spatial and temporal domains. In this work, we explore the use of Karhunen-Loeve (KL) transform to provide temporal

smoothing in the sinogram domain. This technique has been applied previously to dynamic image sequences in PET. We apply this technique separately to various clusters in the sinogram domain, sharing the same temporal variation. We find that the cluster-based KL transform method reduced the root mean square error in simulated time attenuation curves across a range of flow states by an average of about 35% for reduced time sampling. We will apply several quantitative blood flow models to estimate MBF from these TACs and determine which smoothing method provides the most accurate and precise MBF estimates.

9034-72, Session PSMon

#### Implementation of compressive sensing for preclinical cine-MRI

Elliot Tan, Princeton Univ. (United States); Ming Yang, Univ. of Missouri, Dept. of Radiology, Nuclear Science and Engineering Institute (United States) and Harry S. Truman Veterans Hospital (United States); Lixin Ma, Univ. of Missouri-Columbia, Dept. of Radiology, Nuclear Science and Engineering Institute (United States) and Harry S. Truman Veteran Hospital (United States); Yahong R. Zheng, Missouri Univ. of Science and Technology (United States)

This paper presents a practical implementation of Compressive Sensing (CS) for a preclinical MRI machine to acquire randomly undersampled k-space data in cardiac function imaging applications. First, random undersampling masks were generated based on Gaussian, Cauchy, wrapped Cauchy and von Mises probability distribution functions by the inverse transform method. The best masks for undersampling ratios of 0.3, 0.4 and 0.5 were chosen for animal experimentation, and were programmed into a Bruker Avance III BioSpec 7.0T MRI system through method programming in ParaVision. Three undersampled mouse heart datasets were obtained using a fast low angle shot (FLASH) sequence, along with a control undersampled phantom dataset. ECG and respiratory gating was used to obtain high quality images. After CS reconstructions were applied to all acquired data, resulting images were quantitatively analyzed using the performance metrics of reconstruction error and Structural Similarity Index (SSIM). The comparative analysis indicated that CS reconstructed images from MRI machine undersampled data were indeed comparable to CS reconstructed images from retrospective undersampled data, and that CS techniques are practical in a preclinical setting. The implementation achieved 2 to 4 times acceleration for image acquisition and satisfactory quality of image reconstruction.

9034-73, Session PSMon

#### Analytic heuristics for a fast DSC-MRI

Marco Virgulin, Marco Castellaro, Fabio Marcuzzi, Enrico Grisan, Univ. degli Studi di Padova (Italy)

Hemodynamics of the human brain may be studied with Dynamic Susceptibility Contrast MRI (DSC-MRI) imaging. The sequence of volumes obtained exhibits a strong spatiotemporal correlation, that can be exploited to predict which measurements will bring mostly the new information contained in the next frames.

In general, the sampling speed is an important issue in many applications of the MRI, so that the focus of many current researches is to study methods to reduce the number of measurement samples needed for each frame without degrading the image quality. For the DSC-MRI, the frequency under-sampling of single frame can be exploited to make more frequent space or time acquisitions, thus increasing the time resolution and allowing the analysis of fast dynamics not yet observed.

Generally (and also for MRI), the recovery of sparse signals has been achieved by Compressed Sensing (CS) techniques, which are based on statistical properties rather than deterministic ones..











By studying analytically the compound Fourier+Wavelet transform, involved in the processes of reconstruction and sparsification of MR images, we propose a deterministic technique for a rapid-MRI, exploiting the relations between the wavelet sparse representation of the recovered and the frequency samples.

We give results on artificial phantoms with and without added noise, showing the superiority of the methods both with respect to classical Iterative Hard Thresholding (IHT) and to Location Constraint Approximate Message Passing (LCAMP) reconstruction algorithms.

9034-74, Session PSMon

## Resolving complex fiber architecture by means of sparse spherical deconvolution in the presence of isotropic diffusion

Oleg V. Michailovich, Quan Zhou, Univ. of Waterloo (Canada); Yogesh Rathi, Harvard Medical School, Brigham and Women's Hospital (United States)

As compared to more traditional diffusion tensor imaging (DTI), high angular resolution diffusion imaging (HARDI) is capable of resolving the orientations of crossing and branching neural fibre tracts in the brain. HARDI data is collected over a single spherical shell in the q-space, and is usually used as an input to q-ball imaging (QBI) which, in turn, provides estimation of the diffusion orientation distribution functions (ODFs). Unfortunately, the nature of single-shell sampling imposes limitations on the accuracy with which the ODFs can be recovered. As a result, the estimated ODFs may not always possess sufficient resolution to reveal the orientations of fibre tracts crossing each other at acute angles. A possible solution to the problem of limited resolution of QBI is provided by means of spherical deconvolution (SD). Even though SD methods are capable to yield high-resolution reconstructions over spatial locations corresponding to white matter, such methods tend to become unstable when applied to anatomical regions dominated by isotropic diffusion (as it is the case, e.g., in grey matter). To resolve this problem, in this paper, a new deconvolution approach is proposed, which takes advantage of a bounded variation assumption on the isotropic component of cerebral

Apart from being uniformly stable across the whole brain, the proposed method allows one to quantify the isotropic component of cerebral diffusion, which is known to be a useful diagnostic measure by itself.

9034-75, Session PSMon

### Adaptive multi-scale total variation minimization filter for low dose CT imaging

Alexander A. Zamyatin, Toshiba Medical Research Institute USA (United States); Gene Katsevich, Princeton Univ. (United States); Roman Krylov, Univ. of Central Florida (United States); Bibo Shi, Ohio Univ. (United States); Zhi Yang, Toshiba Medical Research Institute USA (United States)

Total Variation (TV) minimization is a well known technique in image processing for image denoising. It has been used in Computed Tomography (CT) imaging, but its use for diagnostic purposes has been very limited because TV processed images are perceived as "plastic" or "unnatural". In this work we revisit the TV filter and propose an improved version that is tailored to diagnostic CT purposes. (1) We revise the TV cost function, which results in symmetric gradient function that leads to more natural noise texture. (2) We apply a multi-scale approach to resolve noise grain issue in CT images. Note that image noise grain is determined by a fixed detector element size, and zoomed images have larger noise grain than full FOV images. (3) We discuss potential acceleration by Nesterov and Conjugate Gradient methods. We perform a thorough image quality evaluation with 20 clinical datasets corresponding to

different body parts, using both visual inspection and quantitative image quality metrics.

9034-76, Session PSMon

### Semi-supervised clustering for parcellating brain regions based on resting state fMRI data

Hewei Cheng, Yong Fan, Institute of Automation (China)

Many unsupervised clustering techniques have been adopted for parcellating the brain into functionally homogeneous region to better understand the functional neuroanatomy based on resting state fMRI data, including Gaussian mixture model (GMM), k-means, hierarchical clustering, and spectral clustering. However, the unsupervised clustering techniques are not able to take advantage of exiting knowledge about the functional neuroanatomy obtained from studies of cytoarchitectonic parcellation or meta-analysis of the literature. In this study, we propose a semi-supervised clustering method for parcellating amygdala into functionally homogeneous subregions based on resting state fMRI data. Particularly, the semi-supervised clustering is implemented as a graph partition problem by modeling each voxel as one node of the graph and connecting each pair of voxels with an edge weighted by a similarity measure between their functional signals. In the graph partition, a cytoarchitectonic parcellation result of amygdala is adopted as prior information and a spatial consistent constraint is adopted as a regularization term to achieve spatially contiguous clustering. The graph partition problem is solved using an efficient algorithm similar to the well-known weighted kernel k-means algorithm. Our method has been validated for the parcellation of amygdala with three subregions for 28 subjects based on their resting state fMRI data. The experiment results indicate that the proposed method could parcellate the amygdala into centromedial (CM), laterobasal (LB) and superficial (SF) parts with improved functionally homogeneity. The distinct structural connectivity patterns of these subregions, derived from diffusion tensor MR imaging (dMRI) data, further demonstrated the validity of the parcellation results.

9034-77, Session PSMon

## Sparse and shrunken estimates of MRI networks in the brain and their influence on network properties

Rafael Romero-Garcia, Univ. Pablo de Olavide (Spain); Line H. Clemmensen, Technical Univ. of Denmark (Denmark)

Morphometric relationships between cortical regions is a widely used approach to identify and characterize structural connectivity. The elevated number of regions that can be considered in a whole-brain correlation analysis might lead to overfitted models that can be controlled by using regularization methods. We found that, as expected, nonregularized correlations had low variability when a scarce number of variables were considered. However, a slight increase of variables led to an increase of variance of several magnitude orders. On the other hand, the regularized approaches showed more stable results with a relative low variance at the expense of a little bias. Interestingly, topological properties as local efficiency estimated in networks constructed from traditional non-regularized correlations also showed higher variability when compared to those from regularized networks. Our findings suggest that a population-based connectivity study can achieve a more robust description of cortical topology through regularization of the correlation estimates. Four regularization methods were examined: Two with shrinkage, one with sparsity and one with both shrinkage and sparsity. Furthermore, the different regularizations resulted in different correlation estimates as well as network properties. The shrunken estimates resulted in lower variance of the estimates than the sparse estimates.











9034-78, Session PSMon

#### Frequency-selective quantification of skin perfusion behavior during allergic testing using photoplethysmography imaging

Nikolai Blanik, RWTH Aachen (Germany); Claudia Blazek, Kantonsspital Aarau AG (Switzerland); Carina B. Pereira, Vladimir Blazek, Steffen Leonhardt, RWTH Aachen (Germany)

The diagnosis of allergic immediate-type reactions is dependent on the visual assessment of the attending physician. With our novel non-obtrusive, camera-based Photoplethysmography Imaging (PPGI) setup, the perfusion in the allergic testing area can be quantified and the results be displayed with spatial resolution in functional mappings. Thereby, each PPGI camera pixel can be assumed as a classical skin attached reflective mode PPG sensor. An algorithm for post-processing of collected PPGI video sequences was developed to transfer blackand-white PPGI images in to virtual 3D perfusion maps. For the first time, frequency selected perfusion quantification was assessed. For the presented study we use PPGI data, collected in a first clinical study [1]. For this purpose, different concentrations of histamine dilutions are administered on 27 healthy volunteers. Our results shows clear trends in an increase of heart beat synchronous perfusion rhythms and parallel, a decrease of lower frequency vasomotor rhythms in these areas. The presented results, publish for the first time, allow new insights in the distribution of skin perfusion dynamics and demonstrate the intuitive clinical usability of the proposed system.

9034-79, Session PSMon

#### Characterizing human retinotopic mapping with conformal geometry: a preliminary study

Duyan Ta, Arizona State Univ. (United States); Brian Barton, Alyssa Brewer, Univ. of California, Irvine (United States); Zhong-Lin Lu, The Ohio State Univ. (United States); Jie Shi, Yalin Wang, Arizona State Univ. (United States)

Functional magnetic resonance imaging (fMRI) has been widely used to measure the retinotopic organization of early visual cortex in the human brain. Previous studies have identified multiple visual field maps (VFMs) based on statistical analysis of fMRI signals, but the resulting geometry has not been fully characterized with mathematical models. Here we test whether VFMs V1 and V2 obey the least restrictive of all geometric mappings; that is, whether they are angle-preserving and therefore maintain conformal mapping. We measured retinotopic organization in individual subjects using standard traveling-wave fMRI methods. Visual stimuli consisted of black and white, drifting checkerboards comprising rotating wedges and expanding rings to measure the cortical representations of polar angle and eccentricity, respectively. These representations were then projected onto a 3D cortical mesh of each hemisphere. By generating a mapped unit disk that is conformal of the VFMs using spherical stereographic projection and computing the parameterized coordinates of the eccentricity and polar angle gradients, we computed Beltrami coefficients to check whether the mapping from the visual field to the V1 and V2 cortical representations is conformal. We find that V1 and V2 exhibit local conformality. Our analysis of the Beltrami coefficient shows that selected regions of V1 and V2 that contain reasonably smooth eccentricity and polar angle gradients do show significant local conformality, warranting further investigation of this approach for analysis of early and higher visual cortex. These results suggest that such a mathematical model can be used to characterize the early VFMs in human visual cortex.

9034-80, Session PSMon

#### Fusion of digital breast tomosynthesis images via wavelet synthesis for improved lesion conspicuity

Harishwaran Hariharan, Victor V. Pomponiu, Univ. of Pittsburgh (United States); Bin Zheng, The Univ. of Oklahoma (United States); Bruce R. Whiting, David Gur, Univ. of Pittsburgh (United States)

Full-field digital mammography (FFDM) is the most common screening procedure for detecting early breast cancer. However, due to complications such as overlapping breast tissue in projection images, the efficacy of FFDM reading is reduced. Recent studies have shown that digital breast tomosynthesis (DBT), in combination with FFDM, increases detection sensitivity considerably while decreasing false-positive, recall rates. There is a huge interest in creating diagnostically accurate 2-D interpretations from the DBT slices. Most of the 2-D syntheses rely on visualizing the maximum intensities (brightness) from each slice through different methods. We propose a wavelet based fusion method, where we focus on preserving holistic information from larger structures such as masses while adding high frequency information that is relevant and helpful for diagnosis. This method enables the spatial generation of a 2D image from a series of DBT images, each of which contains both smooth and coarse structures distributed in the wavelet domain. We believe that the wavelet-synthesized images, generated from their DBT image datasets, provide radiologists with improved lesion and microcalcification conspicuity as compared with FFDM images. The potential impact of this fusion method is (1) Conception of a device-independent. data-driven modality that increases the conspicuity of lesions, thereby facilitating early detection and potentially reducing recall rates; (2) Reduction of the accompanying radiation dose to the patient.

9034-81, Session PSMon

#### Combination of graph theoretic grouping and time-frequency analysis for image segmentation with an example for EDI-OCT

Rahele Kafieh, Hossein Rabbani, Isfahan Univ. of Medical Sciences (Iran, Islamic Republic of)

We introduce a nonparametric approach to multiscale segmentation of images using a hierarchical matrix analysis framework called diffusion wavelets that tries to benefit from the advantages of both graph theory and wavelet transform. Till now a broad range of multiscale transforms like wavelets (and other x-lets) have been introduced for image segmentation task. Furthermore, graph theoretic formulation of grouping is also well-known to deal with this problem. The combination of multiscale transforms and graph based partitioning results in a scale-spectral method exploring through different scales of the image, over a great deal of spectral methods in graph partitioning. The method constructs multiscale basis functions and a series of dilation and orthogonalizations build a hierarchy, automatically. At each level, a set of basis functions is build by applying dyadic powers of a diffusion operator on the basis at the lower level. Two approaches are proposed for multiscale segmentation of images using diffusion wavelets. The first method is based on extended basis functions at each level and designing a competition between the basis value for partitioning. The second approach is defining a new distance for each level and clustering based on such distances. An example of application in Enhanced Depth Imaging Optical Coherence Tomography (EDI-OCT) is shown in this paper. The retinal structure containing inner, outer and choroidal layers of retina are segmented apart from the background by applying diffusion wavelet in a scale that produces 3 clusters.











9034-82, Session PSMon

### Smoothing fields of weighted collections with applications to diffusion MRI processing

Gunnar A. Sigurdsson, Jerry L. Prince, Johns Hopkins Univ. (United States)

Using modern diffusion weighted magnetic resonance imaging protocols, the orientations of multiple neuronal fiber tracts within each voxel can be estimated. Further analysis of these populations, including application of fiber tracking and tract segmentation methods, is often hindered by lack of spatial smoothness of the estimated orientations. For example, a single noisy voxel can cause a fiber tracking method to switch tracts in a simple crossing tract geometry. In this work, a generalized spatial smoothing framework that handles multiple orientations as well as their fractional contributions within each voxel is proposed. The approach estimates an optimal fuzzy correspondence of orientations and fractional contributions between voxels and smooths only between these correspondences. Avoiding a requirement to obtain exact correspondences of orientations reduces smoothing anomalies due to propagation of erroneous correspondences around noisy voxels. Phantom experiments are used to demonstrate both visual and quantitative improvements in postprocessing steps. Improvement over smoothing in the measurement domain is also demonstrated using both phantoms and in vivo human data.

9034-84, Session PSMon

## Image restoration using the total variational deconvolution in optical coherence tomography

Kuanhong Xu, Qiang Wang, Xiaotao Wang, Ping Guo, Haibing Ren, Samsung Advanced Institute of Technology (China); Jaeguyn Lim, Woo-Young Jang, Samsung Advanced Institute of Technology (Korea, Republic of)

Optical coherence tomography has been a new medical imaging instrument with high sensitivity and resolution and has been applied in a wide variety of applications. The OCT signals are the convolution between the impulse response of the samples and the depth point spread function (PSF); nevertheless, the signals are readily distorted by the depth PSF because of the finite width and the non-Gaussian shape envelope of the light source. Although the traditional deconvolution technique can compensate for this distortion, the noise existing in the signals will lead to ill-posedness problem in deconvolution process, which means that in this case the deconvolution result will be far away from the ideal values. In this paper, we develop an OCT image restoration approach using the joint deconvolution and noise reduction. The deconvolution is solved as an inverse problem and the total variation (TV) is introduced as a regularization to overcome the ill-posedness problem and reduce the noise. This inverse problem is solved using the Split Bregman method, which has been demonstrated to be an efficient tool to solve total variation norm minimization problems. Our algorithm can eliminate the distortion of the convolution and reduce the noise concurrently. Compared with the latest image restoration experimental results in OCT (Jun Ke, Biomedical Optics Express, 2012), our algorithm can achieve better image restoration results and the speed is nearly 700 times faster than Ke's algorithm (3 s/frame vs 2066 s/frame, image size 512\*512, Matlab code, Intel(r) Core(TM) i3 CPU 550 @ 3.20 GHz).

9034-85, Session PSMon

### Non-local total variation method for despeckling of ultrasound images

Jianbin Feng, Mingyue Ding, Xuming Zhang, Huazhong Univ. of Science and Technology (China)

Despeckling of ultrasound images, as a very active topic research in medical image processing, plays an important or even indispensable role in subsequent ultrasound image processing. The non-local total variation (NLTV) method has been widely applied to denoising images corrupted by Gaussian noise, but it cannot provide satisfactory restoration results for ultrasound images corrupted by speckle noise. To address this problem, a novel non-local total variation despeckling method is proposed for speckle reduction. In the proposed method, the non-local gradient is computed on the images restored by the optimized Bayesian non-local means (OBNLM) method and it is introduced into the total variation method to suppress speckle in ultrasound images. Comparisons of the restoration performance are made among the proposed method and such state-of-the-art despeckling methods as the squeeze box filter (SBF), the non-local means (NLM) method and the OBNLM method. The quantitative comparisons based on synthetic speckled images show that the proposed method can provide higher peak signal-to-noise ratio (PSNR) and structure similarity (SSIM) than compared despeckling methods. The subjective visual comparisons based on synthetic and real ultrasound images demonstrate that the proposed method outperforms other compared algorithms in that it can achieve better performance of noise reduction, artifact avoidance, edge and texture preservation.

9034-86, Session PSMon

## Stent enhancement using a locally adaptive unsharp masking filter in digital X-ray fluoroscopy

Yuhao Jiang, Eranda Ekanayake, Univ. of Central Oklahoma (United States)

Low exposure X-ray fluoroscopy is used to guide some complicate interventional procedures. Due to the inherent high levels of noise, improving the visibility of some interventional devices such as stent will greatly benefit those interventional procedures. Stent, which is made up of tiny steel wires, is also suffered from contrast dilutions of large flat panel detector pixels. A novel adaptive unsharp masking filter has been developed to improve stent contrast in real-time applications. In unsharp masking processing, the background is estimated and subtracted from the original input image to create a foreground image containing objects of interest. A background estimator is therefore critical in the unsharp masking processing. In this specific study, orientation filter kernels are used as the background estimator. To make the process simple and fast, the kernels average along a line of pixels. A high orientation resolution of 18? is used. A nonlinear operator is then used to combine the information from the images generated from convolving the original background and noise only images with orientation filters. A computerized Monte Carlo simulation followed by ROC study is used to identify the best nonlinear operator. We then apply the unsharp masking filter to the images with stents present. It is shown that the locally adaptive unsharp making filter is an effective filter for improving stent visibility in the interventional fluoroscopy. We also apply a spatio-temporal channelized human observer model to quantitatively optimize and evaluate the filter.











9034-87, Session PSMon

### A local technique for contrast preserving medical image enhancement

Suresh R. Pant, Deepak Ghimire, Keunho Park, Joonwhoan Lee, Chonbuk National Univ. (Korea, Republic of)

The main objective of the contrast enhancement is to improve some characteristics of an image. The local contrast enhancement of medical image, preserving the local detail is useful and important to the medical diagnosis. Histogram equalization is widely used for contrast enhancement. However it tends to change the brightness of an image and hence not suitable for images where preserving the original brightness is essential. Contrast Limited Adaptive Histogram Equalization (CLAHE) computes several histograms corresponding to the distinct section of the image. CLAHE limits the amplification by clipping the histogram at a predefined value before computing the cumulative distribution function (CDF). The over-enhancement may cause the clinical information loss and increase the gain of local noise. The local image contrast preserving dynamic range compression method preserve local image contrast based on luminance ratio of pixel to its local surround. This paper presents a method that incorporates CLAHE and local image contrast preserving dynamic range compression. The proposed method controls the amplification while preserving the local contrast of the image. The range of the gain parameter for local contrast enhancement varies from one image to another. The local contrast enhancement at any pixel position depends on the corresponding pixel neighborhood edge density. We have performed several experiments based on different image quality measures. Our proposed method provides more information about the image detail which affects the medical diagnosis. The experimental results by different image quality measures show that the output image quality of our proposed method is better than the CLAHE output.

9034-88, Session PSMon

## Robust isotropic super-resolution by maximizing a Laplace posterior for MRI volumes

Xian-Hua Han, Yutaro Iwamoto, Ritsumeikan Univ. (Japan); Akihiko Shiino, Shiga Univ. of Medical Science (Japan); Yen-Wei Chen, Ritsumeikan Univ. (Japan)

Magnetic resonance imaging can only acquire volume data with finite resolution due to various factors. In particular, the resolution in one direction (such as the slice direction) is much lower than others (such as the in-plane direction), yielding un-realistic visualizations. This study explores to reconstruct MRI isotropic resolution volumes from three orthogonal scans. This proposed super-resolution reconstruction is formulated as a maximum a posterior (MAP) problem, which relies on the generation model of the acquired scans from the unknown high-resolution volumes. Generally, the deviation ensemble of the reconstructed high-resolution (HR) volume from the available LR ones in the MAP is represented as a Gaussian distribution, which usually results in some noise and artifacts in the reconstructed HR volume. Therefore, this paper investigates a robust super-resolution by formulating the deviation set as a Laplace distribution, which assumes sparsity in the deviation ensemble based on the possible insight of the appeared large values only around some unexpected regions. In addition, in order to achieve reliable HR MRI volume, we integrates the priors such as bilateral total variation (BTV) and non-local mean (NLM) into the proposed MAP framework for suppressing artifacts and enriching visual detail. We validate the proposed robust SR strategy using MRI mouse data with high-definition resolution in two direction and low-resolution in one direction, which are imaged in three orthogonal scans: axial, coronal and sagittal planes. Experiments verifies that the proposed strategy can achieve much better HR MRI volumes than the conventional MAP method even with very high-magnification factor.

9034-89, Session PSMon

# New multiscale speckle suppression and edge enhancement with nonlinear diffusion and homomorphic filtering for medical ultrasound imaging

JinBum Kang, Yangmo Yoo, Sogang Univ. (Korea, Republic of)

Speckle, shown as a granular pattern, considerably degrades the image quality of ultrasound B-mode imaging and lowers the performance of image segmentation and registration techniques. Thus, speckle reduction while preserving the tissue structure (e.g., edges and boundaries of lesions) is essential for ultrasound B-mode imaging. In this paper, a new approach for speckle reduction and edge enhancement based on laplacian pyramid nonlinear diffusion and homomorphic filtering (LPNDHF) is proposed for ultrasound B-mode imaging. In LPNDHF, nonlinear diffusion with a weighting factor is applied in multi-scale domain (i.e., laplacian pyramid) for effectively suppressing the speckle. In addition, in order to overcome the drawback from the previous LPND method, i.e., blurred edges, homomorphic filtering for edge and contrast enhancement is applied from a finer scale to a coarser scale. From the simulation study, the proposed LPNDHF method showed the higher edge preservation and structure similarity values compared to the LPND and LPND with shock filtering (LPNDSF). Also, the LPNDHF provided the higher CNR values compared to LPND and LPNDSF, i.e., 5.02 vs. 3.66 and 2.91, respectively. From the tissue mimicking phantom study, the similar improvement in CNR was achieved from the LPNDHF over LPND and LPNDSF, i.e., 2.35 vs. 1.83 and 1.30. Similarly, the consistent result was obtained with the in vivo abdominal study. These preliminary results demonstrate that the proposed LPNDHF can improve the image quality of ultrasound B-mode imaging by increasing contrast and enhancing the specific signal details by effectively suppressing speckle.

9034-90, Session PSMon

## Magnetic resonance and computed tomography fusion using improved guided filter

Amina Jameel, Abdul Ghafoor, Muhammad Mohsin Riaz, National Univ. of Sciences and Technology (Pakistan)

Improved guided fusion for magnetic resonance and computed tomography imaging is proposed. Medical images are usually of low quality due to noise artifacts. Especially the Magnetic resonance images are often corrupted by Rician noise which results in random fluctuations and reduced contrast. Existing guided filtering scheme uses Gaussian filter and two level weight maps, due to which the scheme has limited performance for noisy medical images. Gaussian filter is not suitable for Rician noise removal, hence is replaced by linear minimum mean square error estimator based filter, consequently improving the fused image quality. The main issue with binary weight assignment (in existing guided fusion scheme) arises when different images have approximately equal saliency values. In such cases, one value is totally discarded, which results in degraded fused image. Furthermore, for noisy Magnetic resonance images, the saliency value may be higher at a pixel due to noise; in that case the noisy value will be selected (which is not desirable). Multiple level weight maps are proposed to ensure that maximum information is transferred to the fused image. The proposed scheme overall produces better fusion results and minimize the inherited noise effects. Simulation results based on visual analysis and variety of quantitative measure show the significance of proposed scheme.











9034-91, Session PSMon

#### Evaluating the predictive power of multivariate tensor-based morphometry in Alzheimer's disease progression via convex fused sparse group Lasso

Sinchai Tsao, The Univ. of Southern California (United States); Niharika Gajawelli, Univ of Southern California (United States); Jiayu Zhou, Jie Shi, Jieping Ye, Yalin Wang, Arizona State Univ. (United States); Natasha Lepore, The Univ. of Southern California (United States)

Tensor-based morphometry (TBM) usually involves a non-linear image registration between multiple subjects and a global tem-plate. The deformations from this operation allow us to detect regional changes in brain volume or surface in a cohort. TBM has been extensively applied in neuroimaging field for disease burden identification, correlation with other imaging biomarkers and disease classification. Past work on TBM or multivariate TBM (mTBM) has shown that these features when applied to the cortical surface outperforms standard volumetric or other features when used for disease diagnosis. However, there is not much work on its statistical power for disease progression research. Previous work by Zhou et al. 2013 has shown that a multi-task learning framework can be used to encode both sparsity as well as temporal smoothness in predicting cognitive outcomes of Alzheimer's Disease Neu-roimaging Initiative (ADNI) subjects based on MRI baseline features as well as other biological information from these subjects. In this work, we combine this multi-task framework with a novel mTBM applied on to hippocampal surface to improve the prediction performance of cognitive scores 6, 12, 24, 36 and 48 months from baseline. We also assess the pre-dictive power of these novel features relative to existing imaging-based features provided by FreeSurfer as well as non-imaging features such as age, sex, baseline test scores and genetic information. We have achieved encouraging results, which show the great potential of TBM for disease progression research.

9034-92, Session PSMon

### Recognizing patterns of visual field loss using unsupervised machine learning

Siamak Yousefi, Michael H. Goldbaum M.D., Linda M. Zangwill, Univ. of California, San Diego (United States); Felipe A. Medeiros, Univ. of California at San Diego (United States); Christopher Bowd, Univ. of California, San Diego (United States)

Glaucoma is a potentially blinding optic neuropathy that results in a decrease in visual sensitivity. Visual field abnormalities (decreased visual sensitivity on psychophysical tests) are the primary means of glaucoma diagnosis. One form of visual field testing is Frequency Doubling Technology (FDT) that tests sensitivity at 52 points within the visual field. Like other psychophysical tests used in clinical practice, FDT results yield specific patterns of defect indicative of the disease. We used Gaussian Mixture Model with Expectation Maximization (GMM-EM), (EM is used to estimate the model parameters) to automatically separate FDT data into clusters of normal and abnormal eyes. Principal component analysis (PCA) was used to decompose each cluster into different axes (patterns).

FDT measurements were obtained from 1,190 eyes with normal FDT results and 786 eyes with abnormal (i.e., glaucomatous) FDT results, recruited from a university-based, longitudinal, multi-center, clinical study on glaucoma. The GMM-EM input was the 52-point FDT threshold sensitivities for all eyes.

The optimal GMM-EM model separated the FDT fields into 3 clusters. Cluster 1 contained 94% normal fields (94% specificity) and clusters 2 and 3 combined, contained 77% abnormal fields (77% sensitivity). For clusters 1, 2 and 3 the optimal number of PCA-identified axes were 2, 2 and 5, respectively.

GMM-EM with PCA successfully separated FDT fields from healthy and glaucoma eyes and identified familiar glaucomatous patterns of loss.

9034-93, Session PSMon

## False positive reduction of microcalcification cluster detection in digital breast tomosynthesis

Ning Xu, Univ. of Illinois at Urbana-Champaign (United States) and GE Global Research (United States); Sheng Yi, Paulo Mendonca, Tai-peng Tian, GE Global Research (United States); Ravi K. Samala, Heang-Ping Chan, Univ. of Michigan Health System (United States)

Digital breast tomosynthesis (DBT) is a new modality that has strong potential in improving the sensitivity and specificity of breast mass detection. However, the detection of microcalcifications (MCs) in DBT is challenging because radiologists have to search for the often subtle signals in many slices. We are developing a computer-aided detection (CAD) system to assist radiologists in reading DBT. The system consists of four major steps, namely: image enhancement; pre-screening of MC candidates; false-positive (FP) reduction, and detection of MC clusters candidates of clinical interest. We propose an algorithm for reducing FP by using 3D characteristics of MC clusters in DBT. The proposed method takes the MC candidates from the pre-screening step as input, which are then iteratively clustered to provide training samples to a random-forest classifier and a rule-based classifier. The random-forest classifier is used to learn a discriminative model of MC clusters using 3D texture features, whereas the rule-based classifier revisits the initial training samples and enhances them by combining median filtering and graph-cut-based segmentation followed by thresholding on the final number of MCs belonging to the candidate cluster. The outputs of these two classifiers are combined according to the prediction confidence of the randomforest classifier. We evaluate the proposed FP-reduction algorithm on a data set of two-view DBT from 40 breasts with biopsy-proven MC clusters. The initial MC candidates were detected in a prescreening stage. The experimental results demonstrate a significant reduction in FP detections, with a final sensitivity of 92.2% for a FP rate of 50%.

9034-94, Session PSMon

# Unsupervised nonlinear dimensionality reduction machine learning methods applied to multiparametric MRI in cerebral ischemia: preliminary results

Vishwa S. Parekh, Jeremy R. Jacobs, Michael A. Jacobs, Johns Hopkins Univ. (United States)

The evaluation and treatment of acute cerebral ischemia requires a technique that can determine the total area of tissue at risk for infarction using diagnostic magnetic resonance imaging (MRI) sequences. Typical MRI data sets consist of T1- and T2-weighted imaging (T1WI, T2WI) along with advanced MRI parameters of diffusion-weighted imaging (DWI) and perfusion methods. Each of these parameters has distinct radiological-pathological meaning. For example, DWI interrogates the movement of water in the tissue and perfusion gives an estimate of the blood flow, both are critical measures during stroke. In order to integrate these data and give an estimate of the tissue damage, we have developed advanced machine learning methods based on unsupervised non-linear dimensionality reduction (NLDR) techniques. NLDR methods are a class of algorithms that uses mathematically defined manifolds for statistical sampling of multidimensional classes to generate a discrimination rule of guaranteed statistical accuracy and they can generate a two- or three-dimensional map, which represents the prominent structures of the data and provides an embedded image of











meaningful low-dimensional structures hidden in their high-dimensional observations. In this manuscript, we develop NLDR methods on high dimensional MRI data sets of a group of preclinical animals and patients with stroke. On analyzing the performance of these methods, we observed that there was a high of similarity between multi-parametric embedded and the ADC map and perfusion map. It was also observed that embedded scattergram of abnormal (infarcted or at risk) tissue can be visualized and provides a mechanism for automatic methods to delineate potential stroke volumes and early tissue at risk.

9034-96, Session PSMon

### On study design in neuroimaging heritability analyses

Mary E. Koran, Bo Li, Vanderbilt Univ. (United States); Neda Jahanshad, Univ. of California, Los Angeles (United States); Tricia A. Thornton-Wells, Vanderbilt Univ. (United States); David C. Glahn, Yale Univ. (United States); Paul M. Thompson, Univ. of California, Los Angeles (United States); John Blangeroe, Texas Biomedical Research Institute (United States); Thomas E. Nichols, The Univ. of Warwick (United Kingdom); Peter Kochunov, Maryland Psychiatric Research Ctr. (United States); Bennett A. Landman, Vanderbilt Univ. (United States)

Imaging genetics is an emerging methodology that combines genetic information with imaging-derived metrics to understand how genetic factors impact observable structural, functional, and quantitative phenotypes. Many of the most well-known genetic studies are based on Genome-Wide Association Studies (GWAS), which use large populations of related or unrelated individuals to associate traits such as disorders with individual genetic factors. Merging imaging and genetics may potentially lead to improved power of association because imaging traits may be more sensitive phenotypes, being closer to underlying genetic mechanisms. We are developing SOLAR-ECLIPSE (SE) imaging genetics software. SE is capable of performing genetic analysis in the pedigrees of random complexity. Importantly, it estimates a traditional additive genetic model including calculation of phenotypic variability that is explained by the genetic commonality among subjects. The central factor of interest, known as heritability, offers bounds on the direct genetic influence over observed phenotypes. In order for a trait to be a good phenotype for GWAS, at least some proportion of its variance must be due to genetic influences, and therefore it must be heritable. Different family structures are most commonly used for estimating heritability yet the variability and biases for each as a function of the sample size are unknown. Herein, we investigate heritability models based on simulated imaging data. Specifically, we use Monte Carlo methods to characterize the bias and the variability of heritability as a function of sample size and pedigree structure (including twins, siblings, nuclear families, and nuclear families with grandparents).

9034-98. Session PSMon

### Determination of the intervertebral disc space from CT images of the lumbar spine

Robert Korez, Univ. of Ljubljana (Slovenia); Darko Stern, Graz Univ. of Technology (Austria); Boštjan Likar, Franjo Pernuš, Univ. of Ljubljana (Slovenia); Tomaž Vrtovec, Univ. of Ljubljana (Slovenia)

Degenerative changes of the intervertebral disc are among the most common causes of low back pain, where for individuals with significant symptoms surgery may be needed. One of the interventions is the total disc replacement surgery, where the degenerated disc is replaced by an artificial implant. For designing implants with good bone contact and continuous force distribution, the morphology of the intervertebral disc

space and vertebral body endplates is of considerable importance. In this study we propose a method for the determination of the intervertebral disc space from three-dimensional (3D) computed tomography (CT) images of the lumbar spine. The first step of the proposed method is the construction of a model of vertebral bodies in the lumbar spine. For this purpose, a chain of five elliptical cylinders is initialized in the 3D image and then deformed to resemble vertebral bodies by introducing 25 shape parameters. The parameters are obtained by aligning the chain to the vertebral bodies in the CT image according to image intensity and appearance information. The determination of the intervertebral disc space is finally achieved by finding the planes that fit the endplates of the obtained parametric 3D models, and placing points in the space between the planes of adjacent vertebrae that enable surface reconstruction of the intervertebral disc space. The morphometric analysis of images from 20 subjects yielded 11.3  $\pm$  2.6, 12.1  $\pm$  2.4, 12.8  $\pm$  2.0 and 12.9  $\pm$  2.7 cm<sup>3</sup> in terms of L1-L2, L2-L3, L3-L4 and L4-L5 intervertebral disc space volume, respectively.

9034-99, Session PSMon

### Blood flow quantification using 1D CFD parameter identification

Richard Brosig, Technische Univ. München (Germany); Markus Kowarschik, Siemens AG (Germany); Peter Maday, Amin Katouzian, Stefanie Demirci, Nassir Navab, Technische Univ. München (Germany)

Patient-specific measurements of cerebral blood flow provide valuable diagnostic information concerning cerebrovascular diseases rather than visually driven qualitative evaluation.

In this paper, we present a quantitative method to estimate blood flow parameters with high temporal resolution from digital subtraction angiography (DSA) image sequences.

Using a 3D DSA dataset and a 2D+t DSA sequence, the proposed algorithm employs a 1D Computational Fluid Dynamics (CFD) model for estimation of time-dependent flow values along a cerebral vessel, combined with an additional Advection Diffusion Equation (ADE) for contrast agent propagation.

A CFD system, followed by an ADE is solved with a finite volume approximation, which ensures the conservation of mass.

Instead of defining a new imaging protocol to obtain relevant data, our cost function optimizes the bolus arrival time (BAT) of the contrast agent in 2D+t DSA sequences.

The visual determination of BAT is common clinical practice and can be easily derived from and be compared to values, generated by a 1D-CFD simulation.

Using this strategy, we ensure that our proposed method fits best to clinical practice and does not require any changes to the medical workflow.

Synthetic experiments show that the recovered flow estimates match the ground truth values with less than 12% error in the mean flow rates.

9034-100, Session PSMon

## Arterial tree tracking from anatomical landmarks in magnetic resonance angiography scans

Alison O'Neil, Erin Beveridge, Toshiba Medical Visualization Systems Europe, Ltd. (United Kingdom); Graeme Houston, Lynne McCormick, Univ. of Dundee (United Kingdom); Ian Poole, Toshiba Medical Visualization Systems Europe, Ltd. (United Kingdom)











This paper reports on arterial tree tracking in 14 Contrast Enhanced MRA volumetric scans, given the positions of a pre-defined set of vascular landmarks, using an efficient variant of Dijkstra's Shortest Path algorithm to find the optimal path for each vessel based on voxel intensity and a learnt vascular probability atlas.

Following manual or automatic identification of all landmarks present in a scan, vessels are tracked independently in the following manner. Firstly, the scan is pre-processed using the top-hat transform with a cubic structuring element of size approximating the vessel diameter. Next Dijkstra's shortest path algorithm is run using a linear cost function based on a vascular probability atlas in conjunction with estimates of the vessel intensity and the degree of noise in the scan, found by intensity histogram analysis and Canny edge detection respectively. Finally, the path is centered using 2D contour analysis.

Tracking results are presented for all major arteries excluding those in the upper limbs. The results were validated by comparison with manually generated vessel center lines. The mean error was 1.7mm with a standard deviation of 0.88mm.

In conclusion, a method for vessel tracking has been developed which exploits the contextual information available when tracking between a pair of defined landmarks.

9034-101, Session PSMon

### Automated volumetric breast density derived by shape and appearance modeling

Serghei Malkov, Karla Kerlikowske, John A. Shepherd, Univ. of California, San Francisco (United States)

The image shape and texture (appearance) estimation designed for facial recognition is a novel and promising approach for application in breast imaging. The purpose of this study was to apply a shape and appearance model to automatically estimate percent fibroglandular volume (%FGV) using digital mammograms. We built a shape and appearance model using 2000 full-field digital mammograms from San Francisco Mammography Registry with known %FGV. An affine transformation was used to remove rotation, translation and scale. Principal Component Analysis (PCA) was applied to extract significant and uncorrelated components. To build an appearance model, we transformed the breast images into the mean texture image by piecewise linear image transformation. Using PCA the image pixels grey-scale values are converted into a reduced set of the shape and texture features. The stepwise regression with forward selection and backward elimination was used to estimate the outcome %FGV with shape and appearance features and other system parameters. The shape and appearance scores were found to correlate moderately to breast %FGV, dense tissue and actual volumes, BMI and age. The highest Pearson correlation coefficient was equal 0.77 for the first shape PCA component and actual breast volume. The stepwise regression method with ten-fold crossvalidation to predict %FGV from shape and appearance variables and other system outcome parameters generated a model with a correlation of r2 = 0.8. In conclusion, a shape and appearance model demonstrated excellent feasibility to extract variables useful for automatic %FGV estimation. Further exploring and testing of this approach is warranted.

9034-102, Session PSMon

### Multiple-model strategy improves sensitivity in automatic anatomy recognition via fuzzy models

Leticia Rittner, Univ. Estadual de Campinas (Brazil); Jayaram K. Udupa, Univ. of Pennsylvania (United States)

Computerized automatic anatomy recognition (AAR) is an essential step to make quantitative radiology a reality. Our strategy to automatically identify and delineate various organs in different given body regions is based on fuzzy models and an organ hierarchy. In previous years, the basic algorithms of our AAR methodology involving model building, object recognition and delineation were described and tested. In the present paper, we propose to replace the single fuzzy model built for each organ by a set of models built for the same organ. Based on a dataset composed of CT images of the Thorax region of 50 subjects and involving 11 organs, our experiments indicate that recognition performance improves when using multiple models compared to a single model for each organ.

9034-103, Session PSMon

## An artifact-robust technique for the automatic segmentation of the labyrinth in post-cochlear-implantation CT

Fitsum Akilu Reda, Jack H. Noble, Vanderbilt Univ. (United States); Robert F. Labadie M.D., Vanderbilt Univ. Medical Ctr. (United States); Benoit M. Dawant, Vanderbilt Univ. (United States)

A cochlear implant (CI) is a device that restores hearing using an electrode array that is surgically placed in the cochlea. After placement, the device is programmed to attempt to optimize hearing outcome. Currently, we are developing an image-guided CI programming (IGCIP) technique that relies on knowledge of the spatial relationship between the electrodes and internal structures of the cochlea. IGCIP is enabled by a number of algorithms we previously developed that permit determination of the positions of the electrodes relative to intra-cochlear anatomy using a pre- and a post-implantation CT. One issue with this technique is that it cannot be used for many subjects for whom a pre-implantation CT was not acquired. This is because it is difficult to localize the intra-cochlear structures in post-implantation CTs alone due to the image artifacts that obscure the cochlea in the image. We are currently developing a technique that can be used to localize the intra-cochlear structures even when no pre-implantation image is available. The approach we propose is to first identify the labyrinth and use its position as a landmark structure to estimate the position of the intra-cochlear anatomy. This article details the technique we have developed for the automatic segmentation of the labyrinth. We validated our method by segmenting post-implantation CTs of five bilateral CI recipients for whom a pre-implantation CT was available to provide a ground truth. Mean and maximum segmentation errors with our technique are 0.248 and 0.69 mm, respectively. These results indicate that our automatic method is accurate enough to be used for determining the position of the intra-cochlear anatomy using the labyrinth as a landmark structure, thereby allowing us to apply our IGCIP technique to individuals for whom no pre-implantation CT is available.

9034-104, Session PSMon

## Measurement of blood flow velocity in vivo video sequences with motion estimation methods

Yansong Liu, Rochester Institute of Technology (United States); Angela Glading, Univ. of Rochester (United States); Eli Saber, Maria Helguera, Rochester Institute of Technology (United States)

Measurement of blood flow velocity in vivo microscopy video is an approach for research of microcirculation system, which has been applied in clinic analysis and physiology study. The video sequence investigated in this paper utilizes standard video frame rate (30 frames/sec), therefore the accuracy and feasibility by using motion estimation methods need to be evaluated. We have investigated both current optical flow and particle image velocimety (PIV) techniques based on cross-correlation by applying both methods to simulated vessel images and in vivo microscopy video sequences. The estimated results from an in vivo video sequence are highly dependent on image structure,











therefore factors that affect the accuracy of each method are examined, including the width of the vessels, vascular structures and noise. The accuracy analysis is investigated by applying both methods to simulated vessel image sequences. The issue of spurious motion generated by microscopy video noise is addressed in this paper and its statistical distribution has been discussed. A temporal post-processing scheme is proposed to effectively reduce the noisy outlier vectors in the velocity field. By applying the iterative PIV algorithm and optical flow method, dense velocity fields therefore can be obtained. A new approach of region fitting window size cross-correlation method is proposed for overcoming the drawbacks of using fixed window size used in most PIV techniques. Limitations of applying motion estimation algorithms to standard microscopy video sequences are addressed and thoroughly discussed in terms of spurious noise, the effect of large displacement and vascular structures.

9034-105, Session PSMon

### Interpolation of longitudinal shape and image data via optimal mass transport

Yi Gao, Liangjia Zhu, The Univ. of Alabama at Birmingham (United States); Sylvain Bouix, Harvard Medical School (United States); Allen Tannenbaum, The Univ. of Alabama at Birmingham (United States)

Longitudinal analysis of medical imaging data has become central to the study of many disorders. Unfortunately, various constraints (study design, patient availability, technological limitations) restrict the acquisition of data to only a few time points, limiting the study of continuous disease/ treatment progression. Having the ability to produce a sensible time interpolation of the data can lead to improved analysis, such as intuitive visualizations of anatomical changes, or the creation of more samples to improve statistical analysis. In this work, we model interpolation of medical image data, in particular shape data, using the theory of optimal mass transport~(OMT), which can construct a continuous transition from two time points while preserving "mass" (e.g., image intensity, shape volume) during the transition. The theory even allows a short extrapolation in time and may help predict short-term treatment impact or disease progression on anatomical structure. We apply the proposed method to the hippocampus-amygdala complex in schizophrenia, the heart in atrial fibrillation, and full head MR images in traumatic brain injury.

9034-106, Session PSMon

## Respiratory motion variations from skin surface on lung cancer patients from 4D CT data

Nicolas Gallego, Jonathan Orban de Xivry, Antonin Descampe, Samuel Goossens, Univ. Catholique de Louvain (Belgium); Xavier Geets M.D., Cliniques Univ. Saint-Luc (Belgium); Guillaume Janssens, IBA SA (Belgium); Benoît M. Macq, Univ. Catholique de Louvain (Belgium)

In radiation therapy of thorax and abdomen regions, knowing how respiratory motion modifies tumor position and trajectory is crucial for accurate dose delivery to tumors while avoiding healthy tissue and organs at risk. This study compares motion amplitudes measured from the skin surface and internal tumor trajectory, internal/external correlations and characterizes tumor trajectory baseline shift. Four male patients with lung cancer with three repeated 4D CT scans, taken on different treatment days, were studied. Surfaces were extracted from 4D CTs by segmentation. Motion over specific regions of interest was analyzed with respect to the motion of the tumor center of mass and correlation coefficient was computed. Tumor baseline shifts were analyzed after rigid registration based on vertebrae and surface

registration. External amplitude variations were observed between fractions. Correlation coefficients of internal trajectories and external distances are greater than 0.6 in the abdomen. This correlation was observable and significant for all patients showing that the external motion is a good surrogate for internal movement on an intra-fraction basis. However for the inter-fraction case, external amplitude variations were observed between fractions and no correlation was found with the internal amplitude variations. Moreover, baseline shifts after surface registration were greater than those after vertebrae registration and the mean distance between surfaces after registration was not correlated to the importance of the baseline shift. These two observations show that, with the current representation of the external surface, inter-fraction variations are not detectable on the surface.

9034-107, Session PSMon

### Motion estimation for nuclear medicine: a probabilistic approach

Rhodri L. Smith, Univ. of Surrey (United Kingdom); Ashrani Aizuddin Abdul Rahni, Univ. Kebangsaan Malaysia (Malaysia); Kevin Wells, Univ. of Surrey (United Kingdom); John Jones, Fatemeh Tahavori, Univ of Surrey (United Kingdom)

Accurate, Respiratory Motion Modelling of the abdominal-thoracic organs serves as a pre-requisite for motion correction of Nuclear Medicine (NM) Images. The work described here is formulated to estimate respiratory motion using a probabilistic framework based on a Hidden Markov Model. This allows the implementation of Bayesian learning and inference to estimate internal motion from external surrogate signals. The structure of models built during an initial training phase (that consists of one respiratory cycle) can be adapted using an expectation maximization (EM) algorithm. This allows estimation of internal motion with varying amplitude and frequency compared to that of the training cycle. A measure of the accuracy of the model fit can be determined from the loglikelihood. This provides a mechanism to assess the applicability of the motion model in the clinical setting. The framework is initially tested on an anthropomorphic test object (XCAT phantom) with varying respiratory motion. For visualization of the effectiveness of our correction approach, a simulated Nuclear Medicine study is performed with four 16mm diameter implanted lung lesions. Results demonstrate the framework is capable of reducing motion, on average, to less than 2mm. This results in an average increase in contrast resolution of lung lesions of 20%. An initial comparison is made with a static total least squares based approach. The Kalman model offers an adaptive, flexible method which which is easily implemented(?) in the clinical setting.

9034-108, Session PSMon

## Automatic lobar segmentation for diseased lungs using an anatomy-based priority knowledge in low-dose CT images

Sang Joon Park, Jung Im Kim, Seoul National Univ. Hospital (Korea, Republic of); Jin Mo Goo, Seoul National Univ. College of Medicine (Korea, Republic of); Doohee Lee, Seoul National Univ. Hospital (Korea, Republic of)

Lung lobar segmentation in CT images is a challenging tasks because of the limitations in image quality inherent to CT image acquisition, especially low-dose CT for clinical routine environment. Besides, complex anatomy and abnormal lesions in the lung parenchyma makes segmentation difficult because contrast in CT images are determined by the differential absorption of X-rays by neighboring structures, such as tissue, vessel or several pathological conditions. Thus, we attempted to develop a robust segmentation technique for normal and diseased lung parenchyma. To evaluate performance of these techniques, we obtained 20 anonymous subjects (10 normals and 10 with lung diseases). The











images were obtained with low-dose chest CT using soft reconstruction kernel (Sensation 16, Siemens, Germany). The voxel size was 0.75 mm x 0.75 mm x 1.00 mm in x, y, and z direction respectively. Our PC-based in-house software segmented bronchial trees and lungs with intensity adaptive region-growing technique. Then the horizontal and oblique fissures were detected by using eigenvalues-ratio of the Hessian matrix in the lung regions which were excluded from airways and vessels. To enhance and recover the faithful 3-D fissure plane, our proposed fissure enhancing filter were applied to the images. After finishing above steps, for careful smoothening of fissure planes, 3-D rolling-ball algorithm in xy and xz coordinate planes are performed, respectively. Results show that success rate of our proposed scheme was achieved up to 89.5.% in the diseased lung parenchyma.

9034-109, Session PSMon

### Splitting of overlapping nuclei guided by robust combinations of concavity points

Marina Plissiti, Eleni Louka, Christophoros Nikou, Univ. of Ioannina (Greece)

In this work, we propose a novel and robust method for the accurate separation of elliptical overlapped nuclei in

microscopic images. The method is based on both the information provided by the global boundary of the nuclei cluster and the detection of concavity points along this boundary. The number of the nuclei and the area of each nucleus included in the cluster are estimated automatically by exploiting the different parts of the cluster boundary demarcated by the concavity points. More specifically, based on the set of concavity points detected in the image of the clustered nuclei, all the possible configurations of candidate ellipses that fit to them are estimated by least squares fitting. For each configuration, an index measuring the fitting residual is computed and the configuration providing the minimum error is selected. The method may successfully separate multiple (more than two) clustered nuclei as the fitting residual is a robust indicator of the number of overlapping elliptical structures even if many erroneous concavity points are present due to noise. Moreover, the algorithm has been evaluated on

cytological images of conventional Pap smears and compares favorably with state of the art methods both in terms of accuracy and execution time.

#### 9034-110, Session PSMon

### Brain tumor locating in 3D MR volume using symmetry

Pavel Dvorak, Institute of Scientific Instruments of the ASCR, v.v.i. (Czech Republic) and Brno Univ. of Technology (Czech Republic); Karel Bartusek, Academy of Sciences of the Czech Republic (Czech Republic)

This work deals with the automatic determination of a brain tumor location in 3D magnetic resonance volumes. The aim of this work is not the precise segmentation of the tumor and its parts but only the detection of its location. This work is the first step in the automatic tumor segmentation process. The algorithm expects 3D magnetic resonance volumes of brain containing a tumor. The detection is based on locating the area that breaks the left-right symmetry of the brain. This is done by multi-resolution comparing of corresponding regions in the left and right hemispheres. The output of the computation is the probabilistic map of the tumor location. Except the brain tumor, the proposed method can find other anomalies of the brain, such as cerebral edema, but the main purpose of the algorithm is the brain tumor detection for subsequent segmentation. Another possible application is a notification of anomaly presence.

The created algorithm was tested on 80 volumes from publicly available

BRATS databases containing multi-contrast 3D brain volumes afflicted by a brain tumor. These pathological structures had various sizes and shapes and were located in various parts of the brain. The overall performance of the algorithm was 97%.

#### 9034-111, Session PSMon

#### CT image noise reduction using rotationalinvariant feature in Stockwell transform

Jian Su, Zhoubo Li, Joshua D. Warner, Lifeng Yu, Daniel J. Blezek, Bradley J. Erickson M.D., Mayo Clinic (United States)

Iterative reconstruction and other noise reduction methods have been employed in CT to improve image quality and to reduce radiation dose. The non-local means (NLM) filter emerges as a popular choice for image-based noise reduction in CT. However, the original NLM method cannot incorporate similar structures if they are in a rotational format, resulting in ineffective denoising in some locations of the image and non-uniform noise reduction across the image. We have developed a novel rotational-invariant image texture feature derived from the multiresolutional Stockwell-transform (ST), and applied it to CT image noise reduction so that similar structures can be identified and fully utilized even when they are in rotated. We performed a computer simulation study in CT to demonstrate better efficiency in terms of utilizing redundant information in the image and more uniform noise reduction achieved by ST than by NLM.

#### 9034-112, Session PSMon

### An automated algorithm for the identification of choriocapillaris in 2D-OCT images

Sumohana Channappayya, Indian Institute of Technology Hyderabad (India); Siva Teja Kakileti, Indian Institute of Technology Guwahati (India); Ashutosh Richhariya, Jay Chhablani, LV Prasad Eye Institute (India)

Age-related macular degeneration (AMD) is characterized by changes in the structures of the retinal pigment epithelial (RPE) cells and the choriocapillaris (CC) region of the choroid. Typically, 2D-OCT scans of the choroid are analyzed manually to identify changes to these structures and diagnose the onset of degeneracy. The manual analysis makes diagnosis slow and possibly erroneous. To address this issue, we present an automated two-stage algorithm for the identification of the CC region in 2D-OCT images. In the first stage, the algorithm identifies the bright RPE cell layer to segment the image and identify the region of interest. In the second stage, the algorithm uses a gradient based method to identify the upper and lower edges of the CC region. The second stage is guided by the structure of the choroid and its relation to the RPE. The proposed algorithm is both accurate and computationally very efficient thereby making it potentially useful in diagnostic applications.

#### 9034-113, Session PSMon

#### Robust vessel detection and segmentation in ultrasound images by a data-driven approach

Ping Guo, Qiang Wang, Xiaotao Wang, Zhihui Hao, Kuanhong Xu, Haibing Ren, Samsung Advanced Institute of Technology (China); Jung-Bae Kim, Youngkyoo Hwang, Samsung Advanced Institute of Technology (Korea, Republic of)

This paper presents a learning based automatic vessel detection and segmentation method in real-patient ultrasound (US) liver images. We aim at detecting multiple shaped vessels robustly and automatically, including vessels with weak and ambiguous boundaries. Firstly, vessel











candidate regions are detected by a data-driven approach where multi-channel vessel enhancement maps are generated and aggregated under a Conditional Random Field (CRF) framework. Vessel candidates are then obtained by thresholding the saliency map. Secondly, regional features are extracted and the probability of each region being a vessel is modeled by random forest regression. Finally, a fast level set method is developed to refine vessel boundaries. Experiments have been carried out on an US liver dataset with 490 images from 98 patients. Experiment result shows that the proposed method achieves significantly better result than existing Hessian filtering based methods, especially in cases of vessels with weak and ambiguous boundaries.

Contributions of this paper are twofold. Firstly, a robust vessel detection and segmentation system is proposed for automatic segmentation of vessels with various shapes. The system contains three main modules which are vessel candidate detection by saliency aggregation, vessel classification by random regression and boundary refinement by fast levelset. Secondly, in order to detect vessel candidates, a data-driven saliency aggregation method is developed for vessel enhancement under a CRF framework. Compared with traditional methods like Hessian, our method is more robust to noise, can detect multiple shaped vessels, and is able to detect vessels with weak and ambiguous boundaries. The vessel enhancement method in this paper not only improves the vessel candidate detection result, but also helps the vessel classification. Compared to Hessian based method, the proposed method in this paper promotes the average precision by 56 percents and 7.8 percents for vessel detection and classification, respectively. Although this work focuses on vessel detection and segmentation in 2D US liver images, we believe that it can be extended to 3D vessels and other medical features as well as other modality images.

#### 9034-114, Session PSMon

## Enhancement of 3D modeling and classification of microcalcification's clusters in breast computed tomography (BCT)

Hiam H. Alquran, Univ. of Massachusetts Lowell (United States); Eman Shaheen, Katholieke Univ. Leuven (Belgium); J. Michael O'Connor, Univ. of Massachusetts Medical School (United States); Mufeed M. Mahmoud, Univ. of Massachusetts Lowell (United States)

#### Introduction:

Current computer aided detection (CADe) software for digital mammography rely mainly on 2D techniques. With the emergence of three-dimensional (3D) breast imaging modalities such as breast Computed Tomography (BCT), there is an opportunity to analyze 3D features for use in calcification classification methods.

#### Methods:

We have previously reported our initial work on automated 3D feature detection and classification based on morphological description. The work was based on models derived from biopsy specimens containing microcalcification clusters imaged by a micro-CT. We are now proposing the expansion of the 3D pattern recognition methods to include novel features. First, replacing the 2D Radon transform by a 3D Radon transform to improve shape discrimination. Second, the addition of cluster spatial feature detection to the previous set of individual calcifications features.

#### Results:

Preliminary results show that the classification rate improved from a total of 546 to 556 correctly classified calcification out of 635 by just applying the 3D Radon transform."

#### Conclusion:

In this study, we have updated our analysis of individual calcification morphology to use entirely 3D features. In addition, one extra morphological class (Le Gal I) was added. We implemented 3D spatial features that we believe will be useful in further cluster

based classification work. Currently, the work is limited by our own understanding of how clinicians interpret 3D pattern features. For future work, feedback from clinicians on the utility of our newly implemented cluster pattern features is the next step. After those discussions we hope to include those features in our SVM.

#### 9034-115, Session PSMon

## Quantitative analysis of rib movement based on dynamic chest bone images: preliminary results

Rie Tanaka, Shigeru Sanada, Makoto Oda, Mitsutaka Suzuki, Kanazawa Univ. (Japan); Kenji Suzuki, The Univ. of Chicago (United States); Keita Sakuta, Kanazawa Univ. (Japan); Hiroki Kawashima, Kanazawa Univ. School of Medicine (Japan)

Purpose: Rib movement during respiration is one of the diagnostic criteria in pulmonary impairments. In general, the rib movement is assessed in fluoroscopy. However, the shadows of lung vessels and bronchi overlapping ribs prevent accurate quantitative analysis of rib movement. Recently, an image-processing technique for separating bones from soft tissue in static chest radiographs, called "virtual dual-energy imaging", has been developed. Our purpose in this study was to evaluate the usefulness of dynamic bone images created by the virtual dual-energy imaging in quantitative analysis of rib movement.

Methods and Materials: Dynamic chest radiographs of 10 patients were obtained using a dynamic flat-panel detector (FPD). Virtual dual-energy imaging based on a massive-training artificial neural network (MTANN) was applied to the dynamic chest images to create bone images. Velocity vectors were measured in local areas on the dynamic bone images, which formed a map. The velocity maps obtained with bone and original images for scoliosis and normal cases were compared to assess the advantages of bone images.

Results: With dynamic bone images, we were able to quantify and distinguish movements of ribs from those of other lung structures accurately. Limited rib movements of scoliosis patients appeared as reduced rib velocity vectors. Vector maps in all normal cases exhibited left-right symmetric distributions, whereas those in abnormal cases showed nonuniform distributions.

Conclusion: Dynamic bone images were useful for accurate quantitative analysis of rib movements: Limited rib movements were indicated as a reduction of rib movement and left-right asymmetric distribution on vector maps. Thus, dynamic bone images can be a new imaging tool for quantitative analysis of rib movements without additional radiation dose.

#### 9034-116, Session PSMon

## Quantifying and visualizing variations in sets of images using continuous linear optimal transport

Soheil Kolouri, Gustavo K. Rohde, Carnegie Mellon Univ. (United States)

Modern advancements in imaging devices have enabled us to explore the subcellular structure of living organisms and extract vast amounts of information. However, interpreting the biological information mined in the captured images is not a trivial task. Utilizing predetermined numerical features is usually the only hope for quantifying this information. Nonetheless, direct visual or biological interpretation of results obtained from these selected features is non-intuitive and difficult. In this paper, we describe an automatic method for modeling visual variations in a set of images, which allows for direct visual interpretation of the most significant differences, and lifts the need for predefined features. The method is based on a linearized version of the continuous optimal transport (OT) metric, which provides a natural linear embedding for











the image data set, in which linear combination of images leads to a visually meaningful image. This enables us to apply linear geometric data analysis techniques such as PCA and LDA in the linearly embedded space and visualize the most prominent modes, as well as the most discriminant modes, in the dataset. Using the continuous OT framework, we are able to analyze variations in shape and texture in a set of images utilizing each image at full resolution, that otherwise cannot be done by existing methods. The proposed method is applied to a set of nuclei images segmented from Feulgen stained liver tissues in order to discover the major visual differences in chromatin distribution of Fetal-Type Hepatoblastoma (FHB) cells compared to the normal cells.

#### 9034-117, Session PSMon

## Context based algorithmic framework for identifying and classifying embedded images of follicle units

Md Mahbubur Rahman, S. S. S. Iyengar, Wei Zeng, Frank Hernandez, Florida International Univ. (United States); Bernard P. Nusbaum, Paul Rose, Hair Transplant Institute of Miami (United States)

Medical image processing has been very emerging research areas in recent days. These types of images are naturally so noisy. To count the target objects is never easy. But the proper treatment depends on the accuracy of the successful locating and counting of the desired objects in an image. Some research work can do this type of segmentation of images, but they include so many constraints on the input images that these solutions cannot be applied in a generalized way to most of the images. Even a slight variation in nature of an input image can lead to a major incorrectness of the result. So we developed a generalized way to count a very noisy part of human body, the hair follicle on the scalp. The objective of this research is to count the number of hair follicle groups and the number of follicles into each group in a microscopic image of human scalp. The follicles are nonstandard in shape i.e. they do not maintain any standard shape like rectangle, oval, circle etc. Moreover the follicles are overlapping with one another in many cases. So it is hard to separate them. Here we will present a technique to count the number of follicle group as well as number of follicles in each group. We also developed a new technique to cluster the objects detected and a method to generate a neighboring connected graph in order to calculate the inter object distances.

#### 9034-118, Session PSMon

### A framework for retinal layer intensity analysis for retinal artery occlusion patient based on 3D OCT

Jianping Liao, Guangxi Univ. (China); Haoyu Chen, Joint Shantou International Eye Ctr. (China); Chunlei Zhou, Ganzhou Tiantangniao Co. (China); Xinjian Chen, Soochow Univ. (China)

Retina is an important extension of brain and responsible for the transduction of light into visual signal. The blood supply to retina is an end artery. Occlusion of retinal artery will lead to severe ischemia and dysfunction of retina. Therefore, quantitative analysis of the reflectivity in the retina is very needed to quantitative assessment of the severity of retinal ischemia. In this paper, we proposed a framework for retinal layer intensity analysis for retinal artery occlusion patient based on 3D OCT images. The proposed framework consists of four main steps. First, a pre-processing step is applied to the input OCT images. During the pre-processing step, we applied a Gaussian filter to the image to reduce the noise. Second, a graph based method, graph search, was applied to segment multiple surfaces in OCT images. Third, the RAO region was detected based on texture classification method. For each voxel, many of textural, structural and positional features are calculated, such as

eigenvalues of the Hessian matrices, output of a Gaussian filter bank, mean intensity, etc. Finally, the intensity analysis (such as mean, stddev. etc) of retinal layer was performed. The proposed method was tested on tested on 27 clinical Spectral domain OCT images. The preliminary results show the feasibility and efficiency of the proposed method.

#### 9034-119. Session PSMon

### Single 3D cell segmentation from optical CT microscope images

Yiting Xie, Anthony P. Reeves, Cornell Univ. (United States)

The automated segmentation of the nucleus and cytoplasm regions in 3D optical CT microscope images has been achieved with two methods, a gradient base approach and a graph-cut approach. Image segmentation of single cells is important for automated disease diagnostic systems. The first method computes a merit curve containing gradient information. Then the first two peaks of the merit curve are selected as the threshold for cytoplasm and nucleus segmentation. The second method applies a graph-cut segmentation twice: the first identifies the nuclear region and the second identifies the cytoplasm.

The segmentation methods were evaluated with 200 3D images consisting of 40 samples of 5 different cell types. The cell types consisted of columnar, macrophage, metaplastic and squamous human cells and cultured A549 cancer cells. The segmented cells were compared with both 2D and 3D reference images and the quality of segmentation was determined by the Dice Similarity Coefficient (DSC).

In general, the graph-cut method had a superior performance to the gradient-based method. The graph-cut method achieved an average DSC of 86% and 72% in nucleus and cytoplasm segmentation respectively for the 2D reference images and 83% and 75% for the 3D references. The gradient method achieved an average DSC of 72% and 51% for nucleus and cytoplasm segmentation for the 2D references and 71% and 51% for the 3D references. The DSC of cytoplasm segmentation was significantly lower than for the nucleus since the cytoplasm was not differentiated as well by image intensity from the background.

#### 9034-120, Session PSMon

# Method for traversing and labeling complex vascular tree structures from 3D medical images: description, validation and application

Walter G. O'Dell, Univ. of Florida (United States); Sindhuja Govindarajan, Athinoula A. Martinos Ctr. for Biomedical Imaging (United States); Ankit Salgia, Johnson & Johnson (India); Satya Hegde M.D., Sreekala Prabhakaran M.D., Univ. of Florida (United States); Ender Finol, The Univ. of Texas at San Antonio (United States); R. James White M.D., Univ. of Rochester Medical Ctr. (United States)

Characterization of pulmonary vascular anatomy has important applications for detection and diagnosis in a variety of vascular diseases. Until now, the emphasis in the field has been to use vessel segmentation to gather information on the number or branches, number of bifurcations, branch length and volume. But to-date there has not been a careful consideration for accurate traversal of the vessel tree to correctly label branch generations and identify and repair erroneous interconnections between adjacent trees. A more comprehensive strategy for traversing and labeling vascular trees has been conceived and a manifestation has been successfully implemented for application to pulmonary vessels observed using three-dimensional X-ray computed tomography (CT) images of the chest. The method has been validated in series of increasingly complex 2D virtual test data sets, and demonstrated on











conventional CT data sets obtained from a healthy adult human and of a pediatric patient. Finally, the method is also applied on a 3D micro-CT data set of the pulmonary arterial tree of a rat. The outputted simulated vessel tree reconstructions appear to faithfully depict the extracted vessel tree structures they are associated with. This represents the first successful approach to distinguishing individual vascular trees from amongst a complex intermingling of trees and is expected to improve our ability to characterize changes in the vascular structure in disease and in response to therapy.

9034-121, Session PSMon

### Standardized anatomic space for abdominal fat quantification

Yubing Tong, The Univ. of Pennsylvania Health System (United States); Jayaram K. Udupa, Univ. of Pennsylvania (United States); Drew A. Torigian, Hospital of the Univ. of Pennsylvania (United States)

Traditionally, fat quantification is performed by estimating the fat distribution on one axial MRI or CT slice at an arbitrary anatomic location, such as between L4 and L5 vertebrae. The optimal location can potentially be obtained by assessing the correlations between fat area at the same anatomic location across all subjects and fat volumes, where the location with maximum correlation can be chosen as the optimal site for abdominal fat quantification. However, correlation will have no meaning if every subject requires a slice at a different anatomic location for correlation calculation. We therefore propose a method for anatomic space standardization for abdomen fat quantification. The main idea behind this method is to map or deform the slice locations for every subject so that they match a mean/standardized slice location determined through training. The actual matching is based on certain landmarks identified with the slice location. The sites of best correlation have not been studied in the past. With this method, the slices of every subject within the same body region are mapped into the same standardized anatomic space and used for correlation calculation. Experimental results on 47 abdominal CT images show that the standardized anatomic mapping of slices with non-linear mapping achieves better anatomic localization of slices via landmarks than linear mapping. Also, the sites of optimal correlation for subcutaneous and visceral components of fat are not the same, contrary to common assumption.

9034-122, Session PSMon

## Registration of segmented histological images using thin plate splines and belief propagation

Jan Kybic, Czech Technical Univ. in Prague (Czech Republic)

We register images based on their multiclass segmentations, for cases when correspondence of local features cannot be established. The relation between classes can be probabilistic as discrete class mutual information is used as a similarity criterion. Because the number of classes is small, this criterion is fast and robust. For speed, the criterion is only evaluated at a sparse set of locations on the interfaces between classes. A thin-plate spline regularization matrix is first factorized using randomized SVD and the subspace of the orthogonality conditions is identified. This leads to a low-rank approximation of the smoothness matrix, which is further approximated by a set of squared pairwise displacement differences. The problem is cast into a discrete setting and the maximum displacement is limited. Taking advantage of the specific form of the regularization criterion, the minimization is solved efficiently by belief propagation. Further speedup and robustness is provided by a multiresolution framework, which requires additional modification of the belief propagation. The method is tested on differently stained histological slices of human prostate and rat kidney. The images

were segmented by the llastik tool into four classes with minimum manual interaction and the proposed algorithm was used to align them. As a reference method, we have used a standard ITK B-spline elastic registration. From visual inspection, both registration results are acceptable and have similar geometric accuracy. However, the proposed method is faster by a factor of 10 to 50. Further speedup is likely using an optimized and multithreaded code.

9034-123, Session PSMon

## Accurate, fully-automated registration of coronary arteries for volumetric CT digital subtraction angiography

Brian Mohr, Marco Razeto, Toshiba Medical Visualization Systems Europe, Ltd. (United Kingdom); Kazumasa Arakita, Toshiba Medical Systems Corp. (Japan); J. D. D. Schuijf, Toshiba Medical Systems Europe B.V. (Netherlands); Andreas Fuchs M.D., Jørgen Tobias Kühl M.D., Rigshospitalet (Denmark); Marcus Chen M.D., National Institutes of Health (United States); K. F. F. Kofoed M.D., Rigshospitalet (Denmark)

Diagnosis of coronary artery disease with Coronary Computed Tomography Angiography (CCTA) is complicated by the presence of significant calcification or stents. Volumetric CT Digital Subtraction Angiography (CTDSA) has recently been shown to be effective at overcoming these limitations. Precise registration of structures is essential as any misalignment can produce artifacts potentially inhibiting clinical interpretation of the data. The fully-automated registration method described in this paper addresses the problem by combining a dense deformation field with rigid-body transformations where calcifications/ stents are present. The method contains non-rigid and rigid components. Non-rigid registration recovers the majority of motion artifacts and produces a dense deformation field valid over the entire scan domain. Discrete domains are identified in which rigid registrations very accurately align each calcification/stent. These rigid-body transformations are combined within the immediate area of the deformation field using a distance transform to minimize distortion of the surrounding tissue. A recent clinical feasibility study using a second-generation 320-row CT detector evaluated reader confidence and diagnostic accuracy using CTDSA registered with this method compared to conventional CCTA. The feasibility study also performed conventional invasive coronary angiography for corroboration and included 27 patients in which 130 lesions were identified. Of 41 lesions with low reader confidence in CCTA, CTDSA improved confidence in 13/36 (36%) of segments with severe calcification and 3/5 (60%) of segments with coronary stents. Also, the false positive rate of CTDSA was reduced compared to conventional CCTA from 18% (24/130) to 14% (19/130).

9034-124, Session PSMon

#### A multi-resolution strategy for a multiobjective deformable image registration framework that accommodates large anatomical differences

Tanja Alderliesten, Academisch Medisch Ctr. (Netherlands); Peter A. N. Bosman, Ctr. voor Wiskunde en Informatica (Netherlands); Jan-Jakob Sonke, The Netherlands Cancer Institute (Netherlands); Arjan Bel, Academisch Medisch Ctr. (Netherlands)

Currently, two major challenges dominate the field of deformable image registration. The first challenge is related to the tuning of the developed methods to specific problems (i.e. how to best combine different objectives such as similarity measure and transformation effort). This is one of the reasons why, despite significant progress, clinical implementation of such techniques has proven to be difficult.











The second challenge is to account for large anatomical differences (e.g. large deformations, (dis)appearing structures) that occurred between image acquisitions. In this paper, we study a framework based on multi-objective optimization to improve registration robustness and to simplify tuning for specific applications. Within this framework we specifically consider the use of an advanced model-based evolutionary algorithm for optimization and a dual-dynamic transformation model (i.e. two "non-fixed" grids: one for the source- and one for the target image) to accommodate for large anatomical differences. The framework computes and presents multiple outcomes that represent efficient trade-offs between the different objectives (a so-called Pareto front). In image processing it is common practice, for reasons of robustness and accuracy, to use a multi-resolution strategy. This is, however, only wellestablished for single-objective registration methods. Here we describe how such a strategy can be realized for our multi-objective approach and compare its results with a single-resolution strategy. For this study we selected the case of prone-supine breast MRI registration. Results show that the well-known advantages of a multi-resolution strategy are successfully transferred to our multi-objective approach, resulting in superior (i.e. Pareto-dominating) outcomes.

#### 9034-125, Session PSMon

# An adaptive patient specific deformable registration for breast images of positron emission tomography and magnetic resonance imaging using finite element approach

Cheng Xue, Fuk-hay Tang, The Hong Kong Polytechnic Univ. (Hong Kong, China)

Image registration of Positron Emission Tomography (PET) and Magnetic Resonance imaging (MRI) is an emerging approach for breast imaging as it combined metabolic and functional information with precise soft tissue delineation. As breast is an easily deformed structure, we proposed a registration method by combining surface-based registration with biomechanical modeling.

Fifty cases of patients with PET and MR breast images were obtained. The images were firstly segmented by k-means algorithm and tetrahedral meshes were built based on segmented images. Vertices on those meshes were surface points. 500 among surface points were selected as boundary points. As exaction of one to one corresponding point is difficult, a robust point matching algorithm was applied to detect corresponding boundary points between two surfaces in different imaging modalities, rather than placing invasive extrinsic landmarks. Steady-state heat transfer finite element analysis was performed with an analogy between displacement vector components and temperature field distribution, without assigning material properties which is individual different. Similarity Index and Receiver operating characteristic (ROC) analysis evaluation was conducted to compare our model with a traditional model.

Results show that the average similarity index is S=0.92 and S=0.88 respectively. The average area value under the binominal ROC curve with our methods and a traditional methods is 0.95 and 0.90 respectively.

In conclusion, we have demonstrated a image registration model suitable for breast image using biomechanical modeling approach. This method can provide clinicians an automatical image registration of breast images with combined PET and MRI information with high accuracy and efficiency.

9034-126, Session PSMon

## Computed tomography lung iodine contrast mapping by image registration and subtraction

Keith Goatman, Costas Plakas, Toshiba Medical Visualization Systems Europe, Ltd. (United Kingdom); Joanne Schuijf, Toshiba Medical Systems Europe B.V. (Netherlands); Erin Beveridge, Toshiba Medical Visualization Systems Europe, Ltd. (United Kingdom); Mathias Prokop M.D., Radboud Univ. Nijmegen Medical Ctr. (Netherlands)

Pulmonary embolism (PE) is a relatively common and potentially life threatening disease, affecting around 600,000 people annually in the United States. Prompt treatment using anticoagulants is effective and saves lives, but unnecessary treatment risks life threatening haemorrhage. The specificity of any diagnostic test is therefore as important as its sensitivity.

Computed tomography (CT) angiography is routinely used to diagnose PE. However, there are concerns it may over-report the condition. Additional information about the severity of an occlusion can be obtained from an iodine contrast map that represents tissue perfusion. Such maps tend to be derived from dual-energy CT acquisitions. However, they may also be calculated by subtracting pre- and post-contrast scans. There are technical advantages to such a subtraction approach, including better contrast-to-noise ratio and bone suppression. However, subtraction relies on accurate image registration.

This paper presents a framework for the automatic alignment of preand post-contrast lung volumes prior to subtraction. The registration accuracy is evaluated for seven subjects for whom pre- and postcontrast helical CT scans were acquired using a Toshiba Aquilion ONE scanner. One hundred corresponding points were annotated on the preand post-contrast scans, distributed throughout the lung volume. Before registration the mean alignment error was 1.9mm (range 1.2--3.5mm) and following registration the mean error was 0.6mm (range 0.4--0.8mm). There was a commensurate reduction in visual artefacts following registration.

In conclusion, a framework for pre- and post-contrast lung registration has been developed that is sufficiently accurate for lung subtraction iodine mapping.

#### 9034-127, Session PSMon

### A hybrid biomechanical intensity based deformable image registration of lung 4DCT

Navid Samavati, Mike Velec, Univ. of Toronto (Canada); Kristy K. Brock, Univ. of Michigan (United States)

Deformable Image Registration (DIR) has been extensively studied over the past two decades due to its essential role in many image-guided interventions, however the potential for clinically significant errors often remain in some regions of each registration. Morfeus is a DIR algorithm that incorporates finite element biomechanical modeling that includes modeling the contact surface between the lungs and the chest wall. However, it currently excludes image contrast, which may aid in ensuring low maximum registration errors in all regions of the image. A hybrid biomechanical intensity-based method is proposed to address this potential limitation. Inhale and exhale 4DCT lung images of 26 patients were initially registered using Morfeus. The acquired deformations using Morfeus were refined using Drop (Munich, Germany). Important parameters in Drop including grid spacing, number of pyramids, and regularization coefficient were optimized for 10 randomly chosen patients (out of 26). The remaining parameters were selected empirically. Target Registration Error (TRE) was calculated by measuring the Euclidean distance of common anatomical points on both images before and after registration. For each patient a minimum of 30 points/lung were used.











The hybrid method resulted in mean±SD (90th%) TRE of 1.5±1.4 (3.0) mm compared to 3.1±2.0 (5.8) using Morfeus and 2.7±2.9 (6.9) using Drop-alone. Average mean TRE among the patients using hybrid was significantly smaller than that of both Morfeus and Drop-alone, p-values of 1.3E-11 and 4.2E-7 (1-tail student t-test), respectively. The average 90th% TRE of all patients using hybrid was significantly smaller than that of both Morfeus and Drop-alone, p-values of 4.9E-8 and 1.5E-5, respectively.

9034-128, Session PSMon

### Two-step FEM-based Liver-CT registration: improving internal and external accuracy

Cristina Oyarzun Laura, Klaus Drechsler, Stefan Wesarg, Fraunhofer-Institut für Graphische Datenverarbeitung (Germany)

The exact location of the internal structures of the organs, especially the vasculature, is of great importance for the clinicians. This information allows them to know which vessels will be affected by the therapy and therefore to better treat the patients. However the use of internal structures for registration is often disregarded especially in physical based registration methods. In this paper we propose an algorithm that uses finite element methods to carry out a registration of liver volumes that will not only have accuracy in the boundaries of the organ but also in the interior. Therefore a graph matching algorithm is used to find correspondences between the vessel trees of the two livers to be registered. In addition to this an adaptive volumetric mesh is generated that contains nodes in the locations in which correspondences were found. The displacements derived from those correspondences are the input for the initial deformation of the model. The first deformation brings the internal structures to their final deformed positions and the surfaces close to it. Finally, thin plate splines are used to refine the solution at the boundaries of the organ achieving an improvement in the accuracy of 75.8%. The algorithm has been evaluated in CT clinical images of the abdomen.

9034-129. Session PSMon

# Normal distributions transform in multi-modal image registration of optical coherence tomography and computed tomography datasets

Jesús Díaz Díaz, Mauro H. Riva, Leibniz Univ. Hannover (Germany); Omid Majdani M.D., Medizinische Hochschule Hannover (Germany); Tobias Ortmaier, Leibniz Univ. Hannover (Germany)

In recent years, optical coherence tomography (OCT) has gained increasing attention not only as an imaging device, but also as a navigation system for surgical interventions. This approach demands to register intra-operative OCT to pre-operative computed tomography (CT) data. In this study, we evaluate algorithms for multi-modal image registration of OCT and CT data of a human temporal bone specimen. We focus on similarity measures that are common in this field, e.g., normalized mutual information, normalized cross correlation, and iterative closest point. We evaluate and compare their accuracies to the relatively new normal distribution transform (NDT), which is very common in simultaneous localization and mapping applications, but is not widely used in image-based registration. Registration is realized considering appropriate image pre-processing, the aforementioned similarity measures, and different local optimization algorithms, as well as line search optimization. For evaluation purpose, the results of a point-based registration with fiducial landmarks are regarded as ground truth. First results indicate that state of the art similarity functions do not perform with the desired accuracy, when applied to unprocessed image data. In contrast, NDT seems to achieve higher registration accuracy.

9034-130, Session PSMon

## Automatic registration of imaging mass spectrometry data to the Allen Brain Atlas transcriptome

Walid M. Abdelmoula, Ricardo J. Carreira, Reinald Shyti, Benjamin Balluff, Else Tolner, Arn M. J. M. van den Maagdenberg, Boudewijn P. F. Lelieveldt, Liam McDonnell, Jouke Dijkstra, Leiden Univ. Medisch Ctr. (Netherlands)

Imaging Mass Spectrometry (IMS) is an emerging molecular imaging technology that provides spatially resolved information on biomolecular structures; each image pixel effectively represents a molecular mass spectrum. By combining the histological images and IMS-images, neuroanatomical structures can be distinguished based on their biomolecular features as opposed to morphological features. The combination of IMS data with spatially resolved gene expression maps of the mouse brain, as provided by the Allen Mouse Brain atlas, would enable comparative studies of spatial metabolic and gene expression patterns in life-sciences research and biomarker discovery. As such, it would be highly desirable to spatially register IMS slices to the Allen Brain Atlas (ABA).

In this paper, we propose a multi-step automatic registration pipeline to register ABA histology to IMS-images. Key novelty of the method is the selection of the best reference section from the ABA, based on pre-processed histology sections. First, we extracted a hippocampus-specific geometrical-feature from the given experimental histological section to initially localize it among the ABA sections. Then, feature-based linear registration is applied to the initially localized section and its two neighbors in the ABA to select the most similar reference section. A non-rigid registration yields a one-to-one mapping of the experimental IMS slice to the ABA. The pipeline was applied on 6 coronal sections from two mouse brains, showing high anatomical correspondence, demonstrating the feasibility of complementing biomolecule distributions from individual mice with the genome-wide ABA transcriptome.

9034-131, Session PSMon

### Wavelet based free-form deformations for nonrigid registration

Wei Sun, Erasmus MC (Netherlands); Wiro J. Niessen, Erasmus MC (Netherlands) and Technische Univ. Delft (Netherlands); Stefan Klein, Erasmus MC (Netherlands)

In nonrigid registration, deformations may take place on the coarse and fine scales. For the conventional B-spline based free-form deformation (FFD) registration, these coarse- and fine-scale deformations are all represented by basis functions of a single scale.

Wavelets have been proposed as a signal representation suitable for multi-scale problems. Wavelet analysis leads to a unique decomposition of a signal into its coarse- and fine-scale components. Potentially, this could therefore be useful for image registration. In this work, we investigate whether a wavelet-based FFD model has advantages for nonrigid image registration. We use a B-spline based wavelet, as defined by Cai and Wang. This wavelet is expressed as a linear combination of B-spline basis functions. Derived from the original B-spline function, this wavelet is smooth, differentiable, and compactly supported. The basis functions of this wavelet are orthogonal across scales in Sobolev space. This wavelet was previously used for registration in computer vision, in 2D optical flow problems, but it was not compared with the conventional B-spline FFD in medical image registration problems. An advantage of choosing this B-spline based wavelet model is that the space of allowable deformation is exactly equivalent to that of the traditional B-spline. The wavelet transformation is essentially a (linear) reparametrization of the B-spline transformation model.

Experiments on 10 CT lung and 18 T1-weighted MRI brain datasets show











that wavelet based registration leads to smoother deformation fields than traditional B-spline based registration, while achieving similar accuracy.

9034-132, Session PSMon

### Non-rigid target tracking in 2D ultrasound images using hierarchical grid interpolation

Lucas Royer, Alexandre Krupa, INRIA Rennes (France); Marie Babel, Institut National des Sciences Appliquées de Rennes (France)

In this paper, a new non-rigid target tracking method within 2D ultrasound image sequence is presented. In order to make the method work in real-time, we based our approach on an algorithm typically used for video compression purposes. Toward that end, a dedicated hierarchical grid interpolation algorithm (HGI) is employed.

A grid of control point is first defined. Then, a motion vector for each control point is estimated by using a local approach. Each pixel has its own motion vector through a bilinear interpolation. In this way, this algorithm can represent a large variety of deformations compared to other motion estimation algorithms such as Overlapped Block Motion Compensation (OBMC), or Block Motion Algorithm (BMA). The selected similarity criteria is the sum of squared difference of image intensity because it provides a trade-off between computation time and motion estimation quality. In addition, the size of the grid is locally adapted in order to be robust to the noisy structure of ultrasound images. Contrary to the other methods proposed in the literature, this method allows to distinguish the rigid and the non-rigid motions that are typically observed in ultrasound image modality.

This technique does not take into account any prior knowledge about the target such as elasticity information or prior dynamics of a contour. Finally, a technique aiming at identifying the main phases of a periodic motion (e.g. breathing motion) is introduced. This new approach is validated from 2D ultrasound images of real human tissues which undergo rigid and non-rigid deformations.

9034-133. Session PSMon

## Spectral embedding-based registration (SERg) aligning multimodal prostate histology and MRI

Eileen Hwuang, Sudha Karthigeyan, Shannon C. Agner, Rutgers, The State Univ. of New Jersey (United States); Mirabela Rusu, Case Western Reserve Univ. (United States); Rachel E. Sparks, Rutgers, The State Univ. of New Jersey (United States); Natalie Shih, Hospital of the Univ. of Pennsylvania (United States); John E. Tomaszewski M.D., Univ. at Buffalo (United States); Mark Alan Rosen M.D., Hospital of the Univ. of Pennsylvania (United States); Michael D. Feldman, The Univ. of Pennsylvania Health System (United States); Anant Madabhushi, Case Western Reserve Univ. (United States)

One challenge of multimodal image registration is that typical similarity measures rely on statistical correlations between image intensities to determine anatomical alignment. Therefore, alternate representations can be constructed to improve the mapping of intensities such that images belonging to different modalities appear more similar. In this work, we present a spectral embedding based registration (SERg) method that uses alternate representations to facilitate multimodal image registration. Spectral embedding leverages a set of computerextracted features derived from image intensities to calculate a parametric eigenvector image representation. This accentuates areas of salience based on modality-invariant structural information and therefore better identifies corresponding regions in both the template and target images. SERg

is implemented using Thirion's Demons registration scheme, which is traditionally known for its limitation to monomodal registration due to sensitivity of its squared difference metric to image intensities. We demonstrate that when registering synthetic T1-weighted to T2-weighted brain magnetic resonance images (MRI) under five levels of noise (0%, 1%, 3%, 5%, and 7%) and two levels of bias field (20% and 40%) with and without noise, SERg yields a mean squared error (MSE) that is 81.51  $\pm$  6.09% lower than that of traditional Demons. SERg of six ex vivo prostate histology to in vivo T2-weighted MRI studies increases the Dice similarity coefficient (DSC) of the prostate gland by 5.3  $\pm$ 0.42%.

9034-134, Session PSMon

### A constrained registration problem based on Ciarlet-Geymonat stored energy

Ratiba Derfoul, Institut National des Sciences Appliquées de Rouen (France) and IFP Energies Nouvelles (France); Carole Le Guyader, Institut National des Sciences Appliquées de Rouen (France)

In this paper, we address the issue of designing a theoretically well-motivated registration model capable of handling large deformations and including geometrical constraints, namely landmark points to be matched, in a variational framework.

The theory of linear elasticity being unsuitable in this case, since assuming small strains and the validity of Hooke's law, the introduced functional is based on nonlinear elasticity principles. More precisely, the shapes to be matched are viewed as Ciarlet-Geymonat materials. We demonstrate the existence of minimizers of the related functional minimization problem and prove a convergence result when the number of geometric constraints increases.

We then describe and analyze a numerical method of resolution based on the introduction of an associated decoupled problem under inequality constraint in which an auxiliary variable simulates the Jacobian matrix of the deformation field. A theoretical result is established. We then provide preliminary 2D results of the proposed matching model for the registration of mouse brain gene expression data to a neuroanatomical mouse atlas.

9034-135, Session PSMon

### Automatic 3D segmentation of spinal cord MRI using propagated deformable models

Benjamin De Leener, Julien Cohen-Adad, Samuel Kadoury, Ecole Polytechnique de Montréal (Canada)

Spinal cord diseases or injuries can cause dysfunction of the sensory and locomotor systems. Segmentation of the spinal cord provides measures of atrophy and allows group analysis of multi-parametric MRI via intersubject registration to a template. All these measures were shown to improve diagnostic and surgical intervention. We developed a framework to automatically segment the spinal cord on T2-weighted MR images, based on the propagation of deformable models. The algorithm is divided into three parts: firstly, an initialization step approximates the spinal cord position and orientation by using the Hough transform on several axial slices around the middle slice in the inferior-superior direction and builds an initial tubular mesh. Secondly, the low-resolution deformable model is propagated along the spinal cord. To deal with highly variable contrast levels between the spinal cord and the cerebrospinal fluid, the deformation is coupled with a contrast adaptation at each iteration. Thirdly, a refinement process and a final deformation are applied on the low-resolution mesh to provide an accurate segmentation of the spinal cord. Our method was evaluated against a semi-automatic edge-based snake method implemented in ITK-SNAP (with manual adjustment) by computing the 3D Dice coefficient, mean and maximum distance errors. Accuracy and robustness were assessed from 8 healthy











subjects. Each subject had two volumes: one at the cervical and one at the thoracolumbar region. Results show a precision of  $0.30\pm0.05$  mm (mean absolute distance error) in the cervical region and  $0.27\pm0.06$  mm in the thoracolumbar region. The 3D Dice coefficient was of 0.93 for both regions.

9034-136, Session PSMon

### Interactive approach to segment organs at risk in radiotherapy treatment planning

Jose Dolz, Hortense A Kirisli, Romain Viard, Laurent Massoptier, AQUILAB (France)

Accurate delineation of organs at risks (OARs) is required for radiation treatment planning (RTP). However, it is a very time consuming and tedious task. The use in clinic of Image Guided Radiation Therapy (IGRT) becomes more and more popular, thus increasing the need of (semi-) automatic method for delineation of the OAR. In this work, an interactive segmentation approach to delineate OAR is proposed and validated. The method is based on the combination of watershed transformation, which groups small areas of similar intensities in homogeneous labels, and graph cuts approach, which uses these labels to create the graph. Segmentation information can be added in any view - axial, sagittal or coronal -, making the interaction with the algorithm easier and faster. Subsequently, this information is propagated within the whole volume, providing a spatially coherent result. Manual delineations made by experts over a set of 9 computed tomography (CT) scans of 6 OARs lungs, kidneys, liver, spleen, heart and aorta - were used to evaluate the proposed approach. With a maximum of 4 interactions, a Dice Similarity Coefficient (DSC) over 0.87 was obtained, which demonstrates that the proposed segmentation approach requires few interactions to provide similar results as the manual delineations. The integration of this method in the RTP process may save a considerable amount of time, and reduce the annotation complexity.

9034-137, Session PSMon

### Auxiliary anatomical labels for joint segmentation and atlas registration

Tobias Gass, Gàbor Székely, Orcun Goksel, ETH Zurich (Switzerland)

This paper studies improving joint segmentation and registration by introducing auxiliary labels for anatomy that has similar appearance to the target anatomy while not being part of that target. Such auxiliary labels help avoid false positive labeling of non-target anatomy by resolving ambiguity. A known registration of a segmented atlas can help identify where a target segmentation should lie. Conversely, segmentations of anatomy in two images can help them be better registered. Joint segmentation and registration is then a method that can leverage information from both registration and segmentation to help one another. It has received increasing attention recently in the literature. Often, merely a single anatomy of interest is labelled in the atlas. In the presence of other anatomy with similar appearance, this leads to ambiguity in intensity based segmentation; for example, when segmenting individual bones in CT images where other bones share the same intensity profile. To alleviate this problem, we introduce automatically-generated multilabel segmentation of atlases, by marking similar-appearance non-target anatomy with an auxiliary label. Information from the auxiliary-labeled atlas segmentation is incorporated by using a novel coherence potential, which penalizes differences between the deformed atlas segmentation and the target segmentation estimate. We validated this on a common joint approach that iteratively alternates between registering an atlas and segmenting the target image to find a final anatomical segmentation. The results show that an auxiliary-labeled atlas outperforms its single-label counterpart, for both a mandibular bone segmentation task in 3D-CT and a corpus callosum segmentation task in 2D-MRI.

9034-138, Session PSMon

# Improving accuracy in coronary lumen segmentation via explicit calcium exclusion, learning-based ray detection and surface optimization

Felix Lugauer, Friedrich-Alexander-Univ. Erlangen-Nürnberg (Germany) and Siemens Corp., Corporate Technology (Germany); Jingdan Zhang, Yefeng Zheng, Siemens Corp., Corporate Technology (United States); Joachim Hornegger, Friedrich-Alexander-Univ. Erlangen-Nürnberg (Germany); Michael Kelm, Siemens Corp., Corporate Technology (Germany)

Invasive cardiac angiography (catheterization) is still the standard in clinical practice for diagnosing coronary artery disease (CAD) but it involves a high amount of risk and cost. New generations of CT scanners can acquire high-quality images of coronary arteries which allow for an accurate identification and delineation of stenoses. Recently, computational flow dynamics (CFD) simulation has been applied to coronary blood flow using geometric lumen models extracted from CT angiography (CTA). The computed pressure drop at stenoses proved to be indicative for ischemia-causing lesions, leading to non-invasive Fractional Flow Reserve derived from CTA (FFRCT). Since the diagnostic value of non-invasive procedures for diagnosing CAD relies on an accurate extraction of the lumen, a precise segmentation of the coronary arteries is crucial.

As manual segmentation is tedious, time-consuming and subjective, automatic procedures are desirable. We present a novel fully-automatic method to accurately segment the lumen of coronary arteries in the presence of calcified and non-calcified plaque. Our segmentation framework is based on three main steps: boundary detection, calcium exclusion and surface optimization. A learning-based boundary detector enables a robust lumen contour detection via dense ray-casting.

The exclusion of calcified plaque is assured through a novel calcium exclusion technique which allows us to accurately capture stenoses of diseased arteries. The boundary detection results are incorporated into a closed set formulation whose minimization yields an optimized lumen surface. On standardized tests with clinical data, a segmentation accuracy is achieved which is comparable to clinical experts and superior to current automatic methods.

9034-139, Session PSMon

## Surface-based reconstruction and diffusion MRI in the assessment of gray and white matter damage in multiple sclerosis

Matteo Caffini, Politecnico di Milano (Italy); Niels Bergsland, Politecnico di Milano (Italy) and Fondazione Don Carlo Gnocchi (Italy); Marcella Lagana, Eleonora Tavazzi, Paola Tortorella, Marco Rovaris, Fondazione Don Carlo Gnocchi (Italy); Giuseppe Baselli, Politecnico di Milano (Italy)

Nonconventional MRI techniques have greatly improved the knowledge of multiple sclerosis (MS) pathogenetic mechanisms, revealing, for example, a diffuse damage of white matter (WM) and grey matter (GM) occurring outside focal lesions. Moreover, the role of GM in determining disability from the early stages of the disease has been better understood. Despite these advances, there are still many unanswered questions, such as the relationship between GM and WM damage. Some authors hypothesize an independent process affecting both of them in parallel while others suggest that GM axonal loss is secondary to Wallerian and retrograde axonal degeneration occurring in the WM. The study of the motor system in all its components, including the corticospinal tract (CST) WM pathway and the corresponding cortical GM area, would have a significant clinical impact especially considering that











disability in MS is mainly related to motor deficits.

Diffusion tensor-based tractography allows the identification of specific WM tracts of interest and measure their integrity with two principal parameters, mean diffusivity (MD) and fractional anisotropy (FA). FreeSurfer provides a useful set of tools for automatic segmentation of brain structures, fine identification of cortical areas and estimation of cortical thickness and curvature. We applied these two advanced techniques to the study of the CST and primary motor cortex in a group of patients affected by MS, with the aim to better understand the relationship between GM and WM damage in a clinically relevant system.

9034-140, Session PSMon

### Uterus segmentation in dynamic MRI using LBP texture descriptors

Rafael Namias, CIFASIS (Argentina); Marc-Emmanuel Bellemare, Mehdi Rahim, Lab. des Sciences de l'Information et des Systèmes (France); Nicolas Pirró, Hôpital de la Timone (France)

Pelvic floor disorders cover pathologies of which physio-pathology is not well understood. However cases get prevalent with an aging population. Within the context of a project aiming at modelization of the dynamics of pelvic organs, we have developed an efficient segmentation process. It aims at alleviating the radiologist with a tedious one by one image analysis. From a first contour delineating the uterus-vagina set, the organ border is tracked along a dynamic {MRI} sequence. The process combines movement prediction, local intensity and texture analysis and active contour geometry control. Movement prediction allows a contour initialization for next image in the sequence. Intensity analysis provides image-based local contour detection enhanced by local binary pattern (LBP) texture descriptors. Geometry control prohibits self intersections and smooths the contour. Results show the efficiency of the method with images produced in clinical routine.

9034-142, Session PSMon

### Robust automated lymph node segmentation with random forests

David I. Allen, The Univ. of Texas at Dallas (United States) and National Institutes of Health (United States); Le Lu, Jiamin Liu, Jianhua Yao, Evrim Turkbey, Ronald M. Summers M.D., National Institutes of Health (United States)

Identification and measurement of the lymph nodes provides radiologists with essential biomarkers for diagnosing disease as enlarged lymph nodes may indicate the presence of illness. Radiologists must often spend a great deal of time detecting and measuring lymph nodes by manually searching CT scan images. Due to an often large volume of CT scan data, there is high demand for automated computational methods to assist radiologists in this task. Automating such a task faces a number of challenges as lymph nodes are often very small and have a highly variable shape. We turn to supervised statistical machine learning methods as a solution to this problem. One such method that has recently gained much attention is the random forest algorithm. This machine learning technique employs an ensemble of decision trees that are trained on labeled multi-class data to recognize the data features that can be used to distinguish each class. The trained forest can then be applied to previously unseen data to obtain a set of probability distributions that can be used to assign class labels to each unlabeled data point. We use this machine learning technique to teach a classifier how to recognize and classify lymph nodes in a CT volume on a per-voxel basis. We show that the random forest algorithm can easily be adapted to this task and has great potential to perform this labeling accurately and efficiently.

9034-143, Session PSMon

#### Joint image segmentation and feature parameter estimation using expectation maximization: application to transrectal ultrasound prostate imaging

Mahdi Orooji, Rachel E. Sparks, Anant Madabhushi, Case Western Reserve Univ. (United States)

Prostate needle biopsy guided by transrectal ultrasound (TRUS) is the current gold standard for prostate cancer (CaP) diagnosis. An accurate detection of the prostate volume and boundary is significantly influential on diagnosis, treatment and follow up of CaP. In this work we present a joint image segmentation-feature parameter estimation method leveraging log-likelihood maximization applied to TRUS images for prostate segmentation. The focus of the presented algorithm is on feature-based voxel segmentation. However, the method is generalizable to any hybrid image segmentation method that jointly considers the image features and other criteria such as maximum allowed distance among voxels belonging to the object, continuity of the object segmentation, and morphology of the segmentation. We theoretically show that the optimum solution (in the sense of minimizing the Bayesian error rate) for this problem by deriving the corresponding likelihood function. We demonstrate that the log-likelihood function maximization problem cannot be solved analytically. Hence, we utilize the expectationmaximization algorithm to iteratively maximize the likelihood function. We also show that increasing the number of features necessarily reduces the Bayesian error rate, regardless of the discriminability of the features. Particularly for prostate segmentation in TRUS, we have shown employing union of Haralick features and first-order statistics features outperforms the case where they are employed individually. The qualitative and quantitative results calculated for expertly segmented prostate across 6 patient studies show the validity of the presented segmentation. The convergence of the variance of estimated parameters to the Cramer-Rao lower bound illustrates the proficiency of our

9034-144, Session PSMon

## Combining watershed and graph cuts methods to segment organs at risk in radiotherapy

Jose Dolz, Hortense A Kirisli, Romain Viard, Laurent Massoptier, AQUILAB (France)

Computer-aided segmentation of anatomical structures in medical images is a valuable tool for efficient Radiation Therapy Planning (RTP). As delineation errors highly affect the radiation oncology treatment, it is crucial to delineate geometric structures accurately. In this paper, a semi-automatic segmentation approach for computed tomography (CT) images, based on watershed and graph-cuts methods, is presented. The watershed pre-segmentation groups small areas of similar intensities in homogeneous labels, which are subsequently used as input for the graph-cuts algorithm. This methodology does not require of prior knowledge of the structure to be segmented; even so, it demonstrated to work well with complex shapes and low intensity. The presented method also allows the user to add foreground and background strokes in any view - axial, sagittal or coronal -, making the interaction with the algorithm easier and faster. Hence, the segmentation information is propagated within the whole volume, providing a spatially coherent result. The proposed algorithm has been evaluated using 9 CT images, by comparing its segmentation performance over several organs - lungs, liver, spleen, heart and aorta - to those of manual delineation from experts. With these experiments, it has been proved that the proposed approach works well for all the anatomical structures analyzed, providing a Dice's coefficient higher than 0.87 in all the cases. Due to the quality of the results, the introduction of the proposed approach in the RTP process will be a helpful tool for organs at risk (OARs) segmentation.











9034-145, Session PSMon

## Interactive segmentation of tongue contours in ultrasound video sequences using quality maps

Sarah Ghrenassia, École de Technologie Supérieure (Canada); Lucie Ménard, Univ. du Québec à Montréal (Canada); Catherine Laporte, Ecole de Technologie Supérieure (Canada)

Ultrasound (US) imaging is an effective and non invasive way of studying

the tongue motions involved in normal and pathological speech, and the results of US studies are of interest for the development of new strategies in speech therapy. State-of-the-art tongue shape analysis techniques based on US images depend on semi-automated tongue segmentation and tracking techniques. Recent work has mostly focused on improving the accuracy of the tracking techniques themselves. However, occasional errors remain inevitable, regardless of the technique used, and the tongue tracking process must thus be supervised by a speech scientist who will correct these errors manually or semi-automatically. This paper proposes an interactive framework to facilitate this process. In this framework, the user is guided towards potentially problematic portions of the US image sequence by a segmentation quality map that is based on the normalized energy of an active contour model and automatically produced during tracking. When a problematic segmentation is identified, corrections to the segmented contour can be made on one image and propagated both forward and backward in the problematic subsequence, thereby improving the user experience. The interactive tools were tested

in combination with two different tracking algorithms. Preliminary results

illustrate the potential of the proposed framework, suggesting that the

proposed framework generally improves user interaction time, with little

9034-146, Session PSMon

change in segmentation repeatability.

## Automatic FDG-PET-based tumor and metastatic lymph node segmentation in cervical cancer

Didac Rodriges, Henrik G. Jensen, Univ. of Copenhagen (Denmark); Annika L. Jacobsen, Per Munck af Rosenschöld, Rigshospitalet (Denmark); Anders E. Hansen, Christian Igel, Sune Darkner, Univ. of Copenhagen (Denmark)

Diagnosis and treatment of cervical cancer, one of the three most often diagnosed cancers worldwide, often rely on delineations of the tumor and metastases based on PET imaging using the contrast agent 18F-Fluorodeoxyglucose (FDG). We present a robust automatic segmentation algorithm for the gross tumor volume (GTV) and metastatic lymph nodes in such images. As the cervix is located next to the bladder and FDG is washed out through the urine, the positive GTV and the bladder cannot be easily separated. Our processing pipeline starts with a histogram-based region of interest detection followed by Chan-Vese level set segmentation. After that, morphological image operations combined with clustering, region growing, and nearest neighbor labeling allow to remove the bladder and to identify the tumor and metastatic lymph nodes. The proposed method was applied to 125 patients, and no failure could be detected by visual inspection. We compared our segmentations with results from manual delineations of corresponding MR and CT images, showing that the detected GTV lay within the MR/CT delineations. We conclude that the algorithm has a very high potential for substituting the tedious manual delineation of PET positive areas.

9034-147, Session PSMon

### MRI brain tumor segmentation and necrosis detection using adaptive Sobolev snakes

Arie Nakhmani, The Univ. of Alabama at Birmingham (United States); Ron Kikinis, Brigham and Women's Hospital (United States); Allen Tannenbaum, The Univ. of Alabama at Birmingham (United States)

Brain tumor segmentation in brain MRI volumes is used in neurosurgical planning and illness staging. It is important to explore the tumor shape and necrosis regions at different points of time to evaluate the disease progression. We propose an algorithm for semi-automatic tumor segmentation and necrosis detection. Our algorithm consists of three parts: conversion of MRI volume to a probability space based on the on-line learned model, tumor probability density estimation, and adaptive segmentation in the probability space. We use manually selected acceptance and rejection classes on a single MRI slice to learn the background and foreground statistical models. Then, we propagate this model to all MRI slices to compute the most probable regions of the tumor. Anisotropic 3D diffusion is used to estimate the probability density. Finally, the estimated density is segmented by the Sobolev active contour (snake) method to select smoothed regions of the maximum tumor probability. The segmentation approach is robust to noise and not very sensitive to the manual initialization in the volumes tested. Also, it is appropriate for low contrast imagery. The irregular necrosis regions are detected by using the outliers of the probability distribution inside the segmented region. The necrosis regions of small width are removed due to a high probability of noisy measurements. The MRI volume segmentation results obtained by our algorithm are very similar to expert manual segmentation.

9034-148, Session PSMon

### Real-time 3D medical structure segmentation using fast evolving active contours

Xiaotao Wang, Qiang Wang, Zhihui Hao, Kuanhong Xu, Ping Guo, Haibing Ren, Samsung Advanced Institute of Technology (China); Woo-Young Jang, Jung-Bae Kim, Samsung Advanced Institute of Technology (Korea, Republic of)

Segmentation of 3D medical structures in real-time is an important as well as intractable problem for clinical applications due to the high computation and memory cost. We propose a novel fast evolving active contour model in this paper to reduce the requirements of computation and memory. The basic idea is to evolve the brief represented dynamic contour interface as far as possible per iteration. Our method encodes zero level set via a single unordered list, and evolves the list recursively by adding activated adjacent neighbors to its end, resulting in active parts of the zero level set moves far enough per iteration along with list scanning. To guarantee the robustness of this process, a new approximation of curvature for integer valued level set is proposed as the internal force to penalize the list smoothness and restrain the list continual growth. Besides, list scanning times are also used as an upper hard constraint to control the list growing. Together with the internal force, efficient regional and constrained external forces, whose computations are only performed along the unordered list, are also provided to attract the list toward object boundaries. Specially, our model calculates regional force only in a narrowband outside the zero level set and can efficiently segment multiple regions simultaneously as well as handle the background with multiple components. Compared with stateof-the-art algorithms, our algorithm is one-order of magnitude faster with similar segmentation accuracy and can achieve real-time performance for the segmentation of 3D medical structures on a standard PC.











9034-149, Session PSMon

### Finding seed points for organ segmentation using example annotations

Ranveer R. Joyseeree, ETH Zurich (Switzerland) and Univ. of Applied Sciences Western Switzerland (Switzerland); Henning Müller, Univ. of Applied Sciences Western Switzerland (Switzerland) and Univ. of Geneva (Switzerland)

Organ identification and segmentation is important in diagnostic medicine to make current decision-support tools more effective and efficient. Performing it automatically would save time and labor. In this paper, a pilot study for the automatic identification of seed points for segmentation and identification of organs in three-dimensional (3D) non-annotated, full-body magnetic resonance (MR) and computed tomography (CT) volumes is presented. It uses 3D MR and CT acquisitions along with corresponding organ annotations from the VISCERAL project.

A training volume is first registered affinely with a carefully-chosen reference volume. The registration transform obtained is then used to warp the annotations of the training volume. For a chosen organ, an overlap volume is created by combining the warped training annotation and the reference annotation. The process is repeated for several training volumes.

Next, a 3D probability map for the location of the organ on the reference volume is derived from the overlap volume. Its centroid is determined and it serves as the seed point for segmentation of the organ. The approach yields very promising initial results.

Afterwards, the reference volume may be affinely mapped onto any non-annotated volume and the mapping applied to the pre-computed volume containing the centroid and the probability distribution for an organ of interest. Segmentation on the non-annotated volume may then be started using existing state-of-the-art algorithms with the warped centroid as the seed point and the warped probability distribution as an aid to the stopping criterion. Finally, the organ may be identified using the segmented data.

9034-150, Session PSMon

## Atherosclerotic carotid lumen segmentation in combined B-mode and contrast enhanced ultrasound images

Zeynettin Akkus, Diego D. B. Carvalho, Stefan Klein, Stijn C. H. van den Oord, Arend F. L. Schinkel, Nico de Jong, Antonius F. W. van der Steen, Johan G. Bosch, Erasmus MC (Netherlands)

Patients with carotid atherosclerotic plaques carry an increased risk of cardiovascular events such as stroke. Ultrasound has been employed as a standard for diagnosis of carotid atherosclerosis. To assess atherosclerosis, the intima contour of the carotid artery lumen should be accurately outlined. For this purpose, we (simultaneously) acquired side-by-side longitudinal contrast enhanced ultrasound (CEUS) and B-mode ultrasound (BMUS) images and exploit the information in the two imaging modalities for accurate lumen segmentation. First, nonrigid motion compensation was performed on both BMUS and CEUS image sequences, followed by averaging over the 150 time frames to produce an image with improved signal-to-noise ratio (SNR). After that, we segmented the lumen from these images using a novel method based on dynamic programming which uses the joint histogram of the CEUS and BMUS pair of images to distinguish between background, lumen, tissue and artifacts. Finally, the obtained lumen contour in the improved-SNR mean image was transformed back to each time frame of the original image sequence. Validation was done by comparing manual lumen segmentations of two independent experts with automated lumen segmentations in the improved-SNR images of 11 carotid arteries from 9 patients. The root mean square error between the two experts

was 0.25±0.17 mm and between automated and average of manual segmentation of two experts was 0.31±0.08 mm. In conclusion, we present a robust and accurate carotid lumen segmentation method which overcomes the complexity of anatomical structures, noise in the lumen, artifacts and echolucent plaques by exploiting the information in two imaging modalities.

9034-151, Session PSMon

### Shape-constrained multi-atlas segmentation of spleen in CT

Zhoubing Xu, Bo Li, Swetasudha Panda, Andrew J. Asman, Kristen L. Merkle, Peter L. Shanahan, Richard G. Abramson, Bennett A. Landman, Vanderbilt Univ. (United States)

Spleen segmentation on clinically acquired CT data is a challenging problem given the complicity and variability of abdominal anatomy. Multiatlas segmentation is a potential method for robust estimation of spleen segmentations, but can be negatively impacted by registration errors. Although labeled atlases explicitly capture information related to feasible organ shapes, multi-atlas methods have largely used this information implicitly through registration. We propose to integrate a level set shape model into the traditional label fusion framework to create a shapeconstrained multi-atlas segmentation framework. Briefly, we (1) adapt two alternative atlas-to-target registrations to obtain the loose bounds on the inner and outer boundaries of the spleen shape, (2) project the fusion estimate to registered shape models, and (3) convert the projected shape into shape priors. With the constraint of the shape prior, our proposed method offers a statistically significant improvement in spleen labeling accuracy with an increase in DSC by 0.06, a decrease in symmetric mean surface distance by 4.01 mm, and a decrease in symmetric Hausdorff surface distance by 23.21 mm when compared to a locally weighted vote (LWV) method.

9034-152, Session PSMon

### Multi-atlas segmentation with particle-based group-wise image registration

Joohwi Lee, The Univ. of North Carolina at Chapel Hill (United States); Ilwoo Lyu, The Univ. of North Carolina at Charlotte (United States); Martin A. Styner, The Univ. of North Carolina at Chapel Hill (United States)

We present a novel image registration method based on B-spline free-form deformation that simultaneously opti- mizes particle correspondence and image similarity metrics. Different from previous B-spline based registration methods optimized w.r.t. the control points, the deformation in our method is estimated from a set of dense unstructured pair of points, which we refer as corresponding particles. As intensity values are matched on the corresponding location, the registration performance is iteratively improved. Moreover, the use of corresponding particles naturally extends our method to a group-wise registration by computing a mean of particles. In this paper, multiple of atlases are used to construct a training set, and a novel image is segmented using this group- wise registration together with pre-existing atlases. We demonstrate the results of our method in an application of rodent brain structure segmentation and show that our method provides better accuracy in two structures compared to other registration methods.











9034-153, Session PSMon

#### Development of automated extraction method of biliary tract from abdominal CT volumes based on local intensity structure analysis

Kusuto Koga, Yuichiro Hayashi, Tomoaki Hirose, Masahiro Oda, Nagoya Univ. (Japan); Takayuki Kitasaka, Aichi Institute of Technology (Japan); Tsuyoshi Igami, Masato Nagino, Kensaku Mori, Nagoya Univ. (Japan)

In this paper, we describe an automated biliary tract extraction method from abdominal CT volumes. The biliary tract has linear structures and intensities of the biliary tract are low in CT volumes. We use a dark linear structure enhancement (DLSE) filter based on a local intensity structure analysis method using the eigenvalues of the Hessian matrix for extraction of the biliary tract. The proposed method consists of two steps including an extraction of the intrahepatic bile duct (IHBD) and an extraction of the extrahepatic biliary tract (EHBT). The IHBD are extracted by applying the DLSE filter to a CT volume. In the EHBT extraction step, we generate a modified CT volume by enhancing CT values of soft tissues and biliary walls from the CT volume. The EHBT are extracted by applying the DLSE filter to the modified CT volumes. We applied the proposed method to sixteen cases of CT volumes. The experimental results showed that the proposed method could extract the biliary tract regions from CT volumes.

9034-154, Session PSMon

## Automatic detection of mitochondria from electron microscope tomography images: a curve fitting approach

Serdar S. Tasel, Reza Z. Hassanpour, Çankaya Univ. (Turkey); Erkan U. Mumcuoglu, Middle East Technical Univ. (Turkey); Guy Perkins, Maryann E. Martone, Univ. of California, San Diego (United States)

Mitochondria are sub-cellular components which are mainly responsible for synthesis of adenosine tri-phosphate (ATP) and involved in the regulation of several cellular activities such as apoptosis. The relation between some common diseases of aging and morphological structure of mitochondria is gaining strength by an increasing number of studies. Electron microscope tomography (EMT) provides high-resolution images of the 3D structure and internal arrangement of mitochondria. Studies that aim to reveal the correlation between mitochondrial structure and its function require the aid of special software tools for manual segmentation of mitochondria from EMT images. Automated detection and segmentation of mitochondria is a challenging problem due to the variety of mitochondrial structures, the presence of noise, artifacts and other sub-cellular structures. Segmentation methods reported in the literature require human interaction to initialize the algorithms. In our previous study, we focused on 2D detection and segmentation of mitochondria using an ellipse detection method. In this study, we propose a new approach for automatic detection of mitochondria from EMT images. First, a preprocessing step was applied in order to reduce the effect of non-mitochondrial sub-cellular structures. Then, a curve fitting approach was presented using a Hessian-based ridge detector to extract membrane-like structures and a curve-growing scheme. Finally, an automatic algorithm was employed to detect mitochondria which are represented by a subset of the detected curves. The results show that the proposed method is more robust in detection of mitochondria in consecutive EMT slices as compared with our previous automatic method.

9034-155, Session PSMon

## Automatic segmentation of vertebral arteries in CT angiography using combined circular and cylindrical model fitting

Min Jin Lee, Helen Hong, Seoul Women's Univ. (Korea, Republic of); Jin Wook Chung, Seoul National Univ. Hospital (Korea, Republic of)

For the visualization and analysis of vertebral arteries in CT angiography, an accurate segmentation of enhanced vessels is an essential process. However, the vertebral arteries pass through the transverse foramen in the cervical vertebra and they have significant overlapping density distribution with surrounding cervical vertebra. Thus, we propose an automatic vessel segmentation method of vertebral arteries in CT angiography using combined circular and cylindrical model fitting. First, initial vessel candidates are segmented using adaptive thresholding and starting points of vertebral arteries are automatically detected by fitting circle model to the initial vessel candidates in axial slice where shoulder landmark is detected. Second, the initial vessel candidates are tracked using circular model fitting. Since boundaries of the vertebral arteries are ambiguous in case the arteries pass through the transverse foramen in the cervical vertebra, the circle model is extended along z-axis to cylinder model for considering additional vessel information of neighboring slices. Finally, the boundaries of the vertebral arteries are detected using graphcut optimization. From the experiments, the proposed method provides accurate results without bone artifacts and eroded vessels in the cervical vertebra.

9034-156, Session PSMon

#### Three Dimensional Level Set Based Semiautomatic Segmentation of Atherosclerotic Carotid Artery Wall Volume Using 3D Ultrasound Imaging

Md Murad Hossain, Khalid Aimuhanna, George Mason Univ. (United States); Limin Zhao, Brajesh Lal, Univ. of Maryland Medical Ctr. (United States); Siddhartha Sikdar, George Mason Univ. (United States)

3D segmentation of carotid plaque from ultrasound images is challenging due to image artifacts and poor boundary definition. Semiautomatic segmentation algorithms have been proposed for the common carotid artery (CCA) but they have rarely been applied to plaques in the internal carotid artery (ICA). In this work, we describe a 3D segmentation algorithm that is robust to shadowing and missing boundaries. Our algorithm uses distance regularized level set method with edge and region based energy to segment media-adventitia (MAB) and lumenintima (LIB) boundary of plaques in the CCA and ICA. The algorithm is initialized by manually placing points on the boundary of a subset of transverse slices with an interslice distance of 5mm. We propose two novel energy terms for minimization, one constraining the MAB to an elliptical shape, and another utilizing a user defined stopping surface to prevent bleeding across poorly defined boundaries. Validation was performed against manual segmentation using 3D US volumes acquired from asymptomatic patients with carotid stenosis using a linear 4D probe. 30 cross sectional images were selected from the whole volume with an interslice distance of 1mm using carotid bifurcation as the landmarks. The Dice similarity coefficient (DSC), Hausdorff distance (HD) and modified HD (MHD) were used to compare algorithm results against manual boundaries on representative cross sectional image planes. Results from two subjects with >50% carotid stenosis showed good agreement to manual segmentation in the ICA with DSC: 82.55 ± 2.9 (MAB),  $81.05 \pm 6.5$  (LIB); MHD:  $0.55 \pm 0.15$  (LIB),  $0.49 \pm 0.14$  (MAB); HD;  $0.87 \pm 0.24$  (MAB),  $0.9 \pm 0.26$  (LIB) in whole volume. The algorithm performs better in CCA than ICA. Analysis on additional patients is











currently underway. The proposed 3D semiautomatic segmentation is first step towards full characterization of 3D plaque progression and longitudinal monitoring.

9034-157, Session PSMon

## Bladder segmentation in MR images with watershed segmentation and graph cut algorithm

Thomas Blaffert, Steffen Renisch, Nicole Schadewaldt, Heinrich Schulz, Philips Research (Germany)

Prostate cancer diagnosis and treatment planning that is based on MR images benefits from superior soft tissue contrast compared to CT images. For these images an automatic delineation of the prostate and the organs at risks such as the bladder is highly desirable. This paper describes a method for bladder segmentation that is based on a watershed transform and gray value valleys and the classification of the watershed regions into bladder and tissue with a graph cut algorithm. The obtained results are superior if compared to a simple region-afterregion classification.

9034-159, Session PSMon

### Neurosphere segmentation in brightfield images

Jierong Cheng, Wei Xiong, Shue Ching Chia, Joo Hwee Lim, Institute for Infocomm Research (Singapore); Shvetha Sankaran, Sohail Ahmed, A\*STAR Institute of Medical Biology (Singapore)

The challenge of segmenting neurospheres (NSPs) from brightfield images includes uneven background illumination (vignetting), low contrast and shadow-casting appearance near the well wall. We propose a pipeline for neurosphere segmentation in brightfield images, focusing on shadow-casting removal. Firstly, we remove vignetting by creating a synthetic blank field image from a set of brightfield images of the whole well. Then, the region with shadow-casting effect is Polar-transformed and undergoes high-pass filtering to create a flat background. Line integration is applied in the horizontal direction of the Polar image to remove the shadow-casting and therefore facilitate automatic segmentation. To suppress the accumulation of noise along the integration path and the inclusion of slowly-varying image components, integrating along two opposite paths with an exponential decay factor (bi-directional decay) is required. Furthermore, a weighted bi-directional decay function is introduced to prevent undesired gradient effect of line integration on NSPs without shadow-casting. Afterward, the local maxima of multiscale Laplacian of Gaussian (LoG) response identify candidate NSPs with its location, size, and filter responses known. Finally, localized region-based level set is used to detect the NSP boundaries. Experimental results show that our proposed radial line integration method (RLI) achieves higher detection accuracy over existing methods in terms of precision, recall and F-score with less computational time.

9034-160, Session PSMon

## 3D pre- versus post-season comparisons of surface and relative pose of the corpus callosum in contact sport athletes

Yi Lao, Children's Hospital Los Angeles (United States) and The Univ. of Southern California (United States); Niharika Gajawelli, The Univ. of Southern California (United States) and Children's Hospital Los Angeles (United States); Lauren Hass, Bryce

Wilkins, Darryl Hwa Hwang, Sinchai Tsao, The Univ. of Southern California (United States); Yalin Wang, Arizona State Univ. (United States); Meng Law, The Univ. of Southern California (United States); Natasha Lepore, The Univ. of Southern California (United States) and Children's Hospital Los Angeles (United States) and The Univ. of Southern California (United States)

Mild traumatic brain injury (TBI) or concussive injury affects 1.7 million Americans annually, of which 300,000 are due to recreational activities and contact sports, such as football, rugby, and boxing[1]. Finding the neuroanatomical correlates of brain TBI non-invasively and precisely is crucial for diagnosis and prognosis. Several studies have shown the influence of traumatic brain injury on the integrity of brain WM[5,8]. The vast majority of these works focus on athletes with diagnosed concussions. However, in contact sports, athletes are subjected to repeated hits to the head throughout the season, and we hypothesize that these have an influence on white matter integrity. In particular, the corpus callosum (CC), as a small structure connecting the brain hemispheres, may be particularly affected by torques generated by collisions, even in the absence of full blown concussions.

Here, we use a combined surface-based morphometry and relative pose analyses, applying on the point distribution model (PDM) of the CC, to investigate TBI related brain structural changes between 9 pre-season and 9 post-season contact sport athletes from MRI. All the data are fed into surface based morphometry analysis and relative pose analysis. The former looks at surface area and thickness changes between the two groups, while the latter consists of detecting the relative translation, rotation and scale between them.

9034-161, Session PSMon

#### A versatile tomographic forward- and backprojection approach on Multi-GPUs

Andreas Fehringer, Technische Univ. München (Germany); Tobias Lasser, Technische Univ. München (Germany) and Helmholtz Zentrum München GmbH (Germany); Irene Zanette, Peter B. Noël, Franz Pfeiffer, Technische Univ. München (Germany)

Iterative tomographic reconstruction gets more and more into the focus of interest for x-ray computed tomography as parallel high-performance computing finds its way into compact and affordable computing systems in form of GPU devices. However, when it comes to the point of highresolution x-ray computed tomography, e.g. measured at synchrotron facilities, the limited memory and bandwidth of such devices are soon stretched to their limits. Especially keeping the core part of tomographic reconstruction, the projectors, both versatile and fast for large datasets is quite a challenge. Therefore, we demonstrate a multi-GPU accelerated forward- and backprojector based on projection matrices and taking advantage of two concepts to distribute large datasets into smaller units. The first concept involves splitting up the volume into chunks of slices perpendicular to the axis of rotation. The result is many perfectly independent tasks which then can be solved by distinct GPU devices. A novel ultrafast precalculation kernel prevents unnecessary data transfers for cone-beam geometries. Datasets with a great number of projections can additionally take advantage of the second concept, a split-up into angular wedges. We demonstrate the portability of our projectors to multiple devices and the associated speedup on a high-resolution liver sample measured at the synchrotron. With our splitting approaches, we gained factors of 3.5 - 3.9 on a system with four and 7.5 - 8.0 with eight GPUs resulting in a computing time of 2.94s instead of 23.5s in the latter











9034-162, Session PSMon

## Genomic connectivity networks based on the BrainSpan atlas of the developing human brain

Ahmed Mahfouz, Technische Univ. Delft (Netherlands) and Leids Univ. Medisch Ctr. (Netherlands); Mark N Ziats, National Institute of Child Health and Human Development, National Institutes of Health (United States) and University of Cambridge (United Kingdom) and Baylor College of Medicine (United States); Owen M. Rennert, National Institute of Child Health and Human Development (United States); Boudewijn P.F. Lelieveldt, Department of Radiology, Leiden University Medical Center (Netherlands) and Department of Intelligent Systems, Delft University of Technology (Netherlands); Marcel J.T. Reinders, Delft Bioinformatics Lab, Delft University of Technology (Netherlands)

The human brain comprises systems of networks that span the molecular, cellular, anatomic and functional levels. Molecular studies of the developing brain have focused on elucidating networks among gene products that may drive cellular brain development by functioning together in biological pathways. On the other hand, studies of the brain connectome attempt to determine how anatomically distinct brain regions are connected to each other, either anatomically (diffusion tensor imaging) or functionally (functional MRI and EEG), and how they change over development. A global examination of the relationship between gene expression and connectivity in the developing human brain is necessary to understand how the genetic signature of different brain regions instructs connections to other regions. Furthermore, analyzing the development of connectivity networks based on the spatio-temporal dynamics of gene expression provides a new insight into the effect of neurodevelopmental disease genes on brain networks.

In this work, we construct connectivity networks between brain regions based on the similarity of their gene expression signature, namely: Genomic Connectivity Networks (GCNs). Genomic connectivity networks were constructed based on the BrainSpan atlas, which provides a transcriptome-wide expression data of the developing human brain. The main goal is to understand how the genetic signature of each brain region instructs its connections with other regions across development. Additionally, we assess the differences in connectivity patterns of networks constructed based on genes associated with a neurodevelopmental disorder (autism spectrum disorder; ASD). Using a graph theoretical approach, we characterized the neurodevelopmental changes in these networks.

9034-163, Session PSMon

### Wavelets based algorithm for the evaluation of enhanced liver areas

Matheus Alvarez, UNESP (Brazil); Diana R. Pina, UNESP (Brazil); Fernando Romeiro, UNESP (Brazil); Sérgio B. Duarte, Centro Brasileiro de Pesquisas Físicas (Brazil); José Ricardo A. Miranda, Guilherme Giacomini, Seizo Yamashita, UNESP (Brazil)

Background: Hepatocellular carcinoma is a primary tumor of the liver and involves different treatment modalities according to the tumor stage. After local therapies, the tumor evaluation is based on the mRECIST criteria, which involves the measurement of the maximum diameter of the viable lesion. This paper describes a computed methodology to measure through the contrasted area of the lesions the maximum diameter of the tumor by a computational algorithm.

Methods: 63 computed tomography (CT) slices from 23 patients were assessed. Non-contrasted liver and HCC typical nodules were evaluated, and a virtual phantom was developed for this purpose. Optimization of

the algorithm detection and quantification was made using the virtual phantom. After that, we compared the algorithm findings of maximum diameter of the target lesions against radiologist measures.

Results: Computed results of the maximum diameter are in good agreement with the results obtained by radiologist evaluation, indicating that the algorithm was able to detect properly the tumor limits. A comparison of the estimated maximum diameter by radiologist versus the algorithm revealed differences on the order of 0.25 cm for large-sized tumors (diameter > 5 cm), whereas agreement lesser than 1.0cm was found for small-sized tumors.

Conclusions: Differences between algorithm and radiologist measures were accurate for small-sized tumors with a trend to a small decrease for tumors greater than 5 cm. Therefore, traditional methods for measuring lesion diameter should be complemented non-subjective measurement methods, which would allow a more correct evaluation of the contrastenhanced areas of HCC according to the mRECIST criteria.

9034-164, Session PSMon

### 3D segmentation of masses in DCE-MRI images using FCM and adaptive MRF

Chengjie Zhang, Li Hua Li, Hangzhou Dianzi Univ. (China)

Dynamic contrast enhanced magnetic resonance imaging (DCE-MRI) is a sensitive imaging modality for the detection of breast cancer. Automated segmentation of breast lesions in DCE-MRI images is challenging due to inherent signal-to-noise ratios and high inter-patient variability. A novel 3D segmentation method based on FCM and MRF is proposed in this study. In this method, a MRI image is segmented by spatial FCM, firstly. And then MRF segmentation is conducted to refine the result. We combined with the 3D information of lesion in the MRF segmentation process by using segmentation result of contiguous slices to constraint the slice segmentation. At the same time, a membership matrix of FCM segmentation result is used for adaptive adjustment of Markov parameters in MRF segmentation process. The proposed method was applied for lesion segmentation on 145 breast DCE-MRI examinations (86 malignant and 59 benign cases). An evaluation of segmentation was taken using the traditional overlap rate method between the segmented region and hand-drawing ground truth. The average overlap rates for benign and malignant lesions are 0.764 and 0.755 respectively. Then we extracted five features based on the segmentation region, and used an artificial neural network (ANN) to classify between malignant and benign cases. The ANN had a classification performance measured by the area under the ROC curve of AUC=0.73. The positive and negative predictive values were 0.86 and 0.58, respectively. The results demonstrate the proposed method not only achieves a better segmentation performance in accuracy also has a reasonable classification performance.

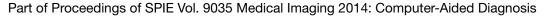








Tuesday - Thursday 18-20 February 2014





9035-2, Session 2

### Multi-fractal texture features for brain tumor and edema segmentation

Syed Reza, Khan M. Iftekharuddin, Old Dominion Univ. (United States)

This basic idea of this work is based on our novel multi-resolution fractal based brain tumor segmentation works. In our prior works, we exploit SVM as weak classifier with a novel modified Adaboost algorithm for tumor and other tissue segmentation. In contrast, this work uses Random Forests for brain tumor & edema classification. We obtain 2D MRI slices from 3D volume MRI for subsequent processing. Since BRATS 2012 dataset is already skull stripped and co-registered, we restrict our preprocessing steps to bias and inhomogeneity correction only.

9035-3, Session 2

## Ischemic Stroke Lesion Segmentation in Multi-spectral MR Images with Support Vector Machine Classifiers

Oskar Maier, Matthias Wilms, Janina von der Gablentz, Ulrike Krämer, Heinz Handels, Univ. zu Lübeck (Germany)

Rationale and objective:

Automatic segmentation of ischemic stroke lesions in magnetic resonance (MR) images is important in clinical practice and for cognitive neuroscience trials. The key problem is to detect largely inhomogeneous regions of varying sizes, shapes and locations.

Materials and methods:

We present a stroke lesion segmentation method based on local features extracted from multi-spectral MR data that are selected to model a human observer's discrimination criteria. A support vector machine classifier is trained on expert-segmented examples and then used to classify formerly unseen images.

Results and conclusion:

Each MR sequence's contribution is closely examined and justified. None is found to be redundant. Leave-one-out cross validation on eight datasets with lesions of varying appearances is performed, showing our method to compare favourably with other published approaches in terms of accuracy and robustness.

9035-4, Session 2

### A ROC-based feature selection method for computer-aided detection and diagnosis

Songyuan Wang, Fourth Military Medical Univ. (China) and Xidian Univ. (China); Guopeng Zhang, Fourth Military Medical Univ. (China); Junying Zhang, Xidian Univ. (China); Qimei Liao, Hongbing Lu, Fourth Military Medical Univ. (China); Chun Jiao, Fourth Military Medical Univ (China)

Image-based computer-aided detection and diagnosis (CAD) has been a very active research topic aiming to assist physicians to detect lesions and distinguish them from benign to malignant. However, the datasets fed into a classifier usually suffer from small number of samples, as well as significantly less samples available in one class (have a disease) than the other, resulting in the classifier's suboptimal performance. How to identifying the most characterizing features of the observed data for lesion detection is critical to improve the sensitivity and minimize false

positives of a CAD system. In this study, we propose a novel feature selection method mR-FAST that combines the minimal-redundancy-maximal relevance (mRMR) framework with a selection metric FAST (feature assessment by sliding thresholds) based on the area under a ROC curve (AUC) generated on optimal simple linear discriminants. With three feature datasets extracted from CAD systems for colon polyps and bladder cancer, we show that the space of candidate features selected by mR-FAST is more characterizing for lesion detection with higher AUC, enabling to find a compact subset of superior features at low cost.

9035-5, Session 2

### Change detection of medical images using dictionary learning techniques and PCA

Varvara Nika, York Univ. (Canada); Paul Babyn, Royal Univ. Hospital (Canada); Hongmei Zhu, York Univ. (Canada)

Automatic change detection methods for identifying the changes of serial MR images taken at different times are of great interest to radiologists. The majority of existing change detection methods in medical imaging, and those of brain images in particular, include many preprocessing steps and rely mostly on statistical analysis of MRI scans. Although most methods utilize registration software, tissue classification remains a difficult and overwhelming task. Recently, dictionary learning techniques are used in many areas of image processing, such as image surveillance, face recognition, remote sensing, and medical imaging. In this paper we present Eigen-Block Change Detection algorithm (EigenBlockCD), which performs local registration and identifies the changes between consecutive MR images of the brain. Blocks of pixels from one scan are used as training samples for detecting the changes in the follow up scan. We use PCA to reduce the dimensionality of the local dictionaries and the redundancy of data. Choosing the appropriate distance measure significantly affects the performance of our algorithm. We examine the differences between L1 and L2 norms as two possible similarity measures in EigenBlockCD. We show the advantages of L2 norm over L1 norm both theoretically and numerically. We also demonstrate the performance of EigenBlockCD algorithm for detecting changes of MR images and compare our results with those provided in recent literature. Experimental results with both simulated and real MRI scans show that EigenBlockCD outperforms the previous methods. It detects clinical changes while ignoring the changes due to patient's position and other acquisition artifacts.

9035-6, Session 2

## Segmentation and automated measurement of chronic wound images: probability map approach

Mohammad Faizal Ahmad Fauzi, Ohio State Univ. (United States) and Multimedia Univ. (Malaysia); Ibrahim Khansa, Karen Catignani, Gayle Gordillo M.D., Chandan K. Sen, Metin N. Gurcan, The Ohio State Univ. (United States)

A chronic wound, as defined by the Wound Healing Society, is a wound that has not healed in a timely fashion. An estimated 6.5 million patients in the United States are affected by chronic wounds, with more than 25 billion US dollars and countless hours spent annually for all aspects of chronic wound care. There is need to develop software tools to analyze wound images that segment wounds, measure their characteristics, and monitor the changes over time. These processed, when done manually, are time-consuming and subject to intra- and inter-reader variability. In this paper, we propose a method that can segment chronic wounds containing granulation, slough and eschar tissues. First, we generate a Red-Yellow-Black (RYK) probability map, which then guides the region growing segmentation process. The red, yellow and black probability











map is designed to handle the granulation, slough and eschar tissues, respectively found in wound tissues. The innovative aspects of this work include: 1) Definition of a wound characteristics specific probability map for segmentation, 2) Computationally efficient regions growing with channel selection; 3) Auto-calibration of measurements with the content of the image. The method was applied on 30 wound images provided by the Ohio State University Wexner Medical Center, with the ground truth independently generated by two clinicians. The ground truth was generated as the consensus of these clinicans. While the inter-reader agreement between the reader is 85.5%, the computer achieves an accuracy of 82.4%.

9035-79, Session 2

## Early detection of Alzheimer's disease using histograms in a dissimilarity-based classification framework

Anne Luchtenberg, Rita Simões, Univ. Twente (Netherlands); Anne-Marie van Cappellen van Walsum, Univ. Twente (Netherlands) and Radboud Univ. Nijmegen Medical Ctr. (Netherlands); Cornelis H. Slump, Univ. Twente (Netherlands)

Early detection of Alzheimer's disease is expected to aid in the development and monitoring of more effective treatments. Classification methods have been proposed to distinguish Alzheimer's patients from normal controls using Magnetic Resonance images.

Dissimilarity-based classification consists of representing objects based on their distance to a representative set of objects, rather than on a set of pre-defined features. In particular, dissimilarity-based classification has been applied to the early detection of Alzheimer's using a pairwise deformation-based distance measure. However, this approach is not only computationally expensive but it also considers large-scale alterations in the brain only.

In this work, we propose the use of gray level histograms, determined both globally and locally, to detect very mild to mild Alzheimer's disease. We hypothesize that groupwise differences in shape and volume are also reflected in intensity differences. Our results show that this approach achieves an accuracy of 70-76% when considering the entire brain, outperforming the traditional classification approach, which uses the histograms as feature vectors. Additionally, using an ensemble of local patches over the entire brain, we obtain an accuracy of 84% (sensitivity 80% and specificity 88%). Finally, we are able to detect which regions contribute the most to the classification. As expected, these lie mostly in the medial-temporal lobe, particularly near the hippocampi.

9035-7, Session 3

### Reference-tissue correction of T2-weighted signal intensity for prostate cancer detection

Yahui Peng, Yulei Jiang, Aytekin Oto, The Univ. of Chicago Medical Ctr. (United States)

Purpose: To investigate whether correction of T2-weighted MR image signal intensity (SI) against reference tissue improves its effectiveness for region of interest (ROI)-based classification of prostate cancer (PCa) vs. normal tissue.

Materials and Methods: We retrospectively collected two 1.5T MR image datasets: 71 cases acquired with GE scanners (dataset A), and 59 cases with Philips scanners (dataset B). Through consensus histology-MR correlation review, 175 PCa and 108 normal-tissue ROIs were identified. Reference-tissue ROIs were selected from the internal obturator muscle, urinary bladder, and pubic bone. Corrected T2 SI was calculated as the ratio of the average T2 SI within a PCa or normal-tissue ROI to that of a reference-tissue ROI. Area under the receiver operating characteristic curve (AUC) was used to evaluate the effectiveness of the T2 SIs for differentiation of PCa from normal-tissue ROIs.

Results: AUC ( $\pm$  standard error) for uncorrected T2 SIs was 0.78 $\pm$ 0.04 (datasets A) and 0.65 $\pm$ 0.05 (datasets B). AUC for T2 SIs corrected with reference muscle, bladder, and bone ROIs was 0.77 $\pm$ 0.04 (p=1.0), 0.77 $\pm$ 0.04 (p=1.0), and 0.75 $\pm$ 0.04 (p=0.8), respectively, for dataset A; and 0.81 $\pm$ 0.04 (p=0.002), 0.78 $\pm$ 0.04 (p<0.001), and 0.79 $\pm$ 0.04 (p<0.001), respectively, for dataset B. Correction in reference to the internal obturator muscle yielded the most consistent results between GE and Phillips images.

Conclusion: Correction of T2-weighted SI in reference to three extraprostatic tissue types can improve its effectiveness for differentiation of PCa from normal-tissue ROIs, and correction in reference to the internal obturator muscle can produce consistent T2-weighted SIs between GE and Phillips MR images.

9035-8, Session 3

# Computer-extracted texture features on T2w MRI to predict biochemical recurrence following radiation therapy for prostate cancer

Shoshana Ginsburg, Mirabela Rusu, Case Western Reserve Univ. (United States); John Kurhanewicz, Univ. of California, San Francisco (United States); Anant Madabhushi, Case Western Reserve Univ. (United States)

In this study we explore the ability of computer-extracted features describing prostate cancer morphology on T2w MRI to predict whether a patient will respond well to radiotherapy or develop biochemical recurrence (BcR) within five years despite radiotherapy. Currently, the Kattan nomogram is used to predict BcR following radiotherapy; the Kattan nomogram incorporates several clinical factors to predict the probability of recurrence-free survival following radiotherapy but has limited prediction accuracy. While the correlation between BcR and factors like tumor stage, Gleason grade, extracapsular spread are well-documented, it is less clear how to predict BcR in the absence of extracapsular spread and for small tumors fully contained in the capsule. This work seeks to identify the role of morphologic traits, quantified via T2w MRI, in predicting BcR risk and to establish T2w MRI texture as a potential independent prognostic marker of PSA failure. In this study we extract a total of 440 intensity features, edge descriptors, co-occurrence features, and Gabor wavelet features from T2w MRI and implement Isomap to embed the data in a low-dimensional space where classification can be performed. We previously developed a method, called variable importance in nonlinear kernels (VINK), for quantifying the contributions of individual features to classification on an Isomap embedding and thereby identifying the few features that play the greatest role in predicting BcR. Using VINK we identify a diagonal gradient feature and a Gabor wavelet feature that together provide an area under the receiver operating characteristic curve of 0.82 for predicting the probability of BcR following radiotherapy in 16 patients. In comparison to the Kattan nomogram, the superior ability of these two computerextracted features to differentiate the survival curves of BcR and non-BcR patients is also demonstrated.

9035-9, Session 3

#### Multi-atlas propagation via a manifold graph on a database of both labeled and unlabeled images

Qinquan Gao, Tong Tong, Daniel Rueckert, Philip Edwards, Imperial College London (United Kingdom)

We present a framework for multi-atlas based segmentation in situations where we have a small number of segmented atlas images, but a large database of unlabeled images is also available. The novelty lies in the











application of graph-based registration on a manifold to the problem of multi-atlas registration. The approach is to place all the images in a learned manifold space and construct a graph connecting near neighbors. Atlases are selected for any new image to be segmented based on the shortest path length along the manifold graph. A multi-scale non-rigid registration takes place via each of the nodes on the graph. The expectation is that by registering via similar images, the likelihood of misregistrations is reduced. Having registered multiple atlases

via the graph, patch-based voxel weighted voting takes place to provide the \_nal segmentation. We apply this approach to a set of T2 MRI images of the prostate, which is a notoriously di\_cult segmentation task. On a set of 25 atlas images and 85 images overall, we see that registration via the manifold graph improves the Dice coefficient from 0.82 to 0.86. This is a modest but potentially useful improvement in a difficult set of images. It is expected that our approach will provide similar improvement to any multi-atlas segmentation task where a large number of unsegmented images are available.

9035-10, Session 3

## Automated polyp measurement based on colon structure decomposition for CT colonography

Huafeng Wang, Stony Brook Univ. (United States); Lihong C. Li, College of Staten Island (United States); Hao Han, Hao Peng, Bowen Song, Stony Brook Univ. (United States); Xinzhou Wei, New York City College of Technology (United States); Zhengrong Liang, Stony Brook Univ. (United States)

Accurate assessment of colorectal polyp size is of great significance for early diagnosis and management of colorectal cancers. Due to the complexity of colon structure, polyps with diverse geometric characteristics grow from different landform surfaces. In this paper, we present a new colon decomposition approach for polyp measurement. We first apply an efficient maximum a posteriori expectationmaximization (MAP-EM) partial volume segmentation algorithm to achieve an effective electronic cleansing on colon. The global colon structure is then decomposed into different kinds of morphological shapes, e.g. haustral folds or haustral wall. Meanwhile, the polyp location is identified by an automatic computer aided detection algorithm. By integrating the colon structure decomposition with the computer aided detection system, a patch volume of colon polyps is extracted. Thus, polyp size assessment can be achieved by finding abnormal protrusion on a relative uniform morphological surface from the decomposed colon landform. We evaluated our method via physical phantom and clinical datasets. Experiment results demonstrate the feasibility of our method in consistently quantifying the size of polyp volume and, therefore, facilitating characterizing for clinical management.

9035-11, Session 3

# An improved high order texture features extraction method with application to pathological diagnosis of colon lesions for CT colonography

Bowen Song, Stony Brook Medicine (United States); Guopeng Zhang, Hongbing Lu, Fourth Military Medical Univ. (China); Huafeng Wang, Fangfang Han, Stony Brook Medicine (United States); Zhu Wei, Stony Brook Univ. (United States); Zhengrong Liang, Stony Brook Medicine (United States)

Differentiation of colon lesions into different pathological phases, e.g., neoplastic and non-neoplastic, is of fundamental importance for computer-aided diagnosis task. Geometric features, which are widely

employed for detection phase, do not perform well in the diagnosis task and more and more attention is given to texture features as they are believed to be a more useful biomarker for the differentiation task. In this paper, we first propose Haralick texture feature extraction method based on higher order images, i.e., gradient image (1st order) and curvature image (2nd order), and then briefly introduce our manually lesion volume segmentation method. We applied the higher order texture features extracted from 3D lesion volume and compared itwith the density based Haralick texture features. SVM-based classifier and ROC analysis were employed for the evaluation. The results shows that after applying high order features the AUC improved from 0.7403 to 0.8525 in differentiating non-neoplastic lesions, e.g., Hyperplastic lesions, from neoplastic ones, e.g., Tubular Adenoma, Tubulovillous Adenoma and Adenocarcinoma lesions. The improved results demonstrate that high order texture feature can help the computer-aided diagnosis task. Using texture biomarker with high order image information for CTC based pathology analysis is promising.

9035-12, Session 4

## An image-based software tool for screening retinal fundus images using vascular morphology and network transport analysis

Richard D. Clark III, Constellation Research, LLC (United States); Daniel J. Dickrell III, Univ. of Florida (United States); David L. Meadows, Constellation Research, LLC (United States)

As the number of digital retinal fundus images taken each year grows at an increasing rate, there exists a similarly increasing need for automatic eye disease detection through image-based analysis. A new method has been developed for classifying standard color fundus photographs into both healthy and diseased categories. This classification was based on the calculated network fluid resistance, a function of the geometry and connectivity of the vascular segments. To evaluate the network resistance, the retinal vasculature was first manually separated from the background to ensure an accurate representation of the geometry and connectivity. The arterial and venous networks were then semi-automatically separated into two separate binary images. The connectivity of the arterial network was then determined through a series of morphological image operations. The network comprised of segments of vasculature and points of bifurcation, with each segment having a characteristic geometric and fluid properties. Based on the connectivity and fluid resistance of each vascular segment, an arterial network flow resistance was calculated, which described the ease with which blood can pass through a vascular system. In this work, 26 eyes (13 healthy and 13 diabetic) from patients roughly 65 years in age were evaluated using this methodology. Healthy arterial networks exhibited a fluid resistance of 0.86  $\pm$  0.49 kPa-s/?L while the average network fluid resistance of the diabetic set was 2.60 ± 0.81 Kpa-s/?L. The results of this new imagebased software demonstrated an ability to automatically, quantitatively and efficiently screen diseased eyes from color fundus imagery.

9035-13, Session 4

## An automatic machine learning system for coronary calcium scoring in clinical non-contrast enhanced, ECG-triggered cardiac CT

Jelmer M. Wolterink, Tim Leiner M.D., Richard A. P. Takx M.D., Max A. Viergever, Ivana Isgum, Univ. Medical Ctr. Utrecht (Netherlands)

Presence of coronary artery calcium (CAC) is a strong and independent predictor of cardiovascular events. We present a system using a forest of extremely randomized trees to automatically identify and quantify CAC in routine cardiac non-contrast enhanced CT. Candidate lesions the system could not label with high certainty were automatically identified and











presented to an expert who could relabel them to achieve high scoring accuracy with minimal effort.

The study included 200 consecutive non-contrast enhanced ECG-triggered cardiac CTs (120 kV, 55 mAs, 3 mm section thickness). Expert CAC annotations made as part of the clinical routine served as the reference standard. CAC candidates were extracted by thresholding (130 HU) and 3-D connected component analysis. They were described by shape, intensity and spatial features calculated using multi-atlas segmentation of coronary artery centerlines from ten CTA scans.

CAC was identified using a randomized decision tree ensemble classifier in a ten-fold stratified cross-validation experiment and quantified in Agatston and volume scores for each patient. After classification, candidates with posterior probability indicating uncertain labeling were selected for further assessment by an expert.

Images with metal implants were excluded. In the remaining 164 images, Spearman's rho between automatic and reference scores was 0.94 for both Agatston and volume scores. On average 1.8 candidate lesions per scan were subsequently presented to an expert. After correction, Spearman's rho was 0.98.

We have described a system for automatic CAC scoring in cardiac CT images which is able to effectively select difficult examinations for further refinement by an expert.

9035-14, Session 4

### Automated coronary artery calcification detection on low-dose chest CT images

Yiting Xie, Cornell Univ. (United States); Matthew D. Cham M.D., Claudia I. Henschke M.D., David F. Yankelevitz M.D., Icahn School of Medicine at Mount Sinai (United States); Anthony P. Reeves, Cornell Univ. (United States)

Coronary artery calcification (CAC) measurement from low-dose CT images can be used to assess the risk of coronary artery disease [1-2]. This paper presents a fully automatic algorithm to detect and measure CAC from low-dose non-contrast non-ECG gated chest CT scans. Based on the automatically detected CAC, the Agatston score (AS), mass and volume score are computed. They are then compared with scores obtained manually from standard-dose ECG gated and low-dose ungated scans of the same patient obtained within a short time interval of each other.

To segment CAC, the automated segmentation of the heart is performed based on constraints from pre-segmented organs to determine general coronary mask. All voxels greater than 180HU within the mask region are considered as CAC candidates. Finally mitral valve and aortic valve calcification is identified and excluded. The remaining candidates are considered as CAC.

The algorithm was evaluated on 41 low-dose non-contrast CT scans. Each scan has a corresponding standard-dose ECG gated CT scan of the same patient taken within a short time. Manual markings were performed on both scans. Using linear regression, the automatic AS were 86% correlated with the standard dose manual scores and 91% correlated with the low-dose manual scores. Standard risk categories were also computed. Compared to standard-dose markings, the automated method correctly assigned the risk categories of 25 cases while 14 cases were 1 category off. Compared to low-dose markings, the automated method correctly assigned the risk categories of 33 cases while 7 cases were 1 category off.

9035-15, Session 4

## Supervised pixel classification for segmenting geographic atrophy in fundus autofluorescene images

Zhihong Hu, Doheny Eye Institute (United States); Gerard G. Medioni, Matthias Hernandez, The Univ. of Southern California (United States); Sadda R. SriniVas, Doheny Eye Institute (United States)

Geographic atrophy (GA) is a manifestation of the advanced or latestage of the age-related macular degeneration (AMD), which may result in severe vision loss and blindness. Techniques to rapidly and precisely quantify atrophic lesions would appear to be of value in advancing the understanding of the pathogenesis of GA lesions and the management of GA progression. The purpose of this study is to develop an automated supervised pixel classification approach for segmenting GA including uni-focal and multi-focal atrophic patches in fundus autofluorescene (FAF) images. The image features include region wise intensity measures (mean and variance), gray level co-occurrence matrix measures (angular second moment, entropy, and inverse difference moment), and Gaussian filter banks. A k-nearest-neighbor (k-NN) pixel classifier is applied to obtain a GA probability map, representing the likelihood that the image pixel belongs to a region of GA. A voting binary iterative hole filling filter is then applied to fill in the small holes. Sixteen randomly chosen FAF images were obtained from sixteen subjects with GA. The algorithmdefined GA regions are compared with manual delineation performed by certified expert graders. Two-fold cross-validation is applied for the evaluation of the classification performance. The mean Dice similarity coefficients (DSC) between the algorithm- and manually-defined GA regions are  $0.84 \pm 0.06$  for one test and  $0.83 \pm 0.07$  for the other test and the area correlations between them are 0.99 (p < 0.05) and 0.94 (p < 0.05) respectively.

9035-16, Session 5

### Opportunities and challenges for diagnostic decision support systems (Keynote Presentation)

Nico Karssemeijer, Radboud Univ. Nijmegen Medical Ctr. (Netherlands)

More than ten years after the successful introduction of computer aided detection (CAD) systems for mammography, expectations among radiologists about the potential of CAD have been lowered considerably. Development of mammography CAD has been stalled for many years and new successful applications have not emerged. Despite a strong increase in CAD research in academic centers, translation from research to clinical practice appears to be highly challenging. In this talk some major causes for the low acceptance of CAD will be discussed. But prospects for large scale use of intelligent software in medical imaging remain good. Developers have to move away though from existing paradigms and explore novel ways to assist clinicians in image interpretation and diagnostic decision making. For instance, it is well known that in many tasks two readers perform better than a single reader. Hence, the value of CAD as a second reader should be evident if CAD on its own was as good as a reader. Unfortunately, this is not yet the case for the majority of CAD applications. Thus, a major challenge will be the improvement of CAD algorithms to reach at least the performance of experienced human readers. Challenges further include integration of CAD in the clinical workflow and improvement of the regulatory process. When these challenges can be overcome, there are big opportunities for automated diagnostic support systems. The availability of huge imaging data archives, quantitative imaging techniques, and increasing knowledge in machine learning will contribute to the development of effective CAD systems in many domains, including radiology, ophthalmology, and pathology.











9035-17, Session 6

#### Detection, modeling and matching of pleural thickenings from CT data towards an early diagnosis of malignant pleural mesothelioma

Kraisorn Chaisaowong, RWTH Aachen (Germany); Thomas Kraus, Univ. Hospital Aachen (Germany)

Pleural thickenings are caused by asbestos exposure and may evolve into malignant pleural mesothelioma. While an early diagnosis plays the key roll to an early treatment, and therefore helping to relieve the morbidity, the growth rate of a pleural thickening can be in turn essential evidence to an early diagnosis of the pleural mesothelioma. The detection of pleural thickenings is today done by a visual inspection of CT data, which is time-consuming and underlies the physician's subjective judgment. Computer-assisted diagnosis systems to automatically assess pleural mesothelioma have been reported worldwide. But in this paper, an image analysis system to automatically detect pleural thickenings and measure their volume is described. We first delineate automatically the pleural contour in the CT images. An adaptive surface-base smoothing technique is then applied to the pleural contours to identify all potential thickenings. A following tissue-specific topology-oriented detection based on a probabilistic Hounsfield Unit model of pleural plagues specify then the genuine pleural thickenings among them. The assessment of the detected pleural thickenings is based on the volumetry of the 3D model, created by mesh construction algorithm followed by Laplace-Beltrami eigenfunction expansion surface smoothing technique. Finally, the spatiotemporal matching of pleural thickenings from consecutive CT data is carried out based on the semi-automatic lung registration towards the assessment of its growth rate. With these methods, a new computerassisted diagnosis system is presented in order to assure a precise and reproducible assessment of pleural thickenings towards the diagnosis of the pleural mesothelioma in its early stage.

9035-18, Session 6

## Automatic localization of IASLC-defined mediastinal lymph node stations on CT images using fuzzy models

Monica M. S. Matsumoto, Jayaram K. Udupa, Steven Archer, Drew A. Torigian, Univ. of Pennsylvania (United States)

Lung cancer is associated with the highest mortality rates among men and women in the United States. The accurate and precise identification of the lymph node stations on computed tomography (CT) images is important for uniform staging and attempts at prognosticating outcome in patients with lung cancer, as well as for pretreatment planning and response assessment purposes. To facilitate standard means of referring to lymph nodes, recently the International Association for the Study of Lung Cancer (IASLC) has proposed a definition of the different stations and zones in the thorax. However, this is typically performed manually by qualitative visual assessment in clinical radiology practice. Therefore, we present a method of automatically recognizing the mediastinal IASLCdefined lymph node stations by modifying a hierarchical fuzzy modeling approach previously developed for body-wide automatic anatomy recognition (AAR) in medical imagery. Our AAR-lymph node (AAR-LN) system follows the AAR methodology and consists of two steps. In the first step, the various lymph node stations are manually delineated on a set of CT images following the IASLC definitions. These delineations are then used to build a fuzzy hierarchical model of the stations. In the second step, the stations are automatically located on any given CT image of the thorax by using the hierarchical fuzzy model and object recognition algorithms. Based on 20 datasets used for model building, 21 datasets for testing purposes, and 9 tested lymph node stations, a mean localization accuracy of within 5-6 voxels has been achieved by the AAR-LN system.

9035-19, Session 6

### Computer detection system for malpositioned endotracheal tubes

Zhimin Huo, Jing Zhang, Carestream Health, Inc. (United States); Hongda Mao, Rochester Institute of Technology (United States); Anne-Marie Sykes, Mayo Clinic (United States); John Wandtke M.D., Univ. of Rochester (United States); David H. Foos, Carestream Health, Inc. (United States)

Portable chest radiographic images play a critical role in examining and monitoring the condition and progress of critically ill patients in intensive care units (ICUs). For example, portable chest images are acquired to ensure that tubes inserted into the patients are properly positioned for effective treatment. In this paper, we present a system that automatically detects the position of an endotracheal tube (ETT), which is inserted into the trachea to assist patients who have difficulty breathing. A properly positioned ETT should be placed 3-5 cm above the carina, which lies at the site of the tracheal bifurcation at the lower end of the trachea. Our approach includes the detection of the lung, spine line, and aortic arch. These landmarks are used to identify regions of interest (ROIs) for ETT and carina detection. Once the ROI is determined for each, a templatematching technique is applied. Our ETT and carina detection methods were developed and tested on 145 CR images and 217 DR images. The locations of the ETTs and carina were identified by an experienced radiologist for the purpose of evaluation. Our ETT detection achieved an average sensitivity of 85% at 0.1 or lower false-positive detections per image. The carina approach correctly identified the carina location within a 10 mm distance from the truth for 79% of the 217 DR images. We expect our system will assist ICU clinicians in detecting malpositioned ETTs in a timely manner as malpositioned ETTs can result in collapsed lungs, which can be life threatening.

9035-20, Session 6

## Artificial neural networks for automatic modelling of the pectus excavatum corrective prosthesis

Pedro L. Rodrigues, António H. J. Moreira, Univ. do Minho (Portugal); Nuno F. Rodrigues, Univ. do Minho (Portugal) and Instituto Politecnico do Cavado e do Ave (Portugal); Antonio C. M. Pinho, Jaime C. Fonseca, Jorge Correia-Pinto, Univ. do Minho (Portugal); João L. Vilaça, Univ. do Minho (Portugal) and Instituto Politecnico do Cavado e do Ave (Portugal)

Pectus excavatum is the most common deformity of the thorax, usually comprising Computed Tomography (CT) examination for preoperative diagnosis. Aiming at the elimination of the high amounts of CT radiation exposure, this work presents a novel methodology for the replacement of CT by a laser scanner (radiation-free) in the treatment of pectus excavatum using personally modeled prosthesis. The complete elimination of CT involves an accurate determination of ribs position and prosthesis placement region, based on chest wall skin surface information, acquired by a laser scanner. The developed solution resorts to artificial neural networks (ANN) trained with data vectors from 165 patients. Each training vector contains information from a patient chest wall skin surface and ribs position, determined using CT images. The training procedure was performed using the soft tissue thicknesses, determined using image processing techniques that automatically segment the skin and rib cage. The developed solution was then used to determine the ribs outline, using data from 20 patient scanners. Scaled Conjugate Gradient, Levenberg-Marquardt, Resilient Back propagation and One Step Secant gradient learning algorithms were used. Tests revealed that ribs position can be estimated with an average error of 4.9±3.23mm and 5.1±3.98mm for the left and right side of the patient. Such an error range is well below current prosthesis manual modeling,











indicating a considerable step forward towards CT replacement for prosthesis personalization.

9035-21, Session 6

## Mediastinal lymph node detection on thoracic CT scans using spatial prior from multi-atlas label fusion

Jiamin Liu, Jocelyn Zhao, Joanne Hoffman, Jianhua Yao, Weidong Zhang, Evrim B. Turkbey, Shijun Wang, Christine Kim, Ronald M. Summers M.D., National Institutes of Health (United States)

Lymph nodes play an important role in clinical practice but detection is challenging due to low contrast surrounding structures and variable size and shape. We propose a fully automatic method for mediastinal lymph node detection on thoracic CT scans. First, lungs are automatically segmented to locate the mediastinum region. Shape features by Hessian analysis, local scale, and circular transformation are computed at each voxel. Spatial prior distribution is determined based on the identification of multiple anatomical structures (esophagus, aortic arch, heart etc) by using multi-atlas with local adaptive label fusion. Shape features and spatial prior are then integrated for lymph node detection. The detected candidates are segmented by curve evolution. Characteristic features are calculated on the segmented lymph nodes and support vector machine is utilized for classification and false positive reduction. We applied our method to 20 patients with 62 enlarged mediastinal lymph nodes. The system achieved a significant improvement with 80% sensitivity at 7 false positives per patient with spatial prior compared to 50% sensitivity at 7 false positives per patient without a spatial prior.

9035-22, Session 6

### Estimation of cartilaginous region in noncontrast CT of the chest

Qian Zhao, Nabile M. Safdar M.D., Children's National Medical Ctr. (United States); Glenna Yu, Children's National Medical Ctr. (United States) and Princeton Univ. (United States); Emmarie Myers, Anthony Sandler, Marius George Linguraru, Children's National Medical Ctr. (United States)

Pectus excavatum is a posterior depression of the sternum and adjacent costal cartilages and is the most common congenital deformity of the anterior chest wall. Its surgical repair can be performed via minimally invasive procedures that involve sternum and cartilage relocation and benefit from adequate surgical planning. In this study, we propose a method to estimate the cartilage regions in thoracic CT scans, which is the first step of statistical modeling of the osseous and cartilaginous structures for the rib cage. The ribs and sternum are first segmented by using interactive region growing and removing the vertebral column with morphological operations. The entire chest wall is also segmented to estimate the skin surface. After the segmentation, surface meshes are generated from the volumetric data and the skeleton of the ribs is extracted using surface contraction method. Then the cartilage surface is approximated via contracting the skin surface to the osseous structure. The ribs' skeleton is projected to the cartilage surface and the cartilages are estimated using cubic interpolation given the joints with the sternum. The final cartilage regions are formed by the cartilage surface inside the convex hull of the estimated cartilages. The method was validated with the CT scans of two pectus excavatum patients and three healthy subjects. The average distance between the estimated cartilage surface and the ground truth is 2.89 mm. The promising results indicate the effectiveness of cartilage surface estimation using the skin surface.

9035-24, Session 7

### Automated aortic calcification detection in low-dose chest CT images

Yiting Xie, Cornell Univ. (United States); Yu Maw Htwe, Icahn School of Medicine at Mount Sinai (United States); Jennifer Padgett, Cornell Univ. (United States); Claudia I. Henschke M.D., David F. Yankelevitz M.D., Icahn School of Medicine at Mount Sinai (United States); Anthony P. Reeves, Cornell Univ. (United States)

Extent of aortic calcification has been shown to be a risk indicator for vascular events including cardiac. We have developed a fully automated computer algorithm to segment and measure aortic calcification in low-dose non-contrast, non-ECG gated chest CT scans. The algorithm first segments the aorta using a pre-computed Anatomy Label Map (ALM). Then based on the segmented aorta, aortic calcification is detected and measured in terms of the Agatston score, mass score and volume score. The automated scores are compared with reference scores obtained from manual markings.

For aorta segmentation, the aorta is modeled as a series of discrete overlapping cylinders and the aortic centerline is determined using a cylinder-tracking algorithm. Then the aortic surface location is detected using the centerline and a triangular mesh model. The segmented aorta is used as a mask for the detection of aortic calcification.

For calcification detection, the image is first filtered. Then an elevated threshold of 160HU is used in the mask region to reduce the effect of noise in low-dose scans. Finally non-aortic calcification voxels (bony structures, calcification in other organs) are eliminated and the remaining candidates are considered as true aortic calcification.

The computer algorithm is evaluated on 45 scans. Using linear regression, the automated Agatston score is 98.15% correlated with the reference Agatston score. The automated mass and volume score is respectively 98.18% and 98.00% correlated with the reference mass and volume score.

9035-25, Session 7

### Segmentation and separation of venous vasculatures in liver CT images

Lei Wang, Christian Hansen, Stephan Zidowitz, Horst K. Hahn, Fraunhofer MEVIS (Germany)

The computer-aided analysis of venous vasculatures including hepatic vein and portal vein is important in liver surgery planning. The analysis normally consists of two important pre-processing tasks: segmenting both vasculatures and separating them from each other by assigning different labels. During the acquisition of multi-phase CT images, both of these venous vessels are enhanced by injected contrast agents and acquired either in a common phase or in two individual phases. The enhanced signals established by contrast agents are often not stably acquired due to non-optimal acquisition time. The inadequate contrast and the presence of large lesions in oncological patients, make the segmentation task quite challenging. To overcome these difficulties, we propose a framework with minimal user interactions to analyze venous vasculatures in multi-phase CT images. Firstly, presented vasculatures are automatically segmented incorporating an efficient multi-scale Hessian-based vesselness filter. The initially segmented vessel tree structures are then converted to a graph representation, on which a series of graph filters are applied in post-processing steps to rule out irrelevant tube-like structures. Eventually, we propose a semi-automatic workflow to refine the segmentation in the areas of inferior vena cava and entrance of portal vein and to separate hepatic vein from portal vein. The segmentation quality was evaluated with intensive tests enclosing 60 CT images from both healthy liver donors and oncological patients. Quantitative measurements dedicated to assess the similarities between segmented and reference vessel trees were designed and calculated.











9035-26, Session 7

## Computerized luminal analysis for detection of non-calcified plaques in coronary CT angiography

Jun Wei, Chuan Zhou, Heang-Ping Chan, Aamer R. Chughtai, Smita Patel, Prachi Agarwal, Jean W. Kuriakose, Lubomir M. Hadjiiski, Ella A. Kazerooni M.D., Univ. of Michigan Health System (United States)

We are developing machine-learning techniques for a computeraided detection system to assist radiologists in detection of NCPs in coronary CTA (cCTA). A quantitative luminal analysis was designed for false positive (FP) reduction. A total of 113 NCPs were identified by experienced cardiothoracic radiologists in 83 cCTA volumes retrospectively collected with IRB approval. Coronary arteries were tracked, segmented and reformatted to a straightened volume with resampled slices perpendicular to the vessel centerline. Coronary arterial segments with diameters greater than about 2 mm were considered for NCP detection. Prescreening achieved a sensitivity of 92.9% (105/113) with a total of 1189 FPs (14.3 FPs/scan). We extracted 9 geometric features and 6 gray-level features, to quantify the differences between NCPs and FPs. The gray-level features included 4 features to measure local statistical characteristics and 2 asymmetry features to measure the asymmetric spatial location of gray-level density along the vessel centerline. The geometric features included a radius differential feature and 8 features extracted from two transformed volumes: the volumetric shape indexing and the gradient direction mapping volumes. The AUC values of individual features ranged from 0.59 to 0.76. On average, 6 features were selected during 10-fold cross-validation training. The average training and test AUC values were 0.87±0.01 and 0.85±0.01, respectively. Using the NCP score from combined feature sets, the FP rates were reduced to 3.49, 2.36, and 1.27 FPs/scan at sensitivities of 90%, 80%, and 70%, respectively, for testing. The study indicated that our computerized luminal analysis was effective for detection of NCPs in

9035-27, Session 7

## Automated discovery of structural features of the optic nerve head on the basis of image and genetic data

Mark A. Christopher, Li Tang, John H. Fingert, Todd E. Scheetz, Michael D. Abràmoff M.D., The Univ. of Iowa (United States)

Evaluation of optic nerve head (ONH) structure is a commonly used clinical technique for both diagnosis and monitoring of glaucoma. Glaucoma is associated with characteristic changes in the structure of the ONH. We present a method for computationally identifying ONH structural features using both imaging and genetic data from a large cohort of participants at risk for primary open angle glaucoma (POAG). Using 1057 participants from the Ocular Hypertension Treatment Study, ONH structure was measured by application of a stereo correspondence algorithm to stereo fundus images. In addition, the presence or absence of a known POAG risk factor associated with the gene TMCO1 was considered for each participant. ONH structural features were discovered using both a principal component analysis approach to identify the major modes of variance within structural measurements and a linear discriminant analysis approach to capture the relationship between the presence of the genetic risk factor and ONH structure. The identified ONH structural features were evaluated based on association with development of POAG by the end of the OHTS study. The identified ONH structural features were found to have significant associations (p < 0.05) with the development of POAG after Bonferroni correction. Further, incorporation of genetic risk status was found to substantially increase performance of early POAG prediction. These results suggest that incorporation of additional genetic information could lead to even greater power to predict the development of POAG.

9035-113, Session 7

# A joint estimation detection of Glaucoma progression in 3D spectral domain optical coherence tomography optic nerve head images

Akram Belghith, Christopher Bowd, Robert N. Weinreb, Linda M. Zangwill, Univ. of California, San Diego (United States)

Glaucoma is an ocular disease characterized by distinctive changes in the optic nerve head (ONH) and visual field. Glaucoma can strike without symptoms and causes blindness if it remains without treatment. Therefore, an early disease detection is important so that treatment can be initiated and blindness prevented from blindness. In this context, important advances in technology for non-invasive imaging of the eye have been made providing quantitative tools to measure structural changes in ONH topography, an essential element for glaucoma detection and monitoring its progression. In particular, 3D spectral domain optical coherence tomography (SD-OCT), an optical imaging technique, has been commonly used to discriminate glaucomatous from healthy subjects. In this paper, we present a new framework for detection of glaucoma progression using the 3D SD-OCT images. In contrast to previous works that use the retinal nerve fiber layer (RNFL) thickness measurement provided by commercially available spectraldomain optical coherence tomograph, we consider the whole 3D volume for change detection. To integrate a priori knowledge and in particular the spatial voxel dependency in the change detection map, we propose the use of the Markov Random Field to handle a such dependency. To accommodate the presence of false positive detection, the estimated change detection map is then used to classify a 3D SDOCT image into the "non-progressing" and "progressing" glaucoma classes based on a fuzzy logic classifier. We compared the diagnostic performance of the proposed framework to existing methods of progression detection.

9035-28, Session 8

## Using undiagnosed data to enhance computerized breast cancer analysis with a three stage data labeling method

Wenqing Sun, Tzu-Liang B. Tseng, The Univ. of Texas at El Paso (United States); Bin Zheng, University of Oklahoma (United States); Flemin Lure, University of Texas at El Paso (United States); Teresa Wu, Arizona State University (United States); Giulio Francia, University of Texas at El Paso (United States); Sergio D. Cabrera, Jianying Zhang, Miguel Vélez-Reyesv, Wei Qian, The Univ. of Texas at El Paso (United States)

A novel three stage Semi-Supervised Learning (SSL) approach is proposed for improving performance of computerized breast cancer analysis with undiagnosed data. These three stages include: (1) Instance selection, which is barely used in SSL or computerized cancer analysis systems, (2) Feature selection and (3) Newly designed 'Divide Co-training' data labeling method. 379 suspicious early breast cancer area samples from 121 mammograms were used in our research. Our proposed 'Divide Co-training' method is able to generate two classifiers through split original diagnosed dataset (labeled data), and label the undiagnosed data (unlabeled data) when they reached an agreement. The highest AUC (Area Under Curve, also called Az value) using labeled data only was 0.832 and it increased to 0.889 when undiagnosed data were included. The results indicate instance selection module could eliminate untypical data or noise data and enhance the following semi-supervised data labeling performance. Based on analyzing different data sizes, it can be observed that the AUC and accuracy go higher with the increase of either diagnosed data or undiagnosed data, and reach the best improvement (△AUC = 0.078, △Accuracy = 7.6%) with 40 of labeled data and 300 of unlabeled data.











9035-29, Session 8

#### A method for simultaneous detection, segmentation and classification of lesions in breast ultrasound images by learning with exemplars

Lidan Zhang, Haibing Ren, Zhihua Liu, Chuan Zhao, YongNan Ji, Samsung Advanced Institute of Technology (China)

In radiology, a Computer-Aided Diagnosis (CAD) system is designed to help human evaluation by providing three important functionalities: detecting lesion, segmenting and distinguishing whether the detected lesion is benign or malignant. In this work, a method is proposed which considered the above three problems at the same time. A lesion is detected if it has similar visual appearance with a specific instance which has been learned before. Specifically, a classifier is independently trained for each exemplar in order to learn the object as a whole as well as its partial features within the object. Once a lesion is detected, it would be associated with a training lesion whose boundary has been manually delineated. Given the pair of detected and exemplar lesions, the contour of the former one can be easily found by transferring geometric knowledge of the latter one. In the same way, we can distinguish whether the detected lesion is benign or malignant in accordance with the diagnosis of the exemplar. Finally experiments on clinical cases have proved that our methods outperformed the state-of-the-art approaches in terms of both the three individual tasks and the overall problem.

9035-30. Session 8

### Tumor detection in 3D ultrasound using phase-based features and Haar-like features

Chuan Zhao, Haibing Ren, YongNan Ji, Lidan Zhang, Zhihua Liu, Hongwei Zhang, Samsung Advanced Institute of Technology (China)

3D ultrasonography has attracted a great deal of interest these years. It has all the advantages of 2D ultrasound, such as imaging in realtime, free of harmful radiation and easy to perform. Besides, it offers a more efficient screening alternative than 2D ultrasound which makes researchers optimistic about its potential for widespread clinical use. Advanced 3D image processing becomes a critical need to make 3D Ultrasound more valuable. In this work, we present a new automatic approach for tumor detection in 3D ultrasound. The method combines a new type of phase-based measure and multi-channel Haar-like features to fast and accurately locate breast tumors in 3D ultrasound images. We formulate tumor detection into a multi-stage system. The first stage classifier extracts phase-based features to generate a confidence map indicating the probability of a voxel belonging to tumors. We define a new measure based on local phase incongruence to extract 3D salient bloblike features. The second stage classifier consists of a nested-cascade of Adaboost classifiers trained from multi-channel Haar-like features which are extracted from intensity images and gradient histogram equalization images. The final tumor candidates are given by the fusion of the two classifiers. A learning-based verification is conducted to reduce false alarms subsequently. The proposed approach has been applied on 543 3D breast ultrasound volumes for tumor detection. The results demonstrate the great potential of our method for clinical applications.

9035-31, Session 8

## Fully automated segmentation of whole breast in MR images by use of dynamic programming

Luan Jiang, Yanyun Lian, Shanghai Advanced Research Institute

(China); Yajia Gu, Xiaoxin Hu, Fudan Univ. Shanghai Cancer Ctr. (China); Qiang Li, Shanghai Advanced Research Institute (China)

Breast segmentation is an important and challenging task for computerized analysis of background parenchymal enhancement in dynamic contrast enhanced magnetic resonance images (DCE-MRI). The purpose of this study is to develop and evaluate a fully automated technique for accurate segmentation of whole breast in threedimensional (3-D) DCE-MRI. The whole breast segmentation consists of two steps, i.e., the delineation of breast skin line and the chest wall. A sectional dynamic programming method was first designed in each 2-D slice to trace the upper and/or lower boundaries of the chest wall. The statistical distribution of gray levels of the breast skin line was employed as weighting factor to enhance the skin line, and dynamic programming was then applied to delineate breast skin line slice-by-slice within the extracted volume of interest (VOI). Our method also took advantages of the continuity of chest wall and skin line across adjacent slices. Finally, the segmented breast skin line and the detected chest wall were connected to create the whole breast segmentation. The preliminary results on 70 cases show that the proposed method can obtain accurate segmentation of whole breast based on subjective observation. With the manually delineated region of 16 breasts in 8 cases, our method achieved Dice overlap measure of 92.1% ± 1.9% (mean ± SD) and volume agreement of 91.6% ± 4.7% for whole breast segmentation. It took approximately 4 minutes and 2.5 minutes for our method to segment the breast in an MR scan of 160 slices and 108 slices, respectively.

9035-32, Session 8

# Sparse representation of multi parametric DCE-MRI features using K-SVD for classifying gene expression based breast cancer recurrence risk

Majid Mahrooghy, Ahmed B. Ashraf, Dania Daye, Carolyn Mies, Mark Alan Rosen M.D., Michael D. Feldman, Despina Kontos, Univ. of Pennsylvania (United States)

We evaluate the prognostic value of sparse representation-based features by applying the K-SVD algorithm on multi-parametric kinetic, textural, and morphologic features in breast dynamic contrast-enhanced magnetic resonance imaging (DCE-MRI). K-SVD is an iterative dimensionality reduction method that optimally reduces the initial feature space by updating the dictionary columns jointly with the sparse representation coefficients. Therefore, by using K-SVD, we not only provide sparse representation of the features and condense the information in a few coefficients but also we reduce the dimensionality. The extracted K-SVD features are evaluated by a machine learning algorithm including a logistic regression classifier for the task of classifying high versus low breast cancer recurrence risk as determined by a validated gene expression assay. The features are evaluated using ROC curve analysis and leave one-out cross validation for different sparse representation and dimensionality reduction numbers. Optimal sparse representation is obtained when the number of dictionary elements is 4 (K=4) and maximum non-zero coefficients is 2 (L=2). We compare K-SVD with ANOVA based feature selection for the same prognostic features. The ROC results show that the AUC of the K-SVD based (K=4, L=2), the ANOVA based, and the original features (i.e., no dimensionality reduction) are 0.78, 0.71. and 0.68, respectively. From the results, it can be inferred that by using sparse representation of the originally extracted multiparametric, high-dimensional data, we can condense the information on a few coefficients with the highest predictive value. In addition, the dimensionality reduction introduced by K-SVD can prevent models from over-fitting.











9035-33, Session 8

## Digital breast tomosynthesis: effects of projection-view distribution on computer-aided detection of microcalcification clusters

Ravi K. Samala, Heang-Ping Chan, Yao Lu, Lubomir M. Hadjiiski, Jun Wei, Mark A. Helvie, Univ. of Michigan Health System (United States)

We investigated the effect of projection view (PV) distribution on detectability of microcalcification clusters (MC) in digital breast tomosynthesis (DBT) by a computer-aided detection (CAD) system. With IRB approval, DBT of breasts with biopsy-proven MCs were acquired with 60° tomographic angle, 21 PVs, and 3° increment (full set). The DBT volume was reconstructed using simultaneous algebraic reconstruction technique (SART) with multiscale bilateral filtering (MSBF) regularization. Three subsets simulating acquisition with 11, 9 and 11 PVs at tomographic angle and angular increment of (30°, 3°), (24°, 3°) and (60°, 6°), respectively, were also reconstructed with MSBF-regularized SART at several iterations. The subsets therefore had about half the dose of the full set. Prescreening of the microcalcification candidates was performed in the enhancement-modulated multiscale calcification response volume. Iterative thresholding in combination with region growing identified the potential microcalcification candidates. The prescreening sensitivity was analyzed using the mean and standard deviation of the signal-to-noise ratio (SNR) of the microcalcification candidates and rank-sensitivity plot. The MCs were detected by dynamic clustering using SNR and distance criteria. No additional FP reduction steps were performed to avoid the variability due to parameter tuning for a small data set. For the three subsets, view-based FROC analysis showed that the lowest FP rates at 75% sensitivity was achieved at 3.73, 4.54 and 5.92 per volume, respectively, compared to that of the full set at 2.64. The (30°, 3°) set performed better than the other two subsets.

9035-34, Session 9

## Reducing false positives of small bowel segmentation on CT scans by localizing colon regions

Weidong Zhang, Jiamin Liu, Jianhua Yao, Ronald M. Summers M.D., National Institutes of Health (United States)

Automated small bowel segmentation is essential for computer-aided diagnosis (CAD) of small bowel pathology, such as tumor detection and pre-operative planning. We previously proposed a novel method [1, 2] to segment the small bowel using the mesenteric vasculature as a roadmap. The method performed well on small bowel segmentation but produced many false positives, most of which were located on the colon [2]. To improve the accuracy of small bowel segmentation, we propose a semiautomated method with minimum interaction to distinguish the colon from the small bowel. The method utilizes anatomic knowledge about the mesenteric vasculature and a statistical method of colon detection. First, anatomic labeling of the mesenteric arteries [3] is used to identify the arteries supplying the colon. Second, a statistical detector is created by combining two colon probability maps. One probability map is of the colon location and is generated from colon centerlines generated from CT colonography (CTC) data. Another probability map is of 3D texture of the colon using Haralick features and support vector machine (SVM) classifiers. The two probability maps are combined to localize colon regions, i.e., voxels having high probabilities on both maps were labeled as colon. Third, colon regions identified by anatomical labeling and the statistical detector are removed from the original results of small bowel segmentation. The method was evaluated on 11 abdominal CT scans of patients suspected of having carcinoid tumors. The reference standard consisted of manually-labeled small bowel segmentation. The method reduced the voxel-based false positive rate of small bowel segmentation from  $19.7\% \pm 3.9\%$  to  $5.9\% \pm 2.3\%$ , with two-tailed P value < 0.0001.

9035-35, Session 9

## An adaptive approach for centerline extraction on CT colonography based on MAP-EM segmentation and distance field

Hao Peng, Stony Brook Univ. (United States); Lihong C. Li, College of Staten Island (United States); Huafeng Wang, Hao Han, Stony Brook Univ. (United States); Perry J. Pickhardt M.D., Univ. of Wisconsin-Madison (United States); Zhengrong Liang, Stony Brook Medicine (United States)

In this paper, we present an adaptive approach for fully automatic centerline extraction and small intestine removal based on MAP-EM partial volume segmentation algorithm and distance field. The computed tomographic colonography (CTC) volume image is first segmented for the colon wall mucosa layer, which represents the partial volume effects around the colon wall. Following that, we applied centerline extraction method and adaptively selected an intermediate layer on the extracted colon wall. Afterwards, branches are separated and small intestines are cleansed. We further examined its potential to solve the challenging touching and colon collapse problems in CTC. Experimental results based on 24 patient scans demonstrated that 100% of the small intestine data had been removed, among which 16 could be dealt with isolated component method, while the other 8 sets of data are cleansed via our proposed method. The voxel by voxel marking procedure preserves the topology and validity of the colon structure. The marked boundary and cleansed colon are very close to those labeled by the experts. Experimental results demonstrated its robustness and efficiency.

9035-36, Session 9

## Improved parameter extraction and classification for dynamic contrast enhanced MRI of prostate

Nandinee F. Haq, Piotr Kozlowski, Edward C. Jones, Silvia D. Chang, S. Larry Goldenberg, Mehdi Moradi, The Univ. of British Columbia (Canada)

Magnetic resonance imaging, particularly dynamic contrast enhanced (DCE) imaging, has shown great potential in prostate cancer diagnosis and prognosis. The time course of the DCE images provides measures of the contrast agent uptake kinetics. Also, using pharmacokinetic modeling, one can extract parameters from the DCE-MR images that characterize the vascularization and can be used to detect cancer. A requirement for calculating the pharmacokinetic DCE parameters is estimating the Arterial Input Function (AIF). One needs an accurate segmentation of the cross section of the descending femoral artery to obtain the AIF. In this work we report semi-automatic segmentation of the cross section of the femoral artery, using circular Hough transform, in the sequence of DCE images. We also report a machine-learning framework to combine pharmacokinetic parameters with the model-free contrast agent uptake kinetic parameters extracted from the DCE time course into a nine-dimensional feature vector. This combination of features is used with random forest and with support vector machine classification for cancer detection. The MR data is obtained from patients prior to radical prostatectomy. After the surgery, wholemount histopathology analysis is performed and registered to the DCE-MR images as the diagnostic reference. We show that the use of a combination of pharmacokinetic parameters and the model-free parameters extracted from the time course of DCE results in improved cancer detection compared to the use of each group of features separately. We also validate the proposed method for calculation of AIF based on comparison with the manual











9035-37, Session 9

## Distinguishing prostate cancer from benign confounders via a cascaded classifier on multi-parametric MRI

Geert Litjens, Radboud Univ. Nijmegen Medical Ctr. (Netherlands); Robin Elliott, Case Western Reserve Univ. (United States); Natalie Shih, Michael D. Feldman, Univ. of Pennsylvania (United States); Jelle O. Barentsz M.D., Christina A. Hulsbergenvan de Kaa, Iringo Kovacs, Henkjan J. Huisman, Radboud Univ. Nijmegen Medical Ctr. (Netherlands); Anant Madabhushi, Case Western Reserve Univ. (United States)

In this paper a new cascaded classifier is introduced to separate prostate cancer and benign confounders on MRI. Specific features to distinguish each of the benign classes will be selected in each step of the cascade, as opposed to a single-shot classifier, which only has the opportunity to learn features common to all confounders, or a multi-class classifier, which tries to learn all distinguishing features at once. Learning how to separate benign confounders from prostate cancer is important because the imaging characteristics of these confounders are poorly understood. The diagnostic uncertainty this causes leads to unnecessary biopsies and overtreatment. We used an annotated prostatectomy data set of 31 patients with multi-parametetric MRI to identify specific features for benign prostatic hyperplasia (BPH), high-grade prostatic intraepithilial neoplasia (HGPIN), atrophy and inflammation. The prostatectomy slides were carefully co-registered to the corresponding MRI slices using an elastic registration technique. We extracted texture, pharmacokinetic and intensity features for each of the confounder classes and prostate cancer. Relevant features for each of the classes were selected using maximum relevance minimum redundancy feature selection. The selected features were then incorporated in a cascading classifier, which can focus on easier subtasks at each stage, leaving the more difficult-to-separate classes for later stages. Results show that distinct features are relevant for each of the benign classes. Furthermore, the cascaded classifier outperforms both multi-class and one-shot classifiers in overall accuracy: 0.76 versus 0.71 and 0.62.

9035-38, Session 9

### A prostate MRI atlas of biochemical failures following radiotherapy

Mirabela Rusu, Case Western Reserve Univ. (United States); John Kurhanewicz, Univ. of California, San Francisco (United States); Anant Madabhushi, Case Western Reserve Univ. (United States)

Radiation therapy (RT) is a common treatment for prostate cancer (PCa), that has a high failure rate (>25%).

Early identification of RT failure can enable the use of more aggressive or neo-adjuvant therapies.

Moreover, predicting RT failure prior to treatment may spare the patient from a procedure that is unlikely to be successful and that also may have side effects.

RT failure is characterized by biochemical recurrence (BcR) which is typically defined relative to prostate specific antigen (PSA) concentration and its variation following treatment.

In this work, we use an anatomically constrained registration framework to construct prostate MRI atlases of BcR and non-BcR following RT.

Specifically, the BcR MRI atlas includes 12 subjects with BcR within 5 years of RT, while the non-BcR MRI atlas was built based on 20 subjects without BcR at 5 years following RT.

The atlas based co-registration bringing the MRI scans into the same canonical space, allows us to preform voxel-by-voxel comparisons and assess statistical differences between the BcR and non-BcR populations.

Furthermore, the statistical shape of the prostate derived from the MRI atlas facilitated the quantitative analysis of the variability in gland morphology between the BcR and non-BcR populations.

To assess whether the differences were valid, we performed an experiment whereby we constructed sub-population atlases by randomly sampling patients within each of the two cohorts to construct BcR and non-BcR atlases.

The differences between the two cohorts in terms of shape appeared to be consistent across these sub-population atlases. Our study suggested that the gland shape varies more in the non-BcR population, particularly in proximity of the apex.

9035-39, Session 10

## Dynamic automated synovial imaging (DASI) for differential diagnosis of rheumatoid arthritis

Enrico Grisan, Univ. degli Studi di Padova (Italy); Bernd Raffeiner, Univ. degli Studi di Padova (Italy) and Ospedale di Bolzano (Italy); Alessandro Coran, Univ. degli Studi di Padova (Italy); Luca Ciprian, Giovanni XXIII Nursing Home (Italy); Roberto Stramare, Univ. degli Studi di Padova (Italy)

Inflammatory rheumatic diseases are leading causes of disability and constitute a frequent medical disorder, leading to inability to work, high comorbidity and increased mortality. The gold-standard for diagnosing and differentiating arthritis is based on patient conditions and radiographic findings, as joint erosions or decalcification. However, early signs of arthritis are joint effusion, hypervascularization and synovial hypertrophy. In particular, vascularization has been shown to correlate with arthritis' destructive behavior, more than clinical assessment.

Contrast Enhanced Ultrasound (CEUS) examination of the small joints is emerging as a sensitive tool for assessing vascularization and disease activity. The evaluation of perfusion pattern rely on subjective semi-quantitative scales, that are able to capture the macroscopic degree of vascularization, but are unable to detect the subtler differences in kinetics perfusion parameters that might lead to a deeper understanding of disease progression and a better management of patients.

We show that after a kinetic analysis of contrast agent appearance, providing the the quantitative features characterizing the perfusion pattern of the joint, it is possible to accurately discriminate RA from PSA by building a random forest classifier on the computed features. We compare its accuracy with the assessment performed by expert radiologist blinded of the diagnosis.

9035-40, Session 10

### Automated identification of spinal cord and vertebras on sagittal MRI

Chuan Zhou, Heang-Ping Chan, Qian Dong, Bo He, Jun Wei, Lubomir M. Hadjiiski, Daniel Couriel, Univ. of Michigan Health System (United States)

We are developing an automated method for the identification of the spinal cord and the vertebras on spinal MR images, which is an essential step for computerized analysis of bone marrow diseases.

The spinal cord segment was first enhanced by a newly developed hierarchical multiscale tubular (HMT) filter that utilizes the complementary hyper- and hypo- intensities in the T1-weighted (T1W) and STIR MRI sequences. An Expectation-Maximization (EM) analysis method was then applied to the enhanced tubular structures to extract candidates of the spinal cord. The spinal cord was finally identified by a maximum-likelihood registration method by analysis of the features extracted from the candidate objects in the two MRI sequences. Using the identified











spinal cord as a reference, the vertebras were localized based on the intervertebral disc locations extracted by another HMT filter applied to the T1W images.

In this study, 10 and 61 MRI scans from 64 patients who were diagnosed with multiple myeloma disease were collected retrospectively with IRB approval as training and test set, respectively. The vertebras manually outlined by a radiologist were used as reference standard. A total of 852 vertebras were marked in the 61 test cases.

For the 61 test cases, 100% (61/61) of the spinal cords were correctly segmented with 6 false positives (FPs) mistakenly identified on the back muscles in 6 scans. A sensitivity of 94.0% (801/852) was achieved for the identification of vertebras, and 16 FPs were marked in 6 scans with an average FP rate of 0.26 FPs/scan.

9035-41, Session 10

#### Adaptive geodesic transform for segmentation of vertebrae on CT images

Bilwaj K. Gaonkar, Siemens Medical Solutions USA, Inc. (United States) and Univ. of Pennsylvania (United States); Liao Shu, Gerardo Hermosillo Valadez, Yiqiang Zhan, Siemens Medical Solutions USA, Inc. (United States)

Vertebral segmentation is a critical first step in any quantitative evaluation of vertebral pathology using CT images. This is especially challenging because bone marrow tissue has the same intensity profile as the muscle surrounding the bone. Thus simple methods such as thresholding or adaptive k-means fail to accurately segment vertebrae. While several other algorithms such as level sets may be used for segmentation any algorithm that is clinically deployable has to work in under a few seconds. To address these dual challenges we present here, a new algorithm based on the geodesic distance transform that is capable of segmenting the spinal vertebrae in under one second. To achieve this we extend the theory of the geodesic distance transforms proposed incite{toiv} to incorporate high level anatomical knowledge through adaptive weighting of image gradients. Such knowledge may be provided by the user directly or may be automatically generated by another algorithm. We incorporate information 'learnt' using a previously published machine learning algorithm to segment the L1 to L5 vertebrae. While we present a particular application here, the adaptive geodesic transform is a generic concept which can be applied to segmentation of other organs as well.

9035-42, Session 10

## 2D segmentation of intervertebral discs and its degree of degeneration from T2-weighted magnetic resonance images

Isaac Castro-Mateos, José Maria Pozo, The Univ. of Sheffield (United Kingdom); Áron Lazary, National Ctr. for Spinal Disorders (Hungary); Alejandro F. Frangi, The Univ. of Sheffield (United Kingdom)

Low back pain is a disorder suffered by hundreds of millions of people around the world. As intervertebral disc (IVD) degeneration is considered one of the key factors causing this illness, its early diagnosis could help prevent this disorder. Clinicians base their diagnosis on visual inspection of 2D slices of Magnetic Resonance (MR) images, which is subject to large inter-observer variability. In this work, an automatic classification method is presented, which provides the Pfirrmann degree of degeneration from a mid-sagittal MR slice.

The proposed method utilizes Active Contour Models, with a new geometrical energy, to achieve an initial segmentation, which is further improved using fuzzy C-means. Then, IVDs are classified according to their degree of degeneration. This classification is attained by means of Adaboost and five especial features, the mean and the variance of the

probability map of the nucleus using two different approaches and the eccentricity of the fitting ellipse to the contour of the IVD.

The classification method was evaluated using a cohort of 150 intervertebral discs assessed by three experts, resulting in a mean specificity (93%) and sensitivity (83%) similar to the one provided by every expert with respect to the most voted value. The segmentation accuracy was evaluated using the Dice Similarity Index (DSI) and Root Mean Square Error of the point-to-contour distance. The mean DSI  $\pm$  2? standard deviation was 91.7%  $\pm$  5.6% and the mean RMSE was 0.82mm and the 95 percentile was 1.36mm. These results were found accurate when comparing to the state-of-the-art.

9035-43, Session 10

### Prediction of treatment response and metastatic disease in soft tissue sarcoma

Hamidreza Farhidzadeh, Mu Zhou, Dmitry B. Goldgof, Lawrence O. Hall, Univ. of South Florida (United States); Meera Raghavan, Robert A. Gatenby, H. Lee Moffitt Cancer Ctr. & Research Institute (United States)

Soft tissue sarcomas (STS) are a heterogenous group of malignant tumors comprised of more than 50 histologic subtypes. Based on spatial variations of the tumor, predictions of the development of necrosis in response to therapy as well as eventual progression to metastatic disease are made. Optimization of treatment as well as management of therapy-related side effects may be improved with information earlier in the course of therapy. Multi-modality pre- and post-gadolinium enhanced magnetic resonance images (MRI) were taken before and after treatment for 30 patients. Regional variations in the tumor bed were measured quantitatively. The voxel values from the tumor region were used as features and a fuzzy clustering algorithm was used to segment the tumor into three spatial regions. The regions were given labels of high, intermediate and low based on the average signal intensity of pixels from the post-contrast T1 modality. These spatially distinct regions were viewed as essential meta-features to predict the response of the tumor to therapy based on necrosis (percentage of dead tissue of tumor) and metastatic disease (spread of tumor to sites other than the primary). The best feature was the difference in the number of pixels in the highest intensity regions of tumors before and after treatment. This enabled prediction of patients with metastatic disease and lack of positive treatment response (i.e. less necrosis). The best accuracy, 73.33%, is achieved by a Support Vector Machine in a leave-one-out cross validation on 30 cases predicting necrosis < 90% post treatment and metastasis.

9035-44, Session 10

## Automatic detection and segmentation of liver metastatic lesions on serial CT examinations

Avi Ben Cohen, Idit Diamant, Tel Aviv Univ. (Israel); Eyal Klang, Michal Amitai, Sheba Medical Ctr. (Israel); Hayit Greenspan, Tel Aviv Univ. (Israel)

In this paper we present a novel automated method for detection and segmentation of liver metastases on serial CT examinations (portal phase) given a 2D baseline segmentation mask. Our database contains 27 CT scans, baselines and follow-ups, of 12 patients and includes 22 test cases. Our method is based on the information given in the baseline CT scan which contains the lesion's segmentation mask marked manually by a radiologist. We use the 2D baseline segmentation mask to identify the lesion location in the follow-up CT scan using non-rigid image registration. The baseline CT scan is also used to locate regions of tissues surrounding the lesion and to map them onto the follow-up CT scan, in order to reduce the search area on the follow-up CT scan.











Finally, adaptive region-growing and mean-shift segmentation are used to obtain the final lesion segmentation. The segmentation results are compared to those obtained by a human radiologist. Compared to the reference standard our method made a correct RECIST 1.1 assessment for 21 out of 22 test cases. The average Dice index was  $0.83 \pm 0.07$ , average Hausdorff distance was  $7.85 \pm 4.84$  mm, average sensitivity was  $0.87 \pm 0.11$ , average false positive ratio was  $0.22 \pm 0.15$  and average false negative ratio was  $0.13 \pm 0.11$ . The segmentation performance and the RECIST assessment results look promising. We are pursuing the methodology further with expansion to 3D segmentation while increasing the dataset we are collecting from the CT abdomen unit at Sheba medical center.

9035-45, Session 11

## Identification of corresponding lesions in multiple mammographic views using starshaped iso-contours

Rafael Wiemker, Dominik Kutra, Harald S. Heese, Thomas Buelow, Philips Research (Germany)

It is common practice to assess lesions in two different mammographic views of each breast: medio-lateral oblique (MLO) and cranio-caudal (CC). We investigate methods that aim to automatically identify a lesion which was indicated by the user in one view in the other view of the same breast. Automated matching of user indicated lesions has slightly different objectives than lesion segmentation or matching for improved computer aided detection, leading to different algorithmic choices. A novel computationally efficient algorithm is presented which is based on detection of star-shaped iso-contours with high sphericity and local consistency. The lesion likelihood is derived from purely geometrically based figures of merit and thus is invariant against monotonous intensity transformations (e.g. non-linear LUTs). Validation was carried out by virtue of FROC curves on a public database consisting of entirely digital mammograms with expert-delineated match pairs, showing superior performance as compared to gradient-based minimum cost path algorithms, with computation times faster by an order of magnitude.

9035-46, Session 11

#### Boosting classification performance in computer aided diagnosis of breast masses in raw full-field digital mammography using processed and screen film images

Thijs Kooi, Nico Karssemeijer, Radboud Univ. Nijmegen Medical Ctr. (Netherlands)

The introduction of Full-Field Digital Mammography (FFDM) in breast screening has brought with it several advantages in terms and processing facilities and image quality. A major drawback however, is that raw FFDM data is still relatively scarce and therefore, training of a computer aided detection (CAD) system is limited by the lack of data. In this paper, we explore the usage of old Screen Film Mammograms (SFM) and FFDM processed by the manufacturer, which are more ubiquitous, in training a system for the detection of tumour masses. We compute a small set of additional features in the raw data, that make use of the log-linearity of the energy imparted on the detector in raw FFDM. We subsequently combine three classifiers, where classifier for raw FFDM has a higher dimensional feature space. We explore four different fusion methods: a weighted average, a majority vote, a convex combination of classifier outputs, based on the training error and an additional classifier, that combines the output of the three individual label estimates. Results are evaluated based on the Partial Area Under the Curve (PAUC) around a clinically relevant operating point. All fusion methods perform better than any of the individual classifiers and combining the classifiers based on their error on the training set outperforms the other methods.

9035-47, Session 11

### Lesion classification using clinical and visual data fusion by multiple kernel learning

Pavel Kisilev, IBM Research - Haifa (Israel); Sharbell Hashoul M.D., Carmel Medical Ctr. (Israel); Eugene Walach, Asaf Tzadok, IBM Research Haifa (Israel)

To overcome operator dependency and to increase diagnosis accuracy in breast ultrasound (US), a lot of effort has been devoted to developing computer-aided diagnosis (CAD) systems for breast cancer detection and classification. Unfortunately, the efficacy of such CAD systems is limited since they rely on correct automatic lesions detection and localization, and on robustness of features computed based on the detected areas.

In this paper we propose a new approach to boost the performance of a Machine Learning based CAD system, by combining visual and clinical data from patient files. We compute a set of visual features from breast ultrasound images, and construct the textual descriptor of patients by extracting relevant keywords from patients' clinical data files. We then use the Multiple Kernel Learning (MKL) framework to train SVM based classifier to discriminate between benign and malignant cases. We investigate different types of data fusion methods, namely, early, late, and intermediate (MKL-based) fusion. Our database consists of 408 patient cases, each containing US images, textual description of complaints and symptoms filled by physicians, and confirmed diagnoses. We show experimentally that the proposed MKL-based approach is superior to other classification methods. Even though the clinical data is very sparse and noisy, its MKL-based fusion with visual features yields significant improvement of the classification accuracy, as compared to the image features only based classifier.

9035-48, Session 11

## Breast density and parenchymal texture measures as potential risk factors for Estrogen-Receptor positive breast cancer

Brad M. Keller, Jinbo Chen, Univ. of Pennsylvania School of Medicine (United States); Emily F. Conant M.D., The Univ. of Pennsylvania Health System (United States); Despina Kontos, Univ. of Pennsylvania School of Medicine (United States)

Accurate assessment of a woman's risk to develop specific subtypes of breast cancer is critical for appropriate utilization of chemopreventative measures, such as with tamoxifen in preventing estrogen-receptor positive breast cancer. In that context, we investigate quantitative measures of breast density and parenchymal texture, measures of glandular tissue content and tissue structure, as risk factors for estrogenreceptor positive (ER+) breast cancer. Mediolateral oblique (MLO) view digital mammograms of the contralateral breast from 106 women with unilateral invasive breast cancer were retrospectively analyzed. Breast density and parenchymal texture were analyzed via fully-automated, software. Logistic regression with feature selection and was performed to predict ER+ versus ER- cancer status. A combined model considering all imaging measures extracted was compared to baseline models consisting of density-alone and texture-alone features. Area under the curve (AUC) of the receiver operating characteristic (ROC) and Delong's test were used to compare the models' discriminatory capacity for receptor status. The density-alone model had a discriminatory capacity of 0.62 AUC (p=0.05). The texture-alone model had a higher discriminatory capacity of 0.70 AUC (p=0.001), which was not statistically different compared to the density-alone model (p=0.37). In contrast the combined density-texture logistic regression model had a discriminatory capacity of 0.82 AUC (p<0.001), which was statistically significantly higher than both the density-alone (p<0.001) and texture-alone regression models (p=0.04). The combination of breast density and texture measures may have the potential to identify women specifically at risk for estrogenreceptor positive breast cancer and could be useful in triaging women into appropriate risk-reduction strategies.











9035-49, Session 11

### Ultrasound breast lesion segmentation using adaptive parameters

Baek Hwan Cho, Yeong Kyeong Seong, Junghoe Kim, Samsung Advanced Institute of Technology (Korea, Republic of); Zhihua Liu, Zhihui Hao, Samsung Advanced Institute of Technology (China); Eun Young Ko M.D., SAMSUNG Medical Ctr. (Korea, Republic of); Kyoung-Gu Woo, Samsung Advanced Institute of Technology (Korea, Republic of)

In computer aided diagnosis for ultrasound images, breast lesion segmentation is an important but intractable procedure. Although active contour models with level set energy function have been proposed for breast ultrasound lesion segmentation, those models usually select and fix the weight values for each component of the level set energy function empirically. The fixed weights might affect the segmentation performance since the characteristics and patterns of tissue and tumor differ between patients. Besides, there is observer variability in probe handling and ultrasound machine gain setting. Hence, we propose an active contour model with adaptive parameters in breast ultrasound lesion segmentation to overcome the variability of tissue and tumor patterns between patients. The main idea is to estimate the optimal parameter set automatically for different input images. We used regression models using 27 numerical features from the input image and an initial seed box. Our method showed better results in segmentation performance than the original model with fixed parameters. In addition, it could facilitate the higher classification performance with the segmentation results. In conclusion, the proposed active contour segmentation model with adaptive parameters has the potential to deal with various different patterns of tissue and tumor effectively.

9035-50, Session 12

## Comparison of CLASS and ITK-SNAP in segmentation of urinary bladder in CT urography

Kenny Cha, Lubomir M. Hadjiiski, Heang-Ping Chan, Elaine M. Caoili M.D., Richard H. Cohan M.D., Chuan Zhou, Univ. of Michigan (United States)

We are developing a computerized method for bladder segmentation in CTU for computer-aided diagnosis of bladder cancer. We have developed a Conjoint Level set Analysis and Segmentation System (CLASS) consisting of four stages: preprocessing and initial segmentation, 3D and 2D level set segmentation, and post-processing. In case the bladder contains regions filled with IV contrast and without contrast, CLASS segments the non-contrast (NC) region and the contrast (C) filled region separately and conjoins the contours. In this study, we compared the performance of CLASS to ITK-SNAP 2.4, which is a publicly available software application for segmentation of structures in 3D medical images. ITK-SNAP performs segmentation by using the edge-based level set on preprocessed images. The level set were initialized by manually placing a sphere at the boundary between the C and NC parts of the bladders with C and NC regions, and in the middle of the bladders that had only C or NC region. Level set parameters and the number of iterations were chosen after experimentation with bladder cases. Segmentation performances were compared using 30 randomly selected bladders. 3D hand segmented contours were obtained as reference standard, and computerized segmentation accuracy was evaluated in terms of the average volume intersection %, average % volume error, average absolute % volume error, average minimum distance, and average Jaccard index. For CLASS, those values were 79.0±8.2%, 16.1±16.3%, 19.9±11.1%, 3.5±1.3 mm, 75.7±8.4%, respectively. For ITK-SNAP, those values were 78.8±8.2%, 8.3±33.1%, 24.2±23.7%, 5.2±2.6 mm, 71.0±15.4%, respectively. CLASS on average performed better and exhibited less variations than ITK-SNAP for bladder segmentation.

9035-51, Session 12

#### Abdominal lymphadenopathy detection using random forest

Kevin M. Cherry, Shijun Wang, Evrim B. Turkbey, Ronald M. Summers M.D., National Institutes of Health (United States)

In this paper we propose a new method for detecting abdominal lymphadenopathy by utilizing a random forest statistical classifier to create voxel-level lymph node predictions, i.e. initial detection of enlarged lymph nodes. The framework permits the combination of multiple statistical lymph node descriptors and appropriate feature selection in order to improve lesion detection beyond traditional enhancement filters. We show that Hessian blobness measurements alone are inadequate for detecting lymph nodes in the abdominal cavity. Of the features tested here, intensity proved to be the most important predictor for lymph node classification. For initial detection, candidate lesions were extracted from the 3D prediction map generated by random forest. Statistical features describing intensity distribution, shape, and texture were calculated from each enlarged lymph node candidate. In the last step, a support vector machine (SVM) was trained and tested based on the calculated features from candidates and labels determined by two experienced radiologists. The computer-aided detection (CAD) system was tested on a dataset containing 30 patients with 119 enlarged lymph nodes. Our method achieved an AUC of 0.762±0.022 and a sensitivity of 79.8% with 14.5 false positives suggesting it can aid radiologists in finding enlarged lymph nodes.

9035-52, Session 12

#### A new classifier fusion method based on confusion matrix and classification confidence for recognizing common CT imaging signs of lung diseases

Ling Ma, Xiabi Liu, Li Song, Yu Liu, Beijing Institute of Technology (China); Chunwu Zhou, Xinming Zhao, Yanfeng Zhao, Chinese Academy of Medical Sciences (China)

Common CT Imaging Signs of Lung Diseases (CISL) are defined as the imaging signs that frequently appear in lung CT images from patients and play important roles in the diagnosis of lung diseases. This paper proposes a new method of multiple classifier fusion to recognize the CISLs, which is based on the confusion matrices of the classifiers and the classification confidence values outputted by the classifiers. The confusion matrix reflects the historical reliability of decision-making of a classifier, while the difference between the classification confidence values for competing classes reflects the current relia-bility of its decision-making. The two factors are merged to obtain the weights of the classifiers' classification confidence values for the input pattern. Then the classifiers are fused in a weighted-sum form. In our experiments of CISL rec-ognition, we combine three types of classifiers: the Max-Min posterior Pseudo-probabilities (MMP), the Support Vector Machine (SVM) and the Bagging. Our method behaved better than not only each of the three single classifier but also the AdaBoost with SVM based weak learners. It shows that the proposed method is effective and promising.

9035-53, Session 12

# Automated detection and quantification of micronodules in thoracic computed tomography scans to identify subjects at risk for silicosis

Colin Jacobs, Radboud Univ. Nijmegen Medical Ctr.











(Netherlands); Sjoerd H. T. Opdam, Technische Univ. Eindhoven (Netherlands); Eva M. van Rikxoort, Radboud Univ. Nijmegen Medical Ctr. (Netherlands); Onno M. Mets, Academisch Medisch Centrum (Netherlands); Jos M. Rooijackers, Utrecht Univ. (Netherlands) and Netherlands Expertise Ctr. for Occupational Respiratory Disorders (Netherlands); Pim A. de Jong, Univ. Medical Ctr. Utrecht (Netherlands); Mathias Prokop M.D., Bram van Ginneken, Radboud Univ. Nijmegen Medical Ctr. (Netherlands)

Silica dust-exposed individuals are at high risk of developing silicosis, a fatal and uncurable lung disease. The presence of disseminated micronodules on thoracic CT is the radiological hallmark of silicosis but finding small numbers of micronodules, to identify subjects at risk, is difficult and tedious work for human observers. We present a computer-aided detection scheme to automatically find and quantify micronodule load. The system uses lung segmentation, template matching, and features analysis. The system achieved a promising sensitivity of 84% at an average of 8.4 false positive marks per scan. In an independent data set of 54 CT scans where we defined four risk categories, the CAD system automatically classified 83% of subjects correctly, and obtained a weighted kappa of 0.76.

9035-54, Session 12

### Multiple-instance learning for computer-aided detection of tuberculosis

Jaime Melendez, Clarisa I. Sánchez, Rick Philipsen, Pragnya Maduskar, Bram van Ginneken, Radboud Univ. Nijmegen Medical Ctr. (Netherlands)

Detection of tuberculosis (TB) in chest radiographs (CXRs) is a hard problem. Therefore, to help radiologists or even take their place when they are not available, computer-aided detection (CAD) systems are being developed. In order to reach a performance comparable to that of human experts, the pattern recognition algorithms of these systems are typically trained on large CXR databases that have been manually annotated to indicate the abnormal lung regions. However, manually outlining those regions constitutes a time-consuming process that, besides, is prone to inconsistencies and errors introduced by interobserver variability and the absence of an external reference standard. In this paper, we investigate an alternative pattern classification method, namely multiple-instance learning (MIL), that does not require such detailed information for a CAD system to be trained. We have applied this alternative approach to a CAD system aimed at detecting textural lesions associated with TB. Only the case (or image) condition (normal or abnormal) was provided in the training stage. We compared the resulting performance with those achieved by several variations of a conventional system trained with detailed annotations. A database of 917 CXRs was constructed for experimentation. It was divided into two roughly equal parts that were used as training and test sets. The area under the receiving operating characteristic curve was utilized as a performance measure. Our experiments show that, by applying the investigated MIL approach, comparable results as with the aforementioned conventional systems are obtained in most cases, without requiring condition information at the lesion level.

9035-55, Session 12

### Seamless insertion of real pulmonary nodules in chest CT exams

Aria X. Pezeshk, Berkman Sahiner, Rongping Zeng, Adam Wunderlich, Weijie Chen, Nicholas A. Petrick, U.S. Food and Drug Administration (United States)

Size and representativeness of the training and test datasets are critical factors in the design and performance estimation of Computer Aided Diagnosis (CAD) systems. However, collection of large repositories of clinical images is hindered by the high cost and difficulties associated with both the accumulation of data and establishment of the ground truth. To address this problem, we are developing an image composition tool that allows users to modify or supplement existing datasets by seamlessly inserting a real lesion extracted from a source image into a different location on a target image. In this study we focus on the application of this tool to pulmonary nodules in chest CT exams. We minimize the impact of user skill on the perceived quality of the composite image by limiting user involvement to two simple steps: the user first draws a casual boundary around the nodule of interest in the source, and then selects the center of desired paste area in the target. We demonstrate examples of the performance of the proposed system on samples taken from the Lung Image Database Consortium (LIDC) dataset. Finally, we compare the detectability of native and inserted nodules in phantoms simulated under different photon counts by analyzing the Area Under the ROC Curve (AUC) of the Hotelling Observer (HO) for a binary classification task involving native and inserted nodules. Our results indicate that the AUC for the HO is close to 0.5 even when the source and target photon counts are not matched, indicating that the HO cannot distinguish between the two classes.

9035-56, Session PSWed

# Classification based micro-calcification detection using discriminative restricted Boltzmann machine in digitized mammograms

Seung Yeon Shin, Seoul National Univ. (Korea, Republic of); Soochahn Lee, Samsung Electronics Co., Ltd. (Korea, Republic of); Il Dong Yun, Hankuk Univ. of Foreign Studies (Korea, Republic of)

We present a new approach for automatic detection of micro-calcifications. The proposed method is based on Discriminative Restricted Boltzmann Machine (DRBM) which automatically learns a variety of morphologies of the micro-calcifications. From raw image patches containing micro-calcifications and those with normal tissues, DRBM automatically captures low level structures of micro-calcifications and uses those as features without appropriate feature selection. Therefore, no expert knowledge and time-consuming hand-tuning are required on making discriminative features for micro-calcifications. The experiments were conducted on the 33 mammograms and the performance was measured by means of the Receiver Operating Characteristics (ROC) analysis. The area under the curve of the proposed method was 0.8294, which showed the feasibility of the proposed method.

9035-57, Session PSWed

## Automatic ultrasound image enhancement for 2D semi-automatic breast-lesion segmentation

Kongkuo Lu, Christopher S. Hall, Philips Research North America (United States)

Breast cancer is the fastest growing form of cancer and second leading cause of cancer death among women in the United States and worldwide. Among different image modalities, ultrasound (US) has been used, as an indispensable tool for breast cancer detection/diagnosis and treatment. In computer-aided assistance, lesion segmentation is a preliminary but vital step, but the task is quite challenging in US images, due to imaging artifacts that complicate detection and measurement of the suspect lesions. The lesions usually present with poor boundary











features and vary significantly in size, shape, and intensity distribution between cases. Automatic methods are highly application dependent while manual tracing methods are extremely time consuming and have a great deal of intra- and inter- observer variability. Semi-automatic approaches are designed to counterbalance the advantage and drawbacks of the automatic and manual methods. However, considerable user interaction might be necessary to ensure reasonable segmentation for a wide range of lesions. This work proposes an automatic enhancement approach to improve the boundary searching ability of the live wire method to reduce necessary user interaction while keeping the segmentation performance. Based on the results of segmentation of 50 2D breast lesions in US images, less user interaction is required to achieve desired accuracy, i.e. >80%, when auto-enhancement is applied for live-wire segmentation.

9035-58, Session PSWed

### A content based framework for mass retrieval in mammograms

Simranjit Kaur, Vipul Sharma, Sukhwinder Singh, Savita Gupta, Panjab Univ. (India) and Univ. Institute of Engineering and Technology (India)

In the recent years, there has been a phenomenal growth in the size of digital mammograms produced in hospitals and medical centers. Thus, there is a need to create efficient access methods or retrieval tools to search, browse and retrieve images from large repositories to aid diagnoses and research. In medical imaging, mammography is considered as a key screening tool to detect any kind of abnormality in breast tissue. This paper presents a Content Based Medical Image Retrieval (CBMIR) system for mass retrieval in mammograms using a two stage framework. Shape features are extracted at the first stage to find similar shape lesions and the second stage further refines the results by finding similar pathology bearing lesions using texture features. Various shape features used in this study are Compactness, Convexity, Spicularity, Radial Distance (RD) based features, Zernike Moments (ZM) and Fourier Descriptors (FD). Further, the texture of mass lesions is characterized by Gray Level Co-occurrence Matrix (GLCM) features, Gray Level Run Length Matrix (GLRLM) features and Fourier Power Spectrum (FPS) features. In this paper, feature selection is done by Correlation based Feature Selection (CFS) technique to select the best subset of shape and texture features as high dimensionality of feature vector may limit computational efficiency. This study used the DDSM database to evaluate the retrieval performance of various shape and texture features. Also, for mass segmentation, a semi-automatic method based on Seed Region Growing approach is proposed. From the experimental results, it has been found that CBIR system using merely the compactness or shape features selected by CFS provided better distinction among four categories of mass shape (Round, Oval, Lobulated and Irregular) at the first stage and FPS based texture features provided better distinction between pathology (Benign and Malignant) at the second stage.

9035-59, Session PSWed

#### Development of a computer tool to detect and classify nodules in ultrasound breast images

Karem D. Marcomini, Antonio O. Carneiro, Homero Schiabel, Univ. de São Paulo (Brazil)

Due to the high incidence rate of breast cancer in women, many procedures have been developed to assist the diagnosis and early detection. Currently, ultrasonography has proved as a useful tool in distinguishing benign and malignant masses. In this context, the computer-aided diagnosis schemes have provided to the specialist a second opinion more accurately and reliably, minimizing the visual subjectivity between observers. Thus, we propose the application of an

automatic detection method based on the use of the technique of active contour in order to show precisely the contour of the lesion and provide a better understanding of their morphology. For this, a total of 144 images of phantoms were segmented and submitted to morphological operations of opening and closing for smoothing the edges. Then morphological features were extracted and selected to work as input parameters for the neural classifier Multilayer Perceptron which obtained 95.34% correct classification of data and Az of 0.96.

9035-60, Session PSWed

### A new mass classification system derived from multiple features and a trained MLP model

Maxine Tan, The Univ. of Oklahoma (United States); Jiantao Pu, Univ. of Pittsburgh (United States); Bin Zheng, The Univ. of Oklahoma (United States)

High false-positive recall rate is an important clinical issue that reduces efficacy of screening mammography. Aiming to help improve accuracy of classification between the benign and malignant breast masses and then reduce false-positive recalls, we developed and tested a new computer-aided diagnosis (CAD) system for mass classification using a database including 600 verified mass regions. The mass regions were segmented from regions of interest (ROIs) with a fixed size of pixels. The mass regions were first segmented by an automated scheme, with manual corrections to the mass boundary performed if there was noticeable segmentation error. We randomly divided the 600 ROIs into 400 ROIs (200 malignant and 200 benign) for training, and 200 ROIs (100 malignant and 100 benign) for testing. We computed and analyzed 124 shape, texture, contrast, and spiculation based features in this study. Combining with previously computed 27 regional and shape based features for each of the ROIs in our database, we built an initial image feature pool. From this pool of 151 features, we extracted 13 features by applying the Sequential Forward Floating Selection algorithm on the ROIs in the training dataset. We then trained a multilayer perceptron model using these 13 features, and applied the trained model to the ROIs in the test set. Receiver operating characteristic (ROC) analysis was used to evaluate classification accuracy. The area under the ROC curve was 0.8814±0.025 for the test dataset. The results show a higher CAD mass classification performance, which needs to be further validated in a more comprehensive study.

9035-61, Session PSWed

## Automated breast tissue density assessment using high order regional texture descriptors in mammography

Yan Nei Law, Bioinformatics Institute (Singapore); Monica K. Lieng, Juniata College (United States); Jingmei Li, Genome Institute of Singapore (Singapore); David Aik-Aun Khoo, Bioinformatics Institute (Singapore)

Breast cancer is the most common cancer and second leading cause of cancer death among women in the US. The relative survival rate is lower among women with a more advanced stage at diagnosis. Early detection through screening is vital. Mammography is the most widely used and only proven screening method for reliably and effectively detecting abnormal breast tissues. In particular, mammographic density is one of the strongest breast cancer risk factors, after age and gender, and can be used to assess the future risk of disease before individuals become symptomatic. A reliable method for automatic density assessment would be beneficial and could assist radiologists in the evaluation of mammograms. To address this problem, we propose a density classification method which uses statistical features from different parts of the breast. Our method is composed of three parts: breast region











identification, feature extraction and building ensemble classifiers for density assessment. It explores the potential of the features extracted from second and higher order statistical information for mammographic density classification. We further investigate the registration of bilateral pairs and time-series of mammograms. The experimental results on 322 mammograms demonstrate that (1) a classifier using features from dense regions has higher discriminative power than a classifier using only features from the whole breast region; (2) these high-order features can be effectively combined to boost the classification accuracy; (3) a classifier using these statistical features from dense regions achieves 75% accuracy, which is a significant improvement from 70% accuracy obtained by the existing approaches.

9035-62, Session PSWed

### Improving breast mass detection using histogram of oriented gradients

Victor V. Pomponiu, Harishwaran Hariharan, Univ. of Pittsburgh (United States); Bin Zheng, The Univ. of Oklahoma (United States); David Gur, Univ. of Pittsburgh School of Medicine (United States)

In this paper we present a novel technique that can be employed to filter the output of the computerized mass detection schemes. The sensitivity of computer-aided detection (CAD) systems is high; nevertheless specificity is not due to high false positive (FP) detection rates. Our approach is based on Histogram of Oriented Gradients (HOG) descriptor for filtering the mass and normal tissue regions. After the descriptors are computed, Support Vector Machines (SVM) are applied to classify the identified masses. The devised technique was tested on 1881 regions of interest (ROIs) acquired using a previously proposed CAD system. Extensive simulations are conducted to illustrate the capacity of the HOG descriptor to improve the performances of mass detection systems.

9035-63, Session PSWed

# Detection of the nipple in automated 3D breast ultrasound using coronal slab-average-projection and cumulative probability map

Hannah Kim, Seoul Women's Univ. (Korea, Republic of); Helen Hong, Seoul Women's Univ. (Korea, Republic of)

In 3D ABUS images, nipple position is an effective landmark for registration in different modalities and it is used to compare the symmetry between left and right breasts and measure the distance from the tumors. However, the shape of nipple is unclear in some slices due to speckle noise and the identification between nipple and areola is difficult due to their similar intensity. Thus, we propose an automatic method for nipple detection on 3D ABUS images using coronal slab-average-projection and cumulative probability map. First, to identify coronal images that appeared remarkable distinction between nipple-areola region and skin, skewness of each coronal image is measured and the negatively skewed images are selected. Second, to enhance the edges of nippleareola region and weaken edges of breast boundary, glandular and fatty tissues, coronal slab-average-projection-image is reformatted from the selected images. Then elliptical ROI covering nipple-areola region is defined by using Sobel edge detection and Hough ellipse transform. Third, to separate the nipple from areola and glandular tissue, 3D Otsu's thresholding is applied to the elliptical ROI and cumulative probability map in the elliptical ROI is generated by assigning high probability to low intensity region. Finally, false detected small components are eliminated using morphological opening and the center point of the detected nipple region is calculated. Experimental results show that our method provides 94.4% nipple detection rate without wrongly detected breast boundary, glandular and fatty tissues. Our method can be used as an landmark for

comparing symmetry between left and right breasts and as a reference point for measuring tumor location in breast CAD.

9035-64, Session PSWed

### Bilateral image subtraction features for multivariate automated classification of breast cancer risk

José M. Celaya-Padilla, Juan R. Rodriguez Sr., Jorge I. Galván-Tejada, Antonio Martínez-Torteya Sr., Victor M. Treviño-Alvarado Sr., José G. Tamez-Peña, Tecnológico de Monterrey (Mexico)

Early tumor detection is key in reducing breast cancer deaths and screening mammography is the most widely available method for early detection. However, mammogram interpretation is based on human radiologist, whose radiological skills, experience and workload makes radiological interpretation inconsistent. In an attempt to make mammographic interpretation more consistent, computer aided diagnosis (CADx) systems has been introduced. This paper presents an CADx system aimed to automatically triage normal mammograms form suspicious mammograms. The CADx system co-reregister the left and breast images, then extracts image features from the co-registered mammographic bilateral sets. Finally, an optimal logistic multivariate model is generated by means of an evolutionary search engine. In this study, 440 subjects form the DDSM public data sets were used: 44 normal mammograms, 201 malignant mass mammograms, and 196 mammograms with malignant calcifications. The results showed a cross validation accuracy of 0.88 and an area under receiver operating characteristic (AUROC) of 0.89 for the calcifications vs. normal mammograms. The optimal mass vs. normal mammograms model obtained an accuracy of 85% and an AUROC of 0.88

9035-65. Session PSWed

# Roles of biologic breast tissue composition and quantitative image analysis of mammographic images in breast tumor characterization

Karen Drukker, Maryellen L. Giger, The Univ. of Chicago Medical Ctr. (United States); Fred Duewer, Serghei Malkov, Christopher Flowers, Bonnie Joe, Karla Kerlikowske, Univ. of California, San Francisco (United States); Jennifer S. Drukteinis, H. Lee Moffitt Cancer Ctr. & Research Institute (United States); John A. Shepherd, Univ. of California, San Francisco (United States)

Purpose. Investigate whether knowledge of the biologic image composition of mammographic lesions provides image-based biomarkers above and beyond those obtainable from quantitative image analysis (QIA) of X-ray mammography.

Methods. The dataset consisted of 45 in vivo breast lesions imaged with the novel 3-component breast (3CB) imaging technique based on dual-energy mammography (15 malignant, 30 benign diagnoses). The 3CB composition measures of water, lipid, and protein thicknesses were assessed and 24 mathematical descriptors, '3CB features', were obtained for the lesions and their periphery. The raw low-energy mammographic images were analyzed with an established in-house QIA method obtaining 32 'QIA features' describing morphology and texture. We investigated the correlation within the '3CB features', within the 'QIA features', and between the two. In addition, the merit of individual features in the distinction between malignant and benign lesions was assessed.

Results. Whereas many descriptors within the '3CB features' and 'QIA features' were, often by design, highly correlated, correlation between descriptors of the two feature groups was much weaker (maximum











absolute correlation coefficient 0.58, p<0.001) indicating that 3CB and QIA-based biomarkers largely provided independent information. Single descriptors from 3CB and QIA appeared equally well-suited for the distinction between malignant and benign lesions, with maximum area under the ROC curve 0.71 for a protein feature (3CB) and 0.71 for a texture feature (QIA).

Conclusions. In this pilot study analyzing the new 3CB imaging modality, knowledge of breast tissue composition appeared additive in combination with existing mammographic QIA methods for the distinction between benign and malignant lesions.

9035-66, Session PSWed

## New method for predicting estrogen receptor status utilizing breast MRI texture kinetic analysis

Baishali Chaudhury, Dmitry B. Goldgof, Lawrence O. Hall, Univ. of South Florida (United States); Robert A. Gatenby, Jennifer S. Drukteinis, Robert J. Gillies, H. Lee Moffitt Cancer Ctr. & Research Institute (United States)

Magnetic Resonance Imaging (MRI) of breast cancer typically demonstrates heterogeneous tumors with spatial variations in blood flow and cell density. Here we examine the potential link between clinical tumor imaging and the underlying evolutionary dynamics behind heterogeneity in the cellular expression of estrogen receptors (ER) in breast cancer. We assume, in an evolutionary environment, that ER expression will only occur in the presence of significant concentrations of estrogen, which is delivered via the blood stream. Thus, we hypothesize, the expression of ER in breast cancer cells will correlate with blood flow on gadolinium enhanced breast MRI. To test this hypothesis, we performed quantitative analysis of blood flow on dynamic contrast enhanced MRI (DCE-MRI) and correlated it with the ER status of the tumor. Here we present our analytic methods, which utilized a novel algorithm to analyze 20 volumetric DCE-MRI breast cancer tumors. The algorithm generates post initial enhancement (PIE) maps from DCE-MRI and then performs texture features extraction from the PIE map, feature selection, and finally classification of tumors into ER positive and ER negative status. This combined gray level co-occurrence matrices, gray level run length matrices and local binary pattern histogram features to quantify breast tumor heterogeneity. The algorithm predicted ER expression with an accuracy of 85% using Naives Bayes classifier in leave-one-out cross-validation. Hence, we conclude that our data supports the hypothesis that imaging characteristics can, through application of evolutionary principles, provide insights into the cellular and molecular properties of cancer cells.

9035-67, Session PSWed

### Exploring perceptually similar cases with multidimensional scaling

Juan Wang, Yongyi Yang, Miles N. Wernick, Illinois Institute of Technology (United States); Robert M. Nishikawa, The Univ. of Chicago (United States)

Retrieving a set of known lesions similar to the one being evaluated might be of value for assisting radiologists to distinguish between benign and malignant clustered micro-calcifications (MCs) in mammograms. In this work, we investigate how perceptually similar cases with clustered MCs may relate to each other in terms of their underlying characteristics (from disease condition to image features). We first conduct an observer study to collect similarity scores from a group of readers (five radiologists and five non-radiologists) on a set of 2,000 image pairs, which were selected from 222 cases (110 malignant, 112 benign) based on their images features. We then explore the potential relationship among the different cases as revealed by their similarity ratings. Specifically, we apply the

multi-dimensional scaling (MDS) technique to embed all the cases in a 2-D plot, in which perceptually similar cases are placed in close vicinity of each other based on their level of similarity. Our results show that cases having different characteristics in their clustered MCs are accordingly placed in different regions in the plot. Moreover, cases of same pathology tend to be clustered together locally, and neighboring cases (which are more similar) tend to be also similar in their clustered MCs (e.g., cluster size and shape). These results indicate that the subjective similarity ratings from the readers are well correlated with the image features of the underlying MCs in the cases, and that perceptually similar cases could be of diagnostic value for discriminating between malignant and benign cases.

9035-68, Session PSWed

# Application of computer-extracted breast tissue texture features in predicting false-positive recalls from screening mammography

Shonket Ray, Jae Young Choi, Univ. of Pennsylvania (United States); Brad M. Keller, Jinbo Chen, Univ. of Pennsylvania School of Medicine (United States); Emily F. Conant M.D., Despina Kontos, The Univ. of Pennsylvania Health System (United States)

Mammographic texture features has been shown to have value in breast cancer risk assessment. Previous models have also been developed that use computer-extracted mammographic features of breast tissue complexity to predict the risk of false-positive (FP) recall from breast cancer screening with digital mammography. This work details a novel locally-adaptive parenchymal texture analysis algorithm that identifies and extracts mammographic features of local parenchymal tissue complexity potentially relevant for false-positive biopsy prediction. This algorithm has two important aspects: (1) the adaptive nature of automatically determining an optimal number of region-of-interests (ROIs) and each ROI's corresponding size based on the parenchymal tissue portion and distribution over the whole breast region and (2) characterizations of both local and global mammographic appearances of the parenchymal tissue that could provide more discriminative information for FP biopsy risk prediction. Preliminary results show that this locally-adaptive texture analysis algorithm in conjunction with logistic regression can predict the likelihood of false-positive biopsy with an ROC performance value of AUC=0.92 (p<0.001) with a 95% confidence interval [0.77, 0.94]. Significant texture feature predictors (p<0.05) included contrast, sum variance and difference average. Sensitivity for false-positives was 51% at the 100% cancer detection operating point. Although preliminary, clinical implications of using prediction models incorporating these texture features may include the future development of better tools and guidelines regarding personalized breast cancer screening recommendations. Further studies are warranted to prospectively validate our findings in larger screening populations and evaluate their clinical utility.

9035-69, Session PSWed

## Chest wall segmentation in automated 3D breast ultrasound images using thoracic volume classification

Tao Tan, Jan van Zelst, Radboud Univ. Nijmegen Medical Ctr. (Netherlands); Wei Zhang, QView Medical, Inc. (United States); Ritse M. Mann M.D., Bram Platel, Nico Karssemeijer, Radboud Univ. Nijmegen Medical Ctr. (Netherlands)

Computer-aided detection (CAD) systems are expected to improve effectiveness and efficiency of radiologists in reading automated 3D breast ultrasound (ABUS) images. One challenging task on developing











CAD is to reduce a large number of false positives. A large amount of false positives originate from acoustic shadowing caused by ribs. Therefore determining the location of the chestwall in ABUS is necessary in CAD systems to remove these false positives. Additionally it can be used as a anatomical landmark for inter- and intra-modal image registration. In this work, we extended our previous developed chestwall segmentation method that fits a cylinder to automated detected rib-surface points and we fit the cylinder model by minimizing a cost function which adopted a term of region cost computed from a thoracic volume classifier to improve segmentation accuracy. We examined the performance on a dataset of 52 images where our previous developed method fails. Using region-based cost, the average mean distance of the annotated points to the segmented chest wall decreased from 7.57+/-2.76 mm to 6.22+/-2.86 mm.

9035-70, Session PSWed

#### Classification of breast lesions presenting as mass and non-mass lesions

Cristina Gallego, Anne L. Martel, Univ. of Toronto (Canada) and Sunnybrook Research Institute (Canada)

We aim to develop a CAD system for robust and reliable differential diagnosis of breast lesions, in particular non-mass lesions. A necessary prerequisite for the development of a successful CAD system is the selection of the best subset of lesion descriptors. But an important methodological concern is whether the selected features are influenced by the model employed rather than by the underlying characteristic distribution of descriptors for positive and negative cases. Another interesting question is how a particular classifier exploits the relationships between descriptors to increase the accuracy of the classification. In this work we set to: (1) Characterize kinetic, morphological and textural features among mass and non-mass lesions; (2) Examine feature spaces and compare selection of subset of features based on similarity of feature importance across feature rankings; (3) Compare two classifier performances namely binary Support Vector Machines (SVM) and Random Forest (RF) for the task of differentiating between positive and negative cases when using binary classification for mass and non-mass lesions separately or when employing a multi-class classification. Breast MRI datasets consists of 243 (173 mass and 70 non-mass) lesions. Results show that RF variable importance used with RF-binary based classification optimized for mass and non-mass lesions separately offers the best classification accuracy.

#### 9035-23, Session PSWed

## Computer-based assessment of left ventricular regional ejection fraction in patients after myocardial infarction

Soo Kng Teo, Yi Su, A\*STAR Institute of High Performance Computing (Singapore); Ru-San Tan, Liang Zhong, National Heart Centre, Singapore (Singapore)

After myocardial infarction (MI), the left ventricle (LV) undergoes progressive remodeling which adversely affects heart function and may lead to development of heart failure. There is an escalating need to accurately depict the LV remodeling process for disease surveillance and monitoring of therapeutic efficacy. Current practice of using ejection fraction to quantitate LV function is less than ideal as it obscures regional variation and anomaly. Therefore, we sought to (i) develop a quantitative method to assess LV regional ejection fraction (REF) using a 16-segment method, and (ii) evaluate the effectiveness of REF in discriminating 10 patients 1-3 months after MI and 9 normal control (sex- and agematched) based on cardiac magnetic resonance (CMR) imaging. Late gadolinium enhancement (LGE) CMR scans were also acquired for the MI patients to assess scar extent. We observed that the REF at the basal, mid-cavity and apical regions for the patient group is significantly

lower as compared to the control group (P < 0.001 using a 2-tail student t-test). In addition, we correlated the patient REF over these regions with their corresponding LGE score in terms of 4 categories – High LGE, Low LGE, Border and Remote. We observed that the median REF decreases with increasing severity of infarction. The results suggest that REF could potentially be used as a discriminator for MI and employed to measure myocardium homogeneity with respect to degree of infarction. The computational performance per data sample took approximately 25 sec, which demonstrates its clinical potential as a real-time cardiac assessment tool.

9035-72, Session PSWed

### Can grey matter in hippocampus and parahippocampus be taken as features of Alzheimer's disease?

Yan'e Guo, Zengqiang Zhang, Bo Zhou, Pan Wang, Hongxiang Yao, Chinese PLA General Hospital (China); Mingshao Yuan, Jimo People's Hospital (China); Ningyu An, Haitao Dai, Luning Wang, Xi Zhang, Chinese PLA General Hospital (China)

Purpose: Alzheimer's disease (AD), clinically characterized by progressive impairment of cognitive function and behavior, is the most common form of dementia in elderly people. The evolution of grey matter atrophy pattern could be traced by voxel-based morphometric (VBM) method which is hypothesis-free, time-efficient, and sensitive to localizing small scale regional differences in grey matter and more easily implied. The hippocampus and parahippocampus are the earliest affected regions in AD. The hippocampus or medial temporal lobe atrophy might be potential biomarker of AD. In present study, we want to evaluate whether grey matter volume in hippocampus and parahippocampus are potential biomarker for AD.

Material and Method: Previous studies also suggested that different part of hippocampus may play different functional roles. In order to achieve more exact features, we divided the bilateral hippocampus and parahippocampus into 4 subregions (head, part 1 and part 2 of the main body, tail) based on the structural MRI data obtained from 35 subjects with AD, 27 age- and gender-matched normal controls (NC). Then Fisher's linear discriminative and leave one-to-five out cross-validation analyses were performed.

Results: In each subregion of the bilateral hippocampus and parahippocampus, the grey matter volume is significantly decreased in AD (P<0.05, FDR corrected) in comparison with normal controls. The classification and cross validation analysis demonstrated that we were able to distinguish the AD patients from the normal controls at a higher correct ratio (higher than 82%).

Significance: The present study provides a simple and easy performed classification protocol for diagnosing AD based on brain imaging.

9035-73, Session PSWed

# Toward early diagnosis of arteriosclerotic diseases: collaborative detection of carotid artery calcifications by computer and dentists on dental panoramic radiographs

Chisako Muramatsu, Ryo Takahashi, Takeshi Hara, Gifu Univ. School of Medicine (Japan); Tatsuro Hayashi, Media Co., Ltd. (Japan); Akitoshi Katsumata D.D.S., Asahi Univ. (Japan); Xiangrong Zhou, Hiroshi Fujita, Gifu Univ. School of Medicine (Japan)

Several studies have reported the presence of carotid artery calcifications (CACs) on dental panoramic radiographs (DPRs) as a possible sign of arteriosclerotic diseases. However, CACs are not easily visible at











the common window level for dental examinations, and dentists, in general, are not looking for CACs. Computerized detection of CACs may help dentists in referring patients with a risk of arteriosclerotic diseases. Downside of our previous method was a relatively large number of false positives (FPs). In this study, we attempted to reduce FPs by including an additional feature and selecting effective features for the classifier. A hundred DPRs including 34 cases with calcifications were included. Initial candidates were detected by thresholding the output of top-hat operation. For each candidate, 10 features and a new feature characterizing the relative position of a CAC with reference to the lower mandible edge were determined. After the rule-based FP reduction, candidates were classified into CACs and FPs by support vector machine. Based on the 10 randomized 2-fold cross-validation evaluations, an average number of FPs was 3.1 per image at 90% sensitivity using seven features selected by the backward selection. Compared to our previous method, the number of FPs was reduced by 38% at the same sensitivity level. In addition, the variation between the results of 10 randomized trials was reduced. The proposed method has a potential in identifying patients with a risk of arteriosclerosis early via general dental examinations.

9035-74, Session PSWed

## Automatic classification of schizophrenia using resting-state functional language network via an adaptive learning algorithm

Maohu Zhu, Nanfeng Jie, Tianzi Jiang, Institute of Automation (China)

A reliable and precise classification of schizophrenia is significant for its diagnosis and treatment of schizophrenia. Functional magnetic resonance imaging (fMRI) is a novel tool increasingly used in schizophrenia research. Recent advances in statistical learning theory have led to applying pattern classification algorithms to access the diagnostic value of functional brain networks, discovered from resting state fMRI data. The aim of this study was to propose an adaptive learning algorithm to distinguish schizophrenia patients from normal controls using resting-state functional language network. Furthermore, here the classification of schizophrenia was regarded as a sample selection problem where a sparse subset of samples was chosen from the labeled training set. Using these selected samples, which we call informative vectors, a classifier for the clinic diagnosis of schizophrenia was established. We experimentally demonstrated that the proposed algorithm incorporating resting-state functional language network achieved 83.6% leave-one-out accuracy on resting-state fMRI data of 27 schizophrenia patients and 28 normal controls. In contrast with Support Vector Machine (SVM) and K-Nearest-Neighbor (KNN), our method vielded better classification performance. Moreover, our results indicated that a dysfunction of resting-state functional language network plays an important role in the clinic diagnosis of schizophrenia.

9035-75, Session PSWed

# Accurate discrimination of Alzheimer's disease from other dementia and/or normal subjects using SPECT specific volume analysis

Hitoshi Iyatomi, Hosei Univ. (Japan); Jun Hashimoto M.D., Fumuhito Yoshii M.D., Toshiki Kazama M.D., Shuichi Kawada M.D., Tetsu Niwa M.D., Yutaka Imai M.D., Tokai Univ. School of Medicine (Japan)

Discrimination between Alzheimer's disease and other dementia is clinically significant, however it is often difficult. In this study, we developed classification models among Alzheimer's disease (AD), other dementia (OD) and/or normal subjects (NC) using patient factors and

indices obtained by SPECT scan such as commonly used distribution of cerebral blood flow (CBF) and those from statistical parametric mapping of specific involved areas (SPM). We investigated a total of 150 cases (50 cases each for AD, OD, and NC) from Tokai University Hospital, Japan. In each case, we used a total of 127 candidate parameters from: (A) 2 patient factors (age and sex), (B) 12 CBF parameters and 113 SPM parameters including (C) 3 from specific volume analysis (SVA), and (D) 110 from voxel-based analysis stereotactic extraction estimation (vbSEE). We built linear classifiers with a statistical stepwise feature selection and evaluated the performance with the leave-one-out cross validation strategy. Our classifiers achieved very high classification performances with reasonable number of selected parameters. In the most significant discrimination in clinical, namely those of AD from OD, our classifier achieved both sensitivity (SE) and specificity (SP) of 96%. In a similar way, our classifiers achieved a SE of 90% and a SP of 98% in AD from NC, as well as a SE of 88% and a SP of 86% in AD from OD and NC cases. Introducing SPM indices such as SVA and vbSEE, classification performances improved around 7-15%. We confirmed that these SPM factors are quite important for diagnosing Alzheimer's disease.

9035-76, Session PSWed

### Automatic pathology classification using a single feature machine-learning support-vector machines

Fernando Yepes-Calderon, Univ. de Barcelona (Spain); Fabian Pedregosa, Bertrand Thirion, INRIA Saclay - Île-de-France (France); Yalin Wang, Arizona State Univ. (United States); Natasha Lepore, Children's Hospital Los Angeles (United States)

Magnetic resonance imaging is highly popular and its growing use in the clinic is producing vast amounts of data. This sotred data is often difficult to interpret visually, and, after the initial reading, does not currently provide added clinical value other than as a retrospective reference for patients and clinicians. However, from the perspective of machine learning, it could be the keystone for accelerating the diagnosis of pathologies. Moreover, this technique can be applied to generate accurate prognosis, provided that a previous classification stage is accomplished with rigorousness. The accuracy of a machine learning implementation increases with the number of independent features that it can learn from and the number of training sets that it is fed. Clinically, hospitals can provide a large source of data as training set. Here, we present a machine learning - support vector machines design that is able to classify subjects into Alzheimer disease, mild cognitive impairment and controls by limiting itself to four individual geometrical measurements among 35 cortical regions in the brain, hence providing usefulness in the clinical setting. Our formulation is motivated by the real clinical scenario, where the measurements have to be simple, intuitive and explainable. On a significantly large imaging dataset consisting of over 200 subjects per group (Total of 829 subjects) taken from the Alzheimers Disease Neuroimaging Initiative (ADNI) database, classification-success indexes of up to 85.6% are reached with single measurement.

9035-77, Session PSWed

### Fiber-based representation and supervised classification of diffusion tensor MRI brain scans

Gali Zimmerman Moreno, Tel Aviv Univ. (Israel); Dafna Ben Bashat, Moran Artzi, Beatrice Nefussy, Tel-Aviv Sourasky Medical Ctr. (Israel); Vivian Drory, Tel Aviv Univ. (Israel); Orna Aizenstein, Tel-Aviv Sourasky Medical Ctr. (Israel); Hayit Greenspan, Tel Aviv Univ. (Israel)

A novel method is proposed for representation and classification of Diffusion Tensor Imaging (DTI) brain scans. Diffusion tensor imaging











allows the reconstruction of the white matter fibers in the brain via a process named tractography. The resulting sets of fibers usually differ both in the number of extracted fibers and in the fibers shape. The various diffusion-based measures along these fibers are indicative of the fibers integrity. Our method represents each brain by a single high dimensional feature vector, which preserves the diffusion-based measures information from most of the brains fibers. The number of features is constant which allows for convenient incorporation in various learning and classification frameworks. The individual tractographies and the parameters sampling are done in each brains native space and no non-linear registration is needed. A standard template fiber-set is used as a geometric reference for creating all the feature vectors.

The derived representation has many potential uses, such as brain classification and retrieval. In this work we use the representations to train a supervised classifier between a group of healthy subjects and a group of patients with Amyotrophic Lateral Sclerosis (ALS). A leave-one-out experiment with this data set yields high precision and recall values (above 90%).

9035-78, Session PSWed

## MRI signal and texture features for the prediction of MCI to Alzheimer's disease progression

Antonio Martínez-Torteya, Juan A. Rodriguez-Rojas, José M. Celaya-Padilla, Jorge I. Galván-Tejada, Victor M. Treviño-Alvarado Sr., José G. Tamez-Peña, Tecnológico de Monterrey (Mexico)

An early diagnosis of Alzheimer's disease (AD) confers many benefits. Several biomarkers from different information modalities have been proposed for the prediction of MCI to AD progression, where features extracted from MRI have played an important role. However, studies have focused almost exclusively in the morphological characteristics of the images. This study aims to determine whether features relating to the signal and texture of the image could add predictive power. Baseline clinical, biological and PET information, and MP-RAGE images for 62 subjects from the Alzheimer's Disease Neuroimaging Initiative were used in this study. Images were divided into 83 regions and 50 features were extracted from each one of these. A multimodal database was constructed, and a feature selection algorithm was used to obtain an accurate and small logistic regression model, which achieved a crossvalidation accuracy of 0.96. These model included six features, five of them obtained from the MP-RAGE image, and one obtained from genotyping. A risk analysis divided the subjects into low-risk and highrisk groups according to a prognostic index, showing that both groups are statistically different (p-value of 2.04e-11). The results demonstrate that features related to MRI signal and texture add MCI to AD predictive power, and support the idea that multimodal biomarkers outperform single-modality biomarkers.

#### 9035-80, Session PSWed

### Volume curtaining: a focus+context effect for multimodal volume visualization

Ross Maciejewski, Adam J. Fairfield, Jonathan D. Plasencia, Arizona State Univ. (United States); Yun Ho Jang, Sejong Univ. (Korea, Republic of); Nicholas Theodore, Barrow Neurosurgical Associates (United States); Neil Crawford, St. Joseph's Hospital and Medical Ctr. (United States); David H. Frakes, Arizona State Univ. (United States)

In surgical preparation, physicians will often utilize multimodal imaging scans to capture complementary information to improve diagnosis and to drive patient-specific treatment. These imaging scans may consist of

data from magnetic resonance imaging (MRI), computed tomography (CT), or other various sources. The challenge in using these different modalities is that the physician must mentally map the two modalities together during the diagnosis and planning phase. Furthermore, the different imaging modalities will be generated at various resolutions as well as slightly different orientations due to patient placement during scans. In this work, we present an interactive system for multimodal data fusion, analysis and visualization. Our proposed approach integrates interactive multi-modal co-registration and uses arbitrary clipping combined with transfer function tools for multi-volume visualization. This process can be divided into two steps: co-registration of the volumes and visualization of the aligned volumes. Our work focuses on multi-modal scans of the same patient in the same region, but at different resolutions and varying angles of acquisition. Primarily, we concentrate on visualizing breaks in the craniocervical region of the spine. By partnering with researchers in biomedical engineering and surgeons who will ultimately employ this software, we present a single software tool that allows doctors to transition from medical image volume slices to analyzing registered 3D projections. The proposed system combines interactive co-registration, linked 3D volume rendering and interactive 2D slice exploration incorporating interactive segmentation via transfer functions, arbitrary clipping and multi-modal viewing.

9035-81, Session PSWed

### Multilevel image recognition using discriminative patches and kernel covariance descriptor

Le Lu, Jianhua Yao, Evrim B. Turkbey, Ronald M. Summers M.D., National Institutes of Health (United States)

Computer-aided diagnosis of medical images has emerged as an important tool to objectively improve the performance, accuracy and consistency for clinical workflow. To computerize the medical image diagnostic recognition problem, there are three fundamental problems: where to look (i.e., where is the region of interest from the whole image/ volume), image feature description/encoding, and similarity metrics for classification or matching. In this paper, we exploit the motivation, implementation and performance evaluation of task-driven iterative, discriminative image patch mining; covariance matrix based descriptor via intensity, gradient and spatial layout; and Log-Euclidean distance kernel for Support Vector Machine, to address these three aspects respectively. To cope with often visually ambiguous image patterns for the region of interest in medical diagnosis, discovery of multilabel selective discriminative patches is desired. Covariance of several image statistics summarizes their second order interactions within an image patch and is proved as an effective image descriptor, with low dimensionality compared with joint statistics and fast computation regardless of the patch size. We extensively evaluate two extended Gaussian kernels using Affine-invariant Riemannian Metric or Log-Euclidean Metric with support vector machines (SVM), on two medical image classification problems of degenerative disc disease (DDD) detection on cortical shell unwrapping CT map and colitis detection on CT key images. The proposed approach is validated with promising quantitative results on these challenging tasks. Our experimental findings and discussion also unveil some interesting insights on the covariance feature composition with or without spatial layout for classification and retrieval, and different kernel constructions for SVM. This will also shed some light on future work using covariance feature and kernel classification for medical image analysis.











9035-82, Session PSWed

## Surgical retained foreign object (RFO) prevention by computer aided detection (CAD)

Theodore C. Marentis, Lubomir M. Hadjiyski, Lucas Rondon, Amrita R. Chaudhury, Univ. of Michigan Health System (United States); Nikolaos Chronis, Univ. of Michigan (United States); Heang-Ping Chan, Univ. of Michigan Health System (United States)

Retained Foreign Objects (RFOs) during surgery, also called gossypbiomas, are associated with mortality rates between 11 and 35%. There is a gap in surgical practice in how objects are accounted for in the operating room (OR) and a perceptual gap for radiologists identifying RFOs on radiographs as they are malleable and have variable appearance. We developed a Gossypiboma Micro Tag (GµT) that comprises of High Contrast Tags (HCTags) to label potential RFOs. Images of RFOs were acquired by imaging the GµTs over cadavers. To ensure random orientation we encapsulate the GµT in an opaque sphere that can roll. Under IRB we estimate the incidence of lines, tubes, and other man-made objects on intraoperative radiographs and replicate it on cadaver images. A statistician randomizes where the GµT and other foreign objects are placed in the abdomen in a 4 x 5 grid. We have created a large data set of 1,100 images with 3D GµT, 652 of which contains the  $G\mu T$  and the remaining without. The CAD involves the following key steps: (1) Preprocessing, (2) GµTs candidate labeling and segmentation, (3) false positive (FP) reduction, and (4) GµT detection. The CAD system can be operated at a high-sensitivity mode of 95% at a false positive rate of 0.94/image or a high-specificity mode of 0.08/image at 86% sensitivity. Studies are underway to further improve its sensitivity and specificity.

#### 9035-83, Session PSWed

## Quantitative characterization of brain β-amyloid using a joint PiB/FDG PET image histogram

Jon J. Camp, Mayo Clinic (United States); Dennis P. Hanson, Mayo Clinic (United States); David R. Holmes III, Bradley J. Kemp, Mayo Clinic (United States); Matthew L Senjem, Melissa Murray, Dennis W Dickson M.D., Joseph Parisi M.D., Mayo Clinic (United States); Ronald C. Petersen M.D., Val J. Lowe M.D., Mayo Clinic (United States); Richard A. Robb M.D., Mayo Clinic College of Medicine (United States)

A complex analysis performed by spatial registration of PiB and MRI patient images in order to localize the PiB signal to specific brain regions has been proven effective(2) in the diagnosis of Alzheimer's Disease (AD) and Lewy Body Disease (LBD).

This paper presents an original method of diagnosis and stratification of amyloid-related brain disease based on the use of PiB PET images in conjunction with 18F-FDG PET images (without MR images) to unambiguously identify the PiB signal arising from the cortex.

Rigid registration of PiB and FDG images is relatively straightforward, and in registration, the FDG signal serves to identify the cortical region in which the PiB signal is relevant. The brightest pixels in the FDG image represent the cortex. The correlation of the brightest PiB voxels with the brightest FDG values indicates the presence of Amyloid protein in the cortex in disease states, while correlation of the brightest PiB voxels with mid-range FDG values indicates only nonspecific binding in the white matter.

9035-84, Session PSWed

## Differentiating recurrent glioblastoma multiforme from radiation induced effects via texture analysis on multi-parametric MRI

Pallavi Tiwari, Case Western Reserve Univ. (United States); Lisa Rogers, Leo Wolansky, Andrew Sloan, Mark Cohen, Univ. Hospitals of Cleveland (United States); Anant Madabhushi, Case Western Reserve Univ. (United States)

We present a novel approach to identify computer extracted texture descriptors (CETDs) on multi-parametric MRI to distinguish radiation necrosis (RN) from recurrent glioblastoma multiforme (rGBM) postchemo-radiation. Differentiating these two conditions (RN, rGBM) on standard MRI is clinically challenging, primarily because the morphological appearance of RN closely mimics that of rGBM. The underlying hypothesis of this study is that CETDs on MRI can capture subtle, multi-scale morphologic attributes for distinguishing RN versus rGBM, features that may not be visually appreciable via qualitative inspection on traditional MRI. 17 patients were analyzed with Gd-T1 contrast, T2-FLAIR, T2w, apparent diffusion coefficient (ADC, derived from diffusion weighted imaging), and T1w protocols. A set of 400 CETDs (co-occurrence matrix homogeneity, neighboring gray-level dependence matrix, multi-scale Gaussian derivatives, and Law features) for modeling macro and micro-scale morphologic changes within the treated lesion area for each MRI protocol were extracted. Triplets of CETDs from the set of 400 were chosen via randomized selection over 10000 iterations. Silhouette Index (SI), a measure to quantify separation between clusters (RN, rGBM) by computing distance between cluster centers (normalized between 0 (no separation between clusters) and 1 (perfect separation)) was recorded for every feature triplet at every iteration. The triplets with highest SI were identified. The three sets of feature descriptors with the highest SI were consistently identified as gradient (edge-based), law, and co-occurrence feature sets with SI of 0.4, 0.38, and 0.35. Law texture descriptors appeared to capture soap-bubble enhancement (ring patterns), spreading wave front (ripple patterns), and swiss-cheese effect (splotched spots), qualitative observations previously described on MRI to distinguish RN from rGBM.

9035-85. Session PSWed

## Efficient 3D texture feature extraction from CT images for computer-aided diagnosis of pulmonary nodules

Fangfang Han, Northeastern Univ. (China) and Neusoft Corp. (China); Huafeng Wang, Stony Brook Univ. (United States); Bowen Song, Stony Brook Medicine (United States); Guopeng Zhang, Hongbing Lu, Fourth Military Medical Univ. (China); William Moore M.D., Zhengrong Liang, Stony Brook Medicine (United States); Hong Zhao, Northeastern Univ. (China) and Neusoft Corp. (China)

Texture feature from chest CT images for malignancy assessment of pulmonary nodules has become an un-ignored and efficient factor in Computer-Aided Diagnosis (CADx). In this paper, we focus on extracting as fewer as needed efficient texture features, which can be combined with other classical features (e.g. size, shape, growing rate, etc.) for assisting lung nodule diagnosis. Based on a typical calculation algorithm of texture features, namely Haralick features achieved from the graytone spatial-dependence matrices, we calculated two dimensional (2D) and 3D Haralick features from the CT images of 905 nodules. All of the CT images were selected from the Lung Image Database Consortium and Image Database Resource Initiative (LIDC-IDRI), which is the largest public chest database. 3D Haralick feature model of thirteen directions contains more information from the relationships on the neighbor voxels of different slices than 2D features from only four directions. After











comparing the efficiencies of 2D and 3D Haralick features applied on the diagnosis of nodules, principal component analysis (PCA) algorithm was used to extract as fewer as needed efficient texture features. To achieve an objective assessment of the texture features, the support vector machine classifier was trained and tested repeatedly for one hundred times. And the statistical results of the classification experiments were described by an average receiver operating characteristic (ROC) curve. The mean value (0.8776) of the area under the ROC curves in our experiments can show that the two extracted 3D Haralick projected features have the potential to assist the classification of benign and malignant nodules.

#### 9035-86, Session PSWed

### A novel computer-aided detection system for pulmonary nodule identification in CT images

Hao Han, Stony Brook Univ. (United States); Lihong C. Li, College of Staten Island (United States); Huafeng Wang, Hao Zhang, Stony Brook Univ. (United States); William Moore M.D., Zhengrong Liang, Stony Brook Medicine (United States)

Computer-aided detection (CAD) of pulmonary nodules from computer tomography (CT) scans is critical for assisting radiologists to identify lung lesions at an early stage. In this paper, we propose a novel approach for CAD of lung nodules based on a two-stage vector quantization (VQ) scheme. The proposed system was validated on 100 cases selected from the publicly available Lung Image Database Consortium (LIDC) database, where the 252 nodules were annotated by at least three radiologists. Compared to the commonly-used thresholding approach, the firststage VQ is more efficient to extract lung from the chest volume. For the detection of initial nodule candidates (INCs) within the extracted lung volume, the second-stage VQ proved to be much faster than existing approaches, with a detection rate of 92.1%. False-positive (FP) reduction of INCs were conducted via expert filtering in combination with a featurebased support vector machine (SVM) classifier. The present expert filtering rules significantly reduced the average FPs from 1297.8/scan to 55.3/scan while maintaining a high sensitivity of 85.8%. The subsequent 2-fold cross validation of SVM showed that our system could achieve a detection rate of 81.2% at 5 FPs/scan, and a higher sensitivity of 90.4% at 9 FPs/scan.

#### 9035-87, Session PSWed

### Comparison of biophysical factors influencing on emphysema quantification with low-dose CT

Changyong Heo, Seoul National Univ. (Korea, Republic of); Jonghyo Kim, Seoul National Univ (Korea, Republic of)

Emphysema Index(EI) measurements in MDCT is known to be influenced by various biophysical factors such as total lung volume(TLV), and body size. We investigated the association of the confounding biophysical factors with emphysema index in low-dose MDCT. In particular, we attempt to identify a potentially stronger biophysical factor than total lung volume. A total of 855 low-dose MDCT volumes taken at 120kVp, 40mAs, 1mm thickness, and B30f reconstruction kernel were included from the lung cancer screening database in Seoul National University Hospital. The lungs, airways, and pulmonary vessels were automatically segmented, and two Emphysema Indices, RA950 and Perc15, were extracted from the segmented lungs. The biophysical factors such as total lung volume(TLV), mode of lung attenuation(ModLA), effective body diameter(EBD), and the water equivalent body diameter(WBD) were estimated from the segmented lung and body area. The association of biophysical factors with emphysema indices were evaluated by correlation coefficients. The mean emphysema indices were 8.3±5.3(%) in RA950, and -931±18(HU) in Perc15. The estimates of biophysical

factors were 4.8±1.1(L) in TLV, -901±21(HU) in ModLA, 25.0±2.6(cm) in EBD, and 27.1±2.5(cm) in WBD. The correlation coefficients of biophysical factors with RA950 were 0.69 in TLV, 0.85 in ModLA, 0.23 in EBD, and 0.1 WBD, the ones with Perc15 were 0.71 in TLV, 0.98 in ModLA, 0.17 in EBD, and 0.33 WBD. Study results revealed that two biophysical factors, TLV and ModLA, mostly affects the emphysema indices. In particular, the ModLA exhibited strongest correlation of 0.98 with Perc15, which indicating the ModLA is the most significant confounding biophysical factor in emphysema indices measurement, and thus warrants further investigation to explore a technique to compensate its impacts.

#### Description of Purpose:

1. To investigated the association of the confounding biophysical factors with emphysema index in low-dose MDCT.

#### Methods:

- 1. Dataset
- 855 cases taken in Seoul National University Hospital.
- low-dose lung cancer screening dataset.
- 120kVp, 40mAs, 1mm thickness, B30f reconstruction kernel.
- 24 ~ 76 years old.
- 2. Analysis procedure (Figure 1.)
- Airway segmentation.
- Lung segmentation.
- Measurement of Emphysema features, emphysema indices and biophysical factors.
- 3. Application
- The lungs, airways, and pulmonary vessels were automatically segmented, and two Emphysema Index, RA950 and Perc15, were extracted from the segmented lungs.
- 4. Performance evaluation
- The biophysical factors such as total lung volume(TLV), mode of lung attenuation(ModLA), effective body diameter(EBD), and the water equivalent body diameter(WBD) were estimated from the segmented lung and body area.
- The association of biophysical factors with emphysema indices were evaluated by correlation coefficients.

#### Results:

- The mean emphysema indices were  $8.3\pm5.3(\%)$  in RA950, and  $-931\pm18(HU)$  in Perc15.
- The estimates of biophysical factors were  $4.8\pm1.1(L)$  in TLV,  $-901\pm21(HU)$  in ModLA,  $25.0\pm2.6(cm)$  in EBD, and  $27.1\pm2.5(cm)$  in WBD.
- The correlation coefficients of biophysical factors with RA950 were 0.69 in TLV, 0.85 in ModLA, 0.23 in EBD, and 0.1 WBD, the ones with Perc15 were 0.71 in TLV, 0.98 in ModLA, 0.17 in EBD, and 0.33 WBD.

New or breakthrough work to be presented:

1. We attempt to identify a potentially stronger biophysical factor than total lung volume.

#### Conclusion:

Study results revealed that two biophysical factors, TLV and ModLA, mostly affects the emphysema indices. In particular, the ModLA exhibited strongest correlation of 0.98 with Perc15, which indicating the ModLA is the most significant confounding biophysical factor in emphysema indices measurement, and thus warrants further investigation to explore a technique to compensate its impacts.

#### 9035-88. Session PSWed

## Microstructure analysis of the pulmonary lung of the secondary lobulus by a synchrotron radiation CT

Yasunori Fukuoka, Yoshiki Kawata, Noboru Niki, Univ. of











Tokushima (Japan); Keiji Umetani, Japan Synchrotron Radiation Research Institute (Japan); Yasutaka Nakano, Shiga Univ. of Medical Science (Japan); Noriyuki Moriyama, Hironobu Ohmatsu, National Cancer Ctr. Hospital East (Japan); Harumi Itoh, Univ. of Fukui (Japan)

The conversion of images at micro level of the normal lung and those with very early stage lung disease and the quantitative analysis of morphology on the images can contribute to the chest image diagnosis of the next generation. The collection of very minute CT images is necessary in using high luminance synchrotron radiation CT for converting the images. The purpose of this study is to analyze the structure of secondary pulmonary lobule of the lung. We also show the structure of the secondary pulmonary lobule by means of extending our vision to a wider fieldthrough theimage reconfigurationfrom the projection image of synchrotron radiation CT.

#### 9035-89, Session PSWed

### Wavelet based rotation invariant texture feature for lung tissue classification and retrieval

Jatindra K. Dash, Sudipta Mukhopadhyay, Rahul Das Gupta, Indian Institute of Technology Kharagpur (India); Mandeep K. Garg, Nidhi Prabhakar, Niranjan Khandelwal, Postgraduate Institute of Medical Education & Research (India)

This paper evaluates the performance of recently proposed rotation invariant texture feature extraction method for the classification and retrieval of lung tissues affected with Interstitial Lung Diseases (ILDs). The method makes use of principle texture direction as the reference direction and extracts texture features using Discrete Wavelet Transform (DWT). A private database containing high resolution computed tomography (HRCT) images belonging to five category of lung tissue is used for the experiment. The experimental result shows that the rotation invariant feature used achieves better retrieval as well as classification accuracy.

#### 9035-90, Session PSWed

### Effect of image variation on computer aided detection systems

Parisa Rabbani, KTH Royal Institute of Technology (Sweden); Pragnya Maduskar, Rick Philipsen, Laurens E. Hogeweg, Bram van Ginneken, Radboud Univ. Nijmegen Medical Ctr. (Netherlands)

As the importance of Computer Aided Detection (CAD) systems application is rising in medical imaging field due to the advantages they generate; it is essential to know their weaknesses and try to find a proper solution for them. A common possible practical problem that affects CAD systems performance is: dissimilar training and testing datasets declines the efficiency of CAD systems. In this paper normalizing images is proposed, three different normalization methods are applied on chest radiographs namely (1) Simple normalization (2) Local Normalization (3) Multi Band Local Normalization. The supervised lung segmentation CAD system performance is evaluated on normalized chest radiographs with these three different normalization methods in terms of Jaccard index. As a conclusion the normalization enhances the performance of CAD system and among these three normalization methods Local Normalization and Multi band Local normalization improve performance of CAD system more significantly than the simple normalization.

9035-91, Session PSWed

### 3D mapping of airway wall thickening in asthma with MSCT: a level set approach

Catalin Fetita, Télécom SudParis (France); Pierre-Yves Brillet, Univ. Paris 13 (France); Ruth A Hartley, Glenfield Hospital, University of Leicester (United Kingdom); Philippe Grenier, Univ. Pierre et Marie Curie (France); Christopher Brightling, Glenfield Hospital, University of Leicester (United Kingdom)

Assessing the airway wall thickness in multi slice computed tomography (MSCT) as image marker for airway disease phenotyping such asthma and COPD is a current trend and challenge for the scientific community working in lung imaging. This paper addresses the same problem from a different point of view: considering the expected wall thickness ratio for a normal subject as known and constant throughout the airway lumen dimensions, the aim is to build up a 3D map of airway wall regions of larger thickness and to define an overall score able to highlight a pathological status. In this respect, the local dimension (caliber) of the previously segmented airway lumen is obtained on each point by exploiting the granulometry morphological operator. A level set function is defined based on this caliber information and on the expected wall thickness ratio, which allows to obtain a good estimate of the airway wall throughout all segmented lumen generations. Next, the vascular (or mediastinal dense tissue) contact regions are automatically detected and excluded from analysis. For the remaining airway wall border points, the real wall thickness is estimated based on the tissue density analysis in the airway radial direction; thick wall points are highlighted on a 3D representation of the airways and the percent of thick wall areas is set-up as assessment score. The proposed approach is fully automated and was evaluated (proof of concept) on a patient selection (10) coming from different databases including mild, severe asthmatics and normal cases. This preliminary evaluation confirms the discriminative power of the proposed approach regarding different phenotypes and is currently extending to larger cohorts.

9035-92, Session PSWed

### 3D intrathoracic region definition and its application to PET-CT analysis

Ronnarit Cheirsilp, The Pennsylvania State Univ. (United States); Rebecca Bascom, Thomas W Allen, The Pennsylvania State Univ (United States); William E. Higgins, The Pennsylvania State Univ. (United States)

Recently developed integrated PET-CT scanners give co-registered multimodal data sets that offer complementary three-dimensional (3D) digital images of the chest. PET (positron emission tomography) imaging gives highly specific functional information of suspect cancer sites, while CT (X-ray computed tomography) gives associated anatomical detail. Because the 3D CT and PET scans generally span the body from the eyes to the knees, accurate definition of the intrathoracic region is vital for focusing attention to the central-chest region. In this way, diagnostically important regions of interest (ROIs), such as central-chest lymph nodes and cancer nodules, can be more efficiently isolated. We propose a method for automatic segmentation of the intrathoracic region from a given co-registered 3D PET-CT study. Using the 3D CT scan as input, the method begins by finding an initial intrathoracic region boundary for a given 2D CT section. Next, active contour analysis, driven by a cost function depending on local image gradient, gradientdirection, and contour shape features, iteratively estimates the contours spanning the intrathoracic region on neighboring 2D CT sections. This process continues until the complete region is defined. We next present an interactive system that employs the segmentation method for focused 3D PET-CT chest image analysis. A validation study over a series of PET-CT studies reveals that the segmentation method gives a Dice index accuracy of >98%. In addition, further results demonstrate the utility of











the method for focused 3D PET-CT chest image analysis, ROI definition, and visualization.

9035-93, Session PSWed

#### Lung texture classification using bag of visual words

Marina Asherov, Idit Diamant, Hayit Greenspan, Tel Aviv Univ. (Israel)

Interstitial lung diseases (ILD) are a group of around 150 disorders of the lung parenchyma. High-Resolution Computed Tomography (HRCT) is the most important modality in ILD diagnosis. Classification of various lung tissue patterns caused by ILD is still quite challenging task. The main challenges are that different lung texture look very similar and there are various texture patterns representing specific tissue type. This work focuses on classification of five most common categories of lung tissues of ILD on HRCT images: normal, emphysema, ground glass, fibrosis and micronodules. Our objective in this study is to classify the annotated region of interest (AROI) using a bag of visual words (BoVW) framework. The image is divided to small patches. A collection of representative patches are defined as visual words. This procedure of dictionary construction is performed for every lung texture category in order to balance the feature space in case of an unbalanced dataset. The assumption is that different lung textures are represented by different visual word distributions. The classification is performed using an SVM classifier with histogram intersection kernel. In order to estimate the generalization performance of the classification of AROI, a leave-onepatient-out cross validation (LOPO CV) is used. Dataset of 1018 AROIs from 95 patients is used. We experiment with various parameters in order to optimize the system performance and achieve an overall classification accuracy of 79%, which compares with the state-of-the-art in this domain. Additional experimentation is underway to augment the feature representation and attempt to increase the accuracy further.

9035-94, Session PSWed

### Automated segmentation of murine lung tumors in X-ray micro-CT images

Joshua K. Y. Swee, Imperial College London (United Kingdom) and Siemens Corporate Research (United States); Clare Sheridan, Elza de Bruin, Julian Downward, Francois Lassaily, Cancer Research UK (United Kingdom); Luis Pizarro Quiroz, Imperial College London (United Kingdom)

Recent years have seen micro-CT emerge as a means of providing imaging analysis in pre-clinical study, with micro-CT having been shown to be particularly applicable to the examination of murine lung tumors. Despite this, existing studies have involved substantial human intervention during the image analysis process, with the use of fullyautomated aids found to be almost non-existent. We present a new approach to automate the segmentation of murine lung tumors designed specifically for micro-CT-based pre-clinical lung cancer studies that addresses the specific requirements of such study, as well as the limitations human-centric segmentation approaches experience when applied to micro-CT data. Our approach consists of three distinct stages, and begins by utilizing edge enhancing and vessel enhancing non-linear anisotropic diffusion filters to extract anatomy masks (lung/ vessel structure) in a pre-processing stage. Initial candidate detection is then performed through ROI reduction utilizing obtained masks and a two-step automated segmentation approach that aims to extract all disconnected objects within the ROI, and consists of Otsu thresholding, mathematical morphology and marker-driven watershed. False positive reduction is finally performed on initial candidates through randomforest-driven classification using the shape, intensity, and spatial features of candidates. We provide validation of our approach using data from an associated lung cancer study, showing favorable results both in

terms of detection (sensitivity=86%, specificity=89%) and structural recovery (Dice Similarity=0.88) when compared against manual specialist annotation.

9035-95, Session PSWed

#### Longitudinal follow-up study of smokinginduced emphysema progression in low-dose CT screening of lung cancer

Hidenobu Suzuki, Yoshiki Kawata, Noboru Niki, Univ. of Tokushima (Japan); Yasutaka Nakano, Shiga Univ. of Medical Science (Japan); Hironobu Ohmatsu, Masahiko Kusumoto, Takaaki Tsuchida, National Cancer Ctr. Hospital East (Japan); Kenji Eguchi, Teikyou Univ. (Japan); Noriyuki Moriyama, National Cancer Ctr. Hospital East (Japan)

Chronic obstructive pulmonary disease is a major public health problem that is predicted to be third leading cause of death in 2030. Although spirometry is traditionally used to quantify emphysema progression, it is difficult to detect the loss of pulmonary function by emphysema in early stage, and to assess the susceptibility to smoking. This study presents quantification method of smoking-induced emphysema progression based on annual changes of low attenuation area (LAA) by each lung lobe acquired from low-dose CT images in lung cancer screening. The method consists of three steps. First is segmentation of lung lobes using interlobar fissures extracted by enhancement filter based on four-dimensional curvature. Second is segmentation of LAA by each lung lobe. Finally, smoking-induced emphysema progression is assessed by statistical analysis of the annual changes represented by linear regression of LAA percentage in each lung lobe. This method was applied to 256 participants in lung cancer CT screening for 6 years. The results showed that LAA progressions of nonsmokers, past smokers, and current smokers are different in terms of pack-year and smoking cessation duration. This study demonstrates effectiveness in diagnosis and prognosis of early emphysema in lung cancer CT screening.

9035-96, Session PSWed

# Potential usefulness of a topic model-based categorization of lung cancers as quantitative CT biomarkers for predicting the recurrence risk after curative resection

Yoshiki Kawata, Noboru Niki, Univ. of Tokushima (Japan); Hironobu Ohamatsu, Keiju Aokage, Mitsuo Satake, Masahiko Kusumoto, Takaaki Tsuchida, National Cancer Ctr. Hospital East (Japan); Kenji Eguchi, Teikyou Univ. School of Medicine (Japan); Masahiro Kaneko, Tokyo Health Service Association (Japan); Noriyuki Moriyama, Tokyo Midtown Medical Ctr. (Japan)

Lung cancer is the leading cause of cancer mortality worldwide. A high proportion of non-small-cell lung cancer (NSCLC) patients exhibit with symptoms in advanced disease stage. The recent release of positive results from the National Lung Screening Trial (NLST) in the US delivered that CT screening does in fact have a positive impact on the reduction of lung cancer-related mortality. While this study does show the efficacy of CT based screening, physicians often face the problem of deciding appropriate management strategies for maximizing patient survival and for preserving lung function. Distinguishing a subset of patients with less invasive nodules and a better prognosis remains a substantial and challenging problem. In this work, we investigate a potential usefulness of the topic model-based categorization of lung cancers as quantitative CT biomarkers for predicting the recurrence risk after curative resection. The elucidation of the subcategorization of a pulmonary nodule type in CT images is an important preliminary step towards developing the











nodule managements that are specific to each patient. We categorize lung cancers by analyzing volumetric distributions of CT values within lung cancers via a topic model such as latent Dirichle allocation. We calculate the association of recurrence with prognostic factors including categorization, gender, age, tumor diameter, smoking status, disease stage, histological type, lymphatic permeation, and vascular invasion using a multivariate Cox proportional hazards model. Using 454 CT images of NSCLCs (maximum lesion size of 3 cm), we determine the predictive accuracy and discriminative ability of the model using time-dependent concordance index and calibration curve through bootstrap resampling to illustrate the potential usefulness of the topic model-based categorization of lung cancers as quantitative CT biomarkers.

9035-97, Session PSWed

## Computerized organ localization in abdominal CT volume with context-driven generalized Hough transform

Jing Liu, Qiang Li, Shanghai Advanced Research Institute (China)

Fast localization of organs is a key step in computer-aided detection of lesions and in image guided radiation therapy. We developed a contextdriven Generalized Hough Transform (GHT) for robust localization of an organ-of-interests (OOIs) in a CT volume. Conventional GHT locates the center of an organ by looking-up center locations of pre-learned organs with "matching" edges. It often suffers from mislocalization because "similar" edges in vicinity may attract the pre-learned organs towards wrong places. The proposed method not only uses information from organ's own shape but also takes advantage of nearby "similar" edge structures. First, multiple GHT co-existing look-up tables (cLUT) were constructed from a set of training shapes of different organs. Each cLUT represented the spatial relationship between the center of the OOI and the shape of a co-existing organ. Second, the OOI center in a test image was determined using GHT with each cLUT separately. Third, the final localization of OOI was based on weighted combination of the centers obtained in the second stage. The training set consisted of 10 CT volumes with manually segmented OOIs including liver, spleen and kidneys. The method was tested on a set of 25 abdominal CT scans. Context-driven GHT correctly located all OOIs in the test image and gave localization errors of 19.5±9.0, 12.8±7.3, 9.4±4.6 and 8.6±4.1 mm for liver, spleen, left and right kidney respectively. Conventional GHT mislocated 8 out of 100 organs and its localization errors were 26.0±32.6, 14.1±10.6, 30.1±42.6 and 23.6±39.7mm for liver, spleen, left and right kidney respectively.

9035-98, Session PSWed

## Segmentation of urinary bladder in CT urography (CTU) using CLASS with enhanced contour conjoint procedure

Kenny Cha, Lubomir M. Hadjiiski, Heang-Ping Chan, Richard H. Cohan M.D., Elaine M. Caoili M.D., Chuan Chou, Univ. of Michigan (United States)

We are developing a computerized method for bladder segmentation in CTU for computer-aided diagnosis of bladder cancer. A challenge for computerized bladder segmentation in CTU is that the bladder often contains regions filled with IV contrast and without contrast. Previously, we proposed a Conjoint Level set Analysis and Segmentation System (CLASS) consisting of four stages: preprocessing and initial segmentation, 3D and 2D level set segmentation, and post-processing. In case the bladder is partially filled with contrast, CLASS segments the non-contrast (NC) region and the contrast (C) filled region separately and conjoins the contours. The NC and C Contour Conjoint Procedure (CCP) is not trivial. Inaccuracies in the NC and C contours may cause CCP to exclude portions of the bladder. To alleviate this problem, we

implemented model-guided refinement to propagate the C contour if the level set propagation in the region stops prematurely due to substantial non-uniformity of the contrast. An enhanced CCP with regularized energies further propagates the conjoint contours to the correct bladder boundary. Segmentation performance was evaluated using 172 cases: 81 training cases and 92 test cases. For all cases, 3D hand segmented contours were obtained as reference standard, and computerized segmentation accuracy was evaluated in terms of average volume intersection %, average % volume error, and average minimum distance. With enhanced CCP, those values were  $78.0\pm14.7\%$ ,  $16.4\pm16.9\%$ ,  $3.8\pm2.3$  mm, respectively, for the test set. With CLASS, those values were  $67.3\pm14.3\%$ ,  $29.3\pm15.9\%$ ,  $4.9\pm2.6$  mm, respectively. The enhanced CCP improved bladder segmentation significantly (p<0.001) for all three performance measures.

9035-99, Session PSWed

## Level-set based free fluid segmentation with improved initialization using region growing in 3D ultrasound sonography

Dae Hoe Kim, KAIST (Korea, Republic of); Konstantinos N. Plataniotis, Univ. of Toronto (Canada); Yong Man Ro, KAIST (Korea, Republic of)

In this study, new free fluid segmentation method is proposed, aiming to increase segmentation accuracy on free fluids, at the same time, decrease processing time, regardless of the accuracy of initial seeds. In order to segment free fluid regions fast and accurate, we propose a new free fluid segmentation based on Chan-vese level-set with an improved initialization using minimum variance region growing. The proposed method is devised to take complementary effects on both methods. In experiments, the effectiveness of the proposed method is demonstrated with 3D US volumes in terms of Dice's coefficient, volume difference, Hausdorff distance and processing time. Results show that the proposed method outperforms CVLS and MVRG in terms of processing time as well as segmentation accuracy.

9035-100, Session PSWed

## Performance of an automated renal segmentation algorithm based on morphological erosion and connectivity

Benjamin Abiri, New York Univ. School of Medicine (United States); Brian Park, New York Univ. (United States); Hersh Chandarana, Artem Mikheev, New York Univ. Langone Medical Ctr. (United States); Vivian S. Lee, Univ. of Utah Health Systems (United States); Henry Rusinek, New York Univ. Langone Medical Ctr. (United States)

The precision, accuracy, and efficiency of a novel semi-automated segmentation technique for VIBE (volumetric interpolated breath-hold sequence) MRI sequences was analyzed using 7 clinical datasets. Two observers performed whole-kidney segmentation using EdgeWave segmentation software based on constrained morphological growth. Ground truths were prepared by manual tracing of kidney on each of approximately 40 slices. Using the software, the average inter-observer disagreement was 2.7% ± 2.12% for whole kidney volume, 2.1% ± 1.77% for cortex, and 4.1% ± 3.18% for medulla. In comparison to the ground truth kidney volume, the error was 2.8% ± 2.5% for whole kidney volume, 3.1%± 1.75% for cortex, and 3.6%±.3.1% for medulla. It took an average of 4:14 +/- 1:42 minutes of operator time, plus 2:56 +/- 1:23 minutes of computer time to perform segmentation of one whole kidney, cortex, and medulla. Segmentation speed, inter-observer agreement and accuracy were several times better than those of our existing graph-cuts segmentation technique requiring approximately 20 minutes per case











and with 7-10% error. With the expedited image processing, high interobserver agreement, and volumes closely matching true values, kidney volumetry becomes a reality in many clinical applications.

9035-101, Session PSWed

### COMPASS based ureter segmentation in CT urography (CTU)

David W. Zick, Lubomir M. Hadjiyski, Heang-Ping Chan, Richard H. Cohan M.D., Elaine M. Caoili M.D., Chuan Zhou, Jun Wei, Univ. of Michigan Health System (United States)

We are developing a computerized system for automated segmentation of ureters in CTU, referred to as COmbined Model-guided Path-finding Analysis and Segmentation System (COMPASS). Ureter segmentation is a critical component for computer-aided diagnosis of ureter cancer. A challenge for ureter segmentation is the presence of regions not well opacified with intravenous (IV) contrast. COMPASS consists of three stages: (1) adaptive thresholding and region growing, (2) path-finding and propagation, and (3) edge profile extraction and feature analysis. 124 ureters, in 79 CTU scans with IV contrast were collected from 79 patient files. On average, the ureters spanned 283 CT slices (range:116 to 399, median:301). More than half of the ureters contained malignant or benign lesions and some had ureter wall thickening due to malignancy. A starting point for each of the 124 ureters was selected manually to initialize the tracking by COMPASS. Path-finding and segmentation were guided by the anatomical knowledge of ureters in CTU. The segmentation performance was quantitatively assessed by estimating the percentage of the length that was successfully tracked and segmented for each ureter. Of the 124 ureters, 120 (97%) were segmented completely (100%), 121 (98%) were segmented through at least 70% of its length, and 123 (99%) were segmented at least 50%. In comparison, using our previous method, 85 (69%) ureters were segmented completely (100%), 100 (81%) were segmented through at least 70% of its length, and 107 (86%) were segmented at least 50%. COMPASS improved significantly the ureter tracking, including regions across ureter lesions, wall thickening and the narrowing of the lumen.

9035-102. Session PSWed

### Ultrasound based computer-aided-diagnosis of kidneys for pediatric hydronephrosis

Juan J. Cerrolaza, Craig A. Peters, Aaron D. Martin, Emmarie Myers, Nabile M. Safdar M.D., Marius George Linguraru, Children's National Medical Ctr. (United States)

Ultrasound is the mainstay of imaging for pediatric hydronephrosis, though its potential as diagnostic tool is limited by its subjective assessment, and lack of correlation with renal function. Therefore, all cases showing signs of hydronephrosis undergo further invasive studies, like diuretic renogram, in order to assess the actual renal function. Under the hypothesis that renal morphology is correlated with renal function, a new ultrasound based computer-aided diagnosis (CAD) tool for pediatric hydronephrosis is presented. From 2D ultrasound, a novel set of morphological features of the renal collecting systems and the parenchyma, is automatically extracted using image analysis techniques. From the original set of features, including size, geometric and curvature descriptors, a subset of ten features are selected as predictive variables, combining a feature selection technique and area under the curve filtering. Using the washout half time (T1/2) as indicative of renal obstruction, two groups are defined. Those cases whose T1/2 is above 30 minutes are considered to be severe, while the rest would be in the safety zone, where diuretic renography could be avoided. Two different classification techniques are evaluated (logistic regression, and support vector machines). Adjusting the probability decision thresholds to operate at the point of maximum sensitivity, i.e., preventing any severe case be misclassified, specificities of 53%, and 75% are achieved, for the logistic

regression and the support vector machine classifier, respectively. The proposed CAD system allows to establish a link between non-invasive non-ionizing imaging techniques and renal function, limiting the need for invasive and ionizing diuretic renography.

9035-103, Session PSWed

### Automated abdominal lymph node segmentation based on RST analysis and SVM

Yukitaka Nimura, Yuichiro Hayashi, Nagoya Univ. (Japan); Takayuki Kitasaka, Aichi Institute of Technology (Japan); Kazuhiro Furukawa M.D., Nagoya Univ. (Japan); Kazunari Misawa M.D., Aichi Cancer Ctr. Research Institute (Japan); Kensaku Mori, Nagoya Univ. (Japan)

This paper describes a segmentation method for abdominal lymph node (LN) using radial structure tensor analysis (RST) and support vector machine. LN analysis is one of crucial parts of lymphadenectomy, which is a surgical procedure to remove one or more LNs in order to evaluate them for the presence of cancer. Several works for automated LN detection and segmentation have been proposed. However, there are a lot of false positives (FPs). The proposed method consists of LN candidate segmentation and FP reduction. LN candidates are extracted using RST analysis in each voxel of CT scan. RST analysis can discriminate between difference local intensity structures without influence of surrounding structures. In FP reduction process, we eliminate FPs using support vector machine with shape and intensity information of the LN candidates. The experimental result reveals that the sensitivity of the proposed method was 82.0 % with 21.6 FPs/case.

9035-104, Session PSWed

## A universal approach for automatic organ segmentations on 3D CT images based on organ localization and 3D GrabCut

Xiangrong Zhou, Gifu Univ. School of Medicine (Japan); Takaaki Ito, Gifu Univ. (Japan); Xinxin Zhou, Nagoya Bunri Univ. (Japan); Huayue Chen, Gifu Univ. School of Medicine (Japan); Takeshi Hara, Gifu Univ. (Japan); Ryujiro Yokoyama, Gifu Univ. School of Medicine (Japan); Masayuki Kanematsu, Hiroaki Hoshi, Gifu Univ. (Japan); Hiroshi Fujita, Gifu Univ. School of Medicine (Japan)

This paper describes a universal approach to accomplish the automatic segmentation for different organ regions on 3D CT scans. The proposed approach combines the organ localization and 3D GrabCut techniques to achieve an automatic and quick segmentation process. The basic idea of proposed method is to detect 3D bounding-box of a 3D target region on CT images firstly, and segment the target organ region in the boundingbox by using a 3D GrabCut algorithm. A machine-learning method was used to train a detector to localize the 3D bounding-box of the target organ through a template matching on a feature space expanded by local binary patterns. A 3D GrabCut algorithm was used for further organ segmentation by iteratively estimating the CT number distributions of the target organ and backgrounds with a graph-cuts optimization. We applied this approach to segment 12 kinds of principle organ and tissue regions independently on torso CT scans. In our experiments, we randomly selected 300 CT scans (with human indicated organ and tissue locations) for training the 2D detectors, and then, applied the proposed approach to localize and segment each of the target regions on the other 1,000 CT scans for performance evaluation. The good performance and usefulness were shown in the experimental results.











9035-105, Session PSWed

## A novel colonic polyp volume segmentation method for computer tomographic colonography

Huafeng Wang, Stony Brook Medicine (United States); Lihong C. Li, College of Staten Island (United States); Hao Han, Bowen Song, Hao Peng, Stony Brook Medicine (United States); Yunhong Wang, Lihua Wang, BeiHang Univ. (China); Zhengrong Liang, Stony Brook Medicine (United States)

Colorectal cancer is the third most common type of cancer. However, this disease can be prevented by detection and removal of precursor adenomatous polyps after the diagnosis given by experts on computer tomographic colonography (CTC). During CTC diagnosis, the radiologist looks for colon polyps and measures not only the size but also the malignancy. It is a common sense that to segment polyp volumes from their complicated growing environment is of much significance for accomplishing the CTC based early diagnosis task. Previously, the polyp volumes are mainly given from the manually or semi-automatically drawing by the radiologists. As a result, some deviations cannot be avoided since the polyps are usually small (6~9mm) and the radiologists' experience and knowledge are varying from one to another. In order to achieve automatic polyp segmentation carried out by the machine, we proposed a new method based on the colon decomposition strategy. We evaluated our algorithm on both phantom and patient data. Experimental results demonstrate our approach is capable of segment the small polyps from their complicated growing background.

9035-106, Session PSWed

# Progressive region-based colon extraction for computer-aided detection and quantitative imaging in cathartic and non-cathartic CT colonography

Janne J. Näppi, Massachusetts General Hospital (United States) and Harvard Medical School (United States); Yasuji Ryu, Massachusetts General Hospital (United States); Hiroyuki Yoshida, Massachusetts General Hospital (United States) and Harvard Medical School (United States)

Accurate automated extraction of the region of colon is an important first step for practical computer-aided detection (CADe) and quantitative imaging (QI) in computed tomographic colonography (CTC). We developed a progressive region-based (PRB) method for colon extraction to minimize the presence of extra-colonic components in comparison with our previously developed lumen-based tracking (LBT) method and to provide quantitative information for automated estimation of the quality of bowel preparation. In the first part, extra-colonic components other than small bowel are excluded from the abdominal region by use of dedicated anatomy-based methods. In the second part, the region of colon is separated from small bowel by reconstruction of a pathway from anus to cecum based on the remaining abdominal lumen regions by use of anatomy-based landmarks, segmental features, and region-based lumen-tracking algorithms, where algorithms of progressively increasing complexity are used as needed depending on the complexity of the individual extraction task. Finally, the extracted lumen region is tested for potentially missing complementary segments that should still be included in the final region. The method was tested with 15 challenging cathartic and non-cathartic fecal-tagging CTC cases, where the previous LBT method had included extra-colonic components. Preliminary results indicate that the PRB outperforms the LBT by minimizing extra-colonic regions and that it can also be used to provide meaningful quantitative information about the quality of bowel preparation.

9035-107, Session PSWed

### GISentinel: a software platform for automatic ulcer detection on capsule endoscopy videos

Steven Yi, Heng Jiao, Fan Meng, Xyken, LLC (United States); Jonathan A. Leighton, Pasha Shabana, Lauri Rentz, Mayo Clinic (United States)

In this paper, we present a novel and clinically valuable software platform for automatic ulcer detection on gastrointestinal (GI) tract from Capsule Endoscopy (CE) videos. Typical CE videos take about 8 hours. They have to be reviewed manually by physicians to detect and locate diseases such as ulcers and bleedings. The process is time consuming. Moreover, because of the long-time manual review efforts, it is prone to miss-finding. Working with our collaborators, we developed a software platform which can fully automated GI tract ulcer detection and classification. For this presentation, we focus on ulcer detection algorithm design and the software performance results. This software includes 3 parts: the frequency based Log-Gabor filter regions of interest (ROI) extraction or segmentation, unique feature selection and validation, and the cascade SVM-logic based classification for identifying ulcers under various challenging situations such as appearance alike normal tissues, food particles, bubbles, fluid, and specular reflection). Initial evaluations show descent results. In occurring instance-wise, the ulcer detection rate is 88.1%. The false alarm rate is 25.24%. Given that ulcer is among the most difficult diseases to locate and identify in the videos, the results have exceeded our expectations. This work is a part of our innovative 2D/3D based GI tract disease detection software platform. The final goal of this SW is to find and classification of major GI tract diseases intelligently, such as bleeding, ulcer, and polyp from the CE videos. This paper will mainly describe the automatic ulcer detection functional

9035-108, Session PSWed

### Retinal image quality assessment using generic features

Mahnaz Fasih, J. M. Pierre Langlois, Ecole Polytechnique de Montréal (Canada); Houssem Ben Tahar, DIAGNOS Inc. (Canada); Farida Cheriet, Ecole Polytechnique de Montréal (Canada)

Automated retinal image quality assessment is an important step in automatic eye disease diagnosis. Diagnosis accuracy is highly dependent on the quality of retinal images, because poor image quality might prevent the observation of significant eye features and disease manifestations. A robust algorithm is therefore required in order to quickly evaluate the quality of images inside a large database. We developed a fast algorithm for assessment of retinal image quality based on generic features that is independent from segmentation methods. The local sharpness and texture features were evaluated by applying the cumulative probability of blur detection metric and run-length encoding algorithm, respectively. Based on the recommendation of medical experts, these features were applied on the macula and optic disc regions. The quality features are combined to evaluate the image suitability for diagnosis purposes. The support vector machine method with radial basis function was used as a nonlinear classifier in order to categorize images to gradable and ungradable groups. We successfully applied our methodology on 65 images of size 2592?1944 pixels that had been manually graded by a medical expert. The expert evaluated 38 images as gradable and 27 as ungradable. The results indicate a very good agreement between the proposed algorithm predictions and the medical expert judgment: sensitivity 96.15% and specificity 94.74%. The developed algorithm demonstrates sufficient robustness to identify relevant images for an automatic diagnosis.











9035-110, Session PSWed

### A boosted optimal linear learner for retinal vessel segmentation

Enrico Grisan, Enea Poletti, Univ. degli Studi di Padova (Italy)

Ocular fundus images provide important information about retinal degeneration, which may be related to acute pathologies or to early signs of systemic diseases. An automatic and quantitative assessment of vessel morphological features, such as diameters and tortuosity, can improve clinical diagnosis and evaluation of retinopathy. We propose a data-driven approach, in which the system learns a set of optimal discriminative convolution kernels (linear learner). The set is progressively built based on a ADA-boost sample weighting scheme, providing seamless integration between linear learner estimation and classification. At variance with available methods that resort in using the green channel alone, we make full use of the color information, estimating the kernels on the RGB data of the training samples. The set is employed as a rotating bank of matched filters, whose response is used by the boosted linear classifier to provide a classification of each image pixel into the two classes of interest (vessel/background). In order to test the generality of the approach, we assessed the performance of the proposed method on fundus images using the DRIVE dataset. We show that the segmentation performance yields an accuracy of 0.94.

9035-111, Session PSWed

### Glaucoma detection based on local binary patterns in fundus photographs

Maya Alsheh Ali, Thomas Hurtut, Univ. Paris Descartes (France) and Ecole Polytechnique de Montréal (Canada); Timothée Faucon, DIAGNOS Inc. (Canada); Farida Cheriet, Ecole Polytechnique de Montréal (Canada)

Glaucoma, a group of diseases that lead to optic neuropathy, is one of the most common reasons for blindness worldwide. Glaucoma rarely causes symptoms until the later stages of the disease. Early detection of glaucoma is very important to prevent visual loss since optic nerve damages cannot be reversed. To detect glaucoma, purely data-driven techniques have advantages, especially when the disease characteristics are complex and when precise image-based measurements are difficult to obtain. In this paper, we present our preliminary study for glaucoma detection using an automatic method based on local texture features extracted from fundus photographs. It implements the completed modeling of Local Binary Patterns (CLBP) to capture representative texture features from the whole image. A local region is represented by three operators: its central pixel (LBPC) and its local differences as two complementary components, the sign (LPB) and the magnitude (LBPM). An image texture is finally described by both the distribution of LBP and the joint-distribution of LBPM and LBPC. Our images are then classified using a nearest-neighbor method with a leave-one-out validation strategy. On a sample set of 41 fundus images (13 glaucomatous, 28 non-glaucomatous), our method achieves 95.1% success rate with a specificity of 92.3% and a sensitivity of 96.4%. This study proposes a reproducible glaucoma detection process that could be used in a lowpriced medical screening, thus avoiding the inter-experts variability issue.

9035-112, Session PSWed

## Automatic multiresolution age-related macular degeneration detection from fundus images

Mickaël Garnier, Thomas Hurtut, Univ. Paris Descartes (France) and Ecole Polytechnique de Montréal (Canada); Houssem Ben Tahar, DIAGNOS Inc. (Canada); Farida Cheriet, Ecole

Polytechnique de Montréal (Canada)

Age-related Macular Degeneration (AMD) is a leading cause of legal blindness. As the disease progress, visual loss occurs rapidly, therefore early diagnosis is required for timely treatment. Automatic, fast and robust screening of this widespread disease should allow an early detection. Most of the automatic diagnosis methods in the literature are based on a complex segmentation of the drusen, targeting a specific symptom of the disease. In this paper, we present a preliminary study for AMD detection from color fundus photographs using a multiresolution texture analysis. We analyze the texture at several scales by using a wavelet decomposition in order to identify all the relevant texture patterns. Textural information is captured using both the sign and magnitude components of the completed model of Local Binary Patterns. An image is finally described with the textural pattern distributions of the wavelet coefficient images obtained at each level of decomposition. We use a Linear Discriminant Analysis for feature dimension reduction to avoid the curse of dimensionality problem and image classification. Experiments were conducted on a dataset containing 45 images (23 healthy and 22 diseased) of variable quality and captured by different cameras. Our method achieved a recognition rate of 93.3%, with a specificity of 95.5% and a sensitivity of 91.3%. This approach shows promising results at low costs that in agreement with medical experts as well as robustness to both image quality and fundus camera model.

#### 9035-114, Session PSWed

#### Preliminary study on differentiation between glaucomatous and non-glaucomatous eyes on stereo fundus images using cup gradient models

Chisako Muramatsu, Gifu Univ. School of Medicine (Japan); Yuji Hatanaka, Univ. of Shiga Prefecture (Japan); Kyoko Ishida, Akira Sawada, Tetsuya Yamamoto M.D., Hiroshi Fujita, Gifu Univ. School of Medicine (Japan)

Glaucoma is one of the leading causes of blindness in Japan and the US. One of the indices for diagnosis of glaucoma is the cup-todisc ratio (CDR). We have been studying a computerized method for measuring CDR on stereo fundus photographs. Although our previous study indicated that the method may be useful, cup determination was not always successful, especially for the normal eyes. In this study, we investigated a new method to quantify the likelihood of glaucomatous disc based on the similarity scores to the glaucoma and non-glaucoma models. Eighty-seven images, including 40 glaucomatous eyes, were included in this study. Only one eye from each patient was used. Using two images captured from different angles, a depth image was created by finding the local corresponding points. One of the characteristics of a glaucomatous disc can be not only that the cup is enlarged but it has an acute slope. On the other hand, a non-glaucomatous cup generally has a gentle slope. Therefore, our models were constructed by averaging the depth gradient images. In order to account for disc size, disc outline was automatically detected, and all images were registered by warping the disc outline to a circle with a predetermined diameter using thin plate splines. Similarity scores were determined by multiplying a test case with both models. With the sensitivity of 90%, the specificity was 83.0% using the CDR, whereas it was improved to 97.9% by the model-based method. The proposed method may be useful for differentiation of glaucomatous eyes.











9035-115, Session PSWed

## Segmentation of enhanced depth imaging optical coherence tomography images using wavelet based graph cut algorithm

Hossein Rabbani, Isfahan Univ. of Medical Sciences (Iran, Islamic Republic of)

Limited numbers of non-invasive imaging techniques are available for assessing the choroid, a structure that may be affected by a variety of retinal disorders or become primarily involved in conditions such as polypoidal choroidal vasculopathy and choroidal tumors. The introduction of enhanced depth imaging optical coherence tomography (EDI-OCT) has provided the advantage of in vivo cross-sectional imaging of the choroid, similar to the retina, with standard commercially available spectral domain OCT machines. A texture-based algorithm is introduced in this paper for fully automatic segmentation of choroidal images obtained from a 1060 nm optical coherence tomography (OCT) system. Dynamic programming is utilized to determine the location of the retinal pigment epithelium (RPE). The Bruch's membrane (BM) is the blood-retina barrier that separates the RPE cells of the retina from the choroid and can be segmented by searching for the pixels with the biggest gradient value below the RPE. A novel method is proposed to segment the choroidsclera interface (CSI), which employs the wavelet based features to construct a Gaussian mixture model (GMM). The model is then used in a s-t cut graph for segmentation of the choroidal boundary. The proposed algorithm is compared with the manual segmentation and the results show an unsigned error of 1.71±0.91 pixels for BM extraction and 7.65±3.96 pixels for choroid detection.

9035-116, Session PSWed

## From medical imaging to computer simulation of fractional flow reserve in four coronary artery trees

Simone Melchionna, Stefania Fortini, Massimo Bernaschi, Mauro Bisson, Consiglio Nazionale delle Ricerche (Italy); Nahyup Kang, Hyong-Euk Lee, Samsung Advanced Institute of Technology (Korea, Republic of)

We present the results of a computational study of coronary trees obtained from CT acquisition at resolution of  $0.35\,\mathrm{mm}\times0.35\,\mathrm{mm}\times0.4\,\mathrm{mm}$  and presenting significant stenotic plaques. We analyze the cardiovascular implications of stenotic plaques for a sizeable number of patients and show that the standard clinical criterion for surgical or percutaneous intervention, based on the Fractional Flow Reserve (FFR), is well reproduced by simulations in a range of inflow conditions that can be finely controlled. The relevance of the present study is related to the reproducibility of FFR data by simulating the coronary trees at global level via high performance simulation methods. In particular, the data show that controlling the flow Reynolds number is a viable procedure to account for FFR as heart-cycle time averages and maximal hyperemia, as measured in vivo. The reproducibility of the clinical data with simulation offers a systematic approach to measuring the functional implications of stenotic plaques.

9035-117, Session PSWed

## Learning-based automatic detection of severe coronary stenoses in CT angiographies

Imen Melki, GE Healthcare (France) and Univ. Paris-Est Marnela-Vallée (France); Cyril Cardon, Nicolas Gogin, GE Healthcare

(France); Hugues Talbot, Laurent Najman, Univ. Paris-Est Marnela-Vallée (France)

3D cardiac computed tomography angiography (CCTA) is becoming a standard routine for non-invasive heart diseases diagnosis thanks to fast and continuous progress. Due to its high negative predictive value, CCTA can be used to decide whether or not the patient should be considered for invasive angiography. However, an accurate assessment of cardiac lesions using this modality is still a time-consuming task and needs a high degree of clinical experience. Thus, providing automatic tool to assist clinicians during the diagnosis task is highly desirable. In this work, we propose a fully automatic approach for accurate severe cardiac stenosis detection. Our algorithm uses the Random Forest classification to detect stenotic areas. First, the classifier is trained on an 18 CT cardiac exam with CTA reference standard. Then, then classification result is used to detect severe stenoses (with a narrowing degree higher than 50%) in a 30 cardiac CT exam database. Features that best capture the different stenosis configurations are extracted along the vessel centerlines at different scales. To ensure the accuracy against the vessel direction and scale changes, we extract features inside "cylindrical" patterns with variable directions and radii. Thus, we avoid ROIs containing structures other than the vessel walls. The algorithm is evaluated using the Rotterdam Coronary Artery Stenoses Detection and Quantification Evaluation Framework. The evaluation is performed using reference standard quantifications obtained from quantitative coronary angiography (QCA) and consensus reading of CTA. The obtained results show that we can reliably detect severe stenosis with a sensitivity of

9035-118. Session PSWed

### Time-resolved volumetric MRI blood flow: a Doppler ultrasound perspective

Roy van Pelt, Technische Univ. Eindhoven (Netherlands); Javier Olivan-Bescos, Philips Healthcare (Netherlands); Eike Nagel M.D., King's College London (United Kingdom); Anna Vilanova, Technische Univ. Eindhoven (Netherlands)

Hemodynamic information is increasingly inspected to assess cardiovascular disease. Abnormal blood-flow patterns include high-speed jet flow and regurgitant flow. Such pathological blood-flow patterns are nowadays mostly inspected by means of color Doppler ultrasound imaging. To date, Doppler ultrasound has been the prevailing modality for blood-flow analysis, providing non-invasive and cost-effective blood-flow imaging. Since recent years, magnetic resonance imaging (MRI) is increasingly employed to measure time-resolved blood-flow data. Albeit more expensive, MRI enables volumetric velocity encoding, providing true vector-valued data with less noise. Domain experts in the field of ultrasound and MRI have extensive experience in the interpretation of blood-flow information, although they employ different analysis techniques.

We devise a visualization framework that extends on common Doppler ultrasound visualizations, exploiting the added value of MRI velocity data, and aiming for synergy between the domain experts. Our framework enables experts to explore the advantages and disadvantages of the current renditions of their imaging data. Furthermore, it facilitates the transition from conventional Doppler ultrasound images to present-day high-dimensional velocity fields. To this end, we present a virtual probe that enables direct exploration of MRI-acquired blood-flow velocity data using user-friendly interactions. Based on the probe, Doppler ultrasound inspired visualizations convey both in-plane and through-plane bloodflow velocities. In a compound view, these two-dimensional visualizations are linked to state-of-the-art three-dimensional blood-flow visualizations. In addition, we introduce a novel volume rendering of the blood-flow velocity data that emphasizes anomalous blood-flow patterns. The visualization framework was evaluated by the involved domain experts, and we present their feedback.











9035-120, Session PSWed

## Description of patellar movement by 3D parameters obtained from dynamic CT acquisition

Marina F. S. de Sá Rebelo, Ramon A. Moreno, Marco A. Gutierrez, Riccardo G. Gobbi, Luiz F. R. Avila, Gilberto L. Camanho, Marco K Demange, Univ. de São Paulo (Brazil); Jose R Pecora, Univ de São Paulo (Brazil)

The patella femoral joint is critical in the biomechanics of the knee. The patella femoral instability is one condition that generates pain, functional impairment and often requires surgery as part of orthopedic treatment. The analysis of the patella femoral dynamics has been performed by several medical image modalities. The clinical parameters assessed are mainly based on 2D measurements, such as the patellar tilt angle and the lateral shift among others. Besides, the acquisition protocols are mostly performed with the leg laid static at fixed angles. The use of helical multi-detector row CT scanner can allow the capture and display of the joint's movement performed actively by the patient. However, the orthopedic applications of this scanner have not yet been standardized or widespread. In this work we present a method to evaluate the biomechanics of the patella femoral joint during active contraction using multi slice CT images. This approach can greatly improve the analysis of patellar instability by displaying physiology during muscle contraction. The movement was evaluated by computing its 3D displacements and rotations from leg's original angle to a posterior one. The first processing step registered the images in both angles based on the femur's position. The transformation matrix of the patella from the images was then calculated, which provided the rotations and translations performed by the patella from its position in the first image to its position in the second image. Analyses of these parameters for all frames provided real 3D information about the patellar displacement.

9035-121. Session PSWed

### Wide association study of radiological features that predict future knee OA pain: data from the OAI

Jorge I. Galván-Tejada, José M. Celaya-Padilla, Antonio Martínez-Torteya Sr., Juan A. Rodriguez-Rojas, Victor M. Treviño-Alvarado Sr., José G. Tamez-Peña, Tecnológico de Monterrey (Mexico)

Knee pain is a common and one of the most important symptoms in Osteoarthritis (OA), due to its nature, pain is a debilitating feature of OA. The joint pain is a late manifestation of osteoarthritis, in early stages of the disease, changes in joint structures are shown, some of the most common, formation of bony osteophytes, cartilage degradation and joint space reduction, among others. Knowing that joint space reduction and osteophyte formation are clearly symptoms of radiological OA, the objective of this study is to achieve an association between the radiological features with a late OA symptom, the joint pain. Using public data from the Osteoarthritis initiative (OAI), a multivariate study was performed on Bioinformatics tools to determine a relationship of future pain with the radiological evidence of the disease. A case-control study was done using available data form participates in OAI databases. All case-control subjects present no evidence of pain, no medication for pain, and no symptomatic status, case subjects developed pain in some time point of the study. Radiological information was evaluated with a quantitative and a semi-quantitative score by OAI radiologist groups. The multivariate models obtained in the Bioinformatics study suggest that can exist an association between some of the early joint changes and the presence of future pain. To develop an image based biomarker in early stages can be a useful tool to improve the future quality of life in people with OA.

9035-122, Session PSWed

### vertebral degenerative disc disease severity evaluation using random forest classification

Hector E. Munoz, Jianhua Yao, National Institutes of Health (United States); Joseph E. Burns, Yasuyuki Pham, Univ. of California, Irvine (United States); James Stieger, Ronald M. Summers M.D., National Institutes of Health (United States)

Degenerative disc disease (DDD) develops in the spine as vertebral disks degenerate and bony growths form to restabilize the spine. The bony growths are hyperdense spurs localized to the cortical shell of the vertebral body. DDD naturally occurs in patients with increasing age. Bony growths may continue to worsen or stabilize as the spine reaches a new equilibrium point. We have previously created a CAD system that detects DDD and in this paper present a new system to determine the severity of DDD of individual vertebral levels. This will be useful to monitor the progress of developing DDD, as rapid growth may indicate that there is a greater stabilization problem that needs to be addressed. The existing DDD CAD system extracts the spine from CT images and segments the cortical shell of individual levels with a dual-surface model. The cortical shell is unwrapped, and is analyzed to detect the hyperdense regions of DDD. With the aid of a scoring atlas, two radiologists scored the severity of DDD of each disk space of 46 CT scans. A random forest classifier is trained using the radiologists' score as references and features generated from the detections to determine the severity of individual vertebral disk levels. The agreement of the two readers was evaluated and had a linearly-weighted Cohen's kappa of 0.30. The agreement between the computer severity score and radiologist's had Cohen's kappa of 0.28.

9035-123, Session PSWed

### Registration and color calibration for dermoscopy images in time-course analysis

Daiji Furusho, Hitoshi Iyatomi, Hosei Univ. (Japan)

Since melanomas grow and metastasize rapidly, the mutation in their appearance is much larger than that of nevi.

If the variation can be evaluated quantitatively in automated system, it is of substantial help. However, photographic conditions of skin tumor are in most cases not uniform during the follow-up. In this study, we proposed a fully automated image registration and color calibration method between dermoscopy images in time-course analysis. In the registration process, parameters for geometrical correction such as offset, differences of magnification and rotation were estimated by the scale-invariant feature transform (SIFT) and the bi-weight method and the registration was performed by the similarity transform. In the color calibration process, it is needed to calibrate colors of the dermoscopy image with the careful consideration for the actual variation of tumor color. Our process stands on the idea that an area with few appearance changes during the time course should originally have an almost same color. We found these stable areas as the basis regions and the cumulative brightness transfer function (CBTF) were calculated to perform calibration. Our registration algorithm achieved a precision of 95.4±3.2% and a recall of 92.4±6.5%, respectively where the manual alignment using the Exif data as a reliable reference did both indices of 91.6±5.1% and 95.7±5.9%, respectively. Our color calibration method largely reduced the color difference between time-course images  $\Delta E$  from 10.9±5.6 to 3.9±1.7. These results showed that proposed method was effective to compensate both geometrical and chronological changes between dermoscopy images in time-course analysis.











9035-124, Session PSWed

### Towards quantitative assessment of calciphylaxis

Thomas M. Deserno, István Sárándi, Daniel Haak, Stephan Jonas, Paula Specht, Vincent Brandenburg, RWTH Aachen (Germany)

Calciphylaxis is a rare disease that has devastating conditions associated with high morbidity and mortality. Calciphylaxis is characterized by systemic medial calcification of the arteries yielding necrotic skin ulcerations. In this paper, we aim at supporting the installation of multi-center registries for calciphylaxis, which includes a photographic documentation of skin necrosis. However, photographs acquired in different centers under different conditions using different equipment and photographers cannot be compared quantitatively. For normalization, we use a simple color pad that is placed into the field of view, segmented from the image, and its color fields are analyzed. In total, 24 colors are printed on that scale. A least squares approach is used to determine the linear color transform. The method is evaluated using in total 10 images of two sets of different captures of the same necrosis. The variability of quantitative measurements based on free hand photography is assessed regarding geometric and color distortions before and after our simple calibration procedure. Using automated image processing, the standard deviation of measurements is significantly reduced. The coefficients of variations yield 5-20% and 2-10% for geometry and color, respectively. Hence, quantitative assessment of calciphylaxis becomes practicable and will impact a better understanding of this rare but fatal disease.

9035-125, Session PSWed

### Towards robust identification and tracking of Nevi in sparse photographic time series

Jakob Vogel, Alexandru O. Duliu, Technische Univ. München (Germany); Yuji Oyamada, School of Fundamental Science and Engineering, Waseda Univ. (Japan); Jose Gardiazabal, Technische Univ. München (Germany); Tobias Lasser, Technische Univ. München (Germany) and Helmholtz Zentrum München GmbH (Germany); Mahzad Ziai, Rüdiger Hein, Nassir Navab, Technische Univ. München (Germany)

In dermatology, photographic imagery is acquired in large volumes in order to monitor the progress of diseases, especially melanocytic skin cancers. For this purpose, overview (macro) images are taken of the region of interest and used as a reference map to re-localize highly magnified images of individual lesions. The latter are then used for diagnosis. These pictures are acquired at irregular intervals under only partially constrained circumstances, where patient positions as well as camera positions are not reliable. In the presence of a large number of nevi, correct identification of the same nevus in a series of such images is thus a time consuming task with ample chances for error.

This paper introduces a method for largely automatic and simultaneous identification of nevi in different images, thus allowing the tracking of a single nevus over time, as well as pattern evaluation. The method uses a rotation-invariant feature descriptor that uses the local neighborhood of a nevus to describe it. The texture, size and shape of the nevus are not used to describe it, as these can change over time, especially in the case of a malignancy. We then use the Random Walks framework to compute the correspondences based on the probabilities derived from comparing the feature vectors. Evaluation is performed on synthetic and patient data at the university clinic.

9035-126, Session PSWed

## Evaluation of a computer-aided skin cancer diagnosis system for conventional digital photography with manual segmentation

Adam Huang, National Central Univ. (Taiwan); Wen-Yu Chang, I-Shou Univ. (Taiwan); Cheng-Han Hsieh, Hsin-Yi Liu, National Central Univ. (Taiwan); Gwo-Shing Chen, Kaohsiung Medical Univ. (Taiwan)

We evaluate a computer-aided diagnosis (CADx) system developed for both melanocytic and non-melanocytic skin lesions by using conventional digital photographs with lesion boundaries manually marked by a dermatologist. Clinical images of skin lesions taken by conventional digital cameras can capture useful information such as shape, color, and texture for diagnosing skin cancer. However, shape features are difficult to analyze automatically because skin surface reflections may change skin color and make segmentation a challenging task. In this study, two non-medical users manually mark the boundaries of a dataset of 769 (174 malignant, 595 benign) conventional photographs of melanocytic and non-melanocytic skin lesions. A state-of-the-art software system for segmenting color images, JSEG, is also tested on the same dataset. Their results are compared to a dermatologist's markings, which are used as the gold standard in this study. The human users' markings are relatively close to the gold standard and achieve an overlapping rate of 70.4% (+/- 15.3%, std) and 74.6% (+/- 14.4%, std). Compared to human users, JSEG only succeeds in segmenting 636 (82.7%) out of 769 lesions and achieves an overlapping rate of 72.2% (+/-20.7%) for these 636 lesions. The estimated area under the receiver operating characteristic curve (AUC) of the CADx by using lesion boundary markings of users 1, 2, and JSEG are 0.915, 0.940, and 0.857 respectively. Our preliminary results indicate that manual segmentation can be repeated relatively consistent compared to automatic segmentation.

9035-127. Session PSWed

### Computer-aided diagnosis of diabetic peripheral neuropathy

Viktor Chekh, The Univ. of New Mexico (United States); Peter Soliz, Elizabeth McGrew, Simon Barriga, VisionQuest Biomedical, LLC (United States); Mark R. Burge, Shuang Luan, The Univ. of New Mexico (United States)

Diabetic peripheral neuropathy (DPN) refers to the nerve damage that can occur in diabetic patients. It most often affects the extremities, such as the feet, and can lead to peripheral vascular disease, deformity, infection, ulceration, and even amputation. The key to managing diabetic foot is prevention and early detection. Unfortunately, current existing diagnostic techniques are mostly based on patient sensations and exhibit significant inter- and intra-observer differences. We have developed a computer aided diagnostic (CAD) system for diabetic peripheral neuropathy. The thermal response of the feet of diabetic patients following cold stimulus is captured using an infrared camera. The plantar foot in the images from a thermal video are segmented and registered for tracking points or specific regions. The temperature recovery of each point on the plantar foot is extracted using our bio-thermal model and analyzed. The regions that exhibit abnormal ability to recover are automatically identified to aid the physicians to recognize problematic areas. The key to our CAD system is the segmentation of infrared video. The main challenges for segmenting infrared video compared to normal digital video are (1) as the foot warms up, it also warms up the surrounding, creating an ever changing contrast; and (2) there may be significant motion during imaging. To overcome this, a hybrid segmentation algorithm was developed based on a number of techniques such as continuous maxflow, model based segmentation, shape preservation, convex hull, and temperature normalization. Verifications of the automatic segmentation and registration using manual segmentation and markers show good agreement.











9035-128, Session PSWed

#### An automatic early stage alveolar-boneresorption evaluation method on digital dental panoramic radiographs

Min Zhang, Gifu Univ. School of Medicine (Japan); Akitoshi Katsumata D.D.S., Asahi Univ. (Japan); Chisako Muramatsu, Takeshi Hara, Gifu Univ. School of Medicine (Japan); Hiroshi Fujita, Gifu Univ. School of Medicine (Japan)

Automatically evaluating alveolar-bone resportion is very important. The purpose of this study was to propose a novel system for automatic alveolar-bone-resorption evaluation for digital panoramic radiograph. An alveolar bone is a specialized type of bone which is designed to accommodate teeth. Damage to the alveolar bone can have serious consequences, including the risk of loss of teeth and septicemia if the damage is caused by an infection. The proposed system enables visualization and quantification of resorption of alveolar bone surrounding and between the roots of teeth. It has the following procedures: (1) pre-processing for atest image; (2) detection of teeth root apex with Gabor filter and curving fitting for the root apex line; (3) detection of features related with alveolar bone by using image phase congruency map and curve fitting for the alveolar line; (4) detection of occlusion line with selected Gabor filter; (5) the quantitative alveolar-bone-resorption degree evaluation. The initial trial on 29 test cases that the quantitative evaluation results of alveolar bone resportion is highly correlated to the clinic diagnositic results and may has potential clinical practicability.

9035-129, Session PSWed

## A method for automatic liver segmentation from multi-phase contrast-enhanced CT images

Rong Yuan, Ming Luo, Huazhong Univ. of Science and Technology (China); Luyao Wang, Wuhan National Lab. for Optoelectronics (China) and Huazhong Univ. of Science and Technology (China); Shaofa Wang, Tongji Medical College (China); Qingguo Xie, Huazhong Univ. of Science and Technology (China) and Wuhan National Lab. for Optoelectronics (China)

Liver segmentation is a basic and fundamental function in systems of computer aided liver surgery, and it is crucial for volume calculation, operation designing and risk evaluation. Traditionally, liver in computed tomography (CT) images is segmented manually, which is timeconsuming because of the huge amount of images and the complicated contours of liver. In this paper, an automatic method was proposed to segment the liver from multi-phase contrast-enhanced CT images. An anisotropic filter is applied to decrease the image noise while maintaining clear edges. Based on the fact that liver is the largest internal organ of the body, the range of the gray values of liver parenchyma is estimated by plotting the 3D-histogram of all images from one phase. Then, four series of binary images are produced for finding the certain pixels of liver as the initial segmentation, an under-segmented result. Lastly, we use the compensating algorithm to the details like edges, cusps and holes to get an accurate result. Fifteen sets of clinical abdomens CT images of five patients were segmented by our algorithm. The running-time is about 30 seconds for a set of images from single-phase which includes more than 200 slices. The results were evaluated by an experienced surgeon and were considered acceptable. In the following work, the qualitative and quantitative evaluation of our algorithm will be performed by comparing with manual segmentation and other method results. More clinical cases will be taken into account to prove the robustness as well.

9035-130, Session PSWed

### Classification of weak specular reflections in laparoscopic images

Bidisha Chakraborty, J. Marek Marcinczak, Rolf-Rainer Grigat, Technische Univ. Hamburg-Harburg (Germany)

Specular reflections are present in the majority of laparoscopic videos. If not considered they will affect all further image analysis and registration algorithms. In most state-of-the-art algorithms, segmentation of specular reflections is done by intensity thresholding. However, the strong reflections are detected but the weak reflections are missed. The proposed method automatically detects the contour boundaries belonging to specular reflections by an SVM classifier. The algorithm improves the detection of small weak reflections by training on contours of specular reflections with a combination of intensity and shape descriptors. Segmentation is done on contours by intensity thresholding and morphological operations. A comparative analysis of the proposed method with existing methods is presented. The ground truth for the test images are manually labeled for evaluation. The database contains 702 specular reflections present in 132 images and they are taken from 31 patients. This method improves the sensitivity in detection of weak reflections by 15% compared to the best known method and 7% for all reflections.

9035-131, Session PSWed

### Active shape models incorporating isolated landmarks for medical image annotation

Tobias Norajitra, Hans-Peter Meinzer, Bram Stieltjes, Klaus H. Maier-Hein, Deutsches Krebsforschungszentrum (Germany)

Apart from their robustness in anatomic surface segmentation, purely surface based 3D Active Shape Models lack the ability to automatically detect and annotate non-surface key points of interest. However, annotation of anatomic landmarks is desirable, as it yields additional anatomic and functional information, e.g. in computer-aided diagnosis tasks. Moreover, landmark detection might help to further improve accuracy during ASM segmentation. We present an extension of surface-based 3D Active Shape Models incorporating isolated nonsurface landmarks. Positions of isolated and surface landmarks are modeled conjoint within a point distribution model. Isolated landmark appearance is described by a set of Haarlike Features, supporting local landmark detection on the PDM estimates using a kNN-Classifier. Landmark detection was evaluated in a leave-one-out cross validation on a reference dataset comprising 45 CT volumes of the human liver after shape space projection. Our experiments have shown an improvement in detection accuracy compared to the position estimates delivered by the PDM. Our results encourage further research with regard to the combination of shape priors and machine learning for landmark detection within the Active Shape Model Framework.

9035-132, Session PSWed

#### Texture feature based liver lesion classification

Yeela Doron, Nitzan Mayer-Wolf, Idit Diamant, Tel Aviv Univ. (Israel); Hayit Greenspan, Tel Aviv Univ. (Israel) and ICSI (United States)

Liver lesion classification is a difficult clinical task. Computerized analysis can support clinical workflow by enabling more objective and reproducible evaluation, and may reduce the number of required tissue biopsies. In this paper, we evaluate the contribution of several types of texture features for the optimization of a computer-aided diagnostic (CAD) system which automatically classifies liver lesions from CT images.











Based on the assumption that liver lesions of various classes differ in their texture features, different texture features were examined as lesion descriptors. Although texture features are often used for this task, there is currently a lack of detailed research focusing on the comparison across different texture features, or their combinations, on a given liver lesions dataset. In the current work we investigated the performance of GLCM, LBP and Gabor texture features, separately and combined. Regions of interest (ROI's) taken from CT images of hepatic Cysts, Metastases, Hemangiomas and healthy tissues were used as an input to the proposed system (112 ROI's in total). The system consists of a feature extraction module and a classification module. The feature extraction module computes GLCM, LBP and Gabor texture features obtained from the ROI's, as well as their grey-level intensity values. For the classification module, SVM and KNN classifiers were examined. Best results were obtained with Gabor filtering and SVM classification (91% accuracy). Combination of the Gabor with LBP and Intensity features improved the results, to a final 97% accuracy.

9035-133, Session PSWed

### Automatic seed selection for segmentation of liver cirrhosis in laparoscopic sequences

Rahul Sinha, J. Marek Marcinczak, Rolf-Rainer Grigat, Technische Univ. Hamburg-Harburg (Germany)

For computer aided diagnosis based on laparoscopic sequences, image segmentation is one of the basic steps which define the success of all further processing. However, many image segmentation algorithms require prior knowledge which is given by interaction with the clinician. We propose an automatic seed selection algorithm for segmentation of liver cirrhosis in laparoscopic sequences which assigns each pixel a probability of being cirrhotic liver tissue or background tissue.

Our approach is based on a trained classifier using SIFT features and PCA. Due to the unique illumination conditions in laparoscopic sequences of the liver, a very low dimensional feature space can be used for classification via logistic regression.

The methodology is evaluated on 718 cirrhotic liver and background patches that are taken from laparoscopic sequences of 7 patients. Using a linear classifier we achieve a precision of 91% in a leave-one-patient-out cross-validation. Furthermore, we demonstrate that with logistic probability estimates, seeds with high certainty of being cirrhotic liver tissue can be obtained. For example, our precision of liver seeds increases to 99% if only seeds with more than 95% probability of being liver are used. Finally, these automatically selected seeds can be used as priors in Graph Cuts which is demonstrated in this paper.

9035-134, Session PSWed

### Infective endocarditis detection through SPECT/CT images digital processing

Albino Moreno-Gómez, Raquel Valdes-Cristerna, Luis Jiménez-Ángeles, Univ. Autónoma Metropolitana-Iztapalapa (Mexico); Enrique Vallejo, Univ. Nacional Autónoma de México (Mexico); Salvador Hernández Sandoval, Gabriel Soto, Instituto Nacional de Cardiología - Ignacio Chávez (Mexico)

Infective endocarditis (IE) is a pathology manifested as an infection of the membrane that covers the heart cavities or heart valves interior. For the medical imaging of infective processes the radiopharmaceutical UBI-29-41 Tc-99m has proved to have, a high specificity in the infected regions and a quick body elimination. The authors proposed a new semiautomatic tool for IE diagnosis based on the digital processing of SPECT/CT images with the use of a 99mTc UBI 29 41 radiopharmaceutical based on the segmentation of the CT images.

Were processed the SPECT/CT studies of 16 patients with IE clinical diagnosis that were admitted at the Instituto Nacional de Cardiología "Ignacio Chávez" and the studies for 5 control subjects. The SPECT images were preprocessed with a wavelet shrinkage filtering algorithm. The CT images were segmented with a weighted mean-shift filtering. For the images analysis, it was used a CT images volume segmented in the sections of 5 slices taking as reference the heart valves and recovering only the heart and right lung regions. When calculating the histogram of each ROI, it is used 1% of the higher intensity pixels of the heart and the first quartile pixels on lung region. With the calculated averages of both ROI, the heart/lung rate was figured. There were no statistically significant differences between the heart/lung rates values of a group of patients diagnosed with IE (2.62+-0.47) and a group of control subjects (2.84+-0.68).

9035-136, Session PSWed

## A preliminary study for fully automated quantification of psoriasis severity using image mapping

Kazuhiro Mukai, Hitoshi Iyatomi, Hosei Univ. (Japan)

Psoriasis is a common chronic skin disease and detracts patients' QoL seriously. Since there is no known cure so far, controlling appropriate disease condition is necessary and therefore quantification of its severity is important. In clinical, PASI (psoriasis area and severity index) is commonly used for abovementioned purpose, however it is often subjective and troublesome. A fully automatic computer-assisted area and severity index (CASI) was proposed to make an objective quantification of skin disease. It investigates size and density of erythema based on digital image analysis, however it does not consider various inadequate effects caused by different geometrical conditions under clinical follow-up (i.e. variability in direction and distance between camera and patient). In this study, we proposed an image alignment method for soft skin images and investigated to quantify severity of psoriasis under follow-up combined with the idea of CASI. The proposed method aligns images with finding the "same" points among images with SIFT (Scale-Invariant-Feature-Transform) and Affine transform in ROI with respect to pixel. We used clinical images from 7 patients with psoriasis lesions on their trunk under clinical follow-up were used. In each series, we align images for their first image with the proposed image alignment method. Our proposed method aligned images appropriately on visual assessment and confirmed that psoriasis areas were properly extracted using the approach of CASI. Although we could not compare PASI and CASI directly due to their different ROI, we confirmed that there was a strong correlation between those scores with our image alignment











Tuesday - Thursday 18-20 February 2014

Part of Proceedings of SPIE Vol. 9036 Medical Imaging 2014: Image-Guided Procedures, Robotic Interventions, and Modeling

9036-1, Session 1

### Innovative approach for in-vivo ablation validation on multimodal images

Osama Shahin, Univ. zu Lübeck (Germany); Georgios Karagkounis, Daniel Carnegie, Johns Hopkins Univ. (United States); Alexander Schlaefer, Univ. zu Lübeck (Germany); Emad M. Boctor, Johns Hopkins Outpatient Ctr. (United States)

Radio frequency ablation (RFA) is an important therapeutic procedure for small hepatic tumors. To make sure that the target tumor is effectively treated, RFA monitoring is essential. While several imaging modalities can observe the ablation procedure, it is not clear how ablated lesions on the images correspond to actual necroses. This uncertainty contributes to the high local recurrence rates (up to 55%) after radio frequency ablative therapy. This study investigates a novel approach to correlate images of ablated lesions with actual necroses. We mapped both intraoperative images of the lesion and a slice through the actual necrosis in a common reference frame. An electromagnetic tracking system was used to accurately macth lesion slices from different imaging modalities. To minimize the liver deformation effect, the tracking reference frame was defined inside the tissue by anchoring an electromagnetic sensor adjacent to the lesion. A validation test was performed using a phantom and proved that the end-to-end accuracy of the approach was within 2 mm. In an in-vivo experiment, intra-operative magnetic resonance imaging (MRI) and ultrasound (US) ablation images were correlated to gross and histopathology. The results indicate that the proposed method can accurately correlate in-vivo ablations on different modalities. Ultimately, this will improve the interpretation of the ablation monitoring and reduce the recurrence rates associated with RFA.

9036-2, Session 1

## Model-based formalization of medical knowledge for context-aware assistance in laparoscopic surgery

Darko Katic, Karlsruher Institut für Technologie (Germany); Anna-Laura Wekerle, UniversitätsKlinikum Heidelberg (Germany); Fabian Gärtner, Karlsruher Institut für Technologie (Germany); Hannes Kenngott M.D., Ruprecht-Karls-Univ. Heidelberg (Germany); Beat Peter Müller-Stich M.D., Heidelberg School of Medicine (Germany); Rüdiger Dillmann, Stefanie Speidel, Karlsruher Institut für Technologie (Germany)

The increase of technological complexity in surgery has created a need for novel man-machine interaction techniques. Specifically, context-aware systems which automatically adapt themselves to the current circumstances in the OR have great potential in this regard. To create such systems, models of surgical procedures are vital, as they allow analyzing the current situation and assessing the context. For this purpose, we have developed a Surgical Process Model based on Description Logics. It incorporates general medical background knowledge as well as intraoperatively observed situational knowledge. The representation consists of three parts: the Background Knowledge Model, the Preoperative Process Model and the Integrated Intraoperative Process Model. All models depend on each other and create a concise view on the surgery. As a proof of concept, we applied the system to a specific intervention, the laparoscopic distal pancreatectomy.

9036-3, Session 1

#### Software-assisted post-interventional assessment of radiofrequency ablation

Christian Rieder, Benjamin Geisler M.D., Fraunhofer MEVIS (Germany); Philipp Bruners M.D., RWTH Aachen (Germany); Peter Isfort M.D., Hong-Sik Na, RWTH Aachen (Germany); Andreas H. Mahnken M.D., Univ. Hospital Aachen (Germany); Horst K. Hahn, Fraunhofer MEVIS (Germany)

Radiofrequency ablation (RFA) is becoming a standard procedure for minimally invasive tumor treatment in clinical practice. Due to it's common technical procedure, low complication rate, and low cost, RFA has become an alternative to surgical resection. To evaluate the therapy success of RFA, thorough follow-up imaging is essential. Conventionally, shape, size, and position of tumor and coagulation are visually compared in a side-by-side manner using pre- and post-interventional images. To objectify the verification of the treatment success, a novel software system allowing for fast and accurate comparison of tumor and coagulation is proposed.

In this work, the clinical value of the proposed assessment software is evaluated. In a retrospective clinical study, 39 cases of hepatic tumor ablation were evaluated using the prototype software and conventional image comparison by four radiologists with different levels of experience. Cases were randomized and evaluated in two sessions to avoid any recall-bias. Self-confidence of correct diagnosis (local recurrence vs. no local recurrence) on a six-point scale was given for each case by the radiologists. Sensitivity, Specificity, positive and negative predictive values as well as receiver operating curves are calculated for both methods. It is shown that the software-assisted method allows physicians to correctly identify local tumor recurrence with a higher percentage than the conventional method (sensitivity:~0.6 vs.~0.35), whereas the percentage of correctly identified successful ablations is slightly reduced (specificity:~0.83 vs.~0.89)

9036-4, Session 1

### Anatomical parameterization for volumetric meshing of the liver

Sergio Vera, Alma IT Systems (Spain); Miguel Angel González Ballester, Alma IT Systems (Spain) and ICREA - Catalan Institution for Research and Advanced Studies (Spain) and Univ. Pompeu Fabra (Spain); Debora Gil, Univ. Autònoma de Barcelona (Spain)

A coordinate system parameterizing the interior of organs is a powerful tool for a systematic localization of injured tissue. If the same coordinate values are assigned to specific anatomical sites, parameterizations ensure integration of data across different medical image modalities. Harmonic mappings have been used to produce parametric meshes over the surface of anatomical shapes, given their flexibility to set values at specific locations through boundary conditions. However, most of the existing implementations in medical imaging restrict to either anatomical surfaces, or the depth coordinate with boundary conditions is given at sites of limited geometric diversity. In this paper we present a method for anatomical volumetric parameterization that extends current harmonic parameterizations to the interior anatomy using information provided by the volume medial surface.

We have applied the methodology to define a common reference system for the liver shape and functional anatomy. This reference system sets a solid base for creating anatomical models of the patient's liver, and











allows comparing livers from several patients in a common framework of reference.

9036-5, Session 1

## Preliminary clinical trial in percutaneous nephrolithotomy using a real-time navigation system for percutaneous kidney access

Pedro L. Rodrigues, António H. J. Moreira, Univ. do Minho (Portugal); Nuno F. Rodrigues, Univ. do Minho (Portugal) and Instituto Politécnico do Cávado e do Ave (Portugal); Antonio C. M. Pinho, Jaime C. Fonseca, Estevão Lima, Univ. do Minho (Portugal); João L. Vilaça, Univ. do Minho (Portugal) and Instituto Politécnico do Cávado e do Ave (Portugal)

Background: Precise needle puncture of renal calyces is a challenging and essential step for successful percutaneous nephrolithotomy. This work tests and evaluates, through a clinical trial, a real-time navigation system to plan and guide percutaneous kidney puncture.

Methods: A novel system, entitled i3DPuncture, was developed to aid surgeons in establishing the desired puncture site and the best virtual puncture trajectory, by gathering and processing data from a tracked needle with optical passive markers. In order to navigate and superimpose the needle to a preoperative volume, the patient, image data and tracker system were previously registered intraoperatively using seven points that were strategically chosen based on rigid bone structures and nearby kidney area. In addition, relevant anatomical structures for surgical navigation were automatically segmented using a multi-organ segmentation algorithm that clusters volumes based on statistical properties and minimum description length criterion. For each cluster, a rendering transfer function enhanced the visualization of different organs and surrounding tissues.

Results: One puncture attempt was sufficient to achieve a successful kidney puncture. The puncture took 265 seconds, and 32 seconds were necessary to plan the puncture trajectory. The virtual puncture path was followed correctively until the needle tip reached the desired kidney calveed.

Conclusions: This new solution provided spatial information regarding the needle inside the body and the possibility to visualize surrounding organs. It may offer a promising and innovative solution for percutaneous punctures.

9036-6, Session 2

### Construction of a multimodal CT-video chest model

Patrick Byrnes, William E. Higgins, The Pennsylvania State Univ. (United States)

Bronchoscopy enables a number of minimally invasive chest procedures for diseases such as lung cancer and asthma. For example, using the bronchoscope's continuous video stream as a guide, a physician can navigate through the lung airways to examine general airway health, collect tissue samples, or administer a disease treatment. In addition, physicians can now use new image-guided intervention (IGI) systems, which draw upon both three-dimensional (3D) multi-detector computed tomography (MDCT) chest scans and bronchoscopic video, to assist with bronchoscope navigation. Unfortunately, little use is made of the acquired video stream, a potentially invaluable source of information. In addition, no effort has been made to link the bronchoscopic video stream to the detailed anatomical information given by a patient's 3D MDCT chest scan. We propose a method for constructing a multimodal CT-video model of the chest. After automatically computing a patient's 3D MDCT-based airway-tree model, the method next parses the available video data to generate a positional linkage between a sparse set of

key video frames and airway path locations. Next, a fusion/mapping of the video's color mucosal information and MDCT-based endoluminal surfaces is performed. This results in the final multimodal CT-video chest model. The data structure constituting the model provides a history of those airway locations visited during bronchoscopy. It also provides for quick visual access to relevant sections of the airway wall by condensing large portions of endoscopic video into representative frames containing important structural and textural information. When examined with a set of interactive visualization tools, the resulting fused data structure provides a rich multimodal data source. The model has potential for improving the efficiency of diagnostic bronchoscopies that require a detailed examination of the airway tree. In addition, for patients requiring follow-up bronchoscopies, the model could help directly compare the impact of treatment at specific endoluminal locations. We demonstrate the potential of the multimodal model with both phantom and human

9036-7, Session 2

### Visual tracking of da Vinci instruments for laparoscopic surgery

Stefanie Speidel, Enrico Kuhn, Karlsruher Institut für Technologie (Germany); Sebastian Bodenstedt, Karlsruhe Institute of Technology (Germany); Sebastian Röhl, Karlsruher Institut für Technologie (Germany); Hannes Kenngott M.D., Ruprecht-Karls-Univ. Heidelberg (Germany); Beat Peter Müller-Stich M.D., Heidelberg School of Medicine (Germany); Rüdiger Dillmann, Karlsruher Institut für Technologie (Germany)

Intraoperative tracking of laparoscopic instruments is a prerequisite to realize further assistance functions. Since endoscopic images are always available, this sensor input can be used to localize the instruments without special devices or robot kinematics. In this paper, we present an image-based markerless 3D tracking of different da Vinci instruments in near real-time without an explicit model. The method is based on different visual cues to segment the instrument tip, calculates a tip point and uses a multiple object particle filter for tracking. The accuracy and robustness is evaluated with in vivo data. The method shows promising results for tracking of the highly articulated and dynamic instruments without an explicit model.

9036-8, Session 2

## Computer-assisted polyp matching between optical colonoscopy and CT colonography: a phantom study

Holger R. Roth, Univ. College London (United Kingdom); Thomas E Hampshire, Centre for Medical Image Computing, University College London (United Kingdom); Emma Helbren, Centre for Medical Imaging, University College London (United Kingdom); Mingxing Hu, Centre for Medical Image Computing, University College London (United Kingdom); Roser Vega, Gastrointestinal Services, University College Hospital (United Kingdom); Steve Halligan, Centre for Medical Imaging, University College London (United Kingdom); David J Hawkes, Centre for Medical Image Computing, University College London (United Kingdom)

Potentially precancerous polyps detected with CT colonography (CTC) need to be removed subsequently using an optical colonoscope (OC). Due to large colonic deformations induced by the colonoscope, even very experienced colonoscopists find it difficult to pinpoint the exact location of the colonoscope tip in relation to polyps reported on CTC. This can cause unduly prolonged OC examinations that are stressful for the patient, colonoscopist and supporting staff.











We developed a method based on monocular 3D reconstruction from OC images that automatically matches polyps observed in OC with polyps reported on prior CTC. A matching cost is computed using rigid point-based registration between surface point clouds extracted from both modalities. A 3D printed and painted phantom of a 25 cm long transverse colon segment was used to validate the method on two medium sized polyps. Results indicate that the matching cost is smaller at the correct corresponding polyp between OC and CTC: the value is 3.9 times higher at the in-correct polyp, comparing the correct match between polyps to the incorrect match. Furthermore, we compare to matching the reconstructed polyp from OC with other colonic endoluminal surface structures such as haustral folds and show that there is a minimum at the correct polyp from CTC.

Automated matching between polyps observed in OC and prior CTC would facilitate the biopsy or removal of true-positive pathology or exclusion of false-positive CTC findings, and will reduce colonoscopy false-negative (missed) polyps. Ultimately such a method might reduce healthcare costs, patient inconvenience and discomfort.

9036-9, Session 2

## Adaptive fiducial-free registration using multiple point selection for real-time electromagnetically navigated endoscopy

Xiongbiao Luo, Kensaku Mori, Nagoya Univ. (Japan)

This paper proposes an adaptive fiducial-free registration method that uses a multiple point selection strategy based on sensor orientation and endoscope radius information. To develop a flexible endoscopy navigation system, since we use an electromagnetic tracker with positional sensors to estimate bronchoscope movements, we must synchronize such tracker and pre-operative image coordinate systems using either marker-based or fiducial-free registration methods. Fiducialfree methods assume that bronchoscopes are operated along bronchial centerlines. Unfortunately, such an assumption is easily violated during interventions. To address such a tough assumption, we utilize an adaptive strategy that generates multiple points in terms of sensor measurements and bronchoscope radius information. From these generated points, we adaptively choose the optimal point, which is the closest to its assigned bronchial centerline, to perform registration. The experimental results from phantom validation demonstrate that our proposed adaptive strategy significantly improved the fiducial-free registration accuracy from at least 5.4 to 2.2 mm compared to current available methods.

9036-10, Session 2

## Physiological factors of small intestine in experimentation of virtual video capsule endoscope

Liang Mi, Guanqun Bao, Kaveh Pahlavan, Worcester Polytechnic Institute (United States)

Wireless capsule endoscope plays an increasingly important role in assisting clinical diagnosis of disease and abnormality inside human small intestine. Based on endoscopic images, researchers have attempted to use motion tracking methods to explore its further application of localization of the wireless capsule in order to indicate the location of the abnormality. Usually, validity of their methods was tested using a virtual testbed because carrying out experiments on the human body is extremely costly and restricted by law. However, when setting up the testbeds, most researchers assumed the small intestine to be a straight tube with a constant radius, which was far from the reality. In our previous work, a virtual environment that could simulate intestinal contraction was built and validated with a velocity estimation algorithm. In this paper, the influence of intestinal contraction on motion tracking algorithm is further studied. According to clinical data and geometric

models, the relation between the degree of intestinal contraction and the size of black hole in the center of the endoscopic images is explored. Based on the analysis, a motion tracking algorithm that was designed in our previous work is improved by making it self-adaptable to intestinal contraction. Moreover, the relation between the shape and position of the black hole and the curvature of the small intestine is also studied and the potential of this relation to help predict the direction of motion of the wireless capsule is explored. Experiments for validation of our methods are being conducted using a virtual testbed.

9036-11, Session 2

#### Motion magnification for endoscopic surgery

A. Jonathan McLeod, Terry M. Peters, Robarts Research Institute (Canada)

Endoscopic and laparoscopic surgeries are used for many minimally invasive procedures but limit the visual and haptic feedback available to the surgeon. This can make vessel sparing procedures particularly challenging to perform. Previous approaches have focused on hardware intensive intraoperative imaging or augmented reality systems that are difficult to integrate into the operating room. This paper presents a simple approach where motion is visually enhanced in the endoscopic video to reveal pulsating arteries. This is accomplished by amplifying subtle, periodic changes in intensity coinciding with the patient's pulse. This method is then applied to two procedures to illustrate its potential. The first, endoscopic third ventriculostomy, is a neurosurgical procedure where the floor of the third ventricle must be fenestrated without injuring the basilar artery. The second, nerve-sparing robotic prostatectomy, involves removing the prostate while limiting damage to the neurovascular bundles. In both procedures, motion magnification can enhance subtle pulsation of the respective arteries to aid in identifying and avoiding these vessels.

9036-12. Session 3

## Reconstruction and feature selection for desorption electrospray ionization mass spectroscopy imagery

Yi Gao, Liangjia Zhu, The Univ. of Alabama at Birmingham (United States); Isaiah Norton, Brigham and Women's Hospital (United States); Nathalie Y. R. Agar, Harvard Medical School (United States); Allen Tannenbaum, The Univ. of Alabama at Birmingham (United States)

Desorption electrospray ionization mass spectrometry (DESI-MS) provides a highly sensitive imaging technique for differentiating normal and cancerous tissue at the molecular level. This can be very useful, especially under intra-operative conditions where the surgeon has to make crucial decision about the tumor boundary. In such situations, the time it takes for imaging and data analysis becomes a critical factor. Therefore, in this work we utilize compressive sensing to perform the sparse sampling of the tissue, which halves the scanning time. Furthermore, sparse feature selection is performed, which not only reduces the dimension of data from about \$10^4\$ to less than 50, and thus significantly shortens the analysis time. This procedure also identifies biochemically important molecules for further pathological analysis. The methods are validated on brain and breast tumor data sets.











9036-13, Session 3

## Automatic standard plane adjustment on mobile C-Arm CT images of the calcaneus using atlas-based feature registration

Michael Brehler, German Cancer Research Center (DKFZ) (Germany); Joseph Görres, Deutsches Krebsforschungszentrum (Germany); Ivo Wolf, Hochschule Mannheim (Germany); Jochen Franke M.D., Jan von Recum, Paul A. Gruetzner M.D., BG Unfallklinik (Germany); Hans-Peter Meinzer, Diana Wald, Deutsches Krebsforschungszentrum (Germany)

The workflow for treating calcaneal fractures is an osteosynthesis followed by intraoperative imaging to validate the repositioning of bone fragments. C-Arm CT offers surgeons the possibility to directly verify the alignment of the fracture parts in 3D. Although the device provides more mobility, there is no information about the device-to-patient orientation for standard plane reconstruction. Hence, physicians have to manually align the planes in a position that intersects with the articular surfaces. This can be a time-consuming step and imprecise adjustments lead to diagnostic errors. We address this issue by introducing novel semi-/ automatic methods for adjustment of the standard planes on mobile C-Arm CT images. With our semi-automatic method, physicians can quickly adjust the planes by setting six points based on anatomical landmarks. The automatic method reconstructs the standard planes in two steps, first SURF keypoints (2D and newly introduced pseudo-3D) are generated for each image slice; secondly, these features are registered to an atlas point set and the parameters of the image planes are transformed accordingly. The accuracy of our method was evaluated on 51 C-Arm CT images from clinical routine with manually adjusted standard planes by three physicians of different expertise. The average time of the experts (46s) deviated from the intermediate user (55s) by 9 seconds. By applying 2D SURF keypoints 88% of the articular surfaces were intersected correctly by the transformed standard planes with a calculation time of 10 seconds. The pseudo-3D features performed even better with 91% and 8 seconds.

9036-14, Session 3

#### Mechanically assisted 3D ultrasound for pre-operative assessment and guiding percutaneous treatment of focal liver tumors

Hamid Sadeghi Neshat, Robarts Research Institute (Canada); Jeffery S. Bax, Ctr. for Imaging Technology Commercialization (Canada); Kevin Barker, Lori Gardi, Robarts Research Institute (Canada); Nirmal Kakani, The Univ. of Western Ontario (Canada); Aaron Fenster, Robarts Research Institute (Canada)

Image-guided percutaneous ablation is the standard treatment for focal liver tumors deemed inoperable and used to maintain eligibility for patients on transplant waitlists. Radiofrequency (RFA), microwave (MWA) and cryo-ablation technologies are all delivered via a needleshaped probe inserted directly into the tumor. Planning is mostly based on contrast CT/MRI. While intra-procedural CT (iCT) is commonly used to confirm the intended probe placement, 2D ultrasound (US) remains the main imaging modality for needle guidance, and in some centers is the only modality used. Correlation of the intraoperative 2D US with iCT or pre-operative imaging is essential for accurate needle placement, however, correspondence can be challenging given the limited field-ofview (FOV) in 2D US. We have developed a passive tracking arm with a motorized scan-head and software tools to improve guiding capabilities of conventional US by large FOV 3D US scans that can be overlaid and compared to planning and intra-procedural CT. The tracker arm is used to scan the whole liver with a high geometrical accuracy that facilitates multi-modality landmark based image registration. Software tools are provided to assist with the segmentation of the ablation probes and

tumors, find the 2D US plane that best shows the probe(s) from a 3D US image and the corresponding image from planning CT scans. Results from laboratory testing and a phase 1 clinical trial for planning and guiding RFA and MWA procedures will be presented. Early clinical results show comparable and in some cases additional information to CT/iCT.

9036-15, Session 3

### Optoacoustic sensing for target detection inside cylindrical catheters

Behnoosh Tavakoli, Xiaoyu Guo, Russell H. Taylor, Jin U. Kang, Johns Hopkins Univ. (United States); Emad M. Boctor, Johns Hopkins Outpatient Ctr. (United States)

Optoacoustic sensing is a hybrid technique that combines the advantages of high sensing depth of ultrasound with contrast of optical absorption. In this study a miniature optoacoustic probe that can characterize the target properties located at the distal end of a catheter is investigated. The probe includes an optical fiber to illuminate the target with the pulsed laser light and a hydrophone to detect the generated optoacoustic signal. The probe is designed for the forward-sensing and therefore the acoustic signal propagates along the tube before being detected. Due to the circular geometry, the waves inside the tube are highly complex. A three dimensional numerical simulation is performed to model the optoacoustic wave generation and propagation inside the water filled cylindrical tubes. The effect of the boundary condition, tube diameter and target size on the detected signal is systematically evaluated. A prototype of the probe is made and tested for detecting an absorbing target inside a 2mm diameter tube submerged in water. The preliminary experimental results corresponding to the simulation is acquired. Although many different medical applications for this miniature probe may exist, our main focus is on detecting the occlusion inside the ventricular shunts. These catheters are used to divert the excess cerebrospinal fluid to the absorption site and regulate inter cranial pressure of hydrocephalous patients. Unfortunately the malfunction rate of these catheters due to blockage is very high. This sensing tool could locate the occluding tissue non-invasively and can potentially characterize the occlusion composites by scanning at different wavelengths of the light.

9036-16, Session 3

## Polarization-sensitive multispectral tissue characterization for optimizing intestinal anastomosis

Jaepyeong Cha, Johns Hopkins Univ. (United States); Brian Triana, Children's National Medical Ctr. (United States) and Princeton Univ. (United States); Azad Shademan, Axel Krieger, Peter C. W. Kim, Children's National Medical Ctr. (United States); Jin U. Kang, Johns Hopkins Univ. (United States)

In bowel anastomosis, poor suture placements could result in postsurgery complications. Several factors contribute to these complications,
e.g., thin tissue and blood vein tear. Optical imaging is capable of
perceiving anatomical characteristics invisible to human vision. Despite
this, most recent advancements in surgical vision have been geared
towards improving what the surgeon sees, but not the quantitative
assessments of the surgical field that enhances the surgeon's perception.
In this work, a novel imaging system that recommends anastomosis
placements to surgeons is developed. This is achieved by integrating a
multispectral imaging system coupled with polarizers and multispectral
image analysis software. The presented platform provides both spectral
properties and depth information of the tissue at the measured area.
We performed preliminary imaging of ex vivo porcine intestine tissue to
evaluate the system capability. Different tissue status (naïve, resected,
post-suture in/outside) were examined and processed for the future











analysis. As a result, vulnerable tissue regions including blood vessels, which should be avoided when suturing, were successfully identified and differentiated. In addition, by using a region-based supervised classification, different tissue regions were successfully segmented. Finally, thickness difference between tissue regions were visualized and compared to ground truth measurements using optical coherence tomography (OCT). Preliminary data suggest that our imaging platform and analysis algorithm may be useful in avoiding blood vessels, identifying optimal regions, and locating suture placements to perform safer operations in possibly reduced time.

9036-17, Session 4

## Optical surface scanning for respiratory motion monitoring in radiotherapy: a feasibility study

Susanne L. Bekke, Univ. Hospital Herlev (Denmark) and Technical Univ. of Denmark (Denmark); Faisal Mahmood, Univ. Hospital Herlev (Denmark); Jakob Helt-Hansen, Technical Univ. of Denmark (Denmark); Claus F. Behrens, Univ. Hospital Herlev (Denmark)

Purpose: We evaluated the feasibility of a marker-less optical surface scanning system (OS) to track the motion of the patient surface. Motion tracking is needed in deep inspiration breath-hold (DIBH) radiotherapy for breast cancer patients. DIBH is used to reduce the radiation dose to the heart and lungs. Compared to competing marker-based systems (MBs), OS does not require an object-marker on the patient's skin and enables motion tracking using two different spatial points simultaneously.

Materials & Methods: A phantom, created from a CPR dummy, was designed to simulate sinusoidal breathing. The motion signal was measured with the phantom's head placed at isocenter, and with lateral, longitudinal and vertical phantom movement of  $\pm 75$  and  $\pm 150$  mm.

The MB and OS were used to determine the amplitude, period and baseline (signal at end-expiration) for each phantom position. The amplitude and period were estimated by fitting a sine-curve to the measured signals.

Results: For all phantom positions the period was estimated to 6.3±0.007 s (mean±standard deviation, N=25) for both systems, and the amplitude was estimated to 8.1±0.9 mm and 4.9±0.9 mm for the OS and MB, respectively. Visual check showed an amplitude around 8 mm. The MB amplitude-error may be introduced by tilting of the object-marker during breathing. The largest baseline shift was 39.5 mm for MB and 0.7 mm for OS (all phantom positions).

Conclusion: OS can potentially be used as an alternative to MB. The amplitude estimates are more accurate and the baseline shifts are smaller with OS compared to MB.

9036-18, Session 4

## Statistical analysis of surrogate signals to incorporate respiratory motion variability into radiotherapy treatment planning

Matthias Wilms, Jan Ehrhardt, Univ. zu Lübeck (Germany); René Werner, Univ. Medical Ctr. Hamburg-Eppendorf (Germany); Mirko Marx, Heinz Handels, Univ. zu Lübeck (Germany)

Respiratory motion and its variability lead to location uncertainties in radiation therapy (RT) of thoracic and abdominal tumors. Current approaches for motion compensation in RT are usually driven by respiratory surrogate signals, e.g., spirometry. In this contribution, we present an approach for statistical analysis, modeling and subsequent simulation of surrogate signals on a cycle-by-cycle basis. The simulated signals represent typical patient-specific variations of, e.g., breathing

amplitude and cycle period. For the underlying statistical analysis, all breathing cycles of an observed signal are consistently parameterized using approximating B-spline curves. Statistics on breathing cycles are then performed by using the parameters of the B-spline approximations. Assuming that these parameters follow a multivariate Gaussian distribution, realistic simulated surrogate signals can be generated and used to incorporate patient-specific information about motion variability into treatment planning. The signal values are first related to internal motion by establishing a correspondence model, which is then applied to calculate tumor appearance probabilities and to estimate dosimetric effects of motion variability.

9036-19, Session 4

### Marker-less respiratory motion modeling using the Microsoft Kinect for Windows

Fatemeh Tahavori, Kevin Wells, Univ. of Surrey (United Kingdom)

Respiratory motion can obfuscate tumor delineation which impacts both radiotherapy planning and the associated delivery. Much work in this area relies on the use of as assumed single averaged cycle. The aim of this work is to examine subject-specific external respiratory motion and its drift from such an assumed average cycle.

External respiratory motion was acquired from a group of 20 volunteers using a marker-less 3D depth camera, Kinect for Windows, each captured for 300s. Then, the anterior surface was divided into thoracic and abdominal components and in each region PCA has been performed to investigate the dominant variation. The first principal component typically describes more than 95% of data variance in the thoracic and abdominal surfaces. Across all of the subjects used in this study, 58% of subjects demonstrate largely abdominal breathing and 33% exhibit thoracic dominated breathing. In most cases there is observable drift in respiratory motion during the 300s capture period, which is quantified using Kernel Density Estimation. This study demonstrates that for this cohort of apparently healthy volunteers, there is significant respiratory motion drift in most cases, in terms of amplitude and relative displacement between the thoracic and abdominal respiratory components. This has implications for any motion correction/prediction methodology that relies on an assumed average cycle.

9036-20, Session 4

## Separating complex compound patient motion tracking data using independent component analysis

Clifford Lindsay, Worcester Polytechnic Institute (United States); Karen Johnson, Michael A. King, Univ. of Massachusetts Medical School (United States)

In SPECT imaging, motion from respiration and body motion can reduce image quality by introducing motion-related artifacts. A minimallyinvasive way to track patient motion is to attach external markers to the patient's body and record their location throughout the imaging study. If a patient exhibits multiple movements simultaneously, such as respiration and body-movement, each marker location data will contain a mixture of these motions. Decomposing this complex compound motion into separate simplified motions can have the benefit of applying a more robust motion correction to the specific type of motion. Most motion tracking and correction techniques target a single type of motion and either ignore compound motion or treat it as noise. Few methods account for compound motion exist, but they fail to disambiguate superposition in the compound motion (i.e. inspiration in addition to body movement in the positive anterior/posterior direction). We propose a new method for decomposing the complex compound patient motion using an unsupervised learning technique called Independent Component Analysis (ICA). Our method can automatically detect and separate











different motions while preserving nuanced features of the motion without the drawbacks of previous methods. Our main contributions are the development of a method for addressing multiple compound motions, the novel use of ICA in detecting and separating mixed independent motions, and generating motion transform with 12 DOFs to account for twisting and shearing. We show that our method works with clinical datasets and can be employed to improve motion correction in single photon emission computed tomography (SPECT) images.

9036-21, Session 5

#### Surgical screw segmentation for mobile C-arm CT devices

Joseph Görres, Michael Brehler, Deutsches Krebsforschungszentrum (Germany); Jochen Franke M.D., BG Unfallklinik (Germany); Ivo Wolf, Hochschule Mannheim (Germany); Sven Y. Vetter M.D., Paul A. Gruetzner M.D., BG Unfallklinik (Germany); Hans-Peter Meinzer, Diana Wald, Deutsches Krebsforschungszentrum (Germany)

Calcaneal fractures are commonly treated by open reduction and internal fixation. An anatomical reconstruction of involved joints is mandatory to prevent cartilage damage and premature arthritis. In order to avoid intraarticular screw placements, the use of mobile C-arm CT devices is required. However, for analyzing the screw placement in detail, a timeconsuming human-computer interaction is necessary to navigate through 3D images and therefore to view a single screw in detail. Established interaction procedures of repeatedly positioning and rotating sectional planes are inconvenient and impede the intraoperative assessment of the screw positioning. To simplify the interaction with 3D images, we propose an automatic screw segmentation that allows for an immediate selection of relevant sectional planes. Our algorithm consists of three major steps. At first, cylindrical characteristics are determined from local gradient structures with the help of RANSAC. In a second step, a DBScan clustering algorithm is applied to group similar cylinder characteristics. Each detected cluster represents a screw, whose determined location is then refined by a cylinder-to-image registration in a third step. Our evaluation with 309 screws in 50 images shows robust and precise results. The algorithm detected 98% (303) of the screws correctly. Thirteen clusters led to falsely identified screws. The mean distance error for the screw tip was  $0.8 \pm 0.8$  mm and for the screw head  $1.2 \pm 1$  mm. The mean orientation error was  $1.4 \pm 1.2$  degrees.

9036-22, Session 5

### A Compact Method for Prostate Zonal Segmentation on Multi-parametric MRIs

Yanling Chi, Singapore Bioimaging Consortium (Singapore); Henry Ho, Yan Mee Law, Singapore General Hospital (Singapore); Qi Tian, Singapore Bioimaging Consortium (Singapore); Hongjun Chen, Biobot Surgical Pte. Ltd. (Singapore); Kae Jack Tay, Singapore General Hospital (Singapore); Jimin Liu, Singapore Bioimaging Consortium (Singapore)

Prostate cancer is the second most common cancer in men. The occurrence of prostatic cancers varies in zones. Statistically, 70-75% of prostate cancers occur in the peripheral zone. The knowledge of the zonal anatomy is useful in targeting the lesions during the image-guided interventions of the prostate. Automatic segmentation of prostate zones has great potential of improving the intervention's accuracy. In this paper, we present a novel compact method to segment the prostatic zones using multi-parametric magnetic resonance imaging (MRI). The proposed method first builds a probabilistic atlas of the prostate/structure using ten sets of pre-labeled T2-weighted MRIs. Second, it registers T1-weighted images, the apparent diffusion coefficient (ADC) map and 3D prostate/

structure atlas to T2-weighted images using Plastimatch software package [1]. Third, it represents the prostatic tissues using a Gaussian mixture model (GMM) in terms of density features, texture features, hessian-based blobness, and apparent diffusion coefficients. GMM parameters are estimated from 10 sets of training data using the iterative Expectation-Maximization (EM) algorithm. Fourth, a fuzzy classifier is employed to delineate the prostate and the central zone hierarchically, with the shape constrains of the built 3D prostate/structure probabilistic atlas. Morphological operations are finally conducted to fine tune the segmentation results. The peripheral zone can be obtained by subtracting the central zone from the prostate. The proposed method is tested on ten sets of multi-parametric MRIs to obtain primitive results. In this work, with the advantages of the image analysis techniques, the anatomical priors and multi-parametric MRIs of the prostate are combined to do the zonal segmentation. The contributions of individual components: T1-weighted, T2-weighted, diffusion MRIs, the 3D prostatic probabilistic atlas, and the image features, to the segmentation of prostatic structures will be studied.

9036-23, Session 5

### Segmentation of risk structures for otologic surgery using the Probabilistic Active Shape Model

Meike Becker, Matthias Kirschner, Georgios Sakas, Technische Univ. Darmstadt (Germany)

Our research project investigates a multi-port approach for minimally-invasive otologic surgery. For planning such a surgery, an accurate segmentation of the risk structures is crucial. However, the segmentation of these risk structures is a challenging task: The anatomical structures are very small and some have a complex shape, low contrast and vary both in shape and appearance. Therefore, prior knowledge is needed which is why we apply model-based approaches.

In the present work, we use the Probabilistic Active Shape Model (PASM) which is a more flexible and specific variant of the Active Shape Model (ASM) to segment the following risk structures: cochlea, semi-circular canals, facial nerve, chorda tympani, ossicles, internal auditory canal, external auditory canal and internal carotid artery. For the evaluation, we trained and tested the algorithm on 42 computed tomography data sets using leave-one-out tests. By visual assessing the results, one sees in general a good agreement of manual and algorithmic segmentations. Further, we achieve a good Average Symmetric Surface Distance while the maximum error is comparatively large due to low contrast at start and end points. Furthermore, we compare the PASM to the standard ASM and show that the PASM leads to a higher accuracy.

9036-24, Session 5

## Semi-automatic segmentation of vertebral bodies in volumetric MR images using a statistical shape+pose model

Amin Suzani, Abtin Rasoulian, Sidney Fels, Robert N. Rohling, Purang Abolmaesumi, The Univ. of British Columbia (Canada)

In recent years, there has been a significant surge of interest in using magnetic resonance (MR) for imaging spine. Segmentation of vertebral structures in MR images is challenging because of poor contrast between bone surfaces and surrounding soft tissue. This paper describes a semi-automatic method for segmenting vertebral bodies in multi-slice MR images. In order to achieve a fast and reliable segmentation, the method takes advantage of correlation between shape and pose of different vertebrae in the same patient by using a statistical multi-vertebrae anatomical shape+pose model. Given a multi-slice MR image of the spine, we initially reduce the intensity inhomogeneity in the image using an intensity-correction algorithm. Then a 3D anisotropic











diffusion algorithm is applied for smoothing the image. Afterwards, we extract edges from a relatively small region of the pre-processed image with a simple user interaction. Subsequently, an iterative Expectation Maximization technique is used to register the statistical multi-vertebrae anatomical model to the extracted edge points in order to achieve a fast and reliable segmentation for lumbar vertebral bodies. We evaluate our method in terms of speed and accuracy by applying it to volumetric MR images of the spine acquired from nine patients. Quantitative and visual results demonstrate that the method is promising for segmentation of vertebral bodies in volumetric MR images.

9036-26, Session 6

## Piecewise-rigid 2D-3D registration for pose estimation of snake-like manipulator using an intraoperative X-ray projection

Yoshito Otake, Johns Hopkins Univ. (United States); Ryan J. Murphy, Michael D. Kutzer, Johns Hopkins Univ. (United States); Armand Mehran, Johns Hopkins Univ. Applied Physics Lab. (United States)

Snake-like dexterous manipulator may offer significant advantages in minimally-invasive surgery in the areas not reachable with conventional tools. Precise control of a wire-driven manipulator is challenging due to deterioration of calibration associating the wire tension and kinematic configuration, thus requires correcting the calibration intraoperatively by determining the actual pose of the manipulator. A method for simultaneously estimating pose and kinematic configuration of a piecewise-rigid object such as a snake-like manipulator from a single x-ray projection is presented. The method parameterizes kinematics using a small number of variables (e.g., 5), and optimizes them simultaneously with the 6 degree-of-freedom pose parameter of the base link using an image similarity between digitally reconstructed radiographs (DRRs) of the manipulator's attenuation model and the real projection. Simulation studies assumed various geometric magnifications (1.2-2.6) and out-of-plane angulations (0 deg-90 deg) in a scenario of hip osteolysis treatment, which demonstrated the median joint angle error was 0.04 deg (for 2.0 magnification, +-10 deg out-of-plane rotation). Average computation time was 57.6 sec with 82,953 function evaluations on a mid-range GPU. The joint angle error remained lower than 0.07o while out-of-plane rotation was 0 deg-60 deg. An experiment using video images of a real manipulator demonstrated a similar trend as the simulation study except for slightly larger error around the tip attributed to accumulation of errors induced by deformation around each joint not modeled with a simple pin joint. Potential applications of the proposed approach include pose estimation of vertebrae in spine and a series of electrodes in coronary sinus catheter.

9036-27, Session 6

## Deformable registration for image-guided spine surgery: preserving rigid body vertebral morphology in free-form transformations

Sureerat Reaungamornrat, Ali Uneri, Yoshito Otake, Zhe Zhao, Adam S. Wang, Akhil J. Khanna, Jeffrey H. Siewerdsen, Johns Hopkins Univ. (United States)

Purpose: Accurate localization of target and critical anatomy in imageguided spine surgery is challenged by deformation associated with patient positioning and the intervention itself. Conventional nonrigid registration fails to preserve rigid anatomy and can cause distortions that confound high-precision surgery. We propose a registration method incorporating a rigidity constraint that preserves rigid morphology in bones while allowing deformation of surrounding soft tissues.

Method: The deformable registration aligns preoperative images to

intraoperative cone-beam CT (CBCT) using free-form deformation (FFD) with a local rigidity penalty. The penalty enforces 3 rigid transformation via orthogonality, affinity, and/or properness according to a simple intensity threshold. The method was evaluated against unconstrained FFD (uFFD) and Demons registration in simulation and cadaver studies in terms of target registration error (TRE) and preservation of rigid morphology.

Result: The orthogonality-constrained deformation (oFFD) demonstrated improved performance compared to uFFD and Demons. The TRE for oFFD, uFFD, and Demons was 1.0, 1.7, and 2.2 mm, respectively, in simulation studies, and only oFFD preserved rigid morphology at near-ideal values of zero orthogonality and unity Jacobian determinant. Similar results were found in an ovine spine specimen and a human cadaver under varying conditions of scoliosis, kyphosis, and lordosis, with oFFD providing equivalent or improved TRE and near-perfect preservation of rigid morphology.

Conclusions: A promising method for CBCT-guided spine surgery has been identified incorporating a constrained FFD to preserve bone morphology. The approach could overcome distortions intrinsic to unconstrained FFD and facilitate high-precision image-guided spine surgery.

9036-28, Session 6

# Hyperspectral imaging for surgical margin delineation of head and neck cancer: registration of hyperspectral and histological images

Guolan Lu, Emory Univ. (United States) and Georgia Insitute of Technology (United States); Luma V. Halig, Dongsheng Wang, Zhuo Georgia Chen, Emory Univ. (United States); Baowei Fei, Emory Univ. (United States) and Georgia Institute of Technology (United States)

The determination of head and neck tumor margins during surgical resection remains a challenging task. The complete removal of malignant tissue and conservation of healthy tissue is important for the preservation of organ function, patient satisfaction, and quality of life. Visual inspection and palpation is not sufficient for discriminating between malignant and normal tissue types. Hyperspectral imaging (HSI) technology has the potential to noninvasively delineate surgical tumor margin and can be used as an intra-operative visual aid tool. Since histological images provide the ground truth of cancer margins, it is necessary to warp the cancer regions in ex vivo histological images to in vivo HSI images in order to validate the HSI tumor margins and to optimize the imaging parameters. In this paper, principal component analysis is utilized to extract the principle component bands of the HSI images, which is then used to register HSI images with the corresponding histological image. Affine registration is chosen to model the global transformation. The B-spline free form deformation (FFD) method is used to model the local non-rigid deformation. Registration experiment was performed on animal hyperspectral and histological images. Experimental results from animals demonstrated the feasibility of the hyperspectral imaging method for cancer margin detection.

9036-29, Session 6

### Dynamic tracking of a deformable tissue based on 3D-2D MR-US image registration

Bahram Marami, McMaster Univ. (Canada) and Robarts Research Institute (Canada); Shahin Sirouspour, McMaster Univ. (Canada); Aaron Fenster, Robarts Research Institute (Canada); David W. Capson, Univ. of Victoria (Canada)











Real-time registration of pre-operative computed tomography (CT) or magnetic resonance (MR) images with intra-operative Ultrasound (US) images can be a valuable tool in image-guided therapies and interventions. This paper presents an automatic method for dynamically tracking the deformation of a soft tissue based on registering preoperative three-dimensional (3D) MR images to intra-operative twodimensional (2D) US images. The registration algorithm is based on concepts in state estimation where a dynamic finite element (FE)based linear elastic deformation model correlates the imaging data in the spatial and temporal domains. A Kalman-like filtering process estimates the unknown deformation states of the soft tissue using the deformation model and a measure of error between the predicted and the observed intra-operative imaging data. The error is computed based on an intensity-based similarity measure, namely, modality independent neighborhood descriptor (MIND), and no segmentation or feature extraction from images is required. The performance of the proposed method is evaluated by dynamically deforming 3D preoperative MR images of a breast phantom tissue based on real-time 2D images obtained from an US probe. Experimental results on different registration scenarios showed that deformation tracking converges in a few iterations. The average target registration error on the plane of 2D US images for manually selected fiducial points was between 0.3 and 1.5 mm depending on the size of deformation.

9036-30, Session 6

### Target registration error for rigid shape-based registration with heteroscedastic noise

Burton Ma, Joy Choi, Hong M. Huai, York Univ. (Canada)

We propose an analytic equation for approximating expected root mean square (RMS) target registration error (TRE) for rigid shape-based registration where measured noisy data points are matched to a rigid shape. The noise distribution of the data points is assumed to be zeromean, independent, and non-identical; i.e., the noise covariance may be different for each data point. The equation was derived by extending a previously published spatial stiffness model of registration. The equation was validated by performing registration experiments with both synthetic registration data and data collected using an optically tracked pointing stylus. The synthetic registration data were generated from the surface of an ellipsoid. The optically tracked data were collected from three plastic replicas of human radii and registered to isosurface models of the radii computed from CT scans. Noise covariances for the data points were computed by considering the pose of the tracked stylus, the positions of the individual fiducial markers on the stylus coordinate reference frame, and the calibrated position of the stylus tip; these quantities and an estimate of the fiducial localization covariance of the tracking system were used as inputs to a previously published algorithm for estimating the covariance of TRE for point-based (fiducial) registration. Registration simulations were performed using a modified version of the iterated closest point algorithm and the resulting RMS TREs were compared to the values predicted by our analytic equation.

9036-31, Session 6

### Registration of liver images to minimally invasive intraoperative surface and subsurface data

Yifei Wu, Vanderbilt Univ. (United States); Daniel C. Rucker, Vanderbilt Univ. (United States) and The Univ. of Tennessee Knoxville (United States); Rebekah H. Conley, Thomas S. Pheiffer, Amber L. Simpson, Vanderbilt Univ. (United States); Sunil K. Geevarghese M.D., Vanderbilt Univ. Medical Ctr. (United States) and Vanderbilt Univ. School of Medicine (United States); Michael I. Miga, Vanderbilt Univ. (United States)

Laparoscopic liver resection is increasing accepted as a standard of care with results comparable to open cases while incurring less trauma and reducing recovery time. The tradeoff is increased difficulty due to limited visibility and restricted freedom of movement. Image-guided surgical navigation systems can help localize anatomical features to improve patient safety and achieve negative surgical margins.

Previous research has demonstrated that intraoperative surface data can be used to drive a finite element tissue mechanics organ model such that high resolution preoperative scans are registered and visualized in the context of the current surgical pose. In this paper we present an investigation of using sparse data as imposed by laparoscopic limitations to drive a registration model. Surface swabs and subsurface data were used in tandem to reconstruct a displacement field on the posterior of the organ to optimize the fit between the intraoperative data and the preoperative liver model.

Tests based on laboratory phantoms were used to validate the potential of this approach. Experimental results based on a liver phantom demonstrate that Target Registration Errors (TRE) on the order of 6mm were achieving using only surface swab data, while use of only subsurface data yielded errors on the order of 7mm. Registrations using a combination of both datasets achieved TRE on the order or 2.5mm and represent a sizeable improvement over either dataset alone.

9036-32, Session 7

### **Engineering therapeutic processes: from research to commodity** (Keynote Presentation)

Robert L. Galloway Jr., Vanderbilt Univ. (United States)

Three of the most important forces driving medical care are: patient specificity, treatment specificity and the move from discovery to design. Engineers while trained in specificity, efficiency, and design are often not trained in either biology or medical processes. Yet they are increasing critical to medical care. For example, modern medical imaging at US hospitals generates 1 exabyte (10^18 bytes) of data per year clearly beyond unassisted human analysis. It is not desirable to involve engineers in the acquisition, storage and analysis of this data, it is essential. While in the past we have nibbled around the edges of medical care, it is time and perhaps past time to insert ourselves more squarely into medical processes, making them more efficient, more specific and more robust. This requires engineers who understand biology and physicians who are willing to step away from classic medical thinking to try new approaches. But once the idea is proven in a laboratory, it must move into use and then into common practice. This requires additional engineering to make the process robust to noisy data and imprecise practices as well as workflow analysis to get the new technique into operating and treatment rooms. True innovation and true translation will require physicians, engineers, other medical stakeholders and even corporate involvement to take a new, important idea and move it not just to a patient but to all patients.

9036-33, Session 7

#### Integration and visualization of intraoperative stereovision imaging for brain shift compensation during image-guided cranial procedures

Timothy J. Schaewe, Medtronic, Inc. (United States); Xiaoyao Fan, Songbai Ji, Thayer School of Engineering at Dartmouth (United States); David W. Roberts M.D., Dartmouth Hitchcock Medical Ctr. (United States); Keith D. Paulsen, Thayer School of Engineering at Dartmouth (United States); David Simon, Medtronic, Inc. (United States)

Dartmouth and Medtronic Navigation have established an academic-











industrial partnership to develop, validate, and evaluate a multi-modality neurosurgical image-guidance platform for brain tumor resection surgery that is capable of updating the spatial relationships between preoperative images and the current surgical field. A stereovision system has been developed and optimized for intraoperative use through integration with a surgical microscope and an image guided surgery system. The microscope and stereovision CCD sensors are localized relative to the surgical field using optical tracking and can efficiently acquire stereo image pairs from which a localized 3D profile of the exposed surface is reconstructed. This paper reports the first demonstration of intraoperative acquisition, reconstruction and visualization of 3D stereovision surface data in the context of an industry-standard neuronavigation platform. We present our methods for conversion of the dense point cloud data that is produced by the stereovision reconstruction process to data objects that can be readily merged with preoperative imaging and are efficiently rendered in the 2D and 3D views of the navigation system. Surgical cases during which the stereovision system has been employed to estimate brain shift at the post dural opening time point are presented. Visualization of these data provides valuable information to the surgeon at the earliest stage of the resection procedure, significantly improving the accuracy of image-based guidance and reducing the extrapolation required by the surgeon to achieve maximum surgical accuracy.

9036-34, Session 7

## Stereoscopic augmented reality using ultrasound volume rendering for laparoscopic surgery in children

Jihun Oh, Xin Kang, Emmanuel Wilson, Craig A. Peters, Timothy D. Kane, Raj Shekhar, Children's National Medical Ctr. (United States)

In laparoscopic surgery, live laparoscopic video provides visualization of exposed organ surfaces in the surgical field, but is unable to show internal structures beneath those surfaces. The laparoscopic ultrasound is often used to visualize those structures, but its use is limited to intermittent confirmation because of the need for an extra hand to maneuver the ultrasound probe. Other limitations of ultrasound are difficulty of interpretation, a need for an extra port, and the size of ultrasound transducer that may be too large for use in small children. In this paper, we investigated an augmented reality (AR) system that features continuous hands-free volumetric ultrasound scanning and a stereoscopic laparoscope. The 3D ultrasound acquisition is accomplished externally by back-and-forth movement of a laparoscopic transducer mounted on a slider of a linear stage and the volume is updated. An overlay of maximum intensity projection of the ultrasound volume on the laparoscopic stereo video through geometric transformations promises an AR system particularly suitable for children because ultrasound is radiation-free and provides higher-quality images in small patients, and this AR representation is better than the AR using ultrasound slice-video overlay.

9036-35, Session 8

### Localization accuracy of sphere fiducials in computed tomography images

Jan-Philipp Kobler, Jesús Díaz Díaz, Leibniz Univ. Hannover (Germany); J. Michael Fitzpatrick, Vanderbilt Univ. (United States); G. Jakob Lexow, Omid Majdani M.D., Medizinische Hochschule Hannover (Germany); Tobias Ortmaier, Leibniz Univ. Hannover (Germany)

In recent years, bone-attached robots and microstereotactic frames have attracted increasing interest due to the promising targeting accuracy they provide. Such devices attach to a patient's skull via bone anchors, which are used as landmarks during intervention planning as well. However,

as simulation results reveal, the performance of such mechanisms is limited by errors occurring during the localization of their bone anchors in preoperatively acquired computed tomography images. Therefore, it is desirable to identify the most suitable fiducials as well as the most accurate method for fiducial localization. We present experimental results of a study focusing on the fiducial localization error (FLE) of spheres. Two phantoms equipped with fiducials made from ferromagnetic steel and titanium, respectively, are used to compare two clinically available imaging modalities (multi-slice CT (MSCT) and cone-beam CT (CBCT)), three localization algorithms as well as two methods for approximating the FLE. Furthermore, the impact of cubic interpolation applied to the images is investigated. Results reveal that, generally, the achievable localization accuracy in CBCT image data is significantly higher compared to MSCT imaging. The lowest FLEs (approx. 50 µm) are obtained using spheres made from titanium, CBCT imaging, template matching based on cross correlation for localization, and interpolating the images by a factor of sixteen. Nevertheless, the achievable localization accuracy of spheres made from steel is only slightly inferior. The outcomes of the presented study will be valuable considering the optimization of future microstereotactic frame prototypes as well as the operative workflow.

9036-36, Session 8

#### On the accuracy of a video-based drillguidance solution for orthopedic and trauma surgery: preliminary results

Jessica Magaraggia, Friedrich-Alexander-Univ. Erlangen-Nürnberg (Germany); Gerhard Kleinszig, Wei Wei, Markus Weiten, Rainer Graumann, Siemens AG (Germany); Elli Angelopoulou, Joachim Hornegger, Friedrich-Alexander-Univ. Erlangen-Nürnberg (Germany)

Over the last years, several solutions have been proposed to guide the physician during reduction and fixation of bone fractures. Available solutions often use bulky instrumentation inside the operating room (OR). The latter ones usually consist of a stereo camera, placed outside the operative field, and optical markers directly attached to both the patient and the surgical instrumentation, held by the surgeon. Recently proposed solutions try to reduce both the required additional instrumentation and the radiation exposure to both patient and physician. In this paper, we present the adaptation and the first implementation of our recently proposed video camera-based solution for screw fixation guidance. Based on the simulations conducted in our previous work, we mounted a small camera on a drill in order to recover its tip position and axis orientation w.r.t our custom-made drill sleeve with attached markers. Since drill-position accuracy is critical, we thoroughly evaluated the accuracy of our implementation. We used an optical tracking system as ground truth. For this purpose, we built a custom plate reference system and attached reflective markers to both the instrument and the plate. Free drilling was then performed 19 times. The position of the drill axis was continuously recovered using both our video-camera solution and the tracking system for comparison. The recorded time covered targeting, perforation of the surface bone by the drill bit and bone drilling. The orientation of the instrument axis and the position of the instrument tip were recovered with an accuracy of  $1.60 \pm 1.22^{\circ}$  and  $2.03 \pm 1.36$  mm respectively.

9036-37, Session 8

## In vivo reproducibility of robotic probe placement for an integrated US-CT image-guided radiotherapy system

Muyinatu A. Lediju Bell, H. Tutkun Sen, Iulian I. Iordachita, Peter Kazanzides, John Wong, Johns Hopkins Univ. (United States)











Ultrasound (US) has potential to provide real-time monitoring of radiation therapy, but the tissue deformations caused by US probes could result in mismatches between patient anatomy at the time of treatment delivery, when compared to treatment planning anatomy. If the US probe is placed to achieve similar deformations for planning purposes, its presence causes streak artifacts in the CT images required for treatment planning. To overcome these challenges, we propose robot-assisted placement of a real ultrasound probe, followed by placement of a geometricallyidentical, CT-compatible model probe. This work is the first to investigate the in vivo reproducibility of tissue deformations with robotic probe placement using this approach. Following an IACUC-approved protocol, a canine prostate was implanted with three 2.38-mm spherical metallic markers, and the US probe was placed to visualize implanted markers. The real and model probes were automatically removed and returned to the same position, and CT images were acquired with each probe placement. The model probe was also removed and returned with the same force normal to the probe to investigate this alternate positioning approach if there are large day-to-day patient setup errors. Marker positions in CT images were analyzed to determine repeatability. Results indicate that tissue deformations were repeatable under position control with median 3D errors of 0.6 and 0.7 mm with the real and model probes, respectively. The median 3D error between real and model probes was 0.2 mm under position control and 0.6 mm under force control. Results are promising for organs similar to the dog prostate.

9036-38, Session 8

## Workflow assessment of 3T MRI-guided transperineal targeted prostate biopsy using a robotic needle guidance

Sang-Eun Song, Kemal Tuncali M.D., Junichi Tokuda, Andriy Fedorov, Brigham and Women's Hospital (United States); Tobias Penzkofer M.D., Brigham and Women's Hospital (United States) and Univ. Hospital Aachen (Germany); Fiona Fennessy M.D., Clare Tempany M.D., Brigham and Women's Hospital (United States); Kitaro Yoshimitsu, Brigham and Women's Hospital (United States) and Tokyo Women's Medical Univ. (Japan); John Magill, Physical Sciences Inc. (United States); Nobuhiko Hata, Brigham and Women's Hospital (United States)

Magnetic resonance imaging (MRI) guided transperineal targeted prostate biopsy has become a valuable instrument for detection of prostate cancer in patients with continuing suspicion for aggressive cancer after transrectal ultrasound guided (TRUS) guided biopsy. The MRI-guided procedures are performed using mechanical targeting devices or templates, which suffer from limitations of spatial sampling resolution and/or manual in-bore adjustments. To overcome these limitations, we developed and clinically deployed an MRI-compatible piezoceramic-motor actuated needle guidance device, Smart Template, which allows automated needle guidance with high targeting resolution for use in a wide closed-bore 3-Tesla MRI scanner. One of the main limitations of the MRI-guided procedure is the lengthy procedure time compared to conventional TRUS-guided procedures. In order to optimize the procedure, we assessed workflow of 30 MRI-guided biopsy procedures using the Smart Template with focus on procedure time. An average of 3.4 (range: 2~6) targets were preprocedurally selected per procedure and 2.2 ± 0.8 biopsies were performed for each target with an average insertion attempt of  $1.9 \pm 0.7$  per biopsy. The average technical preparation time was  $14 \pm 7$  min and the in-MRI patient preparation time was  $42 \pm 7$  min. After  $21 \pm 7$  min of initial imaging,  $64 \pm 12$  min of biopsy was performed yielding an average of  $10 \pm 2$  min per tissue sample. The total procedure time occupying the MRI suite was  $138 \pm 16$  min. No noticeable tendency in the length of any time segment was observed over the 30 clinical cases.

9036-39, Session 8

#### A user-friendly automated port placement planning system for laparoscopic robotic surgery

Luis G. Torres, The Univ. of North Carolina at Chapel Hill (United States); Hamidreza Azimian, The Hospital for Sick Children (SickKids) (Canada); Andinet Enquobahrie, Kitware, Inc. (United States)

Laparoscopic surgery is a minimally invasive surgical approach in which surgical instruments are passed through ports placed at small incisions. This approach can benefit patients by reducing recovery times and scars. Surgeons have also gained greater dexterity, accuracy, and vision through adoption of robotic surgical systems. However, in some cases a pre-selected set of ports cannot be accommodated by the robot; the robot's arms may cause collisions during the procedure, or the surgical targets may not be reachable through the selected ports. In this case, the surgeon must either make more incisions for more ports, or even abandon the laparoscopic approach entirely. To assist in this, we are building an easy-to-use system which, given a surgical task and preoperative medical images of the patient, will recommend a suitable port placement plan for the robotic surgery. This work bears two main contributions: 1) a high level user interface that assists the surgeon in operating the complicated underlying planning algorithm; and 2) an interface to assist the surgical team in implementation of the recommended plan in the operating room. We believe that such an automated port placement system would reduce setup time for robotic surgery and reduce the morbidity to patients caused by unsuitable surgical port placement.

9036-40, Session 8

#### Preliminary testing of a compact, boneattached robot for otologic surgery

Neal P. Dillon, Vanderbilt Univ. (United States); Ramya Balachandran, Vanderbilt Univ. Medical Ctr. (United States); Antoine Motte dit Falisse, Univ. Catholique de Louvain (Belgium); Thomas J. Withrow, Vanderbilt Univ. (United States); George B. Wanna, Robert F. Labadie M.D., Vanderbilt Univ. Medical Ctr. (United States); J. Michael Fitzpatrick, Robert J. Webster III, Vanderbilt Univ. (United States)

Otologic surgery often involves mastoidectomy procedure, which is drilling away part of the temporal bone, in order to visualize critical structures embedded in the bone and safely access the middle and the inner ear. We propose to automate this portion of the surgery using a compact, bone-attached milling robot. A high level of accuracy is required to avoid damage to critical structures. In this study, several of the design considerations are discussed and a robot design and prototype are presented. The prototype is a 4 DOF robot similar to a four-axis milling machine that mounts to the patient's skull. A positioning frame, containing fiducial markers and attachment points for the robot, is attached to the skull and scanned with the patient. The target bone volume is manually segmented by the surgeon and automatically converted to a milling path and robot trajectory. The robot is then attached to the positioning frame and the procedure begins. An initial phantom test was performed to verify the surgical workflow and robot kinematics.











9036-41, Session 9

## Breast deformation modeling: comparison of methods to obtain a patient specific unloaded configuration

Bjoern Eiben, Vasileios Vavourakis, John H. Hipwell, Univ. College London (United Kingdom); Sven Kabus, Cristian Lorenz, Thomas Buelow, Philips Research (Germany); David J. Hawkes, Univ. College London (United Kingdom)

In biomechanical simulations of the human breast, the analyzed geometry is often reconstructed from in vivo medical imaging procedures. For example in dynamic contrast enhanced magnetic resonance imaging (DCE-MRI), the acquired geometry of the patient's breast when lying in the prone position represents a deformed configuration that is prestressed by typical in vivo conditions and gravity. Thus, physically realistic simulations require consideration of this loading and, hence, establishing the undeformed configuration is an important task for accurate and reliable biomechanical modelling of the breast.

We compare three different numerical approaches to recover the unloaded configuration from the loaded geometry given patient specific biomechanical models built from prone and supine MR images. Compared algorithms are: (i) the simple inversion of gravity without the consideration of pre-stresses, (ii) a fixed point type iterative approach which uses only forward simulations and (iii) the inverse finite element formulation.

It is shown that the iterative and the inverse approach produce similar zero-gravity estimates, whereas the simple inversion of gravity is only appropriate for small deformations.

9036-42, Session 9

#### Intraoperative measurement of indenterinduced brain deformation

Songbai Ji, Xiaoyao Fan, Thayer School of Engineering at Dartmouth (United States); David W. Roberts M.D., Dartmouth Hitchcock Medical Ctr. (United States); Keith D. Paulsen, Thayer School of Engineering at Dartmouth (United States)

Accurate measurement of soft tissue material properties is critical for characterizing its biomechanical behaviors but can be challenging especially for the human brain in vivo. In this study, we investigated the feasibility of inducing and detecting cortical surface deformation intraoperatively for patients undergoing open skull neurosurgeries. A custom disk-shaped indenter made of high-density tungsten (diameter of 15 mm with a thickness of 6 mm) was used to induce deformation on the brain cortical surface immediately after dural opening. Sequences (typically 250 frames at 15 frames-per-second, or ~17 seconds) of highresolution stereo image pairs were acquired to capture the harmonic motion of the exposed cortical surface as a result of blood pressure pulsation before and after indentation. For each sequence with the first left image serving as a baseline, rigid registration was performed using features outside the exposed craniotomy to compensate for any microscopic motion when needed. An optical-flow motiontracking algorithm was then used to detect in-image cortical surface deformation. The resulting displacements of the exposed features within the craniotomy were spatially averaged to identify the temporal frames corresponding to motion peak magnitudes. Corresponding image pairs were then selected to reconstruct full-field three-dimensional (3D) cortical surfaces before and after indentation, respectively, from which full 3D displacement fields were obtained. With one clinical patient case, we illustrate the feasibility of the technique in detecting indenter-induced cortical surface deformation in order to allow subsequent processing to determine material properties of the brain in vivo in the future.

9036-43, Session 9

#### Virtual estimates of fastening strength for pedicle screw implantation procedures

Cristian A. Linte, Mayo Clinic College of Medicine (United States); Jon J. Camp, Kurt E. Augustine, Paul M. Huddleston, David R. Holmes III, Mayo Clinic (United States); Richard A. Robb M.D., Mayo Clinic College of Medicine (United States)

Traditional 2D images provide limited use for accurate planning of spine interventions, mainly due to the complex 3D anatomy of the and spine, and close proximity of nerve bundles and vascular structures that must be avoided during the procedure. Our previously developed and disseminated clinician-friendly platform for spine surgery planning takes advantage of 3D pre-operative images, to enable oblique reformatting and 3D rendering of individual or multiple vertebrae, interactive templating, and placement of virtual pedicle implants. Here we extend the capabilities of the planning platform and demonstrate how the virtual templating approach not only assists with the selection of the optimal implant size and trajectory, but can also provide surrogate estimates of the fastening strength of the implanted pedicle screws based on implant dimension and bone mineral density of the displaced bone substrate. According to the failure theories, each screw withstands a maximum holding power (i.e., maximum pull-out force) that is directly proportional to the screw diameter (D), the bone-inserted screw length (L), and the specific gravity (i.e., bone mineral density) of the pedicle body. In this application, voxel intensity is used as a surrogate measure of the bone mineral density (BMD) of the pedicle body segment displaced by the screw. We conducted an initial assessment of the developed platform using retrospective pre- and postoperative clinical 3D CT data from five patients who underwent spine surgery, consisting of a total of 28 pedicle screws implanted in the lumbar spine. The Fastening Strength of the planned implants was directly assessed by estimating the intensity - area product across the pedicle volume displaced by the virtually implanted screw. For post-operative assessment, each vertebra was registered to its homologous counterpart in the pre-operative image using an intensity-based rigid registration followed by minimal manual adjustment. Following registration, the Fastening Strength was computed for each displaced bone segment. According to our preliminary clinical study, a comparison between Fastening Strength, displaced bone volume and mean voxel intensity showed no statistical difference (p > 0.1) as far as these three parameters between the virtually templated proposed planned and the traditional clinical approach. This study has demonstrated the feasibility of the platform in providing the surgeon with estimates of the pedicle screw fastening strength in response to the virtual implantation, given the intrinsic vertebral geometry and bone mineral density.

9036-44, Session 9

## A cost effective and high fidelity fluoroscopy simulator using the image-guided surgery toolkit (IGSTK)

Ren Hui Gong, Brad Jenkins, Raymond W. Sze, Ziv R. Yaniv, Children's National Medical Ctr. (United States)

Medical training is primarily based on the apprenticeship model. The main issue with this approach is that it exposes patients to potential harm associated with the training process. Use of simulation enables the trainees to improve their skills prior to providing clinical care, thus reducing potential harm to patients. As a consequence simulation is an attractive alternative, primarily at the early stages of training. Ideally a simulation system mimics the clinical setup with high fidelity. Unfortunately, such systems come with high financial costs. In this work we describe a low cost, high fidelity X-ray fluoroscopy simulation system. Our system enables operators to practice their skills using the clinical device, with simulated X-rays and a virtual patient instead of real











X-rays and a physical patient. The virtual patient is represented using a set of temporal computed tomography (CT) images, corresponding to the underlying dynamic processes. Digitally Reconstructed Radiographs (DRRs) are generated from the CT images using ray casting based on the fluoroscopy imaging parameters. To establish the spatial relationship between the CT and the fluoroscopy device, the CT is virtually attached to a patient phantom, and a webcam is used to track the phantom's pose on the patient bed. The webcam is mounted on the image intensifier, and the fluoroscope's pose with respect to the webcam is obtained by using a calibration phantom. To control image-acquisition the operator moves the fluoroscope as they would do in its normal operation mode. To control zoom, collimation and image saving the operator uses a keypad that we mount alongside the device's control panel. Software implementation is based on the open source image-guided surgery toolkit (IGSTK), and use of the graphics processing unit (GPU) to accelerate DRR generation. Our preliminary experiments show that highly realistic DRRs can be obtained from CT in real-time.

9036-45, Session 9

### Cochlear implant simulator for surgical technique analysis

Rebecca L. Turok, Vanderbilt Univ. (United States); Robert F. Labadie M.D., George B. Wanna, Vanderbilt Univ. Medical Ctr. (United States); Benoit M. Dawant, Jack H. Noble, Vanderbilt Univ. (United States)

Cochlear Implant (CI) surgery is a procedure in which an electrode array is inserted into the cochlea. The electrode array is used to stimulate auditory nerve fibers and restore hearing for people with severe to profound hearing loss. The primary goals when placing the electrode array are to fully insert the array into the cochlea while minimizing trauma to the cochlea. Studying the relationship between surgical outcome and various surgical techniques has been difficult since trauma and electrode placement are generally unknown without histology. Our group has created a CI placement simulator that combines an interactive 3D visualization environment with a haptic-feedback-enabled controller. Surgical techniques and patient anatomy can be varied between simulations so that outcomes can be studied under varied conditions. With this system, we envision that through numerous trials we will be able to statistically analyze how outcomes relate to surgical techniques. As a first test of this system, in this work, we have designed an experiment in which we compare the distribution of forces imparted to the cochlea in the array insertion procedure when using two different but commonly used surgical techniques for cochlear access, called round window and cochleostomy access. Our results suggest that CIs implanted using round window access may cause less trauma to deeper intra-cochlear structures than cochleostomy techniques. This result is of interest because it challenges traditional thinking in the otological community but might offer an explanation for recent anecdotal evidence that suggests that round window access techniques lead to better outcomes.

9036-46, Session 10

## Fast segmentation of the prostate for brachytherapy based on joint fusion of images and labels

Saman Nouranian, Mahdi Ramezani, S. Sara Mahdavi, The Univ. of British Columbia (Canada); Ingrid Spadinger, William J. Morris, British Columbia Cancer Agency (Canada); Septimiu E. Salcudean, Purang Abolmaesumi, The Univ. of British Columbia (Canada)

Brachytherapy as one of the treatment methods for prostate cancer takes place by implantation of radioactive seeds inside the gland. The standard of care for this treatment procedure is to acquire transrectal

ultrasound images of the prostate which are segmented in order to plan the appropriate seed placement. The segmentation process is usually performed either manually or semi-automatically and is associated with subjective errors because the prostate visibility is limited in ultrasound images. The current segmentation process also limits the possibility of intra-operative delineation of the prostate to perform real-time dosimetry. In this paper, we propose a computationally inexpensive and fully automatic segmentation approach that takes advantage of previously segmented images to form a joint space of images and their segmentations. We utilize joint Independent Component Analysis method to generate a model which is further employed to produce a probability map of the target segmentation. We evaluate this approach on the transrectal ultrasound volume images of 60 patients using a leaveone-out cross-validation approach. The results are compared with the manually segmented prostate contours that were used by clinicians to plan brachytherapy procedures. We show that the proposed approach is fast with comparable accuracy and precision to those found in previous studies on TRUS segmentation.

9036-47, Session 10

## Evaluating the utility of 3D TRUS image information in guiding intra-procedure registration for motion compensation

Tharindu S. De Silva, Derek W. Cool M.D., Cesare Romagnoli M.D., Aaron Fenster, Aaron D. Ward, The Univ. of Western Ontario (Canada)

In targeted 3D transrectal ultrasound (TRUS)-guided biopsy, patient and prostate movement during the procedure can cause target misalignments that hinder accurate sampling of pre-planned suspicious tissue locations. Multiple solutions have been proposed for motion compensation via registration of intra-procedural TRUS images to a baseline 3D TRUS image acquired at the beginning of the biopsy procedure. While 2D TRUS images are widely used for intra-procedural guidance, some solutions utilize richer intra-procedural images such as bi- or multi-planar TRUS or 3D TRUS, acquired by specialized probes. In this work, we measured the impact of such richer intra-procedural imaging on motion compensation accuracy, to evaluate the tradeoff between cost and complexity of intra-procedural imaging versus improved motion compensation. We acquired baseline and intra-procedural 3D TRUS images from 29 patients at standard sextant-template biopsy locations. We used the planes extracted from the 3D intra-procedural scans to simulate 2D and 3D information available in different clinically relevant scenarios for registration. The registration accuracy was evaluated by calculating the target registration error (TRE) using manually identified homologous fiducial markers (micro-calcifications). Our results indicate that TRE improves gradually when the number of intra-procedural imaging planes used in registration is increased. Full 3D TRUS information helps the registration algorithm to robustly converge to more accurate solutions. These results can also inform the design of a fail-safe workflow during motion compensation in a system using a tracked 2D TRUS probe, by prescribing rotational acquisitions that can be performed quickly and easily by the physician immediately prior to needle targeting.

9036-48, Session 10

## Toward 3D-guided prostate biopsy target optimization: an estimation of tumor sampling probabilities

Peter R. Martin, Western Univ. Canada (Canada); Derek W. Cool M.D., Robarts Research Institute (Canada); Cesare Romagnoli M.D., The Univ. of Western Ontario (Canada) and London Health Sciences Ctr. (Canada); Aaron Fenster, Robarts Research Institute (Canada); Aaron D. Ward, The Univ. of Western Ontario (Canada) and Western Univ. Canada (Canada)











Magnetic resonance imaging (MRI)-targeted, 3D transrectal ultrasound (TRUS)-guided "fusion" prostate biopsy aims to reduce the ~23% false negative rate of clinical 2D TRUS-guided sextant biopsy. Although it has been reported to double the positive yield, MRI-targeted biopsy still yields false negatives. Therefore, we propose optimization of biopsy targeting to meet the clinician's desired tumor sampling probability, optimizing needle targets within each tumor and accounting for uncertainties due to guidance system errors, image registration errors, and irregular tumor shapes. We obtained multiparametric MRI and 3D TRUS images from 49 patients. A radiologist and radiology resident contoured 81 suspicious regions, yielding 3D surfaces that were registered to 3D TRUS. We estimated the probability, P, of obtaining a tumor sample with a single biopsy. Given an RMS needle delivery error of 3.5 mm for a contemporary fusion biopsy system,  $P \ge 95\%$  for 21 out of 81 tumors when the point of optimal sampling probability was targeted. Therefore, more than one biopsy core must be taken from 74% of the tumors to achieve  $P \ge 95\%$  for a biopsy system with an error of 3.5 mm. Our experiments indicated that the effect of error along the needle axis on the percentage of core involvement (and thus the measured tumor burden) was mitigated by the 18 mm core length.

9036-49, Session 10

#### Distinguishing benign confounding treatment changes from residual prostate cancer on MRI following laser ablation

Geert Litjens, Henkjan J. Huisman, Radboud Univ. Nijmegen Medical Ctr. (Netherlands); Robin Elliott, Case Western Reserve Univ. (United States); Natalie Shih, Hospital of the Univ. of Pennsylvania (United States); Michael D. Feldman, The Univ. of Pennsylvania Health System (United States); Satish E. Viswanath, Case Western Reserve Univ. (United States); Jurgen Futterrer, Joyce Bomers, Radboud Univ. Nijmegen Medical Ctr. (Netherlands); Anant Madabhushi, Case Western Reserve Univ. (United States)

Laser interstitial thermotherapy (LITT) is a relatively new focal therapy technique for the ablation of localized prostate cancer. In this study we are for the first time integrating ex-vivo pathology and MRI to assess the imaging characteristics of prostate cancer and benign confounding treatment changes following LITT on 3 Tesla multi-parametric MRI. Via a unique clinical trial, which gave us the availability of ex-vivo histology and pre- and post-LITT MRI, we (1) investigated the imaging characteristics of treatment effects and residual disease, (2) evaluated treatment induced feature changes in the ablated area relative to the residual disease. Towards this end first a pathologist annotated the ablated area and the residual disease on the ex-vivo histology and then we transferred the annotations to the post-LITT MRI using semi-automatic elastic registration. The pre- and post-LITT MRI were subsequently registered and features extracted. A scoring metric based on change in median pre- and post-LITT feature values was introduced, which allowed us to identify the most treatment responsive features. Finally, we combined this knowledge in a clustering algorithm. Our results show that (1) image characteristics for treatment effects and residual disease are different, (2) change of feature values between pre- and post-LITT MRI can be a quantitative biomarker for treatment response and (3) a clustering approach to separate treatment effects and residual disease incorporating both (1) and (2) yielded a maximum area under the ROC curve of 0.97 over 3 studies.

9036-51, Session 10

## EM-navigated catheter placement for gynecologic brachytherapy: an accuracy study

Alireza Mehrtash, Brigham and Women's Hospital (United States) and Harvard Medical School (United States); Antonio Leonardo Damato, Guillaume Pernelle, Lauren Ashley Barber, Nabgha Farhat, Akila Ninette Viswanathan, Robert A Cormack, Tina Kapur, Brigham and Women's Hospital (United States)

Gynecologic malignancies, which include cervical, endometrial, ovarian, vaginal and vulvar cancers, cause significant mortality in women worldwide. The standard care for many primary and recurrent gynecologic cancers consists of chemoradiation followed by brachytherapy. In high dose rate (HDR) brachytherapy, sources that deliver high doses of radiation are placed directly inside the cancerous tissue using intracavitary applicators or interstitial applicators with catheters. While technology for navigation of catheters and needles is well developed for procedures such as prostate biopsy, brain biopsy, and cardiac ablation, it is notably lacking for gynecologic HDR brachytherapy. We developed a method for evaluating image-guided catheter placement accuracy in a benchtop experiment that closely mimics the clinical interstitial gynecologic brachytherapy procedure. A future bedside translation of this technology offers the potential benefit of maximizing tumor coverage during catheter placement while avoiding adjacent organs, the bladder and the rectum. In the experiment, five catheter insertions procedures were performed on a phantom model; the first to create a target configuration and the rest to test targeting accuracy. The experiment was carried out on a laptop computer (2.1GHz Intel Core i7 computer, 8GB RAM, Windows 7 64-bit), using an EM Aurora tracking system with a 1.3mm diameter 6 DOF sensor, 6F brachytherapy catheters, inserted through a Syed-Neblett applicator. All software was written using the 3D Slicer and PLUS open source software. The mean targeting error was 2.89mm and the standard deviation was 1.93mm in all 48 catheter placements by 3 different operators, which is comparable to targeting errors in commercial clinical navigation systems.

9036-68, Session 10

## MRI-guided prostate focal laser ablation therapy using a mechatronic needle guidance system

Jeremy J. Cepek, Robarts Research Institute (Canada); Uri Lindner, Sangeet Ghai, Sean R. H. Davidson, John Trachtenberg M.D., Univ. Health Network (Canada); Aaron Fenster, Robarts Research Institute (Canada)

Focal therapy of localized prostate cancer is receiving increased attention due to its potential for providing effective cancer control in select patients with minimal treatment-related side effects. Magnetic resonance imaging (MRI)-guided focal laser ablation (FLA) is an attractive modality for such an approach. In FLA therapy, accurate placement of laser fibers is critical to ensuring that the full tumor volume is ablated. In practice, error in needle placement is invariably present due to pre- to intraoperative image registration error, needle deflection, prostate motion, and variability in interventionalist skill. In addition, some of these sources of error are difficult to control, since the available workspace and patient positions are restricted within a clinical MRI bore. In an attempt to take full advantage of the utility of intra-operative MRI, while minimizing error in needle placement, we developed an MRI-compatible mechatronic system for guiding needles to the prostate for FLA therapy. The system has been used to place interstitial catheters for MRI-guided FLA therapy in eight subjects in an ongoing Phase I/II clinical trial. Data from these cases has provided quantification of the level of uncertainty in needle placement error. To relate needle placement error to clinical outcome, we











developed a model for predicting the probability of achieving complete index tumor ablation for a family of parameterized treatment plans. Results from this work have enabled the specification of evidence-based selection criteria for the maximum tumor size that can be confidently ablated using this technique, and a systematic method of generating patient-specific treatment plans.

9036-52, Session 11

### In vivo validation of a 3D ultrasound system for imaging the lateral ventricles of neonates

Jessica Kishimoto, Aaron Fenster, Robarts Research Institute (Canada); Nancy Chen, Western Univ. Canada (Canada); David S. Lee, London Health Research Ctr. (Canada); Sandrine de Ribaupierre, London Health Research Ctr. (Canada) and Western Univ. Canada (Canada)

Dilated lateral ventricles in neonates can be due to many different causes, such as brain loss, congenital malformation, or from blockage of the flow of CSF. Such enlargement can raise intracranial pressure resulting in brain damage, and up to 25% of patients with severely enlarged ventricles have epilepsy in later life. Ventricle enlargement is clinically monitored using 2D US through the fontanels. The sensitivity of 2D US to dilation is poor because it cannot provide accurate measurements of irregular volumes such as the ventricles, so most clinical evaluations are of a qualitative nature.

We developed a 3DUS system to image the cerebral ventricles of neonates within the confines of incubators and can be easily translated to more open environments. Ventricle volumes can be segmented from these images giving a quantitative volumetric measurement of ventricle enlargement without moving the patient into an imaging facility.

In this paper, we report on in vivo validation studies 1) comparing 3DUS ventricle volumes before and after clinically necessary interventions removing CSF and 2) comparing 3DUS ventricle volumes to those from MRI. Post-intervention ventricle volumes were less than pre-intervention measurements for all patients and all interventions. We found high correlations (R = 0.97) between the difference in ventricle volume and the reported removed CSF with the slope not sig different than 1 (p < 0.05). Comparisons between ventricle volumes from 3DUS and MR images taken 4 ( $\pm$ 3.8) days of each other failed to show significant difference (p=0.44) between 3DUS and MRI through paired t-test.

9036-53, Session 11

### Visualizing positional uncertainty in freehand 3D ultrasound

Houssem-Eddine Gueziri, Ecole de Technologie Supérieure (Canada); Michael J McGuffin, Catherine Laporte, École de Technologie Supérieure (Canada)

The freehand 3D ultrasound technique relies on position sensors attached to the probe to register the location of each image to a 3D space. However, the imprecision of the position sensors reduces the reliability of estimated image locations. In this paper, we propose a novel method to compute the positional uncertainty of an image plane. First, we use rigid body point-based registration to compute the error produced by each pixel of the image during the tracking. The Target Registration Error (TRE) is used to compute the covariance matrix of errors at each pixel position. This covariance matrix is then decomposed as a 3D orientation error, in the x, y and z directions. Considering a volume around the image, we introduce the Image Plane Crossing Probability (IPCP) to determine the probability that the plane passes through each voxel. The result is a point cloud probability around the image plane, where each voxel contains the crossing probability and the contribution of each direction of the error. Finally, a simple volume rendering technique is used to visualize the uncertainty of the plane

position. The results are validated in two steps. The first step is a Monte Carlo simulation to validate the estimate of the TRE covariance for the tracking errors. The second step simulates TRE errors on a plane and validates the associated positional uncertainty.

9036-54, Session 11

### Synthetic aperture imaging in ultrasound calibration

Golafsoun Ameri, John S. H. Baxter, A. Jonathan McLeod, Uditha L. Jayaranthe, Elvis C. S. Chen, Terry M. Peters, Robarts Research Institute (Canada)

Ultrasound calibration allows for ultrasound images to be incorporated into a variety of interventional applications. Traditional Z-bar calibration procedures rely on wired phantoms with an a priori known geometry. The line fiducials produce small, localized echoes which are then segmented from an array of ultrasound images from different tracked probe positions. In conventional B-mode ultrasound, the wires at greater depths appear blurred and are difficult to segment accurately, limiting the accuracy of ultrasound calibration. This paper presents a novel ultrasound calibration procedure which takes advantage of synthetic aperture imaging to reconstruct high resolution ultrasound images at all depths. In these images, line fiducials are much more readily and accurately segmented, leading to decreased calibration error. The proposed calibration technique is compared to a one based on B-mode ultrasound. The fiducial localization was improved from 0.24 mm in conventional B-mode images to 0.18 mm in synthetic aperture images corresponding to an improvement of 27%. This resulted in an overall reduction of calibration error from a fiducial registration error of 1.56 mm to 1.42 mm, an improvement of 9%. Synthetic aperture images display greatly improved segmentation capabilities due to their improved resolution and interpretability resulting in improved calibration.

9036-56, Session 12

### Toward standardized mapping for left atrial analysis and cardiac ablation guidance

Maryam E. Rettmann, David R. Holmes III, Mayo Clinic (United States); Cristian A. Linte, Mayo Clinic College of Medicine (United States); Douglas L. Packer, Mayo Clinic (United States); Richard A. Robb M.D., Mayo Clinic College of Medicine (United States)

In catheter-based cardiac ablation, the pulmonary vein ostia are important landmarks for guiding the ablation procedure, and for this reason, have been the focus of many studies quantifying their size, structure, and variability. Analysis of pulmonary vein structure, however, has been limited by the lack of a standardized reference space for population based studies. In this work, we describe a novel technique for computing flat maps of left atrial anatomy in a standardized space. A flat map of left atrial anatomy is created by casting a single ray through the volume and systematically rotating the camera viewpoint to obtain the entire field of view. The technique is validated by assessing preservation of relative surface areas and distances between the original 3D geometry and the flat map geometry. The proposed methodology is demonstrated on 10 subjects which are subsequently combined to form a probabilistic map of anatomic location for each of the pulmonary vein ostia and the boundary of the left atrial appendage. The probabilistic map demonstrates that the location of the inferior ostia have higher variability than the superior ostia and the variability of the left atrial appendage is similar to the superior pulmonary veins. This technique also has potential application in mapping electrophysiology data, radio-frequency ablation burns, or treatment planning in cardiac ablation therapy.











9036-57, Session 12

## Intraoperative measurements on the mitral apparatus using optical tracking: a feasibility study

Sandy Engelhardt, Deutsches Krebsforschungszentrum (Germany); Raffaele De Simone, Ruprecht-Karls-Univ. Heidelberg (Germany); Diana Wald, Deutsches Krebsforschungszentrum (Germany); Norbert Zimmermann, Sameer Al Maisary, Carsten J. Beller, Matthias Karck, Ruprecht-Karls-Univ. Heidelberg (Germany); Hans-Peter Meinzer, Deutsches Krebsforschungszentrum (Germany); Ivo Wolf, Deutsches Krebsforschungszentrum (Germany) and Hochschule Mannheim (Germany)

Mitral valve reconstruction is a widespread surgical method to repair incompetent mitral valves.

During reconstructive surgery the judgement of mitral valve geometry and subvalvular apparatus is mandatory in order to choose for the appropriate repair strategy. To date, intraoperative analysis of mitral valve is merely based on visual assessment and simple inaccurate sizer devices, which do not allow for any accurate measurement of the complex three-dimensional anatomy. We propose a new intraoperative computer-assisted method for mitral valve measurements using a pointing instrument together with an optical tracking system. Sixteen anatomical points were defined on the mitral apparatus. The feasibility and the reproducibility of the measurements have been tested on a rapid prototyping heart model and a freshly exercised porcine heart. Four heart surgeons repeated the measurements three times on each heart. Morphologically important distances between the measured points are calculated. We achieved an interexpert variability mean of 2.28  $\pm$  1.13 mm for the 3D-printed heart and  $2.45 \pm 0.75$  mm for the porcine heart. The overall time to perform a complete measurement is 1-2 minutes, which makes the method viable for virtual annuloplasty during an intervention.

9036-58, Session 12

## Ultrasound based mitral valve annulus tracking for off-pump beating heart mitral valve repair

Feng P. Li, Martin Rajchl, John T. Moore, Terry M. Peters, Robarts Research Institute (Canada)

Mitral regurgitation (MR) occurs when the mitral valve cannot close properly during systole. The NeoChord© tool aims to repair the regurgitating leaflets by implanting an artificial chorda tendinea on a beating heart without a cardiopulmonary bypass. Image guidance is crucial for such a procedure due to lack of direct vision of the targets or instruments. While this procedure is currently guided solely by transesophageal echocardiography (TEE), our previous work has demonstrated that guidance safety and efficiency can be significantly improved by employing augmented virtuality in terms of virtual presentation of mitral valve annulus (MVA) and tools in the system. However, real-time mitral annulus tracking is still a challenge. In this paper, we describe an image-based approach to rapidly track MVA points on 2D/biplane TEE images. This approach is composed of two components: an image-based phasing component identifying images at optimal cardiac phases for tracking, and a registration component updating the coordinates of MVA points. Preliminary validation has been performed on porcine data with an average difference between manually and automatically identified MVA points of 2.5mm. Using a parallelized implementation, this approach is able to track the mitral valve at up to 10 images per second.

9036-59, Session 12

## Patient-specific left atrial wall-thickness measurement and visualization for radiofrequency ablation

Jiro Inoue, Robarts Research Institute (Canada); Allan C. Skanes, Western Univ. Canada (Canada); James A. White, Robarts Research Institute (Canada) and Western Univ. Canada (Canada); Martin Rajchl, Maria Drangova, Robarts Research Institute (Canada)

Introduction: For radiofrequency (RF) catheter ablation of the left atrium, safe and effective dosing of RF energy requires transmural left atrium ablation without injury to extra-cardiac structures. The thickness of the left atrial wall may be a key parameter in determining the appropriate amount of energy to deliver. While left atrial wall thickness is known to amount of energy to deliver. While left atrial wall thickness is known to the current clinical workflow. Our goal is to develop a tool for presenting patient-specific left atrial thickness information to the clinician in order to assist in the determination of the proper RF energy dose.

Methods: We use an interactive segmentation method with manual correction to segment the left atrial blood pool and myocardium from contrast-enhanced cardiac CT images. We then create a mesh from the segmented blood pool and determine the myocardial thickness, on a per-vertex basis, orthogonal to the mesh surface. The thickness measurement is visualized by assigning colors to the vertices of the blood pool mesh. We applied our method to 5 contrast-enhanced cardiac CT images.

Results: Left atrial wall-thickness measurements were generally consistent with published thickness ranges. Variations were found to exist between patients, and between regions within each patient.

Conclusion: It is possible to visually determine areas of thick vs. thin myocardium with high resolution in a patient-specific manner.

9036-60, Session 12

## Mapping cardiac fiber orientations from high resolution DTI to high frequency 3D ultrasound

Xulei Qin, Silun Wang, Ming Shen, Xiaodong Zhang, Mary B. Wagner, Emory Univ. (United States); Baowei Fei, Emory Univ. (United States) and Georgia Insitute of Technology (United States)

The orientation of cardiac fibers in the heart affects the cardiac anatomical, mechanical, and electrophysiologic properties. Although echocardiography is the most common imaging modality in clinical cardiac examination, it can only provide the cardiac geometry or motion information without cardiac fiber orientations. If the patient's cardiac fiber orientations can be mapped to his/her echocardiography images in the clinical examinations, it may provide quantitative and comprehensive parameters for diagnosis, personalized modeling, and image-guided cardiac therapies. Therefore, this project addresses the feasibility of mapping the personalized cardiac fiber orientations to 3D ultrasound volumes. First, the geometry of the heart extracted from the MRI is translated to 3D ultrasound by rigid and deformable registration. After the registration, the deformable fields between both geometries from MRI and ultrasound are obtained. In the registration step, three different deformable registration methods were utilized and their corresponding volume Dice similarity scores were all over 90% and the corresponding target errors were less than 0.25 mm. Finally, the cardiac fiber orientations imaged by DTI are mapped to ultrasound volumes based on the extracted deformation fields between both geometries from MRI and ultrasound. The proposed approach can provide cardiac fiber orientations to ultrasound images and can have many potential applications in cardiac imaging and image-guided procedures.











9036-72, Session 12

## Efficient feature-based 2D/3D registration of transesophageal echocardiography to x-ray fluoroscopy for cardiac interventions

Charles R. Hatt, Michael A. Speidel, Amish N. Raval, Univ. of Wisconsin-Madison (United States)

We present a novel 2D/3D registration algorithm for fusion between transesophageal echocardiography (TEE) and X-ray fluoroscopy (XRF). The TEE probe is modeled as a subset of 3D gradient and intensity point features, which facilitates efficient 3D-to-2D perspective projection. A novel cost-function, based on a combination of intensity and edge features, evaluates the registration cost value without the need for time-consuming generation of digitally reconstructed radiographs. Validation experiments were performed with simulations and phantom data. Simulations found a target registration error of 1.08(1.93) mm for biplane(monoplane) geometries. Our feature-based registration method greatly reduces computational load, which is necessary for achieving the goal of real-time, accurate image based registration between TEE and XRF.

#### 9036-25, Session PSWed

## Automatic thoracic anatomy segmentation at CT using hierarchical fuzzy models and registration

Kaioqiong Sun, Nanchang Hangkong Univ. (China); Jayaram K. Udupa, Dewey Odhnera, Univ. of Pennsylvania (United States); Yubing Tong, The Univ. of Pennsylvania Health System (United States)

This paper proposes a thoracic anatomy segmentation method based on hierarchical recognition and delineation guided by built model. Labeled binary samples for each organ are registered and aligned into a 3-d fuzzy set representing the shape model for the organ. The gray intensity distributions of the corresponding regions of the organ in original image are recorded in the model. The hierarchical relation and mean location relation between different organs are also concentrated in the model. Following the model, different organs in target image are registered into the corresponding shape model based on the hierarchical structure and location relation in the model. Fuzzy connected delineation method is then used to obtain the last segmentation result of organs with seed point provided by recognition. The 3d model combined with affine register method ensures that accurate recognition can be obtained for both nonsparse and sparse organ. The hierarchical structure and location relation integrated in the model provides the initial parameters of the affine transform and makes the registration fast and accurate. The results on real angiogram are presented.

#### 9036-50, Session PSWed

## Towards Enabling Ultrasound Guidance in Cervical Cancer High-Dose-Rate Brachytherapy

Adrian Wong, Samira Sojoudia, The Univ. of British Columbia (Canada); Marc Gaudet, British Columbia Cancer Agency (Canada); Wan Wan Yap, British Columbia Cancer Agency (Canada) and Division of Radiation Oncology, BC Cancer Agency (Canada); Silvia D Chang, Purang Abolmaesumi, The Univ. of British Columbia (Canada); Christina Aquino-Parsons, British Columbia Cancer Agency (Canada); Mehdi Moradi, The Univ. of British Columbia (Canada)

MRI and computed tomography (CT) are used in image-based solutions for guiding high dose rate (HDR) brachytherapy treatment of cervical cancer. MRI is costly and CT exposes the patients to ionizing radiation. Ultrasound, on the other hand, is affordable and safe. The long term goal of our work is to enable the use of multiparametric ultrasound imaging in image-guided HDR for cervical cancer. In this paper, we report the development of enabling technology for ultrasound guidance and tissue typing. We report a system to obtain the 3D freehand transabdominal ultrasound RF signals and B-mode images of the uterus, and a method for registration of ultrasound to MRI. MRI and 3D ultrasound images of the female pelvis were registered by contouring the uterus in the two modalities, creating a surface model, followed by rigid and B-spline deformable registration. The resulting transformation was used to map the location of the tumor from the T2-weighted MRI to ultrasound images and to determine cancerous and normal areas in ultrasound. B-mode images show a contrast for cancer vs. normal tissue. Our study shows the potential and the challenges of ultrasound imaging in guiding cervical cancer treatments.

#### 9036-61, Session PSWed

### Detection of tooth fractures in CBCT images using attention index estimation

Andre Souza, Carestream Health, Inc. (United States); Alexandre X. Falcão, Univ. Estadual de Campinas (Brazil); Lawrence A. Ray, Carestream Health, Inc. (United States)

The attention index ( $\phi$ ) is a number from zero to one that indicates a possible fracture detected inside a selected tooth. The higher the  $\phi$ number, the greater the likelihood for needed attention in the visual examination. The method developed for  $\phi$  estimation extracts a connected component with image properties that are similar to those of a typical tooth fracture. That is, in cone-beam computed tomography (CBCT) images, it appears as a dark canyon inside the tooth. The method also provides a plane across the geometric center of the suspicious fracture component, which maximizes the number of pixels from that component inside the plane, in order to start the visual examination process. During visual examination, the user (doctor) can change plane orientations and locations by manipulating the mouse toward different graphical elements that represent the plane on a 3D rendition of the tooth, while the corresponding image of the plane is shown at its side. The visual examination aims at confirming or disproving the fracturedetection event. We have designed and implemented these algorithms using the image foresting transform methodology.

#### 9036-62, Session PSWed

## Segmentation of 3D ophthalmic CT images based on the analytic eye model for the purposes of proton therapy planning

Anastasia Makarova, Dmitrij Orlov, Igor Erokhin, Mihail Lomanov, Institute for Theoretical and Experimental Physics (Russian Federation)

In the course of proton therapy planning of ophthalmic malignancies the structure identification is difficult due to relative tissue homogeneity. The uncertainties in a dosimetric plan caused by imperfect segmentation affect the positioning time as well as accuracy of dose delivery. Our investigation is based on using of extended analytic eye model for an image registration in the new application aimed to reduce the difficulty of the segmentation process. The new detailed eye model was developed based on Gullstrand model. It provides continuous linking of eye structures and takes into account the age of a patient and eye ametropia. The model includes following parameters: standard (table data averaged over the age group), topometric (measured individually by physician) and calculated. The task is implemented with use of Insight Segmentation and Registration Toolkit (ITK) and Visualization Toolkit (VTK) C++ libraries.











The stack of CT images is displayed with volume rendering technique. The hierarchical structure of the model is realized through ITK Spatial Object class and its subclasses. ITK model based registration abilities are implemented for automatic registration of an eye model to CT image. Spatial Object is converted to VTK Polygonal Data for visualization. Manual adjustment of the model parameters is provided by VTK cell picking classes. The adjusted model is converted to voxel structure for dose calculations. Finally, the treatment plans implementing the new eye model are evaluated in comparison with previously planned procedures.

9036-63, Session PSWed

# Updating a preoperative surface model with information from real-time tracked 2D ultrasound using a Poisson surface reconstruction algorithm

Deyu Sun, Maryam E. Rettmann, David R. Holmes III, Mayo Clinic (United States); Cristian A. Linte, Mayo Clinic College of Medicine (United States); Douglas L. Packer, Mayo Clinic (United States); Richard A. Robb M.D., Mayo Clinic College of Medicine (United States)

In this work, we propose a method to for intraoperative reconstruction of a left atrial surface model for the application of cardiac ablation therapy. In this approach, the intraoperative point cloud is acquired by tracked, ECG-gated 2D freehand intra-cardiac echocardiography device, which is registered and merged with a preoperative, high resolution left atrial surface model built from CT. For the surface reconstruction, we introduce a novel method to estimate the normal vector of the point cloud from the preoperative left atrial model, which is required for the Poisson Equation Reconstruction algorithm. In the current work, the algorithm is evaluated using a preoperative surface model from patient CT data and simulated intraoperative ultrasound data. Factors such as intraoperative deformation of the left atrium, proportion of the left atrial surface sampled by the ultrasound, sampling resolution, sampling noise, and registration error were considered through a series of simulation experiments.

9036-64, Session PSWed

### Hand-eye calibration using dual quaternions in medical environment

Danilo Briese, Siemens AG (Germany) and Otto-von-Guericke-Univ. Magdeburg (Germany); Christine Niebler, Siemens AG (Germany); Georg Rose, Otto-von-Guericke-Univ. Magdeburg (Germany)

Nowadays medical interventions are often supported by localization systems using different measurement tools (MT). This requires to register the MT coordinate sytem to the world coordinate system used by the medical device. The hand-eye calibration is a well-known method from robotics to estimate the transformation between the gripper of a robot (hand) and a MT (eye) rigidly attached to the robot. Using a calibration tool (e.g. checker board) one can obtain the hand-eye transformation using known relative movements of the robot and the data from the MT. The approach can also be used for MT located elsewherefootnote [E.,g. a ceiling mounted camera system with optical markers} using markers on the device. The position of the markers is not required to be known since they are rigid during the motions. Based on prior work using dual quaternions to represent transformations in the SE(3) we not only took into account movements between immediate neighbour positions P<sub>i</sub> and P<sub>i</sub>, but combined all positions to gain (P<sub>2</sub>) submotions in every subset  $\Sigma_{p}^{p}=3(p)^{+}$  footnote{With P is the number of conducted positions.} without increasing the number of positions conducted during the calibration. We took into account the unity constraint for dual quaternions since only those represent rigid motions in space. We performed simulations

that show the advantage of our algorithm. Additionally we gained experimental data which supported the outcome of the simulations. We can outline that our approach achieves more accurate results estimating the hand-eye transformation than the aforementioned algorithms.

9036-65, Session PSWed

## Distribution of guidance models for cardiac resynchronization therapy in the setting of multi-center clinical trials

Martin Rajchl, Kamyar Abhari, John Stirrat, Eranga Ukwatta, Diego Cantor-Rivera, Feng P. Li, Terry M. Peters, James A. White, Robarts Research Institute (Canada)

Multi-center trials provide the unique ability to investigate novel techniques across a range of geographical sites with sufficient statistical power, the inclusion of multiple operators determining feasibility under a wider array of clinical environments and workflows. For this purpose, we introduce a new means of distributing pre-procedural cardiac models for image-guided interventions across a large scale multi-center trial. In this method, a single core facility is responsible for image processing, employing a novel web-based interface for model visualization and distribution. The requirements for such an interface, being WebGL-based, are minimal and well within the realms of accessibility for participating centers. We then demonstrate the accuracy of our approach using a single-center pacemaker lead implantation trial with generic planning models.

9036-66, Session PSWed

# Open framework for management and processing of multi-modality and multidimensional imaging data for analysis and modeling muscular function

David García, Univ. Hospital of Geneva (Switzerland); Bénédicte M. A. Delattre, Philips Healthcare (Switzerland); Sara Trombella, Univ. Hospital of Geneva (Switzerland); Sean Lynch, Medizinische Hochschule Hannover (Germany); Matthias Becker, Univ. of Geneva (Switzerland); Hon Fai Choi, Univ. of Geneva (Switzerland); Osman Ratib, Univ. Hospital of Geneva (Switzerland)

Musculoskeletal disorders (MSD) are becoming a big healthcare economical burden in developed countries with aging population. Classical methods like biopsy or EMG used in clinical practice for muscle assessment are invasive and not accurately sufficient for measurement of impairments of muscular performance. Non-invasive imaging techniques can nowadays provide effective alternatives for static and dynamic assessment of muscle function. In this paper we present work aimed toward the development of a generic data structure for handling n-dimensional metabolic and anatomical data acquired from hybrid PET/ MRI scanners. Special static and dynamic protocols were developed for assessment of physical and functional images of individual muscles of the lower limb. In an initial stage of the project a manual segmentation of selected muscles was performed on high-resolution 3D static images and subsequently interpolated to full dynamic set of contours from selected 2D dynamic images across different levels of the leg. This results in a full set of 4D data of lower limb muscles at rest and during exercise. These data can further be extended to a 5D data by adding metabolic data obtained from PET images. Our data structure and corresponding image processing extension allows for better evaluation of large volumes of multidimensional imaging data that are acquired and processed to generate dynamic models of the moving lower limb and its muscular function.











9036-67, Session PSWed

### Innovation in aortoiliac stenting, an in vitro comparison

Erik Groot Jebbink, Univ. Twente (Netherlands) and Rijnstate Hospital (Netherlands); Peter C. J. M. Goverde, Vascular Clinic ZNA (Belgium); Jacques A. van Oostayen, Michel M. P. J. Reijnen, Rijnstate (Netherlands); Cornelis H. Slump, Univ. Twente (Netherlands)

Aortoiliac occlusive disease (AIOD) may cause disabling claudicatio, due to progression of atherosclerotic plaque. Bypass surgery to treat AIOD has unsurpassed patency results, with 5-year patency rates up to 86%, at the expense of high complication rates. Therefore, less invasive, endovascular treatment of AOID with stents in both iliac limbs is the first choice in many cases, however, with limited results (5-year patency: 63%). Changes in blood flow due to an altered geometry of the bifurcation is likely to be one of the contributing factors. The aim of this study is to compare the geometry and hemodynamics of various aortoiliac stent configurations in vitro.

Transparent vessel phantoms mimicking the anatomy of the aortoiliac bifurcation are created to accommodate stent configurations. Bare metal kissing stents (BMK), kissing covered (KC) stents and the Covered Endovascular Reconstruction of the Aortic bifurcation (CERAB) configuration are investigated. Ellipses fitted to axial CT slices of the stent lumen provide a measure for stent conformation ratio (D-ratio). Furthermore the area between the vessel and stent (mismatch areas) are determined. The phantoms are placed in a flow rig, to obtain flow patterns from dye injection.

The proximal D-ratios for the BMK, KC, CERAB are 1.6, 1.13 and 1.45 respectively. The proximal mismatch area, in mm?, is 24.75, 56.68 and 4.04. Dye injection reveals flow disturbances near the neobifurcation of both BMK and KC stents.

Although, BMK stents have a high D-ratio, the lowest radial mismatch was found in the CERAB configuration. The flow perturbations seen with the KC and BMK configuration are surmounted by the CERAB configuration.

9036-69, Session PSWed

### Preliminary study of rib articulated model based on dynamic fluoroscopy images

Pierre-Frederic Villard, LORIA (France); Pierre Escamilla, GE Healthcare (France); Erwan Kerrien, INRIA (France); Sébastien Gorges, Yves L. Trousset, GE Healthcare (France); Marie-Odile Berger, INRIA (France)

We present in this paper a preliminary study of rib motion tracking during Interventional Radiology (IR) fluoroscopy guided procedures. It consists in providing a physician with moving rib three-dimensional (3D) models projected in the fluoroscopy plane during a treatment. The strategy is to help to quickly recognize the target and the no-go areas i.e. the tumor and the organs to avoid. The method consists in i) elaborating a kinematic model of each rib from a preoperative computerized tomography (CT) scan, ii) processing the on-line fluoroscopy image and iii) optimizing the parameters of the kinematic law such as the transformed 3D rib projected on the medical image plane fit well with the previously processed image.

In order to have an initial idea of the expected signal linked to the respiration cycle, we plot the diaphragm motion by taking a craniocaudal point displacement with respect to the time. A periodic breathing cycle is recognizable and there are around six respiration cycles during the nine seconds of the experiment giving a respiration rate between 30 and 40.

The optimization process has been performed on four ribs. The results show a visually good rib tracking. For each of them we plot the angle

evolution with each time step of the fluoroscopy image. Rib motion has been quantitatively validated by checking the correspondence with the diaphragm motion signal. The six breathing phases are synchronized. In order to quantify it we analyzed the signal with a Fourier power transform that shows a good synchronism between ribs.

9036-70, Session PSWed

## Solving for free-hand and real-time 3D ultrasound calibration with anisotropic orthogonal Procrustes analysis

Elvis C. S. Chen, Robarts Research Institute (Canada); A. Jonathan McLeod, Uditha L. Jayarathne, Western Univ. Canada (Canada); Terry M. Peters. Robarts Research Institute (Canada)

In the context of ultrasound calibration, we present a novel plane-based phantom for real-time 3D ultrasound calibration. Exploiting on the concept of mathematical fiducial, i.e. that the intersection of any 3 non-parallel planes is a point, this phantom allows for automatic and robust fiducial localization. We also present a novel numerical solution to solve for the calibration parameters (comprising of anisotropic scales, rotation, and translation) using recent advancements in the field of Orthogonal Procrustes Analysis. Based on the Majorization Principle, this algorithm is guaranteed to converge monotonically towards the global optimum from any initialization. This algorithm is used to solve for fiducial-based calibration for both free-hand 2D and real-time 3D ultrasound.

9036-71, Session PSWed

### Motion and deformation compensation for freehand prostate biopsies

Siavash Khallaghi, Saman Nouranian, Samira Sojoudi, Hussam A. Ashab, Lindsay Machan, Silvia D. Chang, Peter Black, Martin Gleave, Larry Goldenberg, Purang Abolmaesumi, The Univ. of British Columbia (Canada)

In this paper, we present a registration pipeline to compensate for prostate motion and deformation during a targeted freehand prostate biopsies. We perform 2D-3D registration by reconstructing a thin-volume around the real-time 2D ultrasound imaging plane. Constrained Sum of Squared Differences (SSD) and gradient descent optimization are used to rigidly align the moving volume to the fixed thin-volume. Subsequently, B-spline deformable registration is performed to compensate for remaining non-linear deformations. SSD and zero-bounded Limited memory Broyden Fletcher Goldfarb Shannon (LBFGS) optimizer are used to find the optimum B-spline parameters. Registration results are validated on three prostate biopsy patients. Initial experiments suggest thin-volume-to-volume registration to be more effective than slice-to-volume registration. Also, a consistent 3 mm improvement of Target Registration Error (TRE) is achieved following the deformable registration.

9036-73, Session PSWed

### Effects of intraoperative CT scanning on the accuracies of electromagnetic tracking

Elodie Lugez, Queen's Univ. (Canada); David R. Pichora, Kingston General Hospital (Canada); Selim G. Akl, Randy E. Ellis, Queen's Univ. (Canada)

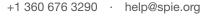
Tracking during surgeries that use intraoperative CT scanning is technically challenging. Each step and component of scan acquisition, from the type of table to X-ray generation inside the CT gantry, may have an effect on electromagnetic tracking. In this study, we investigated four states of mobile-gantry CT scanning: static CT gantry with X-ray













scanning; static CT gantry with X-ray idle; moving CT gantry with X-ray scanning; moving CT gantry with X-ray idle.

We examined the variations of position measurement accuracies as a function of the sensor location within the measured volume, and then as a function of the sensor orientation within the sensed volume. In addition, we assessed the variations of orientation measurement accuracies as a function of the sensor's location and sensor's orientation within the sensed volume. In doing so, two devices were manufactured to respectively translate or rotate a sensor.

Although some of the paths of the orienting scaffold were not detectable by the tracking system, we observed consistent results in the four states assessed. The position RMS accuracy was 5.1 mm when translating the sensor and 26.6 mm when rotating the sensor. The orientation RMS accuracy was 1.6 degrees when translating the sensor, and 5.6 degrees when rotating the sensor.

These results suggest that the state of the CT scanner did not influence EM tracking performance. However, the inherent properties of the CT gantry greatly affected the EM measurement accuracies, especially when the orientation of the sensor varied.

9036-74, Session PSWed

### SimITK: model driven engineering for medical imaging

Melissa Trezise, Queen's Univ. (Canada); David Gobbi, Univ. of Calgary (Canada); James Cordy, Queen's Univ. (Canada); Purang Abolmaesumi, The Univ. of British Columbia (Canada); Parvin Mousavi, Queen's Univ. (Canada)

The Insight Segmentation and Registration Toolkit (ITK) is a highly utilized open source medical imaging library providing chiefly the functionality to register, segment, and filter medical images. Although extremely powerful, ITK has a steep learning curve for users with little or no background in programming. It was for this reason that SimITK was developed. SimITK wraps ITK into the model driven engineering environment Simulink, a part of the Matlab development suite. The first released version of SimITK was a proof of concept, and demonstrated that ITK could be wrapped successfully in Simulink.

In this paper a new version of SimITK is presented where ITK classes are wrapped using a fully automated process. SimITK includes thirty-seven image filters, twelve optimizers, and nineteen transform classes from ITK version 4 which are successfully wrapped and tested, and can be quickly and easily combined to perform medical imaging tasks. These classes were chosen to represent a broad range of usability and to allow for greater flexibility when creating registration pipelines. Many improvements were also implemented including real-time monitoring of the optimization process for image registration. SimITK has the potential to reduce the learning curve for ITK and allow the user to focus on developing workflows and algorithms. A release of SimITK along with tutorials and videos are available at www.simitkvtk.com.

9036-75, Session PSWed

### Automatic labeling and segmentation of vertebrae in CT images

Abtin Rasoulian, Robert N. Rohling, Purang Abolmaesumi, The Univ. of British Columbia (Canada)

Labeling and segmentation of the spinal column from CT images is a pre-processing step for a range of image-guided interventions. State-of-the art techniques have focused either on image feature extraction or template matching for labeling of the vertebrae followed by segmentation of each vertebra. Recently, statistical multi-object models have been introduced to extract common statistical characteristics among several anatomies. In particular, we have created models for segmentation of the lumbar spine which are robust, accurate, and computationally tractable.

In this paper, we reconstruct a statistical multi-vertebrae pose+shape model and utilize it in a novel framework for labeling and segmentation of vertebra in a CT image. We validate our technique in terms of accuracy of the labeling and segmentation of CT images acquired from 56 subjects. The method correctly labels all vertebrae in 70% of patients and is one level off for the remaining 30%. The mean distance error achieved for the segmentation is 2.1(0.7) mm.

9036-76, Session PSWed

### Design and development of an ultrasound calibration phantom and system

Alexis Cheng, Martin K. Ackerman, Gregory S. Chirikjian, Johns Hopkins Univ. (United States); Emad M. Boctor, Johns Hopkins Outpatient Ctr. (United States)

Image-guided surgery systems are often used to provide surgeons with informational support. Due to several unique advantages such as there being no ionizing radiation, ease of use, and real-time images, ultrasound is a common medical imaging modality used in image-guided surgery systems. To perform advanced forms of guidance with ultrasound, such as virtual image overlays or automated robotic actuation, an ultrasound calibration process must be performed. This process recovers the rigid body transformation between a tracked marker attached to the ultrasound transducer and the ultrasound image. A phantom or model with known geometry is also required. In this work, we design and test an ultrasound calibration phantom and software. The two main considerations in this work are utilizing our knowledge of ultrasound physics to design the phantom and delivering an easy to use calibration process to the user. We explore the use of a three-dimensional printer to create the phantom in its entirety without need for user assembly. We have also developed software to automatically segment the threedimensional printed rods from the ultrasound image by leveraging knowledge about the shape and scale of the phantom. In this work, we present preliminary results from using this phantom to perform ultrasound calibration. We match the projection of the points segmented from the image to the known model and calculated a sum squared difference between each point of 1.6mm ± 1.2mm. Future work will compare calibration using our phantom and software with other conventional methods.

9036-77. Session PSWed

### Computational modeling and analysis for left ventricle motion using CT/Echo image fusion

Ji-Yeon Kim, Nahyup Kang, Hyoung-Euk Lee, James D. K. Kim, Samsung Advanced Institute of Technology (Korea, Republic of)

In order to diagnose heart disease such as myocardial infarction, 2D strain through the speckle tracking echocardiography (STE) or the tagged MRI is often used. However out-of-plane strain measurement using STE or tagged MRI is inaccurate. Therefore, strain for whole organ which are analyzed by simulation of 3D cardiac model can be applied in clinical diagnosis. To simulate cardiac contraction in a cycle, cardiac physical properties should be reflected in cardiac model. The myocardial wall in left ventricle is represented as a transversely orthotropic hyperelastic material, with the fiber orientation varying sequentially from the epicardial surface, through about 0° at the midwall, to the endocardial surface. A time-varying elastance model is simulated to contract myocardial fiber, and physiological intraventricular systolic pressure curves are employed for the cardiac dynamics simulation in a cycle. And an exact description of the cardiac motion should be acquired in order that essential boundary conditions for cardiac simulation are obtained effectively. Real time cardiac motion can be acquired by using echocardiography and exact cardiac geometrical 3D model can be reconstructed using 3D CT data. In this research, image fusion technology from CT and echocardiography is employed in order to consider patient-specific left ventricle movement.











Finally, longitudinal strain from STE which is known to fit relatively well actual result is used to verify these results.

9036-78, Session PSWed

## Colonoscope navigation system using colonoscope tracking method based on line registration

Masahiro Oda, Hiroaki Kondo, Nagoya Univ. (Japan); Takayuki Kitasaka, Aichi Institute of Technology (Japan); Kazuhiro Furukawa M.D., Ryoji Miyahara M.D., Nagoya Univ. Graduate School of Medicine (Japan); Yoshiki Hirooka M.D., Nagoya Univ. Hospital (Japan); Hidemi Goto M.D., Nagoya Univ. Graduate School of Medicine (Japan); Nassir Navab, Technische Univ. München (Germany); Kensaku Mori, Nagoya Univ. (Japan)

This paper presents a new colonoscope navigation system, CT colonography is utilized for colon diagnosis based on CT images. If polyps are found while CT colonography, colonoscopic polypectomy can be performed to remove them. While performing a colonoscopic examination, a physician controls colonoscope based on his/her experience. Inexperienced physicians may occur complications such as colon perforation while colonoscopic examinations. To reduce complications, a navigation system of colonoscope while performing the colonoscopic examinations is necessary. We propose a colonoscope navigation system. This system has a new colonoscope tracking method. This method obtains a colon centerline from a CT volume of a patient. A curved line (colonoscope line) representing the shape of colonoscope inserted to the colon is obtained by using electromagnetic sensors. A coordinate system registration process that employs the ICP algorithm is performed to register the CT and sensor coordinate systems. The colon centerline and colonoscope line are registered by using a line registration method. The position of the colonoscope tip in the colon is obtained from the line registration result. Our colonoscope navigation system displays virtual colonoscopic views generated from the CT volumes. A viewpoint of the virtual colonoscopic view is a point on the centerline that corresponds to the colonoscope tip. Experimental results using a colon phantom showed that the proposed colonoscope tracking method can track the colonoscope tip with small tracking errors.

#### 9036-79, Session PSWed

#### Intraoperative imaging of cortical perfusion by time-resolved thermography using cold bolus approach

Julia Hollmach, Christian Schnabel, Nico Hoffmann, Yordan Radev, Stephan B. Sobottka, Matthias Kirsch, Gabriele Schackert, Edmund Koch, Gerald Steiner, Technische Univ. Dresden (Germany)

In the past decades, thermographic cameras with high thermal and temporal resolution of up to 30 mK and 50 Hz, respectively, have been developed. These sophisticated camera systems are able to reveal thermal variations and heterogeneities of tissue and blood. Thus, they provide a sensitive, noninvasive, label-free, and fast application to investigate blood perfusion and to detect perfusion disorders. Therefore, time-resolved thermography is evaluated and tested for intraoperative imaging of the cerebral cortex during neurosurgeries.

The motivation of this study is the intraoperative evaluation of the cortical perfusion by observing the temporal temperature curve of an intravenously applied cold bolus. The temperature curve of a cold bolus is influenced by thermodilution, depending on the temperature difference to the system, the course of the path and mixing.

In this initial study, a flow phantom was used in order to determine the

temperature variations of cold boli under stable conditions in a vascular system. The typical temperature profile of cold water passing by can be approximated by a bi-Gaussian function involving a set of four parameters. These parameters can be used to assess the cold bolus, since they provide information about its intensity, duration and arrival time. The findings of the flow phantom can be applied, under certain conditions, to thermographic measurements of the human cortex. The results demonstrate that time-resolved thermographic imaging is a suitable method to detect cold boli not only at a flow phantom but also at the human cortex.

9036-80, Session PSWed

## Registration based filtering: an acceptable tool for noise reduction in left ventricular dynamic rotational angiography images?

Jean-Yves Wielandts M.D., Stijn De Buck, Joris Ector M.D., Dieter Nuyens M.D., Frederik Maes, Hein Heidbuchel M.D., Katholieke Univ. Leuven (Belgium)

VT ablations could benefit from Dynamic 3D (4D) left ventricle (LV) visualization as road-map for anatomy-guided procedures. We developed a registration-based method that combines information of several cardiac phases to filter out noise and artifacts in low-dose 3D Rotational Angiography (3DRA) images. This also enables generation of accurate multi-phase surface models by semi-automatic segmentation (SAS). The method uses B-spline non-rigid inter-phase registration (IPR) and subsequent averaging of the registered 3DRA images of 4 cardiac phases, acquired with a slow atrial pacing protocol, and was validated on data from 5 porcine experiments. IPR parameter settings were optimized against manual delineations of the LVs using a composed similarity score (Q), dependent on DICE-coefficient, RMSDistance, Hausdorff (HD) and the percentage of inter-surface distances <3mm and <4mm. The latter are clinically acceptable error cut-off values. Validation was performed after SAS for varying voxel intensity thresholds (ISO), by comparison between models with and without prior use of IPR. Distances to the manual delineations at optimal ISO were reduced to  $\leq$ 3mm for 95.6±2,7% and to  $\leq$ 4mm for 97.1±2.0% of model surfaces. Improved quality was proven by significant mean Q-increase irrespective of ISO (7.75% at optimal ISO (95%CI 4.60-10.90, p<0.0001). Quality improvement was more important at suboptimal ISO values. Significant (p<0.0001) differences were also noted in HD (-21,35%; 95%CI -18,61%--24,10%), RMSD (-32,60%; 95%CI -29,79%--35,41%) and DICE (+4,33%; 95%CI +2,85%-+5,82%). Generating 4D LV models proved feasible, with sufficient accuracy for clinical applications, opening the perspective of more accurate overlay and guidance during ablation in locations with high degrees of movement.

9036-81, Session PSWed

#### Dimensional accuracy of 3D printed vertebra

Kent M. Ogden, Nathaniel Ordway, Dalanda Diallo, Gwen Tillapaugh-Fay, SUNY Upstate Medical Univ. (United States); Can Asian, Syracuse Univ. (United States)

3D printer applications in the biomedical sciences and medical imaging are expanding and will likely have an important impact on the practice of medicine. Orthopedic surgery has been an obvious area for development of 3D printer applications as the segmentation of bony anatomy is relatively straightforward. There are important issues that should be addressed when using 3D printed models for applications that may affect patient care; in particular the dimensional accuracy of the printed parts needs to be accurate to avoid poor decisions being made prior to surgery or therapeutic procedures. In this work, the dimensional accuracy of a 3D printed vertebral body derived from CT data for a cadaver spine is compared with direct measurements on the ex-vivo vertebra and with measurements made on the 3D rendered vertebra using commercial 3D











image processing software. The vertebra was printed on a consumer grade 3D printer using an additive print process using PLA (polylactic acid) filament. Measurements were made for 15 different anatomic features of the vertebral body, including vertebral body height, endplate width and depth, pedicle height and width, and spinal canal width and depth, among others. It is shown that for the segmentation and printing process used, the results of measurements made on the 3D printed vertebral body are substantially the same as those produced by direct measurement on the vertebra and measurements made on the 3D rendered vertebra.

9036-82, Session PSWed

### A tool for intraoperative visualization of registration results

Franklin King, Andras Lasso, Csaba Pinter, Gabor Fichtinger, Queen's Univ. (Canada)

PURPOSE: Validation of image registration algorithms is frequently accomplished by the visual inspection of the resulting linear or deformable transformation due to the lack of ground truth information. Visualization of transformations produced by image registration algorithms during image-guided interventions allows for a clinician to evaluate the accuracy of the result transformation. Software packages that perform the visualization of transformations exist, but are not part of a comprehensive and extensible application framework or otherwise have other shortcomings. We present a tool that visualizes both linear and deformable transformations and is integrated in an open-source software application framework suited for intraoperative use. METHODS: Visualization of transformations is accomplished by representing the transformation as a vector field with a choice of six different modes. Glyph visualization mode uses oriented and scaled glyphs, such as arrows, to represent the deformation field in 3D whereas glyph slice visualization mode creates arrows that can be seen as a 2D vector field. Grid visualization mode creates deformed grids shown in 3D whereas grid slice visualization mode creates a series of 2D grids. Block visualization mode creates a deformed rectangular model. Finally, contour visualization mode creates isosurfaces and isolines that visualize the magnitude of deformation across a volume. The transform visualizer was implemented as a plugin for the application 3D Slicer. 3D Slicer is a comprehensive open-source application framework developed for medical image computing. RESULTS: The transform visualizer tool fulfilled the requirements for quick evaluation of intraoperative image registrations. The plugin is freely available as an extension for 3D Slicer. CONCLUSION: A tool for the visualization of deformation fields was created and integrated into 3D Slicer, facilitating the validation of image registration algorithms within a comprehensive application framework suited for intraoperative use.

9036-83, Session PSWed

# Effects of deformable registration algorithms on the creation of statistical maps for preoperative targeting in deep brain stimulation procedures

Yuan Liu, Pierre-François D'Haese, Benoit M. Dawant, Vanderbilt Univ. (United States)

Deep brain stimulation, which is used to treat various neurological disorders, involves implanting a permanent electrode into precise targets deep in the brain. Accurate pre-operative localization of the targets is difficult to achieve, as these are typically located in homogenous regions with poor contrast. Population-based statistical atlases are often used to assist with this process. These atlases are created by acquiring the location of efficacious target points in many subjects and projecting these onto reference image volumes using non-rigid registration algorithms. The registration algorithm used in the normalization process

may bias the atlases and it is thus important to study how different deformable registration methods may affect the process. In this paper, we have qualitatively and quantitatively compared six well-known deformable registration methods using various metrics designed to measure the centroid, spread, and shape of the statistical maps. This study is conducted on a large-scale dataset which includes 100 patient volumes and three additional volumes used as references, resulting in a total of 1800 deformable registrations. Results show that statistical atlases constructed by different deformable registration methods share comparable centroids and spreads with marginal differences in their shape. Among the six methods being studied, Diffeomorphic Demons performs the most differently with centroids being furthest apart and largest spreads, but differences between mean spread values are not found to be significant.

9036-84, Session PSWed

### Design of a tracked ultrasound calibration phantom made of LEGO bricks

Ryan A. Walsh, Marie Soehl, Adam Rankin, Andras Lasso, Queen's Univ. (Canada); Gabor Fichtinger, Queen's Univ. (Canada) and Cancer Care Ontario (Canada)

PURPOSE: This paper presents a low cost, available N-wire phantom for tracked ultrasound calibration made from LEGO bricks. A phantom constructed from widely available materials allows a lower cost, more available and modifiable model that can be built in less time compared to 3D printed phantom models. METHODS: To affirm the phantom's reproducibility and build time, ten builds were done by first-time users. The phantoms were used for a tracked ultrasound calibration by an experienced user. The success of each user's build was determined by the lowest root mean square (RMS) wire reprojection error of three calibrations. RESULTS: The phantom was successfully built by all ten first-time users in an average time of 18.8 minutes. It cost \$10.60 CAD for the required LEGO® bricks and averaged a 0.69mm of error for ultrasound calibrations. It is one third the cost of similar 3D printed phantoms and takes much less time to build. CONCLUSION: It was found that the phantom could be reproduced more easily, was one third the cost, more accessible and faster to build than similar 3D printed models. The proposed phantom was found to be capable of producing equivalent calibrations to 3D printed phantoms.

9036-85, Session PSWed

### SPECT-US image fusion and clinical applications

Johann B. Hummel, Marcus Kaar, Rainer Hoffmann, Wolfgang Birkfellner, Thomas Beyer, Anton Staudenherz, Michael Figl, Medizinische Univ. Wien (Austria)

Because scintigraphic images lack anatomical information, single photon emission tomography (SPECT) and positron emission tomography systems (PET) are combined physically with CTs to compensate for this drawback. In our work, we present a method where the CT is replaced by a 3D ultrasound device. Because in this case a mechanical linkage is not possible, we use an additional optical tracking system (OTS) for spatial correlation of the SPECT or PET information and the US. To enable image fusion between the functional SPECT and the anatomical US we first calibrate the SPECT by means of the optical tracking system. This is done by imaging a phantom with SPECT and scanning the surface of the phantom using a calibrated stylus of the OTS. Applying an iterative closest point (ICP) algorithm results in the transformation between the optical coordinate system and the SPECT coordinate system. When a patient undergoes a SPECT scan, a 3D US image is taken immediately after the scan. Since the scan head of the US is also tracked by the OTS, the transformation between OTS and SPECT can be calculated straight forward. For clinical intervention, the patient is again imaged with











the US and a 3D/3D registration between the two US volumes allows to transform the functional information of the SPECT to the current US image in real time.

We found a mean distance between the point cloud of the optical stylus and the segmented surface of the phantom of 2.3 mm while the maximum distance was found to be 6.9 mm. The 3D3D registration between the two US images was accomplished with an error of 2.1 mm.

9036-86, Session PSWed

#### Dual-projection 3D-2D registration for surgical guidance: preclinical evaluation of performance and minimum angular separation

Ali Uneri, Yoshito Otake, Adam S. Wang, Johns Hopkins Univ. (United States); Gerhard Kleinszig, Sebastian Vogt, Siemens Healthcare (Germany); Gary L. Gallia, Daniele Rigamonti, Jean-Paul Wolinsky, Ziya L. Gokaslan, Akhil J. Khanna, Johns Hopkins Univ. (United States); Jeffrey H. Siewerdsen, Johns Hopkins Univ. (United States)

An algorithm for 3D-2D registration of CT and x-ray projections has been developed using dual projection views to provide 3D localization with accuracy exceeding that of conventional tracking systems. The registration framework employs a normalized gradient information (NGI) similarity metric and covariance matrix adaptation evolution strategy (CMA-ES) to solve for the patient pose in 6 degrees of freedom. Registration performance was evaluated in anthropomorphic head and chest phantoms, as well as a human torso cadaver, using C-arm projection views acquired at angular separations ( $\Delta\theta$ ) ranging from 0° to 178°. Registration accuracy was assessed in terms target registration error (TRE) and compared to that of an electromagnetic tracker. Studies evaluated the influence of C-arm magnification, x-ray dose, and preoperative CT slice thickness on registration accuracy and the minimum angular separation required to achieve TRE  $\sim 1-3$ mm. The results indicate that  $\Delta\theta$  as small as ~10–20° is adequate to achieve TRE <2 mm with 95% confidence, comparable or superior to that of commercial trackers. The method allows direct registration of preoperative CT and planning data to intraoperative fluoroscopy. providing 3D localization free from conventional limitations associated with external fiducial markers, stereotactic frames, trackers, and manual registration. The studies support potential application to percutaneous spine procedures and intracranial neurosurgery.

9036-87, Session PSWed

### Feasibility of a touch-free user interface for ultrasound snapshot-guided nephrostomy

Simon Kotwicz, Andras Lasso, Tamas Ungi, Gabor Fichtinger, Queen's Univ. (Canada)

PURPOSE: Clinicians are often required to interact with visualization software during image-guided medical interventions, but sterility requirements forbid the use of traditional keyboard and mouse devices. In this study we attempt to determine the feasibility of using a touchfree interface in a real time procedure by creating a full gesture-based guidance module for ultrasound snapshot-guided percutaneous nephrostomy. METHODS: The workflow for this procedure required a gesture to select between multiple options, a "back" and "next" gesture, a "reset" gesture and a way to mark a point on an image. Using an orientation sensor mounted on the hand as input device, gesture recognition software was developed based on yaw, pitch and roll angles. Five operators were recruited to train the developed gesture recognition software. The participants performed each gesture ten times and placed three points on predefined target positions. They also performed tasks

unrelated to the sought after gestures to evaluate the vulnerability of the software to false positives. The orientation sensor measurements and the position of the marked points were recorded. The recorded data was used to establish threshold values and optimize the gesture recognition algorithm. RESULTS: For the "back", "reset" and "select option" gesture, a 100% recognition rate was achieved. For the "next" gesture, a 92% recognition rate was obtained. With the optimized gesture recognition software no false positives were observed when performing the gestures or when performing actions unrelated to the sought after gestures. The mean point placement error was 0.55 mm with a standard deviation of 0.30 mm. The mean placement time was 4.79 seconds. CONCLUSION: The system that was developed is promising and demonstrates potential for touch-free interfaces in the operating room.

9036-88, Session PSWed

## Active shape models with optimized texture features for radiotherapy planning of prostate cancer

Kun Cheng, Yang Feng, Dean Montgomery, Edinburgh Cancer Research UK Ctr. (United Kingdom) and The Univ. of Edinburgh (United Kingdom); Duncan B. McLaren, Edinburgh Cancer Research UK Ctr. (United Kingdom); Stephen McLaughlin, Heriot-Watt Univ. (United Kingdom); William H. Nailon, Edinburgh Cancer Research UK Ctr. (United Kingdom)

There is now considerable interest in radiation oncology on the use of shape models of anatomy to improve target delineation and assess anatomical disparity at time of radiotherapy. In this paper a texture based active shape model (ASM) is presented for automatic delineation of the gross tumor volume (GTV), containing the prostate, on computed tomography (CT) images of prostate cancer patients. The model was trained on two-dimensional (2D) contours identified by a radiation oncologist on sequential CT image slices. A three-dimensional (3D) GTV shape was constructed from these and iteratively aligned using Procrustes analysis. To train the model the shape deformation variance was learnt using the Active Shape Model (ASM) approach. In a novel development to this approach a profile feature was selected from precomputed texture features by minimizing the Mahalanobis distance to obtain the most distinct feature for each landmark. The interior of the GTV was modelled using quantile histograms to initialize the shape model on new cases. From the archive (num=42) of contoured CT scans 32 cases were randomly selected for training and 10 for evaluating performance. The gold standard was taken as the contour defined by the radiation oncologist. The shape model achieved an overall dice coefficient of 0.81 for all test cases. Performance was found to increase, mean DC of 0.87, when the volume size of the new case was similar to the mean shape of the model. With further work the approach has the potential to be used in real-time delineation of target volumes.

9036-89, Session PSWed

## Heuristic estimation of electromagnetically tracked catheter shape for image-guided vascular procedures

Fuad N. Mefleh, Clemson Univ. (United States); George H. Baker M.D., Medical Univ. of South Carolina (United States); David M. Kwartowitz, Clemson Univ. (United States) and Medical Univ. of South Carolina (United States)

In our previous work we presented a novel image-guided surgery (IGS) system, Kit for Navigation by Image Focused Exploration (KNIFE). KNIFE has been demonstrated to be effective in guiding mock clinical procedures with the tip of an electromagnetically tracked catheter overlaid onto a pre-captured bi-plane fluoroscopic loop. Representation











of the catheter in KNIFE differs greatly from what is captured by the fluoroscope, due to distortions and other properties of fluoroscopic images. When imaged by a fluoroscope, catheters can be visualized due to the inclusion of radiopaque materials (i.e. Bi, Ba, W) in the polymer blend. However, in KNIFE catheter location is determined using a single tracking seed located in the catheter tip that is represented as a single point overlaid on pre-captured fluoroscopic images.

To bridge the gap in catheter representation between KNIFE and traditional methods we constructed a catheter with five tracking seeds positioned along the distal 70 mm of the catheter. We have currently investigated the use of four spline interpolation methods for estimation of true catheter shape. Currently data from this initial investigation have not been generated. Further studies will assess more complex spline generation algorithms as well as determine acceptable levels of shape estimation error.

9036-90, Session PSWed

# A dimensionless dynamic contrast enhanced MRI parameter for intra-prostatic tumor target volume delineation: initial comparison with histology

Thomas Hrinivich, Western Univ. Canada (Canada) and Robarts Research Institute (Canada) and London Regional Cancer Program (Canada); Eli D. Gibson, Western Univ. Canada (Canada) and Robarts Research Institute (Canada); Mena Gaed M.D., Western Univ. Canada (Canada) and Robarts Research Institute (Canada) and Lawson Health Research Institute (Canada); José A. Gomez-Lemus M.D., Madeleine Moussa M.D., Western Univ. Canada (Canada); Charlie McKenzie, Western Univ. Canada (Canada) and Robarts Research Institute (Canada); Glenn S. Bauman, The Univ. of Western Ontario (Canada) and London Regional Cancer Program (Canada) and Lawson Health Research Institute (Canada); Aaron D. Ward, The Univ. of Western Ontario (Canada) and London Regional Cancer Program (Canada); Aaron Fenster, Western Univ. Canada (Canada) and Robarts Research Institute (Canada) and Lawson Health Research Institute (Canada); Eugene Wong, Western Univ. Canada (Canada) and London Regional Cancer Program (Canada) and Lawson Health Research Institute (Canada)

Purpose: T2 weighted and diffusion weighted magnetic resonance imaging (MRI) show promise in isolating prostate tumours. Dynamic contrast enhanced (DCE)-MRI has also been employed as a component in multi-parametric tumour detection schemes. Model-based parameters such as Ktrans are conventionally used to characterize DCE images and require arterial contrast agent (CR) concentration. A robust parameter map that does not depend on arterial input may be more useful for target volume delineation or patient specific Ktrans quality assurance (QA). We present a dimensionless parameter (Wio) that characterizes CR washin and wash-out rates without requiring arterial CR concentration. Wio is compared to Ktrans in terms of ability to discriminate cancer in the prostate, as demonstrated via comparison with histology.

Methods: 3 subjects underwent DCE-MRI using gadolinium contrast and 7 s imaging temporal resolution. A pathologist identified cancer on whole-mount histology specimens, and slides were deformably registered to MR images. The ability of Wio maps to discriminate cancer was determined using an ROC analysis.

Results: There is a trend that Wio shows greater mean area under the ROC curve than Ktrans, but the difference was not statistically significant based on a Wilcoxon rank-sum test (p = 0.47).

Conclusions: Preliminary results indicate that Wio shows potential as a tool for Ktrans QA, showing similar ability to discriminate cancer in the prostate as Ktrans without requiring arterial CR concentration.

9036-91, Session PSWed

### 3D non-rigid surface-based MR-TRUS registration for image-guided prostate biopsy

Yue Sun, Wu Qiu, Robarts Research Institute (Canada); Cesare Romagnoli M.D., The Univ. of Western Ontario (Canada); Aaron Fenster, Robarts Research Institute (Canada)

Two dimensional (2D) transrectal ultrasound (TRUS) guided prostate biopsy is the standard approach for definitive diagnosis of prostate cancer (PCa) and guiding biopsy needles to suspicious regions in the prostate. However, due to the lack of image contrast of prostate tumors needed to clearly visualize early-stage PCa, prostate biopsy often results in false negatives, requiring repeat biopsies. Magnetic Resonance Imaging (MRI) has been considered to be the most promising imaging modality for noninvasive identification of PCa, since it can provide a high sensitivity and specificity for the detection of early stage PCa. Our main objective is to develop and validate a registration method of 3D MR-TRUS images, allowing generation of volumetric 3D maps of targets identified in 3D MR images to be biopsied using 3D TRUS images. Our registration method first makes use of an initial rigid registration of 3D MR images to 3D TRUS images using 6 manually placed approximately corresponding landmarks in each image. Following the manual initialization, two prostate surfaces are segmented from 3D MR and TRUS images and then non-rigidly registered using a thin-plate spline (TPS) algorithm. The registration accuracy was evaluated using 4 patient images by measuring target registration error (TRE) of manually identified corresponding intrinsic fiducials (calcifications and/or cysts) in the prostates. Experimental results show that the proposed method yielded an overall mean TRE of 2.05 mm, which is favorably comparable to a clinical requirement for an error of less than 2.5 mm.

9036-92, Session PSWed

#### A New CT prostate segmentation for Ultrasound-guided CT-based HDR brachytherapy

Xiaofeng Yang, Peter Rossi, Tomi Ogunleye, Walter Curran, Tian Liu, Emory Univ. (United States)

High-dose-rate (HDR) brachytherapy has become a popular treatment modality for intermediate or high risk prostate cancer. Prostate HDR treatment involves placing 10 to 20 catheters (needles) into the prostate gland, and then delivering radiation dose to the cancerous regions through these catheters. These catheters are often inserted with transrectal ultrasound (TRUS) guidance and the HDR treatment plan is based on the CT images. The main challenge for CT-based HDR planning is to accurately segment prostate volume in CT images due to the poor soft tissue contrast and additional artifacts introduced by the catheters. To overcome these limitations, we propose a novel approach to segment the prostate in CT images through TRUS-CT deformable registration based on the catheter locations. In this approach, the HDR catheters are reconstructed from the intra-operative TRUS and post-operative CT images and used as landmarks for the TRUS-CT image registration. We then use the prostate contour generated from the TRUS images captured during ultrasound-guided HDR procedure to segment the prostate on the CT images through deformable registration. A prostate-phantom study demonstrated a sub-millimeter accuracy of our method. A pilot study of 10 prostate-cancer patients was conducted to further test its clinical feasibility. All patients had 3 gold markers implanted in the prostate that were used to evaluate the registration accuracy, as well as previous diagnostic MR images that were used as the gold standard to assess the prostate segmentation. For the 10 patients, the mean gold-marker displacement was 1.2 mm; the prostate volume difference between our approach and the MRI was 7.3%, and the Dice volume overlap was 91.9%. Our proposed method will improve prostate delineation, enable accurate dose planning and delivery, and potentially enhance prostate HDR treatment outcome.











9036-93, Session PSWed

## Identifying MRI markers to evaluate early treatment related changes post laser ablation for cancer pain management

Pallavi Tiwari, Case Western Reserve Univ. (United States); Shabbar Danish, Univ. of Medicine & Dentistry of New Jersey (United States); Anant Madabhushi, Case Western Reserve Univ. (United States)

Laser interstitial thermal therapy (LITT) has recently emerged as a new treatment modality for cancer pain management that targets the cingulum (pain center in the brain) via MRI-guided focused laser ablation. Unfortunately the effects of laser ablation on the cingulum are currently unknown. We present a novel approach at evaluating early ablation treatment changes via identification of computerized MRI descriptors that can better capture subtle morphological changes that occur post-LITT, as compared to raw MR intensity images. A retrospective cohort of studies comprising pre- and 24-hour post-LITT T1-weighted (T1w), T2w, T2-GRE, and T2-FLAIR acquisitions was considered. Our scheme involved (1) inter-protocol as well as inter-acquisition registration of pre- and post-LITT MRI, (2) quantitation of MRI parameters by correcting for intensity drift in order to examine tissue-specific response, and (3) quantification of MRI maps via texture and intensity features. Quantitative, voxel-wise comparison of the changes in MRI features indicated that steerable and non-steerable gradient texture features were highly sensitive as well as specific in predicting subtle micro-architectural changes within and around the ablation zone pre- and post-LITT. The highest ranked texture feature was identified for FLAIR which yielded a normalized percentage change of 360% within the ablation zone relative to its pre-LITT value. A relative change of 140%, 96% and 75% was reported within the ablation zone for T2w, GRE, and T1w MRI respectively. Our preliminary results thus indicate great potential for non-invasive computerized MRI features in determining localized micro-architectural focal treatment related changes post-LITT.

9036-94, Session PSWed

#### Development and evaluation of optical needle depth sensor for percutaneous diagnosis and therapies

Keryn Palmer, David Alelyunas, Connor McCann, Kitaro Yoshimitsu, Brigham and Women's Hospital (United States); Takahisa Kato, Brigham and Women's Hospital (United States) and Canon U.S.A, Inc. (United States); Sang-Eun Song, Nobuhiko Hata, Brigham and Women's Hospital (United States)

Current methods of needle insertion during percutaneous CT and MRI guided procedures lack precision in needle depth sensing. The depth of the needle insertion is currently monitored through depth markers drawn on the needle and later confirmed by intra-procedural imaging; until this confirmation, the physicians' judgment that the target is reached is solely based on the depth markers, which are not always clearly visible. We have therefore designed an optical sensing device which provides continuous feedback of needle insertion depth and degree of rotation throughout insertion.

An optical mouse sensor was used in conjunction with a microcontroller board, Arduino Due, to acquire needle position information. The device is designed to be attached to a needle guidance robot developed for MRI-guided prostate biopsy in order to aid the manual insertion. An LCD screen and three LEDs were employed with the Arduino Due to form a hand-held device displaying needle depth and rotation. Accuracy of the device was tested to evaluate the impact of insertion speed and rotation.

Unlike single dimensional needle depth sensing developed by other researchers, this two dimensional sensing device can also detect the rotation around the needle axis. The combination of depth and rotation

sensing would be greatly beneficial for the needle steering approaches that require both depth and rotation information. Our preliminary results indicate that this sensing device can be useful in detecting needle motion when using an appropriate speed and range of motion.

9036-95, Session PSWed

#### Image to physical space registration of supine breast MRI for image guided breast surgery

Rebekah H. Conley, Vanderbilt Univ. (United States); Ingrid M. Meszoely M.D., Vanderbilt Univ. Medical Ctr. (United States); Thomas S. Pheiffer, Logan W. Clements, Jared A. Weis, Thomas E. Yankeelov, Michael I. Miga, Vanderbilt Univ. (United States)

Breast conservation therapy (BCT) is a popular option for many women diagnosed with early stage breast cancer and involves a lumpectomy followed by radiotherapy. However, only approximately 50% of eligible women will elect this procedure over mastectomy despite equal survival benefit due to uncertainty in outcome with regards to complete excision of cancerous cells, risk of local recurrence, and cosmesis. Determining surgical margins intraoperatively is difficult and achieving negative margins is not as robust as it needs to be, resulting in high re-operation rates and often mastectomy. Magnetic resonance images (MRI) can provide detailed information about tumor extents, however diagnostic images are acquired in a fundamentally different patient presentation than that used in surgery. Therefore, the high quality diagnostic MRIs taken in the prone postion are not optimal for use in surgical planning due to the drastic shape change between preoperative images and the common supine surgical position. This work proposes to investigate the value of supine MRI in an effort to localize tumors intraoperatively using image-guidance. Mock intraoperative setups (realistic patient positioning in non-sterile environment) and preoperative imaging data were collected from a patient scheduled for lumpectomy. The mock intraoperative data included a tracked laser range scan of the patient's breast surface, tracked center points of MR visible fiducials on the patient's breast, and tracked B-mode ultrasound and strain images. The preoperative data included a supine MRI with visible fiducial markers. Fiducial markers localized in the MRI were rigidly registered to their mock intraoperative counterparts using an optically tracked stylus. After an initial rigid registration, an iterative closest point registration algorithm was used to align the surface extracted from the MRI and the point cloud acquired by the laser range scanner. The root mean square (RMS) registration error using the tracked markers was 3.4mm. Following closest point registration, the average closest point distance was 1.76±0.502 mm.

9036-96, Session PSWed

### A global CT to US registration of the lumbar spine

Simrin Nagpal, Queen's Univ. (Canada); Ilker Hacihaliloglu, The Univ. of British Columbia (Canada); Tamas Ungi, Queen's Univ. (Canada); Abtin Rasoulian, The Univ. of British Columbia (Canada); Jill Osborn, St. Paul's Hospital (Canada); Victoria A Lessoway, British Columbia Women's Hospital (Canada); Robert N Rohling, University of British Columbia (Canada); Dan P. Borschneck, Kingston General Hospital (Canada); Purang Abolmaesumi, The Univ. of British Columbia (Canada); Parvin Mousavi, Queen's Univ. (Canada)

Spine needle injections are widely applied for analgesia and anesthesia. Current treatment is performed either blindly or using fluoroscopy or computed tomography (CT). Alternatively, ultrasound (US) guidance for spine needle procedures is becoming more prevalent since US is a non-ionizing and more accessible image modality. An inherent challenge











to US imaging of the spine is the acoustic shadows created by the bony structures of the vertebra limiting visibility. It is challenging to use US as the sole imaging modality for intraoperative guidance of spine needle injections. However, aligning the preoperative CT with the intraoperative US augments anatomical visualization for the clinician during spinal interventions. To align the preoperative CT and intraoperative US, a novel registration pipeline is presented that involves automatic global and multi vertebrae registration. The registration pipeline is composed of two distinct phases: preoperative and intraoperative. Preoperatively, spring points are selected between adjacent vertebrae. Intraoperatively, the lumbar spine is first aligned between the CT and US followed by a multi vertebrae registration. The springs are used to constrain the movement of the individually transformed vertebrae to ensure the optimal alignment is a pose of the lumbar spine that is physically possible. Validation of the algorithm was performed on five clinical patient datasets. The registration pipeline is able to register the datasets from initial misalignments of up to 25 mm with a mean TRE of 1.17 mm. From these results, it is evident that the proposed registration pipeline offers an automatic robust registration between clinical CT and US data.

9036-97, Session PSWed

#### Rigid point registration circuits

J. Michael Fitzpatrick, Vanderbilt Univ. (United States)

In 1996 Freeborough proposed a method for estimating target registration error (TRE) when no ground truth is available. In his approach, a circuit of registrations is performed using the same registration method on multiple poses of the same object: P1-to-P2, P2-to-P3, ..., PNc-to-P1, with Nc > 2 , where the last registration completes the circuit. Any difference between the original and final positions, which we call the "Circuit TRE", indicates that the registration method suffers from TRE; Freeborough estimated that the true TRE = Circuit TRE /  $\!\sqrt{3}$ . The current work shows both by theoretical derivation and by computer simulation that Freeborough's approach greatly underestimates TRE for rigid point registration.

9036-98. Session PSWed

#### Needle localization using a moving stylet/ catheter in ultrasound-guided regional anesthesia: a feasibility study

Parmida Beigi, Robert N. Rohling, The Univ. of British Columbia (Canada)

Despite the wide range and long history of ultrasound guided needle insertions, an unresolved issue in many cases is clear needle visibility. A well-known ad hoc technique to detect the needle is to move the stylet and look for changes in the needle appearance. We present a new method to automatically locate a moving stylet/catheter within a stationary cannula using motion detection. We then use this information to detect the needle trajectory and the tip. The differences between the current frame and the previous frame are detected and localized, to minimize the influence of tissue global motions. A polynomial fit based on the detected needle axis determines the estimated stylet shaft trajectory, and the extent of the differences along the needle axis represents the tip. Over a few periodic movements of the stylet including its full insertion into the cannula to the tip, a combination of polynomial fits determines the needle trajectory and the last detected point represents the needle tip. Experiments are conducted in water bath and bovine muscle tissue for several stylet/catheter materials. Results show that a plastic stylet has the best needle shaft and tip localization accuracy in the water bath with RMSE = 0.16 mm and RMSE = 0.51 mm, respectively. In the bovine tissue, the needle tip was best localized with the plastic catheter with RMSE = 0.33 mm. The stylet tip localization was most accurate with the steel stylet, with RMSE = 2.81 mm and the shaft was best localized with the plastic catheter, with RMSE = 0.32 mm.

9036-99, Session PSWed

### Tracked ultrasound calibration studies with a phantom made of LEGO bricks

Marie Soehl, Ryan A. Walsh, Adam Rankin, Andras Lasso, Gabor Fichtinger, Queen's Univ. (Canada)

PURPOSE: In this study, spatial calibration of tracked ultrasound was compared by using a calibration phantom made of LEGO bricks and two 3-D printed N-wire phantoms. METHODS: The accuracy and variance of calibrations were compared under a variety of operating conditions. Twenty trials were performed using an electromagnetic tracking device with a linear probe and three trials were performed using varied probes, varied tracking devices and the three aforementioned phantoms. The accuracy and variance of spatial calibrations found through the standard deviation and error of the 3-D image reprojection were used to compare the calibrations produced from the phantoms. RESULTS: This study found no significant difference between the measured variables of the calibrations. The average standard deviation of multiple 3-D image reprojections with the highest performing printed phantom and those from the phantom made of LEGO bricks differed by 0.05 mm and the error of the reprojections differed by 0.13 mm. CONCLUSION: Given that the phantom made of LEGO bricks is significantly less expensive, more readily available, and more easily modified than precision-machined N-wire phantoms, it prompts to be a viable calibration tool especially for quick laboratory research and proof of concept implementations of tracked ultrasound navigation.

9036-100, Session PSWed

#### Mapping surgical fields by moving a laserscanning multimodal scope attached to a robot arm

Yuanzhen Gong, Timothy D. Soper, Vivian W. Hou, Danying Hu, Blake Hannaford, Eric J. Seibel, Univ. of Washington (United States)

Endoscopic visualization in brain tumor removal is challenging because tumor tissue is often visually indistinguishable from healthy tissue. Fluorescence imaging can improve tumor delineation, though this impairs reflectance-based visualization of gross anatomical features. To accurately navigate and resect tumors, we created an ultrathin/flexible, scanning fiber endoscope (SFE) that acquires reflectance and fluorescence wide-field images at high-resolution. Furthermore, our miniature imaging system is affixed to a robotic arm providing precise and programmable motion of SFE, from which we generate multimodal surface maps of the surgical field.

To test this system, synthetic phantoms of debulked tumor from brain are fabricated having spots of fluorescence representing residual tumor. 3D surface maps of this surgical field are produced by moving the SFE over the phantom during concurrent reflectance and fluorescence imaging (30Hz video). SIFT-based feature matching between reflectance images is implemented to select a subset of key frames, which are reconstructed in 3D by bundle adjustment. The resultant reconstruction yields a multimodal 3D map of the tumor region that can improve visualization and robotic path planning.

Efficiency of creating these maps is important as they are generated multiple times during tumor margin clean-up. By using pre-programmed vector motions of the robot arm holding the SFE, the computer vision algorithms are optimized for efficiency by reducing search times. Preliminary results indicate that times for creating these 3D multimodal maps of the surgical field can be reduced to one third (<1 minute) by using known trajectories of the surgical robot moving the image-guided tool.











Sunday - Monday 16-17 February 2014

Part of Proceedings of SPIE Vol. 9037 Medical Imaging 2014: Image Perception, Observer Performance, and Technology Assessment

9037-1, Session 1

### Visual search from lab to clinic and back (Keynote Presentation)

Jeremy M. Wolfe, Harvard Medical School (United States) and Brigham and Women's Hospital (United States)

Many of the tasks of medical image perception can be understood as demanding visual search tasks (especially if you happen to be a visual search researcher). In this talk I will discuss the profitable dialogue between the practical demands of search in radiology and the fundamental principles of search, uncovered by basic research in visual attention. There are three 'take-home'" messages. (1) Humans have a search engine that comes with impressive capabilities and equally impressive limitations. (2) Medical image perception tasks are imperfectly matched to those capabilities and can be vulnerable to those limitations. (3) Introspection, even by highly-trained experts, is not an adequate guide to performance in radiological search tasks. These 'messages' will be illustrated with examples from the clinic and the lab.

9037-2, Session 1

### Effect of mammographic breast density on radiologists' visual search pattern

Dana Al Mousa, Patrick C. Brennan, Elaine Ryan, The Univ. of Sydney (Australia); Warwick B. Lee, Cancer Institute NSW (Australia); Mariusz W. Pietrzyk, Warren M. Reed, Maram M. Alakhras, Yanpeng Li, Claudia R. Mello-Thoms, The Univ. of Sydney (Australia)

This study investigates the impact of breast density on visual searching pattern. A set of 74 one-view malignancy containing mammographic images were examined by 7 radiologists. Eye position was recorded and visual search parameters such as total time examining a case, time to hit the lesion, dwell time and number of hits per area were collected. Fixations were calculated in 3 areas of interests: background breast parenchyma, dense areas of parenchyma and lesion. Significant increases in dwell time and number of hits in dense areas of parenchyma were noted for the high compared to low mammographic density images when the lesion overlay the fibroglandular tissue (p<0.01). When the lesion was outside the fibroglandular tissue, significant increase in dwell time and number of hits in dense areas of parenchyma in high compared to low mammographic density images was observed (p<0.01). No significant difference has been found in total time examining a case, time to first fixate the lesion, dwell time and number of hits in background breast parenchyma and lesion areas. In conclusion, our data suggests that dense areas of breast parenchyma attract radiologists' visual attention. Lesions overlaying the fibroglandular tissue were faster to be detected, therefore lesion location, whether overlaying or outside the fibroglandular tissue, appeared to have an impact on radiologists' visual searching pattern.

9037-3, Session 1

# Laparoscopic surgical skills training: an investigation of the potential of using surgeons' visual search behavior as a performance indicator

Yan Chen, Leng Dong, Alastair G. Gale, Loughborough Univ.

(United Kingdom); Benjamin Rees, Charles Maxwell-Armstrong M.D., Queen's Medical Ctr. (United Kingdom)

Laparoscopic surgery is a difficult perceptual-motor task and effective and efficient training in the technique is important. Viewing previously recorded laparoscopic operations is a standard training technique for surgeons to increase their knowledge of such 'minimal access surgery (MAS). It is not known whether this is a useful technique, how effective it is or what effect it has on the surgeon watching the recorded video. As part of an on-going series of studies into laparoscopic surgery, an experiment was conducted to examine whether surgical skill level has an effect on the visual search behaviour of individuals of different surgical experience when they examine such imagery. Medically naive observers (computer science research students), medical students, junior surgeons and experienced surgeons viewed laparoscopic recordings of two recent operations. Initial analyses of the recorded eye movement data indicated commonalities between all observers, largely irrespective of surgical experience. This, it is argued, is due to visual search in this situation largely being driven by the dynamic nature of the images. However, when the recordings were broken down into meaningful surgical segments, as defined by an independent expert surgeon, then search differences were apparent, related to surgical expertise. Consequently, it is argued that monitoring the eye movements of surgeons whilst they watch prerecorded operations is a useful adjunct to existing training regimes.

9037-4, Session 2

### Adaptive controller for volumetric display of neuroimaging studies

Ben Bleiberg, National Intrepid Ctr. of Excellence (United States); Justin Senseney, National Institutes of Health (United States); Jesus J. Caban, National Intrepid Ctr. of Excellence (United States)

Volumetric display of medical images is an increasingly relevant method for examining an imaging acquisition as the prevalence of thin-slice imaging increases in clinical studies. Current mouse and keyboard implementations for volumetric control provide neither the sensitivity nor specificity required to manipulate a volumetric display for efficient reading in a clinical setting. Solutions to efficient volumetric manipulation provide more sensitivity by removing the binary nature of actions controlled by keyboard clicks, but specificity is lost because a single action may change display in several directions. When specificity is then further addressed by re-implementing hardware binary functions through the introduction of mode control, the result is a cumbersome interface that fails to achieve the revolutionary benefit required for adoption of a new technology. We address the specificity versus sensitivity problem of volumetric interfaces by providing adaptive positional awareness to the volumetric control device by manipulating communication between hardware driver and existing software methods for volumetric display of medical images. This creates a tethered effect for volumetric display, providing a smooth interface that improves on existing hardware approaches to volumetric scene manipulation.

9037-5, Session 2

### Preference and performance regarding different image sizes when reading cranial CT

Antje C. Venjakob, Technische Univ. Berlin (Germany); Tim Marnitz, Charité Universitätsmedizin Berlin (Germany); Claudia R. Mello-Thoms, The Univ. of Sydney (Australia)











Image size is an important factor for the interpretation of medical images and has shown to impact performance. The experiment conducted at the Berlin university hospital Charité compared performance, visual search and preference of 21 radiologists who interpreted cranial CT cases of two different sizes. No impact on performance was found when comparing the JAFROC figure of merit and reading time. However, small images were associated with more false positive decisions, whereas large images generated more false negative decisions. The results of the eye movement analysis suggest that detection of perturbed sites was facilitated in small images, possibly due to enhanced motion detection. This could be shown by faster time to first fixation for true as well as false positive decision sites in small images as well as by longer fixations that span more slices. However, when asked to indicate on a scale from 0 to 10 how much they liked each image size, large images were on average rated as more preferable compared to small images. The individual preference ratings did not correlate with the participants' performance, indicating that preference may not be the best selection criterion when reading medical images. The experiment is currently being replicated at a university hospital in Sydney. The newly acquired data will be integrated into the presentation and discussion of this experiment.

9037-6, Session 2

#### Gaze as a biometric

Hong-Jun Yoon, Oak Ridge National Lab. (United States); Tandy Carmichael, Tennessee Technological Univ. (United States); Georgia D. Tourassi, Oak Ridge National Lab. (United States)

Two people may analyze a visual scene in two completely different ways. Our study sought to determine whether human gaze may be used to establish the identity of an individual. To accomplish this objective we investigated the gaze pattern of twelve individuals viewing different still images with different spatial relationships. Specifically, we created 5 visual "dot-pattern" tests to be shown on a standard computer monitor. These tests challenged the viewer's capacity to distinguish proximity, alignment, and perceptual organization. Each test included 50 images of varying difficulty (total of 250 images). Eye-tracking data were collected from each individual while taking the tests. The eye-tracking data were converted into gaze velocities and analyzed with Hidden Markov Models to develop personalized gaze profiles. Using leave-one-out cross-validation, we observed that these personalized profiles could differentiate among the 12 users with classification accuracy ranging between 53% and 76%, depending on the test. This was statistically significantly better than random guessing (i.e., 8.3% or 1 out of 12). Classification accuracy was higher for the tests where the users' average gaze velocity per case was lower. The study findings support the feasibility of using gaze as a biometric or personalized biomarker. These findings could have implications in Radiology training and the development of personalized e-learning environments.

9037-7, Session 2

## Going on with false beliefs: What if satisfaction of search was really suppression of recognition?

Claudia R. Mello-Thoms, Phuong Dung Trieu, Patrick C. Brennan, The Univ. of Sydney (Australia)

Satisfaction of search (SOS) is a well known phenomenon in radiology, in which the detection of one abnormality facilitates the neglect of other abnormalities. Over the years SOS has been thoroughly studied primarily in chest and in trauma, and it has been found to be an elusive effect, appearing in some settings but not in others. Unfortunately, very little is known about SOS in mammography. In this study we will explore SOS in breast cancer detection by considering a case set of digital mammograms as interpreted by breast radiologists. However, we will also attempt to challenge the core of the paradigm; for decades, many

have associated SOS with incomplete search, but as Kundel has put eloquently when addressing the SPIE in 2004, "observers do not stop viewing when one abnormality has been found on an image with multiple abnormalities". What else could cause SOS then? According to our previous work, the first "perceived" abnormality reported by a radiologist has an influential role in the report of any other "perceived" abnormalities on the case, which supports the idea that perhaps SOS is caused a perceptual suppression of the recognition of different abnormalities. In other words, once the radiologist has made a first report (regardless of whether that first report is a TP or FP), detection and hence reporting of other abnormalities present in the case are greatly dependent on whether these associated abnormalities "fit the profile" of what has been already found.

9037-8, Session 2

### Pilot reader studies to compare digital microscopic images versus the microscope

Brandon D. Gallas, Marios A. Gavrielides, U.S. Food and Drug Administration (United States) and Ctr. for Devices and Radiological Health (United States); Jason Hipp, National Cancer Institute (United States) and National Institutes of Health (United States); Adam Wunderlich, U.S. Food and Drug Administration (United States); Stephen M. Hewitt, National Cancer Institute (United States) and National Institutes of Health (United States)

#### Purpose:

Microscopic whole slide imaging (WSI) scanners have the potential to help pathologists be more effective, more efficient, and have more impact. However, none of these benefits can be fully realized until it is demonstrated that pathologists can be as effective with digital WSI images as they are with the microscope and the glass slides.

#### Methods:

The key element in our methodology is the registration of a glass slide and its digital (whole slide imaging, WSI) scanned version, the WSI image. Registration reduces or eliminates location variability (what readers are looking at) that arises from expertise, training, and execution. Correspondingly, we reduced the task from cell search and classification to just classification by targeting small ROIs that contain 1-6 candidate cells. We use inter- and intra-pathologist agreement, within and across modalities (modality 1: pathologists using digital images, modality 2: pathologists using the optical microscope).

#### Results:

Round 1 of our pilot studies indicated the following: our registration precision degrades as the stage moves, readers possibly needed help scoring cells on a 100-point scale, and classifying cells as plasma cells or not appeared to be a task more ready for a pivotal study than classifying cells as mitotic figures or not.

#### Conclusions:

We are in the process of improving registration. We are also adding training on scoring on a 100-point scale and improving the training of the classification tasks. We intend to report results of Round 2 of our pilot studies and compare them to results of Round 1.

9037-9, Session 2

### Visual quality assessment of H.264/AVC compressed laparoscopic video

Asli E. Kumcu, Klaas Bombeke, Univ. Gent (Belgium); Heng Chen, Vrije Univ. Brussel (Belgium); Ljubomir Jovanov, Ljiljana Platisa, Hiêp Q. Luong, Jan Van Looy, Univ. Gent (Belgium); Yves Van Nieuwenhove, Univ. Ziekenhuis Gent (Belgium); Peter Schelkens, Vrije Univ. Brussel (Belgium); Wilfried Philips, Univ.











#### Gent (Belgium)

Ongoing advances in video processing are bringing the digital revolution to the operating room, giving rise to new opportunities such as telesurgery and tele-collaboration. However, applications such as minimally invasive surgery, robotic surgery, and wireless endoscopy generate large video streams that demand gigabytes of storage and transmission capacity. While data compression can be used to enable efficient data handling, it must avoid reducing the image quality to clinically unacceptable levels. In this study we assess the quality of compressed laparoscopy video using a subjective evaluation study and state-ofthe-art objective metrics. Test sequences were High-Definition videos captures of four laparoscopic surgery procedures. Raw sequences were processed with H.264/AVC IPPP-CBR at four compression levels (20, 5.6, 2.9, and 1.82 Mbps) chosen with a pilot study. 16 naive observers and 4 laparoscopic surgeons evaluated the quality and suitability for surgery (surgeons only) using Single Stimulus Continuous Quality Evaluation (SSCQE) methodology. PSNR, VQM, and HDR-VDP scores were also computed. Preliminary analysis indicates that the observers noticed a statistically significant drop in quality only at 2.9 and 1.82 Mbps, compared to the reference, for all four scenes. The objective measures reported quality degradation at every level of compression and thus do not exhibit a linear relationship with human observers in absolute terms. Currently the study with experts is ongoing and will be reported at the conference. We are investigating whether quality judgments are contentindependent, whether objective measures can be used to predict expert judgment, and if naive observers could be used a surrogates for experts.

9037-10, Session 3

## Investigating links between emotional intelligence and observer performance by radiologists in mammography

Sarah J. Lewis, Claudia R. Mello-Thoms, Steven Cumming, Patrick C. Brennan, The Univ. of Sydney (Australia); Kevin Keane, Univ. College Dublin (Ireland); Mark F. McEntee, The Univ. of Sydney (Australia); Stuart J. Mackay, Univ. of Liverpool (United Kingdom)

A novel direction of mammography/radiology research is better understanding the links between cognitive factors and radiologists' accuracy and performance. This study examines relationships between El scores and observer performance by radiologists in breast cancer detection.

Three separate samples were collected with Australian and US breast imaging radiologists. The radiologists were asked to undertake a mammographic interpretation task to identify malignant breast lesions and localise the lesions using a confidence rating scale. Following this activity, the radiologists were administered the El Trait (TElQue) questionnaire. The Trait El test gives a Global El score and 4 sub-scores in Well-being, Self-Control, Emotionality and Sociability.

Sample 1 (Darling Harbour 2012) radiologists were divided into 2 experience bands; radiologists <13 years as "less" experience and >13 years as "more". There was a significant Pearsons correlation (r = 0.849, p =0.012) between Self control and Location Sensitivity in the "less" experience band however there was little correlation (r = 0.09) between this El trait in "more" experience. In the second sample (Darwin 2013) radiologists were divided into 3 groups: high, medium, low experience; however there were no statistically significant correlation between El and performance. Analysis of the US radiologists (Sample 3: Louisville) scores is ongoing; however there is a significant difference between the El scores of US and Australian radiologists in terms of the El traits Wellbeing (5.86, 5.50, p<0.03) and Self-Control (4.89, 4.70, p<0.04).

El is correlated to observer performance in lesser experienced radiologists. It is suggested that tasks perceived as more difficult by less experienced radiologists may evoke more emotion (uncertainty, frustration, pressure). As experience increases radiologists may develop an ability to control their emotions or emotional intelligence becomes less important in decision making.

9037-11, Session 3

## How does radiology report format impact reading time, comprehension and visual scanning?

Elizabeth A. Krupinski, The Univ. of Arizona (United States); Bruce Reiner, Eliot Siegel, University of Maryland (United States)

This study examined whether radiology report format influences reading time and comprehension of information. Three reports were reformatted to conventional free text, structured text organized by organ system, and hierarchical structured text organized by clinical significance. Five attending radiologists, 5 radiology residents, 5 internal medicine attendings and 5 internal medicine residents read the reports and answered a series of questions about them. Reading was timed and participants reported reading preferences. For reading time there was no significant effect for format, but there was for attending versus resident, and radiology versus internal medicine. For percent correct scores there was no significant effect for report format or for attending versus resident, but there was for radiology versus internal medicine with the radiologists scoring better overall. Report format does not appear to impact viewing time or percent correct answers, but there are differences in both for specialty and level of experience. There were also differences between the four groups of participants with respect to what they focus on in a radiology report and how they read reports (skim versus read in detail). There may not be a "one-size-fits-all" radiology report format as individual preferences differ widely.

9037-12, Session 3

### Bone suppression technique for chest radiographs

Zhimin Huo, Jing Zhang, Huimin Zhao, Carestream Health, Inc. (United States); Susan Hobbs, John Wandtke M.D., Univ. of Rochester (United States); Anne-Marie Sykes, Mayo Clinic (United States); David H. Foos, Carestream Health, Inc. (United States)

Chest radiographs are the most commonly used exams by clinicians for screening and diagnosing lung diseases. Bone structures, such as ribs and clavicles, on chest radiographs are major noise contributors, which significantly reduce the detectability of abnormalities (e.g., nodules). Studies showed that lung nodule detection was significantly improved after the rib structure on chest radiographs was suppressed. We developed innovative approaches to suppress the rib structure seen on chest radiographs. Our rib detection approach includes lung segmentation; initial rib detection based on pixel classification; rib labeling to identify individual ribs; rib modeling to further refine rib detection; and rib-edge detection to accurately trace the rib edge. We evaluated the performance of rib detection by comparing the computerdetected ribs to manually detected rib regions. The rib detection performance was evaluated on 500+ images, including standard posterior-anterior (PA) and portable anterior-posterior (AP) chest images, yielding average sensitivities of 83.06% (±6.59%) and 74.51% (±11.49%) for PA and AP images, respectively. Further, the rib-suppressed images were evaluated in a reader study where radiologists were asked to detect lung nodules on chest radiographic images before and after the rib and clavicle structures were suppressed. Initial pilot reader studies from two readers showed that using rib-suppressed images improved readers' confidence of nodule presence on at least 40% of 27 images. Further, it allowed the readers to agree on nodule detections on six more images (two with only one nodule present) from their initial agreements on 17 images with at least 12% increase in nodule detection.











9037-13, Session 3

## The patterns of false positive lesions for chest radiography observer performance: insights into errors and locations

John W. Robinson, Patrick C. Brennan, Claudia R. Mello-Thoms, Mariusz W. Pietrzyk, Sarah J. Lewis, The Univ. of Sydney (Australia)

CXR interpretation continues to represent an area of radiological error with significant penalty for the late diagnosis of lung cancers. Published data asserts the miss rate on CXR of early lung cancer is 20-50%. In this study, the false positive rates of the radiologist sample have been investigated for patterns in location in both CXRs that contain nodules and those that do not. The effect of perceptual priming in both the rate and location within the chest region are analysed.

Ten radiologists participated in an observer performance task and asked to interpret 40 CXRs. The CXRs were derived from the Japanese Society of Radiologic Technology data base of real cases. The radiologists were shown 40 cases, with 19 abnormal and 21 normal PA images. Radiologists were instructed interpret the images and identify any malignancies using a 2-5 confidence scale (2= least confident case contains malignancy and 5=highest confidence of malignancy). The images were displayed on 3 Megapixel medical-grade monitors with ambient light levels at 30-40 Lux. Radiologists were permitted to window, zoom and pan images and there was no time limit for the study.

The distribution of false positives related to the upper lobes of both lungs related closely to the published miss rates for nodules in the upper lobes. In this study 42% of the false positives in the right lung were related to the upper lobe and 33% of the false positives on the left lung were related to the upper lobe. An analysis of the false positive rate between normal and abnormal CXRs is ongoing.

9037-14, Session 3

## Nonparametric EROC analysis for observer performance evaluation on joint detection and estimation tasks

Adam Wunderlich, U.S. Food and Drug Administration (United States); Bart Goossens, Univ. Gent (Belgium)

The majority of the literature on task-based image quality assessment has focused on lesion detection tasks, using the receiver operating characteristic (ROC) curve, or related variants, to measure performance. However, since many clinical image evaluation tasks involve both detection and estimation (e.g., estimation of kidney stone composition, estimation of tumor size), there is a growing interest in performance evaluation for joint detection and estimation tasks. To evaluate observer performance on such tasks, Clarkson introduced the estimation ROC (EROC) curve, and the area under the EROC curve as a summary figure of merit. In the present work, we propose nonparametric estimators for practical EROC analysis from experimental data, including estimators for the area under the EROC curve and its variance. The estimators are illustrated with a practical example comparing MRI images reconstructed from different k-space sampling trajectories.

9037-15, Session 4

### Non-Gaussian statistical properties of virtual breast phantoms

Craig K. Abbey, Univ. of California, Santa Barbara (United States); Predrag R. Bakic, Univ. of Pennsylvania (United States); David D. Pokrajac, Delaware State Univ. (United States); Andrew

D. A. Maidment, Univ. of Pennsylvania (United States); Miguel P. Eckstein, Univ. of California, Santa Barbara (United States); John M. Boone, UC Davis Medical Ctr. (United States)

Images derived from a "phantom" are useful for characterizing the performance imaging systems. In particular, the modulation transfer properties of imaging detectors are traditionally assessed by physical phantoms consisting of an edge. More recently researchers have come to realize that quantifying the effects of object variability can also be accomplished with phantoms in modalities such as breast imaging where this may be the principal limitation in performance. This is especially true when a virtual phantom can be used in a simulation environment. In breast imaging, several such phantoms have been proposed. In this work, we analyze non-Gaussian statistical properties of virtual phantoms such as these, and compare them to similar statistics derived from a database of breast images.

The virtual phantoms assessed consist of three classes. The first is known as clustered-blob lumpy backgrounds. The second class is "binarized" textures which typically apply some sort of threshold to a stochastic 3D texture intended to represent the distribution of adipose and glandular tissue in the breast. The third approach comes from efforts at the University of Pennsylvania to directly simulate the 3D anatomy of the breast. We use Laplacian fractional entropy (LFE) as a measure of the non-Gaussian statistical properties of each simulation.

Our results show that the simulation approaches differ considerably in LFE with very low scores for the clustered-blob lumpy background to very high values for the UPenn phantom. These results suggest that LFE may have value in developing and tuning virtual phantom simulation procedures.

9037-16, Session 4

## Mammographic density descriptors of novel phantom images: Effect of clustered lumpy backgrounds

Yanpeng Li, Patrick C. Brennan, Elaine Ryan, The Univ. of Sydney (Australia)

Mammographic breast density is a risk factor for breast cancer. In order to accurately quantify the correlations between density descriptors and the fibroglandular tissue, a phantom system has been developed that represents glandular tissue within an adipose tissue structure. Strong correlations have been found between synthesised glandular mass and several image descriptors. The aim of this study is to investigate if the same correlations can be found when strong background noise was added to the phantom images. For a set of one hundred phantom mammographic images, clustered lumpy backgrounds were synthesised. The correlation between the synthesised glandular mass and the descriptors like percentage density, integrated density, and standard deviation of mean grey value of the whole phantom were calculated. The results showed the correlation is still high and statistically significant for the above three descriptors with r is 0.7597, 0.8208, and 0.7167 respectively. This indicates these descriptors may be used to assess breast fibroglandular tissue content using mammographic images.

9037-17, Session 4

### Using image simulation to test the effect of detector type on breast cancer detection

Alistair Mackenzie, Lucy M. Warren, David R. Dance, The Royal Surrey County Hospital NHS Trust (United Kingdom) and Univ. of Surrey (United Kingdom); Dev P. Chakraborty, Univ. of Pittsburgh (United States); Julie Cooke, Jarvis Breast Screening and Diagnostic Ctr. (United Kingdom); Mark D. Halling-Brown, Padraig T. Looney, The Royal Surrey County Hospital NHS Trust











(United Kingdom); Matthew G. Wallis, Cambridge Univ. Hospitals NHS Foundation Trust (United Kingdom) and NIHR Cambridge Biomedical Research Ctr. (United Kingdom); Rosalind M. Given-Wilson, St George's Healthcare NHS Trust (United Kingdom); Gavin G. Alexander, The Royal Surrey County Hospital NHS Trust (United Kingdom); Kenneth C. Young, The Royal Surrey County Hospital NHS Trust (United Kingdom) and Univ. of Surrey (United Kingdom)

The effect that image quality associated with different detectors has on cancer detection in mammography was measured using a novel method for changing the appearance of images. Method: A set of 270 mammography cases (one view, both breasts) was acquired using five Hologic Selenia and two Hologic Dimensions X-ray sets: 80 normal cases, 80 cases with simulated inserted subtle calcification clusters, 80 cases with subtle real non-calcification malignant lesions and 30 cases with biopsy proven benign lesions. The 270 cases (arm 1) were converted to appear as if they had been acquired on three other imaging systems: caesium iodide detector (arm 2), needle image plate computed radiography (CR) (arm 3) and powder phosphor CR (arm 4). Seven experienced mammography readers marked the location of suspected cancers in the images. They classified the degree of visibility of the lesions and whether the lesion would require further investigation (recall) and their confidence in that decision. Statistical analysis was performed using JAFROC analysis. Results: Preliminary results show that some of the differences in lesion visibility and recall between pairs of arms for calcification clusters and non-calcification lesions were statistically significant (p<0.05). A significant relationship between the area under the curve for degree of visibility of calcification clusters and the threshold thickness for 0.25 mm diameter gold disks in the CDMAM test object was found. Conclusions: Detector type is likely to have a significant impact on the detection and recall of subtle calcification clusters and non-calcification cancers for images viewed at the same dose.

9037-18, Session 4

### Task-based optimization of image reconstruction in breast CT

Adrian A. Sanchez, Emil Y. Sidky, Xiaochuan Pan, The Univ. of Chicago Medical Ctr. (United States)

We demonstrate a task-based assessment of image quality in dedicated breast CT in order to optimize the number of projection views acquired. The methodology we employ is based on the Hotelling Observer (HO) and its associated metrics. We consider two tasks: the Rayleigh task of discerning between two resolvable objects and a single larger object, and the signal detection task of classifying an image as belonging to either a signal-present or signal absent hypothesis. HO SNR values are computed for 50, 100, 200, 500, and 1000 projection view images, with the total imaging radiation dose held constant. We use the conventional fan-beam FBP algorithm and investigate the effect of varying the width of a Hanning window used in the reconstruction, since this affects both the noise properties of the image and the under-sampling artifacts which can arise in the case of sparse-view acquisitions. Our results demonstrate that fewer projection views should be used in order to increase HO performance, which in this case constitutes an upper-bound on human observer performance. However, the impact on HO SNR of using fewer projection views, each with a higher dose, is not as significant as the impact of employing regularization in the FBP reconstruction through a Hanning filter.

9037-19, Session 4

## Evaluation of penalty design in penalized maximum-likelihood image reconstruction for lesion detection

Li Yang, Andrea Ferrero, Univ. of California, Davis (United States); Rosalie J. Hagge, University of California Davis (United States); Ramsey D. Badawi, Jinyi Qi, Univ. of California, Davis (United States)

Detecting cancerous lesions is a major clinical application in emission tomography. In previous work, we have studied penalized maximumlikelihood (PML) image reconstruction for the detection task, where we used a multiview channelized Hotelling observer (mvCHO) to assess the lesion detectability in 3D images. It mimics the condition where a human observer examines three orthogonal views of a 3D image for lesion detection. We proposed a method to design a shift-variant quadratic penalty function to improve the detectability of lesion at unknown locations, and validated it using computer simulations. In this study we evaluated the benefit of the proposed penalty function for lesion detection using real patient data. A patient was scanned under GE DST at UC Davis Medical Center. A Na-22 point source was scanned in air at variable locations and the point source data were superimposed onto the patient data as artificial lesions after attenuated by the patient body. Independent Poisson noise was added to high-count sinograms to generate 200 pairs of lesion-present and lesion-absent data sets, each mimicking a 5-minute scans. Lesion detectability was assessed using a multiview CHO and a human observer two alternative forced choice (2AFC) experiment. The results showed that the optimized penalty can improve lesion detection over the conventional quadratic penalty function.

9037-20, Session 4

## Observer assessment of multi-pinhole SPECT geometries for prostate cancer imaging, a simulation study

Faraz Kalantari, Anando Sen, Howard C. Gifford, Univ. of Houston (United States)

Quantitative SPECT imaging using Prostascint (In-111) is a method for detection of prostate tumors and prostate-cancer staging. Poor quality of the scans using conventional medium-energy parallel-hole (MEPAR) collimators inspired us to investigate multipinhole (MPH) imaging for tumor detection. MPH detectors may improve count sensitivity while providing much higher spatial resolution. For this abstract, we compared different MPH configurations for the task of small-tumor detection in the prostate and surrounding lymph nodes. Spherical tumors were placed within the prostate and lymph nodes of a digital anthropomorphic phantom having a typical Prostascint biodistribution. Analytical, kernelbased software was used to create different sets of projections. Different numbers of pinholes were simulated in both 180 and 360-degree orbits for data acquisition. Performance evaluation of each MPH configuration was carried out in a localization ROC (LROC) study with channelized nonprewhitening (CNPW) and visual-search model observers applied to 2D slices extracted from 3D reconstructions.

9037-21, Session 5

Comparing observer models and feature selection methods for a task-based assessment of digital breast tomosynthesis in reconstruction space

Subok Park, George Z. Zhang, Rongping Zeng, Kyle J. Myers,













U.S. Food and Drug Administration (United States)

A task-based assessment of image quality [Barrett and Myers 2004] for DBT can be done in the either projection or reconstructed data space. As the choice of observer models and feature selection methods can vary depending on the type of task and data statistics, we previously investigated the performance of two channelized-Hotelling observer (CHO) models in conjunction with 2D Laguerre-Gauss (LG) and two implementations of partial least squares (PLS) channels along with that of the Hotelling observer in binary detection tasks involving DBT projections [Zhang SPIE2013]. The difference in these observers lies in how the spatial correlation between angular DBT projections is incorporated in the observer's strategy to perform the given task. In the current work, we investigate how these seven observers compare for performing a binary detection task of a spherical signal object embedded in structured breast phantoms with the use of DBT reconstructed slices and incorporating the spatial correlation between different numbers of reconstruction slices. Our preliminary results indicate that either of the LG and PLS channels could be used for optimizing the system but on different tasks. For instance, LG could be good for the detection of the reconstructed signal similar to the original signal shape in the object space whereas PLS is more suitable for the classification of a given image using all signal information including reconstruction artifacts.

9037-22, Session 5

## Polar-map model observers for perfusion defects localization and detection in SPECT myocardial perfusion imaging

Felipe M. Parages, Illinois Institute of Technology (United States); J. Michael O'Connor, Univ. of Massachusetts Medical School (United States) and Univ. of Massachusetts Lowell (United States); Hendrik P. Pretorius, Univ. of Massachusetts Medical School (United States); Jovan G. Brankov, Illinois Institute of Technology (United States)

In medical imaging, model observers (MO) are frequently used to act as surrogates of human observers in task-based image quality assessment. In SPECT myocardial perfusion imaging (MPI), a task-based evaluation involves detection, localization and severity assessment of perfusion defects.

In this paper we propose use of a machine-learning model observer based on naive-bayes classification (NB-MO) which uses features extracted from the polar-map images. The proposed model observer is trained to predict defect localization and severity scores as given by five human observers, for each observer separately, in simulated SPECT myocardial perfusion imaging. Five human observers as well as corresponding model observer data were analyzed with multi-reader multi-case (MRMC) analysis using conventional area under the receiver operating characteristic (ROC) curve and alternative free-response ROC (AFROC) as figures of merit. In this work we also included a comparison with a variation of a previously published scanning linear observer (SLO) adapted to SPECT polar-maps images.

Preliminary results, using simulated data and human observer study from five experienced physicians reading images that included defects with variable: size, location and severity, show excellent agreement between NB-MO and humans observers.

9037-23, Session 5

### Design of a practical image-quality assessment method using real CT data

Hsin-Wu Tseng, College of Optical Sciences, The Univ. of Arizona (United States); Jiahua Fan, GE Healthcare (United States); Matthew A. Kupinski, College of Optical Sciences, The Univ. of

Arizona (United States); Paavana Sainath, GE Healthcare (United States)

The channelized Hotelling observer (CHO) is a powerful method for quantitative image quality evaluations of CT systems and their image reconstruction algorithms. These methods have recently been used to validate the dose reduction achievable using iterative imagereconstruction algorithms. The use of the CHO for routine and frequent system evaluations is desirable both for potential quality assurance evaluations as well as further system optimizations. The use of channels substantially reduces the amount of data required to achieve good estimates of observer performance. However, the number of scans required is still large enough even with channels to make methods impractical for routine use. This work explores different data reduction schemes and designs a new approach that requires only a few CT scans of a phantom. For this work, the leave-one-out likelihood (LOOL) method developed by Hoffbeck and Landgrebe is studied as an efficient method of estimating the covariance matrices needed to compute CHO performance. Three different approaches are included in the study: a conventional estimation technique with a large sample size, a conventional technique with fewer samples, and the new LOOL approach with fewer samples. The mean value and standard deviation of SNR is estimated by shuffle method. Results indicate that an 84% data reduction can be achieved without loss of accuracy making the proposed CHO based approach a practical tool for routine CT system assessment.

9037-24, Session 5

## Comparison of computational to human observer detection for evaluation of CT low dose iterative reconstruction

Brendan L. Eck, Rachid Fahmi, Case Western Reserve Univ. (United States); Kevin M. Brown, Nilgoun Raihani, Philips Healthcare (United States); David L. Wilson, Case Western Reserve Univ. (United States)

Model observers were compared to human detection so as to establish computational methods for assessing low dose iterative CT image reconstruction. A 5-channel Laguerre-Gauss Hotelling Observer (CHO) was used with six models adding noise to decision variable (DV) and/or channel outputs (CO). Models were: (1)DV-noise with constant standard deviation (std), (2)DV-noise with std proportional to DV std, (3)DV-noise with std proportional to DV plus a constant, (4)CO-noise with constant std across channels, (5)CO-noise in each channel with std proportional to CO variance, and (6)combined DV-noise as in (3) and CO-noise as in (5). 4AFC human experiments were performed on target sub-images with a flat background equidistant from the phantom center. Model parameters were estimated from human probability correct (PC) data. PC in human and all model observers increased with dose, contrast, and size, and was much higher for IMR than FBP. In fact, detectability of IMR was better than FPB at 1/3 dose, suggesting significant dose savings with IMR. Model-6 gave the best overall fit to humans across independent variables (dose, size, contrast, and reconstruction) at fixed display window. Model-6 fit the extraordinary difference between IMR and FBP, despite the different noise quality. Model predictability was demonstrated by the favorable comparison of Model-6 with fixed parameters to human detection on blended reconstructions consisting of weighted sums of FBP and IMR. It is anticipated that the model observer will predict results from iterative reconstruction methods having similar noise characteristics, enabling rapid comparison of methods.

9037-25, Session 5

### Assessment of prostate cancer detection with a visual-search human model observer

Anando Sen, Faraz Kalantari, Howard C. Gifford, Univ. of











Houston (United States)

The primary goal of this study is to compare tumor detection performances of human and model observers in prostate SPECT reconstructions. The data acquisition simulated a parallel-hole geometry with medium-energy collimators and reconstructions contained corrections for attenuation and detector response. Tumors were added to the acquired projections. The task of an observer is to test a reconstructed slice for the presence of a single tumor in the prostate or the lymph nodes. Tumors are detected using two model observers, the Channelized Non-Prewhitening (CNPW) scanning observer and a Visual Search (VS) observer. The scanning observer tests every point as a tumor location by projecting it into a space of channels while the VS uses clustering to identify suspicious candidates before applying the scanning observer on them. This is followed by a human observer study for the comparison of results. Both the models and the human study were scored by an LROC curve. The effect of contrast on the model and the human observers is discussed.

9037-26, Session 6

### Does sensitivity measured from screening test-sets predict clinical performance?

BaoLin P. Soh, The Univ. of Sydney (Australia) and Singapore General Hospital (Singapore); Warwick B. Lee, BreastScreen New South Wales (Australia); Claudia R. Mello-Thoms, Kriscia A. Tapia, The Univ. of Sydney (Australia); John T Ryan, Ziltron (Ireland); Wai Tak Hung, Graham J. Thompson, BreastScreen New South Wales (Australia); Rob Heard, Patrick C. Brennan, The Univ. of Sydney (Australia)

Aim: To examine the relationship between sensitivity measured from the BREAST test-set and clinical performance.

Background: Whilst both PERFORMS and BREAST test-set strategies have been regarded by the UK and Australia national breast screening programs as possible methods of estimating readers' clinical efficacy, the relationship between the results obtained from test-set reading and real life performance has never been satisfactorily understood.

Methods: Forty-one radiologists from BreastScreen New South Wales participated in this study. Each radiologist was asked to read a BREAST test-set which consisted of sixty de-identified mammographic examinations gathered from the BreastScreen Digital Imaging Library. Sensitivity measured from the BREAST test-set was compared with screen readers' clinical audit data using Spearman's rank correlation coefficient.

Results: Statistically significant positive moderate correlations were shown between test-set sensitivity and each of the following metrics: rate of invasive cancer per 10 000 reads (r=0.495; p < 0.01); rate of small invasive cancer per 10 000 reads (r=0.546; p < 0.001); detection rate of all invasive cancer and DCIS per 10 000 reads (r=0.444; p < 0.01).

Conclusion: Statistically significant positive moderate correlations were shown between sensitivity measured from the BREAST test-set and real life detection rate which validated that such test-set strategies can reflect readers' clinical performance and be used as a quality assurance tool. The strength of correlation demonstrated in this study was higher than previously found by others.

9037-27, Session 6

# Modeling resident error-making patterns in detection of mammographic masses using computer-extracted image features: preliminary experiments

Maciej A. Mazurowski, Jing Zhang, Joseph Y. Lo, Duke Univ.

(United States); Cherie M. Kuzmiak M.D., The Univ. of North Carolina at Chapel Hill (United States); Sujata V. Ghate M.D., Sora Yoon, Duke Univ. (United States)

Providing high quality mammography education to radiology trainees is essential, as good interpretation skills potentially ensure the highest benefit of screening mammography for patients. We have previously proposed a computer-aided education system that utilizes trainee models, which relate human-assessed image characteristics to interpretation error. We proposed that these models be used to identify the most difficult and therefore the most educationally useful cases for each trainee. In this study, as a next step in our research, we propose to build trainee models that utilize features that are automatically extracted from images using computer vision algorithms. To predict error, we used a random forest classifier which accepts imaging features as input and returns error as output. Reader data from 3 experts and 3 trainees were used. Receiver operating characteristic analysis was applied to evaluate the proposed trainee models. Our experiments showed that, for three trainees, our models were able to predict error better than chance. This is an important step in the development of adaptive computer-aided education systems since computer-extracted features will allow for faster and more extensive search of imaging databases in order to identify the most educationally beneficial cases.

9037-28, Session 6

## Mammographic density measurement: a comparison of automated volumetric density measurement to BIRADS

Christine N. Damases, The Univ. of Sydney (Australia) and Univ. of Namibia (Namibia); Mark F. McEntee, The Univ. of Sydney (Australia)

Breast density is considered a strong cancer risk, however its quantitative assessment is difficult. The aim of this study is to compare mammographic breast density assessment with automated volumetric software with Breast Imaging Reporting and Data System (BIRADS) categorization by radiologists. A data set of 120 mammograms was classified by twenty American Board of Radiology (ABR) Examiners. The mammograms were of 20 women (mean age, 60 years; range, 42-89 years). The data set comprised the left craniocaudal (LCC) and the left mediolateral oblique (LMLO) mammograms for each case. These women were image twice once with GE system and the following year with Hologic system. These images also had their volumetric density classified by using Volpara Density Grade (VDG). The radiologists were asked to estimate the mammographic density according to BIRADS categories (1-4). Statistical tests performed included independent samples t-test, Pearson's coefficient of correlation and Cohen's Kappa for statistical agreement. There was a moderate agreement between VDG classification and radiologist BIRADS density shown with Cohen's Kappa (k = 0.42; p ≤ 0.001). Radiologists estimated percentage density to be lower by an average of 0.44, the radiologist's BIRADS having a mean of 2.13 and the mean VDG higher at 2.57 (t = -15.56; p  $\leq$  0.001). VDG and radiologist's BIRADS showed a positive strong correlation (r = 0.78; p  $\leq$  0.001). Radiologist BIRADS and VDG AvBD% also showed a strong positive correlation (r = 0.86; p  $\leq$  0.001). There was a large spread of radiologist's BIRADS categories for each of the VDG AvBD% classifications.

9037-29, Session 6

## Pursuing optimal thresholds to recommend breast biopsy by quantifying the value of tomosynthesis

Yirong Wu, Oguzhan Alagoz, David J. Vanness, Amy Trentham-Dietz, Univ. of Wisconsin-Madison (United States); Elizabeth S. Burnside, Univ. of Wisconsin Hospital and Clinics (United States)











A 2% threshold has been traditionally used to recommend breast biopsy in mammography. We aim to characterize how the biopsy threshold varies to achieve the maximum expected utility (MEU) of tomosynthesis in breast cancer diagnosis. A cohort of 312 patients, imaged with standard full field digital mammography (FFDM) and digital breast tomosynthesis (DBT), was selected for a reader study. Fifteen readers interpreted each patient's images and estimated the probability of malignancy using two modes: FFDM versus FFDM + DBT. We generated receiver operator characteristic (ROC) curves with the probabilities for all readers combined. We found that FFDM+DBT provided improved accuracy and MEU compared with FFDM alone. When DBT was included in the diagnosis along with FFDM, the optimal biopsy threshold became 2.7% as compared with 2% threshold for FFDM alone. While understanding the optimal threshold from a decision analytic standpoint will not help physicians improve their performance without additional guidance (e.g. decision support to reinforce this threshold), the discovery of this level does demonstrate the potential clinical improvements attainable with DBT. Specifically, DBT has the potential to lead to substantial improvements in breast cancer diagnosis since it could reduce the number of patients recommended for biopsy while preserving the maximal expected utility.

9037-30, Session 6

## Efficacy of digital breast tomosynthesis for breast cancer diagnosis

Maram M. Alakhras, The Univ. of Sydney (Australia); Claudia R. Mello-Thoms, The Univ. of Sydney (Australia) and Univ. of Pittsburgh School of Medicine (United States); Mary Rickard, The Univ. of Sydney (Australia) and Sydney Breast Clinic (Australia); Roger Bourne, Patrick C. Brennan, The Univ. of Sydney (Australia)

Purpose: To compare the diagnostic performance of digital breast tomosynthesis (DBT) in combination with digital mammography (DM) with that of digital mammography alone Materials and Methods: Twenty six experienced radiologists who specialized in breast imaging read 50 cases of patients who underwent DM and DBT. Both exams included the craniocaudal (CC) and mediolateral oblique (MLO) views. 27 (54%) of the cases were cancers and 23 (46%) were non cancer cases, with histopathologic examination established truth in all lesions.

Each case was interpreted once with DM alone and once with DM+DBT, and the observers were asked to mark the location of the lesion, if present, and give it a score based on a five-category assessment by the Royal Australian and New Zealand College of Radiologists (RANZCR). The diagnostic performance of DM compared with that of DM+DBT was evaluated in terms of the difference between areas under receiver-operating characteristic (ROC) curves (AUCs) for RANZCR scores, Jackknife free-response receiver operator characteristics (JAFROC) figure-of-merit, sensitivity, location sensitivity and specificity.

Results: Average AUC and JAFROC for DM versus DM+DBT was significantly different (AUCs 0.690 vs 0.781, p=< 0.0001), (JAFROC 0.618 vs. 0.732, p=< 0.0001) respectively. The use of DBT in combination with DM resulted in an improvement in sensitivity (0.629 vs. 0.701, p=0.0011), location sensitivity (0.548 vs. 0.690, p=< 0.0001) and specificity (0.656 vs. 0.758, p=0.0015) for DM and DM+DBT respectively.

Conclusion: Adding DBT to DM significantly improved ROC, JAFROC, sensitivity, location sensitivity and specificity values. Keywords: Digital breast tomosynthesis. Digital mammography. Cancer. Diagnostic performance.

9037-31, Session 6

### Retrieving phase information in sonography for improved microcalcification detection

Sara Bahramian, Michael F. Insana, Univ. of Illinois at Urbana-Champaign (United States)

The process of echo-signal demodulation within the display stage of ultrasonic image formation discards signal phase. It has long been hypothesized that demodulation could be eliminating important clinical task information but the tools to rigorously study this effect were not developed. We have now developed an information analysis to show how task information flows through different stages of image formation. In this paper, we show how traditional display-stage processing eliminates high spatial-frequency task information, and how simple methods can recover the loss for improved diagnostic performance. We also study the improvement in detecting breast microcalcifications using the proposed method.

Sonographic images are computed from the envelope of the recorded radio-frequency echo signal. The envelope contains information at spatial frequencies limited by the bandwidth of pulse envelope. However, the signal phase of the pre-image echo signal can encode information about tissue structure at up to twice the pulse bandwidth. Even though phase information is eliminated by traditional demodulation methods, through simple modification in display processing we can recover lost information and introduce it back into the B-mode image. We verify these predictions with a set of breast-lesion simulations, where lesions contain microcalcifications that provide high-contrast, high-spatial-frequency detection challenges. We will demonstrate that sonography can increase sensitivity to microcalcifications in a manner accessible to human and model observers. Hence by understanding the information flow of the ideal observer at different stages of image formation, new opportunities for improving diagnostic performance emerge.

9037-32, Session 7

### Alternative applications of spatio-temporal contrast sensitivity in a 3D model observer

Ali N. Avanaki, Kathryn S. Espig, Barco, Inc. (United States); Cedric Marchessoux, Barco N.V. (Belgium); Predrag R. Bakic, Univ. of Pennsylvania (United States); Tom R. Kimpe, Barco N.V. (Belgium); Andrew D. A. Maidment, Univ. of Pennsylvania (United States)

In (A. Avanaki et al SPIE MI 2013), we reported that the results of CSF application with 3D linear filtering only follow the expected observation trend for browsing speed, and not viewing distance, display contrast or luminance. In order to better follow the expected observation trends, we now consider Probability Map (PM) and two versions of Monte Carlo (MC1&2) for application of human contrast sensitivity function (CSF) in a 3D model observer. In PM, the visibility probability for each frequency component of the stack, p, is calculated using Barten's spatio-temoporal CSF, component's modulation, and human's psychometric function. p is then considered to be the perceived amplitude of the frequency component and will be used by a traditional model observer (e.g., LGmsCHO). In MC1&2, a component is randomly kept with probability p or discarded with 1-p. The kept component amplitude is either normalized to unity (MC1) or left as-is (MC2). DBT stacks generated by a breast phantom (P. Bakic et al. Med Phys. 2011) are processed in the same simulation pipeline used in our previous paper but with alternative CSF application methods. Our results indicate MC1 as the most promising method, since it conforms to all four expected observation trends considered: it yields a detection performance that peaks at certain browsing speed and viewing distance, and increases with contrast and luminance. We are also planning to perform psychophysical experiments to validate our conclusion.











9037-33, Session 7

## Discovering common properties of human observers' visual search and mathematical observers' scanning I: theory and conjecture

Xin He, Frank W. Samuelson, Rongping Zeng, Berkman Sahiner, U.S. Food and Drug Administration (United States)

There is a lack of consensus in the objective assessment of observer performance in search tasks. To pursue a consensus, we propose a new principle. In particular, we propose to discover metrics to reflect the intrinsic properties of search observers. These properties, if discovered successfully, should have the ability to predict search observers' performance. The goal of this work is to present a theory and a conjecture toward two intrinsic properties of search observers: detectability (d') and effective uncertainty level (M\*). Detectability (d') quantifies the observer's ability to detect once the location is given and is a well-understood concept. Effective uncertainty level (M\*) quantifies the ability to search. The larger the M\* is, the more difficult it is to search. To objectively assess whether the two properties are "intrinsic", in a companion paper, we investigate their ability in predicting the search performance of both human observers and scanning channelized Hotelling observers.

9037-34, Session 7

### Human template estimation using a Gaussian processes algorithm

Francesc Massanes, Jovan G. Brankov, Illinois Institute of Technology (United States)

In this paper we propose the use of a machine learning algorithm based in Gaussian Processes to estimate a human observer linear template for the detection of a signal in a noisy background. Estimating a human observer template is not novel, however the use of a multi-kernel Gaussian Processes approach is. This model provides spatial smoothing by using a sparse kernel representation. For validation purposes, we train this model observer with the ground truth and the estimated template is actually the same as the statistically optimal detector. Next we presented the human observer template estimated for the detection of a signal on a different power-low background.

9037-35, Session 7

### A stereo matching model observer for stereoscopic viewing of 3D medical images

Gezheng Wen, Mia K. Markey, The Univ. of Texas at Austin (United States); Gautam S. Muralidlhar, VuCOMP (United States)

Stereoscopic viewing of 3D medical imaging data has the potential to increase the detection of abnormalities. We are developing a new stereo model observer inspired by the mechanisms of stereopsis in human vision. Given a stereo pair of images of an object (i.e., left and right images separated by a small displacement), our observer first finds the corresponding points between the two views, and then fuses them together to create the 2D cyclopean view. Assuming that the cyclopean view has extracted most of the 3D information presented in the stereo pair, a channelized Hotelling observer (CHO) can be utilized to make decisions. We conduct a simulation study that attempted to mimic the detection of breast lesions on stereo viewing of breast tomosynthesis projection images. We render voxel datasets that contain random 3D power-law noise to model normal breast tissues. A 3D Gaussian signal is added to some of the datasets to model the presence of a breast lesion. Multiple stereo pairs of projection images are generated for each dataset by changing the separation angle between the two views. The model calculates the disparity maps using Belief-Propagation-based matching,

and a CHO with Laguerre-Gaussian channels is applied to the cyclopean views. The performance of the model is evaluated in terms of the accuracy of binary decisions on the presence of the simulated lesions. ROCs conducted on testing images show that the model achieves the highest average the area under the curve with a separation angle of 8 degree.

9037-36, Session 7

### A model observer based on human perception to quantify the detectability

Georges Acharian, Trixell (France) and Gipsa-lab (France); Nathalie Guyader, Gipsa-lab (France); Jean-Michel Vignolle, Trixell (France); Christian Jutten, Gipsa-lab (France) and Institut Univ. de France (France)

In medical imaging, model observers such as the "Hotelling observer" and the "prewhitening matched filter" have been proposed to predict detectability of objects in X-ray images. These models are based on decision theory applied on the entire image. We developed a model closer to human visual perception in the sense that it takes into account gaze at some particular areas. Hence, the proposed method is locally derived on few areas that correspond to the salient areas of the objects to be detected. The study is divided into two parts: a psychophysical experiment to obtain human's performance and a theoretical part to develop and test the proposed model.

During the experiment, several participants were asked during a free search task to detect particular objects in noisy images. The luminance contrast of objects is adaptively adjusted according to their responses to obtain a percentage of correct detection for each object of 50 %.

The proposed model is based on the decision theory applied on small image areas corresponding to the high visual acuity of foveal vision. Areas were chosen according to their high saliency values computed through a bio-inspired model of visual attention. For each area, we computed the local likelihood ratio and the index of detectability. By supposing statistical independence between areas, we combine the local indexes and the model returns a global detectability index. The results show the proposed model outperforms classical models of the literature.

9037-37, Session 7

#### Detectability and image quality metrics based on robust statistics: following non-linear, noise-reduction filters

J. Eric Tkaczyk, Eri Haneda, GE Global Research (United States); Giovanni J. Palma, Razvan Iordache, Remy Klausz, Mathieu Garayt, GE Healthcare (France); Ann-Katherine Carton, GE Global Research (United States) and GE Healthcare (France)

Non-linear image processing and reconstruction algorithms that have the characteristics of noise reduction while preserving edge detail are currently being evaluated for the medical research field. We have implemented a robust statistics analysis of four widely utilized, methods. This work demonstrates consistent trends in filter impact by which such non-linear algorithms can be evaluated. We calculate the object-mass signal histogram and propose metrics based on measured non-Gaussian distributions that can serve as image quality measures similar to SDNR and detectability. The algorithms studied here vary significantly in their approach to noise reduction. Median filter (MD), bilinear (BL), anisotropic diffusion (AD) and total-variance regularization (TV) are techniques studied here. It is shown that the detectability of objects limited by Poisson noise is not significantly improved. The fraction of correct responses in repeated n-alternate forced choice experiments, for n=2-1000. However, multi-pixel objects or single pixels with contrast above the detectability threshold will benefit from non-linear processing











algorithms by increased median separation of the object-level histogram from the background-level distribution resulting in increased conspicuity.

9037-38, Session 7

# Discovering common properties of human observers' visual search and mathematical observers' scanning II: predicting individual human and mathematical observers' performance

Xin He, Frank W. Samuelson, Berkman Sahiner, U.S. Food and Drug Administration (United States)

We proposed a theory and conjectured two intrinsic properties to characterize the performance of search observers: 1) detectability (d'), which quantifies the ability to detect given the location cue and 2) effective uncertainty level (M"), which quantifies the ability to search. The larger the M\* is, the more difficult it is to search. In this paper, we assessed whether these properties are "intrinsic" by investigating their ability in predicting individual human and scanning channelized Hotelling observers' performance using Gaussian lumpy background images. In particular, for each observer, we designed experiments to measure his/her d' and M\*, which were then used to predict this particular observer's performance in search tasks of other settings. The predictions were then compared to the experimentally measured observer performance and received satisfactory agreement in most cases.

9037-39. Session PSMon

## A comparison of Australian and USA radiologists' performance in detection of breast cancer

Wasfi I. Suleiman, The Univ. of Sydney (Australia); Dianne Georgian-Smith, Brigham and Women's Hospital, Harvard Medical School. (United States); Michael G Evanoff, The American Board of Radiology (United States); Sarah Lewis, The Univ. of Sydney (Australia) and The Brain and Mind Research Institute (Australia); Mark F. McEntee, The Univ. of Sydney (Australia)

The purpose of this study is to compare the performance of expert mammography radiologists from Australia and the USA. A total of 41 radiologists, 21 from Australia and 20 from the USA, independently reviewed 30 mammographic cases containing two views mammograms a cranio-caudal (CC) and a medio-lateral oblique projection (MLO) of the same breast. Twenty cases had abnormal findings and 10 cases had normal findings. The same general procedure was used for both experiments. Readers were asked to locate any visualized cancer, and assign a level of confidence from 1 to 5. A normal image was represented with number 1 and malignant lesions with numbers 2-5. There was no restriction on search time and number of mouse-clicks. A jackknife free-response receiver operating characteristic (JAFROC), sensitivity, specificity and location sensitivity was calculated using Ziltron software and JAFROC V4.1. Radiologists received a measure of their accuracy at the end of the study. A Mann-Whitney test was used to compare the performance of both Australian and USA radiologists. Software (SPSS, version 21.0; SPSS, Chicago, IL) was used. The results of this study showed that the USA radiologists sampled had more years of experience (p  $\leq$  0.01) but read less mammograms per year (p  $\leq$  0.03); when experience and number of mammograms per year were taken into account the Australian radiologists sampled showed significantly higher sensitivity and location sensitivity (p≤0.001).

9037-40, Session PSMon

## Investigations of internal noise levels for different target sizes, contrasts, and noise structures

Minah Han, Shinkook Choi, Jongduk Baek, Yonsei Univ. (Korea, Republic of)

To describe internal noise levels for different target sizes, contrasts, and noise structures, Gaussian targets with four different sizes (i.e., standard deviation of 2,4,6 and 8) and three different noise structures(i.e., white, low-pass, and high-pass) were generated. The generated noise images were scaled to have standard deviation of 0.15. For each noise type, target contrasts were adjusted to have the same detectability based on NPW, and the detectability of CHO was calculated accordingly. For human observer study, 3 trained observers performed 2AFC detection tasks, and correction rate, Pc, was calculated for each task. By adding proper internal noise level to numerical observer(i.e., NPW and CHO), detectability of human observer was matched with that of numerical observers. Even though target contrasts were adjusted to have the same detectability of NPW observer, detectability of human observer decreases as the target size increases. The internal noise level varies for different target sizes, contrasts, and noise structures, demonstrating different internal noise levels should be considered in numerical observer to predict the detection performance of human observer.

9037-41, Session PSMon

## Investigating the visual inspection subjectivity on the contrast-detail evaluation in digital mammography images

Maria A. Sousa, Univ. de São Paulo (Brazil); Regina B. Medeiros, Univ. Federal de São Paulo (Brazil); Homero Schiabel, Univ. de São Paulo (Brazil)

A major difficulty in the interpretation of mammographic images is the low contrast and also, in the case of early detection of breast cancer, the reduced size of the features of malignancy on findings such as microcalcifications. Furthermore, image assessment is subject to significant reliance of the capacity of observation of the expert that will perform it, compromising the final diagnosis accuracy. Thinking about this aspect, this study evaluated the subjectivity of visual inspection to assess the contrast-detail in mammographic images. For this, we compared the human readings of images generated with the CDMAM phantom performed by four observers, enabling to determining a threshold of contrast visibility in each diameter disks present in the phantom. These thresholds were compared graphically and by statistical measures allowing us to build a strategy for use of contrast and detail (dimensions) as parameters of quality in mammography.

9037-42, Session PSMon

# The quest for 'diagnostically lossless' medical image compression: a comparative study of objective quality metrics for compressed medical images

Ilona A. Kowalik-Urbaniak, Dominique Brunet, Jiheng Wang, Univ. of Waterloo (Canada); David Koff, Nadine Smolarski-Koff, McMaster Univ. (Canada); Edward R. Vrscay, Univ. of Waterloo (Canada); Bill Wallace, Agfa HealthCare (Canada); Zhou Wang, Univ. of Waterloo (Canada)

Given the explosive growth of digital image data being generated,











researchers in medical imaging have been investigating the use of lossy compression methods for data storage. Since visual quality may be compromised, it is essential to be able to determine the degree to which a medical image can be compressed before its diagnostic quality is compromised. This study is primarily concerned with improved methods of objectively assessing the diagnostic quality of compressed medical images.

Radiologists most often employ the mean squared error (MSE) and its close relative, PSNR, even though they are known to characterize visual quality quite poorly. A more recent image fidelity measure, the structural similarity (SSIM) index, measures the difference/similarity between two images by combining three components of the human visual system -- luminance, contrast and structure. The result is a much improved assessment of visual quality.

In this paper, we examine whether compression ratio (CR), MSE and PSNR actually serve as reliable indicators of diagnostic quality, i.e., "model the perception of trained radiologists in a satisfactory way." We also examine the quality factor (QF) of the JPEG compression algorithm. The performances of the above indicators are compared to that of SSIM, based on experimental data collected in two experiments involving radiologists.

Analysis of our data in terms of ROC and Kolmogorov-Smirnov statistics reveals that (i) CR demonstrates the poorest performance, (ii) MSE/PSNR perform inconsistently and (iii) SSIM demonstrates the best performance, i.e., it provides the closest match to the subjective assessments of the radiologists.

9037-43, Session PSMon

### A comparison of ROC inferred from FROC and conventional ROC

Mark F. McEntee, Mariusz W. Pietrzyk, Stephen Littlefair, The Univ. of Sydney (Australia) and Brain & Mind Research Institute (Australia)

This study aims to determine whether receiver operating characteristic (ROC) scores inferred from free-response receiver operating characteristic (FROC) were equivalent to conventional ROC scores for the same readers and cases. Thirty-four examining radiologists of the American Board of Radiology independently reviewed 47 PA chest radiographs under at least two conditions. Thirty-seven cases had abnormal findings and 10 cases had normal findings. Half the readers were asked to first locate any visualized lung nodules, mark them and assign a level of confidence [the FROC mark-rating pair] and second give an overall to the entire image on the same scale [the ROC score]. The second half of readers gave the ROC rating first followed by the FROC mark-rating pairs. A normal image was represented with number 1 and malignant lesions with numbers 2-5. A jackknife free-response receiver operating characteristic (JAFROC), and inferred ROC (infROC) was calculated from the mark-rating pairs using JAFROC V4.1 software. ROC based on the overall rating of the image calculated using DBM MRMC software which was also used to compare infROC and ROC AUCs treating the methods as modalities. Pearson's correlations coefficient and linear regression were used to examine their relationship using SPSS, version 21.0; (SPSS, Chicago, IL). The results of this study showed no significant difference between the ROC and Inferred ROC AUCs (p≤0.44). While Pearson's correlation coefficient was 0.7 (p≤0.01). Inter-reader correlation calculated from Obuchowski-Rockette covariance's averaged 0.58 and intra-reader was less than 0.1.

9037-44, Session PSMon

### Visual search behavior during laparoscopic cadaveric procedures

Yan Chen, Leng Dong, Alastair G. Gale, Loughborough Univ. (United Kingdom); Benjamin Rees, Charles Maxwell-Armstrong

M.D., Queen's Medical Ctr. (United Kingdom)

Laparoscopic surgery provides a very complex example of medical image interpretation. The task entails visually examining a display that portrays the laparoscopic procedure from a varying viewpoint, eye-hand coordination, complex 3D interpretation of the 2D display image, efficient and safe usage of appropriate surgical tools, as well as other factors. Training in laparoscopic surgery typically entails practice using a surgical simulator as well as the viewing of previously recorded laparoscopic operations. A study was undertaken to determine whether any differences exist between where surgeons look during actual operations and where they look when simply viewing the same pre-recorded operations. It was hypothesised that differences would exist related to the different experimental conditions; however the relative effect of such differences for training purposes was unknown. The visual search behaviour of two experienced surgeons was recorded as they performed two types of laparoscopic operations on a cadaver. The operations were also digitally recorded. Subsequently they viewed the recording of their operations, again whilst their eye movements were monitored. Differences were found in various eye movement parameters when the two surgeons performed the operations and where they looked when they simply watched the recordings of the operations. It is argued that this reflects the different perceptual motor skills pertinent to the different situations. The importance of this for surgical training is explored. Additionally, the data analyses leads to new ways of considering dynamic medical image inspection and provides further insight into performance and visual search behaviour in such dynamic medical image scenarios.

9037-45, Session PSMon

### Direction of an initial saccade depends on radiological expertise

Mariusz W. Pietrzyk, The Univ. of Sydney (Australia); Mark F. McEntee, The Univ. of Sydney (Australia) and Brain & Mind Research Institute (Australia); Michael E. Evanoff, The American Board of Radiology (United States); Patrick C. Brennan, The Univ. of Sydney (Australia); Claudia R. Mello-Thoms, The Univ. of Sydney (Australia) and Univ. of Pittsburgh (United States)

Aim: To evaluate the role of radiographic details in global impression of chest x-ray images viewed by experts in thoracic and non-thoracic domains.

Background: Kundel and Nodine's seminal work (1) showed that within 200ms, radiologists could achieve a mean ROC score (Az-value) of 0.76 when identifying lung and cardiac abnormalities with similar results being obtained by Oestmann et al a decade later (2). These findings were refined by Carmody, Nodine and Kundel (3) who showed that within 300ms, 40% of subtle tumours in chest radiographs could be detected, but this could be increased to 85% when prior information regarding tumour location was provided. Whilst the methodologies were slightly different among these three studies, the message that the decision-making process depends heavily on information captured during very short image viewing durations that facilitated detection of image abnormalities was consistent, implying that factors other than foveal fixations may be at play when detecting radiologic abnormalities. The minimum duration of image display that is long enough to facilitate a global recognition was found between 240 and 300ms (4).

Method: The study was approved by IRB. Five thoracic and six non-thoracic radiologists participated in two tachistoscopic (one low pass and one with the entire frequency spectrum, each lasting 270ms) each containing 50 PA chest radiographs with 50% prevalence of pulmonary nodule. Eye movements were monitored in order to evaluate a presaccade shift of visual attention, saccade latency, decision time and the time to first fixation on a pulmonary nodule.

Conclusion: Thoracic radiologists benefited from high spatial frequency appearance during a rapid presentation of chest radiograph by allocating pre-saccade attention towards pulmonary nodules. This behaviour correlated with a higher number of correct decisions, followed by higher confidence in the decisions made, and briefer reaction times.













9037-46, Session PSMon

## Complementary Cumulative Precision Distribution: A New Graphical Metric for Medical Image Retrieval System

Jatindra K. Dash, Sudipta Mukhopadhyay, Indian Institute of Technology Kharagpur (India); Niranjan Khandelwal, Post Graduate Institute of Medical Education and Research (India)

Precision vs. recall graph is the most used evaluation measure amongst all graphical measures proposed for evaluating retrieval system. These graphs evaluate different systems by varying the number of top retrieval considered. However, in real life the operating point for different applications are known to prior. This necessitates evaluating retrieval system at a given operating point set by the user. This paper proposes a graphical metric called Complementary Cumulative Precision Distribution (CCPD) that evaluates different systems at a particular operating point considering each images in the database as query.

9037-47, Session PSMon

### Preliminary experiments on quantification of skin condition

Kenzo Kitajima, Hitoshi Iyatomi, Hosei Univ. (Japan)

Evaluation of skin conditions for cosmetic purpose is usually performed by his/herself and sometimes done by experts. It is, however, often subjective. In such a background, development of objective evaluation criteria for skin conditions has been called. In this study, we developed a new assessment method for skin conditions such as a moisturizing property of the skin and its fineness with the image analysis only. We captured a facial images from volunteer subjects aged between 30s and 60s by Pocket Micro® device (Scalar Co., Japan). This device has two image capturing modes; the normal mode and the non-reflection mode with the aid of its polarization filter. We captured images from a total of 68 spots from subjects' face with both modes and accordingly we analyzed a total of 136 skin images. The moisture-retaining property of the skin and subjective evaluation score of the skin fineness in 5-point scale for each case were also obtained in advance as a gold standard and their mean and SD were 35.15±3.22 (?S) and 3.45±1.17, respectively. We extracted a total of 107 image parameters and built linear regression models for estimating abovementioned items with a stepwise feature selection. The developed model for estimating skin moisture achieved the MSE of 1.92 ?S with 6 selected parameters, while the model for doing skin fineness achieved that of 0.51 scales with 7 parameters under the leave-one-out cross validation. We confirmed the developed models predicted the degree of skin moisture and skin fineness appropriately with only captured image.

9037-48, Session PSMon

## Validation and comparison of intensity based methods for change detection in serial brain images

Žiga Lesjak, Univ. of Ljubljana (Slovenia); Žiga Špiclin, Univ. of Ljubljana (Slovenia); Boštjan Likar, Franjo Pernuš, Univ. of Ljubljana (Slovenia)

Detection of morphological changes in the brain over time is a common clinical task when assessing the progress of a neurodegenerative disease such as multiple sclerosis. Morphological changes are usually quantified by manual delineation of lesions in serial magnetic resonance brain images. Several automatic methods for detection and quantification of changes in the brain over time were proposed to speed up the process and make it less susceptible to human errors. The absence of publicly

available image databases with corresponding gold standard of the changes, however, results in the new and existing methods being tested on different databases and even with different performance metrics. This makes direct comparison of existing methods difficult if not nearly impossible. Furthermore, some methods have not yet been tested on clinical images. In this paper, we focus on comparison and validation of three state-of-the-art intensity based methods for detection of changes in the brain over time. We created synthetic and clinical image databases so as to objectively assess the three methods. Our final goal is to make the synthetic and clinical image databases, and the gold standard segmentations, publicly available so as to enable an objective comparison of any existing and new change detection methods. As such, the image databases represent an important tool in translational research, enabling evaluation and selection of the methods for the particular application.

9037-49, Session PSMon

#### Validation of parameter estimation methods for determining optical properties of atherosclerotic tissues in intravascular OCT

Ronny Y. Shalev, Madhusudhana Gargesha, David Prabhu, Kentaro Tanaka, Andrew M. Rollins, Marco Costa M.D., Case Western Reserve Univ. (United States); Hiram G. Bezerra M.D., Univ. Hospitals of Cleveland (United States); Guy Lamouche, National Research Council Canada (Canada); David L. Wilson, Case Western Reserve Univ. (United States)

We compared parameter estimation methods for computing optical attenuation coefficient (u) from intravascular OCT pullbacks. We computed u's from small volumes of interest (VOIs) annotated by experts as calcified, fibrotic, or lipid from cadaver tissue and a specially constructed tissue phantom (Biomedical Optics Express, 3(6):1381). Hundreds of VOI's from multiple pullback datasets were analyzed. We eliminated catheter- and system-dependent response, log-transformed, filtered with average, median, or Lee filters, and estimated u for each VOI using fit to all data (ALL), average of fits to individual A-lines (AVG), parallel line fit (PL), robust average (RAVG), and robust parallel line (RPL). We employed chi-square, coefficient of variation of estimates, and separation of tissue types in multidimensional feature space to inform us about the best method. We observed that filtering was desirable and the preferred estimation methods were: RPL>RAVG>PL>AVG?ALL. With AVG, the following u's were obtained on phantoms: calcified (2.5±0.57/ mm), fibrotic (3.49±0.7/mm), and lipid (6.94±1.22/mm). For RPL, numbers were: calcified (2.3±0.36/mm), fibrotic (3.36±0.53/mm), and lipid (5.65±1.15/mm). A smaller spread in u's for RPL suggests robustness. Also, results were very similar to those obtained for clinical pullbacks, with means roughly within 20%. A per-VOI plot of (u,I') feature space (l'=average VOI intensity) showed non-overlapping clusters for the three phantom tissue types. We believe that the atherosclerotic phantoms used in our study will help fine-tune our computational approaches and enable automated tissue classification in the future.

9037-50, Session PSMon

## Automated stent strut coverage analysis in intravascular OCT images using support vector machine

Hong Lu, Case Western Reserve Univ. (United States); Kentaro Tanaka, Hiram G. Bezerra M.D., Univ. Hospitals Case Medical Ctr. (United States) and Cardiovascular Imaging Core Lab. (United States); Andrew M. Rollins, David L. Wilson, Case Western Reserve Univ. (United States)

Stent implantation is a popular coronary revascularization procedure for











patients with atherosclerosis. Various stent types have been developed to improve treatment efficacy. Stent strut coverage has been one of the major analysis targets of stent device trials. The absence of stent coverage after implantation is a potential biomarker of late stent thrombosis. With ideal resolution and imaging speed, intravascular OCT has been used to assess stent tissue coverage after stent implantation. Currently, intravascular OCT image analysis is primarily done manually, which usually only analyzes every third frame and still time consuming. In addition, inter- and intra-analyst variability is inevitable in manual analysis. We proposed a method to classify stent struts as covered or uncovered automatically. Based on manual criteria for covered and uncovered struts, 8 features were extracted at multiple positions around the struts and a support vector machine classifier was trained with manual ground truth. We performed leave-one-stent-out cross validation on 20 follow-up OCT pullbacks. 10451 covered and 4729 uncovered struts were analyzed in total. We achieved a sensitivity of 80% and a specificity of 82% in identifying uncovered struts. Most of the errors were from struts with tissue coverage thinner than 30 µm. The area under ROC is 0.88. Inter-analyst variability was analyzed by evaluating the performance of two analysts against a "gold standard" established by experienced analysts. The performance of our automated method lies in between the two analysts. With the proposed method, we can analyze all the frames containing struts efficiently and consistently, which will make our software a valuable tool for stent trials and clinical treatment.

9037-51, Session PSMon

### Analysis of temporal dynamics in imagery during acute limb ischemia and reperfusion

John M. Irvine, John Regan, Tammy A. Spain, Draper Lab. (United States); Joseph D. Caruso, Maricela Rodriquez, Rajiv Luthra, Jonathan Forsberg, Nicole J. Crane, Eric Elster, Naval Medical Research Ctr. (United States)

Ischemia and reperfusion injuries present major challenges for both military and civilian medicine. Improved methods for assessing the effects and predicting outcome could guide treatment decisions. Specific issues related to ischemia and reperfusion injury can include complications arising from tourniquet use, such as microvascular leakage in the limb, loss of muscle strength and systemic failures leading to hypotension and cardiac failure. Better methods for assessing the viability of limbs/tissues during ischemia and reducing complications arising from reperfusion are critical to improving clinical outcomes for at-risk patients. The purpose of this research is to develop and assess possible prediction models of outcome for acute limb ischemia using a pre-clinical model. Our model relies only on non-invasive imaging data acquired from an animal study. Outcome is measured by pathology and functional scores. We explore color, texture, and temporal features derived from both color and thermal motion imagery acquired during ischemia and reperfusion. The imagery features form the explanatory variables in a model for predicting outcome. Comparing model performance to outcome prediction based on direct observation of blood chemistry, blood gas, urinalysis, and physiological measurements provides a reference standard. Initial results show excellent performance for the imagery-base model, compared to predictions based direct measurements. This paper will present the models and supporting analysis, followed by recommendations for future investigations.

9037-52, Session PSMon

### Visual perception based x-ray fluoroscopy image enhancement

Santosh Singh, The Shiv Nadar Univ. (India); Ankur Gupta, Samsung Research India (India)

One of the most important points in the clear visibility of structures (especially in fluoroscopic images) is the difference between the

luminance of the foreground object with the background. In the proposed algorithm we are estimating the contrast ratio in between foreground and background as shown in Figure 1. As an example shown in the figure 1, our aim is to enhance the visibility of vessels. Initially we will first segment the vessels using the existing techniques and get the binary image. Once the boundaries of the vessels are detected in that vicinity a suitable size of window is placed to estimate the contrast ratio is that window. Suppose a suitable size window has been selected and placed on the boundary of the vessel. Assuming the contrast ratio between the foreground and background region is CR1, i.e. foreground\_1/ background\_1 = CR1 and when the same window is moved to next adjoining region then the contrast ration in between foreground and background is CR2, i.e. foreground\_2/background\_2 = CR2.

In similar fashion, the contrast ration has been estimated along all the edges of vessels by moving the non-overlapping window. According to the human perception literature, humans perceive the structures better when the contrast ratio is reasonably good in between foreground object in comparison to background. Now let's assume that CR is the ideal contract ratio for the best visibility of the objects in the fluoroscopic images. Also, assume that by moving non-overlapping window for the estimation of the contrast ration and we achieve N different contrast ratios which are different than the ideal contrast ratio, i.e., CR. For all those values which are different than ideal contrast ratios, our aim is to enhance the foreground region everywhere so that the contrast ratio is approximately close to ideal CR, which means CR1, CR2 and so on should be approximately equal to CR.

In the proposed algorithm, we have maintained the contrast ratio among all the non-overlapping windows in a such way that the visual perception of the vessels increases without increasing the x-ray dosage for the fluoroscopic images. Such proposed algorithm has many advantages for diagnostic as well as during the treatment of the disease.

9037-53, Session PSMon

## Clinical compliance of viewing conditions in radiology reporting environments against current quidelines and standards

Shona Daly, Louise A. Rainford, Marie Louise Butler, Univ. College Dublin (Ireland)

#### Background

Several studies have demonstrated the importance of environmental conditions in the radiology reporting environment, with many indicating that incorrect parameters could lead to error and mis-interpretation. Literature is available with recommendations as to the levels that should be achieved in clinical practice, but evidence of adherence to these guidelines in radiology reporting environments is absent. This study audited the reporting environments of four teleradiologist and eight nospital based radiology reporting areas. This audit aimed to quantify adherence to guidelines and identify differences in the locations with respect to layout and design, monitor distance and angle as well as the ambient factors of the reporting environments.

#### Method

In line with international recommendations, an audit tool was designed to enquire in relation to the layout and design of reporting environments, monitor angle and distances used by radiologists when reporting, as well as the ambient factors such as noise, light and temperature. The review of conditions were carried out by the same independent auditor for consistency. The results obtained were compared against international standards and current research. Each radiology environment was given an overall compliance score to establish whether or not their environments were in line with recommended guidelines.

#### Results and Conclusion

Poor compliance to international recommendations and standards among radiology reporting environments was identified. Teleradiology reporting environments demonstrated greater compliance than hospital environments. The findings of this study identified a need for greater











awareness of environmental and perceptual issues in the clinical setting. Further work involving a larger number of clinical centres is recommended.

9037-54, Session PSMon

# Study of quality perception in medical images based on comparison of contrast enhancement techniques in mammographic images

Bruno R. Matheus, Luciana B. Verçosa M.D., Bruno Barufaldi, Homero Schiabel, Univ. de São Paulo (Brazil)

With the absolute prevalence of digital images in mammography several new tools became available for radiologist; such as CAD schemes, digital zoom and contrast alteration. This work focuses in contrast variation and how the radiologist reacts to these changes when asked to evaluated image quality.

Three contrast enhancing techniques were used in this study: conventional equalization, Goes technique [1] – a digitization correction – and value subtraction. A set of 100 images was used in tests from some available online mammographic databases. The tests consisted of the presentation of all four versions of an image (original plus the three contrast enhanced images) to the specialist, requested to rank each one from the best up to worst quality for diagnosis. Analysis of results has demonstrated that Goes technique [1] produced better images in almost all cases. Equalization, which mathematically produces a better contrast, was considered the worst for mammography image quality enhancement in the majority of cases (69.7%). The value subtraction procedure produced images considered better than the original in 84% of cases.

Tests indicate that, for the radiologist's perception, it seems more important to guaranty full visualization of nuances than a high contrast image. Another result observed is that the "ideal" scanner curve does not yield the best result for a mammographic image. The important contrast range is the middle of the histogram, where nodules and masses need to be seen and clearly distinguished.

9037-55, Session PSMon

## CT radiation dose optimization: successful implementation for routine head, chest and abdominal CT examination

Lama Sakhnini, Univ. of Bahrain (Bahrain); Majed Dwaik, King Hamad Univ. Hospital (Bahrain); Jehad Tammous, King Hamad Univ. Hopsital (Bahrain); Rami Alawad, King Hamad Univ. Hospital (Bahrain)

The purpose of this study is to find an optimization approach to minimize the absorbed dose to adult patients undergoing CT examination, while maintain the diagnostic image quality. A single detector CT was considered, to represent typical practice in King Hamad University Hospital. We included 500 patients in this study and investigated radiation dose for three anatomical regions, head, chest and abdomen and pelvis. For each type of CT examination, two groups of patients were considered. 300 patients in Group I: were imaged according to the protocols set by the manufacturer. Group II: 200 patients were imaged according to the protocols set by our team after optimization. We were able to adjust the adjustable factors such as noise index, scan time, pitch, rotation time and slice thickness. For each examination the weighted volume CT dose index (CTDIvol) and dose length product (DLP) were recorded and noise is measured. Each study was also reviewed for image quality. Measured (CTDIvol, DLP) were compared to international reference levels. For Group I, the CTDIvol and DLP values were higher than the reference levels. After Dose optimization the CTDIvol and DLP values were significantly reduced to have lower values than the reference levels. The results of our study showed that the CTDIvol and DLP values taken from images done using the protocols set by the Ct machine developers are higher than the reference levels which indicate that manufacturers are focusing their efforts toward improving image quality rather than the minimizing the dose that can be given to the patient.

9037-56, Session PSMon

### MedXViewer: an extensible web-enabled software package for medical imaging

Padraig T. Looney, The Royal Surrey County Hospital NHS Trust (United Kingdom); Alistair Mackenzie, Kenneth C. Young, The Royal Surrey County Hospital NHS Trust (United Kingdom) and Univ. of Surrey (United Kingdom); Mark D. Halling-Brown, The Royal Surrey County Hospital NHS Trust (United Kingdom)

MedXViewer (Medical Extensible Viewer) is an application designed to allow workstation-independent, PACS-less viewing and interaction with anonymised medical images (e.g. observer studies). The application was initially implemented for use in digital mammography and tomosynthesis but the flexible software design allows it to be easily extended to other imaging modalities.

Regions of interest can be identified by a user and any associated information about a mark, an image or a study can be added. The questions and settings can be easily configured depending on the need of the research allowing both ROC and FROC studies to be performed.

The extensible nature of the design allows for other functionality and hanging protocols to be available for each study. Panning, windowing, zooming and moving through slices are all available while modality-specific features can be easily enabled e.g. quadrant zooming in mammographic studies.

MedXViewer can integrate with a web-based image database allowing results and images to be stored centrally. The software and images can be downloaded remotely from this centralised data-store. Alternatively, the software can run without a network connection where the images and results can be encrypted and stored locally on a machine or external drive.

Due to the advanced workstation-style functionality, the simple deployment on heterogeneous systems over the internet without a requirement for administrative access and the ability to utilise a centralised database, MedXViewer has been used for running remote paper-less observer studies and is capable of providing a training infrastructure and co-ordinating remote collaborative viewing sessions (e.g. cancer reviews, interesting cases).

9037-57, Session PSMon

### Atlas-registration based image segmentation of MRI human thigh muscles in 3D space

Ezak Ahmad, Moi Hoon Yap, Jamie S. McPhee, Hans Degens, Manchester Metropolitan Univ. (United Kingdom)

Automatic segmentation of anatomic structures of magnetic resonance thigh scans can be a challenging task due to the potential lack of precisely defined muscles boundaries and issues related to intensity inhomogeneity or bias field across an image. In this paper, we demonstrate a combination framework of atlas construction and image registration methods to propagate the desired region of interest (ROI) between atlas image and the targeted MRI thigh scans for quadriceps muscles, femur cortical layer and bone marrow segmentations. The proposed system employs a semi-automatic segmentation method on an initial image in one dataset (from a series of images). The segmented initial image is then used as an atlas image to automate the segmentation of other images in the MRI scans (3-D space). The processes include: ROI labeling, atlas construction and registration, and morphological











transform the atlas (template) image to the targeted image based on the prior atlas information and non-rigid registration.

#### INTRODUCTION

Human thigh muscles play an important role in locomotion and body rotation. Thigh muscles consist of two main compartments - the quadriceps muscle group on the anterior and the hamstrings on the posterior. Physical activity levels evidently decrease during aging [1] and the consequent disuse can impact on muscle size and function. The effect of ageing is not only limited to disuse, factors such as hormonal and other endocrine changes also contribute to muscle degenerative [2]. Figure 1, shows a transverse-plane cross section of the mid-thigh in a young (Figure 1(a)) and older (Figure 1 (b)) man and it is clear that the muscles of the older man were smaller and the whole-thigh had more fatty adipose tissue.

Over the past four years, physiologists from the School of Healthcare Science, Manchester Metropolitan University, have coordinated several large-scale research projects to investigate the causes of atrophy and weakness of leg muscles in old age and how this leads to problems in daily life activities. As part of this process, MRI images were collected from around 300 people aged between 18 and 90 years. The MRI images can be analyzed for muscle, fat and connective tissue content by examining pixel areas and pixel intensity, and quantification of the results reveals differences between people and the effects of ageing or disease [3].

Manual segmentation of ROIs within slices is well established, but extremely time consuming, laborious and prone to intra-operator variability [4]. Several studies have developed automated or semi-automated analysis techniques to study MRIs of brain, spinal cord, heart and other internal organs, but few have developed such techniques to study thigh muscles. The study of thigh muscles is a priority due to their importance in locomotion, mobility and metabolism and the extent of deterioration in ageing and disease. A reliable semi-automatic or fully automatic segmentation system is critical for large-scale studies to increase efficiency and reduce analysis time compared to manual segmentation. However, automatic segmentation often proves difficult due to image artifact, noise, echo, overlapping of pixel/voxel intensities and non- uniform 2-D pixel intensity.

#### 9037-58, Session PSMon

### Automatic segmentation of abdominal vessels for improved pancreas localization

Amal Farag, Jiamin Liu, Ronald M. Summers M.D., National Institutes of Health (United States) and Imaging Biomarkers and CAD Lab. (United States)

Accurate automatic detection and segmentation of abdominal organs from CT images is important for quantitative and qualitative organ tissue analysis as well as computer-aided diagnosis. The large variability of organ locations, the spatial interaction between organs that appear similar in medical scans and orientation and size variations are among the major challenges making the task very difficult. The pancreas poses these challenges in addition to its flexibility which allows for the shape of the tissue to vastly change. Due to the close proximity of the pancreas to numerous surrounding organs within the abdominal cavity the organ shifts according to the conditions of the organs within the abdomen, as such the pancreas is constantly changing. Combining these challenges with typically found patient-to-patient variations and scanning conditions the pancreas becomes harder to localize. In this paper we focus on three abdominal vessels that almost always abut the pancreas tissue and as such useful landmarks to identify the relative location of the pancreas. The splenic and portal veins extend from the hila of the spleen and liver, respectively, travel through the abdominal cavity and join at a position close to the head of the pancreas known as the portal confluence. A third vein, the superior mesenteric vein, anastomoses with the other two veins at the portal confluence. An automatic segmentation framework for obtaining the splenic vein, portal confluence and superior mesenteric vein is proposed using 17 (11 female and 6 male patients) contrast enhanced computed-tomography datasets. The proposed method

uses outputs from the multi-organ multi-atlas label fusion (MOMALF) and Frangi vesselness filter to obtain automatic seed points for vessel tracking and generation of statistical models of the desired vessels. The approach shows ability to identify the vessels and improve localization of the pancreas within the abdomen.

#### 9037-59, Session PSMon

## Ensuring consistent color display in medical images: in terms of color calibration, brightness of monitor and ambient light

Daiki Iwai, Nagoya Univ. Graduate School of Medicine (Japan); Minoru Hosoba, Kazuko Ohno, Yutaka Emoto, Yoshito Tabata, Kyoto College of Medical Science (Japan); Norihisa Matsui, Shimadzu Corp. (Japan)

#### **PURPOSE**

It is necessary to ensure consistency of color monitors in medical imaging such as endoscopy and nuclear medicine. However, color image consistency has not been accomplished yet and there is no standardized guideline for quality control of color monitors nor ambient light in image reading. Effects by color calibration, brightness of monitor and ambient light for color display are investigated. Furthermore, we estimate optimal surroundings for color image reading.

#### **METHODS**

We have introduced a simple color calibration device. Then degraded monitor is calibrated. Chromaticity distance is calculated and compared before and after calibration. Furthermore, color nuclear medicine image is compared visually before and after calibration.

To observe effects of monitor's brightness to chromaticity, maximum brightness level of monitor is deliberately changed in several monitors. Chromaticity of 120 colors are measured and mapped to chromaticity diagram and compared each gradation and each brightness levels.

Illumination which surrounds the monitor is deliberately changed at several levels. Chromaticity is compared with dark room in same color. And also brightness of monitor is changed each conditions to estimate effect of relationship between illumination and brightness.

#### RESULTS

Chromaticity distance which indicates color difference is significantly decreased especially in blue color by color calibration.

This trend depends on digital value of color, brightness of monitor and type of color.

#### CONCLUSION

Optimal circumstances for image reading are using color calibration, setting brightness to higher levels of monitor, making room darker as possible to ensure consistent color display. And it is necessary to make guideline for them.

#### 9037-60, Session PSMon

## Laterally extended field of view without geometric distortion using image stitching in open-configuration MRI

Cheol Pyo Hong, Dong-Hoon Lee, Korea Research Institute of Standards and Science (Korea, Republic of); Bong Soo Han, Yonsei Univ. (Korea, Republic of)

Open-configuration MRI for easy patient access causes a restricted imaging field of view and geometrical distortion resulting in reduced reliability of the structural information application, such as the quantitation of tissue segmentation and the planning of radiotherapy treatment. The method proposed in this study is use of MR image











stitching, which is merging divided isocentric images of the same object through the table moving laterally. This stitching procedure results in an elongated field of view and provides a distortion-corrected image due to main field homogeneity and gradient field linearity are guaranteed near the isocenter relative to the far from the magnet isocenter. Simultaneously laterally extended and distortion corrected images were successfully acquired using image stitching procedure. These methods are beneficial towards defining tissue segmentation in large filed of view and the more accurate calculation of adipose tissue levels.

9037-61, Session PSMon

### A new iterative method for liver segmentation from perfusion CT scans

Ahmed Draoua, Univ. d'Auvergne Clermont-Ferrand I (France); Adélaïde Albouy-Kissi, Antoine Vacavant, Univ. d'Auvergne Clermont-Ferrand I (France); Vincent Sauvage, ISIT, UMR6284 CNRS/Université d'Auvergne, F-63001, Clermont-Ferrand, France (France)

Liver cancer is the third most common cancer in the world, and the majority of patients with liver cancer will die within one year as a result of the cancer. Liver segmentation in the abdominal area is critical for diagnosis of tumor and for surgical procedures. Liver segmentation is a challenging task as liver tissue has to be separated from adjacent organs and substantially the heart. In this paper we present a novel liver segmentation iterative method based on Fuzzy C-means (FCM) coupled with a fast marching segmentation and mutual information. However, a prerequisite for this method is the determination of slice correspondences between ground truth that is, a few images segmented by an expert, and images that contain liver and heart at the same time.

#### 1. INTRODUCTION

Liver cancer [1] is the third leading cancer. The efficiency of organ volume quantification highly depends on robust and reliable segmentation methods which are able to extract the desired organs/structures from medical images. The most reliable 3D segmentation methods are iterative methods, but the major drawback of these methods is (a) the oversegmentation they may produce, and (b) they can be time-consuming. Indeed at each iteration, the image has to be recalculated, and users take a long time to choose the parameters that adapt the best to the type of 3D images. In this context, we propose a semi-automatic method which is guided by ground truth, composed of a few images manually segmented by an expert, and Fuzzy C-means clustering to simplify the image by removing heart before the segmentation.

Problem of existence of the liver and heart on the same slices:

The liver is located in the upper right quadrant of the abdomen [4], the right of the stomach and above the intestines. It extends from the abdomen to the thorax which creates slices containing both the liver and heart during a scanning acquisition which is shown in Figure 1. In some sections the problem of differentiation between the liver and the heart is small (Fig.1.a), but in some slices the problem becomes more complicated (Fig.1.b).

Problem of noise in CT images:

Image noise generated by moving the body of patient or by the reconstruction of the perfusion CT images is a major problem in the field of image processing; it disturbs the segmentation in CT images by noising contours which limits growth of segmentation algorithms causing an over-segmentation or a sub-segmentation [5]. In this work we use CT images of the abdomen for extracting the liver where noises have become increasingly important. This forced us to use a preprocessing step (see Fig.2) before the fast marching segmentation, for preserving the data on organs contour.

#### 2. PRESENTATION OF THE PROPOSED METHOD

In this paper the goal of our method is to segment the liver semiautomatically [2], and is based on three main modules. 9037-62, Session PSMon

## Evaluation of correlation between CT image features and ERCC1 ptotein expression in assessing lung cancer prognosis

Maxine Tan, Nastaran Emaminejad, The Univ. of Oklahoma (United States); Wei Qian, The Univ. of Texas at El Paso (United States); Yan Kang, Northeast University (China); Yubao Guan, Guangzhou Medical University (China); Fleming Yuan Ming Lure, The Univ. of Texas at El Paso (United States); Bin Zheng, The Univ. of Oklahoma (United States)

Due to promotion of lung cancer screening using CT images, more Stage I non-small-cell lung cancers (NSCLC) are detected in current clinical practice. However, a high percentage of NSCLC patients will have cancer relapse after surgery. Accurately predicting prognosis of the NSCLC patients is important to optimally treat and manage the patients after surgery to minimize the risk of cancer relapse. Studies have shown that an excision repair cross-complementing 1 (ERCC1) gene was a potentially useful genetic biomarker to predict prognosis of NSCLC patients. In this study, we investigated and evaluated the correlations between the computed CT image features and ERCC1 gene expression. A database involving 133 NSCLC patients was used. Each patient had a thoracic CT examination and ERCC1 genetic test. We applied a computer-assisted scheme to segment lung volume and tumors. We then computed a set of quantitative image features from tumor and lung parenchymal regions. A logistic regression method was applied to analyze the correlation between each computed image feature and ERCC1 expression. The adjust odds ratios were also computed to identify the possibly increasing trend of image features associated with ERCC1 gene expression. The data analysis results showed that tumors with irregular edge and pleural indentation had significant negative correlation with ERCC1 protein expression levels (p<0.05). The normalized odds ratios of ERCC1 negative expression are 2.22 and 7.25 for the cases depicting tumors with lobular and spiculated edge, respectively. The study indicates that CT phenotype features may also be useful to help predict prognosis of NSCLC patients.

9037-63, Session PSMon

### Comparison of two indirect detection flat panel imagers

Kent M. Ogden, Kimball Clark M.D., Andrij R. Wojtowycz M.D., Michele Lisi M.D., Ernest M. Scalzetti M.D., SUNY Upstate Medical Univ. (United States)

As part of an application for FDA clearance for the use of a new flat-panel indirect detection imager, the FDA required the manufacturer to provide evidence of the image quality equivalence of the new detector with an approved predicate detector currently used in the manufacturer's radiographic/fluoroscopic room. To provide evidence of image quality equivalence, observer studies were conducted by four board-certified Radiologists. These studies consisted of two sets of experiments, one in which images from the two detectors were compared side by side and the preference for one of the images was recorded, and a second set in which each individual image was scored for image contrast, noise, and resolution. These individual scores were also used to create a composite overall image quality score for each image. 30 images or fluoro loops were collected from each detector under IRB approval. Images were anonymized and displayed on diagnostic quality dicom calibrated grayscale monitors during the experiments.

In both sets of experiments, statistical analysis of the results showed that there was not a significant difference in the image quality produced by the two detectors. There were slightly higher scores for images from the new experimental detector. Based on the results of these observer studies, FDA approval was applied for and 510k clearance was granted in May 2013.











Sunday - Tuesday 16-18 February 2014

Part of Proceedings of SPIE Vol. 9038 Medical Imaging 2014: Biomedical Applications in Molecular, Structural, and Functional Imaging

9038-1, Session 1

# Abdominal adipose tissue quantification on water suppressed and non-water suppressed MRI at 3T using semi-automated FCM clustering algorithm

Sunil Kumar Valaparla, The Univ. of Texas Health Science Ctr. at San Antonio (United States); Qi Peng, Albert Einstein College of Medicine (United States); Feng Gao, Geoffrey D. Clarke, The Univ. of Texas Health Science Ctr. at San Antonio (United States)

Because excessive body fat is associated with impaired insulin sensitivity, type 2 diabetes mellitus (T2DM) and cardiovascular disease, accurate measurements of human body fat distribution are desirable. In this study, we hypothesized that the performance of water saturated (WS) MRI is superior to non-water saturated (NWS) MRI for volumetric assessment of abdominal subcutaneous (SAT), intramuscular (IMAT), visceral (VAT), and total (TAT) adipose tissues. We acquired T1-weighted images on a 3T MRI system (TIM Trio, Siemens), which was analyzed using semi-automated segmentation software that employs a fuzzy c-means (FCM) clustering algorithm (Zhou A, et al., J Magn Reson Imag, 2011.34: 852). Sixteen contiguous axial slices, centered at the L4-L5 level of the abdomen, were acquired in eight T2DM subjects with water suppression (WS) and without (NWS). Histograms from WS images show improved separation of non-fatty tissue pixels from fatty tissue pixels, compared to NWS images. Paired t-tests of WS versus NWS showed a statistically significant lower volume of lipid in the WS images for VAT (145.3 cc less, p=0.006) and IMAT (305 cc less, p<0.001), but not SAT (14.1 cc more, NS). WS measurements of TAT also resulted in lower fat volumes (436.1 cc less, p=0.002). There is strong correlation between WS and NWS quantification methods for SAT measurements (r=0.999), but poorer correlation for VAT studies (r=0.845). These results suggest that NWS pulse sequences may overestimate adipose tissue volumes and that WS pulse sequences are more desirable due to the higher contrast generated between fatty and non-fatty tissues.

9038-2, Session 1

### Accelerated self-gated UTE MRI of the murine heart

Abdallah G. Motaal, Nils Noorman, Wolter DeGraaf, Luc Florack, Klaas Nicolay, Gustav J. Strijkers, Technische Univ. Eindhoven (Netherlands)

We introduce a new protocol to obtain radial Ultra-Short TE (UTE) MRI Cine of the beating mouse heart within reasonable measurement time. The method is based on a self-gated UTE with and golden angle radial acquisition and compressed sensing reconstruction. The stochastic nature of the retrospective triggering acquisition scheme produces an under-sampled and random kt-space filling that allows for compressed sensing reconstruction, hence reducing scan time. As a standard, an intragate multislice FLASH sequence with an acquisition time of 4.5 min per slice was used to produce standard Cine movies of 3 mice hearts with 15 frames per cardiac cycle. The proposed self-gated sequence is used to produce Cine movies with short echo time. The total scan time was 11 min per slice. 6 slices were planned to cover the heart from the base to the apex. 2X, 4X and 6X under-sampled k-spaces cine movies were produced from 2, 1 and 0.7 min data acquisitions for each slice. The accelerated cine movies of the mouse hearts were successfully reconstructed with a compressed sensing algorithm. Compared to the FLASH cine images, the UTE images showed much less flow artifacts due to the short echo time. Besides, the accelerated movies had high

image quality and the under-sampling artifacts were effectively removed. Left ventricular functional parameters derived from the standard and the accelerated cine movies were nearly identical.

9038-3, Session 1

### Regional cyst concentration as a prognostic biomarker for polycystic kidney disease

Joshua D. Warner, Maria V. Irazabal-Mira, Vicente E. Torres M.D., Bernard F. King M.D., Bradley J. Erickson M.D., Mayo Clinic (United States)

Polycystic kidney disease (PKD) is a leading cause of renal failure. Despite significant recent advances in the molecular and genetic mechanisms for PKD, the functional mechanisms underpinning the declines in renal function observed in the disorder are not well established. One dominant theory asserts that mass effects from growing cysts disrupt or block the function of normal nephrons. If true, the medullary region is hypothesized to be most vulnerable as normal nephrons pass through the medulla three times, via the descending and ascending limbs of the loop of Henle and, finally, the collecting duct. This study introduces regional cyst concentration as a potential new metric for evaluation of patients with PKD. Our results show central cyst concentration correlates with disease progression significantly better than peripheral cyst concentration. These results provide evidence supporting the mass effect hypothesis.

9038-4, Session 1

## Supervised multi-view canonical correlation analysis: fused multimodal prediction of disease prognosis

Asha Singanamalli, Haibo Wang, Case Western Reserve Univ. (United States); George Lee, Rutgers, The State Univ. of New Jersey (United States); Natalie Shih, Amy Ziober, Mark Alan Rosen M.D., Stephen Master, Univ. of Pennsylvania (United States); John E. Tomaszewski M.D., Univ. at Buffalo (United States); Michael D. Feldman, Univ. of Pennsylvania (United States); Anant Madabhushi, Case Western Reserve Univ. (United States)

While the plethora of information from multiple imaging and non-imaging data streams presents an opportunity for discovery of fused multimodal, multiscale biomarkers, they also introduce multiple independent sources of noise that hinder their collective utility. In this work, we introduce supervised multi-view canonical correlation analysis (sMVCCA), a novel data fusion method that attempts to find a common representation for multiscale, multimodal data where class separation is maximized while noise is minimized. Although this method can be applied to any number of modalities, we demonstrate its application in the context of integrating upto four data streams to predict prostate cancer (CaP) aggressiveness pre- and post- radical prostatectomy (RP) using two datasets. The first dataset comprised of 16 CaP patients with primary Gleason grades of 3 and 4 who underwent (i) T2-w and (ii) dynamic contrast enhanced (DCE) magnetic resonance imaging (MRI) prior to RP, upon which (iii) H&E and (iv) vascular (CD31) stained histology were acquired. Textural and contrast kinetic features from MRI were fused with quantitative histomorphometric (Qh) features that quantify gland and microvessel architecture on histology. SVM classifier yielded the highest classification AUC of 0.92 +/- 0.08 in the sMVCCA joint-space representation as











compared with that of MVCCA, PCA and LDA. The second dataset comprised of (i) H&E stained digitized histologic images and (ii) protein expression measurements for 40 intermediate grade CaP patients who were followed up for 5 years to monitor biochemical recurrence (BcR) post RP. Gland Qh features and proteomic features projected onto the sMVCCA subspace provided an AUC of 0.87 +/- 0.09 with SVM classification, significantly higher than that of MVCCA, PCA and LDA. In addition, Kaplan-Meier curves generated based on classifier prediction in the sMVCCA joint subspace showed significant (p < 0.05) differences for patients with and without BcR, unlike those generated from classifier prediction in the feature spaces of individual modalities.

9038-5, Session 1

#### Target image search using fMRI signals

Shi Xiong, SuTao Song, Yu Zhan, Jiacai Zhang, Beijing Normal Univ. (China)

Recent neural signal decoding studies based on functional magnetic resonance imaging(fMRI) have identified the specific image that the subject observed from a set of potential images by decoding brain signals, and some new decoding study have even reconstructed accurate pictures presented to the observer. In this paper, we described a target image searching method based on the relationship between target image stimuli and fMRI activity. The serial visual presentation task contained 16 blocks of runs, and we recorded fMRI data during a serial visual presentation task in each block. In 8 blocks, subjects were asked to press a button, while in the other 8 blocks, subjects were required to just view image stimuli without any response. In the serial visual presentation task, target images in a sequence of non-target distractor images elicited a stereotypical response in the fMRI, which can be detected by multivoxel pattern analysis. Classifiers designed with support vector machine (SVM) used this response to decipher target images. The leave-oneblock-out cross-validation showed that we can pick out the target images with a possibility far above chance level, which indicate that there's an neural signatures correlated with the target image recognition process in the human systems.

9038-6. Session 2

## Different brain activations between own- and other-race face categorization: an fMRI study using group independent component analysis

Wenjuan Wei, Institute of Automation (China); Jiangang Liu, Beijing Jiaotong Univ. (China); Ruwei Dai, Lu Zi Feng M.D., Institute of Automation (China); Ling Li, Beijing Jiaotong Univ. (China); Jie Tian, Institute of Automation (China)

Previous behavioral researches have proved that individuals process own- and other-race faces differently. One well-known effect is the other-race effect (ORE), which indicates that individuals category otherrace faces more accurately and faster than own-race faces. The existed functional magnetic resonance imaging (fMRI) studies of the other-race effect mainly focused on the racial prejudice and the socio-affective differences towards own- and other-race face. In the present fMRI study, we adopted a race-categorization task to determine the activation level differences between categorizing own- and other-race faces. Thirty one Chinese participants who live in China with Chinese as the majority and who had no direct contact with Caucasian individual were recruited in the present study. We used the group independent component analysis (ICA), which is a method of blind source signal separation that has proven to be promising for analysis of fMRI data. We separated the entail data into 56 components which is estimated based on one subject using the Minimal Description Length (MDL) criteria. The components sorted based on the multiple linear regression temporal sorting criteria, and the fit regression parameters were used in performing statistical test to evaluate the taskrelatedness of the components. The one way anova was performed to

test the significance of the component time course in different conditions. Our result showed that the areas, which coordinates are similar to the right FFA coordinates that previous studies reported, were greater activated for own-race faces than other-race faces, while the precuneus showed greater activation for other-race faces than own-race faces.

9038-7, Session 2

# Effects of non-neuronal components for functional connectivity analysis from resting-state functional MRI toward automated diagnosis of schizophrenia

Junghoe Kim, Samsung Advanced Institute of Technology (Korea, Republic of) and Korea Univ. (Korea, Republic of); Jong-Hwan Lee, Korea Univ. (Korea, Republic of)

A functional connectivity (FC) analysis from resting-state functional MRI (rsfMRI) is gaining its popularity toward the clinical application such as diagnosis of neuropsychiatric disease. To delineate the brain networks from rsfMRI data, non-neuronal components including head motions and physiological artifacts mainly observed in cerebrospinal fluid (CSF), white matter (WM) along with a global brain signal have been regarded as nuisance variables in calculating the FC level. However, it is still unclear how the non-neuronal components can affect the performance toward diagnosis of neuropsychiatric disease. In this study, a systematic comparison of classification performance of schizophrenia patients was provided employing the partial correlation coefficients (CCs) as feature elements. Pair-wise partial CCs were calculated between brain regions, in which six combinatorial sets of nuisance variables were considered. The partial CCs were used as candidate feature elements followed by feature selection based on the statistical significance test between two groups in the training set. Once a linear support vector machine was trained using the selected features from the training set, the classification performance was evaluated using the features from the test set (i.e. leave-one-out cross validation scheme). From the results, the error rate using all nonneuronal components as nuisance variables (12.4%) was significantly lower than those using remaining combination of non-neuronal components as nuisance variables (13.8 ~ 20.0%). In conclusion, the non-neuronal components substantially degraded the automated diagnosis performance, which supports our hypothesis that the nonneuronal components are crucial in controlling the automated diagnosis performance of the neuropsychiatric disease using an fMRI modality.

9038-8, Session 2

## Alternations of functional connectivity in amblyopia patients: A resting-state fMRI study

Jieqiong Wang, Institute of Automation (China); Ling Hu, Capital Medical Univ. (China) and Beijing Tongren Hospital (China); Wenjing Li, Institute of Automation (China); Junfang Xian, Beijing Tongren Hospital, Capital Medical University (China); Likun Ai, Capital Medical Univ. (China) and Beijing Tongren Hospital (China); Huiguang He, Institute of Automation (China)

Amblyopia is a common yet hard-to-cure disease in children and results in poor or blurred revision. Some efforts such as voxel-based analysis, cortical thickness analysis have been tried to reveal the pathogenesis of amblyopia. However, few studies focused on whether amblyopes show characteristic alterations in the functional connectivity (FC) patterns. In this study, we performed the analysis of abnormalities between amblyopia patients and normal controls in three levels: (1)seed-based FC with the left/right primary visual cortex, (2)the network constructed throughout the whole brain and (3)the local network constructed within visual-related regions. Experiments showed the following results: (1)For











seed-based FC, FC between superior occipital gyrus and the primary visual cortex was found to significantly decrease in both sides of the primary visual cortex. The abnormalities were also found in lingual gyrus. The results may reflect functional deficits both in dorsal stream and ventral stream. (2)For the whole brain network, decreased FC was mainly observed in the entire brain and regions. The normalized percentage of regions that have decreased FC with insula cortex to is far more than that with the other structures. The results demonstrated that insula cortex plays a special role in amblyopia. (3)In terms of the local network, no significant abnormalities were found. Our findings suggested that using FC is an effective way to explore the pathogenesis of amblyopia.

9038-9, Session 2

#### Longitudinal MR Cortical Thinning of Individuals and Its Correlation with PET Metabolic Reduction - A Measurement Consistency and Correctness Studies

Zhongmin S. Lin, Gopal B. Avinash, Kathryn M. McMillan, Litao Yan, GE Healthcare (United States); Satoshi Minoshima, Univ. of Washington (United States)

Cortical thinning and metabolic reduction can be possible biomarkers for Alzheimer's disease (AD) diagnosis and monitoring. Many techniques have been developed for the cortical measurement and widely used for the clinical statistical studies. However, the measurement consistency of individuals, an essential requirement for a clinically useful technique, requires proper further investigation. Here we leverage our previously developed technique[1] to measure cortical thickness and thinning and use it with longitudinal MRI from ADNI to investigate measurement consistency and spatial resolution. 10 normal, 10 MCI, and 10 AD subjects in their 70s were selected for the study. Consistent cortical thinning patters were observed in all baseline and follow up images. Rapid cortical thinning was shown in some MCI and AD cases. To evaluate the correctness of the cortical measurement, we compared longitudinal cortical thinning with clinical diagnosis and longitudinal PET metabolic reduction measured using 3D-SSP technique[2] for the same person. Severe cortical thinning that might link to disease conversion from MCI to AD was observed in two cases. Longitudinal MR cortical thinning and corresponding PET metabolic reduction showed high level pattern similarity revealing certain correlations worthy of further studies. In summary, our results suggest that consistent cortical measurements using our technique may provide means for clinical diagnosis and monitoring at individual patient's level; MR cortical thinning measurement can supplement PET metabolic reduction measurement.

9038-10, Session 2

## Independent component analysis of DTI data reveals white matter covariances in Alzheimer's disease

OuYang Xin, XiaoYu Sun, Ting Guo, QiaoYue Sun, Beijing Normal Univ. (China); Kewei Chen, Banner Alzheimer's Institute (United States) and Banner Good Samaritan Medical Ctr. (United States); Li Yao, Xia Wu, Xiaojuan Guo, Beijing Normal Univ. (China)

Alzheimer's disease (AD) is a progressive neurodegenerative disease with the clinical symptom of the continuous deterioration of cognitive and memory functions. Multiple diffusion tensor imaging (DTI) index such as fractional anisotropy (FA) and mean diffusivity (MD) can successfully explain the white matter damages in AD patients. However, most studies focused on the univariate measures (voxel-based analysis) to examine the differences between AD patients and normal controls (NC). In this investigation, we applied a multivariate analytic independent component analysis (ICA) to investigate the white matter covariances based on

FA measurement in DTI data in 35 AD patients and 45 NC from the Alzheimer's Disease Neuroimaging Initiative (ADNI) database. We found that six independent components (ICs) showed significant FA reductions in white matter covariances in AD compared with NC, including the genu and splenium of corpus callosum (IC 1 and IC 2), middle temporal gyral of temporal lobe (IC 3), sub-gyral of frontal lobe (IC 4 and IC 5) and sub-gyral of parietal lobe (IC 6). Our findings revealed covariant white matter loss in AD patients and suggest that the unsupervised data-driven ICA method is effective to explore the changes of FA in AD. This study assists us in understanding the mechanism of white matter covariant reductions in the development of AD.

#### Purpose

Using diffusion tensor imaging (DTI) technology, we performed independent component analysis (ICA) to the fractional anisotropy (FA) maps and investigated regional covariance patterns of the white matter associated with Alzheimer's disease (AD).

9038-11, Session 2

### A brain MRI atlas of the common squirrel monkey, Saimiri sciureus

Yurui Gao, Swetasudha Panda, Shweta P. Khare, Ann S. Choe, Iwona Stepniewska, Xia Ll, Zhoahua Ding, Adam Anderson, Bennett A. Landman, Vanderbilt Univ. (United States)

The common squirrel monkey, Saimiri sciureus, is a New World monkey with functional and microstructural organization of central nervous system similar to that of humans. It is one of the most commonly used South American primates in biomedical research. Unlike its Old World macaque cousins, no digital atlases have described the organization of the squirrel monkey brain. Here, we present a multi-modal magnetic resonance imaging (MRI) atlas constructed from the brain of an adult female squirrel monkey. In vivo MRI acquisitions include T2 structural imaging and diffusion tensor imaging. Ex vivo MRI acquisitions include T2 structural imaging and diffusion tensor imaging. Cortical regions were manually annotated on the co-registered volumes based on published histological sections.

9038-12, Session 3

# Incorporation of learned shape priors into a graph-theoretic approach with application to the 3D segmentation of intraretinal surfaces in SD-OCT volumes of mice

Bhavna J. Antony, The Univ. of Iowa (United States); Qi Song, GE Global Research (United States); Michael D. Abràmoff M.D., Eliott H. Sohn, Xiaodong Wu, The Univ. of Iowa (United States); Mona K. Garvin, Iowa City VA Healthcare System (United States)

Spectral-domain optical coherence tomography (SD-OCT) finds widespread use clinically for the detection and management of ocular diseases. This non-invasive imaging modality has also begun to find frequent use in research studies involving animals such as mice. Numerous approaches have been proposed for the segmentation of retinal surfaces in SD-OCT images obtained from human subjects; however, the segmentation of retinal surfaces in mice scans is not as well-studied. In this work, we describe a graph-theoretic segmentation approach for the simultaneous segmentation of 10 retinal surfaces in SD-OCT scans of mice that incorporates learned shape priors. We compared the method to a baseline approach that did not incorporate learned shape priors and observed that the overall unsigned border position errors reduced from 3.58  $\pm$  1.33 ?m to 3.18  $\pm$  0.54 ?m.









### SPIE Medical Imaging

### Conference 9038: Biomedical Applications in Molecular, Structural, and Functional Imaging

9038-13, Session 3

### Atherosclerotic tissue typing using computational intravascular OCT

Madhusudhana Gargesha, Ronny Y. Shalev, David Prabhu, Case Western Reserve Univ. (United States); Kentaro Tanaka, Univ. Hospitals of Cleveland (United States); Andrew M. Rollins, Case Western Reserve Univ. (United States); Marco Costa M.D., Hiram G. Bezerra M.D., Univ. Hospitals of Cleveland (United States); David L. Wilson, Case Western Reserve Univ. (United States)

We are developing computational techniques for atherosclerotic tissue characterization from clinical 3D intravascular OCT (iOCT) pullback image data. We measured optical attenuation (u) and backscattered intensity (I) from small volumes of interest (VOIs) in (r,?) view identified by experts as calcified, fibrotic, or lipid (>240 VOIs from 35 pullbacks). Model parameters of the imaging system response function were estimated and used to correct clinical images. Processing steps were: correct for catheter; take logarithm to enable usage of linear models and convert multiplicative to additive noise; filter with average, median, or Lee filters having variable sized 3D windows; and estimate (u,l) from each VOI using: fit to all data (ALL), average of fits to individual A-lines (AVG), parallel line fit (PL), robust average (RAVG), and robust parallel line (RPL). Following initial experiments, 15 combinations of filter and estimation method were compared for chi-square, coefficient of variation of estimates, separation of tissue types, etc. Preliminary results suggest that filtering is desirable, estimates varied with method, and RPL>RAVG>PL>AVG~ALL. Using RPL, u's were: calcified (2.37±1.86/ mm), fibrotic (1.10±1.05/mm), and lipid (4.30±1.69/mm), similar to previously reported values obtained under different conditions. An average catheter correction was sufficient for VOIs drawn from intermediate r-depths. A per-VOI plot of (u,l') feature space (l'=average VOI intensity) showed good separation of tissue types. Although noise and tissue inhomogeneity are challenges, results suggest that optical properties can be estimated in 3D regions from clinical pullbacks and used in a comprehensive, computational approach to automated tissue classification.

9038-14, Session 3

## 3D graph-based automated segmentation of corneal layers in anterior-segment optical coherence tomography images of mice

Victor A. Robles, Bhavna J. Antony, Demelza R. Koehn, Michael G. Anderson, Mona K. Garvin, The Univ. of Iowa (United States)

Anterior segment optical coherence tomography (AS-OCT) is a noninvasive imaging modality that allows for the quantitative assessment of corneal thicknesses. Automated approaches are not readily available and therefore measurements are often obtained manually. While graphbased approaches that enable the optimal simultaneous segmentation of multiple 3D surfaces have been proposed and applied to 3D optical coherence tomography volumes of the back of the eye, such approaches have not been applied for the segmentation of the corneal surfaces. In this work we propose adapting this graph-based method for the automated 3D segmentation of three corneal surfaces in AS-OCT images and to measure total corneal thickness. The approach is evaluated based on 34 AS-OCT volumes obtained from both eyes of 17 mice with varying degrees of corneal thicknesses. The segmentation accuracy was assessed using unsigned border positioning errors and was found to be 1.78 microns. We also assessed an average relative error in total layer thickness measurements which was found to be 1.76%.

9038-15, Session 3

### Microcystic macular edema detection in retina OCT images

Emily K. Swingle, The Ohio State Univ. (United States); Andrew Lang, Aaron Carass, Howard S. Ying, Peter A. Calabresi, Jerry L. Prince, Johns Hopkins Univ. (United States)

Optical coherence tomography (OCT) is a powerful imaging tool that is particularly useful for exploring retinal abnormalities in ophthalmological diseases. Recently, it has been used to track changes in the eye associated with neurological diseases, such as multiple sclerosis (MS) where certain tissue layer thicknesses have been associated with disease progression. A small percentage of MS patients also exhibit microcystic macular edema (MME), where fluid-like cysts appear in the inner nuclear layer. This work is the first to present a detection algorithm for these cysts and more importantly report on the spatial distribution of these abnormalities. Our approach uses a random forest classifier to detect the cysts based on 14 features computed at each voxel. Despite a small sample size of five subjects, the algorithm correctly identifies 84.6% of cysts. Finally, using our method, we are able to display the spatial distribution of the cysts within the macula.

9038-67, Session 3

# Optic disc boundary segmentation from diffeomorphic demons registration of monocular fundus image sequences versus 3D visualization of stereo fundus image pairs for automated early stage glaucoma assessment

Vijay Gatti, Jason E. Hill, Brian Nutter, Sunanda D. Mitra, Texas Tech Univ. (United States)

Despite the current availability in resource-rich regions of advanced technologies in scanning and 3-D imaging (e.g. OCT and HRT) in current ophthalmology practice, world-wide screening tests for early detection and progression of glaucoma still consist of a variety of simple tools including fundus image based parameters such as CDR (cup to disc diameter ratio) and CAR (cup to disc area ratio), especially in resourcepoor regions. Reliable automated computation of the above parameters from fundus image sequences requires robust nonrigid registration and segmentation techniques. Recent research work demonstrated that proper non-rigid registration of multi-view monocular fundus image sequences could result in acceptable segmentation of cup boundaries for automated computation of CAR and CDR. This research work introduces a composite diffeomorphic demons registration algorithm for segmentation of cup boundaries from a sequence of monocular images and compares the resulting CAR and CDR values with those computed manually by experts and from 3-D visualization of stereo pairs. Our preliminary results show that the automated computation of CDR and CAR from composite diffeomophic segmentation of monocular image sequences yield values comparable with those from the other two techniques and thus may provide global healthcare with a cost-effective yet accurate tool for management of glaucoma in its early stage.

9038-17, Session 4

#### Optimal 4D image construction from freebreathing MRI acquisitions

Yubing Tong, Jayaram K. Udupa, The Univ. of Pennsylvania Health System (United States); Krzysztof C. Ciesielski, West Virginia Univ. (United States); Joseph M. McDonough, The











Children's Hospital of Philadelphia (Zimbabwe) and Ctr. for Thoracic Insufficiency Syndrome (United States); Andrew Mong, Robert M. Campbell, The Children's Hospital of Philadelphia (United States) and Ctr. for Thoracic Insufficiency Syndrome (United States)

4D dynamic imaging of the thorax has many potential applications. CT and MRI offer sufficient speed to acquire motion information via 4D imaging. For pediatric imaging, x-ray radiation becomes a primary concern and MRI remains the de facto choice. Further, the pediatric subjects in our imaging application area often suffer from extreme malformations of their chest wall, diaphragm, and/or spine, as such patient cooperation needed by some of the gating and tracking techniques are difficult to fulfill without causing patient discomfort. Therefore free-breathing MRI acquisition is the ideal modality of imaging for these patients. In our set up, for each coronal (or sagittal) slice position, slice images are acquired at a rate of about 200-300 ms/slice over several breathing cycles. This produces typically several thousands of slices. We present a novel graph-based combinatorial optimization solution for constructing the best possible 4D volume from such data entirely in the digital domain. The nodes of the graph are the acquired slices, and arc weight is decided based on the similarity of slice images, where a variety of similarity criteria can be considered for formulating the weight function. The best 3D spatial volume for each time point is decided by finding optimal paths in this graph, and the best 4D volume is found by choosing the 4D image among all periods that constitutes the smallest total cost. Our preliminary evaluation indicates that the optimal construction method yields much smoother lung objects in space and time compared to random slice stacking.

9038-19, Session 4

# High resolution quantitative imaging of subcellular morphology and cell refractometry in a liquid environment via endogenous mechanism

Kert Edward, The Univ. of the West Indies (Jamaica); Faramarz Farahi, The Univ. of North Carolina at Charlotte (United States)

Biological cells are composed primarily of water and as such are challenging to image since the induced intensity modulations of transmitted light is typically insufficient to permit acceptable contrast for optical imaging. This issue may be resolved with the aid of exogenous contrast agents but this often has a deleterious effect on the cell and precludes in vivo imaging. A unique approach to this problem is afforded by the phase contrast microscope in which optical-path differences in transmitted light is exploited as a contrast mechanism for qualitative imaging. In recent years, several quantitative phase imaging techniques have been developed which allow for diffraction limited endogenouscontrast imaging with excellent temporal imaging. We hereby present a laser scanning technique for quantitative phase imaging which achieves sub-diffraction limited resolution at the expense of temporal resolution. This instrument is based on a stabilized fiber interfometer which is incorporated into an NSOM for trimodal imaging. Our latest results will focus on modifications made to this system to facilitate imaging in a liquid environment. A simple approach for achieving stable shear-force feedback operation in a liquid will be presented. High resolution images of white blood cells reveal detailed sub-cellular features. Acquired images of fibroblast cells in air and in a liquid environment confirms the efficacy of the feedback operation in a liquid. Moreover, we demonstrate cell refractometry capability without the need for ad hoc modifications. These results clearly demonstrate the unique potentially of this instrument for the study of living cells.

9038-20, Session 4

# Effect of injection technique on temporal parametric imaging derived from digital subtraction angiography in patient specific phantoms

Ciprian N. Ionita, Toshiba Stroke & Vascular Research Ctr. (United States); Victor L. Garcia, Univ. at Buffalo (United States); Daniel R. Bednarek, Kenneth V Snyder, Adnan H. Siddiqui M.D., Elad Levy M.D., Stephen Rudin, Toshiba Stroke & Vascular Research Ctr. (United States)

Parametric imaging maps (PIM's) derived from digital subtraction angiography (DSA) for the cerebral arterial flow assessment in clinical settings have been proposed, but experiments have yet to determine the reliability of such studies. For this study, we have observed the effects of different injection techniques on PIM's. A flow circuit set to physiologic conditions was created using an internal carotid artery phantom. PIM's were derived for two catheter positions, two different contrast bolus injection volumes (5ml and 10 ml), and four injection rates (5, 10, 15 and 20 ml/s). Using a gamma variate fitting approach, we derived PIM's for mean-transit-time (MTT), time-to-peak (TTP) and bolus-arrival-time (BAT). For the same injection rates, a larger bolus resulted in an increased MTT and TTP, while a faster injection rate resulted in a shorter MTT, TTP, and BAT. In addition, the position of the catheter tip within the vasculature directly affects the PIM. The experiment showed that the PIM is strongly correlated with the injection conditions, and, therefore, they have to be interpreted with caution. PIM's images must be taken from the same patient to be able to be meaningfully compared. These comparisons can include pre- and post-treatment images taken immediately before and after an interventional procedure or simultaneous arterial flow comparisons through the left and right cerebral hemispheres. Due to the strong correlation between PIM and injection conditions, this study indicates that this assessment method should be used only to compare flow changes before and after treatment within the same patient using the same injection conditions.

9038-21, Session 4

## Challenges and limitations of patient-specific vascular phantom fabrication using 3D Polyjet printing

Ciprian N. Ionita, Toshiba Stroke & Vascular Research Ctr. (United States); Maxim Mokin, Toshiba Stroke and Vascular Research Ctr (United States); Nicole Varble, Daniel R. Bednarek, Jianping Xiang, Kenneth Snyder, Adnan H. Siddiqui M.D., Elad Levy M.D., Stephen Rudin, Toshiba Stroke & Vascular Research Ctr. (United States)

3D printing technology offers a great opportunity towards development of patient-specific vascular anatomic models for medical device testing and physiological condition evaluation. However, the development process is not yet well established and there are various limitations depending on the materials, printing technology and resolution used. Patient specific neuro-vascular anatomy was acquired from computed tomography angiography (CTA) and rotational digital subtraction angiography (DSA). The volumes were imported into a Vitrea 3D workstation (Vital Images Inc.) and the vascular lumen of various vessels and pathologies were segmented using a "marching cubes" algorithm. The results were exported as Stereo Lithographic (STL) files and were further processed by smoothing, trimming, and wall extrusion (to add a custom wall to the model). The models were printed using a Polyjet printer, Eden 260V (Objet-Stratasys). To verify the phantom geometry accuracy, the phantom was reimaged using rotational DSA, and the new data was compared with the initial patient data. The most challenging part of the phantom manufacturing was removal of support material. This aspect could be a











serious hurdle in building very tortuous phantoms or small vessels. The accuracy of the printed models was very good: distance analysis showed average differences of 120 ?m (maximum, 600 ?m) between the patient and the phantom reconstructed volume dimensions. Most errors were due to residual support material left in the lumen of the phantom. Despite the post-printing challenges experienced during the support cleaning, this technology could be a tremendous benefit to medical research such as in device development and testing.

9038-22, Session 4

## Non-invasive computation of aortic pressure maps: a phantom-based study of two approaches

Michael Delles, Sebastian Schalck, Yves Chassein, Karlsruher Institut für Technologie (Germany); Tobias Müller, Deutsches Krebsforschungszentrum (Germany); Fabian Rengier, UniversitätsKlinikum Heidelberg (Germany) and Deutsches Krebsforschungszentrum (Germany); Stefanie Speidel, Karlsruhe Institute of Technology (KIT) (Germany); Hendrik von Tengg-Kobligk, UniversitätsKlinikum Heidelberg (Germany) and Inselspital Bern (Switzerland) and Deutsches Krebsforschungszentrum (Germany); Hans-Ulrich Kauczor, UniversitätsKlinikum Heidelberg (Germany); Rüdiger Dillmann, Roland Unterhinninghofen, Karlsruher Institut für Technologie (Germany)

Patient-specific blood pressure values in the human aorta are an important parameter in the management of cardiovascular diseases. A direct measurement of these values is only possible by invasive catheterization at a limited number of measurement sites. To overcome these drawbacks, two non-invasive approaches of computing patientspecific relative aortic blood pressure maps throughout the entire aortic vessel volume are investigated by our group. The first approach uses computations from complete time-resolved, three-dimensional flow velocity fields acquired by phase-contrast magnetic resonance imaging (PC-MRI), whereas the second approach relies on computational fluid dynamics (CFD) simulations with ultrasound-based boundary conditions. A detailed evaluation of these computational methods under realistic conditions is necessary in order to investigate their overall robustness and accuracy as well as their sensitivity to certain algorithmic parameters. We present a comparative study of the two blood pressure computation methods in an experimental phantom setup, which mimics the human aorta. The comparative analysis includes the investigation of the impact of algorithmic parameters on the MRI-based blood pressure computation and the impact of extracting pressure maps in a voxel grid from the CFD simulations. Overall, a very good agreement between the results of the two computational approaches can be observed despite of the fact that both methods used completely separate measurements as input data. Therefore, the comparative study of the presented work indicates that both non-invasive pressure computation methods show an excellent robustness and accuracy and can therefore be used for research purposes in the management of cardiovascular diseases.

9038-68, Session 4

#### Time analysis of aneurysm wall shear stress for both Newtonian and Casson flows from image-based CFD models

Marcelo A. Castro, Consejo Nacional de Investigaciones Científicas y Técnicas (Argentina); Maria C. Ahumada Olivares, Univ. Favaloro (Argentina); Christopher M. Putman, Texas Neurointerventional Surgery Associates (United States); Juan R. Cebral, George Mason Univ. (United States) The optimal management of unruptured aneurysms is controversial, and current decision making is mainly based on aneurysm size and location. Incidentally detected unruptured aneurysms less than 5mm in diameter should be treated conservatively. However, small unruptured aneurysms also bleed. Risk factors based on the hemodynamic forces exerted over the arterial wall have been investigated using image-based computational fluid dynamic (CFD) methodologies during the last decade. Accurate estimation of wall shear stress (WSS) is required to properly study associations between flow features and aneurysm processes. Previous works showed that Newtonian and non-Newtonian (Casson) models produce similar WSS distributions and characterization, with no significant differences. Other authors showed that the WSS distribution computed from time-averaged velocity fields is significantly higher for the Newtonian model where WSS is low. In this work we reconstructed ten patient-specific CFD models from angiography images to investigate the time evolution of WSS at selected locations such as aneurysm blebs (low WSS), and the parent artery close to the aneurysm neck (high WSS). When averaging all cases it is seen that the estimation of the timeaveraged WSS, the peak WSS and the minimum WSS value before the systolic peak were all higher when the Casson rheology was considered. However, none of them showed statistically significant differences. At the afferent artery Casson rheology systematically predicted higher WSS values. On the other hand, at the selected blebs either Newtonian or Casson WSS estimations are higher in some phases of the cardiac cycle. Those observations differ among individual cases.

9038-23, Session 5

## Dynamic CT myocardial perfusion imaging: detection of ischemia in a porcine model with FFR verification

Rachid Fahmi, Brendan L. Eck, Case Western Reserve Univ. (United States); Xiaorong Zhou, Univ. Hospitals of Cleveland (United States); Mani Vembar, Philips Healthcare (United States); Hiram G. Bezerra M.D., Univ. Hospitals of Cleveland (United States); David L. Wilson, Case Western Reserve Univ. (United States)

Dynamic myocardial CT perfusion (D-MCTP) is a high resolution. non-invasive technique for assessing myocardial blood flow (MBF), which in concert with coronary CT angiography would enable CT to provide a comprehensive, fast analysis of both coronary anatomy and functional flow. We assessed perfusion in a porcine model with and without coronary occlusion. To induce occlusion, each animal underwent LAD stent implantation and angioplasty balloon insertion. Normal flow condition was obtained with balloon completely deflated. Partial occlusion was induced by balloon inflation against the stent with FFR used to assess the extent of occlusion. Prospective ECG-triggered partial scan (180deg + fan angle) images were acquired at end systole (45% R-R) using 256-slice MDCT (Brilliance-iCT, Philips), and 20mL of contrast flushed by 20mL of saline at 4mL/s. Images were reconstructed using FBP and iterative reconstruction (iDose4, Philips). Processing included: beam hardening correction (BHC), registration of image volumes using 3D cubic B-spline normalized mutual-information, and spatio-temporal bilateral filtering to reduce partial scan artifacts. Absolute blood flow was calculated with a deconvolution-based approach using singular value decomposition. Arterial input function was taken from the LV cavity near the aortic valve. ROIs were identified in healthy and ischemic myocardium and compared in normal and occluded conditions. Underperfusion was detected in the correct LAD territory and flow reduction agreed well with FFR measurements. Flow was reduced, on average, in LAD territories by 52%. Reconstruction method and BHC had minimal effects on the relative flow measurements: however BHC removed artifacts in healthy tissue often perceived as under-perfusion.









9038-24, Session 5

### Parametric myocardial perfusion PET imaging using physiological clustering

Hassan Mohy-ud-Din, Nikolaos Karakatsanis, Martin A. Lodge, Johns Hopkins Univ. (United States); Jing Tang, Oakland Univ. (United States); Arman Rahmim, Johns Hopkins Univ. (United States)

We propose a novel framework of robust kinetic parameter estimation applied to absolute flow quantification in dynamic PET imaging. Kinetic parameter estimation is formulated as nonlinear least squares with spatial constraints problem (NLLS-SC) where the spatial constraints are computed from a physiologically driven clustering of dynamic images, and used to to reduce noise contamination. An ideal clustering of dynamic set of images depends on the underlying physiology of functional regions, and in turn, physiological processes are quantified by kinetic parameter estimation.

We perform a physiological driven clustering of dynamic images using K-means algorithm with Kinetic modeling (KM-KM) in an iterative 'handshaking' fashion. This gives a map of labels where each functionally homogenous cluster is represented by mean kinetics (cluster centroid). Parametric images are acquired by solving the NLLS-SC problem for each voxel which penalizes spatial variations from its means kinetics. This substantially reduces noise in the estimation process for each voxel by utilizing kinetic information from physiologically similar voxels (cluster members). Resolution degradation is also substantially minimized as spatial smoothing between heterogeneous functional regions is not performed. The kinetic estimation process requires blood input function which is extracted from the reconstructed set of dynamic images using nonnegative matrix factorization (NMF).

The proposed framework is shown to improve the quantitative accuracy of Myocardial Perfusion (MP) PET imaging, and in turn, has the long-term potential to enhance capabilities of MP PET in the detection, staging and management of coronary artery disease.

9038-25, Session 6

### Advancing technologies for preclinical molecular imaging (Keynote Presentation)

Simon R. Cherry, Univ. of California, Davis (United States)

In vivo molecular imaging technologies have become an indispensable and widely utilized tool for studying animal models of human disease, and in preclinical evaluation of novel therapeutic strategies. The use of highly sensitive assays based on optical or radiotracer methods provide the foundation for many of the existing and emerging technologies used to provide images that elucidate the spatial and temporal distribution of gene expression and protein targets, and that can be used to probe a variety of molecular and metabolic pathways. Many approaches also offer opportunities for clinical translation.

This presentation will review a selection of technologies being used or developed for in vivo molecular imaging, with a focus on highly sensitive radiotracer assays. Recent trends will be explored, including the development of sub-mm positron emission tomography (PET scanners, hybrid systems that integrate PET and magnetic resonance imaging (MRI), optical imaging of radiotracers via Cerenkov luminescence, and high sensitivity single photon imaging without the use of any physical collimation. The strengths and weakness of different approaches will be discussed and a number of remaining challenges in the field identified.

9038-26, Session 6

# Complementary tumor vascularity imaging in a single PET-CT routine using FDG early dynamic blood flow and contrast-enhanced CT texture analysis

Raz Carmi, Philips Healthcare (Israel); Nikolay Yefremov, Hanna Bernstine, David Groshar, Rabin Medical Ctr. (Israel)

A feasibility study of improved PET-CT tumor imaging approach is presented. A single PET-CT routine includes three different techniques: 18F-FDG early dynamic blood flow intended for perfusion assessment; standard late 18F-FDG uptake; and high-resolution contrast-enhanced CT enabling tissue texture analysis. Both PET protocols utilize the same single standard radiotracer dose administration. Quantitative volumetric arterial perfusion maps are derived from the reconstructed dynamic PET images corresponding to successive acquisition time intervals of 3 seconds only. For achieving high accuracy, the analysis algorithm differentiates the first-pass arterial flow from other interfering dynamic effects, and a noise reduction scheme based on adaptive total-variation minimization aims to provide appreciable quantitative map in physical conditions of high noise and low spatial resolution. The CT texture analysis comprises a practical and robust method for generating volumetric tissue irregularity maps. A local map value is represented by the entropy function which is derived from a weighted co-occurrence matrix histogram of the corresponding image voxel three-dimensional vicinity. Unique entropy scaling scheme and parameter optimization process, as well as appropriate scaling for different image noise and varying contrast agent concentrations, improve the results toward quantitative absolute measure with respect to varying scanning conditions and key analysis parameters. Representative imaging results are demonstrated on several clinical cases involving different organs and cancer types. In these cases the quantitative maps show significant tumor characterization, relative to normal surrounding tissues, in all three imaging techniques. This proof of concept can lead the way to a new practical diagnostic imaging application.

9038-27, Session 6

### Biomarker sensing to assess cancer therapy

John B. Weaver, Xiaojuan Zhang, Dartmouth Hitchcock Medical Ctr. (United States); Daniel B. Reeves, Dartmouth College (United States); Irina M. Perreard, Dartmouth Hitchcock Medical Ctr. (United States); Warren C. Kett, Karl E. Griswold, Thayer School of Engineering at Dartmouth (United States); Barjor Gimi, Venkata K. Nemani, Dartmouth Hitchcock Medical Ctr. (United States); Seiko Toraya-Brown, Steven Fiering, Dartmouth College (United States) and Geisel School of Medicine (United States)

We have developed microscopic probes to measure local biomarker concentrations longitudinally over time. Biomarker concentrations are critically important in monitoring therapy because they change so much faster than the physical results of that signaling. For example, the VEGF level provides a very direct evaluation of anti-angiogenic therapies just as heat shock proteins provide a direct evaluation of thermal therapies. We evaluated the sensitivity and specificity of the proposed methods. The potential sensitivity was also estimated. The method uses microscopic probes that are injected in the desired location and can be read out noninvasively longitudinally over time. The probes are magnetic nanoparticles (NPs) encapsulated in a porous alginate shell. The shell keeps the NPs in the location that they were injected and protects them from the immune system. The NPs are coated with antibodies or aptamers for the targeted molecule in a way that the targeted molecule binds NPs together. The number of NPs bound together at any given time is directly proportional to the concentration of the targeted molecule and can be estimated from the rotational freedom of the NPs in a changing magnetic field; free NPs are able to rotate more easily in an alternating











magnetic field. Magnetic spectroscopy of Brownian motion (MSB) characterizes the rotational Brownian motion from the shape of the magnetization. We used MSB to detect concentrations down to 100 pM using the current apparatus but we estimate that the sensitivity should be easily able to measure single digit pM concentrations using microgram quantities of NPs.

9038-28, Session 7

## Early prediction of lung cancer recurrence after stereotactic radiotherapy using second order texture statistics

Sarah A. Mattonen, Western Univ. Canada (Canada); David A. Palma M.D., The Univ. of Western Ontario (Canada) and London Regional Cancer Ctr. (Canada); Cornelis J. Haasbeek, Suresh Senan, Vrije Univ. Medical Ctr. (Netherlands); Aaron D. Ward, The Univ. of Western Ontario (Canada)

Benign radiation-induced lung injury is a common finding following stereotactic ablative radiotherapy (SABR) for lung cancer, and is often difficult to differentiate from a recurring tumour due to the ablative doses and highly conformal treatment with SABR. Current approaches to treatment response assessment have shown limited ability to predict recurrence within 6 months of treatment. The purpose of our study was evaluate the accuracy of second order texture statistics for prediction of eventual recurrence based on computed tomography (CT) images acquired within 6 months of treatment, and compare with the performance of first order appearance and lesion size measures. Consolidative and ground-glass opacity (GGO) regions were manually delineated on post-SABR CT images. Automatic consolidation expansion was also investigated to act as a surrogate for GGO position. The top features for prediction of recurrence were all texture features within the GGO and included energy, entropy, correlation, inertia, and first order texture (standard deviation of density). These predicted recurrence with 2-fold cross validation (CV) accuracies of 70-77% at 2-5 months post-SABR, with energy, entropy, and first order texture having leave-one-out CV accuracies greater than 80%. Our results also suggest that automatic expansion of the consolidation region could eliminate the need for manual delineation, and produced reproducible results when compared to manually delineated GGO. If validated on a larger data set, this could lead to a clinically useful computer-aided diagnosis system for prediction of recurrence within 6 months of SABR and allow for early salvage therapy for patient with recurrence.

9038-29, Session 7

## Dual-energy micro-CT imaging of pulmonary airway obstruction: correlation with micro-SPECT

Cristian T. Badea, Nicholas T. Befera, Darin P. Clark, Yi Qi, G. Allan Johnson, Ctr. for In Vivo Microscopy (United States)

To match recent clinical dual energy (DE) CT studies focusing on the lung, similar developments for DE micro-CT of the rodent lung are required. Our group has been actively engaged in designing pulmonary gating techniques for micro-CT and also introduced the first DE micro-CT imaging method of the rodent lung. The aim of this study was to assess the feasibility of DE micro-CT imaging for the evaluation of airway obstruction in mice and to compare with single photon emission computed tomography (SPECT) using technetium-99m labeled macroaggregated albumin (99mTc-MAA). Our measurements showed that, compared to normal lung regions, there was a 47% higher air fraction in the injured lung regions given via DE micro-CT and this was matched by a relative decrease in lung perfusion of 60 % in micro-SPECT. These results suggest that the pulmonary airway obstructions caused airtrapping similar to asthma or emphysema, resulting in a physiologic

decrease in perfusion to the hypoventilated lung. The proposed DE micro-CT technique for imaging localized airway obstruction performed well in our initial evaluation and gives a higher resolution compared to micro-SPECT. Both DE micro-CT and micro-SPECT provide critical quantitative lung biomarkers for image-based anatomical and functional information in the small animal. The methods are readily linked to clinical methods allowing direct comparison of preclinical and clinical results.

9038-30, Session 7

### Single-shot X-ray measurement of alveolar size distributions

Richard P. Carnibella, Marcus J. Kitchen, Andreas Fouras, Monash Univ. (Australia)

Alveoli are the functional units of respiration, but imaging the lungs at this level is problematic because of the vast difference in scale between the organ as a whole and individual alveoli. While computed tomography and magnetic resonance imaging are capable of the spatial resolution required, neither has a scan speed fast enough to capture a snapshot of the alveoli at a single time point during respiration. Furthermore, the potential dose required for high temporal and spatial resolution computed tomography would be prohibitive.

Here, we present a new technique capable of measuring alveolar dimensions from a single high resolution X-ray image. In projection, a high-resolution image of the lung fields has a speckled appearance, largely due to the superposition of alveoli. We model the alveoli as a system of tightly packed spherical pores and use a genetic algorithm to fit the speckle statistics of this model to those obtained from a region of the lung fields.

We present the results of experiments using lung phantoms, consisting of closely packed samples of microspheres, as validation of the technique. Additionally, we present the results of imaging and analysis of the lung fields of rabbit kittens and compare our findings with measurements made using high-resolution computed tomography.

In this work we demonstrate the ability to regionally measure the distribution of airspace sizes. This is a significant step towards being able to perform dynamic in-vivo measurements, specifically for the purpose of studying alveolar mechanics.

9038-31, Session 7

## Investigation of pulmonary acoustics: comparing airway model generation techniques

Brian Henry, Ying Peng, Zoujun Dai, Thomas Royston, Univ. of Illinois at Chicago (United States); Hansen Mansy, Univ. of Central Florida (United States); Richard Sandler, Nemours Children's Hospital, Orlando (United States)

Alterations in the structure and function of the pulmonary system that occur in disease or injury often give rise to measurable changes, spatially and temporally, in lung sound production and transmission that, if properly quantified, might provide additional information about the etiology, severity and location of trauma injury or other pathology. With this in mind, the authors are developing a comprehensive computer simulation model of pulmonary acoustics, known as The Audible Human Project™. Its purpose is to improve our understanding of pulmonary acoustics and to aid in interpreting measurements of sound and vibration in the lungs generated by airway insonification, natural breath sounds and external stimuli on the torso surface, such as are used in elastography methods. As a part of this development process, finite element (FE) models were constructed of an excised pig lung that also underwent experimental studies. Within these models, the complex airway structure was created via two methods: x-ray CT image segmentation and through an algorithmic means called Constrained











Constructive Optimization (CCO). CCO was implemented to expedite the segmentation process, as airway segments can be grown digitally. These two approaches were used in FE simulations of the surface motion on the lung as a result of sound input into the trachea. Simulation results were compared to experimental measurements. By testing how close these models are to experimental measurements, we are evaluating whether CCO can be used as a means to efficiently construct physiologically relevant airway trees.

9038-32, Session 7

### Automated rat lung segmentation of low resolution CT scans

Benjamin M. Rizzo, Marquette Univ. (United States); Steven T. Haworth, Medical College of Wisconsin (United States) and Zablocki Veterans Affairs Medical Ctr. (United States); Anne V. Clough, Marquette Univ. (United States) and Zablocki Veterans Affairs Medical Ctr. (United States)

Preclinical SPECT imaging of radioactive biomarker uptake within the lung requires accurate identification of the lung boundaries. However, this identification of the lung boundaries and the fissure between the left and right lung is not generally possible. Thus, a rapid low-resolution CT scan is performed, the lung boundaries and fissure are identified in the CT image, and the CT lung region is co-registered with the SPECT volume to obtain the SPECT lung region. Segmentation of rat lungs within the CT volume is particularly challenging due to their unique anatomy, which involves one of the lobes of the right lung crossing over into the left side of the thorax and to the relatively low-resolution of the CT scan. Thus, an automated segmentation algorithm for low resolution rat micro-CT scans was developed. The algorithm first determines the outer boundaries of the lung using standard thresholding techniques. Then depth maps are constructed and utilized to detect fissures on the surface of the lung volume. The fissure's surface location is then used to interpolate the fissure throughout the lung volume. The procedure is implemented as a java plugin to ImageJ. The algorithm is robust, portable, and requires little to no user interaction. The algorithm identifies lung regions that are consistent with the lung anatomy as determined by the relative volumes of the left and right lungs, and which can be used subsequently to identify the lung regions in SPECT images of the same rat.

9038-34, Session 7

# Minimally interactive fuzzy connectedness segmentation of 4D dynamic upper airway MR images

Yubing Tong, Jayaram K. Udupa, Dewey Odhner, Univ. of Pennsylvania (United States); Sanghun Sin, Raanan Arens, Children's Hospital at Montefiore (United States)

There are several disease conditions that lead to upper airway restrictive disorders. In the study of these conditions, it is important to take into account the dynamic nature of the upper airway. Currently, dynamic MRI is the modality of choice for studying these diseases. Unfortunately, the contrast resolution obtainable in the images poses many challenges for an effective segmentation of the upper airway structures. No viable methods have been developed to date to solve this problem. In this paper, we demonstrate the adaptation of the iterative relative fuzzy connectedness (IRFC) algorithm for this application as a potential practical tool. After preprocessing to correct for background image non-uniformities and the non-standardness of intensities, seeds are specified for the airway and its carefully chosen crucial background tissue components. Seed specification is needed on several slices in only the 3D image corresponding to the first time instance of the 4D volume. Subsequently the process runs without human interaction and completes in 1 minute for segmenting the whole 4D volume. Our preliminary

evaluations indicate that the segmentations are of very good quality and the methodology can be used routinely for segmenting 4D MRI volumes.

9038-70, Session 7

#### Development and application of pulmonary structure-function registration methods: towards pulmonary image-guidance tools for improved airway targeted therapies and outcomes

Fumin Guo, Damien Pike, Sarah Svenningsen, Robarts Research Institute (Canada); Harvey O. Coxson, Vancouver General Hospital (Canada); John J. Drozd, Jing Yuan, Aaron Fenster, Grace Parraga, Robarts Research Institute (Canada)

Objectives: Hyperpolarized 3He magnetic resonance imaging (MRI) has emerged as a non-invasive imaging method to measure pulmonary function. Complementary to 3He MRI, x-ray computed tomography (CT) provides high-resolution structural information and has been widely used to provide regional lung morphological information. Our objective was to develop pulmonary imaging registration methods to provide pulmonary structure-function maps to potentially guide targeted pulmonary therapies.

Methods: Proton (1H) and 3He MRI were acquired in 5 ex-smokers and 7 ex-smokers with chronic obstructive pulmonary disease (COPD) in inspiration breath-hold and CT was performed within ten minutes of MRI using the same breath-hold volume and maneuver. Landmark-based non-rigid registration was performed using corresponding fiducial markers in CT and 1H MRI coronal slices. Shape-based non-rigid registration was evaluated by identifying the shapes of the lung cavities manually, and registering the two shapes using affine and thin-plate spline algorithms. We compared registration accuracy for whole lung (WL) and for left and right (LR) lungs independently using the fiducial localization error (FLE) and target registration error (TRE).

Results: For landmark-based registration, TRE was  $7.8\pm4.6$  mm for WL versus  $8.4\pm5.3$ mm for LR registration and these were not significantly different (p=.43). For shape-based registration method, TRE was  $6.9\pm4.4$  for WL versus  $8.0\pm4.6$  mm for LR registration (p=.01). FLE was 1.84 mm and did not dominate the TRE measurement.

Conclusion: There was no significant difference between landmark-based WL and LR registration (p=.43) or between shape and landmark-based WL registration (p=.72). For shape-based registration, LR registration was significantly better (p=.01) than WL registration.

9038-35, Session 8

# Predicting the biomechanical strength of proximal femur specimens with Minkowski functionals and support vector regression

Chien-Chun Yang, Mahesh B. Nagarajan, Markus B. Huber, Univ. of Rochester Medical Ctr. (United States); Julio Carballido-Gamio, Univ. of California, San Francisco (United States); Jan S. Bauer, Thomas H. Baum, Institut für Röntgendiagnostik (Germany); Felix Eckstein, Eva-Maria Lochmüller, Paracelsus Medizinische Privatuniversität (Austria); Thomas M. Link, Univ. of California, San Francisco (United States); Axel Wismüller M.D., Univ. of Rochester Medical Ctr. (United States)

Regional trabecular bone quality estimation for purposes of femoral bone strength prediction is important for improving the clinical assessment of osteoporotic fracture risk. In this study, we explore the ability of 3D Minkowski Functionals derived from multi-detector computed tomography (MDCT) images of proximal femur specimens in predicting











their corresponding biomechanical strength. MDCT scans were acquired for 50 proximal femur specimens harvested from human cadavers. An automated volume of interest (VOI)-fitting algorithm was used to define a consistent volume in the femoral head of each specimen. In these VOIs, the trabecular bone micro-architecture was characterized by statistical moments of its BMD distribution and by topological features derived from Minkowski Functionals. A linear multi-regression analysis and a support vector regression (SVR) algorithm with a linear kernel were used to predict the failure load (FL) from the feature sets; the predicted FL was compared to the true FL determined through biomechanical testing. The prediction performance was measured by the root mean square error (RMSE) for each feature set. The best prediction result was obtained from the Minkowski Functional surface used in combination with SVR, which had the lowest prediction error (RMSE =  $0.939 \pm 0.345$ ) and which was significantly lower than mean BMD (RMSE =  $1.075 \pm 0.279$ , p<0.005). Our results suggest that topological characterization of trabecular bone micro-architecture with Minkowski Functionals on MDCT can contribute to biomechanical strength prediction in proximal femur specimens.

9038-36, Session 8

# Phase contrast imaging X-ray computed tomography: Quantitative characterization of human patellar cartilage matrix with topological and geometrical features

Mahesh B. Nagarajan, Univ. of Rochester Medical Ctr. (United States); Paola Coan, Ludwig-Maximilians-Univ. München (Germany) and European Synchrotron Radiation Facility (France); Markus B. Huber, Univ. of Rochester Medical Ctr. (United States); Paul C. Diemoz, Ludwig-Maximilians-Univ. München (Germany) and European Synchrotron Radiation Facility (France); Axel Wismüller M.D., Univ. of Rochester Medical Ctr. (United States) and Ludwig-Maximilians-Univ. München (Germany)

Current assessment of cartilage is primarily based on identification of indirect markers such as joint space narrowing and increased subchondral bone density on x-ray images. In this context, phase contrast CT imaging (PCI-CT) has recently emerged as a novel imaging technique that allows a direct examination of chondrocyte patterns and their correlation to osteoarthritis through visualization of cartilage soft tissue. This study investigates the use of topological and geometrical approaches for characterizing chondrocyte patterns in the radial zone of the knee cartilage matrix in the presence and absence of osteoarthritic damage. For this purpose, topological features derived from Minkowski Functionals and geometric features derived from the Scaling Index Method (SIM) were extracted from 842 regions of interest (ROI) annotated on PCI-CT images of healthy and osteoarthritic specimens of human patellar cartilage. The extracted features were then used in a machine learning task involving support vector regression to classify ROIs as healthy or osteoarthritic. Classification performance was evaluated using the area under the receiver operating characteristic (ROC) curve (AUC). The best classification performance was observed with highdimensional geometrical feature vectors derived from SIM (0.95 ± 0.06) which outperformed all Minkowski Functionals (p < 0.001). These results suggest that such quantitative analysis of chondrocyte patterns in human patellar cartilage matrix involving SIM-derived geometrical features can distinguish between healthy and osteoarthritic tissue with high accuracy.

9038-37, Session 8

## Bone vascularization: a way to study bone microarchitecture

Pauline Bléry, L'Univ. Nantes Angers Le Mans (France); Florent Autrusseau, LUNAM - Univ. Nantes (France); Eleonore Crauste, Erwan Freuchet, Pierre Weiss, Jean-Pierre V. Guédon, Yves

Amouriq, L'Univ. Nantes Angers Le Mans (France)

Trabecular bone and its microarchitecture are of prime importance for health. Changes of bone microarchitecture are linked to different pathological situations like osteoporosis and begin now to be understood. Conversely, the role of bone vascularization is not really known. A lot of studies showed a relation between osteogenesis and angiogenesis during bone modification, but we actually do not know if a correlation exists between bone microarchitecture and vascular microarchitecture in normal situation, and how the two microarchitectures overlap. Multimodality imaging has given some explanations of the relationships between bone, bone marrow, and blood. So studying bone vascularization represents a good way to better know the relationship between bone microarchitecture and vascular microarchitecture. This study is based on the perfusion of vascularization by a contrast agent before euthanasia on rats. The samples were studied by microCT with a resolution of 9µm. The images obtained were analysed with softwares (NRecon Reconstruction, CtAn, and CtVox) in order to show 3D volumes of bone and vessels, to calculate bone and vessels microarchitecture parameters, and to know if a correlation exist between bone microarchitecture and vascular microarchitecture. The first images of vascular tree were presented. The final paper will show the results of our computations and the quality of the relationships between vascular and bone parameters. The aim of this study is the knowledge of the bone microarchitecture from its vascular microarchitecture and conversely.

9038-38, Session 8

# Automatic classification of squamosal abnormality in micro-CT images for the evaluation of rabbit fetal skull defects using active shape models

Antong Chen, Belma Dogdas, Saurin Mehta, Ansuman Bagchi, Christopher Winkelmann, L. David Wise, Merck & Co., Inc. (United States)

High-throughput micro-CT imaging has been used in our laboratory to evaluate fetal skeletal morphology in developmental toxicology studies. Currently, the volume-rendered skeletal images are visually inspected and observed abnormalities are reported for compounds in development. To improve the efficiency and reduce human error of the evaluation, we implemented a framework to automate the evaluation process. The framework starts by dividing the skull into regions of interest and then measuring various geometrical characteristics. Normal/abnormal classification on the bone segments is performed based on identifying statistical outliers. In pilot experiments using rabbit fetal rabbit skulls, the majority of the skeletal abnormalities can be detected successfully in this manner. However, there are shape-based abnormalities that are relatively subtle and thereby difficult to identify using the geometrical characteristics. To address this problem, we introduced a modelbased approach and applied this strategy on the squamosal bone. We will provide details on this active shape model (ASM) strategy for the identification of squamosal abnormalities and show that this method improved the sensitivity of detecting squamosal-related abnormalities from 0.52 to 0.92.

9038-39, Session 8

# Automated segmentation of knee and ankle regions of rats from CT images to quantify bone mineral density for monitoring treatments of rheumatoid arthritis

Francisco Cruz, Merck & Co., Inc. (United States)

Bone mineral density (BMD) obtained from a CT image is an imaging biomarker used pre-clinically for characterizing the Rheumatoid arthritis











(RA) phenotype. We use this biomarker in animal studies for evaluating disease progression and for testing various compounds. In the current setting, BMD measurements are obtained manually by selecting the regions of interest from three-dimensional (3-D) CT images, which results in a laborious and low-throughput process. Combining image processing techniques, such as intensity thresholding and skeletonization, with mathematical techniques in curve fitting and curvature calculations, we developed an algorithm for quick, consistent, and automatic detection of joints in large CT data sets. The implemented algorithm has reduced analysis time for a study with 200 CT images from 10 days to 3 days and has improved the consistency of the obtained regions of interest compared with manual segmentation. This algorithm has been used successfully in over 40 studies.

9038-40, Session 9

## Hybrid framework based on evidence theory for blood cell image segmentation

Amir Nakib, Univ. Paris-Est Créteil Val de Marne (France) and LISSI (France)

The segmentation of microscopic images is an important issue in biomedical image processing. Many works can be found in the literature; however, there is not a gold standard method that is able to provide good results for all kinds of microscopic images. Then, authors propose methods for a given kind of microscopic images. This paper deals with new segmentation framework based on evidence theory, called ESA (Evidential Segmentation Algorithm) to segment blood cell images. Herein, our goal is to extract the components of a given cell image by using evidence theory, that allows more flexibility to classify the pixels. The obtained results showed the efficiency of the proposed algorithm compared to other competing methods.

9038-41, Session 9

## On the way to a patient table integrated scanner system in magnetic particle imaging

Christian Kaethner, Mandy Ahlborg, Ksenija Gräfe, Gael Bringout, Univ. zu Lübeck (Germany); Timo F. Sattel, Philips Medizin Systeme GmbH (Germany); Thorsten M. Buzug, Univ. zu Lübeck (Germany)

The tomographic imaging modality Magnetic Particle Imaging (MPI) is capable of three-dimensional real time imaging of super-paramagnetic iron oxide nanoparticles. The particles have an inherent non-linear magnetisation, which can be used for signal detection. The spatial encoding is achieved by using an oscillating magnetic field, which is superimposed by a static magnetic gradient field. The latter provides a field free point (FFP), in which the particle response can be used for imaging. The FFP is moved through the field of view (FOV) by the oscillating magnetic field. Due to a high spatial and temporal resolution, the method offers great potential to be used in interventional scenarios, however, the generated FOV needs to be sufficiently large. Generating such a FOV, the commonly used circular shaped coils may exceed the width of a patient table. Therefore, an elliptical and an approximated elliptical topology are compared and presented as alternative coil geometries to the circular shaped coils. The focus of this study is on the generated magnetic fields. Additionally, a design study of integrating an asymmetric MPI scanner into a patient table is proposed in this contribution. Here, an important factor is that the field quality is better than in the circular shaped asymmetric MPI scanner. To investigate this, the magnetic field components and the gradient fields of the two different scanner setups are compared. Promising first results motivate further investigations of a patient table integrated MPI scanner for an application in a catheter lab.

9038-42, Session 9

## Assessment of MR imaging agent targeting of tumor micro-metastases using cryo-imaging

Mohammed Q. Qutaish, Zhuxian Zhou, Mallory R. Busso, Zheng-Rong Lu, David L. Wilson, Case Western Reserve Univ. (United States)

We are developing a platform methodology for the unique, quantitative assessment of emerging targeted theranostics. In this report, we evaluate the ability of CREKA-Gd, a new MR imaging agent, and its red fluorescent counterpart, CREKA-Cy5, to detect even the smallest of tumors in a mouse metastatic breast cancer model. Key is Cryo-imaging (CryoVizTM) which provides microscopic color anatomy and molecular fluorescence images with single tumor cell sensitivity, of an entire mouse via repeated Cryo-sectioning and imaging of the tissue block face. Experimentally, we created green fluorescent metastases by implanting 4T1-GFP cells in fat pads, injected CREKA-Gd and CREKA-Cy5 at 40 days, imaged in MRI (fat suppression T1-weighted flash 3D sequence), sacrificed and froze maintaining nearly exact anatomical pose, and Cryoimaged. Following 3D/3D non-rigid registration of MRI and Cryo-color, we have for each mouse multiple registered volumes (MRI CREKA-Gd, green fluorescence tumor, red fluorescence CREKA-Cy5, and Cryo-color giving fine anatomical details as well as depiction of solid tumors). In analyses, we assess the ability of MRI (CREKA-Gd) and fluorescence (CREKA-Cy5) to detect the green tumors using specially developed software for registration, visualization, segmentation, and statistical analysis of signals. Cryo-imaging typically showed >100 tumor metastases in lungs, liver, bone marrow and adrenal gland, including many micrometastases (<0.125mm3) in lungs and bone marrow. With very careful review, even single cell metastases were found in regions such as the brain. Preliminarily, there was evidence of variable CREKA-Cy5 labeling in nearly every tumor >80%. In MRI, mean contrast to background indicates that nearly every larger metastasis and >65% of very small (<0.1 mm3) metastases were detectable per the Rose criterion. CREKA-Cy5 signal was evident in more small metastases, indicating that improved MR imaging may result in even better detection. This developing platform technology provides a unique, quantitative approach for assessment of tumor targeting of imaging agents and theranostics.

9038-43, Session 9

# A preliminary evaluation of self-made nanobubble in contrast-enhanced ultrasound imaging

Chunfang Li, Kaizhi Wu, Jing Li, Haijuan Liu, Qibing Zhou, Mingyue Ding, Huazhong Univ. of Science and Technology (China)

Nanoscale bubbles (nanobubbles) have been reported to improve the contrast effect of ultrasound imaging due to the enhanced permeation and retention effects at tumor vascular leaks. In this work, a self-made nanobubble ultrasound contrast agent was preliminarily characterized and evaluated in vitro and in vivo. Fundamental properties such as morphology appearance, size distribution, zeta potential, bubble concentration (bubble numbers per milliliter contrast agent suspension) and the stability of nanobubbles were assessed by light microscope and particle sizing analysis. Then the concentration intensity curve and time intensity curves (TICs) were acquired by ultrasound imaging experiment in vitro. Finally, the contrast-enhanced ultrasonography was performed on rat to investigate the procedure of liver perfusion. The results showed that the nanobubbles had good shape and uniform distribution with the average diameter of 507.9 nm, polydispersity index (PDI) of 0.527, and zeta potential of -19.17 mV. Significant contrast enhancement was observed in both in-vitro and in-vivo ultrasound imaging, demonstrating that the self-made nanobubbles can enhance the contrast effect of ultrasound imaging efficiently.











9038-44, Session 9

## Quantum dot-sized organic fluorescent dots for long-term cell tracing

Kai Li, A\*STAR Institute of Materials Research and Engineering (Singapore); Bin Liu, National Univ. of Singapore (Singapore); Ben Zhong Tang, Hong Kong Univ. of Science and Technology (Hong Kong, China)

Fluorescence techniques have been extensively employed to develop non-invasive methodologies for tracking and understanding complex biological processes both in vitro and in vivo, which is of high importance in modern life science research. Among a variety of fluorescent probes, inorganic semiconductor quantum dots (QDs) have shown advantages in terms of better photostability, larger Stokes shift and more feasible surface functionalization. However, their intrinsic toxic heavy metal components and unstable fluorescence at low pH greatly impede the applications of QDs in in vivo studies. In this work, we developed novel fluorescent probes that can outperform currently available QD based probes in practice. Using conjugated oligomer with aggregationinduced emission (AIE) characteristics as the fluorescent domain and biocompatible lipid-PEG derivatives as the encapsulation matrix, the obtained organic dots have shown higher brightness, better stability in biological medium and comparable size and photostability as compared to their counterparts of inorganic QDs. More importantly, unlike QDbased probes, the organic fluorescent dots do not blink, and also do not contain heavy metal ions that could be potentially toxic when applied for living biosubstrates. Upon surface functionalization with a cell-penetrating peptide, the organic dots greatly outperform inorganic quantum dots in both in vitro and in vivo long-term cell tracing studies, which will be beneficial to answer crucial questions in stem cell/immune cell therapies. Considering the customized fluorescent properties and surface functionalities of the organic dots, a series of biocompatible organic dots will be developed to serve as a promising platform for multifarious bioimaging tasks in future.

9038-45, Session 9

## Robust material decomposition for spectral CT

Darin P. Clark, G. Allan Johnson, Cristian T. Badea, Ctr. for In Vivo Microscopy (United States)

Clinical successes with dual energy CT, aggressive development of energy discriminating x-ray detectors, and novel, target-specific, nanoparticle contrast agents promise to establish spectral CT as a powerful functional imaging modality. However, concerns over the radiation dose, photon flux, and sensitivity associated with these applications have arguably stifled development. Here, we propose and demonstrate a post-reconstruction algorithm for robust material decomposition of spectral CT data in the presence of photon noise and angular undersampling to address these issues. Specifically, we combine a Bregman-like optimization strategy with the concepts of kernel regression, joint filtration, and robust principal component analysis to iteratively solve for a material decomposition which is spatially smooth, quantitatively accurate, and minimally biased relative to the source data. We call this algorithm spectral diffusion because it integrates structural information from multiple spectral channels within the framework of diffusion-like denoising algorithms (e.g. anisotropic diffusion, total variation). We demonstrate the application of spectral diffusion to the highly novel, but ill-conditioned triple-energy material decomposition of iodine, gold, and gadolinium concentrations in the mouse kidneys, liver, and spleen to illustrate the potential to resolve target-specific probes in

9038-46, Session 10

## Investigation of the human brainstem with magnetic resonance elastography

Curtis L. Johnson, Joseph L. Holtrop, Univ. of Illinois at Urbana-Champaign (United States); Matthew D. McGarry, Dartmouth College (United States); John B. Weaver, Dartmouth Hitchcock Medical Ctr. (United States); Keith D. Paulsen, Thayer School of Engineering at Dartmouth (United States); Bradley P. Sutton, John G. Georgiadis, Univ. of Illinois at Urbana-Champaign (United States)

Magnetic resonance elastography (MRE) is an emerging medical imaging technique for quantifying the mechanical properties of tissues in vivo. While the mechanical properties of brain tissue have shown sensitivity to neurological diseases, investigation of local properties of specific neuroanatomical features has only been recently possible given the emergence of high-resolution acquisition schemes. The brainstem has not yet been studied due to the need for improved resolution to accurately estimate the very high stiffness of the structure. This work uses a 3D multislab, multishot acquisition to estimate the viscoelasticity of the human brainstem in vivo. The brainstem has a high storage modulus, which agrees with previous ex vivo studies. It also has a low damping ratio, which is indicative of a highly aligned fiber structure. The ability to probe the brainstem with MRE may ultimately improve the study of many neurological conditions, including multiple sclerosis and amyotrophic lateral sclerosis.

9038-47, Session 10

## Imaging hydraulic conductivity in tofu phantoms using poroelastic MR elastography

Keith D. Paulsen, Thayer School of Engineering at Dartmouth (United States) and Dartmouth Hitchcock Medical Ctr. (United States); Adam J. Pattison, Matthew D. McGarry, Thayer School of Engineering at Dartmouth (United States); John B. Weaver, Dartmouth College (United States) and Dartmouth Hitchcock Medical Ctr. (United States)

Magnetic resonance elastography (MRE) is a modality to image the mechanical properties of soft tissue for diagnosis and monitoring of disease. Property distributions are computed from measurements of the tissue motion during mechanical excitation, which requires assuming a set of governing equations linking the motions and a continuum description of tissue properties. Tissue contains both solid and fluid components; a biphasic poroelastic model may describe the mechanical behavior more accurately than single phase viscoelastic models which are commonly employed in MRE. A poroelastic MRE framework also allows imaging of hydrodynamic properties of tissue in addition to the stiffness commonly measured in viscoelastic MRE, and may provide additional valuable diagnostic information. Accurate simultaneous imaging of both shear modulus and hydraulic conductivity is demonstrated in simulated poroelastic phantoms where the simulated data is corrupted with added noise equivalent to MRE motion measurements. A series of phantom experiments demonstrates consistent shear modulus and hydraulic conductivity estimates for three different grades of tofu using spatial priors, and indicate that poroelastic effects may be more apparent at lower frequencies where there is more time for redistribution of fluid to occur. These promising results suggest hydraulic conductivity imaging is achievable for poroelastic tissues such as brain, where changes in hydrodynamic parameters are expected in a range of diseases including hydrocephalus, stroke, traumatic brain injury and edema.









## SPIE Medical Imaging

### Conference 9038: Biomedical Applications in Molecular, Structural, and Functional Imaging

9038-48, Session 10

# Inversion of poroelastic and viscoelastic simulated MR elastography data at high and low actuation frequencies

Matthew D. McGarry, Thayer School of Engineering at Dartmouth (United States); John B. Weaver, Dartmouth Hitchcock Medical Ctr. (United States); Keith D. Paulsen, Thayer School of Engineering at Dartmouth (United States) and Dartmouth Hitchcock Medical Ctr. (United States)

Magnetic resonance elastography (MRE) produces images of the mechanical properties of tissue, and requires selecting a mechanical model relating measurements of tissue motion to continuum mechanical property descriptions. Tissues such as brain have both solid and fluid components, which can be approximated by single phase viscoelasticity (with relatively few unknown properties and simple inversion strategies), or modeled more closely by biphasic poroelasticity (which has more unknown properties and requires nonlinear inversion strategies). Errors in mechanical property estimates resulting from selecting an incorrect mechanical model for MRE inversion are investigated across the spectrum of MRE actuation frequencies using simulated data generated by realistic poroelastic and viscoelastic finite element brain models. Both poroelastic and viscoelastic nonlinear inversion MRE algorithms were applied to each simulated dataset to compare recovered properties with those assigned in the simulation. Under conditions where fluid flow is not significant (such as low poroelastic hydraulic conductivity and/or high actuation frequency), the two models are similar enough to produce accurate results. However, if the timescale of poroelastic fluid redistribution is on the order of the actuation period, model-data mismatch leads to significant inaccuracies in the recovered property images. Similarly, the level of energy loss in cases of heavy viscoelastic damping cannot be adequately represented in a poroelastic material under realistic conditions. Results of this study can be used to predict the conditions where viscoelastic approximations of poroelastic tissue are sufficiently accurate.

9038-49, Session 10

# MRE detection of heterogeneity using quantitative measures of residual error and uncertainty

Ruth J. Okamoto, Washington Univ. in St Louis (United States); Curtis L. Johnson, Univ. of Illinois at Urbana-Champaign (United States); Yuan Feng, Washington Univ. in St. Louis (United States); John G. Georgiadis, Univ. of Illinois at Urbana-Champaign (United States); Philip V. Bayly, Washington Univ. in St. Louis (United States)

In magnetic resonance elastography (MRE), displacement fields from shear waves are inverted to estimate underlying material properties. Modulus differences detected by MRE may be used to distinguish tumors or other localized pathology in tissue. The accuracy of modulus estimates depends on the choice of the assumed constitutive model, as well as on the inversion algorithm, image resolution, and signal-tonoise ratio. In particular, in simpler inversion methods such as direct inversion and three-dimensional local frequency estimation (3D-LFE) the constitutive model is minimal (linear, elastic or viscoelastic, and isotropic) and the simplifying assumption of local homogeneity is usually made. The assumption of local homogeneity is often inaccurate, since the shear wavelength is typically comparable to the size of the structures of interest. Notably, the residual error (in direct inversion) between the model and the experimental data increases sharply at the boundaries of stiff or soft inclusions, while the "certainty" of the 3D-LFE estimate decreases at these boundaries. These error metrics may be used to detect local stiffness heterogeneity, as well as indicate whether candidate constitutive

models are appropriate. The utility of model uncertainty is demonstrated in simulations and with MRE data from a heterogeneous gel phantom.

9038-50, Session 10

# Utilizing a reference material for assessing absolute tumor mechanical properties in modality independent elastography

Dong Kyu Kim, Jared A. Weis, Thomas E. Yankeelov, Michael I. Miga, Vanderbilt Univ. (United States)

There is currently no reliable method for early characterization of breast cancer response to neoadjuvant chemotherapy (NAC) [1,2]. Given that disruption of normal structural architecture occurs in cancer-bearing tissue, we hypothesize that further structural changes occur in response to NAC. Consequently, we are investigating the use of modalityindependent elastography (MIE) [3-8] as a method for monitoring mechanical integrity to predict long term outcomes in NAC. Recently, we have utilized a Demons non-rigid image registration method that allows 3D elasticity reconstruction in abnormal tissue geometries, making it particularly amenable to the evaluation of breast cancer mechanical properties. While past work has reflected relative elasticity contrast ratios [3], this study improves upon that work by utilizing a known stiffness reference material within the reconstruction framework such that a stiffness map becomes an absolute measure. To test, a polyvinyl alcohol (PVA) cryogel phantom and a silicone rubber mock mouse tumor phantom were constructed with varying mechanical stiffness. Results showed that an absolute measure of stiffness could be obtained based on a reference value. This reference technique demonstrates the ability to generate accurate measurements of absolute stiffness to characterize response to NAC. These results support that 'referenced MIE' has the potential to reliably differentiate absolute tumor stiffness with significant contrast from that of surrounding tissue. The use of referenced MIE to obtain absolute quantification of biomarkers is also translatable across length scales such that the characterization method is mechanicsconsistent at the small animal and human application.

9038-51, Session 11

# Method and device for intraoperative imaging of lumpectomy specimens to provide feedback to breast surgeon for prompt reexcision during the same procedure

Andrzej Krol, Susan Hemingway, Kara Kort, Gustavo de la Rosa, Deepa Masrani, David H. Feiglin, SUNY Upstate Medical Univ. (United States); Avice O'Connell, Univ. of Rochester (United States); Mahesh B. Nagarajan, Chien-Chun Yang, Axel Wismüller M.D., Univ. of Rochester Medical Ctr. (United States)

Purpose: To provide intraoperative feedback to breast surgeon on anatomical locations of the positive/close margins in the lump of tissue excised during lumpectomy. Thus allowing for accurate and prompt reexcision during the same procedure to immediately correct the problem without the need of additional surgery days later. Consequently, it could lower the fraction of re-excisions that presently is at 30-50% level.

Methods: We designed, constructed and started testing a device (plastic sphere inside a holder) for micro-CT and micro-MRI imaging of lumpectomy specimens. Surgeon inserts freshly excised specimen into the sphere that can be freely rotated vs. holder. The lesion's spatial orientation vs. patient is preserved. Next, micro-CT or micro-MRI images of the specimen are obtained while the patient is still on the operating table. They are reviewed by a surgeon who marks locations of positive/close margins. Subsequently, computer calculates and displays vector(s) indicating their location(s) vs. patient's breast. Afterwards, surgeon performs re-excision using computer guidance and the whole procedure













is repeated for the re-excised lump of tissue. When all the margins appear as negative in images the procedure is finished.

Results: We performed micro-CT imaging of lumpectomy specimen phantom and determined spatial localization accuracy. We established that the localization error was lower than 10 mm and 10 degrees.

Conclusions: For suitable classes of breast lesions, it could be possible to provide intraoperative feedback to surgeon on anatomical locations of positive/close margins allowing immediate correction of the problem without the need for an additional surgery days later.

9038-52, Session 11

## Ameliorating mammograms by using novel image processing algorithms

Anup Pillai, David M. Kwartowitz, Clemson Univ. (United States)

Mammography is one of the most important tools for the early detection of breast cancer, typically through detection of characteristic masses and/or micro calcifications. Digital mammography has become commonplace in recent years. High quality mammogram images are large in size, providing high-resolution data. Estimates of the false negative rate for cancers in mammography are approximately 10%–30%. This may be due to observer error, but more frequently it is because the cancer is hidden by other dense tissue in the breast and even after retrospective review of the mammogram, cannot be seen.

In this study, we report on the results of novel image processing algorithms that will enhance the images providing decision support to reading physicians. Techniques such as Butterworth high pass filtering, Gabor filter based edge detection will be applied to enhance images and this is followed by segmentation of the region of interest (ROI). Subsequently, the textural features will be extracted from the ROI, which will be used to classify the ROIs as either masses or non-masses. Among the statistical methods most used for the characterization of textures, the co-occurrence matrix makes it possible to determine the frequency of appearance of two pixels separated by a distance, at an angle from the horizontal. This matrix contains a very large amount of information that is not easy to handle. Therefore, it is not used directly but through measurements known as indices of texture such as average, variance, energy, contrast, correlation, normalized correlation and entropy.

9038-53, Session 11

#### Validation and reproducibility assessment of modality independent elastography in a preclinical model of breast cancer

Jared A. Weis, Dong Kyu Kim, Thomas E. Yankeelov, Michael I. Miga, Vanderbilt Univ. (United States)

Clinical observations have long suggested that cancer progression is accompanied by extracellular matrix remodeling and concomitant increases in mechanical stiffness. Elucidation of the mechanobiological basis supporting the association between tumor growth and mechanics continues, with mechanical behavior of the extracellular matrix having been shown to affect growth, differentiation, and motility. Due to strong association of mechanics and tumor progression, there has been considerable interest in incorporating methodologies to diagnose cancer through the use of mechanical stiffness imaging biomarkers, resulting in commercially available US and MR elastography products. Extension of this approach towards monitoring longitudinal changes in mechanical properties along a course of cancer therapy may provide means for assessing early response to therapy; therefore a systematic study of the elasticity biomarker in characterizing cancer for therapeutic

monitoring is needed. The elastography method we employ, modality independent elastography (MIE), can be described as a model-based inverse image-analysis method that reconstructs elasticity images using two acquired image volumes in a pre/post state of compression. In this work, we present preliminary data towards validation and reproducibility assessment of our elasticity biomarker in a pre-clinical model of breast cancer. The goal of this study is to determine the accuracy and reproducibility of MIE and therefore the magnitude of changes required to determine statistical differences during therapy. Our preliminary results suggest that the MIE method can accurately and robustly assess mechanical properties in a pre-clinical system and provides considerable enthusiasm for the extension of this technique towards monitoring therapy-induced changes to breast cancer tissue architecture.

9038-54, Session 11

#### Opto-acoustic breast imaging with coregistered ultrasound

Jason Zalev, Bryan Clingman, Don Herzog, Tom Miller, Michael Ulissey, A. Thomas Stavros, Seno Medical Instruments, Inc. (United States); Alexander A. Oraevsky, TomoWave Laboratories, Inc. (United States); Kenneth Kist, N. Carol Dornbluth, Pamela Otto, The Univ. of Texas Health Science Ctr. at San Antonio (United States)

We present results from a recent study of the Imagio™ Breast Imaging System, which produces real-time two-dimensional color-coded opto-acoustic (OA) images that are co-registered and temporally interleaved with real time gray scale ultrasound using a specialized duplex handheld probe.

The use of dual optical wavelengths provides functional images of breast tissue and tumors displayed with contrast based on total hemoglobin and oxygen saturation of the blood. This provides functional diagnostic information pertaining to tumor metabolism. OA also shows morphologic information about tumor neovascularity that is complementary to the morphological information obtained with conventional grayscale ultrasound. The co-registered dual-modality system conveniently enables analyzing opto-acoustic features on lesions detected by readers familiar with grayscale ultrasound.

We demonstrate co-registered opto-acoustic and ultrasonic images of malignant and benign tumors from a recent clinical study that provide new insight into the function of tumors in-vivo. Results from Feasibility and Verification and Validation Studies show that the technology may have the capability to improve characterization of benign and malignant breast masses over conventional diagnostic breast ultrasound alone, to improve overall accuracy of breast mass diagnosis and to potentially reduce the number of negative biopsies without missing cancers.

9038-16, Session PSMon

# A statistical model for 3D segmentation of retinal choroid in optical coherence tomography images

Hossein Rabbani, Isfahan Univ. of Medical Sciences (Iran, Islamic Republic of)

The choroid is a densely layer under the retinal pigment epithelium (RPE). Its deeper boundary is formed by the sclera, the outer fibrous shell of the eye. However, the inhomogeneity within the layers of choroidal Optical Coherence Tomography (OCT)-tomograms presents a significant challenge to existing segmentation algorithms. In this paper, we performed a statistical study of retinal OCT data to extract the choroid. This model fits a Gaussian mixture model (GMM) to image intensities with Expectation Maximization (EM) algorithm. The goodness of fit for proposed GMM model is computed using Chi-square measure and is











obtained lower than 0.04 for our dataset. After fitting GMM model on OCT data, Bayesian classification method is employed for segmentation of the upper and lower border of boundary of retinal choroid. Our simulations show the signed and unsigned error of -1.44±0.5 and  $1.6\pm0.53$  for upper border,and -5.7±13.76 and 6.3±13.4 for lower border, respectively.

9038-55, Session PSMon

## Model-based motion correction of reduced field of view diffusion MRI data

Jan Hering, Deutsches Krebsforschungszentrum (Germany) and Hochschule Mannheim (Germany); Ivo Wolf, Hochschule Mannheim (Germany) and Deutsches Krebsforschungszentrum (Germany); Hans-Peter Meinzer, Klaus H. Maier-Hein, Deutsches Krebsforschungszentrum (Germany)

In clinical settings, application of the most recent modelling techniques is usually unfeasible due to the limited acquisition time. Localised acquisitions enclosing only the object of interest by reducing the field-of-view (FOV) counteract the time limitation but pose new challenges to the subsequent processing steps like motion correction.

We use datasets from the Human Connectome Project (HCP) to simulate head motion distorted reduced FOV acquisitions and present an evaluation of head motion correction approaches: the commonly used affine registration onto an unweighted reference image guided by the mutual information (MI) metric and a model-based approach, which uses reference images computed from approximated tensor data to improve the performance of the MI metric. While the standard approach using the MI metric yields up to 15% outliers (error>5 mm) and a mean spatial error above 1.5 mm, the model-based approach reduces the number of outliers (1%) and the spatial error significantly (p<0.01). The behavior is also reflected by the visual analysis of the MI metric.

The evaluation shows that the MI metric is of very limited use for reduced FOV data post-processing. The model-based approach has proven more suitable in this context.

9038-56, Session PSMon

## A fully automatic unsupervised segmentation framework for the brain tissues in MR images

Qaiser Mahmood, Chalmers Univ. of Technology (Sweden); Artur Chodorowski, Chalmers Univ. of Technology (Sweden) and Sahlgrenska Univ. Hopsital (Sweden); Babak Ehteshami Bejnordi, Radboud Univ. Nijmegen Medical Ctr. (Netherlands); Mikael Persson, Chalmers Univ. of Technology (Sweden)

This paper presents a novel fully automatic unsupervised automatic framework for the segmentation of brain tissues in magnetic resonance (MR) images. The framework is a combination of our proposed Bayesian based adaptive mean shift (BAMS), a priori spatial tissue probability maps and fuzzy c-means. BAMS is applied to cluster the tissues in the joint spatial-intensity feature space and then a fuzzy c-means algorithm is employed with initialization by a priori spatial tissue probability maps to assign the clusters into three tissue types; white matter (WM), gray matter (WM) and cerebrospinal fluid (CSF). The proposed framework is validated on multimodal synthetic as well as on real T1-weighted MR data with varying noise characteristics and spatial intensity inhomogeneity. The performance of framework is evaluated relative to our previous method BAMS and other existing adaptive mean shift framework. Both of these are based on the pruning and voxel weighted k-means algorithm for classifying the clusters into WM, GM and CSF. The experimental results demonstrate the robustness of proposed framework to noise and spatial intensity inhomogeneity, and that it exhibits a higher degree of segmentation accuracy in segmenting both synthetic and real MR data compared to competing methods.

9038-57, Session PSMon

## Seizures localization using 3D object detection algorithm

Abhinav Bhargava, Jianming Liang, Robert A. Greenes, Arizona State Univ. (United States); David Adelson, Remy Wahnoun, Phoenix Children's Hospital (United States)

Objective: This study describes an automatic 3-Dimensional (3-D) object-detection algorithm used to identify seizure origin from electrocorticography (ECoG) data. Specifically, this method quantitatively localizes seizure foci and surrounding epileptogenic zones to minimize the surgical resection area.

Methods: Seizure data (ECoG, 64-channels) extracted from six patients were assessed. Power was estimated for every seizure using a Short-Time Fourier Transform (STFT); it was then transformed into a binary 3-D image in which black and white pixels represent non-ictal and ictal activity, respectively. The 3-D image maintained the ECoG grid topology with the 3rd dimension representing time; therefore a movie was generated in which each frame represented the power of each electrode in that point in time. A collection of white pixels represented a seizure area, and iterative erosions, or ultimate erosion, were performed on this epileptogenic zone to more accurately detect seizure foci. The spatiotemporal evolution of seizures was visualized through the generated movies as they highlighted the change in seizure areas.

Results: The results are based on those found clinically, which are subject to inaccuracies due to inter- and intra-rater variability; therefore, the true positive rate (TPR) values presented do not represent how accurately this method detects seizure foci. The highest TPR percentage of 38% was found in the frequency range between 65 Hz to 118 Hz. As seizure propagation was not monitored clinically, the accuracy of spatiotemporal evolution detection is undetermined; the results for one patient are presented.

Conclusions: Detection in higher frequencies correlated to higher accuracy than detection in the lower frequencies for 75% of seizures. Suggesting higher frequencies may be a good source of detecting seizure origin. However, TPR value is still not accurate enough to define a relationship between frequency ranges and seizure focus. We believe this is due to high variability in ECoG data. To get a very specific pattern from this technique we need more patients with clear clinical information describing their ictal activity.

9038-58, Session PSMon

# Is there more valuable information in PWI datasets for a voxel-wise acute ischemic stroke tissue outcome prediction than what is represented by typical perfusion maps?

Nils Daniel Forkert, Susanne Siemonsen, Michael Dalski, Tobias Verleger, Andre Kemmling, Jens Fiehler, Univ. Medical Ctr. Hamburg-Eppendorf (Germany)

The acute ischemic stroke is a leading cause for death and disability in the industry nations. In case of a present acute ischemic stroke, the prediction of the future tissue outcome is of high interest for the clinicians as it can be used to support therapy decision making. Within this context, it has already been shown that the voxel-wise multi-parametric tissue outcome prediction leads to more promising results compared to single channel perfusion map thresholding. Most previously published multi-parametric predictions employ information from perfusion maps derived from perfusion-weighted MRI together with other image sequences such as diffusion-weighted MRI. However, it remains unclear if the typically calculated perfusion maps used for this purpose really include all valuable information from the PWI dataset for an optimal tissue outcome prediction. To investigate this problem in more detail,











two different methods to predict tissue outcome using a k-nearestneighbor approach were developed in this work and evaluated based on 18 datasets of acute stroke patients with known tissue outcome. The first method integrates apparent diffusion coefficient and perfusion parameter (Tmax, MTT, CBV, CBF) information for the voxel-wise prediction, while the second method employs also apparent diffusion coefficient information but the complete perfusion information in terms of the voxel-wise residue functions instead of the perfusion parameter maps for the voxel-wise prediction. Overall, the comparison of the results of the two prediction methods for the 18 patients using a leave-one-out cross validation revealed no considerable differences. Quantitatively, the parameter-based prediction of tissue outcome lead to a mean Dice coefficient of 0.474, while the prediction using the residue functions lead to a mean Dice coefficient of 0.461. Thus, it may be concluded from the results of this study that the perfusion parameter maps typically derived from PWI datasets include all valuable perfusion information required for a voxel-based tissue outcome prediction, while the complete analysis of the residue functions does not add further benefits for the voxel-wise tissue outcome prediction.

9038-59, Session PSMon

# Cortical thinning in cognitively normal elderly cohort of 60 to 89 year old from AIBL database and vulnerable brain areas

Zhongmin S. Lin, Gopal B. Avinash, Kathryn M. McMillan, Litao Yan, GE Healthcare (United States)

Age-related cortical thinning has been studied by many researchers using quantitative MR images for the past three decades and quite different results have been reported. Some results have shown age-related cortical thickening in elderly cohort statistically in some brain regions that requires further investigation. This paper leverages our previously reported brain surface intensity model (BSIM)[1] based technique to measure cortical thickness to study cortical changes due to normal ageing. We measured cortical thickness of cognitive normal persons from 60 to 89 years old using Australian Imaging Biomarkers and Lifestyle Study (ABIL) data. MRI brains of 56 healthy people including 29 women and 27 men were selected. We measured average cortical thickness of each individual in eight brain regions: parietal, frontal, temporal, occipital, visual, sensory motor, medial frontal and medial parietal. Unlike the previous published studies, our results showed consistent age-related thinning of cerebral cortex in all brain regions. The parietal, medial frontal and medial parietal showed fast decline rates of 0.14, 0.12 and 0.10 mm/ decade respectively while the visual region showed the slowest decline rate of 0.05 mm/decade. In sensorimotor and parietal areas, women showed higher thinning (0.09 and 0.16 mm/decade) than men while in all other regions men showed higher thinning than women. The average cortical thicknesses of the left brain were slightly thicker than right brain in all brain regions and almost at all ages. These results validate our cortical thickness measurement technique by demonstrating the consistency of the cortical thinning with AIBL database.

9038-60, Session PSMon

# Characterizing the spatial distribution of microhemorrhages resulting from traumatic brain injury (TBI)

Ningzhi Li, Yiyu Chou, Navid Shiee, Leighton Chan, Dzung L. Pham, John A. Butman, National Institutes of Health (United States)

This study examines the spatial distribution of microhemorrhages in 46 TBI patients by investigating their locations on susceptibility weighted images (SWI) and applying region of interest (ROI) analysis using a brain atlas. SWI and 3D T1-weighted images were acquired on a 3T clinical Siemens scanner. A neuroradiologist reviewed all SWI images

on a Carestream PACS workstation and labeled microhemorrhages using the "marker" graphic tool as single voxel. To characterize spatial distribution of microhemorrhages in standard Montreal Neurological Institute (MNI) space, the T1-weighted images was nonlinearly registered to the MNI template. This transformation was applied to the coregistered SWI images and to the marker coordinates. The frequency of microhemorrhages in major brain structures and white matter (WM) tracts were determined from ROIs identified in the digital Talairach brain atlas and diffusion oriented tract segmentations. A total of 629 microhemorrhages were found with an average of 13±34 (range=1-179) in the 24 positive TBI patients. Microhemorrhages mostly congregated around the periphery of the brain and were symmetrically distributed, although a number were found in the corpus callosum. From Talairach ROI analysis, microhemorrhages were most prevalent in the frontal lobes (59.9%). Restricting the analysis to WM tracts, microhemorrhages were primarily found in the corpus callosum (52.5%).

9038-61, Session PSMon

#### Pair-wise Clustering of Large Scale Granger Causality Index Matrices for Revealing Communities

Axel Wismüller M.D., Mahesh B Nagarajan, Univ. of Rochester Medical Ctr. (United States); Herbert Witte, Britta Pester, Lutz Leistritz, Friedrich-Schiller-Univ. Jena (Germany)

To analyze large ensembles of time series is a fundamental challenge in many domains of biomedical image processing applications, ranging from microarray gene expression analysis to functional MRI data processing. We propose a novel approach of applying the linear Granger Causality concept to very high-dimensional time series. The approach is based on integrating dimensionality reduction into a multivariate time series model. If residuals of dimensionality reduced models can be transformed back into the original space, prediction errors in the high-dimensional space may be computed, and a Granger Causality Index (GCI) is properly defined. We provide a proof-of-principle, and compare the results with the classical GCI.

9038-62, Session PSMon

# Automated segmentation of corticospinal tract in diffusion tensor images via multimodality multi-atlas fusion

Xiaoying Tang, Susumu Mori, Michael I. Miller, Johns Hopkins Univ. (United States)

The corticospinal tract (CST) is an important projection fiber tract the primary function of which is to transmit signals for voluntary or willed and skilled movements. In this paper, we proposed a method to automatically segment the CST in diffusion tensor images (DTIs) by incorporating the anatomical features from multi-modality images generated in DTI using multiple DTI atlases. The test subject, and each atlas, was comprised of images with different modality -- the mean diffusivity, the fractional anisotropy, and the images representing the three elements of the primary eigenvector. Each atlas had a paired image containing the manual labels of the three regions of interest - the left and right CST and the background. We solved the problem via maximum a posteriori estimation using generative models. Each image was modeled as a conditional Gaussian mixture random field, conditioned on the atlas-label pair and the change of coordinates of each local label. The expectation-maximization algorithm was used to alternatively estimate the local optimal diffeomorphisms for each atlas and the maximizing segmentations. The algorithm was evaluated on 6 subjects with a wide range of pathology. The proposed method was compared with two state-of-the-art multi-atlas based label fusion methods, against which it displayed a high level of accuracy.











9038-63, Session PSMon

# Metastatic brain cancer: prediction of response to whole-brain helical tomotherapy with simultaneous intralesional boost for metastatic disease using quantitative MR imaging features

Harish A. Sharma, Univ. of Western Ontario (Canada); Glenn S. Bauman, George Rodrigues, The Univ. of Western Ontario (Canada); Robert Bartha, Robarts Research Institute (Canada); Aaron D. Ward, The Univ. of Western Ontario (Canada) and London Health Sciences Ctr. (Canada)

The sequential application of whole brain radiotherapy (WBRT) and more targeted stereotactic radiosurgery (SRS) is frequently used to treat metastatic brain tumors. However, SRS has side effects related to necrosis and edema, and requires separate and relatively invasive localization procedures. Helical tomotherapy (HT) allows for a SRStype simultaneous infield boost (SIB) of multiple brain metastases, synchronously with WBRT and without separate stereotactic procedures. However, some patients' tumors may not respond to HT+SIB, and would be more appropriately treated with radiosurgery or conventional surgery despite the additional risks and side effects. As a first step toward a broader objective of developing a means for response prediction to HT+SIB, the goal of this study was to investigate whether quantitative measurements of tumor size and appearance (including first- and second-order texture features) on a magnetic resonance imaging (MRI) scan acquired prior to treatment could be used to differentiate responder and non-responder patient groups after HT+SIB treatment of metastatic disease of the brain. Our results demonstrated that larger lesions, which may permit a better dose conformation to the target, and those with a more homogeneous pattern of enhancement, which may lack a hypoxic/ necrotic core, may respond better to this form of therapy. With further validation on a larger data set, this approach may lead to a means for prediction of individual patient response based on pre-treatment MRI, supporting appropriate therapy selection for patients with metastatic brain cancer.

#### 9038-64, Session PSMon

## Novel T lymphocyte proliferation assessment using whole mouse Cryo-imaging

Patiwet Wuttisarnwattana, Case Western Reserve Univ. (United States); Syed A. Raza, COMSATS Institute of Information Technology (Pakistan); Saada Eid, Case Western Reserve Univ. (United States); Kenneth R. Cooke M.D., Johns Hopkins Univ. (United States); David L. Wilson, Case Western Reserve Univ. (United States) and Univ. Hospitals of Cleveland (United States) and BioInVision (United States)

To create an in vivo, whole mouse immunological assay with single cell sensitivity, we developed specialized imaging methods and analysis using cryo-imaging (CryoVizTM). Briefly, cryo-imaging provides microscopic color anatomy and molecular fluorescence images with single T-cell sensitivity, of an entire mouse via repeated cryo-sectioning and imaging of the tissue block face. By labeling T-cells with a fluorescent dye, we established a quantitative T-cell proliferation assessment for the secondary lymphoid organs (SLOs) where lymphocytes naturally proliferate. A graft-versus-host-disease (GVHD) model was used. Following bone marrow transplantation, T-cells fluorescently labeled with CFSE dye were infused in syngeneic (without GVHD) and allogeneic (with GVHD) mice. Imaging was performed 1-5 days post-transplant. SLOs such as spleen and lymph nodes were automatically segmented and analyzed using machine learning algorithm. Volumes of red and white pulp were measured. Fluorescent signal in the organ was visualized

as 3D rendering using a color-coded maximum intensity projection algorithm. Since dye dilutes with T-cell clonal expansion, probability density functions and proportion of high intensity voxels (%bright) were estimated from the organ voxel intensities. T-cells were abundantly found in GVHD target organs such as lung, liver, skin and GI-tract. At day 3-5, volumes of SLOs with GVHD were significantly larger than without GVHD. Color-MIPs clearly showed evidence of proliferation, as signal intensity was much lower for animals with GVHD than without. Calculated %bright was also consistent with rapid proliferation in GVHD. Results suggest that this novel approach can be used to reliably assess in vivo T-cell proliferation.

#### 9038-65, Session PSMon

# Comparison analysis of the deterioration in the rat's articular cartilage inducing osteoarthritis CP-FD OCT images with histological images

Sang Hun Park, B. Y. Kim, M. Y. Lee, S. Y. Lee, S. H. Shin, Chonbuk National Univ. (Korea, Republic of); Jeong Hwan Seo, Chonbuk National Univ. Hospital (Korea, Republic of); K. Y Jang, Chonbuk National University Hospital, Dept. of Pathology (Korea, Republic of); W. C. Ham, D. H. Shin, Chonbuk National Univ (Korea, Republic of); Chul-Gyu Song, Chonbuk National Univ. (Korea, Republic of); Jin W kang, Johns Hopkins University (United States)

The objective of this experiment is to compare CP-FD OCT images with histological images, and classify into osteoarthritis (OA) grade. In this study, we induced OA into rat's knee joints and observed the stages of OA at weekly intervals. The progression of OA was monitored by CP-FDOCT. The results using the CP-FDOCT system were compared to biopsy results. A super-luminescent diode (D-855, Superlum Diode Ltd., Ireland) with the central wavelength of 846.5 nm; the spectral full-width at half maximum (FWHM) of ~100 nm was used as the light source; and the axial resolution of our system was found to be 3.153 um. The beam splitter was used a 50/50 coupler (FC850-40-50-APC, Thorlabs Inc., USA) and only one branch on the right side because the reference signal simply used the reflected signal from the distal end of the fiber optic probe. To control the actuators and to perform image processing in our motorized stage-based CP-FDOCT system, OCT acquisition software was developed using the LabVIEW platform. In the histology after 10 days of exposer to MIA, a rough surface of cartilage was shown. In the week-2 image, the right part of the cartilage was degenerated, and the cartilage cell generally was destroyed. In the week-3 image, the whole cartilage surface had degenerated. The thickness of cartilage also was thin, and calcification had progressed too far. The OCT images acquired with the CP-FDOCT system show patterns similar to those in the corresponding histology. In this paper, a technique for the micrometerscale imaging of arthritis cartilage using a high-resolution CP-FDOCT system, which is simpler than the conventional OCT system with two arms, has been proposed. In the OCT image, abnormalities such as cartilage destruction were indicated and matched up with the pattern of the histology. The possibility of having an inexpensive, real-time, high-resolution, nondestructive diagnosis technique for articular cartilage could be realized by combining the use of the endoscope with other clinical imaging techniques. In future work, we plan to make a real-time 3D OCT system for imaging osteoarthritis.

9038-66, Session PSMon

## Comparison of macular OCTs in right and left eyes of normal people

Hossein Rabbani, Isfahan Univ. of Medical Sciences (Iran, Islamic Republic of)











Optical coherence tomography (OCT) is a non-invasive imaging modality being used in the diagnosis and management of a variety of ocular diseases including glaucoma, age-related macular degeneration (AMD) and diabetic macular edema. It is a powerful modality to qualitatively assess retinal features and pathologies or to make quantitative measurements of retinal morphology. Retinal 3D OCT volumes are commonly used for clinical diagnosis or investigation. However accurate and fast analysis of large volumes of data is difficult for clinicians. Therefore, automatic extraction of useful information from OCT images, such as calculating total retinal thickness and retinal nerve fiber layer thickness (RNFLT) have become increasingly significant. Total retinal thickness and nerve fiber layer (NFL) thickness have become useful indices to indicate the progress of glaucoma. While examining RNFL and macular thickness measurements, one cannot help but notice that, besides the fact that the measurements of an individual may be outside the normative database range and thus classified as abnormal, there is tremendous value in evaluating the asymmetry between the two eyes of an individual. Thus the asymmetry analysis can be an important step in the early detection of disease according to the asymmetry of RNFLT in the normal eyes. It is well-known that the loss of ganglion cells (even up to losing 5 layers of these cells), may not be diagnosable through visual field tests. Such a loss can even not be evaluated when we only consider the thickness of one eye since the value of the thickness is dramatically different among individuals. This can simply justify our need to have a comparison between thicknesses of two eyes in symmetricity. Therefore, we have proposed an asymmetry analysis of the retinal nerve layer thickness and total retinal thickness in the around of macula in the normal population of Iranian. In the first step retinal borders and RNFL border are segmented by diffusion map method and thickness profiles were made. We use scaling to shape a square image to be consistent with fundus images. Then we automatically find the middle point of the macula. For this purpose we use a pattern matching scheme. RNFLT and retinal thickness are analyzed by dividing three circle scanning areas (diameter 1, 3, 6 mm) around the macula into 4 quadrants and 9 sectors. Then we obtain the mean and standard deviation of the total thickness and RNFL thickness for the each sector in the right and left eye. The maximums of the average RNFL thickness in right and left eyes are seen in the perifoveal nasal, and the minimums are seen in the fovea. Tolerance limits in RNFL thickness is shown to be between 0.78 to 2.4  $\mu$ m for 19 volunteers used in this study.

9038-69, Session PSMon

# Towards a myocardial contraction force reconstruction technique for heart disease assessment and therapy planning

Seyyed Mohammad Hassan Haddad, Maria Drangova, The Univ. of Western Ontario (Canada); James A White, The Univ. of Calgary (Canada); Abbas Samani, Univ. of Western Ontario (Canada)

Cardiac ischemic injuries can be classified in two main categories: reversible and irreversible. Treatment of reversible damages is possible through revascularization therapies. Clinically, it is quite vital to determine the reversibility of ischemic injuries using early and accurate diagnosis. For this purpose, a number of imaging techniques have been developed. To our knowledge, none of these techniques determine damage reversibility based on a direct measure (e.g. sufficient myocardial contraction forces). Since contraction force generation is a reliable and straightforward mechanical measure for functionality assessment, this research involves developing a new imaging technique for quantification of cardiac contraction forces. This work is also geared towards another application, namely Cardiac Resynchronization Therapy (CRT) and specifically for electrode leads configuration optimization. The latter has not been tackled through a systematic technique thus far. In the proposed method, contraction force reconstruction is accomplished by an inverse problem algorithm solved through an optimization framework which uses iterative forward mechanical modelling of the myocardium. As a result, the method requires a forward mechanical model of the

myocardium which is computationally efficient and robust against divergence. Therefore, we developed such a model which considers all aspects of the myocardial mechanics including hyperelasticity, anisotropy, and active contraction forces of the fibers. This model assumes two major parts for the myocardium consisting background tissue and reinforcement bars simulating myocardial fibers. The finite element (FE) simulations of this model demonstrated quite acceptable performance in mimicking left ventricle (LV) contraction operation.

9038-71, Session PSMon

#### Setting ventilation parameters guided by Electrical Impedance Tomography in an animal trial of Acute Respiratory Distress Syndrome

Michael Czaplik, Univ. Hospital Aachen (Germany) and RWTH Aachen (Germany); Ingeborg Biener, Univ. Hospital Aachen (Germany); Steffen Leonhardt, RWTH Aachen (Germany); Rolf Rossaint M.D., Univ. Hospital Aachen (Germany)

Since mechanical ventilation can cause harm to lung tissue it should be as protective as possible. Whereas numerous options exist to set ventilator parameters, an adequate monitoring is lacking up to date. The Electrical Impedance Tomography (EIT) provides a noninvasive visualization of ventilation which is relatively easy to apply and commercially available. Although there are a number of published measures and parameters derived from EIT, it is not clear how to use EIT to improve clinical outcome of e.g. patients suffering from acute respiratory distress syndrome (ARDS), a severe disease with a high mortality rate. On the one hand, parameters should be easy to obtain, on the other hand clinical algorithms should consider them to optimize ventilator settings. The so called Global inhomogeneity (GI) index bases on the fact that ARDS is characterized by an inhomogeneous injury pattern. By applying positive end-expiratory pressures (PEEP), homogeneity should be attained. In this study, ARDS was induced by a double hit procedure in six pigs. They were randomly assigned to either the EIT or the control group. Whereas in the control group the ARDS network table was used to set the PEEP according to the current inspiratory oxygen fraction, in the EIT group the GI index was calculated during a decremental PEEP trial. PEEP was kept when GI index was lowest. Interestingly, PEEP was significantly higher in the EIT group. Additionally, two of these animals died ahead of the schedule. Obviously, not only homogeneity of ventilation distribution matters but also limitation of over-distension.

9038-72, Session PSMon

# Accurate 3D kinematic measurement of temporomandibular joint using X-ray fluoroscopic images

Takaharu Yamazaki, Akiko Matsumoto, Kazuomi Sugamoto, Ken Matsumoto, Naoya Kakimoto, Yoshiaki Yura, Osaka Univ. Graduate School of Medicine, FOM (Japan)

Accurate measurement and analysis of 3D kinematics of temporomandibular joint (TMJ) is very important for assisting clinical diagnosis and treatment of prosthodontics, orthodontics and oral surgery. This study presents a new 3D kinematic measurement technique of TMJ using X-ray fluoroscopic images, which can easily obtain TMJ kinematic data in natural motion.

In vivo kinematics of TMJ (maxilla and mandibular bone) is determined using a feature-based 2D/3D registration, which uses beads silhouette on fluoroscopic images and 3D surface bone models with beads. The 3D surface models of maxilla and mandibular bone with beads were created from CT scans data of the subject using the mouthpiece with the seven











strategically placed beads. In order to validate the accuracy of pose estimation for the maxilla and mandibular bone, computer simulation test was performed using five patterns of synthetic tantalum beads silhouette images. In the clinical applications, dynamic movement during jaw opening and closing was conducted, and the relative pose of the mandibular bone with respect to the maxilla bone was determined.

The results of computer simulation test showed that the root mean square errors were sufficiently smaller than 1.0 mm and 1.0 degree. In the results of clinical applications, during jaw opening from 0.0 to 36.8 degree of rotation, mandibular condyle exhibited 19.8 mm of anterior sliding relative to maxillary articular fossa, and these measurement values were clinically similar to the previous reports. Consequently, present technique was thought to be suitable for 3D TMJ kinematic analysis.

9038-73, Session PSMon

#### Using Anisotropic 3D Minkowski Functionals for Trabecular Bone Characterization and Biomechanical Strength Prediction in Proximal Femur Specimens

Mahesh B. Nagarajan, Titas De, Univ. of Rochester Medical Ctr. (United States); Eva Lochmüeller, Felix Eckstein, Paracelsus Medizinische Privatuniversität (Austria); Axel Wismüller M.D., Univ. of Rochester Medical Ctr. (United States)

The ability of Anisotropic Minkowski Functionals (AMFs) to capture local anisotropy while evaluating topological properties of the underlying gray-level structures has been previously demonstrated. We evaluate the ability of this approach to characterize local structure properties of trabecular bone micro-architecture in ex vivo proximal femur specimens, as visualized on multi-detector CT, for purposes of biomechanical bone strength prediction. To this end, volumetric AMFs were computed locally for each voxel of volumes of interest (VOI) extracted from the femoral head of 146 specimens. The local anisotropy captured by such AMFs was quantified using a fractional anisotropy measure; the magnitude and direction of anisotropy at every pixel was stored in histograms that served as a feature vectors that characterized the VOIs. A linear multiregression analysis algorithm was used to predict the failure load (FL) from the feature sets; the predicted FL was compared to the true FL determined through biomechanical testing. The prediction performance was measured by the root mean square error (RMSE) for each feature set. The best prediction result was obtained from the fractional anisotropy histogram of AMF Euler Characteristic (RMSE = 1.01 ± 0.13), which was significantly better than MDCT-derived mean BMD (RMSE =  $1.12 \pm 0.16$ , p<0.05). We conclude that such anisotropic Minkowski Functionals can capture valuable information regarding regional trabecular bone quality and contribute to improved bone strength prediction, which is important for improving the clinical assessment of osteoporotic fracture risk.

9038-74, Session PSMon

# The hydration behavior of hydrophilic material in biological samples using ratio of 3-to-2 photon annihilation

Hanan Aldousari, Univ. of Surrey (United Kingdom)

In 2004, the idea of exploiting the unique characteristics of 3? annihilation as a new PET imaging modality (3? PET) was introduced by Kacperski and Spyrou and opened a new scientific field that aims to investigate the 3? yield in hypoxic/normoxic/hyperoxic conditions in tissues for application to oncology. 3? annihilation is considerably higher in a hypoxic environment. In this work, the hydration behaviour in biological samples (blood and serum) of two types of hydrophilic materials, potential candidates for the construction of radiation phantoms, was evaluated. Type A is a HEMA/VP of EWC=38% while type B is an MMA/VP of EWC=75%. The hydrophilic materials dimensions were recorded

after 1, 4, 9, 21, 33, 52, 70, and 97 hours of immersion in blood and serum (at room temperature) in order to observe the changes in shape and level of hydration. The results indicate that the hydration rate is generally higher in serum. The hydration rates for blood and serum were quite similar for sample A; the diffusion coefficients were found to be 0.018 g/h in blood and 0.019 g/h in serum. For sample B, the hydration rate was different for blood and serum; the diffusion coefficients were found to be 0.055 g/h in blood and 0.061 g/h in serum. In conclusion, hydrophilic materials are potentially suitable materials for the construction of hypoxic phantoms as they are tissue equivalent structures in which the hydration level and type of liquid content can be controlled. The peakto-peak method was applied, by using hydrophilic material as a hypoxic phantom, to study the formation and quenching process of positronium that affect the relative yield of 3-to-2 photon annihilation.

9038-75, Session PSMon

#### Investigating the use of texture features for analysis of breast lesions on contrastenhanced cone beam CT

Xixi Wang, Mahesh B. Nagarajan, Univ. of Rochester Medical Ctr. (United States); David Conover, Ruola Ning, Koning Corp. (United States); Avice O'Connell, Axel Wismüller M.D., Univ. of Rochester Medical Ctr. (United States)

Cone beam computed tomography (CBCT) has found use in mammography for imaging the entire breast with sufficient spatial resolution at a radiation dose within the range of that of conventional mammography. Recently, enhancement of lesion tissue through the use of contrast agents has been proposed for cone beam CT. This study investigates whether the use of such contrast agents improves the ability of texture features to differentiate lesion texture from healthy tissue on CBCT in an automated manner. For this purpose, 9 lesions were annotated by an experienced radiologist on both regular and contrastenhanced CBCT images using 2D square ROIs. These lesions were then segmented, and each pixel within the lesion ROI was assigned a label - lesion or non-lesion, based on the segmentation mask. On both sets of CBCT images, four 3-D Minkowski Functionals were used to characterize the local topology at each pixel. The resulting feature vectors were then used in a machine learning task involving support vector regression with a linear kernel to classify each pixel as belonging to the lesion or nonlesion region of the ROI. Classification performance was assessed using the area under the receiver-operating characteristic (ROC) curve (AUC). Minkowski Functionals derived from contrast-enhanced CBCT images were found to exhibit significantly better performance at distinguishing between lesion and non-lesion areas within the ROI when compared to those extracted from CBCT images without contrast enhancement (p < 0.05). Thus, contrast enhancement in CBCT can improve the ability of texture features to distinguish lesions from surrounding healthy tissue.

9038-76, Session PSMon

# A registration-based segmentation method with application to adiposity analysis of mice microCT images

Bing Bai, Anand Joshi, Sebastian Brandhorst, Valter D. Longo, Peter S. Conti, Richard M. Leahy, The Univ. of Southern California (United States)

In this paper we present an automatic, registration-based segmentation method for mouse adiposity studies using microCT images. We coregister the subject CT image and a mouse CT atlas. Our method has three steps. The first step is the reorientation and rigid registration of atlas and CT. Second we apply posture correction using landmark constraints and surface-based warping to match the internal anatomy. Finally a volumetric registration is applied which warps the internal











mouse anatomy of the atlas to match with that of the subject mouse. For method verification we scanned a C57BL6/J mouse from the base of the skull to the distal tibia. We registered the obtained mouse CT image to the Digimouse atlas. Major organs were segmented based on the method described above. Preliminary results show that after the first two steps we can warp the Digimouse atlas image to match the posture and shape of the subject CT image, which has significant differences from the atlas. We will build an atlas with subcutaneous adipose tissue and visceral adipose tissue components and use our software to segment the adipose tissue in order to measure the adiposity of the mouse from microCT images and compare our method with manual segmentation. The software will be used in longitudinal obesity studies using mouse model.

9038-77, Session PSMon

# Relationship of ultrasound signal intensity with SonoVue concentration at body temperature in vitro

Xin Yang, Jing Li, Huazhong Univ. of Science and Technology (China); Xiaoling He, China University of Geosciences (China); kaizhi wu, Yun Yuan, Mingyue Ding, Huazhong Univ. of Science and Technology (China)

In this paper, the relationship between image intensity and ultrasound contrast agent (UCA) concentration is investigated. Experiments are conducted in water bath using a silicon tube filled with UCA (SonoVue) at different concentrations (100?I/I to 6000?I/I) at around 37 °C to simulate the temperature in human body. The mean gray-scale intensity within the region of interest (ROI) is calculated to obtain the plot of signal intensity to UCA concentration. The results show that the intensity firstly exhibits a linear increase to the peak at approximately 1500?I/I then appears a downward trend due to the multiple scattering (MS) effects.

9038-78. Session PSMon

#### A random walk based method for segmentation of intravascular ultrasound images

Jiayong Yan, Hong Liu, Shanghai Medical Instrument Institute (China); Yaoyao Cuicui, Suzhou Institute of Biomedical Engineering and Technology (China)

Intravascular ultrasound (IVUS) is an important imaging technique that is used to study vascular wall architecture for diagnosis and assessment of the cardiovascular diseases. Segmentation of lumen and mediaadventitia boundaries from IVUS images is a basic and necessary step for quantitative assessment of the vascular walls. Due to ultrasound speckles, artifacts and individual differences, automated segmentation of IVUS images represents a challenging task. In this paper, a random walk based method is proposed for fully automated segmentation of IVUS images. Robust and accurate determination of the seed points for different regions is the key to successful use of the random walk algorithm in segmentation of IVUS images and is the focus of our work. The presented method mainly comprises five steps: firstly, the seed points inside the lumen and outside the adventitia are roughly estimated with intensity information, respectively; secondly, the seed points outside the adventitia are refined, and those of the media are determined through the results of applying random walk to the IVUS image with the roughly estimated seed points; thirdly, the media-adventitia boundary is detected by using random walk with the seed points obtained in the second step and the image gradient; fourthly, the seed points for media and lumen are refined; finally, the lumen boundary is extracted by using random walk again with the seed points obtained in the fourth step and the image gradient. The tests of the proposed algorithm on the in vivo dataset demonstrate the effectiveness of the presented IVUS image segmentation approach.











Tuesday - Thursday 18-20 February 2014

Part of Proceedings of SPIE Vol. 9039 Medical Imaging 2014: PACS and Imaging Informatics: Next Generation and Innovations

9039-1, Session 1

## **Re-thinking CAD for the next generation** (Keynote Presentation)

Eliot L. Siegel M.D., Univ. of Maryland Medical Ctr. (United States)

Computer aided detection algorithms have been utilized in radiology for more than two decades, and research about their efficacy has been promising, such as a paper published in Radiology in 1994 suggesting 100% sensitivity and 82% specificity in the detection of spiculated breast cancers. Clinical utilization of CAD, however has plateaued and has largely been limited to mammography. A 2013 SPIE session that focused on challenges in CAD commercialization underscored the fact that despite the large corpus of previous and active research on CAD, incorporation of this technology into clinical practice has been disappointingly slow. A Society of Breast imaging survey found that despite the high penetration of CAD, only 2% of respondents indicated that they always rely on CAD and approximately 50% indicated that they rarely or never rely on CAD in the diagnosis of cancer. The next generation of CAD will reflect the trend toward big data and personalized medicine and shift away from the current second reader approach and toward one in which CAD algorithms increasingly serve as visualization and image measurement/annotation and quantification tools. Computer algorithms will also be increasingly utilized to routinely provide "supplemental" information such as quantification of bone mineral density, interstitial lung disease severity, presence of an aortic aneurysm, coronary artery calcification score, and so on creating a supplemental but not necessarily displayed radiology report. This will allow radiology data to be discoverable by the increasing number of decision support algorithms that will be incorporated into the routine practice of medicine.

9039-2, Session 2

# Development of a web-based DICOM-SR viewer for CAD data of multiple sclerosis lesions in an imaging informatics-based eFolder

Kevin C. Ma, Heng Gao Zhong, Jonathan Wong, Jeffrey Zhang, Brent J. Liu, The Univ. of Southern California (United States)

In the past, we have presented an imaging-informatics based eFolder system for managing and analyzing imaging and lesion data of multiple sclerosis (MS) patients, which allows for data storage, data analysis. and data mining in clinical and research settings. The system integrates the patient's clinical data with imaging studies and a computer-aided detection (CAD) algorithm for quantifying MS lesion volume, lesion contour, locations, and sizes in brain MRI studies. For compliance with IHE integration protocols, long-term storage in PACS, and data query and display in a DICOM compliant clinical setting, CAD results need to be converted into DICOM-Structured Report (SR) format. Open-source dcmtk and customized XML templates are used to convert quantitative MS CAD results from MATLAB to DICOM-SR format. A web-based GUI based on our existing DICOM WADO image viewer has been designed to display the CAD results from generated SR files. The GUI is able to parse DICOM-SR files and extract SR document data, then display lesion volume, location, and brain matter volume along with the referenced DICOM imaging study. In addition, the GUI supports lesion contour overlay, which matches a detected MS lesion with its corresponding DICOM-SR data when a user selects either the lesion or the data. The methodology of converting CAD data in native MATLAB format to DICOM-SR and display of the tabulated DICOM-SR with the patient's clinical information and relevant study images in the GUI will

be presented. The developed SR conversion model and GUI support aim to further demonstrate how to incorporate CAD post-processing components in a PACS and imaging informatics-based environment.

9039-3, Session 2

## Remote volume rendering pipeline for mHealth applications

Ievgeniia Gutenko, Xin Zhao, Ji Hwan Park, Kaloian Petkov, Charilaos Papadopoulos, Arie Kaufman, Stony Brook Univ. (United States); Ronald Cha, Samsung Research America (United States)

We introduce a novel remote volume rendering pipeline for medical visualization targeted for mHealth (mobile health) applications. The necessity of such a pipeline comes from the volume of the medical imaging data produced by current CT and MRI scanners with respect to the complexity of the volumetric rendering algorithms. For example, the resolution of CT Angiography (CTA) data easily reaches 512^3 and up to 6 gigabytes in size by spanning over the time domain while capturing a beating heart. This explosion in data size makes data transfers to mobile devices challenging, and even when the transfer problem is resolved the rendering performance of the device still remains a bottleneck. To deal with this issue, we propose a thin-client architecture, where the entirety of the data resides on a remote server where the image is rendered at and then streamed to the client mobile device. We utilize the display and interaction capabilities of the mobile device, while performing interactive volume rendering on a server capable of handling large datasets. Specifically, upon user interaction the volume is rendered on the server and encoded into an H.264 video stream. H.264 is ubiquitously hardware accelerated, resulting in faster compression and lower power requirements. The choice of low-latency CPU- and GPU-based encoders is particularly important in enabling the interactive nature of our system. We demonstrate a prototype of our framework using various medical datasets on a commodity tablet device.

9039-4, Session 2

## Separation of metadata and pixel data to speed DICOM tag morphing

Mahmoud M. Ismail, James F. Philbin, Johns Hopkins Outpatient Ctr. (United States)

The DICOM information model combines the pixel data with other associated metadata in a single object. It is not possible to access the metadata separately from the pixel data. There are important use cases that only need access to the metadata. The DICOM format increases the running time of those use cases. Tag morphing is an example of one of those applications. Tag or attribute morphing includes deletion, insertion or modification of one or more of the metadata attributes in a study. It is typically used for order reconciliation on study acquisition or to localize the issuer of patient ID (IPID) and the patient ID attributes when data from one Medical Record Number (MRN) domain is transferred to a different domain.

In this work, we propose using the Multi-Series DICOM (MSD) format, which separates metadata from pixel data, while at the same time eliminating duplicate attributes, to reduce the time required for tag morphing. MSD stores studies using two files rather than many single frame files. The first file contains the study metadata and the second contains pixel and other bulk data. The times required updating a set of study attributes in MSD format and the DICOM format are compared. The results show that tag morphing is significantly faster in MSD format.













9039-5, Session 2

## The oncology medical image database (OMI-DB)

Mark D. Halling-Brown, Padraig T. Looney, Mishal N. Patel, Lucy M. Warren, Alistair Mackenzie, Kenneth C. Young, The Royal Surrey County Hospital NHS Trust (United Kingdom)

Current efforts relating to evaluation and research into digital medical imaging require the large-scale collection of images (both unprocessed and processed) and data. This demand has led us to design and implement a flexible oncology image repository, which prospectively collects images and data from multiple sites throughout the UK. This Oncology Medical Image Database (OMI-DB) has been created to support research involving medical imaging and contains unprocessed and processed medical images, associated annotations and data, and where applicable expert-determined ground truths describing features of interest. The process of collection, annotation and storage is almost fully automated and is extremely adaptable, allowing for quick and easy expansion to disparate imaging sites and situations.

Initially the database was developed as part of a large research project in digital mammography (OPTIMAM). Hence the initial focus has been digital mammography; as a result, much of the work described will focus on this field. However, the OMI-DB has been designed to support heterogeneous modalities and is extensible and expandable to store any associated data with full anonymisation. Currently, the majority of associated data is made up of radiological, clinical and pathological annotations extracted from the National Breast Screening System (NBSS). In addition to the data, software and systems have been created to allow expert radiologists to annotate the images with interesting clinical features and provide descriptors of these features. The data from OMI-DB has been used in observer studies and there are several more upcoming studies in progress or planned. To date we have collected 26,740 2D images from 2,623 individuals.

9039-6, Session 2

## A concept of a generalized electronic patient record for personalized medicine

Jens Meier, Univ. Leipzig (Germany); Ruchi R. Deshpande, Brent J. Liu, Image Processing and Informatics Lab. (United States); Thomas Neumuth, Univ. Leipzig (Germany)

The treatment process of tumor patients is supported by different stand-alone ePR and clinical decision support (CDS) systems. We developed a concept for the integration of a specialized ePR for head and neck tumor treatment and a DICOM-RT based CDS system for radiation therapy in order to improve the clinical workflow and therapy outcome. A communication interface for the exchange of information that is only available in the respective other system will be realized. This information can then be used for further assistance and clinical decision support functions. In the first specific scenario radiation therapy related information such as radiation dose or tumor size are transmitted from the CDS to the ePR to extend the information base. This information can then be used for the automatic creation of clinical documents or retrospective clinical trial studies. The second specific use case is the transmission of follow-up information from the ePR to the CDS system. The CDS system, which maintains a database of retrospective treatment planning and outcomes data, uses the current patient's anatomy to search for previous patients with similar anatomical features. The clinician can then look at the outcomes of the resulting set of matched patients from the database, and try to customize the treatment plan for the current patient to ensure the best outcomes. In conclusion this research project shows that centralized information availability in tumor therapy is important for the improvement of the patient treatment process and the development of sophisticated decision support functions.

9039-7, Session 2

# Biomedical image representation and classification using an enntropy weighted probabilistic concept feature space

Mahmudur Rahman, Sameer Antani, Dina Demner-Fushman, George R. Thoma, National Library of Medicine (United States)

This paper presents a novel approach to biomedical image representation for classification by mapping image regions to local concepts and represent images in a weighted entropy based probabilistic feature space. In a heterogeneous collection of medical images, it is possible to identify specific local patches that are perceptually and/or semantically distinguishable. The variation of these patches is effectively modeled as local concepts based on their low-level features as inputs to a multi-class SVM classifier. The probability of occurrence of each concept in an image is measured by spreading and normalizing each region's class confidence score based on the probabilistic output of the classifier. Furthermore, different importance of concepts is measured as Shannon entropy based on pixel values of image patches and used to refine the feature vector to overcome the limitation of the "TF-IDF"-based weighting in commonly used visual words-based image representation, where only frequency of occurrence is considered. Finally, to consider the spatial information about the concepts, each image each segmented into five overlapping regions based on the use of a grid of cells superimposed on the encoded images and local feature vectors are generated from those regions.

The proposed feature extraction and representation scheme is robust against classification and quantization errors and some notion of concept location is taken into account. A systematic evaluation of image classification on two different biomedical image data sets with different imaging modalities and body parts demonstrates improvement of more than 10% for the proposed feature representation approach compared to the commonly used low level features and visual word-based approach.

9039-8, Session 3

# OC To-go: on patient's site integration of images into OpenClinica in clinical trials by mobile devices

Daniel Haak, Stephan Jonas, Johan Gehlen, Thomas M. Deserno, RWTH Aachen (Germany)

Image-based measurements have become an essential surrogate for primary endpoints in controlled clinical trials, but electronic data capture (EDC) systems insufficiently support integration of image files. OpenClinica has established as one of the world's leading EDC systems and is used to collect, manage and store data of clinical trials in electronic case report forms (eCRFs). Integration of mobile devices, which might be used to capture documentary photography, allows instantaneous transfer of images into OpenClinica directly from the patient's bed site. For the communication between mobile application and OpenClinica server, we use web services for metadata and Secure File Transfer Protocol (SFTP) for image file transfer. OpenClinica's web service package (OC WS) already offers web service endpoints, which can be accessed after user's authorization data is captured. The web service endpoints are used to query OpenClinica for context information, such as existing studies, events, subjects and to import data into OpenClinica. For this, a Clinical Data Interchange Standards Consortium Object Data Module (CDISC ODM), connecting eCRF fields with the location of transferred images on the OpenClinica's file system, is generated and sent to OC WS. During image transfer, the progress information (e.g. remaining time) is visualized to the user. The workflow is demonstrated for a European multi-center registry, where patients with calciphylaxis disease are included. The images documenting the skin lesions are captured, transferred and correctly integrated into OpenClinica eCRF immediately during the visit. Furthermore, storage of private health data on the imaging device becomes obsolete.











9039-9, Session 3

#### New approach on secured image distribution

Andreas Thiel, OFFIS e.V. (Germany)

The DICOM standard provides several alternative techniques for communicating images in a secure manner, none of which however is fully applicable to a Grid post-processing scenario. Security in this context primarily means that personal identifying data such as patient demographics need to be kept confidential while images are transmitted or processed outside the generating institution. The most well-known DICOM security extension, also referred to as "DICOM Security Enhancements One", makes use of the Transport Layer Security (TLS) protocol to provide for a secure network transmission by "tunneling" the DICOM protocol through an encrypted connection. While this approach is straightforward, it requires applications to provide explicit support for encrypted DICOM communication, it significantly slows down network transmission over broadband networks, and, most importantly, it does not provide for a secure storage of data at the recipient's side - the recipient always has access to the full, unencrypted DICOM image including all identifying information. Another security technique offered by the DICOM standard called "Attribute Level Confidentiality" seems more promising. With this approach, only the identifying elements are removed from the DICOM image and replaced by "dummy" fields. The original identifying data is encrypted using the Cryptographic Message Syntax and stored as encrypted raw data within the DICOM header. Applications that support this technique and have access to the right encryption key can reconstruct the original object, while all other applications still see a valid DICOM image which is simply anonymized. The problem in the context of the Grid scenario is that DICOM unique identifiers (UIDs) must be seen as identifying information since they might be used to reconstruct the identity of the patient under certain circumstances, and thus be included in the anonymization/encryption process. This means, however, that the post-processing algorithm, which is not supposed to "know" the identity of the patient, only ever sees newly generated UIDs and cannot populate the Source Image Sequence with references to the real original images on which the post-processing was based. This, again, makes it impossible at the originating site to reconstruct the relationship between original images and derived ones.

An extended encryption process has been developed in order to support both the confidentiality requirements and the need for a valid referential integrity of Cloud-based image post-processing. In this approach, instead of a single block or encrypted raw data for the complete anonymized image, each confidential DICOM element value is encrypted and stored separately, along with the attribute tag which is stored in an unencrypted form. This allows the post-processing algorithm to generate two versions of the Source Image Sequence: a clear-text version referring to the temporary UIDs assigned to the original images during anonymization, and one version that contains encrypted information and can be used by the owner of the encryption key to decrypt and reconstruct the real unique identifiers of the original image set and insert that into the Source Image Sequence. The important point is that the post-processing algorithm does not need to be able to ever decrypt the UIDs in order to generate this information. The post-processing only ever has access to the anonymized form of the images, but can copy those encrypted data elements that are needed by the originating site to deanonymize the post-processed images and to reconstruct the referential integrity. This takes place when the post-processed images arrive at the originating site and before they are stored in the local PACS archive, assigned to the right patient and the right study.

9039-10, Session 3

# Medical imaging document sharing solutions for various healthcare services based on IHE XDS/XDS-I profiles

Jianguo Zhang, Yuanyuan Yang, Kai Zhang, Jianyong Sun, Tongue Ling, Shanghai Institute of Technical Physics (China);

Peter R. Bak, McMaster Univ. (Canada)

#### Purpose:

One key problem for continuity of patient care is identification of a proper method to share and exchange patient medical records among multiple hospitals and healthcare providers. This paper focuses in the imaging document component of medical record. The XDS-I (Cross-Enterprise Document Sharing – Image) Profile based on the IHE IT-Infrastructure extends and specializes XDS to support imaging "document" sharing in an affinity domain. In particular, it includes sets of DICOM instances and diagnostic imaging reports. We study image document sharing solutions reveral types of healthcare service and scenario based on IHE XDS/XDS-I profiles. From these studies we conclude if these profiles can be used as the foundation for designing medical image document sharing solutions for various types of regional healthcare service.

#### Methods:

We present three studies. The first one is to adopted the IHE XDS-I integration profile as a technical guide to design and develop image and report sharing mechanisms between hospitals for three types of regional healthcare service and scenario in Shanghai. For image sharing in a large city such as Shanghai for longitude healthcare management, we presented and evaluated the standardized IHE XDS/XDS-I profiles based on image sharing solution between multiple large hospitals and discussed the key issues in this kind type of image sharing application. The second study is for collaborating image diagnosis in regional healthcare services, we introduced grid-based IHE XDS-I implementation to enable imaging diagnosis cross multiple healthcare providers in an affinity domain in Shanghai. The third study of image sharing based on IHE XDS-I profile is to develop a clearinghouse for patient controlled (not well defined? Do you mean the patient population is controlled?) image exchanges between healthcare providers and PHR (definition?) vendors. The latter study is to build clearinghouse for patient controlled image sharing based on XDS-I profile in the RSNA Image Sharing network project.

#### Results:

The pilot testing of the image document sharing with the standardized IHE XDS/XDS-I implementation for longitude healthcare management was done in Shanghai Shen-Kang Hospital Management Center which manages 23 large hospitals in Shanghai city. The grid-based IHE XDS-I implementation for daily collaborative imaging diagnosis cross multiple healthcare providers was evaluated in Zhaibei district and Xuhui District of Shanghai city, which connected 21 community hospitals and three large medical centers. The image exchanging clearinghouse study based on IHE XDS-I has been operated in North America to enable personal controlled image sharing between multiple medical centers and PHR vendors.

New Technology to be presented:

The interface of XDS-I imaging source actor with third party PACS/RIS was recognized as one of key issues in the standardized IHE XDS/XDS-I implementation, and the performance of image retrieval through WADO and other protocols were evaluated. Also, particularly defined IHE ITI-41 transaction was implemented to support data transfer of both imaging document and reports.

#### Conclusions

We designed and evaluated three kinds of image sharing solutions based on IHE XDS/XDS-I profiles. In each solution, some special considerations should be recognized, and the localized implementation of IHE XDS/XDS-I such as metadata definition in both submission set and XDS Registry, and extension of standardized ITI transactions play important roles to achieve success in these applications. From our experience during evaluation and operation, we conclude that the IHE XDS/XDS-I profiles can be used as the foundation to design medical image document sharing solutions for various regional healthcare services.











9039-12, Session 3

### OsiriX Plugin for Integrated Cardiac Imaging research

Markus Huellebrand, Anja B. Hennemuth, Fraunhofer MEVIS (Germany); Daniel Messroghli, Titus Kühne, Deutsches Herzzentrum Berlin (Germany)

Strongly evolving imaging technologies such as e.g. MRI nowadays provide a multitude of new complementary techniques for the analysis of cardiovascular tissue properties, function and hemodynamics. The purpose of the presented work is to provide a research tool, which enables a quick validation of newly developed imaging techniques and supports the co-development of clinically usable analysis tools, which allow an integration with existing complementary examination methods. The concepts combined to this end consist of an integration with the open source research PACS OsiriX, an advanced heuristic DICOM classification and preprocessing as well as an integrative data model, which accumulates patient-specific image data, results and the data relations. Specific processing and analysis plugins can easily be integrated in such a way that they use the data integration and visualization infrastructure as well as results from existing plugins. Presented example applications, such as the evaluation of slice orientations for cardiac function quantification or the integrated analysis of different types of image data for diagnosis of myocarditis show that the provided tool can be successfully used for a multitude of research applications in cardiovascular imaging.

9039-28, Session 3

## Automated collection of medical images for research from heterogeneous systems: trials and tribulations

Mishal N. Patel, Padraig T. Looney, Kenneth C. Young, Mark D. Halling-Brown, The Royal Surrey County Hospital NHS Trust (United Kingdom)

Radiological imaging is fundamental in the healthcare industry and has become routinely adopted for diagnosis, disease monitoring and treatment planning. Over the past two decades both diagnostic and therapeutic imaging have undergone a rapid growth, being able to harness this large influx of medical images can provide an essential resource for research and training. Traditionally, the systematic collection of medical images from heterogeneous sites has not been commonplace within the NHS and is fraught with challenges including, data acquisition, storage, secure transfer and correct anonymisation.

Here, we describe a semi-automated system, which comprehensively oversees the collection of both raw and processed medical images from acquisition to a centralised database. The provision of raw images within our repository enables a multitude of potential research possibilities that utilise the legacy images. Furthermore, we have developed systems and software to integrate these data with their associated clinical data and annotations providing a centralised dataset for research. Currently, we regularly collect digital mammography image from two sites and partially collect from a further three, with efforts to expand into other modalities and sites currently ongoing. At present we have collected 34,014 2D images relating to 2623 individuals. In this paper we describe our medical image collection system and discuss wide spectrum of challenges faced during the design and implementation of such systems.

9039-13, Session 4

# A web-based neurological pain classifier tool utilizing Bayesian decision theory for pain classification in spinal cord injury patients

Sneha K. Verma, Mengyi Wang, The Univ. of Southern California (United States); Sophia Chun M.D., VA Long Beach Healthcare System (United States); Brent J. Liu, The Univ. of Southern California (United States)

Pain is a common complication after spinal cord injury with prevalence estimates ranging 77% to 81%, which highly affects a patient's lifestyle and well being. In the current clinical setting paper-based forms are used to classify pain correctly, however accuracy of diagnoses and optimal management pain largely depend on the expert reviewer, which in many cases not possible because of very few experts in this field. The need for a clinical decision support system that can be used by expert and nonexpert clinicians has been cited in literature, but such a system has not been developed. We have designed and developed a stand-alone tool for correctly classifying pain type in spinal cord injury (SCI) patients, using Bayesian decision theory. Various machine learning simulation methods are used to verify the algorithm using a pilot study data set, which consists of 25 patients data set. The data set consists of the paper-based forms, collected at Long Beach VA clinic with pain classification done by expert in the field. Using the WEKA as the machine learning tool we have tested on the 25 patient dataset that the hypothesis that attributes collected on the forms and the pain location marked by patients have very significant impact on the pain type classification. This system is integrated with the informatics system that will test the effectiveness of using Proton Beam radiotherapy for treating spinal cord injury (SCI) related neuropathic pain as an alternative to invasive surgical lesioning.

9039-14, Session 4

### Wearable technology as a booster of clinical care

Stephan Jonas, Andreas Hannig, Cord Spreckelsen, Thomas M. Deserno, Uniklinik RWTH Aachen (Germany)

In this work, we propose a novel concept for supporting everyday clinical pathways with wearable technology like Google Glass. In contrast to most prior work, we are not focusing on the omnipresent screen to display patient information or images, but are trying to maintain existing workflows. To achieve this, our systems supports clinical staff as an observer and documentor, only intervening adequately if problems are detected. Using the example of medication preparation and administration, a task known to be prone to errors, we demonstrate the full potential of the new device class. Using the built-in camera of Google Glass, patient and medication identifier are captured and the information is send to a transaction server. The server communicates with the hospital information system to obtain patient records and medication information. It then analyses the new medication for possible side-effects and interactions with already administered drugs. The result is sent to the device while encapsulating all sensitive information respecting data security and privacy. The user only sees a traffic light style encoded result of his action to avoid distraction. The server can reduce documentation efforts and reports in real-time on possible problems during medication preparation or administration. In conclusion, we designed a secure system around three basic principles with many applications in everyday clinical work: (i) minimal interaction and distraction; (ii) no patient data is displayed; and (iii) device is pure observer, not part of the workflow. By reducing errors and documentation burden, our approach has the capability to boost clinical care.











9039-15, Session 4

# Development of a user customizable imaging informatics-based intelligent workflow engine system to enhance rehabilitation clinical trials

Ximing Wang, Clarisa Martinez, Jing Wang, Ye Liu, Brent J. Liu, The Univ. of Southern California (United States)

The dramatic changes of technology in the past decade have produced massive amounts of multimedia data and complex workflows in large-scale rehabilitation clinical trials. Because each clinical trial has specific workflow needs, current clinical trial data management requirements are typically met by a custom-built system. Challenges occur because software development can be time-consuming, resource-intensive, and these issues can negatively impact the data collected. As a result, a solution to provide efficient workflow and data management and decision support to serve the clinical trials is urgently needed.

Workflow engines have been shown to improve the efficiency of business through automated processing. Complex clinical study workflows—such as those found in rehabilitation clinical trials—can also benefit from the workflow engine to enhance the efficiency of multimedia data collection, analysis and dissemination across different stages of the workflow. We put forward an intelligent workflow engine cored informatics system for complex randomized control trials.

The system will allow a project coordinator to build a data collection and management system that is customized to the research protocol workflow of a clinical trial, without any previous knowledge of software development needed. The system provides a graphical user interface through which users may pick blocks and modules to customize the workflow. A library of modules can be added to each phase of the workflow. The available modules currently include: treatment effect assessment tools, a web based DICOM viewer for brain images, DICOM uploader, data anonymizer and parser, intervention forms, and a video parser. The system will be evaluated with data from the 14 subjects enrolled in the Dose Optimization of Stroke Evaluation (DOSE) trial. The objective of the DOSE Clinical Trial is to determine prospectively the optimal dose of therapy that will lead to further improvements of upper extremity use for individual patients who have had a stroke. The trial aims to recruit 60 subjects in a 4-year period.

In summary, the intelligent workflow engine provides flexibility in building and tailoring the workflow in various stages of clinical trials. Although the system is designed for a trial of rehabilitation, it may be extended to all other imaging based non-rehabilitation clinical trials.

9039-16, Session 4

## Mapping of ApoE4 related white matter damage using diffusion MRI

Sinchai Tsao, Niharika Gajawelli, Darryl Hwa Hwang, The Univ. of Southern California (United States); Stephen Kriger, San Francisco V. A. Medical Ctr. (United States); Meng Law, Helena C. Chui, The Univ. of Southern California (United States); Michael W. Weiner M.D., San Francisco V. A. Medical Ctr. (United States); Natasha Lepore, The Univ. of Southern California (United States)

ApoliopoproteinE  $_{-\epsilon}4$  (ApoE $_{-\epsilon}4$ ) polymorphism is the most well known genetic risk factor for developing Alzheimers Disease. The exact mechanism through which ApoE  $_{\epsilon}4$  increases AD risk is not fully known, but may be related to decreased clearance and increased oligomerization of Aß. By making measurements of white matter integrity via diffusion MR and correlating the metrics in a voxel-based statistical analysis with ApoE $_{\epsilon}4$  genotype (whilst controlling for vascular risk factor, gender, cognitive status and age) we are able to identify changes in white matter associated with carrying an ApoE $_{\epsilon}4$  allele. We found potentially significant regions (P uncorrected<0.05) near the hippocampus and the posterior cingulum that were independent of voxels that correlated with

age or clinical dementia rating (CDR) status suggesting that ApoE may affect cognitive decline via a pathway in dependent of normal aging and acute insults that can be measured by CDR and Framingham Coronary Risk Score (FCRS).

9039-17, Session 4

# The power of hybrid / fusion imaging metrics in future PACS systems: a case study into the white matter hyperintensity prenumbra using FLAIR and diffusion MR

Sinchai Tsao, Niharika Gajawelli, Samantha J. Ma, Peter A. Michels, The Univ. of Southern California (United States) and Children's Hospital Los Angeles (United States); Meng Law, Helena C. Chui, The Univ. of Southern California (United States); Natasha Lepore, The Univ. of Southern California (United States) and Children's Hospital Los Angeles (United States)

Most white matter related neurological disease exhibit a large number of White Matter Hyperintensities (WMHs) on FLAIR MRI images. However, these lesions are not well understood. At the same time, Diffusion MRI has been gaining popularity as a powerful method of characterizing White Matter (WM) integrity. This work aims to study the behavior of the diffusion signal within the WMH voxels. The goal is to develop hybrid MR metrics that leverage information from multiple MR acquisitions to solve clinical problems. In our case, we are trying to address the WMH penumbra (as defined by Maillard et al 2011) where WMH delineates a foci that is more widespread than than the actual damage area presumably due to acute inflammation. Our results show that diffusion MR metrics may be able to better delineate tissue that is inflamed versus scar tissue but may be less specific to lesions than FLAIR. Therefore, a hybrid metric that encodes information from both FLAIR and Diffusion MR may yield new and novel imaging information about the progression of white matter disease progression. We hope that this work also demonstrates how future PACS systems could have image fusion capabilities that would be able to leverage information from multiple imaging series to yield new and novel imaging contrast.

9039-18, Session 4

#### Local image descriptor-based searching framework of usable similar cases in a radiation treatment planning database for stereotactic body radiotherapy

Ayumi Nonaka, Hidetaka Arimura, Katsumasa Nakamura, Kyushu Univ. (Japan); Yoshiyuki Shioyama, Saga Heavy Ion Medical Accelerator in Tosu (Japan); Mazen Soufi, Kyushu Univ. (Japan); Taiki Magome, The Univ. of Tokyo Hospital (Japan) and Japan Society for the Promotion of Science (Japan); Hiroshi Honda, Hideki Hirata, Kyushu Univ. (Japan)

The radiotherapy treatment planning (RTP) of the stereotactic body radiotherapy (SBRT) was more complex compared with conventional radiotherapy method because of using a number of beam directions in SBRT. We reported that similar planning cases could be helpful for determination of beam directions for treatment planners, who have less experiences of SBRT. The aim of this study was to develop a framework of searching for usable similar cases to an unplanned case in a RTP database based on a local image descriptor. This proposed framework consists of two steps, i.e., searching and rearrangement. In the first step, the RTP database was searched for 5 cases most similar to object cases based on geometric features related to the location, size and shape of the planning target volume, lung and spinal cord. In the second step, the selected 5 cases were rearranged by use of the













Euclidean distance of a local image descriptor, which is a similarity index based on the magnitudes and orientations of image gradients within a region of interest around an isocenter. It was assumed that the local image descriptor represents the information around lung tumors related to treatment planning. The cases, which were selected as cases most similar to test cases by the proposed method, were more resemble in terms of the tumor location than those selected by the method without the local image descriptor. This result suggests that the use of the local image descriptor make it possible to provide more similar cases to the treatment planner.

9039-19, Session 5

# A collaborative framework for contributing DICOM RT PHI (Protected Health Information) to augment data mining in clinical decision support

Ruchi R. Deshpande, Wanwara Thuptimdang, The Univ. of Southern California (United States); John J. DeMarco, Univ. of California, Los Angeles (United States); Brent J. Liu, The Univ. of Southern California (United States)

We have built a decision support system that provides recommendations for customizing radiation therapy treatment plans, based on patient models generated from a database of retrospective planning data. This database consists of relevant metadata and information derived from the following DICOM objects - CT images, RT Structure Set, RT Dose and RT Plan. The usefulness and accuracy of such patient models partly depends on the sample size of the learning data set. Our current goal is to increase this sample size by expanding our decision support system into a collaborative framework to include contributions from multiple collaborators. Potential collaborators are often reluctant to upload even anonymized patient files to repositories outside their local organizational network in order to avoid any conflicts with the HIPAA Privacy and Security Rules. We have circumvented this problem by developing a tool that can parse DICOM files on the client's side and extract de-identified numeric and text data from DICOM RT headers for uploading to a centralized system. As a result, the DICOM files containing PHI remain local to the client side. This is a novel workflow that results in adding only relevant yet valuable data from DICOM files to the centralized decision support knowledge base in such a way that the DICOM files never leave the contributor's local workstation. Such a workflow serves to encourage clinicians to contribute data for research endeavors by ensuring that protection of electronic patient data.

9039-20, Session 5

#### Classification of Visual Signs in Abdominal CT Image Figures in Biomedical Literature

Zhiyun Xue, Daekeun You, Sameer Antani, Rodney Long, Dina Demner-Fushman, George R. Thoma, National Library of Medicine (United States)

"Imaging signs" are a critical part of radiology's language. They not only are important for conveying diagnosis, but may also aid in indexing radiology literature and retrieving relevant cases and images. Here we report our work towards representing and categorizing imaging signs of abdominal abnormalities in figures in the radiology literature. Given a region-of-interest (ROI) from a figure, our goal was to assign a correct imaging sign label to that ROI from the following seven: accordion, comb, ring, sandwich, small bowel feces, target, or whirl. As training and test data, we created our own "gold standard" dataset of regions containing imaging signs. We computed 2997 feature attributes to represent imaging sign characteristics for each ROI in training and test sets. Following feature selection they were reduced to 70 attributes and were input to a Support Vector Machine classifier. We applied image-enhancement

methods to compensate for variable quality of the images in radiology articles. In particular we developed a method for automatic detection and removal of pointers/markers (arrows, arrowheads, and asterisk symbols) on the images. These pointers/markers are valuable for approximately locating ROIs; however, they degrade the classification because they are often (partially) included in the training ROIs. On a test set of 283 ROIs, our method achieved an overall accuracy of 70% in labeling the seven signs, which we believe is a promising result for using imaging signs to search/retrieve radiology literature. This work is also potentially valuable for the creation of a visual ontology of biomedical imaging entities.

9039-21, Session 5

## Incorporating intelligence into structured radiology reports

Charles E. Kahn Jr., Medical College of Wisconsin (United States)

The new standard for radiology reporting templates being developed through the Integrating the Healthcare Enterprise (IHE) and DICOM organizations defines the storage and exchange of reporting templates as Hypertext Markup Language version 5 (HTML5) documents. The use of HTML5 enables the incorporation of "dynamic HTML," in which documents can be altered in response to their content. HTML5 documents can employ the HTML Document Object Model (DOM), Javascript, and external web services to create intelligent reporting templates. Several reporting templates were created to demonstrate the use of scripts to perform in-template calculations. For example, a template for adrenal CT was created to compute contrast washout percentage from input values of precontrast, dynamic postcontrast, and delayed adrenal nodule attenuation values; the washout value can used to classify an adrenal nodule as a benign cortical adenoma. Dynamic templates were developed to compute volumes and to flag abnormal values, such as common bile duct diameter. Reporting templates also can be connected to external web services: a template was created to link values encoded with RadLex terms to the representation state transfer (REST) interface of the Radiology Gamuts Ontology web service, which responds with differential-diagnosis information encoded in Javascript Object Notation (JSON). Although reporting systems need not use a web browser to render the templates or their contents, the use of HTML5 and Javascript creates innumerable opportunities to construct highly sophisticated reporting templates. This report demonstrates the ability to incorporate dynamic content to enhance the use of radiology reporting templates.

9039-22, Session 5

## Pearl trees web-based interface for teaching informatics in radiology residency programs

Mindy Licurse, Hospital of the Univ. of Pennsylvania (United States); Tessa S. Cook, The Univ. of Pennsylvania Health System (United States)

Imaging informatics has rapidly evolved over the past few decades. With the increasing recognition that future growth and maintenance of radiology practices will rely heavily on radiologists with fundamentally sound informatics skills, the onus falls on radiology residency programs to properly implement and execute an informatics curriculum for this objective. In addition, the American Board of Radiology may choose to include informatics on the new board examinations. However, the resources available for didactic teaching and guidance most especially at the introductory level are varied, with few standardized resources. Given the breadth of informatics, a centralized web-based interface designed to serve as an adjunct to standardized informatics curriculums as well as a stand-alone for other interested audiences is desirable. We present the development of a curriculum using PearlTrees, an existing web-interface based on the concept of a visual interest graph that allows users to collect, organize, and share any URL they find online as well











as to upload other personal photos and notes. For our purpose, the group of "pearls" includes informatics concepts linked by appropriate hierarchal relationships. The curriculum is developed using a combination of our institution's current informatics fellowship curriculum as well as the Practical Imaging Informatics textbook (Branstetter et al., 2009). After development of the initial interface and curriculum with didactic webpages, we anticipate that there could be an area dedicated to uploading informatics community news and developments which will help promote collaborations and foster mentorships at all career levels.

9039-23, Session 5

# Pattern search in multi-structure data: a framework for the next-generation evidence-based medicine

Sreenivas R. Sukumar, Keela C. Ainsworth, Oak Ridge National Lab. (United States)

Our goal is to enable medical researchers query and mine patterns in quantitative measurement data (e.g. lab results such as blood cholesterol, sugar, white-blood-cell count, size of calcification, etc.) and qualitative descriptions (e.g. a radiologist's description of masses and calcifications in a mammogram) when posed in context of a clinical ontology. The traditional approach to building intelligent computer-aided diagnosis systems would be to leverage tools such as Excel and MATLAB to build predictive models based on the quantitative measurements. Today, these tools are not able to leverage the qualitative data available to predict disease diagnosis even if it is rich in content and is made available for research. On the other hand, we are seeing the increased use of digital technologies to archive clinical notes of patients and the dissemination of clinical ontologies and knowledgebases capturing disease-management pathways, rules and guidelines. Based on our survey of current practices, and to the best of our knowledge, there is no system that can associate image-data, textual descriptions of the image data, a medical knowledgebase and quantitative measurements to discover and hypothesize patterns of evidence over a patient population. Our efforts described in this paper are a novel step towards such a system. We describe our approach where we stage both qualitative and quantitative descriptors of each patient as a massive heterogeneous graph integrated with the knowledgebase. The knowledgebase could be clinically renowned datasets (such as SNOMED, SemMed, GINI, etc.) or some ontology the researcher has built based on experience. Using scalable algorithms on modern compute infrastructures that can handle massivesize graphs; we mine for patterns formed when patient-attributes are integrated in context to the knowledgebase. We present evidencediscovery results and discuss insights derived using our approach on mammography and traumatic brain injury datasets.

9039-24, Session PSWed

## Image-based improvement of OpenClinica's electronic case-report forms

Xinzhou Xie, Yan Zhang, Fudan Univ. (China); Stephan Jonas, Christian Druyen, Johan Gehlen, Uniklinik RWTH Aachen (Germany); Yuanyuan Wang, Fudan Univ. (China); Nikolaus Marx, Thomas M. Deserno, Uniklinik RWTH Aachen (Germany)

Automatic thumbnails are generated for big signal and image data captured in controlled clinical trials using a client-server system. In a pilot study, large raw electrocardiography (ECG) data is acquired at different trial centers and uploaded to the server using OpenClinica, an open source software for electronic case report forms. However, quality checks and data analysis cannot be performed at the client side due to the high data volume (64 GB). Thus, this software is developed to process the acquired ECG data on the server side and instantaneously generate a thumbnail for visual quality conformation.

Instead of loading the whole ECG signals, which contain up to three days of twelve-channel ECG, small segments are read for displaying as thumbnail. Additionally, relevant meta information including the Patient-ID, date of birth and the recording time is burned into the image bitmap for identification. This software developed in MATLAB is capable of processing several ECG signals. It successfully generates the thumbnail of the big raw ECG data for the quality check. After this software employed, the client-server ECG system may be more practical.

9039-25, Session PSWed

## A service protocol for post-processing of medical images on the mobile device

Longjun He, Xing Ming, Huazhong Univ. of Science and Technology (China); Lang Xu, Huazhong University of Science and Technology (China); Qian Liu, Huazhong Univ. of Science and Technology (China)

With computing capability and display size growing, the mobile device has been used as a tool to help clinicians view patient information and medical images anywhere and anytime. It is uneasy and time-consuming that transferring the medical images with large data size from picture archiving and communication system (PACS) to mobile client, since the wireless network is unstable and limited by the bandwidth. Otherwise, limited by the computing capability, memory and power endurance, it is hard to provide a satisfactory quality of experience for radiologists to handle some complex post-processing of medical images on the mobile device, such as real-time direct interactive three-dimensional visualization.

In this work, the remote rendering technology is employed to implement the post-processing of medical images instead of local rendering, and a service protocol to standardize the communication between the render server and mobile client is developed. In order to make mobile devices with different platforms be able to access post-processing of medical images, the Extensible Markup Language (XML) is taken to describe this protocol, which contains four main parts: user authentication, medical image query/ retrieval, 2D post-processing (e.g. window leveling, pixel values obtained) and 3D post-processing (e.g. maximum intensity projection (MIP), multi-planar reconstruction (MPR), curved planar reformation (CPR) and direct volume rendering (VR)). And then an instance is implemented to verify the protocol. This instance can support the mobile device access post-processing of medical image services on the render server via a client application or on the web page.

9039-26, Session PSWed

## Teleradiology mobile internet system with a new information security solution

Hitoshi Satoh, Tokyo Health Care Univ. (Japan)

We have developed the teleradiology mobile internet system with a new information security solution that provided with web medical image conference system used with mobile tablet. In the teleradiology mobile internet system used with mobile tablet, the security of information network is very important subjects. We are studying the secret sharing scheme and the tokenization as a method safely to store or to transmit the confidential medical information used with the teleradiology mobile internet system. Secret sharing scheme is a method of dividing the confidential medical information into two or more tallies. Our method has the function of automatic backup. With automatic backup technology, if there is a failure in a single tally, there is redundant data already copied to other tally. Confidential information is preserved at an individual Data Center connected through internet because individual medical information cannot be decoded by using one tally at all. Therefore, even if one of the Data Centers is struck and information is damaged due to the large area disaster, the confidential medical information can be decoded by using the tallies preserved at the data center to which it escapes











damage. Moreover, by using tokenization, the history information of dividing the confidential medical information into two or more tallies is prevented from lying scattered by replacing the history information with another character string. As a result, information is available only to those who have rightful access it and the sender of a message and the message itself are verified at the receiving point. We propose a new information transmission method and a new information storage method with a new information security solution.

9039-27, Session PSWed

# Imaging informatics based on method of MR temperature measurement in high-intensity focused ultrasound

Xiangjiao Chen, Jianguo Zhang, Shanghai Institute of Technical Physics (China)

Magnetic resonance Proton resonance frequency in the temperature measurement is used in this research. However due to the organ environment, as well as systematic error, it is difficult to perform temperature measurement precisely from the theoretical calculations of MR imaging pixels phase information of targeted area. The new design of the temperature measurement algorithm is developed based on a large number of imaging experimental data by using statistical analysis. We specifically designed a MR imaging temperature database to process and analysis of the MR imaging data, and then created empirical formula with an experienced database accordingly. Experimental temperature data was received from the heating process of homemade water film at magnetic field strength for 1.5T of magnetic resonance equipment.

After taking many factors into account such as the complexity of the human organ parts or uncertainty of the environment, we obtained a new algorithm by mining useful information from MR temperature database with huge amount of temperature measurement data with a statistical concept. Compared with the original algorithm?new algorithms have improved greatly in accuracy of temperature measurement.

9039-29, Session PSWed

# The conversion of synchrotron radiation biomedical and medical images into DICOM images

Yunling Wang, Jianyong Sun, Lab. for Medical Imaging Informatics (China); Jianqi Sun, Shanghai Jiao Tong Univ. (China); Jianguo Zhang, Lab. for Medical Imaging Informatics (China)

#### Purpose:

A synchrotron radiation (SR) X-ray source is an extraordinary tool for many applications because of the high intensity, the energy spectrum properties, the peculiar laminar beam geometry and the high degree of coherence. In the past years several studies have proven the suitability of SR in the fields of biomedical X-ray imaging, imaging diagnosis and radiotherapy. As a new type of light source with excellent characteristics, there was a lot of imaging methods being used to perform biomedical and medical imaging researches such as X-Ray absorption imaging, phase-contrast imaging and micro-CT imaging. Also, there were a lot medical imaging processing and display software to display and processing DICOM medical images. In this presentation, we present an approach to transform a various kinds of SR images into proper DICOM images so that to use a rich of medical processing display software to process and display SR biomedical and medical images.

#### Materials and Methods:

In this research, the SR images come from Shanghai Synchrotron Radiation Facility (SSRF). The imaging modalities based on SSRF are X-Ray absorption imaging, and X-ray phase-contrast imaging method and micro-CT imaging. In our research, we mostly focus on animal

imaging with various kinds of body parts, such as brain sections and vessels of rats. We designed DICOM information models for SR biomedical and medical images first. Then, we assigned proper meta data into the information models based on imaging targets (human body tissues or animals) or purposes (medical or biomedical). The original image formats of SR images were mostly tiff and bitmap, the converted final DICOM images were lossless JPEG images. The data sets of new converted images include the SR beam line, detector, scan and other settings.

#### Results:

The SR based DICOM image information models were designed and developed. The SR DICOM images with newly structured data sets can be transferred, stored, processed and displayed by using most of commercial medical imaging software.

New Technologies and Results to be Presented:

Differing from common DICOM medical imaging, this research uses synchrotron radiation facilities, and focus on both human tissues and animals. The SR based new DICOM image information models were designed and developed.

#### Conclusion:

In this research, we presented new approach to create DICOM images of the X-Ray absorption imaging, and X-ray phase-contrast imaging method and micro-CT imaging based on SSRF . The SR based DICOM image information models were designed and developed. The SR DICOM images with newly structured data sets can be transferred, stored, processed and displayed by using most of commercial medical imaging software.

9039-30, Session PSWed

# Analysis of scalability of high-performance 3D image processing platform for virtual colonoscopy

Hiroyuki Yoshida, Massachusetts General Hospital (United States) and Harvard Medical School (United States); Yin Wu, Massachusetts General Hospital (United States); Wenli Cai, Massachusetts General Hospital (United States) and Harvard Medical School (United States)

One of the key challenges in three-dimensional (3D) medical imaging is to enable the fast turn-around time, which is often required for interactive or real-time response. This inevitably requires not only high computational power but also high memory bandwidth due to the massive amount of data that need to be processed. For this purpose, we previously developed a software platform for high-performance 3D medical image processing (HPC 3D-MIP) that employs increasingly available and affordable commodity computing systems such as the multi-core, clusters, and cloud computing systems. To achieve scalable high-performance computing, our platform employs size-adaptive, distributable block volumes as a core data structure for efficient parallelization of a wide range of 3D-MIP algorithms, supports task scheduling for efficient load distribution and balancing, and consists of a layered parallel software libraries that allow image processing applications to share the common functionalities. We evaluated the performance of the HPC 3D-MIP platform by applying it to a computationally intensive process in virtual colonoscopy. Experimental results showed a 12-fold performance improvement on a workstation with 12-core CPUs over the original sequential implementation of the process, indicating the efficiency of the platform. Analysis of scalability based on the Amdahl's law for symmetric multicore chips model showed the potential of a high scalability of the HPC 3D-MIP platform when a larger number of cores is available, although the maximum speedup is limited to 24 times that of the single core, when the number of cores reaches 128.











9039-31, Session PSWed

## Analysis of grid performance using an optical flow algorithm for medical image processing

Ramon A. Moreno, Instituto do Coração do Hospital das Clínicas (Brazil); Rita C. P. Cunha, Univ. Federal de São Paulo (Brazil) and Instituto do Coração do Hospital das Clínicas (Brazil); Marco A. Gutierrez, Instituto do Coração do Hospital das Clínicas (Brazil)

The development of bigger and faster computers have not yet provided the computing power needed for medical image processing that is required nowadays. This happens because of several factors, including: i) the increasing number of qualified digital image-related users present in Healthcare institutions; ii) the demand for more performance and quality of results; iii) researchers are addressing problems that were previously considered extremely difficult to achieve; iv) Medical images are produced with higher resolution and on a larger number of people. These factors lead to the need of exploring computing techniques that can boost the computational power of Healthcare Institutions while maintaining a relative low cost. Parallel computing is one of the approaches that can help solving this problem.

Parallel computing can be achieved using multi-core processors, multiple processors, Graphical Processing Units (GPU), clusters or Grids. In order to gain the maximum benefit of parallel computing it is necessary to write programs specific for each environment or divide the data in smaller subsets.

In this article we make an analysis of the performance of the EELA-2 (E-science grid facility for Europe and Latin-America) grid infrastructure compared with a small Cluster (3 nodes x 8 cores = 24 cores) and a regular PC (Intel i3 – 2 cores). As expected the grid had a better performance for a large number of processes, the cluster for a small to medium number of processes and the PC for few processes.

9039-32, Session PSWed

# An Imaging informatics-based system utilizing DICOM objects for treating pain in spinal cord injury patients utilizing proton beam radiotherapy

Sneha K. Verma, Mengyi Wang, The Univ. of Southern California (United States); Sophia Chun M.D., VA Long Beach Healthcare System (United States); Brent J. Liu, The Univ. of Southern California (United States)

Many US combat personnel have sustained nervous tissue trauma during service, which often causes Neuropathic pain as a side effect, which is difficult to manage. However in select patients, synapse lesioning can provide significant pain control. Our goal is to determine the effectiveness of using Proton Beam radiotherapy for treating spinal cord injury (SCI) related neuropathic pain as an alternative to invasive surgical lesioning. The project is a joint collaboration of USC, Spinal Cord Institute VA Healthcare System, Long Beach, and Loma Linda University. This is first system of its kind that supports integration and standardization of imaging informatics data in DICOM format; clinical evaluation forms outcomes data and treatment planning data from the Treatment planning station (TPS) utilized to administer the proton therapy in DICOM-RT format. It also supports evaluation of SCI subjects for recruitment into the clinical study, which includes the development, and integration of digital forms and tools for automatic evaluation and classification of SCI pain. Last year, we presented the concept for the patient recruitment module based on the principle of Bayesian decision theory. This year we are presenting the fully developed patient recruitment module and its integration to other modules. In addition, the DICOM module for integrating DICOM and DICOM-RT-ION data is also developed and integrated. This allows researchers to upload animal/patient study data into the system. The patient recruitment module has been tested using 25 retrospective patient data and DICOM data module is tested using 5 sets of animal data.











Wednesday - Thursday 19-20 February 2014

Part of Proceedings of SPIE Vol. 9040 Medical Imaging 2014: Ultrasonic Imaging and Tomography

9040-1, Session 1

#### A Feasibility Study of Carotid Elastography for Risk Assessment of Atherosclerotic Plaques Validated by Magnetic Resonance Imaging

Xiaochang Pan, Tsinghua Univ. (China); Lingyun Huang, Philips Research (China); Manwei Huang, China Meitan General Hospital (China); Xihai Zhao, Le He, Tsinghua Univ. (China); Chun Yuan, Tsinghua Univ. (China) and Univ. of Washington (United States); Jing Bai, Jianwen Luo, Tsinghua Univ. (China)

Objectives: Conventional B mode ultrasound images and Doppler/color flow measurements are mostly used to evaluate degree of carotid atherosclerotic stenosis. Alternatively, the correspondence between multi-contrast magnetic resonance (MR) imaging features, plaque composition and histology has been well established (Cai et al, Circulation 2002). We proposed to use B mode echogenecity plus ultrasound strain imaging to quantitatively measure grayscale and mechanical properties of carotid atherosclerotic plaques, and correlate them to multi-contrast MR imaging features known to be associated with high risk plaque histo-pathology.

Methods: Sequences of ultrasound radiofrequency (RF) data of Philips iU22 ultrasound system were acquired from 5 human subjects older than 65 years old having carotid plaques with more than 30% stenosis. The inter-frame strain of plaques was estimated to indicate relative stiffness and rupture risk of plaques, using a two-step optical flow algorithm. The same patients received double blinded MR scans on Philips Achieva 3T TX MR system using multi-contrast protocol. 3D MR images were reconstructed and then slices at the same positions of ultrasound incident angles were registered. Carotid plaques tissue composition was characterized using MR images, while echogenecity and strain in the corresponding ultrasound images were investigated and compared to MR results.

Results: 11 plaques from these 5 human subjects were analyzed. Plaques with intra-plaque hemorrhage (IPH) or lipid-rich necrotic core (LRNC) are defined as high risk factors while calcification is a stable factor. In ultrasound results, the calcification area of plaques showed high echogenecity and low deformation (magnitude) less than 0.3%, the IPH showed intermediate echogenecity and deformation around 1%, and the LRNC showed the lowest echogenecity and large deformation more than 1.8%. The locations of ultrasound results are in good agreement with findings on MR results.

Conclusions: Ultrasound quantitative measurements of grayscale and mechanical properties were performed on a small number of human subjects. These preliminary results suggest that it may be feasible to evaluate plaque vulnerability using echogenecity combined with strain values estimated from ultrasound RF data. Statistical results on more subjects will also be shown in the presentation.

9040-2, Session 1

#### Vibro-elastoraphy: direct FEM inversion of the shear wave equation without the local homogeneity assumption

Mohammad Honarvar, Septimiu E. Salcudean, Robert N. Rohling, The Univ. of British Columbia (Canada)

To produce ultrasound images of tissue elasticity, the vibro-elastography technique involves applying a steady-state multi-frequency vibration to tissue, estimating displacements from ultrasound echo data, and using the estimated displacements in an inverse elasticity problem with the shear modulus spatial distribution as the unknown. The governing equation used requires all three displacement components to fully

solve the inverse problem. However, using ultrasound, only the axial component of the displacement can be measured accurately. Therefore, simplifying assumptions must be used. Usually, the equations of motion are transformed into a Helmholtz equation by assuming tissue incompressibility and local homogeneity. In this paper, we remove the local homogeneity assumption which causes significant imaging artifacts in areas of varying elasticity. We introduce a new finite element based direct inversion technique in which only the coupling terms in the equation of motion are ignored, so it can be used with only one component of the displacement. The use of multi-frequency excitation also allows us to obtain multiple measurements and reduce artifacts in areas where the displacement of one frequency is close to zero. The proposed method was tested in simulations and experiments against a conventional approach in which the local homogeneity is used. The results show significant improvements in elasticity imaging with the new method.

9040-3, Session 1

# Prostate clinical study of a full inversion unconstrained ultrasound elastography technique

Seyed Reza Mousavi, Western Univ. Canada (Canada); Ali Sadeghi-Naini, Gregory J. Czarnota, Sunnybrook Health Sciences Ctr. (Canada); Abbas Samani, Western Univ. Canada (Canada)

Prostate cancer detection at early stages is crucial for desirable treatment outcome. Among available imaging modalities, ultrasound (US) elastography is being developed as an effective clinical tool for prostate cancer diagnosis. Current clinical US elastography systems utilise strain imaging where tissue strain images are generated to approximate the tissue elastic modulus distribution. While strain images can be generated in real-time fashion, they lack the accuracy necessary for having desirable sensitivity and specificity. To improve strain imaging, full inversion based elastography techniques were proposed. Among these techniques, a constrained elastography technique was developed which showed promising results as long as the tumor geometry can be obtained accurately from the imaging modality used in conjunction with the elastography system. This requirement is not easy to fulfill, especially with US imaging. To address this issue, we present an unconstrained full inversion prostate elastography method in conjunction with US imaging where knowledge of tissue geometry is not necessary. One of the reasons that full inversion elastography techniques have not been routinely used in the clinic is lack of clinical validation studies. To our knowledge, no quasi-static full inversion based prostate US elastography technique has been applied in vivo before. In this work, the proposed method was applied to clinical prostate data and reconstructed elasticity images were compared to corresponding annotated histopathology images which is the first quasi-static full inversion based prostate US elastography technique applied successfully in vivo. Results demonstrated a good potential for clinical utility of the proposed method.

9040-4, Session 1

## Improved apparatus for predictive diagnosis of rotator cuff disease

Anup Pillai, Clemson Univ. (United States); Charles A. Thigpen, Proaxis Therapy (United States); Brittany Nicole Hall, David M. Kwartowitz, Clemson Univ. (United States)

Rotator cuff disease impacts over 50% of the population over 60, with reports of incidence being as high as 90% within this population, causing pain and possible loss of function. The rotator cuff is composed of muscles and tendons that work in tandem to support the shoulder. Heavy











use of these muscles can lead to rotator cuff tear, with the most common causes is age-related degeneration or sport injuries, both being a function of overuse. Tears ranges in severity from partial thickness tear to total rupture. Diagnostic techniques are based on physical assessment, detailed patient history, and medical imaging; primarily X-ray, MRI and ultrasonography are the chosen modalities for assessment. The final treatment technique and imaging modality; however, is chosen by the clinician is at their discretion.

Ultrasound has been shown to have good accuracy for identification and measurement of full-thickness and partial-thickness rotator cuff tears. In this study, we report on the progress and improvement of our method of transduction and analysis of in situ measurement of rotator cuff biomechanics. We have improved the ability of the clinician to apply a uniform force to the underlying musculotendentious tissues while simultaneously obtaining the ultrasound image. This measurement protocol combined with ROI based image processing will help in developing a predictive diagnostic model for treatment of rotator cuff disease and help the clinicians choose the best treatment technique

9040-42, Session 1

# Characterization of the elasticity of embedded objects' in tissue mimicking phantoms using ultrasound-stimulated vibroacoustography (USVA)

Ashkan Maccabi, Univ. of California, Los Angeles (United States)

Without an imaging technique that provides well-defined margins of malignant regions with high diagnostic accuracy and contrast, surgical oncologists are forced to excise excess benign tissue surrounding the site to ensure complete resection. Current approaches used in the detection of tumor regions include manual palpation and pre-operative diagnostic imaging to pinpoint malignant tissues. However, these approaches suffer from limitations such as minimal specificity and lack of depth of penetration. Lack of specificity results in the production of vague diseased regions and fails to provide a reliable guidance tool for surgeons. The proposed work provides an alternative diagnostic technique, ultrasound-stimulated vibro-acoustography (USVA) that will aid surgeons with detailed images characterized by enhanced structural boundaries and well-defined borders based on viscoelastic properties of tissues. We demonstrate selective imaging using phantom tissue samples of (i) polyvinyl alcohol and (ii) polydimethylsiloxane polymers chemically altered and arranged into unique geometries of varied elastic topology. In addition, the USVA platform was used to successfully differentiate between the bone and muscle regions of steak samples. Moreover, determining the precision and sensitivity of the USVA imaging system in identifying boundary regions as well as intensities of tissue phantom targets may provide additional information to non-invasively assess confined regions of diseased tissues from normal.

9040-6, Session 2

# Advances in acoustic microscopy and high resolution ultrasonic imaging: from principles to new applications (Keynote Presentation)

Roman G. Maev, Univ. of Windsor (Canada)

The goal of this lecture is to provide an overview of the recent advances in high-resolution ultrasonic imaging principles and techniques and their applications to biomaterials evaluation and industrial materials. This lecture will offer a number of new results from leading research groups worldwide who are engaged in aspects of the development of novel physical principles, new methods, or the implementation of modern technological solutions into current high resolution imaging techniques and methods.

Together with the above mentioned academic and practical avenues in

high resolution ultrasonic imaging research, will also be offered intriguing scientific discussions which have recently surfaced and will hopefully continue to bear fruit in the future.

One more goal of this lecture is to encourage a new generation of researchers to be more involved in research and development in the field to realize the great potential of high resolution acoustic imaging and advance the progress into its various biomedical applications.

9040-8, Session 2

#### Quantitative ultrasound monitoring of breast tumor response to chemotherapy by analysis of frequency-dependent attenuation and backscattered power

Hadi Tadayyon, Lakshmanan Sannachi, Gregory J. Czarnota, Univ. of Toronto (Canada)

The traditional assessment of tumour response to anti-cancer therapy is based on measurement of tumour shrinkage. However, tumour shrinkage is typically a late indicator of response (detectable after several weeks to a month), and there is currently no routine imaging modality available to assess tumour response earlier in the course of therapy. This study investigated quantitative ultrasound (QUS) methods for potentially providing an earlier detection of tumour response to chemotherapy, as early as one week from treatment initiation. This study also assessed the effect of attenuation correction of the power spectrum on the ability to differentiate treatment responding tumours from non-responding ones during the course of the treatment.

Radiofrequency ultrasound data were collected from 27 breast cancer patients prior to treatment and at 4 times during the course of their treatment, using a clinical ultrasound scanner operating a 6 MHz linear array probe. For purposes of quantitative ultrasound analysis, subjects were categorized into two groups- responders (N=18) and non-responders (N=9). Corresponding to each tumour, four QUS parameters - attenuation coefficient estimate (ACE), spectral slope (SS), spectral 0-MHz intercept (SI), and midband fit (MBF) were extracted. Analysis results demonstrated increases in ACE, MBF, and SI parameters after treatment whereas non-responders demonstrated little to no increase in these parameters. Overall, the MBF and SI parameters demonstrated a larger separation between responders and non-responders when attenuation correction was incorporated in the spectral analysis. In addition, the ACE itself served as a tissue characterization parameter which aided in differentiating responders from non-responders.

9040-9, Session 2

#### Computed ultrasound tomography in echo mode (CUTE) of speed of sound for diagnosis and for aberration correction in pulse-echo sonography

Michael Jaeger, Martin Frenz, Univ. Bern (Switzerland); Gerrit Held, Stefan Preisser, Sara Peeters, Michael Grünig, University of Bern (Switzerland)

Sound speed as a diagnostic marker for various diseases of human tissue has been of interest since many years. Up to now, only transmission ultrasound computed tomography (UCT) was able to detect sound speed with the spatial resolution required for diagnostic imaging. UCT, however, is limited to acoustically transparent samples such as the breast. We present a novel technique where spatially resolved detection of sound speed can be achieved using conventional pulse-echo equipment in reflection mode. For this purpose, pulse-echo images are acquired under various transmit beam directions and a two-dimensional map of the sound speed is reconstructed from the resulting signal changes using a direct reconstruction method. Phantom studies











demonstrate a high spatial resolution (1 mm) and contrast (better than 0.8 % of average sound speed) suitable for diagnostic purposes. In comparison to previous reflection-mode based methods, CUTE works also in a situation with only diffuse echoes, and its direct reconstruction algorithm enables real-time application. This makes it promising as an addition to conventional clinical ultrasound where it has the potential to benefit diagnosis in a multimodal approach. In addition, knowledge of the spatial distribution of sound speed will allow more accurate aberration correction and thus improved spatial resolution and contrast of conventional B-mode ultrasound.

9040-10, Session 2

# Dynamic subnanosecond time-of-flight detection for ultra-precise diffusion monitoring and optimization of biomarker preservation

Daniel R. Bauer, Benjamin Stevens, Jefferson Taft, David Chafin, Vinnie Petre, Abbey P Theiss, Michael Otter, Ventana Medical Systems, Inc. (United States)

Recently, it has been demonstrated that the preservation of cancer biomarkers, such as phosphorylated epitopes, in formalin-fixed paraffinembedded tissue is highly dependent on the localized concentration of the crosslinking agent. This study details a real-time diffusion monitoring system based on the acoustic time-of-flight (TOF) between 5 horizontal pairs of 4 MHz focused transducers. Diffusion affects TOF because of the distinct acoustic velocities of formalin and interstitial fluid. Tissue is placed between the transducers and vertically translated to obtain TOF values at multiple locations with a spatial resolution of approximately 1mm. Imaging is repeated for several hours until osmotic equilibrium is reached. A post-processing technique, analogous to digital acoustic interferometry, enables detection of subnanosecond TOF differences. Reference subtraction is used to compensate for environmental effects. Finally, experimental results are correlated with a simulation of the expected TOF, calculated from analytical solutions of diffusion, to estimate the tissue's diffusivity constant. Diffusion measurements with TOF monitoring ex vivo human tonsil tissue are well-correlated with a single exponential curve (R2>0.98) with a magnitude of 5-120 ns, depending on the tissue size (2-6mm) and formalin concentration (10-40%). The average exponential decay constant of 2 and 6 mm diameter samples are 20 and 315 minutes, respectively, although times varied significantly throughout the tissue (?max=174 min). The diffusivity constant of tonsil in 10% formalin was estimated to be 0.08 ?m2/ms. This technique can precisely monitor diffusion progression and could be used to mitigate effects from tissue heterogeneity and intersample variability, enabling improved preservation of sensitive cancer biomarkers

9040-54, Session 2

#### Lesion detectability in automated breast ultrasound

Sara Bahramian, Univ. of Illinois at Urbana-Champaign (United States); Keith A. Wear, U.S. Food and Drug Administration (United States)

Automated Breast Ultrasound (ABUS) systems introduce a new Ultrasound technology to address some of the drawbacks of the traditional handheld Ultrasound technology. The detection performance of this new technology is studied. The lesion detectability performance is measured using Monte-Carlo simulation techniques over the synthesized images generated by the automated breast Ultrasound systems. This performance is compared to performance of the detection using handheld Ultrasound images. It is shown that resolution degradation in the synthesize images, results in less reliable detection as compared to the handheld images scanning the same plane.

Lesion detectability is studied by measuring task information available throughout imaging process for each technology. The degradation of the spatial and sampling resolution in generating synthesized images in ABUS technology is considered. . It is shown that some task information is lost as the synthesized images are compared to the conventional handheld B-scans taken in the same plane. Then we look into the effect of this information loss in transferring task information to the B-mode images through different figures of merit namely SNR and area under the ROC curve. We show that loss of information in the RF (radio frequency) data is affecting the detectability of lesion in the synthesized images. So the detectability of the lesion in the synthesized image is degraded as compared to the handheld Ultrasound image. It is also shown that the precision of estimation for figures of merit in the synthesized image is less than the achievable precision for handheld counterpart with the same number of measurements.

9040-11, Session 3

# Software phantom with realistic speckle modeling for validation of image analysis methods in echocardiography

Yuen C. Law, RWTH Aachen (Germany); Daniel Tenbrinck, Xiaoyi Jiang, Westfälische Wilhelms-Univ. Münster (Germany); Torsten Kuhlen, RWTH Aachen (Germany)

Computer-assisted processing and interpretation of medical ultrasound images is one of the most challenging tasks within image analysis. Physical phenomena in ultrasonographic images, e.g., the characteristic speckle noise or shadowing effects make the majority of standard methods from computer vision and mathematical image processing inapplicable. Furthermore, validation of adapted computer vision methods proves to be difficult due to missing ground truth information. There is no widely accepted software phantom in this community and existing software phantoms are not flexible enough to support the use of specific speckle models for different tissue types, e.g., muscle and fat tissue. In this work, we propose a software phantom with a realistic speckle noise simulation to fill this gap and provide a flexible simulation tool for validation purposes in medical ultrasound image analysis. We discuss the generation of speckle patterns and perform statistical analysis of the resulting noise and speckle textures to obtain quantitative measures of the realism regarding the simulated textures.

9040-12, Session 3

## Breast boundary detection with active contours

Ivana Balic, Pulkit Goyal, SonoView Acoustic Sensing Technologies (Switzerland); Olivier Roy, Neb Duric, Delphinus Medical Technologies (United States) and Karmanos Cancer Institute (United States)

Ultrasound tomography is a modality that can be used to image various characteristics of the breast, such as sound speed, attenuation, and reflectivity. In the considered setup, the breast is immersed in water and scanned along the coronal axis from the chest wall to the nipple region. To improve image visualization, it is desirable to remove the water background. To this end, the 3D boundary of the breast must be accurately estimated. We present an algorithm based on active contours that automatically detects the boundary of a breast using a 3D stack of attenuation images obtained from an ultrasound tomography scanner. We build upon an existing method to design an algorithm that is fast, fully automated, and reliable. We demonstrate the effectiveness of the proposed technique using clinical data sets.











9040-14, Session 3

#### A comparison of region-based and pixelbased CEUS kinetics parameters in the assessment of arthritis

Enrico Grisan, Univ. degli Studi di Padova (Italy); Bernd Raffeiner, Univ. degli Studi di Padova (Italy) and General Hospital of Bolzano (Italy); Alessandro Coran, Univ. degli Studi di Padova (Italy); Gaia Rizzo, University of Padova (Italy); Luca Ciprian, Giovanni XXIII (Italy); Roberto Stramare, Univ. degli Studi di Padova (Italy)

Inflammatory rheumatic diseases are leading causes of disability and constitute a frequent medical disorder, leading to inability to work, high comorbidity and increased mortality. The gold-standard for diagnosing and differentiating arthritis is based on patient conditions and radiographic findings, as joint erosions or decalcification. However, early signs of arthritis are joint effusion, hypervascularization and synovial hypertrophy. In particular, vascularization has been shown to correlate with arthritis' destructive behavior, more than clinical assessment.

Contrast Enhanced Ultrasound (CEUS) examination of the small joints is emerging as a sensitive tool for assessing vascularization and disease activity. The evaluation of perfusion pattern rely on subjective semi-quantitative scales, that are able to capture the macroscopic degree of vascularization, but are unable to detect the subtler differences in kinetics perfusion parameters that might lead to a deeper understanding of disease progression and a better management of patients. Quantitative assessment is mostly performed by means of the Qontrast software package, that requires the user to define a region of interest, whose mean intensity curve is fitted with an exponential function. We show that using a more physiologically motivated perfusion curve, and by estimating the kinetics parameters separately pixel per pixel, the quantitative information gathered is able to differentiate more effectively different perfusion patterns.

In particular, we will show that a pixel-based analysis is able to provide significant markers differentiating rheumatoid arthritis from simil-rheumatoid psoriatic arthritis, that have non-significant differences in clinical evaluation (DAS28), serological markers, or region-based parameters.

#### 9040-15, Session 3

#### Calibration of echocardiographic tissue Doppler velocity, using simple, universallyapplicable methods

Niti M. Dhutia, Massoud Zolgharni, Keith Willson, Graham D. Cole, Alexandra N. Nowbar, Charlotte H. Manisty, Darrel P. Francis, Imperial College London (United Kingdom)

Echocardiographers face three major challenges when making tissue Doppler velocity measurements: apparent inconsistency between manufacturers, uncertainty over which part of the trace to make measurements and a lack of local equipment calibration. We develop, test, and make freely available, tools to solve these problems in any echocardiography laboratory.

We designed and constructed an actuator setup to produce automatic reproducible motion, and used it to compare velocities measured using 3 echocardiographic modalities: M-mode, speckle tracking, and tissue Doppler, against a non-ultrasound, optical gold standard. In the clinical phase, 25 patients underwent M-mode, speckle tracking and tissue Doppler measurements of tissue velocities.

In-vitro, the M-mode and speckle tracking velocities were concordant with optical assessment. Of the three possible tissue Doppler measurement conventions (outer, middle and inner line) only the middle line agreed with the optical assessment (discrepancy -0.20 (95%CI -0.44

to 0.03)cm/s, p=0.11, outer +5.19(4.65 to 5.73)cm/s, p=1.2?10-8, inner -6.26(-6.87 to -5.65)cm/s, p=7.2?10-9). A similar pattern occurred across all 4 studied manufacturers. M-mode was therefore chosen as the in-vivo gold standard.

Clinical measurements of tissue velocities by speckle tracking and the middle line of the tissue Doppler showed good agreement with M-mode, while the outer line overestimated significantly (+1.27(0.97to1.57)cm/s, p=2.8?10-8) and the inner line underestimated (-1.81(-2.11to-1.52)cm/s, p=7.0?10-12).

Echocardiographic velocity measurements can be calibrated by simple, inexpensive tools. We found that the middle of the tissue Doppler trace represents velocity correctly. Echocardiographers requiring velocities to match between different equipment, settings or modalities should use the middle line as the "guideline".

#### 9040-58, Session 3

## Minimum variance image blending for robust ultrasound image deconvolution

Sungchan Park, Jooyoung Kang, Yun-Tae kim, Kyuhong kimj, Jung-Ho kim, Jong Keun Song, Samsung Electronics Co., Ltd. (Korea, Republic of)

#### 1. OUR PURPOSE

After receiving ultrasound signal with imaging device, we obtain the low resolution image due to the device and tissue's spatial response. We can denote this response as the point spread function (PSF). If you know the PSF previously and assume that the input image has the convolution model between the PSF and restored image, we can obtain the high resolution image by the deconvolution process. The recent paper has reported that the classification errors of the tissue characterization are reduced with the help of the deconvolution methods. But, when the ultrasound wave propagates the human body, its velocity factors' change, which makes the PSF shape different at each region. To solve the PSF estimation problem, many algorithms have been developed to find its magnitude and phase information. Some algorithms simply eliminate the phase component and estimate the magnitude with the low pass filter. Other algorithms use the phase unwrapping methods which need high computational complexities. They are rarely error free because of the ill-posed problem and produce the PSF estimation errors and make the image overblurred on the deconvolution process.

#### 2. NEW OR BREAKTHROUGH WORK TO BE PRESENTED

To solve this problem, we present a new spatial varying blending scheme based on the minimum variance estimator. The multi window based MV beamformer has high resolution and robustness using the weighted blending of each channel data. In our case, we can obtain high resolution results which suppress the blur artifacts enough at the image post-processing level, although the deconvolution images have the restoration errors. We build the several types of deconvolution images which are used for the blending. Some use the PSFs which are estimated from the input RF images. The other type's one is the beamformed image which is invariant to PSF errors. Thus, in the worst case, it can eliminate artifacts although the restoration errors exist. After brightness alignment between the images, we blend them with the optimal weight of the minimum variance estimator. We measure its noise statistics on the sample space and compute the covariance matrix.

Although there exist cases which have the poor PSF estimation, we can suppress the artifacts efficiently by blending the images based on the MV scheme. Furthermore, we represent a new sparse image restoration method based on the alternating minimization algorithm for the higher resolution restoration.

#### 3. EXPERIMENTAL RESULTS

We verify our algorithm on the real liver and wire phantom data quantitatively and qualitatively. In all the cases, we can observe that the blur artifacts of the images which are produced by the PSF estimation error are suppressed and show the highest resolution among the input candidate images. In the wire phantom, we measure the resolution at











7cm, 10cm and 13 cm depths. On the average, the beamformed image, homomorphic algorithm, minimum phase algorithm and our adaptive blending algorithm have the resolutions 2.5mm, 1.2mm, 1.6mm, 1.2 mm respectively. It is matched to the highest resolution one among candidates.

#### 4. CONCLUSIONS

In this paper, for robust and high resolution deconvolution results, we presented a new minimum variance image blending technique. By blending multiple images optimally, we can suppress the artifacts efficiently and obtain the high resolution simultaneously. In the future, we will consider the low complexity and the parallel algorithm based on the GPU module and try to apply our algorithm to the medical system as the image processing module. The cMUT transducer has the broad band response characteristic. For the high resolution image restoration, it is one of the important factors. We will consider to implement our algorithm on the cMUT system for the high quality ultrasound image.

9040-16, Session 4

# Design and fabrication of a low-frequency (1-3 MHz) ultrasound transducer for accurate placement of screw implants in the spine

Amir Manbachi, Univ. of Toronto (Canada); Mike Lee, F. Stuart Foster, Sunnybrook Research Institute (Canada); Howard J. Ginsberg, St. Michael's Hospital (Canada); Richard S. C. Cobbold, Univ. of Toronto (Canada)

Last year, approximately 800,000 cases of spinal fusion surgeries were performed in the United States, necessitating insertion of screw implants. Their exact placement is critical and made complex due to limited visibility of the spine, continuous bleeding in the exposed regions, and variability in morphologies. The alarmingly high rate of screw misplacements (20-40%) reported in the literature is of major concern since such misplacements can place the surrounding vital structures at risk. A potential guidance method for determining the best screw trajectory is by the use of real-time ultrasound imaging similar to that used for intravascular imaging. A miniaturized transducer could be inserted into the pedicle to image the anatomy from within and identify bone boundaries.

A major challenge of imaging within bone is high attenuation of the signal. The rapid increase of attenuation with frequency requires the use of much lower frequencies (1-3 MHz). This study describes the custom design and fabrication of 2 MHz ultrasound probes (3.5 mm) for pedicle screw guidance. Two transducer designs are explored to provide improved sensitivity and signal to noise ratio, compared to the previously tested transducer within the pedicle. Custom stainless steel housing was fabricated to be compatible with surgical procedure and sterilization process. The performance of the transducers are compared with PiezoCAD simulation tool, a commercial KLM modeling software and future development of an array probe is mentioned. Long-term implications of this study will facilitate a real-time, three-dimensional method of guiding the placement of pedicle screws without incurring any radiation hazard.

9040-17. Session 4

# A synthetic transmit aperture imaging technique using orthogonally band-divided signals to utilize wide bandwidth property of CMUT arrays

Bae-Hyung Kim, Suhyun Park, Kyuhong Kim, Taeho Jeon, Seungheun Lee, Youngil Kim, Kyungil Cho, Jongkeun Song, Samsung Advanced Institute of Technology (Korea, Republic of)

In this paper, a differentiation technique to utilize the wide bandwidth

characteristic of the CMUT arrays is introduced. In theory, synthetic transmit aperture (STA) imaging techniques can produce the same image quality as that of the conventional dynamic focusing (CDF) method, with a smaller number of active channels. STA-SET/MER, a STA imaging method using a single element to transmit a short pulse (SET) and multiple elements to receive echo signals (MER), can achieve a perfect two-way dynamic focusing. In practice, however, it is difficult to achieve such advantages of STA techniques due to the well-known motion artifact. In this work, we present an efficient method to minimize the motion artifact by constructing a single image frame with dramatically reduced transmit/receive (T/R) steps. However, STA-SET/MER also suffers from low SNR problem since the acoustic power transmitted from a single element is limited to avoid electrical breakdown and overheating of array elements. In this work, a novel STA imaging technique using orthogonally band-divided signals to increase SNR and frame rate without sacrificing image resolution is reported. This paper also presents mathematical analyses to show the conditions and methods for designing such orthogonal sub-band signals and a modulation and demodulation process of orthogonal sub-band signals designed within the frequency bandwidth of the CMUT arrays. The presented method is verified by computer simulations using Field II and experiments. Currently, we are extending the presented approach to volumetric ultrasound imaging technique using 2-D CMUT-on-ASIC arrays.

9040-18, Session 4

# A preliminary work on pre-beamformed data acquisition system for ultrasound imaging with 2D transducer

Xu Li, Huazhong Univ. of Science and Technology (China)

This paper present a preliminary work on a pre-beamformed data acquisition ultrasound imaging system for a 3-MHz, 32x32 2-D array tranducer. The row-column addressing scheme is adopted for the transducer fabrication. This scheme provides a simple interconnection, consisting of one top, one bottom single-layer flex circuits. The designed system can acquire pre-beamformed data with 12-bit resolution at 40-MHz sampling rate. The digitized data of all channels are first fed through FPGAs to deserialize and stored in a 4GB RAM buffer. The acquired data can be transferred through a 1000 Mbps Ethernet link to a computer for off-line processing and analysis. The system design is based on high-level commercial integrated circuits to obtain the maximum flexibility and minimum system complexity.

9040-19, Session 4

# Hybrid beamformer architecture to minimize volumetric ultrasound imaging scanners using 2D CMUT-on-ASIC arrays

Bae-Hyung Kim, Taeho Jeon, Jongkeun Song, Seungheun Lee, Suhyun Park, Kyuhong Kim, Youngil Kim, Kyungil Cho, Samsung Advanced Institute of Technology (Korea, Republic of)

Volumetric ultrasound imaging systems using 2-D arrays with thousands of elements necessitate active probes for data acquisition and signal processing that are integrated with front-end electronics. Up-to-date CMUT technologies enable us to minimize the size and cost of ultrasound scanners by integrating front-end ASICs into 2D CMUT arrays. In the previous works, we demonstrated a design prototype of a ultrasound scan-head probe using 2-D phased CMUT-on-ASIC arrays and a hybrid volume beamforming (HVB) technique. In the HVB method, only either elevation or azimuth scan produces a volume image while receive beamforming is firstly performed in elevation (or azimuth) direction by using the analog beamformer, and then the beamformed signals are sent to the digital beamformer of the ASIC to perform dynamic receive beamforming in azimuth (or elevation) direction. In this work, to reduce











HW complexity of the hybrid beamformer, design methods and test results of the analog- and digital-beamformers are reported. A new method and architecture for performing analog beamforming is presented to reduce a required number of hardware devices and a required amount of calculation which is performed by a system and a correspondingly required amount of memory. In addition, a novel lower-bit beamforming method using 3-level quantized samples and its architecture for very small and cheap scanners is proposed. The presented method is verified by computer simulations and experiments. Currently, we are extending the presented architecture to develop a true smart probe by including lower power devices and cooling systems, and bringing wireless data transmission into consideration.

9040-20, Session 4

# A comparison between temporal and subband minimum variance adaptive beamforming

Konstantinos Diamantis, Heriot-Watt Univ. (United Kingdom); Iben K. Holfort-Voxen, Technical Univ. of Denmark (Denmark); Alan H. Greenaway, Heriot-Watt Univ. (United Kingdom); Tom H. Anderson, The Univ. of Edinburgh (United Kingdom); Jørgen A. Jensen, Technical Univ. of Denmark (Denmark); Vassilis Sboros, Heriot-Watt Univ. (United Kingdom)

This paper compares the performance between temporal and subband Minimum Variance (MV) beamformers for medical ultrasound imaging. MV based adaptive beamforming can be implemented in the frequency domain, using the short-time Fourier Transform (STFT). The STFT is employed for broad-band, ultrasound sensor signals that are divided into frequency bands, to ensure that the narrow-band condition of the adaptive beamformer is met. Each subband is processed individually and for each one, an optimized set of complex apodization weights is provided based on the sample covariance matrix estimated from the data. The time-domain implementation calculates the sample covariance matrix directly from the data without the previous requirement of dividing them into separate frequency bands. Therefore, a single set of data-dependent apodization weights is provided instead of one for each segment. The performance of the beamformers is evaluated with simulated synthetic aperture data obtained from Field II and is quantified by the Full-Width-Half-Maximum (FWHM) and the Peak-Side-Lobe level (PSL). From a point phantom, single emission with the central transducer element transmitting and all elements receiving, provides a FWHM of 0.12 mm for both implementations at a depth of 40 mm, 10 times lower than the value achieved by conventional beamforming. The corresponding values of PSL are -31 and -25 dB for frequency subband and time-domain MV beamformers, and from a cyst phantom the contrast level is calculated at -40 and -38 dB, respectively. The comparison demonstrates similar resolution but slightly lower side-lobes for the subband approach at the expense of increased computation time.

9040-21, Session 4

## Development of a novel acoustic lens based pulse echo Ultrasound Imaging system

Saugata Sinha, Navalgund A. Rao, Rochester Institute of Technology (United States)

Acoustic lens based focusing technology where the image reconstruction is achieved through the focusing of an acoustic lens, can potentially replace time consuming and expensive electronic focusing technology for producing high resolution real time ultrasound (US) images. A novel acoustic lens focusing based pulse echo US imaging system is explored here. In this system, a Polyvinylidene fluoride (PVDF) film transducer generates plane wave which is backscattered by the object and focused by a spherical acoustic lens on to a linear array of transducers. To

improve the anticipated low signal to noise ratio (SNR) of the received US signal due to the low electromechanical coupling coefficient of the PVDF film, here we explored the possibility of implementing pulse compression technique using linear frequency modulated (FM) signals or chirp signals. Comparisons among the different SNR values obtained with short pulse and after pulse compression with chirp signal show a clear improvement of the SNR for the compressed pulse. The preliminary results show that the SNR achieved for the compressed pulse depends on time bandwidth product of the input chirp and the spectrum of the US transducers. The axial resolution obtained with compressed pulse improves with increasing sweep bandwidth of input chirp signals, whereas the lateral resolution remains almost the same. This work demonstrates the feasibility of using a PVDF film transducer as an US transmitter in an acoustic lens focusing based imaging system and implementing pulse compression technique into the same setup to improve SNR of the received US signal.

9040-23, Session 5

#### Real-time clutter reduction in epioptoacoustic imaging of human volunteers

Michael Jaeger, Univ. Bern (Switzerland); Kujtim Gashi, Technische Universiteit Eindhoven (Netherlands); Sara Peeters, Univ. Bern (Switzerland); Gerrit Held, Stefan Preisser, University of Bern (Switzerland); Jeffrey C. Bamber, The Royal Marsden NHS Foundation Trust (United Kingdom) and The Institute of Cancer Research (United Kingdom); Martin Frenz, Univ. Bern (Switzerland)

Optoacoustic (OA) imaging allows the display of optical contrast inside tissue based on ultrasound detection after tissue irradiation using short laser pulses. In a multi-modal combination with pulse-echo ultrasound, OA is promising to improve diagnostic accuracy via the display of small blood vessels as well as of the local blood oxygenation level within the anatomical context. Unfortunately, epi-OA image contrast is deteriorated by clutter signals originating from the site of tissue irradiation which often limit imaging depth to around one centimetre. In past years, we have developed displacement-compensated averaging (DCA) for clutter reduction, based on the clutter decorrelation that occurs when palpating the tissue using the ultrasound probe. This method has now been implemented on a research ultrasound system for real time scanning of human volunteers with freehand guidance of the linear probe. In this presentation we will demonstrate that clutter is a real issue in clinical OA imaging, and we will show how DCA significantly improves image contrast as compared to conventional averaging. The results indicate that clutter reduction is a basic requirement for a successful combination of OA imaging with pulse-echo ultrasound. In addition we show recent phantom results of a novel clutter reduction technique where OA signals of interest can be detected free of clutter by tagging them with the localised vibration in the focus of a focused ultrasonic beam. Noiselimited imaging depth could thus be achieved in gelatine phantoms mimicking human soft tissues.

9040-24, Session 5

## Acousto-optic imaging by wavefront adaptive holography using photorefractive crystals

Jean-Baptiste Laudereau, Emilie Benoit, Institut Langevin (France); Vincent Servois, Pascale Mariani, Institut Curie (France); Alexander A. Grabar, Uzhgorod National Univ. (Ukraine); Jean-Luc Gennisson, François Ramaz, Institut Langevin (France)

Biological tissues are very strong light-scattering media. As a consequence, current medical imaging devices do not allow optical imaging of thick samples unless invasive techniques are used. Acousto-optic imaging is a light-ultrasound coupling technique that uses the optical sidebands created by acousto-optic effect to map the local











light intensity inside the medium. It takes advantage of the ballistic propagation of ultrasound in biological tissues to access optical contrast with a millimeter resolution. However, acousto-optic signal is weak and presents a speckle pattern as coherent light sources are used. Consequently, classical detection schemes based on interferometry with plane wave references lead to poor SNR. Thanks to photorefractive crystals, we developed a system based on wavefront adaptive holography that works around 800 nm and allows us to measure the acousto-optic signal on a photodiode with a SNR 10 000 times higher. Due to its working at an appropriate wavelength range inside the optical therapeutic window, such a technique is particularly well-suited for biological applications. We thus developed a multi-modal acousto-optic / ultrasound imaging platform that allows us to perform both techniques at the same time. We tested this technique on ex vivo human liver tumors. Since their mechanical properties are close to those of healthy tissues around, it is difficult to see them with ultrasound. Otherwise, invasive techniques must be used for optical imaging because of their location inside the human body. We thus obtained optical contrast whereas mechanical contrast was not significant.

9040-25, Session 5

#### Frequency analysis of Multispectral Photoacoustic Images for Differentiating Malignant Region from Normal Region in Excised Human Prostate

Saugata Sinha, Navalgund A. Rao, Rochester Institute of Technology (United States); Keerthi S. Valluru, Bhargava K. Chinni, Vikram S. Dogra, Univ. of Rochester (United States); María Helguera, Rochester Institute of Technology (United States)

Frequency domain analysis of the Photoacoustic (PA) radio-frequency signals can potentially be used as a tool for characterizing microstructure of absorbers in tissue. This study investigates the feasibility of analyzing the spectrum of multispectral PA signals generated by excised human prostate tissue samples to differentiate between malignant and normal prostate regions. Photoacoustic imaging at five different wavelengths, corresponding to peak absorption coefficients of deoxyhemoglobin, whole blood, oxyhemoglobin, water and lipid in the near infra red (NIR) (700 nm - 1000 nm) region, was performed on freshly excised prostate specimens taken from patients undergoing prostatectomy for biopsy-confirmed prostate cancer. The PA images were co-registered with the histopathology images of the prostate specimens to determine the region of interest (ROI) corresponding to malignant and normal tissue. The calibrated power spectrum of each PA signal from a selected ROI was fit to a linear model for extracting the corresponding slope, mid-band fit and intercept parameters. Mean value of each parameter corresponding to malignant and adjacent normal prostate ROI was calculated for each of the five wavelengths. The results obtained for 9 different human prostate specimens, show that the mean values of mid-band fit and intercept are significantly different between malignant and normal regions. In addition, the average mid-band fit and intercept values show a decreasing trend with increasing wavelength. These preliminary results suggest that frequency analysis of multispectral PA signals can be used to differentiate malignant region from the adjacent normal region in human prostate tissue.

9040-26, Session 5

# Coherence-based photoacoustic imaging of brachytherapy seeds implanted in a canine prostate

Muyinatu A. Lediju Bell, Danny Y. Song M.D., Emad M. Boctor, Johns Hopkins Univ. (United States)

Prostate brachytherapy is administered by implanting tiny radioactive

seeds to treat prostate cancer. The method currently relies on transrectal ultrasound imaging for intraoperative visualization of the metallic seeds. Photoacoustic (PA) imaging has been suggested as a feasible alternative to ultrasound imaging due to its superior sensitivity to metal surrounded by tissue. However, PA images suffer from poor contrast when there is insufficient laser fluence. A short-lag spatial coherence (SLSC) beamformer was implemented to enhance these low-contrast photoacoustic signals. Performance is compared to a conventional delay-and-sum (DAS) beamformer. An ex vivo dog prostate was implanted with black ink-coated brachytherapy seeds. The implanted brachytherapy seeds were visualized at distances of 13-16 mm from the location of the fiber, and the average energy at the tip of the optical fiber was varied from 7 to 17 mJ. Compared to DAS beamforming, mean contrast, contrast-to-noise, and signal-to-noise ratios were improved by 21-33 dB, 3-4, and 2-4 dB, respectively, with short-lag spatial coherence (SLSC) beamforming applied to the received photoacoustic data, when approximately 10% of the receive aperture elements were included in the short-lag sum. Similar improvements were achieved with brachytherapy seeds implanted in an in vivo canine prostate. Results indicate that the SLSC beamformer holds promise for intraoperative localization of prostate brachytherapy seeds.

9040-27, Session 6

## Ultrasound bent-ray tomography using both transmission and reflection data

Nghia Q. Nguyen, Lianjie Huang, Los Alamos National Lab. (United States)

Ultrasound bent-ray tomography can produce the sound-speed distribution of the breast for detection and diagnosis of breast cancer. However, conventional ultrasound-bent tomography using only transmission data gives low-resolution images. We develop a new ultrasound bent-ray tomography method using both transmission and reflection data to improve sound-speed reconstructions. We employ an ultrasound reflection imaging technique such as Kirchhoff migration to obtain locations of reflectors for calculating arrival times of ultrasound reflector signals. We use both first-arrival times (time-of-flights) of ultrasound transmission data and arrival times of ultrasound reflection data for sound-speed reconstructions. Our numerical examples show that our new ultrasound bent-ray tomography using both transmission and reflection data significantly improves the image resolution and sound-speed reconstructions compared to the conventional ultrasound tomography using only transmission data.

9040-28, Session 6

# Comparison of sound speed measurements on two different ultrasound tomography devices

Mark A. Sak, Karmanos Cancer Institute (United States); Neb Duric, Peter J. Littrup M.D., Karmanos Cancer Institute (United States) and Delphinus Medical Technologies (United States); Lisa Bey-Knight, Karmanos Cancer Institute (United States); Mark E. Sherman, Gretchen Gierach, National Cancer Institute (United States); Antonina Malyarenko, Karmanos Cancer Institute (United States)

Ultrasound tomography (UST) employs sound waves to produce three-dimensional images of breast tissue and precisely measures the attenuation of sound speed secondary to breast tissue composition. High breast density is a strong breast cancer risk factor and sound speed is directly proportional to breast density. UST provides a quantitative measure of breast density based on three-dimensional imaging without compression, thereby overcoming the shortcomings of many other imaging modalities. The quantitative nature of the UST breast density











measures are tied to an external standard, so sound speed measurement in breast tissue should be independent of specific hardware. The work presented here compares breast sound speed measurement obtained with two different UST devices. The Computerized Ultrasound Risk Evaluation (CURE) system located at the Karmanos Cancer Institute in Detroit, Michigan was recently upgraded to the SoftVue ultrasound tomographic device. A total of 12 patients had one or both of their breasts imaged on both systems on the same day. There were 22 sound speed scans analyzed from each system and the average breast sound speeds were compared. The sound speed measurements from each system were strongly and positively correlated with each other. The weighted Spearman's correlation coefficient was found to be rs = 0.808 and the slope of the line of best fit between the two systems was 0.9662. The average difference in sound speed between the two sets of data was 1.4 m/s and this difference was not statistically significant. These results suggest that there is no fundamental difference in sound speed measurement for the two systems and support combining data generated with these instruments in future studies.

9040-29, Session 6

# Breast ultrasound tomography using virtual sources and both transmission and reflection data

Lianjie Huang, Youzuo Lin, Zhigang Zhang, Nghia Q. Nguyen, Yassin Labyed, Kenneth M. Hanson, Los Alamos National Lab. (United States); Daniel Sandoval, Michael Williamson M.D., The Univ. of New Mexico (United States)

Ultrasound tomography has great potential to provide quantitative estimations of mechanical properties of breast tumors for accurate detection and characterization of breast cancers. We design and manufacture a new synthetic-aperture breast ultrasound tomography system with two parallel transducer arrays. The distance of these two arrays is adjustable for scanning different sizes of the breast. The transducer arrays are translated vertically to scan the breast from the chest wall/axillary region to the nipple region to acquire ultrasound transmission and reflection data for whole-breast ultrasound tomography imaging. Our breast ultrasound tomography system uses virtual ultrasound sources to acquire breast ultrasound transmission and reflection data simultaneously. The system is undergoing the final safety test, and the University of New Mexico Hospital will use the system to acquire breast ultrasound tomography data for 200 patients. In addition, we develop a suite of novel ultrasound ray and waveform tomography methods for high-resolution and high-fidelity reconstructions of the breast sound speed. We apply these methods to breast ultrasound data to investigate the capability of our breast ultrasound tomography system for detecting and characterizing small breast tumors. Tomography results demonstrate that our ultrasound ray and waveform tomography methods using both transmission and reflection data greatly improves tomographic reconstructions compared to those obtained using only transmission data or only reflection data.

9040-30, Session 6

# Optimization of the aperture and the transducer characteristics of a 3D ultrasound computer tomography system

Nicole V. Ruiter, Michael Zapf, Torsten Hopp, Robin Dapp, Hartmut E. Gemmeke, Karlsruher Institut für Technologie (Germany)

The aim of this work was to design a new aperture for 3D USCT which extends the properties of the current aperture to a larger ROI fitting the buoyant breast in water, reduces the need for careful patient positioning, and decreases artifacts in transmission tomography. The optimization

resulted in a larger opening angle of the transducers, a larger diameter of the aperture and an approximately homogeneous distribution of the transducers over the aperture, with locally random distances. The described methods enable the automatic generation of an optimized aperture for given diameters of apertures and transducer arrays and number of channels and quantitative comparison to other arbitrary apertures. Thus, during the design phase of the next generation USCT, the image quality can be balanced against the specification parameters and given hardware and cost limitations. The methods can be applied for general aperture optimization only limited by the assumptions of a hemispherical aperture and circular transducer arrays.

9040-31, Session 6

## Breast imaging with SoftVue: initial clinical evaluation

Neb Duric, Peter J. Littrup M.D., Delphinus Medical Technologies (United States) and Karmanos Cancer Institute (United States); Cuiping Li, Olivier Roy, Steven Schmidt, Delphinus Medical Technologies Inc (United States) and Karmanos Cancer Institute (United States); Xiaoyang Cheng, John Seamans, Andrea Wallen, Delphinus Medical Technologies Inc (United States); Lisa Bey-Knight, Karmanos Cancer Institute (United States)

We describe the clinical performance of SoftVue, a breast imaging device based on the principles of ultrasound tomography. Participants were enrolled in a clinical study at Wayne State University. The first step in the analysis was to determine the accuracy with which breast anatomy was rendered. Initial comparisons with MRI suggest that SoftVue can accurately image the same range of breast anatomy. The second step of the analysis focused on imaging masses across the breast density continuum. As in conventional ultrasound, we found that masses are relatively unobscured by dense parenchyma, due to their biomechanical differences relative to background tissue.

9040-32, Session 6

## **GPU** based 3D SAFT reconstruction including phase aberration

Ernst Kretzek, Nicole V. Ruiter, Karlsruher Institut für Technologie (Germany)

3D ultrasound computer tomography (3D USCT) promises reproducible high-resolution images for early detection of breast tumors. The KIT prototype provides three different modalities (reflectivity, speed of sound (SOS), and attenuation).

For high resolution reflectivity images phase aberration correction using the SOS images is necessary. The synthetic aperture focusing technique (SAFT) used for reflectivity image reconstruction is highly compute-intensive but suitable for an accelerated execution on GPUs. In this paper we investigate how the calculation of the phase aberration correction can be optimized and integrated into the SAFT algorithm. We analysed different methods to optimize the trade off between memory requirement and image quality. For 64 slices with 1024? pixels a reconstruction can be done in 30 min on eight GPUs with a performance of 66.4 GV/s. Thereby the average error made by the optimized SOS calculation is negligible.











9040-33, Session 7

# 3D endobronchial ultrasound reconstruction and analysis for multimodal image-guided bronchoscopy

Xiaonan Zang, The Pennsylvania State Univ. (United States); Rebecca Bascom, Christopher R Gilbert, Jennifer W Toth, The Pennsylvania State Hershey Medical Center (United States); William E. Higgins, The Pennsylvania State Univ. (United States)

The current practice for lung-cancer staging draws upon multidetector computed-tomography (MDCT) and bronchoscopy. An MDCT scanner provides a high-resolution three-dimensional (3D) image of the chest that is used for preoperative procedure planning, while bronchoscopy gives live intraoperative video of the endobronchial airway tree structure. State-of-the-art image-guided intervention (IGI) systems bring these two sources - the 3D MDCT image data and endobronchial video together to improve procedure efficacy. Because neither source provides live extraluminal information on suspect nodules or lymph nodes, endobronchial ultrasound (EBUS) is often introduced during a procedure. Unfortunately, existing IGI systems provide no direct synergistic linkage between the MDCT/video data and EBUS data. Hence, EBUS proves difficult to use and can lead to inaccurate interpretations. To address this drawback, we present a prototype of a multimodal IGI system that brings together the various image sources. The system enables 3D reconstruction and visualization of structures depicted in the 2D EBUS video stream. It also provides a set of graphical tools that link the EBUS data directly to the 3D MDCT and bronchoscopic video. Results using human airway tree phantom data indicate that the new system could potentially enable a smoother more natural incorporation of EBUS into the system-level work flow of bronchoscopy.

9040-34, Session 7

# Determining inter-fractional motion of the uterus using 3D ultrasound imaging during radiotherapy for cervical cancer

Mariwan Baker, Claus F. Behrens, Univ. Hospital Herlev (Denmark); Jørgen Arendt Jensen, Center for Fast Ultrasound Imaging, Dept. of Elec. Eng., Technical University of Denmark (Denmark)

#### Purpose

In radiotherapy the uterine positional changes can degrade the accuracy of the treatment plan for cervical cancer patients. The purpose of this study was to; 1) Quantify the inter-fractional uterine displacement using a novel 3D ultrasound (US) imaging system, and 2) Compare the result to the uterine shift determined from Cone-Beam CT (CBCT) imaging.

#### Methods

Four cervical cancer patients underwent CBCT imaging prior to the treatment delivery and the bone matching shift was applied. After the treatment delivery the patients were US scanned. The weekly transabdominal scans were performed using a Clarity US system (Clarity® Model 310C00). Soft-tissue matching was performed and positional shift was recorded for the three orthogonal directions.

#### Results

Overall mean value (±1SD) of US shift was (mm); left-right: (1.6±3.3), anterior-posterior: (-2.1±2.8), inferior-superior (IS): (-3.5±7.5). The variations were larger than CBCT shifts in all directions. The largest inter-fractional displacement was from -11 mm to +14 mm in IS-direction for patient 1. Thus, the CBCT bone matching underestimates the actual uterine positional displacement due to neglecting relative positional change to the bone structures. Since the US images were significantly better than CBCT images in soft-tissue visualization, the US system can be an optional image-guided radiation therapy (IGRT) system. The

operators experienced difficulty in capturing the entire uterus during US scanning.

Conclusion

3D US imaging is superior in soft-tissue visualization, but capturing the entire uterus is a challenge. Ultrasound imaging might be an optional IGRT system to identify the daily uterine positional variations.

9040-35, Session 8

## Rapid measurements of intensities for safety assessment of advanced imaging sequences

Jørgen A. Jensen, Morten F. Rasmussen, Matthias B. Stuart, Borislav G. Tomov, Technical Univ. of Denmark (Denmark)

FDA requires that intensity and safety parameters are measured for all imaging schemes for clinical imaging. This is often cumbersome, since the scan sequence have to be broken apart and measurements conducted for the individually emitted beams.

This necessitates reprogramming the ultrasound scanner and keeping track of the scan sequence, which potentially can lead to errors and wrong measurements.

This paper suggest to use the multi-line sampling capability of modern scanners and research systems, where the intensity is measured for all imaging lines in one emission sequence. This makes it possible to map out the pressure field and hence intensity level for all imaging lines in a single measurement. The approach has several advantages: the scanner does not have to be re-programmed, but can use the scan sequence without modification. The measurements are orders of magnitude faster (minutes rather than hours) and the final intensity level calculation can be made generic. The scheme has been implemented on the Acoustic Intensity Measurement System AIMS III (Onda, Sunnyvale, California, USA).

The research scanner SARUS is used for the experiments, where one of the receive channels records the hydrophone signal. A 3 MHz BK 8820e (BK Medical, Herlev, Denmark) convex array with 192 elements is used. An Onda HFL-0400 hydrophone is used and connected to a pre-amplifier Onda AH-2010. A single emission sequence is used for testing and calibrating the approach. The measurements using the AIMS III software and the SARUS system agree within a relative standard deviation of 0.23%.

9040-36, Session 8

## Hard real-time beam scheduler enables adaptive images in multi-probe systems

Richard J. Tobias, Cephasonics (United States)

Real-time embedded-system concepts were adapted to allow an imaging system to responsively control the firing of multiple probes. Large-volume, operator-independent (LVOI) imaging would increase the diagnostic utility of ultrasound . An obstacle to this innovation is the inability of current systems to drive multiple tiles dynamically. Commercial systems schedule scanning with static lists of beams to be fired and processed; here we allow an imager to adapt to changing beam schedule demands, as an intelligent response to incoming image data. Two situations where automatic scheduling changes are valuable are demonstrated: a flexible duplex mode, and with a two-transducer application mimicking LVOI imaging.

Embedded-system concepts allow an imager to responsively control the firing of multiple probes. Operating systems use powerful dynamic scheduling algorithms, such as fixed priority preemptive scheduling. Even real-time operating systems lack the timing constraints required for ultrasound. Particularly for Doppler modes, events must be scheduled with sub-nanosecond precision, and acquired data is useless without this requirement. A successful scheduler needs unique characteristics.











As a verification example, we demonstrate continuously-variable PRF in Duplex mode. To get close to what would be needed in LVOI imaging, we show two transducers scanning different parts of a subject's leg. When one transducer notices flow in a region their scans overlap in, the system reschedules the other transducer to start flow mode and alter its beams to get a view of the observed vessel and produce a vector flow measurement. This demonstrates key attributes of a successful LVOI system, such as robustness against obstructions and adaptive self-correction.

9040-38, Session 8

# Comparison of vector velocity imaging using directional beamforming and transverse oscillation for a convex array transducer

Jørgen A. Jensen, Technical Univ. of Denmark (Denmark)

Vector velocity imaging can reveal both the magnitude and direction of the blood velocity. Several techniques have been suggested for estimating the velocity and this paper compares the performance for directional beamforming and transverse oscillation (TO) vector flow imaging (VFI).

Data have been acquired using the SARUS experimental ultrasound scanner connected to a BK 8820e (BK Medical, Herlev, Denmark) convex array probe with 192 active elements.

A duplex sequence with 129 B-mode emissions interleaved with 129 flow emissions has been made.

The flow was generated in a recirculating flow rig with a stationary, laminar flow and the volume flow was measured by a MAG 3000 (Danfos, S{o}nderbog, Denmark) magnetic flow meter for reference. Data were beamformed with an optimized transverse oscillation scheme for the TO VFI and standard fourth order estimators were employed for the velocity estimation. Directional RF lines were beamformed along the flow direction and cross-correlation was employed to estimate the velocity magnitude. The velocities were determined for beam-to-flow angles of 60, 75 and 90 degrees. Using 32 emissions the relative standard deviation for TO estimation was 7.0% at a beam-to-flow angle of 75 degrees. This was 3.8% for directional beamforming. At 60 degrees it was 2.2%. The general improvement, however, comes at a substantial increase in calculational load for the directional beamformation compared to the TO method.

9040-39. Session 8

## Investigating a method for non-invasive ultrasound aberration correction through the skull bone

Meaghan A. O'Reilly, Sunnybrook Research Institute (Canada); Ryan M. Jones, Kullervo Hynynen, Sunnybrook Research Institute (Canada) and Univ. of Toronto (Canada)

Ultrasound imaging in the brain suffers from the presence of the skull bone, which strongly aberrates and attenuates sound at ultrasonic frequencies. As a result, ultrasound imaging in the brain has been limited to the use of small aperture arrays through narrow acoustic windows which are minimally perturbing. However, large aperture arrays can offer improved resolution when combined with passive imaging techniques. Robust aberration correction methods are particularly important when imaging over the whole skull surface. In this study, we examined a method for non-invasive aberration correction in which single microbubbles are excited through a human skullcap and their signals used to determine phase and amplitude correction terms for image formation. The correction terms were applied to image tube phantoms through an ex vivo human skull cap. The method was compared with a gold-standard hydrophone-based phase correction. The bubble-based method could correct the image aberration, but resulted in a translation

of the resulting image compared with the hydrophone-based correction. Further experimental work and simulations will examine the potential benefits of a multi-frequency aberration correction approach, the spatial region over which bubble-based corrections are valid, and the effect of the number of bubble events used to calculate the correction terms on the quality of the resulting image.

9040-40, Session 8

## Detection and display of acoustic window for guiding and training cardiac ultrasound users

Sheng-Wen Huang, Emil Radulescu, Shougang Wang, Philips Research North America (United States); Karl E. Thiele, David Prater, Douglas Maxwell, Patrick Rafter, Philips Healthcare (United States); Clement Dupuy, Jeremy Drysdale, Ramon Erkamp, Philips Research North America (United States)

Successful ultrasound data collection strongly relies on user skill. Among different scans, echocardiography is especially challenging as the heart is surrounded by ribs and lung tissue. Less experienced users might acquire compromised images because of suboptimal hand-eye coordination and less awareness of artifacts. Clearly, there is a need for a tool that can guide and train less experienced users to position the probe correctly. We propose to help users with hand-eye coordination by displaying lines overlaid on B-mode images. The lines indicate the edges of blockages (e.g., ribs) and are updated in real time according to movement of the probe relative to the blockages. They provide information about how probe positioning can be improved. To distinguish between blockage and acoustic window, we use coherence, an indicator of channel data similarity after applying focusing delays. Specialized beamforming was developed to estimate coherence. Image processing is applied to coherence maps to detect unblocked beams and the angle of the lines for display. We built a demonstrator based on a Philips iE33 scanner, from which raw data and video output are transferred to a workstation for processing. The detected lines are overlaid on B-mode images and fed back to the scanner display to provide users real-time guidance. Movies showing the demonstrator running live will be presented at the conference. Using such information in addition to B-mode, users will be able to quickly find the right acoustic window for optimal image quality and improve their skill.

9040-74, Session 8

## Increasing the dynamic range of synthetic aperture vector flow imaging

Carlos A. Villagomez Hoyos, Matthias B. Stuart, Jørgen A. Jensen, Technical Univ. of Denmark (Denmark)

Velocity imaging is highly susceptible beam-to-flow angle and the complex geometry of the vessels complicate the measurement. There is therefore a need for a reliable angle estimation for vector blood flow imaging. The use of high frame rate acquisitions techniques such as the synthetic aperture, can increase the frame-to-frame signal correlation of the scatterer displacement. In this approach recursive synthetic aperture acquisition, directional beamforming, and cross-correlations are used to produce B-mode and vector velocities in an interleaved 1-to-1 ratio, providing a high frame rate equal to the effective pulse repetition frequency of each imaging mode. The angle of flow is estimated, and then the flow is determined in that direction. This method works for every angle, including fully axial and fully transverse flows. Field II simulations were performed with a 192 element, 7 MHz linear array with a laminar transverse flow profile phantom, with peaks velocities of 0.5 m/s and 0.05 m/s in each simulated vessel. For the simulated vessel with peak velocity of 0.5 m/s and flow angle of 90, the relative bias is 5.1% and the relative standard deviation is 7.5%. For the simulated vessel with peak velocity of 0.05 m/s and flow angle of -90, the relative bias is -5.0% and the relative standard deviation is 8.1%. The method is able to estimate the flow











angles and flow velocities in the same phantom, and makes possible to present vector flow images with a high dynamic range.

9040-5, Session PSWed

# A new radial strain and strain rate estimation method using autocorrelation for carotid artery

Jihui Ye, Hoonmin Kim, Jongho Park, Sunmi Yeo, Sogang Univ. (Korea, Republic of); Hwan Shim, Hyungjoon Lim, Samsung Electronics Co., Ltd. (Korea, Republic of); Yangmo Yoo, Sogang Univ. (Korea, Republic of)

Atherosclerosis is a leading cause of cardiovascular disease. The early diagnosis of atherosclerosis is of clinical interest since it can prevent any adverse effects of atherosclerotic vascular diseases. In this paper, a new carotid artery radial strain estimation method based on autocorrelation is presented. In the proposed method, the strain is first estimated by the autocorrelation of two complex signals from the consecutive frames. Then, the angular phase from autocorrelation is converted to strain and strain rate and they are analyzed over time. In addition, a 2D strain image over region of interest in a carotid artery can be displayed. To evaluate the feasibility of the proposed radial strain estimation method, radiofrequency (RF) data of 408 frames in the carotid artery of a volunteer were acquired by a commercial ultrasound system equipped with a research package (V10, Samsung Medison, Korea) by using a L5-13IS linear array transducer. From in vivo carotid artery data, the mean strain estimate was -0.1372 while its minimum and maximum values were -2.961 and 0.909, respectively. Moreover, the overall strain estimates are highly correlated with the reconstructed M-mode trace. Similar results were obtained from the estimation of the strain rate change over time. These results indicate that the proposed carotid artery radial strain estimation method is useful for assessing the arterial wall's stiffness noninvasively without increasing the computational complexity.

9040-13. Session PSWed

#### ECG-based frame selection and curvaturebased ROI detection for measuring carotid intima-media thickness

Haripriya Sharma, Ramsri G. Golla, Yu Zhang, Arizona State Univ. (United States); Christopher B. Kendall, Robert T. Hurst, Mayo Clinic Arizona (United States); Nima Tajbakhsh, Jianming Liang, Arizona State Univ. (United States)

Carotid intima-media thickness (CIMT) has proven to be sensitive for predicting individual risk of cardiovascular diseases (CVD). The CIMT is measured based on region of interest (ROIs) in end-diastolic ultrasound frames (EUFs). To interpret CIMT videos, in the current practice, the EUFs and ROIs must be manually selected, a process that is tedious and time consuming. To reduce CIMT interpretation time, this paper presents a novel method for automatically selecting EUFs and determining ROIs in ultrasound videos. The EUFs are selected based on the QRS complex of the ECG signal associated with the ultrasound video, and the ROI is detected based on image intensity and curvature of the carotid artery bulb. Once a EUF is selected and its corresponding ROI is determined, our system measures CIMT using the snake algorithm extended with hard constraints [1,6-7] by computing the average thickness and maximum thickness, calculating the vascular age, and generating a patient's report. In this study, we utilize 23 subjects. Each subject has 4 videos, and approximately 3 EUFs are selected in each video, resulting in a total of 272 ROIs. By comparing with the reference provided by an expert for both frame selection and ROI detection, we achieve 92.96% sensitivity and 97.62% specificity for EUF selection, and 81.25% accuracy in ROI detection.

9040-41, Session PSWed

## Plane wave facing technique for ultrasonic elastography

Mingu Lee, Hwan Shim, Byeong Geun Cheon, Yunsunb Jung, Samsung Electronics Co., Ltd. (Korea, Republic of)

A shear wave generation technique which exploits multiple plane waves facing with each other toward their center line is introduced. Through this line, ultrasonic waves interfere constructively resulting two planar shear waves that propagate to the opposite directions parallel to the transducer instead of oblique wave from multiple point focused pushes due to the temporal inconsistency of the pushes. One advantage of the plane wave facing technique over an unfocused push beam is that it generates much larger shear waves because it actively takes advantage of constructive interference between waves and, moreover, a larger number of elements can be used without diffused beam pattern. Field II simulated intensity maps of the push beams using the proposed method are presented with those of multiple point focusing and unfocusing techniques for comparison. In the simulation, two plane waves are considered for the simplicity, and the number of elements, apodizations, and steering angles for facing are varied as parameters. Also, elasticity images of CIRS 049A phantom are presented using the proposed technique with combshaped push beams, i.e. multiple push beams are used simultaneously at different locations. L7-4 transducer is used for the simulation and elasticity imaging.

#### Description of Purpose:

For elasticity imaging and quantitative measuring of tissues, a recently popular and well accepted method is to generate shear waves and estimate of its speed inside the tissues using ultrasonic pulses. An acoustic radiation force induced by applying ultrasonic waves at a specific tissue area deforms the tissue locally, and when the force is removed shear waves propagate toward perpendicular directions to that of radiation force.

Supersonic shear imaging technique (SSI) [1] applies focused push beams at a set of locations in an axial line to generate shear wave propagations. Because push beams at those locations are temporally separated to each other and a shear wave propagation is basically spherical when the beam is focused at a point, the combined shear wave is naturally oblique to the axial direction which makes the estimation of its speed a little more complicated and narrow the region-of-interest (ROI) in the lateral direction. In addition, the push duration of each push beam is limited due to the same reason, and consequently the advantage of focusing is somewhat weakened in the sense of getting enough acoustic radiation force.

Also the use of unfocused push for inducing acoustic radiation force is introduced [2] which excites several transducer elements to apply pulses with no delay difference, in the case of linear transducer, to make the push beam planar underneath the elements. A main disadvantage of using unfocused push is that it is difficult to generate a shear wave with large amplitude. Exciting more transducer elements to overcome this would only widen the beam and cause inhomogeneity of the beam shape.

The proposed method to generate shear wave in this paper is to steer two or more adjacent plane waves as shown in Fig. 1 to induce constructive interferences in the narrow center line between them and, consequently, make a high intensity push beam. Intense push increases the amplitude of propagating shear wave which results in higher accuracy of elasticity estimation. As well as the constructive interference, the lack of the theoretical limit of the pushing duration, that the multiple point focusing method has, enables the beam more intense with enough duration. Also, the beam profile at the axial center line can be more flattened with appropriate apodization to reduce errors in elasticity estimation as the shear wave can be more planar.











9040-43, Session PSWed

#### Ultrasound 2D strain estimator based on nonrigid registration for ultrasound elastography

Xiaofeng Yang, Mylin Torres, Stephanie Kirkpatrick, Walter Curran, Tian Liu, Emory Univ. (United States)

In this paper, we present a novel approach to calculate 2D strain through registration of the pre- and post-compression (deformation) B-mode image sequences based on an intensity-based non-rigid registration algorithm. Compared with the most commonly used cross-correlation (CC) method, our approach is not constrained to any particular set of directions, and can overcome displacement estimation errors introduced by incoherent motion and variations in the signal under high compression. This method was tested using phantom and in vivo data. The robustness of our approach was demonstrated in axial direction as well as lateral direction, where the standard CC method frequency fails. In addition, our approach copes well under large compression (over 6%). In the phantom study, we computed the strain image under various compressions and calculated the signal-to-noise (SNR) and contrast-tonoise (CNS) ratios. The SNR and CNS values of our method were much higher than those calculated from the CC method. Furthermore, the clinical feasibility of our approach was demonstrated with the in vivo data from patients with arm lymphedema.

9040-44, Session PSWed

### Object detection in ultrasound elastography for use in HIFU treatment of cancer

Alex Huang, San José State Univ. (United States); Soumya Mankani, Anritsu Co. (United States)

High intensity focused ultrasound (HIFU), has applications in treating various cancers, such as prostate, liver and breast cancer. In order for HIFU to be effective and efficient it needs to be guided by an imaging modality. While there are several options for guiding HIFU treatment, one of the most promising is ultrasound elastography. Current commercial devices use B mode imaging or MRI and are manual processes. Ultrasound elastography allows complete automation of HIFU treatment due to the enhanced image that elastography provides. The elastic image provides more information and less noise.

To show that segmentation was possible on elastic images, nine algorithms were implemented in matlab and used on three distinct images for object detection. The three images used, have varying properties regarding object intensity and placement, as well as different noise patterns. Using PSNR, to gauge the effectiveness of each algorithm, it was shown that segmentation was possible on all images using different algorithms. The bilateral shock bilateral algorithm proved to be an overall effective algorithm in every situation with a PSNR of 83.87db on the phantom image. The segmentation results clearly highlight any object in the images. Future work includes fine tuning the algorithm with different phantom images and in-vivo images to distinguish between noise and desired object.

9040-45, Session PSWed

## Synthetic aperture elastography: a GPU based approach

Prashant Verma, Marvin M. Doyley, Univ. of Rochester (United States)

A synthetic aperture (SA) ultrasound imaging system produces high precision axial and lateral displacement estimates [1]; however, low frame rates and large data volumes have hampered its clinical utility. This paper describes a real-time SA ultrasound elastography system

that we have recently developed to overcome these limitations. In this system, we implemented both beamforming and elastographic signal processing methods on an Nvidia GFX 480 graphical processing unit (GPU). One thread per pixel was used during beamforming, whereas axial and lateral displacements were computed in parallel using 2D cross correlation. We compared the quality of elastograms computed with our real-time system relative to those computed using our standard single threaded elastographic imaging methodology. In all studies, we used conventional measures of image quality such as elastographic signal to noise ratio () to evaluate the performance of axial and lateral strain elastograms computed with the GPU setup relative to those computed with our standard computing platform. The results indicate that using our real-time elastography system were comparable to those achieved using our standard elastographic imaging methodology. More specifically, of axial and lateral strain elastograms computed with the real-time system were 36 dB and 23 dB, respectively, which was numerically equal to those computed with our standard approach. Additionally, we achieved a frame rate of 6 frames per second using the GPU-based approach for 16 transmits and kernel size of 60 x 60 pixels, which is 400 times faster than that achieved using our standard protocol.

9040-46, Session PSWed

## 3D ultrasound Nakagami imaging for radiation-induced vaginal fibrosis

Xiaofeng Yang, Emory Univ. (United States); Joseph Shelton, Emory Univ (United States); Peter Rossi, Debrorah Bruner, Srini Tridandapani, Tian Liu, Emory Univ. (United States)

Radiation-induced vaginal fibrosis is a debilitating site-effect, affecting up to 80% of women receiving radiotherapy for their gynecological (GYN) malignancies. Despite the significant incidence and severity, little research has been conducted to identify the pathophysiologic changes of vaginal toxicity. In a previous study, we have demonstrated that ultrasound Nakagami shape and PDF parameters can be used to quantify radiation-induced vaginal toxicity. These Nakagami parameters are derived from the statistics of ultrasound backscattered signals to capture the physical properties (e.g., arrangement and distribution) of the biological tissues. In this paper, we propose to expand this Nakagmi imaging concept from 2D to 3D to fully characterize radiation-induced changes to the entire vaginal wall within the radiation treatment field. A pilot study with 5 post-radiotherapy GYN patients was conducted using a clinical ultrasound scanner (6 MHz) with a mechanical stepper. A serial of 2D ultrasound images, with radio-frequency (RF) signals, were acquired at 1 mm step size. The 2D Nakagami shape and PDF parameters were calculated from the RF signal envelope with a sliding window, and then 3D Nakagami parameter images were generated from the parallel 2D images. This imaging method may be useful as we try to monitor radiation-induced vaginal injury, and address vaginal toxicities and sexual dysfunction in women after radiotherapy for GYN malignancies.

9040-47, Session PSWed

# Quality assurance for ultrasound scanners using a durable tissue-mimicking phantom and radial MTF

Marcus Kaar, Friedrich Semturs, Michael Figl, Rainer Hoffmann, Johann Hummel, Medizinische Univ. Wien (Austria)

For the use in routine technical quality assurance (TQA) we developed a tissue-mimicking phantom and an evaluation algorithm. Key properties of US phantom materials are sound velocity and acoustic attenuation. For daily clinical use the material also has to be nontoxic, durable and easy in handling and maintenance. The base material of our phantom is Poly(vinyl alcohol) (PVA), a synthetic polymer. By freezing the phantom body during the production process, it changes its sound velocity to closely match the one of the human body. The phantom's base form is a











cuboid containing a large anechoic cylindric target.

In routine QA it is required to gain comparable and reproducible results from a single image. To determine spatial resolution of phantom images, we calculate a modulation transfer function (MTF). We developed an algorithm, that calculates a radial MTF from a circular structure representing spatial resolution averaged across all directions. For evaluation of the algorithm, we created a set of synthetic images. A comparison of the results from a traditional slanted edge algorithm and our solution showed a close correlation. The US phantom was imaged with a commercial US-scanner at different sound frequencies. The computed MTFs of higher frequency images show higher transfer percentages in all spatial frequencies than the MTFs of lower frequency images.

The results suggest that the proposed method produces clear statements about the spatial resolution of evaluated imaging devices. We therefore consider the method as suitable for application in technical quality assurance of diagnostic ultrasound scanners.

#### 9040-48, Session PSWed

# Feasibility of using a reliable automated Doppler flow velocity measurements for research and clinical practices

Massoud Zolgharni, Niti M. Dhutia, Graham D. Cole, Keith Willson, Darrel P. Francis, Imperial College London (United Kingdom)

Human factors are a major source of variability in extracting clinical indices from the spectral Doppler envelopes that exhibit different shapes and sizes as a result of various heart conditions, different operators, and different imaging machines or manufactures. To reduce the variability and enhance the reliability of Doppler measurements, we have developed an automated system for detecting envelopes of Doppler traces. The proposed technology, the first of its kind, is capable of analysing long Doppler strips spanning many heartbeats. Two indices of velocity time integral and peak velocity that are used in clinical settings were considered for evaluating the efficiency of the automated measurements. Three cardiologist experts were asked to make similar measurements and the manual values were used as the gold-standard reference data. The results revealed that almost all automated values were within the range of expert measurements. Statistical analyses of linear regression and Bland-Altman showed a good agreement between the two methods. The proposed technology can be applied to clinical settings to reduce the inter- and intra-observer variability, and used in research to quantify different sources of error in Doppler measurements and to acquire more accurate data when required.

#### 9040-49, Session PSWed

# Automated measurement of fetal myocardial performance index in ultrasound Doppler waveforms

Heechul Yoon, Hyuntaek Lee, Samsung Electronics Co., Ltd. (Korea, Republic of); Kang-Won Jeon, Samsung Electronics Co. Ltd. (Korea, Republic of); Hae-kyung Jung, Samsung Electronics Co., Ltd. (Korea, Republic of); Mi-Young Lee, Hye-Sung Won, Eun-Jin Jeon, Asan Medical Ctr. (Korea, Republic of); Eun-Ho Yang, Jin-Young Choi, Soon-Jae Hong, Samsung Electronics Co., Ltd. (Korea, Republic of)

In the paper, we introduce a new automated measurement method for myocardial performance index (MPI), also known as Tei index, which is one of the most substantial indicators in the early screening of fetal heart defects. Since assessing fetal cardiac functions based on MPI has become a routine and significant process for monitoring fetal

conditions, there have been explicit requirements to automate MPI measurements. Due to small heart sizes of fetuses, we focus on the automation of modified MPI (Mod-MPI) measurements which use only a single Doppler gate. The proposed method detects and classifies four valve click signals in Doppler waveforms as crucial landmarks based on various image features. In the study, we use four main features which are extracted by vertical projection of Doppler waveforms after proper transformation. Finally, four features and their gradients determine a final MPI value by coarse-to-fine approach. For performance evaluation, 88 of fetal examinations were collected from commercial ultrasound machine (Accuvix A30, Samsung Medison Co., Ltd, Seoul, Korea), and two clinical experts measured the Mod-MPI both manually and automatically. Quantitative comparisons based on intraclass correlation coefficient (ICC) yield that intra-observer reproducibility is higher when performing the proposed method (ICC=0.951 and 0.932 for observer 1 and 2) comparing to those of manual measurements (ICC=0.868 and 0.857 for observer 1 and observer 2). Thus, our method (ICC=0.962) reveals distinctly superior inter-observer reproducibility than that of manual measurement (ICC=0.597). Although mean difference from observer 2 (?0.062) is over three times larger than that of observer 1 (?0.018) due to different experiences, both of mean differences are acceptable. In conclusion, the proposed MPI measurement method can significantly improve reproducibility while providing reliable results.

#### 9040-51, Session PSWed

# Implementation and optimization of ultrasound signal processing algorithms on mobile GPU

Woo Kyu Kong, Wooyoul Lee, Kyu Cheol Kim, Yangmo Yoo, Tai Kyong Song, Sogang Univ. (Korea, Republic of)

In medical ultrasound imaging, GPGPU has been used for improving computing power of ultrasound signal processing on PC. Recently, mobile GPU become powerful to deal with 3D games and videos at high frame rates on Full HD or HD resolution displays. This paper proposes the method to implement ultrasound signal processing on mobile GPU with programmable shaders on OpenGL ES 2.0. We show that a range of signal processing algorithms readily apply on mobile GPU by conducting B-mode image processing using OpenGL ES 2.0 (Galaxy S4). The beamformed data were captured from V10 (Samsung Medison), using a 2-5 MHz convex array probe with the transmit frequency of 1.6 MHz and the sampling frequencies of 20 MHz. Performance is evaluated by frame rate while varying the range of signal processing blocks. The implementation method of ultrasound signal processing on OpenGL ES 2.0 was verified by analyzing PSNR with MATLAB gold standard which has the same signal path. Other evaluation metrics, CNR was also analyzed to verify the method. From the evaluations, it has been verified that processing on OpenGL ES 2.0 has no significant difference with the processing using MATLAB. In addition, we propose techniques to achieve increased performance with optimization of shader design and load sharing between vertex and fragment shader. Implementation of ultrasound signal processing on OpenGL ES 2.0 minimizes of the size and lowers the cost of the ultrasound system. Thus, anybody who has the smart device can utilize ultrasound signal processing at low cost.

9040-52, Session PSWed

## Automatic estimation of elasticity parameters in breast tissue

Katrin Skerl, Sandy Cochran, Andrew Evans, Univ. of Dundee (United Kingdom)

Shear wave elastography (SWE), a novel ultrasound imaging technique, can provide unique information about cancerous tissue. To estimate elasticity parameters, a region of interest (ROI) is manually positioned over the stiffest part of the shear wave image (SWI). The aim of the work











is to estimate the elasticity parameters i.e. mean elasticity, maximal elasticity and standard deviation, fully automatically.

Ultrasonic SWIs of a breast elastography phantom and breast tissue in vivo were acquired using the Aixplorer system (Supersonic Imagine, Aix-en-Provence, France). First, the SWI within the ultrasonic B-mode image was detected using MATLAB then the elasticity values were extracted. The ROI was automatically positioned over the stiffest part of the SWI and the elasticity parameters were calculated. Finally all values were saved in a spread sheet which also contains the patients study ID. The elasticity values of the examined tissue are automatically estimated and saved to an excel sheet. This excel sheet is easy available for physicians and clinical staff for further estimation. Thereby the efficiency was increased. Especially for the evaluation and performance of clinical trials this algorithm simplifies the handling. The SWE processing method allows physicians easy access to the elasticity parameters of the examined tissues. This reduces clinical time and effort and simplifies evaluation of data in clinical trials.

#### 9040-55, Session PSWed

# Medical ultrasound image reconstruction using compressive sampling and lp-norm minimization

Adrian Basarab, Univ. de Toulouse (France) and Institut de Recherche en Informatique de Toulouse (France) and Univ. Paul Sabatier (France); Alin M. Achim, Univ. of Bristol (United Kingdom); Denis Kouamé, Univ. de Toulouse (France) and Institut de Recherche en Informatique de Toulouse (France) and Univ. Paul Sabatier (France)

In the last four years, a few research groups worked on the feasibility of compressive sampling (CS) in ultrasound medical imaging and several attempts of applying the CS theory may be found in the recent literature. In particular, it was shown that using I\_p-norm minimization with p different from 1 provides interesting RF signals reconstruction results. In this paper, we propose to further improve this technique by processing the reconstruction in the Fourier domain. In addition, ?-stable distributions are used to model the Fourier transforms of the RF lines. The parameter p used in the optimization process is related to the parameter ? obtained by fitting the data (in the Fourier domain) with an ?-stable distribution. The results obtained on two experimental US images show significant reconstruction improvement compared to the previously published approach where the reconstruction was performed in the spatial domain.

#### 9040-56. Session PSWed

## The design of split row-column addressing array for 2D transducer

Yanping Jia, Liushuai Lv, Mingyue Ding, Yuchi Ming, Huazhong Univ. of Science and Technology (China)

Real-time 3D ultrasonic imaging with 2D array is difficult to implement because of the challenge in fabricating and interconnecting the 2D transducer array with a large number of elements. Row-column addressing supplies a simple manufacturing method with 2N connections rather than N2 for an N?N array. The top and bottom electrodes of the transducer are designed to be orthogonal, resulting in essentially two orthogonal1-D arrays in a single transducer. However, this interconnection scheme degrades the image quality because of defocusing in azimuth direction in transmit event. To solve this problem, a split row-column addressing scheme is proposed in this paper. Rather than connecting all the elements in the azimuth direction together, the array is divided into several disconnected blocks. This method can access focusing beams in both azimuth and elevation directions. Selecting an appropriate split scheme is the key to maintaining a

reasonable trade off in image quality and the number of connections. The relation between the number of split and the corresponding main-lobe width is discussed. The simulated point spread functions of 32?32 array with and without split row-column addressing are given out. The result shows the image quality is similar to fully addressing for 32?32 array in case of five blocks with 6,8,4,8, and 6 elements of each block.

#### 9040-57, Session PSWed

# On the spectral response of thick piezoelectric capacitor sensors for arrays in imagenology applications

Bartolome Reyes-Ramírez, Crescencio Garcia-Segundo, Augusto García-Valenzuela, Univ. Nacional Autónoma de México (Mexico)

We investigate the spectral response of thick piezoelectric films to ultrasound perturbations arising from photoacoustic signals resulting from the interaction of laser pulses with neoprene immersed in water. The purpose is to characterize and verify consistency of the fabrication and of the response of capacitive piezoelectric sensors based on Polyvinylidene Fluoride (PVDF). We consider 52 µm thick PVDF films excited by laser pulse. The wavelength of sound waves within the considered spectral bandwidth ranges from equal to smaller than the thickness of the PVDF film. Initially, we analyze theoretically the mechanical-to-electrical transduction as a function of the frequency of sound. Then we present experimental results of the frequency response of a home-made PDVF sensor in water with test signals from 1 to 30 MHz induced by laser pulses. In this way we verify the correspondence of the analytic expression for the frequency dependent transfer function of a piezoelectric film and the experimental response of the test sensors. The tested sensors were encapsulated within a Faraday cage for the purpose of reducing high frequency noise. We compare the measured spectrum and the amplitude of the signal obtained in water for direct laser incidence on the sensor and for a test material pumped with laser pulses with our theoretical predictions.

#### 9040-59, Session PSWed

# Simulation study of real time 3D synthetic aperture sequential beamforming for ultrasound imaging

Martin C. Hemmsen, Morten F. Rasmussen, Matthias B. Stuart, Jørgen A. Jensen, Technical Univ. of Denmark (Denmark)

A simulation study of a wireless real-time three-dimensional (3-D) ultrasound imaging method using an electronically steered 64x64 element 300µm pitch linear array is presented. The wireless and real-time imaging capability is obtained using Synthetic Aperture Sequential Beamforming (SASB). The image quality of the presented 3-D SASB imaging method is compared to parallel beamforming utilizing 16 receive beamformers.

Parallel beamforming is constrained to 256 data transmission lines for a realistic implementation. Both imaging metods are setup with a view field of 60x60 degrees and a scan depth of 10 cm, resulting in 361 emissions for a frame rate of 20 Hz. As one indicator for image quality the C-scan 20 dB cystic resolutions are calculated for a set of scatters from 15 to 95 mm in steps of 10 mm. The set of C-scans are obtained by calculating the sum over a  $\pm 7.5$  mm radial distance for each of the 3-D point spread functions. The simulation results show that SASB has an improved cystic resolution at all depths, and as much as up to 80% reduction in cystic resolution at a depth of 95 mm. The results proves the viability of the method for wireless real-time 3-D ultrasound imaging.











9040-60, Session PSWed

# Optimization of ultrasound data processing with OpenCL for portable low-cost ultrasound system

Norbert Zolek, Krzysztof M. Sielewicz, Mateusz Walczak, Marcin Lewandowski, Institute of Fundamental Technological Research (Poland)

Our aim is to build programmable, portable ultrasound visualization system with full processing based on synthetic aperture (SA) algorithms. We propose optimizations of the ultrasound raw data transfer from the acquisition card and processing allowing to use most of computational power of General Purpose Graphical Processing Units (GPGPU). The parallel and strength reduction as well as polynomial approximations of the computations allow to obtain real-time processing on small low power single board PC based on Accelerated Processing Unit R-252F (AMD) (with Radeon 7400G class with 192 cores of GPGPU built-in processor with power consumption less than 25W). The obtained results of reconstruction, are compared with the visualization quality and visualization performance of a research Verasonics ultrasound acquisition system V-1-128 with V-3 chassis (Verasonics, USA). The results show that the our algorithms with proper optimizations allow to perform calculations for reconstruction of the standard ultrasound signal in real time (with framerate at least 80 fps) without any hardware preprocessing which is faster about 10 fps than framerate obtained from commercial system. The performance obtained allows to include additional postprocessing algorithms to improve image quality and still maintain real time processing.

9040-61, Session PSWed

## Ultrasound waveform tomography with a spatially-variant regularization scheme

Youzuo Lin, Lianjie Huang, Los Alamos National Lab. (United States)

Reliably characterizing small breast tumors is crucial for early cancer detection. The conventional ultrasound waveform tomography with a global regularization parameter may either over-regularize or under-regularize in different regions, leading to inaccurate estimates of breast sound-speed values. We develop a new ultrasound waveform tomography method with a spatially-variant regularization scheme for accurate sound-speed reconstructions, particularly for small breast tumors. Our new method employs different regularization parameters in different regions so that each regularization parameter is optimal for each region. Our numerical examples demonstrate that our new method improves reconstructions of sound-speed values of small breast tumors and greatly reduces image noise and artifacts.

9040-62, Session PSWed

## Real-time bent-ray breast ultrasound tomography using graphical processing units

Yassin Labyed, Lianjie Huang, Los Alamos National Lab. (United States)

We develop a parallel breast ultrasound ray tomography (USRT) algorithm that is optimal for use with graphical processing units (GPUs). Our algorithm generates USRT images of 2D slices of the breast in real time. We test the algorithm using a GPU cluster, each GPU (NVIDIA GTX670) has 1344 cores and 4GB of memory. We use numerical simulations and ultrasound data acquired from a breast tissue-mimicking phantom using our 768-channel breast ultrasound tomography system. We test the frame rate as a function of the size of the sound-speed map (number of

pixels) and the number of GPUs used for tomography reconstruction. Our breast ultrasound ray tomography algorithm achieves a frame rate of 2 Hz for a 400?400 sound-speed map using 8 GPUs. This frame rate is faster than the rate at which our ultrasound tomography system acquires slices of the breast. The frame rate increases with increasing number of GPUs or reducing the size of the sound-speed image. However the frame rate is not a linear function of the number of GPUs and the size of the image. Real-time ultrasound tomography could potentially help translate the breast ultrasound tomography technology into the clinic.

9040-63, Session PSWed

## Efficient implementation of ultrasound waveform tomography using data blending

Zhigang Zhang, Lianjie Huang, Los Alamos National Lab. (United States)

Ultrasound waveform tomography is time-consuming for large datasets acquired using a synthetic-aperture ultrasound tomography system consisting of hundreds to thousands of transducer elements. We develop a new ultrasound waveform tomography method using data blending from multiple sources to greatly improve the computational efficiency. This method simultaneously simulates ultrasound waves emitted from multiple transducer elements. We add a random time-delay to each source to distinguish the effect of different sources. The random time-delay helps eliminate the unwanted cross interference produced by blending data from different sources. This approach greatly reduces the computational time of ultrasound waveform tomography to less than one tenth of that for the original ultrasound waveform tomography, and makes it feasible for ultrasound waveform tomography in clinical applications.

9040-64. Session PSWed

# Toward a practical ultrasound waveform tomography algorithm for improving breast imaging

Cuiping Li, Delphinus Medical Technologies (United States) and Wayne State Univ. (United States); Gursharan S. Sandhu, Wayne State Univ. (United States); Olivier Roy, Delphinus Medical Technologies (United States) and Wayne State Univ. (United States); Neb Duric, Delphinus Medical Technologies (United States) and Karmanos Cancer Institute (United States); Veerendra Allada, Delphinus Medical Technologies (United States); Steven Schmidt, Delphinus Medical Technologies (United States) and Wayne State Univ. (United States)

Ultrasound tomography is an emerging modality for breast imaging. However, current ultrasonic tomography imaging algorithms, historically hindered by the limited memory and processor speed of computers, are based on ray theory and assume a homogeneous background, which is inaccurate for complex heterogeneous regions and fails when the size of lesions is about the same size or smaller than the wavelength of ultrasound used. Therefore, wave theory must be used in ultrasonic imaging algorithms to properly handle the heterogeneous nature of breast tissue and the diffraction effects in order to accurately image small lesions. Moreover, by taking full advantage of the computational architecture of Graphic Processing Units (GPUs), the intensive processing burden of waveform tomography can be greatly alleviated. In this study we develop novel and practical clinical breast imaging methods based on waveform tomography that have the potential to regularly detect lesions before they become metastatic. We implement waveform tomography algorithms by utilizing the Delphinus Medical Technologies SoftVue acquisition geometry and computational architecture, which will be able to produce high-accuracy and high-resolution breast images on clinically relevant time scales. We will show some simulation results and access the resolution and accuracy of our waveform tomography algorithms.











9040-65, Session PSWed

## Investigation of adjoint-state method for ultrasound tomography that eliminates the need for ray-tracing

Fatima Anis, Yang Lou, Mark A. Anastasio, Washington Univ. in St. Louis (United States)

Our work introduces an ultrasound tomography (UST) reconstruction algorithm based on the adjoint method for medical imaging. This method improves current ray-tracing based UST reconstruction algorithm and has been previously applied to seismic travel-time tomography [S. Leung and J. Qian, Comm. Math. Sci. 4 (2006)]. Ultrasound tomography has received wide attention for its ability to help breast cancer diagnosis both by providing speed of sound and attenuation information, as well as providing adjunct imaging data for optoacoustic tomography (OAT). Current image reconstruction algorithms for UST are usually based on ray- tracing and gradient methods. Our investigation shows two drawbacks of these methods that lead to inaccuracy in image reconstruction. First, ray bending in ray-tracing will cause an uneven distribution of ray paths. This will lead to insufficient updates in shadow zones (regions covered by few ray paths) and cause artifacts. While this effect can be compensated by regularization to some extent, we show that it cannot be avoided completely in ray-tracing methods. Second, often, a linear approximation of the gradient objective function is used, which also introduces errors into the gradient descent optimization method. We will demonstrate that using the adjoint method to directly compute the Frechet derivative of the continuous non-linear objective function can circumvent both drawbacks of the ray-tracing method. Numerical simulations are then given to show the improvement of our method over the ray-tracing method.

9040-66, Session PSWed

## Segmentation of 3D ultrasound computer tomography reflection images using edge detection and surface fitting

Torsten Hopp, Michael Zapf, Nicole V. Ruiter, Karlsruher Institut für Technologie (Germany)

An essential processing step for comparison of Ultrasound Computer Tomography images to other modalities, as well as for the use in further image processing, is to segment the breast from the background. In this work we present a (semi-) automated 3D segmentation method which is based on the detection of the breast boundary in coronal slice images and a subsequent surface fitting. The method was evaluated using a software phantom and in-vivo data. The fully automatically processed phantom results showed that a segmentation of approx. 10% of the slices of a dataset is sufficient to recover the overall breast shape. Application to 16 in-vivo datasets was performed successfully using a semi-automated processing. The processing time for the segmentation of a dataset could be significantly reduced compared to a manual segmentation. Comparison to manually segmented images identified a smoother surface for the semi-automated segmentation with an average of 11.0% of differing voxels and an average surface deviation of 2 mm. Limitations of the edge detection may be overcome by future updates of the USCT system, allowing a fully-automated usage of our segmentation approach.

9040-67, Session PSWed

# Intense acoustic burst ultrasound modulated optical tomography for elasticity mapping of soft biological tissue mimicking phantom: a laser speckle contrast analysis study

Mayanglambam S. Singh, Rajan Kanhirodan, Ram Vasu, Indian Institute of Science (India)

This report addresses the assessment of variation in elastic property of soft biological tissues non-invasively using laser speckle contrast measurement. The experimental as well as the numerical (Monte-Carlo simulation) studies are carried out. In this an intense acoustic burst of ultrasound (an acoustic pulse with high power within standard safety limits), instead of continuous wave, is employed to induce large modulation of the tissue materials in the ultrasound insonified region of interest (ROI) and it results to enhance the strength of the ultrasound modulated optical signal in ultrasound modulated optical tomography (UMOT) system. The intensity fluctuation of speckle patterns formed by interference of light scattered (while traversing through tissue medium) is characterized by the motion of scattering sites. The displacement of scattering particles is inversely related to the elastic property of the tissue. We study the feasibility of laser speckle contrast analysis (LSCA) technique to reconstruct a map of the elastic property of a soft tissuemimicking phantom. We employ source synchronized parallel speckle detection scheme to (experimentally) measure the speckle contrast from the light traversing through ultrasound (US) insonified tissuemimicking phantom. The measured relative image contrast (the ratio of the difference of the maximum and the minimum values to the maximum value) for intense acoustic burst is 86.44 % in comparison to 67.28 % for continuous wave excitation of ultrasound. We also present 1-D and 2-D image of speckle contrast which is the representative of elastic property distribution.

9040-68. Session PSWed

### Born-ratio type data normalization improves quantitation in photoacoustic tomography

Mayanglambam S. Singh, Phaneendra K. Yalavarthy, Indian Institute of Science (India)

In this report, we present a Born-ratio type of data normalization for reconstruction of initial acoustic pressure distribution in photoacoustic tomography (PAT). The normalized Born-ratio type of data is obtained as a ratio of photoacoustic pressure obtained with tissue sample in a coupling medium to the one obtained using purely coupling medium. It is shown that this type of data normalization improves the quantitation (intrinsic contrast) of the reconstructed images in comparison to the traditional techniques (unnormalized) that are currently available in PAT. Studies are carried out using various tissue samples. The robustness of the proposed method is studied at various noise levels added to the collected data. The improvement in quantitation can enable accurate estimation of patho-physiological parameter (optical absorption coefficient, µa) of tissue sample under investigation leading to better sensitivity in PAT.

9040-69, Session PSWed

## Multiwavelength photoacoustic microscopy using a custom developed supercontinuum fiber laser

Esra Aytac-Kipergil, Hakan Erkol, Bogaziçi Üniv. (Turkey); Seydi Yavas, Bilkent Univ. (Turkey); Aytac Demirkiran, Nasire Uluc, Mehmet Burcin Unlu, Bogaziçi Üniv. (Turkey)













Photoacoustic imaging is based on reconstruction of optical energy deposition that leads to ultrasound signals through thermal expansion. The signal amplitude is directly proportional to the local fluence and the absorption coeffcient of the target; thus, concurrence of source wavelength with the absorption peak of chromophores is of paramount significance. Here, we report a multiwavelength, very fast photoacoustic microscopy system with ultrabroad (500-1300 nm) spectrum. The laser is fiber-integrated, custom developed especially for photoacoustic excitation with adjustable parameters; pulse duration, energy and repetition frequency independent from each other. Pulse repetition frequency could be varied between 50 kHz to 3 MHz by acousto optic modulator through custom-developed field-programmable gate-array electronics. A 3.5 meter long photonic crystal fiber is spliced to doubleclad Yb-doped fiber of the laser amplifier for supercontinuum generation. The supercontinuum is sent through an acousto-optic tunable filter that enables very rapid wavelength tuning before being focused into the object. The laser system is superior to laser diodes and tunable Q-Switched lasers in the sense that it can provide higher pulse energies and higer repetition frequencies with the choice for a desired wavelength in the visible and near infrared spectral region. Multiwavelength imaging is performed on a phantom comprising multiple polymer tubes with diameters varying from 50 µm to 1mm filled with dyes of known absorption spectra. The tubes are immersed in Intralipid solution to mimic strong optical scattering of tissue, then the phantom is scanned along a line of length 50 mm in steps of 10  $\mu$ m. Taking measurements at multiple wavelengths allows for spectral separation of signals from different absorbers based on their characteristic absorption spectra and enables functional imaging.

9040-70, Session PSWed

# A study on the real-time photoacoustic tomography system for functional imaging and the monitoring of the rat's kidney inflammation

Dong Ho Shin, Sang Hun Park, Chonbuk National Univ. (Korea, Republic of); M.Y. Lee, W.C Ham, H.K Paik, Chonbuk National Univ (Korea, Republic of); Chul-Gyu Song, Chonbuk National Univ. (Korea, Republic of)

In this study, we developed a real-time PAT system for functional imaging in vivo and confirmed the feasibility of the proposed system through phantom test. Also, we have done a comparative analysis the rat's kidney. To quantify the measured photoacoustic signals from the linear array transducer in real-time, a multi-channel DAQ device is necessary. The PCI extensions for an instrumentation(PXI)-platform-based DAQ are used, with 50 MHz sampling frequency, 12 bit resolution, 128 analog input channels and 192 Mb/sec transmission speed, using direct memory access (DMA) method and a control program developed in Labview software. A custom-developed trigger controller is dedicated to laseremitting, and the trigger for acquisition timing generation and a linear array probe (L14-5/28, Ultrasonix) with 5 MHz center frequency and 128 element transducers were used to measure the photoacoustic signal. To amplify and filter the detected signal, a custom-developed pre-amplifier was placed ahead of the DAQ, and had 40 dB gain, 5 MHz passband and 128 channels. The results of phantom test show that our PAT system has enough performance to obtain a 570 \* 300 pixel image at 15 frames/sec with approximately 0.3mm resolution.

Also, we have done a comparative analysis the rat's inflammation of the kidneys. To observe the progression of inflammation, we induced inflammation by injecting the histamine into the right kidney. After the injection of histamine and contrast agency, we sacrificed the rats at intervals of 2 days and obtained histological images. PAT and histological images showed the inflammation of the kidneys progress of similar pattern. These results illustrated the potential for non-invasive diagnosis about the inflammation of the kidneys using PAT.

Also, we have done a comparative analysis the rat's inflammation of the kidneys. To observe the progression of inflammation, we induced inflammation by injecting the histamine into the right kidney. After the injection of histamine and contrast agency, we sacrificed the rats at intervals of 2 days and obtained histological images. PAT and histological images showed the inflammation of the kidneys progress of similar pattern. These results illustrated the potential for non-invasive diagnosis about the inflammation of the kidneys using PAT.

9040-71, Session PSWed

### Software Framework for spatially-tracked pre-beamformed RF data acquisition with a freehand clinical 2D ultrasound transducer

Hyun Jae Kang, Xiaoyu Guo, Alexis Cheng, Emad M. Boctor, Johns Hopkins Univ. (United States)

Acquisition of ultrasound (US) pre-beamformed radio-frequency (RF) data is essential in photoacoustic (PA) imaging research. Moreover, 3D PA imaging can provide volumetric information for a target of interest. However, existing 3D PA systems require specifically designed motion stages, ultrasound scanner and data acquisition system to collect 3D pre-beamformed RF data. These systems are not compatible with clinical ultrasound systems and are difficult to reconfigure and generalize to other PA research. To overcome the limitations of existing 3D PA systems, we propose and develop a software framework for spatially-tracked pre-beamformed RF data acquisition with a freehand conventional 2D ultrasound transducer and external tracking device. We upgraded our previous software framework using task-classes of OpenIGTLinkMUSiiC2.0 and MUSiiCToolkit 2.0. Also, we improved our MUSiiCToolKit 2.0 by adding MUSiiC Notes 2.0, a collection of specific task-classes for US research. MUSiiC DAQ-Server 2.0, MUSiiC Tracker Server and MUSiiCSync are the main modules of our software framework. Spatially-tracked 2D PA frames are collected efficiently using this software framework for 3D PA research and imaging. The software modules of our software framework are based on the concept of network distributed modules and support multiple-client connections via TCP/ IP network simultaneously. Moreover, the collected 2D PA frames are compatible with other modules of MUSiiC ToolKit 2.0 such as MUSiiC Beamform, B-Mode and MUSiiC Image-Viewer modules. These aspects of our software framework allow us to easily reconfigure and generalize our system to other PA or US research.

9040-72, Session PSWed

### Enabling technologies for robot assisted ultrasound tomography: ultrasound calibration

Fereshteh Aalamifar, Rishabh Khurana, Alexis Cheng, Russell H. Taylor, Iulian I. Iordachita, Emad M. Boctor, Johns Hopkins Univ. (United States)

In this study, we are proposing a robot-assisted ultrasound tomography (UT) system that can offer soft tissue tomographic imaging, deeper, and faster scan of the anatomy. This system consists of a robot operated ultrasound probe which tracks the position of another freehand probe, trying to align with it. The main challenge is to have the two ultrasound probes properly aligned. However, the system functionality and design is such that the ultrasound calibration has become a challenging problem too. In this paper, after providing an overview of the proposed robotic ultrasound tomography system, we focus on the ultrasound calibration problem.











9040-73, Session PSWed

### Real-time GPU implementation of transverse oscillation vector velocity flow imaging

David P. Bradway, Michael J. Pihl, Andreas Krebs, Borislav G. Tomov, Technical Univ. of Denmark (Denmark); Carsten S Kjær, Svetoslav I Nikolov, BK Medical (Denmark); Jørgen A. Jensen, Technical Univ. of Denmark (Denmark)

This paper presents a real-time ready implementation of 3-D vector flow image processing using an off-the-shelf AMD graphics processing unit (GPU). When combined with real-time beamforming, this efficient method will enable a 2-D transducer to be used to estimate the three orthogonal velocity components nearly instantaneously, allowing the visualization of complex flow patterns in the heart and arteries. In this work, Open Computing Language (OpenCL) is used to process 3-D M-mode data obtained using the Syntheic Aperture Realtime Ultrasound Scanner (SARUS) to image a carotid artery of a healthy 30-year-old volunteer. Loading and processing data from this 10-second M-Mode acquisition took 1.1 seconds on the GPU compared with 25.3 seconds using Matlab. When only processing time is recorded and file reading is neglected, the running times are 0.7 seconds and 8.25 seconds respectively. The observed percent difference between the OpenCL and Matlab results are 3.2%, 2.1%, and 0.18% for the X, Y, and Z dimensions. This method will enable the estimation of quantitative volumetric flow rates and bed-side examinations of angle-independent flow estimation. There may be important impacts on diagnoses of cardiovascular disease, improved visualization of complex 3-D flow patterns, and an increased understanding of human blood flow and pathology.

#### 9040-75, Session PSWed

### Assessment of aortic pulse wave velocity by ultrasound: a feasibility study in mice

Francesco Faita, Nicole Di Lascio, Francesco Stea, Claudia Kusmic, Rosa Sicari, Consiglio Nazionale delle Ricerche (Italy)

Pulse wave velocity (PWV) is considered a surrogate marker of arterial stiffness and could be useful for characterizing cardiovascular disease progression even in mouse models. Aim of this study was to develop an image process algorithm for assessing arterial PWV in mice using ultrasound (US) images only and test it on the evaluation of age-associated differences in abdominal aorta PWV (aaPWV).

US scans were obtained from six adult (7 months) and six old (19 months) wild type male mice (strain C57BL6) under gaseous anaesthesia. For each mouse, diameter and flow velocity instantaneous values were achieved from abdominal aorta B-mode and PW-Doppler images; all measurements were obtained using edge detection and contour tracking techniques. Single-beat mean diameter and velocity were calculated and time-aligned, providing the InD-V loop. aaPWV values were obtained from the slope of the linear part of the loop (the early systolic phase), while relative distension (reID) measurements were calculated from the mean diameter signal.

aaPWV values for young mice  $(3.5\pm0.52 \text{ m/s})$  were lower than those obtained for older ones  $(5.12\pm0.98 \text{ m/s})$  while reID measurements were higher in young  $(25\%\pm7\%)$  compared with older animals evaluations  $(15\%\pm3\%)$ . All measurements were significantly different between the two groups (P<0.01 both).

In conclusion, the proposed image processing technique well discriminate between age groups. Since it provides PWV assessment just from US images, it could represents a simply and useful system for vascular stiffness evaluation at any arterial site in the mouse, even in preclinical small animal models.

9040-76, Session PSWed

# The effects of probe placement on measured flow velocity in transcranial Doppler ultrasound imaging in vitro and in vivo experiments

Daan L. K. de Jong, Aisha S. S. Meel-van den Abeelen, Joep Lagro, Jurgen Claassen, Radboud Univ. Nijmegen Medical Ctr. (Netherlands); Cornelis H. Slump, Univ. Twente (Netherlands)

The measurement of the blood flow in the middle cerebral artery (MCA) using transcranial Doppler (TCD) ultrasound (US) imaging is considered to be clinically relevant for the study of the cerebral autoregulation. Especially in the aging population, impairment of the autoregulation may coincide or relate to loss of perfusion and consequently loss of brain function. The cerebral autoregulation can be assessed by relating the blood pressure to the blood flow in the brain. The blood pressure is conveniently and non - invasively measured with a finger cuff, the measured blood pressure can be related to the blood pressure in the brain. Doppler US is a widely used, non-invasive method to measure the blood flow in the MCA. However, Doppler flow imaging is known to produce results that are dependent of the operator. The angle of the probe insonation with respect to the centerline of the blood vessel is a well known factor for output variability. In patients also the skull must be traversed and the MCA must be detected, influencing the US signal intensity. In this contribution we report two studies. We describe first an in - vitro setup to study the Doppler flow in a situation where the ground truth is known by applying a flow phantom. Secondly, we report on a study with healthy volunteers where the effects of small probe displacements on the flow velocity signals are investigated. For the latter purpose, a special probe holder was designed to control the experiment.









Sunday - Monday 16-17 February 2014

Part of Proceedings of SPIE Vol. 9041 Medical Imaging 2014: Digital Pathology



9041-1, Session 1

#### **Path**, **present and future** (Keynote Presentation)

Richard M. Levenson M.D., Univ. of California, Davis (United States)

The talk will describe the traditional practice of pathology, with examples of how morphological diagnoses, still the mainstay of patient care, are actually arrived at. Then the role(s) of biomarkers - molecular indicators currently used to explore the complexity of cancer and the specific threats and vulnerabilities of individual tumors will be discussed. Such biomarkers are being tied to the deployment of novel therapeutics and will gate many future decisions as to which patients will (or will not) be treated by what drugs. There is a contest of sorts between tissue-extractbased tests (including proteomics and nucleic acid analyses) that can be both precise and highly multiplexed (tens to thousands of analytes) but are largely devoid of spatial context, and microscopic imaging based assays (like immunohistochemistry) that can have resolution down to the subcellular scale, but can deliver only modest levels of multiplexing. Novel instrumentation, reagents, and importantly, software (including machine learning and artificial intelligence), can help deliver both increasingly reliable assessments of pure morphology-associated features of pathology specimens, in some cases outperforming pathologists, and can also generate accurate and multiplexed, spatially resolved, molecular phenotypes. However, harder than the science and engineering challenges may be the problem of actually deploying such tools in a changing medical, financial and legal landscape.

9041-2, Session 1

### Automatic detection of invasive ductal carcinoma in whole slide images with convolutional neural networks

Angel Cruz Roa, Univ. Nacional de Colombia (Colombia); Ajay N. Basavanhally, Rutgers, The State Univ. of New Jersey (United States); Fabio A. González Osorio, Univ. Nacional de Colombia (Colombia); Hannah Gilmore, Univ. Hospitals of Cleveland (United States); Michael D. Feldman, Hospital of the Univ. of Pennsylvania (United States); Shridar Ganesan, Rutgers Cancer Institute of New Jersey (United States); Natalie Shih, Hospital of the Univ. of Pennsylvania (United States); John E. Tomaszewski M.D., Univ. at Buffalo (United States); Anant Madabhushi, Case Western Reserve Univ. (United States)

Recently many studies have shown that convolutional neural networks (CNN) are able to learn an appropriate task depending data representation for challenging computer vision problems beating the previous state of the art approaches. Here, we present a novel application of CNN for automatic detection of invasive ductal carcinoma (IDC) in whole slide images (WSI), sampling a large amount of image patch regions from WSI to train the CNN model. From the dataset comprises WSI from 40 patients diagnosed with IDC, we selected 28 slides for training and 12 slides for testing. CNN yielded the best quantitative results for automatic detection of IDC in terms of F-measure and balanced accuracy (76.27%, 85.40%), in comparison with the two best handcrafted features Fuzzy Color Histogram (71.06%, 78.74%) and RGB Histogram (69.51%, 77.24%), while the rest of global features, nuclear texture and architectural features did not produce competitive results. Our results also suggest that at least some of the errors (falsepositives and false-negatives) were less from any fundamental problems associated with the approach, than the inherent limitations in obtaining a very highly granular annotation of the diseased area of interest by an expert pathologist.

9041-3, Session 1

## Zooming in: high resolution 3D reconstruction of differently stained histological whole slide images

Johannes Lotz, Judith Berger, Fraunhofer MEVIS (Germany); Benedikt Müller, Kai Breuhahn, UniversitätsKlinikum Heidelberg (Germany); Niels Grabe, Ruprecht-Karls-Univ. Heidelberg (Germany); Stefan Heldmann, André Homeyer, Fraunhofer MEVIS (Germany); Bernd Lahrmann, Ruprecht-Karls-Univ. Heidelberg (Germany) and UniversitätsKlinikum Heidelberg (Germany); Hendrik Laue, Janine Olesch, Michael Schwier, Fraunhofer MEVIS (Germany); Oliver Sedlaczek, Arne Warth, UniversitätsKlinikum Heidelberg (Germany)

Much insight into metabolic interactions, tissue growth, and tissue organization can be gained by analyzing differently stained histological serial sections. One opportunity unavailable to classic histology is three-dimensional (3D) examination and computer aided analysis of tissue samples. In this case, registration is needed to reestablish spatial correspondence between adjacent slides that is lost during the sectioning process. Furthermore, the sectioning introduces various distortions like cuts, folds, tearings, and local deformations to the tissue, which need to be corrected in order to exploit the additional information arising from the analysis of neighboring slide images.

In this paper we present a novel image registration based method for reconstructing a 3D tissue block implementing a zooming strategy around a user-defined point of interest. We efficiently align consecutive slides at increasingly fine resolution up to cell level. We use a two-step approach, where after a macroscopic, coarse alignment of the slides as preprocessing, a nonlinear registration is performed to correct local, non-uniform deformations. Being driven by the optimization of the normalized gradient field (\$mathcal{NGF}\$) distance measure, our method is suitable for differently stained and thus multi-modal slides.

We applied our method to ultra thin serial sections \$(2, mu m)\$ of a human lung tumor and reconstructed the 3D volume. In total 170 slides, stained alternatingly with four different stains, have been registered. Thorough visual inspection of virtual cuts through the reconstructed block perpendicular to the cutting plane shows accurate alignment of vessels and other tissue structures.

Using nonlinear image registration, our method is able to correct locally varying deformations in tissue structures and exceeds the limitations of globally linear transformations.

9041-4, Session 3

### **Detection of felt tip markers on microscope** slides

David Friedrich, Dietrich Meyer-Ebrecht, RWTH Aachen (Germany); Alfred Böcking, Institute of Pathology (Germany); Dorit Merhof, RWTH Aachen (Germany)

Sensitivity and specificity of conventional cytological methods for cancer diagnosis can be raised significantly by applying further adjuvant cytological methods. To this end, the pathologist marks regions of interest (ROI) with a felt tip pen on the microscope slide for further analysis. This paper presents algorithms for the automated detection of these ROIs, which enables further automated processing of these regions by digital pathology solutions and image analysis. For this purpose, an overview scan is obtained at low magnification. Slides from certain manufacturers need to be treated, as they might contain certain regions which need to be excluded from the analysis. Therefore the slide type is identified first. Subsequently, the felt tip marks are detected











automatically, and gaps appearing in the case of ROIs which have been drawn incompletely are closed. Based on the marker detection, the ROIs are obtained. The algorithms have been optimized on a training set of 82 manually annotated images. On the test set, the slide types of all but one out of 81 slides were identified correctly. A sensitivity of 98.31% and a positive predictive value of 97.89% were reached for the detection of ROIs. In combination with a slide loader or a whole slide imaging scanner as well as automated image analysis, this enables fully automated batch processing of slides.

9041-5, Session 3

#### Hot spot detection for breast cancer in Ki-67 stained slides: image dependent filtering approach

Muhammad Khalid Khan Niazi, The Ohio State Univ. Medical Ctr. (United States); Erinn Downs-Kelly M.D., The Cleveland Clinic (United States); Metin N. Gurcan, The Ohio State Univ. Wexner Medical Ctr. (United States)

We present a new method to detect hot spots from breast cancer slides stained for Ki67 expression. It is common practice to use centroid of a nucleus as a surrogate representation of a cell. This often requires the detection of individual nuclei. Once all the nuclei are detected, the hot spots are detected by clustering the centroids. For large size images, nuclei detection is computationally demanding. Instead of detecting the individual nuclei and treating hot spot detection as a clustering problem, we considered hot spot detection as an image filtering problem where positively stained pixels are used to detect hot spots in breast cancer images. The method first segments the Ki-67 positive pixels using the visually meaningful segmentation (VMS) method that we developed earlier [1]. Then, it automatically generates an image dependent filter to generate a density map from the segmented image. The smoothness of the density image simplifies the detection of local maxima. The number of local maxima directly corresponds to the number of hot spots in the breast cancer image. The method was tested on 23 different regions of interest images extracted from 10 different breast cancer slides stained with Ki67. To determine the intra-reader variability, each image was annotated twice for hot spots by a pathologist with two-week interval in between her two readings. A computer-generated hot spot region was considered a true-positive if the hot it agrees with either one of the two annotation sets provided by the pathologist. While the intra-reader variability was 57%, our proposed method can correctly detect hot spots with 81% precision.

9041-6, Session 3

## Breast histopathology using random decision forests-based classification of infrared spectroscopic imaging data

David Mayerich, Univ. of Illinois at Urbana-Champaign (United States); Michael J. Walsh, Andre Kadjacsy-Balla, Univ. of Illinois at Chicago (United States); Shachi Mittal, Indian Institute of Technology Delhi (India); Rohit Bhargava, Univ. of Illinois at Urbana-Champaign (United States)

Breast cancer accounts for approximately 30% of new cancer cases in women, resulting in approximately 40,000 deaths in the United States in 2012. Current methods for cancer detection rely on the clinical application of dyes, often using immunohistochemistry techniques. Pathologists then evaluate the stained tissue in order to determine cancer stage and potential treatment. These methods are commonly used, however they are non-quantitative and it is difficult to control for staining quality across multiple laboratories. In this paper, we propose the use of mid-infrared spectroscopic imaging in order to classify tissue

types in biopsy samples. Our goal is to augment the data available to pathologists by providing them with quantitative chemical information to aid diagnostic activities in clinical and research activities related to breast cancer.

Tissue samples in a tissue microarray (TMAs) format are fixed, sectioned, and placed of substrates. One TMA section is imaged using a Fourier Transform Infrared (FT-IR) imaging system in order to acquire chemical information. Adjacent sections are prepared with a panel of chemical stains commonly used for breast cancer diagnosis. A trained pathologist then uses the stain information to annotate pixels in the adjacent FT-IR image based on tissue type. This annotation, combined with the spectroscopic information, is used to train a statistical classification system. We use a random forest model to perform the classification, showing that this provides robust classification and can be performed quickly in a clinical environment.

9041-7, Session 3

### Quantitative analysis of stain variability in histology slides and an algorithm for standardization

Babak Ehteshami Bejnordi, Nadya Timofeeva, Irene Otte-Höller, Nico Karssemeijer, Jeroen A. van der Laak, Radboud Univ. Nijmegen Medical Ctr. (Netherlands)

This paper presents data on the sources of variation of the widely used hematoxylin and eosin (H&E) histological staining, as well as a new algorithm to reduce these variations in digitally scanned tissue sections. Experimental results demonstrate that staining protocols in different laboratories and staining on different days of the week are the major factors causing color variations in histopathology images. The proposed algorithm for standardizing histology slides is based on an initial clustering of the image into two tissue classes having different tissue absorption characteristics for different stains. The color distribution for each tissue class is standardized by aligning the 2D histogram of color distribution in the hue-saturation-density (HSD) model. Qualitative evaluation of the proposed standardization algorithm shows that color constancy of the standardized images is improved. Quantitative evaluation demonstrates that the algorithm outperforms competing methods. In conclusion, the paper demonstrates that staining variations, which may potentially hamper usefulness of computer assisted analysis of histopathological images, may be reduced considerably by applying the proposed algorithm.

9041-8, Session 3

## Does the choice of display system influence perception and visibility of clinically relevant features in digital pathology images?

Tom R. Kimpe, Johan Rostang, Barco N.V. (Belgium); Ali N. Avanaki, Kathryn S. Espig, Albert Xthona, Barco, Inc. (United States); Ioan Cocuranu, Anil V. Parwani M.D., Liron Pantanowitz, Univ. of Pittsburgh Medical Ctr. (United States)

Digital pathology systems typically consist of a slide scanner, processing software, visualization software, and finally a workstation with display for visualization of the digital slide images. This paper studies whether digital pathology images can look different when presenting them on different display systems, and whether these visual differences can result in different perceived contrast of clinically relevant features.

By analyzing a set of four digital pathology images of different subspecialties on three different display systems, it was concluded that pathology images look different when visualized on different display systems. The importance of these visual differences is elucidated when they are located in areas of the digital slide that contain clinically











relevant features. Based on a calculation of dE2000 differences between background and clinically relevant features, it was clear that perceived contrast of clinically relevant features is influenced by the choice of display system.

Furthermore, it seems that the specific calibration target chosen for the display system has an important effect on the perceived contrast of clinically relevant features. Preliminary results suggest that calibrating to DICOM GSDF calibration performed slightly worse than sRGB, while a new experimental calibration target CSDF performed better than both DICOM GSDF and sRGB. This result is promising as it suggests that further research work could lead to better definition of an optimized calibration target for digital pathology images resulting in a positive effect on clinical performance.

9041-9, Session 4

### Towards automatic patient selection for chemotherapy in colorectal cancer trials

Alexander I. Wright, Derek R. Magee, Philip Quirke, Univ. of Leeds (United Kingdom); Darren E. Treanor, Univ. of Leeds (United Kingdom) and Leeds Teaching Hospitals NHS Trust (United Kingdom)

Colorectal cancer (CRC) is the second largest cause of cancer mortality in the US and UK, with over 51,000 and 16,000 deaths per year respectively. The tumour:stroma ratio (T:S), is defined as the proportion of epithelial to stromal cells within a cancer, and can be quantified using stereometry techniques, such as the RandomSpot system. Since the introduction of this sampling system, research has found that the proportion of tumour to stroma can predict the response to therapy in colorectal cancer patients. Currently, T:S is calculated manually by visually inspecting and classifying systematically placed, equidistant points within the boundaries of a tumour on a virtual slide (referred to as 'spot counting'). By utilising existing pathologist classification data from previous clinical studies, a supervised learning algorithm has been developed in attempt to replicate human scoring. The algorithm extracts features based on colour, texture shape and structure, and uses a random forests implementation for training and testing. Currently the algorithm exhibits a 79% accuracy rate, without incorporating contextual features. Further work is being carried out to account for appropriate contextual information and for identification of virtual slides unsuitable for image analysis.

9041-10, Session 4

## Cascaded ensemble of convolutional neural networks and handcrafted features for mitosis detection

Haibo Wang, Case Western Reserve Univ. (United States); Angel Cruz Roa, Univ. Nacional de Colombia (Colombia); Ajay N. Basavanhally, Rutgers, The State Univ. of New Jersey (United States); Hannah Gilmore, Case Western Reserve Univ. (United States); Fabio A. González Osorio, Univ. Nacional de Colombia (Colombia); Natalie Shih, Hospital of the Univ. of Pennsylvania (United States); Michael D. Feldman, The Univ. of Pennsylvania Health System (United States); John E. Tomaszewski M.D., Univ. at Buffalo (United States); Anant Madabhushi, Case Western Reserve Univ. (United States)

Breast cancer (BCa) grading plays an important role in predicting disease aggressiveness and patient outcome. A key component of BCa grade is mitotic count, which quantifies the number of cells in the process of dividing (i.e. undergoing mitosis) at a specfic point in time. The development of computerized systems for automated detection of mitotic

nuclei is complicated by the highly variable shape and appearance of mitoses. In this paper, we present a cascaded approach for mitosis detection that intelligently combines convolutional neural networks (CNN) and handcrafted features (morphology, color and texture features). Evaluation on the public MITOS dataset yielded an F-measure of 0.7345. Apart from this being the second best performance ever recorded for this MITOS dataset, our approach is faster and requires fewer computing resources compared to extant methods, making this feasible for clinical use.

9041-11, Session 4

## Grading vascularity from histopathological images based on traveling salesman distance and vessel size

Muhammad Khalid Khan Niazi, Jessica Hemminger M.D., Habibe Kurt M.D., Gerard Lozanski M.D., Metin N. Gurcan, The Ohio State Univ. (United States)

Vascularity represents important element of tissue/tumor microenvironment and is implicated in tumor growth, metastatic potential and resistence to therapy. Small blood vessels can be visualized using immunohistochemical stains specific to vascular cells. However, currently used manual methods to assess vascular density are poorly reproducible and are at best semi quantitative. Computer based quantitative and objective methods to measure microvessel density are urgently needed to better understand and clinically utilize microvascular density information. We propose a new method to quantify vascularity from images of bone marrow biopsies stained for CD34 vascular lining cells protein as a model. The method starts by automatically segmenting the blood vessels by methods of maxlink thresholding and minimum graph cuts. The segmentation is followed by morphological postprocessing to reduce blast and small spurious objects from the bone marrow images. To classify the images into one of the four grades, we extracted 20 features from the segmented blood vessel images. These features include first four moments of the distribution of the area of blood vessels, first four moments of the distribution of 1) the edge weights in the minimum spanning tree of the blood vessels, 2) the shortest distance between blood vessels (shortest distance to connect all blood vessels with a constraint that each blood vessel should be visited once), 3) the homogeneity of the shortest distance (absolute difference in distance between consecutive blood vessels along the shortest path) between blood vessels and 5) blood vessel orientation. The method was tested on 26 bone marrow biopsy images stained with CD34 IHC stain, which were evaluated by three pathologists (GL, JH, HK). The pathologists took part in this study by quantifying blood vessel density using gestalt assessment in hematopoietic bone marrow portions of bone marrow core biopsies images. To determine the intra-reader variability, each image was graded twice by each pathologist with two-week interval in between their readings. For each image, the ground truth (grade) was acquired through consensus among the three pathologists at the end of the study. Ranking of the features reveals that the forth moment of the distribution of the area of blood vessels along with first moment of the distribution of the shortest distance between blood vessels can correctly grade 68.18% of the bone marrow biopsies, while the intra- and inter-reader variability among the pathologists are 66.87% and 40%, respectively.

9041-12. Session 4

## Automated high-throughput assessment of prostate biopsy tissue using infrared spectroscopic chemical imaging

Paul Bassan, Ashwin Sachdeva, The Univ. of Manchester (United Kingdom); Jonathan Shanks, The Christie NHS Foundation Trust (United Kingdom); Michael D. Brown, Noel W. Clarke, The Paterson Institute for Cancer Research (United Kingdom) and











The Univ. of Manchester (United Kingdom); Peter Gardner, The Univ. of Manchester (United Kingdom)

Fourier transform infrared (FTIR) chemical imaging has been demonstrated as a promising technique to construct automated systems to compliment histopathological evaluation of biomedical tissue samples. Current histopathology practice involves preparing thin tissue sections and depositing them onto glass slides. After staining, most commonly haematoxylin and eosin (H&E), a histopathologist visually evaluates the tissue. This is a manual process and can be time consuming in cases where several sections using different stains are required. Studies have shown that there is variation in the agreement between operators viewing the same tissue [1] suggesting that a complimentary technique for verification could improve the robustness of the evaluation, and improve patient care. FTIR chemical imaging allows the spatial distribution of chemistry to be rapidly imaged at a high (diffraction limited) spatial resolution where a pixel represents an area of 5.5 ? 5.5 µm2 of tissue. At each pixel there is a full infrared spectrum providing a chemical fingerprint which studies have shown contains the diagnostic potential to discriminate between different cell types, and even the benign or malignant state of prostatic epithelial cells [2-4]. We report a label-free (i.e. no chemical de-waxing, or staining) method of imaging large pieces of prostate tissue (typically 1 cm ? 2 cm) in tens of minutes yielding images containing millions of spectra. Spectra are then automatically classified as one of seven cell-types in prostate tissue in a matter of seconds. This can be extended to classify the tissue as cancerous or non-cancerous and even predict the grade of the cancer.

#### References

- 1. Allsbrook, W.C., et al., Interobserver reproducibility of Gleason grading of prostatic carcinoma: Urologic pathologists. Human Pathology, 2001. 32(1): p. 74-80.
- 2. Fernandez, D.C., et al., Infrared spectroscopic imaging for histopathologic recognition. Nature Biotechnology, 2005. 23(4): p. 469-474.
- 3. Baker, M.J., et al., FTIR-based spectroscopic analysis in the identification of clinically aggressive prostate cancer. British Journal of Cancer, 2008. 99(11): p. 1859-1866.
- 4. Gazi, E., et al., A correlation of FTIR spectra derived from prostate cancer biopsies with Gleason grade and tumour stage. European Urology, 2006. 50(4): p. 750-761.

#### 9041-13, Session 4

## A fast method for approximate registration of whole-slide images of serial sections using local curvature

Nicholas A. Trahearn, David B. Epstein, The Univ. of Warwick (United Kingdom); David Snead, Univ. Hospitals Coventry and Warwickshire NHS Trust (United Kingdom); Ian A. Cree, Nasir M. Rajpoot, The Univ. of Warwick (United Kingdom)

We present a method for fast, approximate registration of whole-slide images (WSIs) of histopathology serial sections. Popular histopathology slide registration methods in the existing literature tend towards intensity-based approaches. Further input, in the form of an approximate initial transformation to be applied to one of the two WSIs, is then usually required, and this transformation needs to be optimised. Such a transformation is not readily available in this context and thus there is a need for fast approximation of these parameters.

Fast registration is achieved by comparison of the external boundaries of adjacent tissue sections, using local curvature on multiple scales to assess similarity. Our representation of curvature is a modified version of the Curvature Scale Space (CSS) image. We substitute zero crossings with signed absolute maxima of curvature to improve the registration's robustness to the subtle morphological differences of adjacent sections. A pairwise matching is made between curvature maxima at scales increasing exponentially, the matching minimises the distance between

maxima pairs at each scale. The boundary points corresponding to the matched maxima pairs are used to estimate the desired transformation.

Our method is highly robust to translation, rotation, and linear scaling, and shows good performance in cases of moderate non-linear scaling. On our set of test images the algorithm shows improved reliability and processing speed in comparison to existing CSS based registration methods.

#### 9041-14, Session 4

# Classification of glioblastoma and metastasis for neuropathology intraoperative diagnosis: a multi-resolution textural approach to model the background

Mohammad Faizal Ahmad Fauzi, The Ohio State Univ. (United States) and Multimedia Univ. (Malaysia); Hamza N. Gokozan, Brad Elder, Vinay K. Puduvalli, Jose J. Otero, Metin N. Gurcan, The Ohio State Univ. (United States)

Brain cancer surgery requires intraoperative consultation by neuropathology to guide surgical decisions regarding the extent to which the tumor undergoes gross total resection. In this context, the differential diagnosis between glioblastoma and metastatic cancer is challenging as the decision must be made during surgery in a short time-frame (typically 30 minutes). We propose a method to classify glioblastoma versus metastatic cancer based on extracting textural features from the non-nuclei region of cytologic preparations. For glioblastoma, these regions of interest are filled with glial processes between the nuclei, which appear as anisotropic thin linear structures. For metastasis, these regions correspond to a more homogeneous appearance, thus suitable texture features can be extracted from these regions to distinguish between the two tissue types. In our work, we use the Discrete Wavelet Frames to characterize the underlying texture due to its multi-resolution capability in modeling underlying texture and its directional nature. The textural characterization is carried out in primarily the non-nuclei regions after nuclei regions are segmented by adapting our visually meaningful decomposition segmentation algorithm to this problem. k-nearest neighbor method with (k=1 or 3) resulted in promising results: 80% accuracy for glioblastomas, 87.5% for metastasis and 83.5% overall. Further studies are underway to incorporate nuclei region features into classification on an expanded dataset.

#### 9041-15. Session 5

## 3D reconstruction of digitized histological sections for vasculature quantification in the mouse hind limb

Yiwen Xu, The Univ. of Western Ontario (Canada); J. Geoffrey Pickering, Zengxuan Nong, Robarts Research Institute (Canada); Eli D. Gibson, Robarts Research Institute (Canada) and The Univ. of Western Ontario (Canada); Aaron D. Ward, The Univ. of Western Ontario (Canada)

In contrast to imaging modalities such as magnetic resonance imaging and micro computed tomography, digital histology reveals multiple stained tissue features at high resolution (0.25µm/pixel). However, the two-dimensional (2D) nature of histology challenges three-dimensional (3D) quantification and visualization of the different tissue components, cellular structures, and subcellular elements. This limitation is particularly relevant to the vasculature, which has a complex and variable structure within tissues. Our objective was to perform an accurate, fully automated 3D reconstruction of mouse hind-limb tissue stained with hematoxylin and immunostained for smooth muscle ?-actin using 3,3'-Diaminobenzidine chromogen. We performed a 3D reconstruction using pairwise rigid registrations of 5µm thick, paraffin-embedded serial











sections, digitized at 0.25µm/pixel. Each registration was performed using the iterative closest points algorithm on blood vessel landmarks. Landmarks were vessel centroids, determined according to a signed distance map of each pixel to a decision boundary in hue-saturationvalue color space; this decision boundary was determined based on manual annotation of a separate training set. Cell nuclei were then automatically extracted and corresponded to refine the vessel landmark registration. Homologous nucleus landmark pairs appearing on not more than two adjacent slides were chosen to avoid registrations which force curved or non-section-orthogonal structures to be straight and section-orthogonal. The median accumulated target registration errors ± interguartile ranges for the vessel landmark registration, and the nucleus landmark refinement were 43.4±42.8µm and 2.9±1.7µm, respectively (p<0.0001). Fully automatic and accurate 3D rigid reconstruction of mouse hind limb histology imaging is feasible based on extracted vasculature and nuclei.

9041-16, Session 5

## Toward digital staining using stimulated Raman scattering and statistical machine learning

Koichi Tanji, Yoichi Otsuka, Shuya Satoh, Hiroyuki Hashimoto, Canon Inc. (Japan); Yasuyuki Ozeki, The Univ. of Tokyo (Japan); Kazuyoshi Itoh, Osaka Univ. (Japan)

Stimulated Raman scattering (SRS) microscopy is a promising imaging modality, which can visualize biological tissues with chemical specificity based on vibrational spectroscopy. PSRS microscopy has been used to obtain two-dimensional spectral images of rat liver tissue, three-dimensional images of a vessel in rat liver, and in vivo spectral images of mouse ear skin. PMeanwhile, various multivariate analysis techniques such as principal component analysis and independent component analysis have been applied to obtain spectral images.

In this study, we propose digital staining method using SRS spectra and statistical machine learning, which makes use of prior knowledge on?spectra patterns corresponding to the spatial composition of tissue samples and obtains digitally stained images without time-consuming chemical staining processes. The method is based on Fisher's linear discriminant analysis and regression models which compensate discriminant function on the whole image region. In addition, we select spectra peaks based on Mahalanobis distance which is defined as a ratio between to within subgroup variation. In this way, subgroups corresponding to each intracellular structure are clearly discriminated in the multidimensional feature space.

We investigated the performance of our method on liver tissue samples. The results show that the proposed method can digitally stain each intracellular structure such as cell nuclei, cytoplasm and erythrocytes separately. We are anticipating applications of our method to pathological diagnosis in the future.

9041-17, Session 5

### Accuracy and variability of tumor burden measurement on multi-parametric MRI

Mehrnoush Salarian, The Univ. of Western Ontario (Canada); Eli D. Gibson, Robarts Research Institute (Canada); Maysam Shahedi, Mena Gaed M.D., José A. Gomez-Lemus M.D., Madeleine Moussa M.D., Cesare Romagnoli M.D., Derek W. Cool M.D., Matthew Bastian-Jordan, Joseph L. Chin, Stephen E. Pautler, Glenn S. Bauman, Aaron D. Ward, The Univ. of Western Ontario (Canada)

Measurement of prostate tumour volume can inform prognosis and treatment selection, including an assessment of the suitability and

feasibility of focal therapy, which can potentially spare patients the deleterious side effects of radical treatment. Prostate biopsy is the clinical standard for diagnosis but provides limited information regarding tumour volume due to sparse tissue sampling. A non-invasive means for accurate determination of tumour burden could be of clinical value and an important step toward reduction of overtreatment. Multi-parametric magnetic resonance imaging (MPMRI) is showing promise for prostate cancer diagnosis. However, the accuracy and inter-observer variability of prostate tumour volume estimation based on separate expert contouring of T2-weighted (T2W), dynamic contrast-enhanced (DCE), and diffusion-weighted (DW) MRI sequences acquired using an endorectal coil at 3T is currently unknown. We investigated this question using a histologic reference standard based on a highly accurate MPMRIhistology image registration and a smooth interpolation of planimetric tumour measurements on histology. Our results showed that prostate tumour volumes estimated based on MPMRI consistently overestimated histological reference tumour volumes. The variability of tumour volume estimates across the different pulse sequences exceeded inter-observer variability within any sequence. Tumour volume estimates on DCE MRI provided the lowest inter-observer variability and the highest correlation with histology tumour volumes, whereas the apparent diffusion coefficient (ADC) maps provided the lowest volume estimation error. If validated on a larger data set, the observed correlations could support the development of automated prostate tumour volume segmentation algorithms as well as correction schemes for tumour burden estimation on MPMRI

9041-18, Session 5

## Ex-vivo optical coherence tomography of the human prostate after radical prostatectomy: preliminary results from a pilot study

Berrend G. Muller, Daniel M. de Bruin, Willemien van den Bos, Martin J. Brandt, Dirk J. Faber, Maria P. Laguna-Pes, Ton G. van Leeuwen, Jean J. de la Rosette, Academisch Medisch Ctr. (Netherlands)

Introduction: Current treatment in prostate cancer aims at systemic or radical procedures, with considerable side effects such as erectile dysfunction and/or incontinence. Current imaging modalities and biopsy protocols are insufficiently accurate to support tailored treatment of lowand intermediate risk prostate cancer. Optical coherence tomography (OCT) provides real-time morphological and quantitative information of tissue with unprecedented resolution. We present ex-vivo quantitative three-dimensional OCT data of prostate tissue by means of the optical attenuation coefficient using a needle-guided imaging probe.

Materials and Methods: A pullback scanning OCT probe and system were used to acquire 540 OCT images over 5.4 mm. Each probe was delivered through a 2.7 FR Venflon™ needle and applied at 6 specific locations per prostate. First, the OCT system and probes were calibrated using increasing concentrations Intralipid™ to assess the system roll-off and point-spread-function in order to optimize the optical attenuation analysis algorithms. Finally, grid-based optical scattering information by means of the optical attenuation coefficient from 6 ex-vivo human prostates were correlated to histo-pathology in 6 ex-vivo prostates to assess diagnostic accuracy per prostate.

#### Results:

3D attenuation visualization was accomplished by the in-house developed software. System calibration showed attenuation coefficients vs. Intralipid concentration which are in accordance with previously published results. The area under the ROC curve of each prostate ranges from 0.54 to 0.8.

Conclusion: Malignant areas were positively correlated to areas with a high attenuation coefficient. Research and analysis methods should be further studied in- and ex vivo to evaluate and improve true imaging accuracy.











9041-19, Session 5

# Enhancing effective depth-of-field using spectra-specific wavelets based multi-focus image fusion for digital pathology applications

Sailesh Conjeti, Biswajoy Ghosh, Sri Phani K. Karri, Debdoot Sheet, Hrushikesh T. Garud, Jyotirmoy Chatterjee, Ajoy K. Ray, Indian Institute of Technology Kharagpur (India)

Optical microscopy at high magnification is limited by a low depth of field (DoF) and prevents capture of clear target images of tissue structures at different depths in thin section histology when its thickness is greater than DoF. In this work, a wavelet-based multi-focus image fusion algorithm using a pixel-by-pixel non-linear fusion schema is presented. The all-in-focus image is generated by selectively fusing multiple partially focussed images. The information to be fused is selected as spectraspecific (R, G, B components) local maxima of wavelet-derived global focus measures (Daubechies 'Db6') estimated over complete z-stack. Following discrete wavelet coefficient extraction, the approximated components are blended as a weighted-average using weights proportional to localized focus measures generated from gradientbased scale-inclusive Gaussian steerable filters. For detail component fusion, the activity level is estimated as a Gaussian-windowed average of absolute coefficient values, followed by fusion using thresholded activity comparison and moving-window based consistency verification. The fused image is generated by inverse wavelet transform of the fusion of approximate and detail components. Multi-focus fusion of histopathological sections stained with Haematoxylin and Eosin are fused using a configuration with Daubechies 'Db4' wavelet basis with average global focus measure improvement of 9.61 dB (Max: 19.14 dB and Min: 4.78 dB). The proposed strategy ensures minimal blurring and preservation of local details in the fused image thus effectively extending the DoF of bright-field optical microscopy. This framework has been successful for histopathological images and can be leveraged for other optical microscopy applications.

9041-20, Session 5

### Tissue imaging using optical projection tomographic microscopy

Qin Miao, Univ. of Washington (United States); Vivan Hu, univeristy of washington (United States); Eric J. Seibel, Univ. of Washington (United States)

Conventional Optical Projection Tomography (OPT) can image tissue samples both in absorption and fluorescence mode. Absorption image can show the anatomical structure of the sample, while fluorescence mode can determine highly specific molecular distribution. The depth of focus (DOF) of the lens in conventional OPT needs to transverse the whole sample of millimeter or centimeter sizes. As a result, resolution will be poor due to the low numerical aperture (NA) needed to generate large DOF. In conventional pathology, the specimens are embedded in wax and sliced into thin slices so that high NA objective lens can be used to image the sections. In this case, the high resolution is obtained by using high NA objective lens, but 3D images can be only obtained by stitching different sections together. Here, we propose a new method that can image entire pathological specimen without sectioning with the same high resolution as the conventional pathology. To produce high resolution that is isotropic, the focal plane of the high NA objective lens is scanned through the entire specimen to produce one in a series of projection images. Then the specimen is rotated so that the subsequent projection is taken at different perspective. After all the projections are taken, 3D images are generated by the filtered back-projection method. Cleared pancreas tissue stained with Aldehyde Fuchsin is imaged.

9041-21, Session PSMon

#### Prostate malignancy grading using glandrelated shape descriptors

Ulf-Dietrich Braumann, Patrick Scheibe, Markus Löffler, Univ. Leipzig (Germany); Glen Kristiansen, Nicolas Wernert, Univ. Bonn (Germany)

The meritorious Gleason grading scheme (1966) relying on microscopy inspection and qualitative analysis of architectural features of prostate cancer tissues inherently is affected by a deficiency of both inter- and intra-observer reproducibility. Even though two revisions (2005, 2010) have reduced these problems, computer-assisted approaches pursuing quantitative histomorphometry are expected to further improve and standardize malignancy analyses.

We have accomplished a proof-of-principle study to assess the descriptive potential of two simple geometric measures applied to sets of segmented glands within images of 125 prostate cancer tissue sections. Respective measures addressing the shape of glands were (i) inverse solidity and (ii) inverse compactness, whereas both measures (obtained as gland-size weighted averaged) were combined using logistic regression in order to differentiate tumor patterns in line with Gleason grades 3 and 4/5. Obtained accuracy has reached 95% for near optimum gland segmentations. As results suggest, this approach not only exhibits good discriminatory properties, but also is robust w.r.t. gland segmentation variations.

Further, we have re-inspected all 5% discordant cases: about half of the them were re-assigned by the uropathologist, since even for an experienced observer it is hard to assign Gleason grade 3 or 4 in the presence of fusing glandular structures. Remaining ambiguities were caused due to similarities between sievelike cancer formations and normal glandular structures.

While our findings suggest that computer-assisted algorithmic differentiation of prostate malignancies using gland-related shape descriptors is promising, the method will be further validated in a large independent series of specimens.

9041-22, Session PSMon

# Multiparametric MR imaging of prostate cancer foci: assessing the detectability and localizability of Gleason 7 peripheral zone cancers based on image contrasts

Eli D. Gibson, Robarts Research Institute (Canada) and The Univ. of Western Ontario (Canada); Mena Gaed M.D., Robarts Research Institute (Canada) and Lawson Health Research Institute (Canada) and The Univ. of Western Ontario (Canada); Thomas Hrinivich, The Univ. of Western Ontario (Canada) and Robarts Research Institute (Canada); José A. Gomez-Lemus M.D., Madeleine Moussa M.D., Cesare Romagnoli M.D., The Univ. of Western Ontario (Canada); Jonathan Mandel, St. Joseph's Hospital (Canada) and The Univ. of Western Ontario (Canada); Matthew Bastian-Jordan, St. Joseph's Hospital (Canada); Derek W. Cool M.D., The Univ. of Western Ontario (Canada) and Robarts Research Institute (Canada); Suha Ghoul, Robarts Research Institute (Canada) and The Univ. of Western Ontario (Canada) and London Health Sciences Ctr. (Canada); Stephen E. Pautler, Lawson Health Research Institute (Canada) and The Univ. of Western Ontario (Canada); Joseph L. Chin, The Univ. of Western Ontario (Canada); Cathie Crukley, Robarts Research Institute (Canada) and Lawson Health Research Institute (Canada); Glenn S. Bauman, The Univ. of Western











Ontario (Canada); Aaron Fenster, Robarts Research Institute (Canada) and The Univ. of Western Ontario (Canada) and Lawson Health Research Institute (Canada); Aaron D. Ward, The Univ. of Western Ontario (Canada) and Lawson Health Research Institute (Canada)

Purpose: Multiparametric magnetic resonance imaging (MPMRI) supports detection and staging of prostate cancer, but the image characteristics needed for tumor boundary delineation to support focal therapy have not been widely investigated. We quantified the detectability (image contrast between tumor and non-cancerous contralateral tissue) and the localizability (image contrast between tumor and non-cancerous neighboring tissue) of Gleason score 7 (GS7) peripheral zone (PZ) tumors on MPMRI using tumor contours mapped from histology using accurate 2D-3D registration. Methods: MPMRI [comprising T2-weighted (T2W), dynamic-contrast-enhanced (DCE), apparent diffusion coefficient (ADC) and contrast transfer coefficient images] and post-prostatectomy digitized histology images were acquired for 6 subjects. Histology contouring and grading (approved by a genitourinary pathologist) identified 7 GS7 PZ tumors. Contours were mapped to MPMRI images using semi-automated registration algorithms (combined target registration error: 2 mm). For each focus, three measurements of mean ± standard deviation of image intensity were taken on each image: tumor tissue (m\_T±s\_T), non-cancerous PZ tissue < 5 mm from the tumor (m\_N±s\_N), and non-cancerous contralateral PZ tissue (m\_C±s\_C). Detectability (D=(m\_T-m\_C)/\(\sigma(s\_T^2+s\_C^2)\) and localizability (L=(m\_T-m\_C)/\(\sigma(s\_T^2+s\_C^2)\)) m\_N) $\sqrt{(s_T^2+s_N^2)}$  were quantified for each focus on each image. Results: T2W images showed the strongest detectability, although detectability |D|≥1 was observed on either ADC or DCE images, or both, for all foci. Localizability on all modalities was variable; however, ADC images showed localizability |L|≥1 for 3 foci. Conclusions: Delineation of GS7 PZ tumors on individual MPMRI images faces challenges; however, images may contain complementary information, suggesting a role for fusion of information across MPMRI images for delineation.

9041-23, Session PSMon

### A generalized framework for stain separation in digital pathology applications

Biswajoy Ghosh, Sailesh Conjeti, Sri Phani K. Karri, Debdoot Sheet, Indian Institute of Technology Kharagpur (India); Hrushikesh T. Garud, Indian Institute of Technology Kharagpur (India) and Texas Instruments (India) Pvt. Ltd. (India); Arindam Ghosh, Sub-Divisional Hospital (India); Jyotirmoy Chatterjee, Ajoy K. Ray, Indian Institute of Technology Kharagpur (India)

Microscopic examination of stained tissue sections obtained from biopsies forms the foundation of pathologically diagnosing diseased organs. Although offering a multi-scale view of the system pathology, interpretation is often subjective. Inter- and intra-observer variation in reporting due to limitations in tissue staining methods accounts for this subjectivity. Variation in stain uptake often leads to spectral overlap, variation in image intensities thus affecting the spectral signatures of imaged section and challenging computer assisted diagnosis. Stain density estimation techniques often referred to as digital stain separation have been introduced to overcome such limitations through quantification of amount of local stain uptake by a tissue. This is achieved by decorrelating the spectrally spread signal received by the color imaging sensor. Both blind and unblinded methods have been proposed with each having its own benefit. We focus on devising a framework for robust estimation of color deconvolution matrices as the basis for unblinded method. Here we propose a generalized framework using the Beer-Lambert intensity decay law for relating the stain uptake at a region to the resulting color and impose a Maxwellian chromaticity based regularization factor for solving the deconvolution matrix. The algorithm is trained and tested over different combinations of HE, VG and PAS stained cervical biopsy samples. The performance is validated using a 6-fold cross validation technique for each stain family and

error in estimation measured across folds using MSE of stain uptake measurement. This generalized framework can be appropriately modified to other histopathological and immunohistochemical compound staining methods in brightfield microscopy.

9041-24, Session PSMon

## Selection of the best features for leukocytes classification in blood smear microscopic images

Omid Sarrafzadeh, Hossein Rabbani, Ardeshir Talebi, Hossein Usefi Banaem, Isfahan Univ. of Medical Sciences (Iran, Islamic Republic of)

Automatic differential counting of leukocytes provides invaluable information to pathologist for diagnosis and treatment of many diseases. The main objective of this paper is to detect leukocytes from a blood smear microscopic image and classify them into their types: Neutrophil, Eosinophil, Basophil, Lymphocyte and Monocyte using features that pathologists consider to differentiate leukocytes. Features include color, geometric and texture features. Colors of nucleus and cytoplasm vary among the leukocytes. Lymphocytes have single, large, round or oval and Monocytes have singular convoluted shape nucleus. Nucleus of Eosinophils is divided into 2 and of Neutrophils into 2 to 5 segments. Lymphocytes often have no granules, Monocytes have tiny granules, Neutrophils have fine granules and Eosinophils have large granules in cytoplasm. We extract 6 color features from both nucleus and cytoplasm, 6 geometric features only from nucleus and 6 statistical features and 7 moment invariants features only from cytoplasm of leukocytes. The features are fed to support vector machine (SVM) classifiers with one to one architecture. The results obtained from applying the proposed method on blood smear microscopic image of 10 patients including 149 white blood cells (WBCs) indicate that correct rate for all classifiers are above 91% which is in a high level in comparison with previous literatures.

9041-25, Session PSMon

### A discriminant multi-scale histopathology descriptor using dictionary learning

David E. Romo, Juan D. García-Arteaga, Univ. Nacional de Colombia (Colombia); Pablo Arbeláez, Univ. of California, Berkeley (United States); Eduardo Romero Castro M.D., Univ. Nacional de Colombia (Colombia)

When examining a histological sample, an expert must not only identify structures at different scale and conceptual levels, i.e. cellular, tissular and organic, but also recognize and integrate the visual cues of specific pathologies and histological concepts such as "gland", "carcinoma" or "collagen". It is necessary then to code the texture and color so that the relevant information present at different scales is emphasized and preserved. In this article we propose a novel multi-scale image descriptor using dictionaries that learn and code discriminant visual elements associated with specific histological concepts. The dictionaries are built separately for each concept using sparse coding algorithms. The descriptor's discrimination capacity is evaluated using a naive strategy that assigns a particular image to the class best represented by a particular dictionary. Results show how, even using this very simple approach, average recall and precision measures of 0.81 and 0.86 were obtained for the challenging problem of classifying epidermis, eccrine glands, hair follicle and nodular carcinoma in basal skin carcinoma images.











9041-26, Session PSMon

### A multiview boosting approach to tissue segmentation

Jin Tae Kwak, Sheng Xu, Peter A. Pinto M.D., Baris Turkbey M.D., Marcelino Bernardo, Peter L Choyke M.D., Bradford J. Wood, National Institutes of Health (United States)

Digitized histopathology images have a great potential for improving or facilitating current assessment tools in cancer pathology. In order to develop accurate and robust automated methods, the precise segmentation of histologic objects such epithelium, stroma, and nucleus is necessary, in the hopes of information extraction not otherwise obvious to the subjective eye. Here, we propose a multivew boosting approach to segment histology objects of prostate tissue. Tissue specimen images are first represented at different scales using a Gaussian kernel and converted into several forms such HSV and La\*b\*. Intensity- and texturebased features are extracted from the converted images. Adopting multiview boosting approach, we effectively learn a classifier to predict the histologic class of a pixel in a prostate tissue specimen. The method attempts to integrate the information from multiple scales (or views). 18 prostate tissue specimens from 4 patients were employed to evaluate the new method. The method was trained on 11 tissue specimens including 75,832 epithelial and 103,453 stroma pixels and tested on 55,319 epithelial and 74,945 stroma pixels from 7 tissue specimens. The technique showed 96.7% accuracy, and as summarized into a receiver operating characteristic (ROC) plot, the area under the ROC curve (AUC) of 0.983 (95% CI: 0.983-0.984) was achieved.

9041-27, Session PSMon

### Cell density in prostate histopathology images as a measure of tumor distribution

Hayley M. Reynolds, Scott Williams, Peter MacCallum Cancer Ctr. (Australia); Alan M. Zhang, Cheng Soon Ong, David J. Rawlinson, Rajib Chakravorty, National ICT Australia (Australia) and The Univ. of Melbourne (Australia); Catherine Mitchell, Peter MacCallum Cancer Ctr. (Australia); Annette Haworth, Peter MacCallum Cancer Ctr. (Australia) and The Univ. of Melbourne (Australia)

We have developed an automatic technique to measure cell density in high resolution histopathology images of the prostate, allowing for quantification of differences between tumour and benign regions of tissue. Haemotoxylin and Eosin (H&E) stained histopathology slides from five patients were scanned at 20x magnification and annotated by an expert pathologist. Colour deconvolution and a radial symmetry transform were used to detect cell nuclei in the images, which were processed as a set of small tiles and combined to produce global maps of cell density. Kolmogorov-Smirnov tests showed a significant difference in cell density distribution between tumour and benign regions of tissue for all images analyzed (p < 0.05), suggesting that cell density may be a useful feature for segmenting tumour in un-annotated histopathology images. ROC curves quantified the potential utility of cell density measurements in terms of specificity and sensitivity and threshold values were investigated for their classification accuracy. Motivation for this work derives from a larger study in which we aim to correlate ground truth histopathology with in-vivo multiparametric MRI (mpMRI) to validate tumour location and tumour characteristics. Specifically, cell density maps will be registered with T2-weighted MRI and ADC maps from diffusion-weighted MRI. The validated mpMRI data will then be used to parameterise a radiobiological model for designing focal radiotherapy treatment plans for prostate cancer patients.

9041-28, Session PSMon

## Type II fuzzy systems for amyloid plaque segmentation in transgenic mouse brains for Alzheimer's disease quantification

April Khademi, PathCore Inc. (Canada) and Univ. of Guelph (Canada); Danoush Hosseinzadeh, PathCore Inc. (Canada)

Alzheimer's disease (AD) is the most common form of dementia in the elderly characterized by extracellular deposition of amyloid plaques (AP). Using animal models, AP loads have been manually measured from histological specimens to understand disease etiology, as well as response to treatment. Due to the manual nature of these approaches, obtaining the AP load is labourious, subjective and error prone. Automated algorithms can be designed to alleviate these challenges by objectively segmenting AP. In this paper, we focus on the development of a novel algorithm for AP segmentation based on robust preprocessing and a Type II fuzzy system. Type II fuzzy systems are much more advantageous over the traditional Type I fuzzy systems, since ambiguity in the membership function may be modeled and exploited to generate excellent segmentation results. The ambiguity in the membership function is defined as an adaptively changing parameter that is tuned based on the local contrast characteristics of the image. Using transgenic mouse brains with AP ground truth, validation studies were carried out showing a high degree of overlap and low degree of oversegmentation (0.8233 and 0.0917, respectively). The results highlight that such a framework is able to handle plaques of various types (diffuse, punctate), plaques with varying A? concentrations as well as intensity variation caused by treatment effects or staining variability

9041-29, Session PSMon

### Novel 3D cryo-histology method for validation of 3D imaging modalities

David Prabhu, Mohammed Q. Quatish, Case Western Reserve Univ. (United States); Emile Mehanna, Univ. Hospitals of Cleveland (United States); Zhuxian Zhou, Madhusudhana Gargesha, Andrew M. Rollins, Case Western Reserve Univ. (United States); Marco Costa M.D., Hiram G. Bezerra M.D., Univ. Hospitals of Cleveland (United States); David L. Wilson, Case Western Reserve Univ. (United States)

We developed a novel 3D histology technique (cryo-histology) and applied it to the validation of OCT image analysis methods and MRI imaging agents. Cryo-imaging (CryoVizTM) provides microscopic color anatomy and molecular fluorescence images, with single cell sensitivity of entire specimens, via repeated cryo-sectioning and tiled imaging of the tissue block face. Additionally, selected tissue sections are acquired via a taping method which ensures spatial fidelity. Histology images are registered to the appropriate color 2D image within the 3D cryo-image volumes. By registering in vivo image volumes to cryo-histology volumes, one can accurately analyze multi-modality data from the macro to the molecular level. In intravascular OCT experiments, 30 segments from 10 ex vivo coronary arteries were imaged using both OCT and cryoimaging. Selected histology sections were acquired and stained with H&E and Masson's Trichrome stains. Using an algorithm accounting for the catheter-centric rather than true-3D imaging with OCT, registration was performed on 15 of the acquired segments. Distance measurements between corresponding side branches was used to assess registration accuracy. Mean differences between these measurements improved from the unregistered data (-0.48  $\pm$  1.12 mm) to the registered data (-0.15 ± 0.41 mm) suggesting an improvement in correlation. Cryo-histology verified the ability of OCT imaging to identify fibrous, lipid, calcium. In targeted MRI imaging agent experiments, we examined targeting of Gd-CREKA to metastatic tumors in mouse tumor model of breast cancer. We acquired MRI, Cryo-brightfield, florescence GFP tumors, Cy5-CREKA, and histology sections. Then, we applied 3D multimodal











registration of MRI, Cryo-brightfield, Cryo-fluorescence and histology sections. Registered histology sections along with other volumes enabled verification of tumor model and assess targeting to metastases on multi-level visualizations from tissue to molecules.

9041-30, Session PSMon

### Perceptual uniformity of commonly used color spaces

Ali N. Avanaki, Kathryn S. Espig, Barco, Inc. (United States); Tom R. Kimpe, Barco N.V. (Belgium); Albert Xthona, Barco, Inc. (United States); Cedric Marchessoux, Johan Rostang, Bastian Piepers, Barco N.V. (Belgium)

Use of color images in medical imaging has increased significantly the last few years. Color information is essential for applications such as ophthalmology, dermatology and clinical photography. Use of color at least brings benefits for other applications such as endoscopy, laparoscopy and digital pathology.

Remarkably, as of today, there is no agreed standard on how color information needs to be visualized for medical applications. This lack of standardization results in large variability of how color images are visualized and it makes quality assurance a challenge. For this reason FDA and ICC recently organized a joint summit on color in medical imaging (CMI) [link]. At this summit, one of the suggestions was that modalities such as digital pathology could benefit from using a perceptually uniform color space (T. Kimpe, "Color Behavior of Medical Displays," CMI presentation, May 2013). Perceptually uniform spaces have already been used for many years in the radiology community where the DICOM GSDF standard [link] provides linearity in luminance but not in color behavior.

In this paper we quantify perceptual uniformity, using CIE's ?E2000 as a color distance metric, of several color spaces that are typically used for medical applications. We applied our method to theoretical color spaces Gamma 1.8, 2.0, & 2.2, standard sRGB, and DICOM (correction LUT for gray applied to all primaries). In addition, we also measured color spaces (i.e., native behavior) of a high-end medical display (Barco Coronis Fusion 6MP DL, MDCC 6130), and a consumer display (Dell 1907FP).

Our results indicate that sRGB & the native color space on the Barco Coronis Fusion exhibit the least non-uniformity within their group. However, the remaining degree of perceptual non-uniformity is still significant and there is certainly room for improvement.

9041-31, Session PSMon

### Feature-enhancing zoom to facilitate Ki-67 hot spot detection

Jesper Molin, Chalmers Univ. of Technology (Sweden) and Linköping Univ. (Sweden) and Sectra Imtec AB (Sweden); Kavitha Shaga Devan, Karin Wårdell, Linköping Univ. (Sweden); Claes Lundström, Linköping Univ. (Sweden) and Sectra Imtec AB (Sweden)

Image processing algorithms in pathology commonly include automated decision points such as classifications. While this enables efficient automation, there is also a risk that errors are induced. A different paradigm is to use image processing for enhancements without introducing explicit classifications. Such enhancements can help pathologists to increase efficiency without sacrificing accuracy. In our work, this paradigm has been applied to Ki-67 hot spot detection. Ki-67 scoring is a routine analysis to quantify the proliferation rate of tumor cells. Cell counting in the hot spot, the region of highest concentration of positive tumor cells, is a method increasingly used in clinical routine. An obstacle for this method is that while hot spot selection is a task suitable for low magnification, high magnification is needed to discern positive

nuclei, thus the pathologist must perform many zooming operations. We propose to address this issue by an image processing method that increases the visibility of the positive nuclei at low magnification levels. This tool displays the modified version at low magnification, while gradually blending into the original image at high magnification. The tool was evaluated in a feasibility study with four pathologists targeting routine clinical use. In a task to compare hot spot concentrations, the average accuracy was  $75\pm4.1\%$  using the tool and  $69\pm4.6\%$  without it (n=4). Feedback on the system, gathered in follow-up interviews, was that the pathologists found the tool useful and fitting in their existing diagnostic process. The pathologists judged the tool to be feasible for implementation in clinical routine.

9041-32, Session PSMon

## Phenotyping TILs in situ: automated enumeration of FOXP3+ and CD69+ T cells in follicular lymphoma

James R. Mansfield, PerkinElmer, Inc. (United States)

#### Background

In many cancers, tumor-infiltrating lymphocytes (TILs) indicate levels of tumor immunogenicity and predict survival. In particular, increased levels of regulatory T cells (Tregs) are associated with poorer prognosis, whilst CD69+ T-cells may also be prognostic. Understanding the phenotype and pattern of TILs in situ within tumors would be advantageous. However, visual TIL assessment cannot easily determine the type of lymphocyte in situ and multimarker quantitation is difficult with standard methods. We present a multi-marker, computer-aided event-counting method for determining the phenotypes of lymphocytes in follicular lymphoma using a multispectral imaging (MSI) automated tissue segmentation and counting approach.

#### Material and methods

A tissue microarray containing follicular lymphoma (FL) cores from 70 patients was chromogenically immunostained for CD3, CD69 and FOXP3, counterstained with hematoxylin, of which 40 cores were informative for both triplex staining and clinical follow-up. Each core was imaged using MSI and the individual staining of each marker separated from each other using spectral unmixing. Images were analyzed using software trained to recognize different tissue compartments based on morphology, specifically based on CD3 rich (extra-follicular) and poor (intra-follicular) areas. The FOXP3 or CD69 status of each CD3+ TIL was then determined and number Treg (FOXP3+/CD3+) and CD69+ T-cells counted in the intra- and extra-follicular areas.

#### Results

The intra-follicular (CD3 poor) and extra-follicular (CD3 rich) regions were accurately recognized within each core, based on abundance of CD3 cells. MSI enabled the accurate quantitation of CD3, CD69 and FOXP3 without crosstalk. The number of FOXP3+/CD3+ Tregs and CD69+ T-cells were counted in each core and used in Kaplan-Meier survival analysis, which demonstrated association of FOXP3+/CD3+ Tregs with favourable outcome in both the intra- (p=0.0173) and extra-follicular (p=0.0173) areas, as well as CD69+ T-cells in intra-follicular (p=0.0175) areas; CD69+ T-cells were not prognostic in extra-follicular areas (p=4509).

#### Conclusions

This study demonstrates use of an automated method for counting Tregs in follicular lymphoma, showing association of FOXP3+ Tregs with good outcome. Given the generic nature of the method automated multiplexed tissue cytometry analyses are feasible for routine clinical studies and work with many multiplexed IHC staining methodologies, of importance for translational cancer studies in general.











9041-33, Session PSMon

## Requirements, desired characteristics and architectural proposal for a visualization framework for digital pathology

Tom R. Kimpe, Barco N.V. (Belgium); Kathryn S. Espig, Ali N. Avanaki, Barco, Inc. (United States); Johan Rostang, Cedric Marchessoux, Bastian Piepers, Barco N.V. (Belgium); Albert Xthona, Barco, Inc. (United States)

Use of color images in medical imaging has increased significantly the last few years. One of the applications in which color plays an essential role is digital pathology. Remarkably, as of today, there is no agreed standard on how color information needs to be processed and visualized for medical imaging applications such as digital pathology. This lack of standardization results into large variability of how color images are visualized and it makes consistency and quality assurance a challenge. For this reason FDA and ICC recently organized a joint summit on color in medical imaging.

This paper focuses on the visualization and display side of the digital pathology imaging pipeline. Requirements and desired characteristics for visualization of digital pathology images are discussed in depth. Several technological alternative solutions and considered. And finally a proposal is made for a possible architecture for a display & visualization framework for digital pathology images. The main goal for making this architectural proposal is to facilitate a discussion that could lead to standardization.

9041-34. Session PSMon

#### Novel computer-aided diagnosis of Mesothelioma using nuclear structure of mesothelial cells in effusion cytology specimens

Akif Burak Tosun, Carnegie Mellon Univ. (United States); Alex Yergiyev, Allegheny General Hospital (United States); Soheil Kolouri, Carnegie Mellon Univ. (United States); Jan F. Silverman, Allegheny General Hospital (United States); Gustavo K. Rohde, Carnegie Mellon Univ. (United States)

Malignant mesothelioma is an uncommon neoplasm with high mortality and short survival. Currently, the gold diagnostic standard is a pleural biopsy with subsequent histologic examination of the tissue demonstrating invasion by the tumor. The diagnostic tissue is obtained through thoracoscopy or open thoracotomy, both being highly invasive procedures. Thoracocenthesis, or removal of effusion fluid from the pleural space, is a far less invasive procedure that can provide material for cytological examination. However, it is insufficient to definitively confirm or exclude the diagnosis of malignant mesothelioma, since tissue invasion cannot be determined. In this study, we present a computerized method to detect and classify malignant mesothelioma based on the nuclear chromatin distribution from digital images of mesothelial cells in effusion cytology specimens. Our method aims at determining whether a set of nuclei belonging to a patient, obtained from effusion fluid images using image segmentation, is benign or malignant, and has a potential to eliminate the need for tissue biopsy. This method is performed by quantifying chromatin morphology of cells using the optimal transportation (Kantorovich-Wasserstein) metric in combination with the modified Fisher discriminant analysis, a k-nearest neighborhood classification, and a simple voting strategy. Our results show that we can classify the data of 10 different human cases with 100% accuracy after blind cross validation. We conclude that nuclear structure alone contains enough information to classify the malignant mesothelioma. We also conclude that the distribution of chromatin seem to be a discriminating feature between nuclei of benign and malignant mesothelioma cells.

9041-36, Session PSMon

#### A Bayesian framework for cell-level protein network analysis for multivariate proteomics image data

Violet N. Kovacheva, Korsuk Sirinukunwattana, The Univ. of Warwick (United Kingdom); Nasir M Rajpoot, The Univ. of Warwick (United Kingdom) and Univ. of Qatar (Qatar)

The recent development of multivariate imaging techniques, such as the Toponome Imaging System (TIS), has facilitated the analysis of co-localization of several protein markers. This could hold the key to understanding complex phenomena such as protein-protein interaction in cancer. In this paper, we propose a Bayesian framework for cell-level network analysis allowing the identification of several protein pairs having significantly higher co-expression levels in cancerous tissue samples when compared to normal colon tissue. It involves segmenting the DAPI-labeled image into cells and determining the cell phenotypes according to their protein-protein dependence profile (PPDP). The cells are phenotyped using Gaussian Bayesian hierarchical clustering (GBHC), assuming a Gaussian distribution for the PPDP. The phenotypes are then analyzed using Difference in Sums of Weighted cO-dependence Profiles (DiSWOP), which detects differences in the co-expression patterns of protein pairs. We demonstrate that the pairs highlighted by the proposed framework have high concordance with recently obtained results in our group. The proposed approach could identify functional protein complexes active in cancer progression and cell differentiation.

9041-37, Session PSMon

#### Automatic scale-independent morphologybased quantification of liver fibrosis

Jérémy Coatelen, HISTALIM (France) and Univ. d'Auvergne (France) and Image Science for Interventional Techniques (France); Adélaïde Albouy-Kissi, Benjamin Albouy-Kissi, Image Science for Interventional Techniques (France) and Univ. d'Auvergne (France); Jean-Philippe Coton, Laurence Sifre, HISTALIM (France); Pierre Dechelotte, Univ. Hospital Estaing (France); Armand Abergel, Univ. Hospital Estaing (France) and Image Science for Interventional Techniques (France) and Univ. d'Auvergne (France)

The pathologists have an expert knowledge of the classification of fibrosis. However, the differentiation of intermediate grades (ex: F2-F3) may cause significant inter-expert variability. A quantitative morphological marker is presented in this paper, introducing a local-based image analysis on human liver tissue slides. Having defined hotspots in slides, the liver collagen is segmented with a color deconvolution technique. After removing the regions of interstitial fibrosis, the fractal dimension of the fibrosis regions is computed by using the box-counting algorithm. As a result, a quantitative index provides information about the grade of the fibrosis regions and thus about the tissue damage. The index does not take account of the pathological status of the patient but it allows to discriminate accurately and objectively the intermediate grades for which the expert evaluation is partially based on the fibrosis development. This method was used on six human liver tissue slides (from six different patients) using constant conditions of preparation, acquisition (same image resolution, magnification x20) and box-counting parameters. The liver tissue slides were labeled by a pathologist using METAVIR scores. A reasonably good correlation is observed between the METAVIR scores and the proposed morphological index. Furthermore, the method is reproducible and scale independent which is appropriate for biological high resolution images. Nevertheless, further work is needed to define reference values for this index is such a way that METAVIR subdomains will be well delimited.











9041-38, Session PSMon

### Color accuracy and reproducibility in whole slide imaging scanners

Prarthana Shrestha, Bas Hulsken, Philips Digital Pathology Solutions (Netherlands)

The digital scanners used in whole slide imaging (WSI) require an accurate and reliable representation of colors, considering their application in clinical diagnosis. In this paper, we propose a workflow for color reproduction in WSI scanners such that the colors in the scanned images are close to the ground truth of the input slide and consistent among scanners. We prepare a color phantom test slide, based on a standard IT8-target transmissive film, whose original colorimetric values for reference are available from the manufacturer. The phantom test slide is used to color calibrate the WSI scanner. The color accuracy of the calibrated scanners is measured by comparing with the reference colorimetric values in terms of DeltaE-2000 metric. We also employ a colorimetric method to render scanner generated RGB colors to the standard display (sRGB) colorspace such that the color difference among the scanners is minimum. The main advantage of the proposed workflow is that it is compliant to the ICC standard, applicable to color management systems in different platforms, and involve no additional color measuring devices. Our test on the reproducibility of the 11 phantom slides show that the prescribed preparation method can produce reliable slides with an average DeltaE below 1. The proposed workflow is implemented and evaluated in 35 WSI scanners, where the average DeltaE between a scanner and the colorimetric reference is 3.5. The DeltaE results on the phantom correlates with the visual color quality of the tissues scans.







